

---

# **Influence of Bridging Groups on the Reactivity of Dinuclear Platinum(II) Complexes with bis(2- pyridylmethyl)amine Chelate Headgroups.**

By

**Allen Mambanda**  
BSc. (Hons.); MSc. (Zimbabwe)

A thesis submitted in partial fulfilment for the **Doctoral of Philosophy** Degree  
to the Faculty of Science and Agriculture, University of KwaZulu-Natal.

For the work carried out in  
The School of Chemistry,  
University of KwaZulu-Natal,  
Pietermaritzburg.  
December 2009.



---

## **Declaration**

**This thesis report is based on results from an original work carried out in the School of Chemistry, University of KwaZulu-Natal, Pietermaritzburg and has not been submitted for the award of a Degree or a Diploma at any University.**

.....  
**A. Mambanda**

**I hereby certify that the statement is true.**

.....  
**Professor D. Jaganyi**  
**Supervisor**

**School of Chemistry**  
**University of KwaZulu-Natal**  
**Pietermaritzburg**  
**December 2009**

---

To my family and dear mum, with lots of love

---

# Table of Contents

<i>Acknowledgements</i>	<b>i</b>
<i>Abstract</i>	<b>ii</b>
<i>List of Abbreviations</i>	<b>viii</b>
<i>List of Figures and Schemes</i>	<b>x</b>
<i>List of Tables</i>	<b>xv</b>
<i>Publications and Conferences contributions</i>	<b>xx</b>

## Chapter One

### Use of Platinum complexes as anticancer pharmaceuticals.

<b>1.0</b>	<b>Mononuclear Pt(II) complexes</b>	<b>1</b>
1.0.1	Introduction	<b>1</b>
1.0.2	Mechanism of action of cisplatin	<b>4</b>
1.0.3	Mechanism of cisplatin resistance	<b>9</b>
1.0.4	The follow-up generations of cisplatin	<b>12</b>
1.0.4.1	<i>Mononuclear platinum drugs with reduced toxic side effects</i>	<b>12</b>
1.0.4.2	<i>Mononuclear platinum drugs designed to overcome cisplatin resistance</i>	<b>13</b>
1.0.4.3	<i>Orally administrable platinum complexes</i>	<b>14</b>
1.0.4.4	<i>Active trans-platinum complexes</i>	<b>15</b>
<b>1.1</b>	<b>Multinuclear Pt(II) complexes</b>	<b>18</b>
1.1.1	Introduction	<b>18</b>
1.1.2	Multinuclear Pt(II) complexes bridged by flexible diamines	<b>19</b>
1.1.3	Multinuclear Pt(II) bridged by rigid linkers	<b>25</b>
<b>1.2</b>	<b>Aims and objectives of the study</b>	<b>31</b>
<b>1.3</b>	<b>References</b>	<b>33</b>

## Chapter Two

A review on the theoretical aspects on the ligand substitution reactions of square-planar Pt(II) complexes focusing on the general role of the non-leaving ligand backbone.

<b>2.0</b>	<b>Theoretical aspects of ligand substitution reactions at a square-planar Pt(II) centre</b>	<b>40</b>
2.0.1	Introduction	<b>40</b>

2.0.2	Chemical bonding in square-planar $d^8$ platinum metal complexes	42
2.0.3	Mechanism labels at a square-planar geometry	45
<b>2.1</b>	<b>Measurements of kinetic parameters of ligand substitution reactions.</b>	<b>49</b>
2.1.1	Measurement of the rate constants	49
2.1.2	Measurement of the activation parameters	53
2.1.2.1	<i>Measurement of Enthalpy of activation (<math>\Delta H^\ddagger</math>) and Entropy of activation (<math>\Delta S^\ddagger</math>)</i>	53
2.1.2.2	<i>Measurement of the activation volume (<math>\Delta V^\ddagger</math>)</i>	55
2.1.3	Instrumentation for studying the kinetics of ligand substitution reactions of Pt(II) complexes	57
2.1.3.1	<i>General experimental considerations for chemical kinetics of substitution reactions</i>	57
2.1.3.2	<i>UV-visible Spectrophotometry</i>	59
2.1.3.3	<i>Flow Methods</i>	61
<b>2.2</b>	<b>General considerations for substitution reactions of Pt(II) complexes.</b>	<b>62</b>
2.2.1	Associative activation at a Pt(II) metal centre	62
2.2.2	Nature of the entering and leaving groups	65
2.2.3	Effect of solvent	68
2.2.4	Nature of the non-leaving coordinated groups	69
<b>2.3</b>	<b>References</b>	<b>77</b>

## Chapter Three

### Tuning the reactivity of chelated dinuclear Pt(II) complexes through a flexible diamine linker. A detailed kinetic and mechanistic study.

<b>3.0</b>	<b>Abstract</b>	<b>81</b>
<b>3.1</b>	<b>Introduction</b>	<b>82</b>
<b>3.2</b>	<b>Experimental</b>	<b>84</b>
3.2.1	Synthesis and characterization of $N,N,N',N'$ -tetrakis(2-pyridylmethyl)- $\alpha,\omega$ -alkyldiamine ligands	84
3.2.2	Synthesis of [ $\{\text{Pt}(\text{Cl})\}_2(N,N,N',N'$ -tetrakis(2-pyridylmethyl)- $\text{N}(\text{CH}_2)_n\text{N}-\text{N}(\text{ClO}_4)_2$ complexes	86
3.2.3	Preparation of aqua Pt(II) complexes and nucleophile solutions	88
3.2.4	Instrumentation and spectrometric measurements	90
3.2.5	Determination of $\text{p}K_a$ value of complexes	90

---

3.2.6	Kinetic measurements	91
3.2.7	Computational details	91
<b>3.3</b>	<b>Results</b>	<b>92</b>
3.3.1	Acid-base equilibria of the aqua Pt(II) complexes	92
3.3.2	Computational calculations	93
3.3.3	Kinetic measurements	100
<b>3.4</b>	<b>Discussion</b>	<b>112</b>
3.4.1	Hydrolysis of complexes	112
3.4.3	Kinetic measurements	113
<b>3.5</b>	<b>Conclusions</b>	<b>117</b>
<b>3.6</b>	<b>References</b>	<b>118</b>
<b>3.7</b>	<b>Supplementary information</b>	<b>121</b>
<b>3.8</b>	<b>Commentary notes</b>	<b>138</b>
3.8.1	X-rays diffraction analysis of ligand L2; L3 and L6.	138
3.8.2	Comment on the crystal structure of ligand L2; L3 and L6.	139
3.8.3	References to the commentary notes	140

## Chapter Four

### Kinetics study of Pt(II) amphiphiles derived from a bis(2-pyridylmethyl)amine chelate headgroup.

<b>4.0</b>	<b>Abstract</b>	<b>141</b>
<b>4.1</b>	<b>Introduction</b>	<b>142</b>
<b>4.2</b>	<b>Experimental</b>	<b>145</b>
4.2.1	Synthesis and characterization of amphiphilic ligands	145
4.2.2	Synthesis characterization of amphiphilic Pt(II) complexes	147
4.2.3	Preparation of aqua Pt(II) complexes	149
4.2.4	Preparation of nucleophiles solutions	150
4.2.5	Physical measurements and instrumentation	150
4.2.5.1	<i>Spectrophotometric measurements</i>	150
4.2.5.2	<i>Kinetics measurements</i>	151
4.2.5.3	<i>DFT Quantum mechanical calculations</i>	151
<b>4.3</b>	<b>Results and Discussion</b>	<b>152</b>
4.3.1	Synthesis and characterization	152

---

4.3.2	Acid-base equilibria of the aqua Pt(II) complexes	152
4.3.3	Computational calculations	156
4.3.4	Kinetics measurements	164
<b>4.4</b>	<b>Conclusions</b>	<b>176</b>
<b>4.5</b>	<b>References</b>	<b>177</b>
<b>4.6</b>	<b>Supplementary information</b>	<b>180</b>
<b>4.7</b>	<b>Commentary notes</b>	<b>197</b>
4.7.1	X-rays diffraction analysis of ligand <b>L4</b>	197
4.7.2	References to the commentary notes	198

## Chapter Five

### Ligand substitution reactions of chelated dinuclear Pt(II) complexes with diaminobenzene and diaminohexane linkers.

<b>5.0</b>	<b>Abstract</b>	<b>199</b>
<b>5.1</b>	<b>Introduction</b>	<b>200</b>
<b>5.2</b>	<b>Experimental</b>	<b>203</b>
5.2.1	Materials and reagents	203
5.2.2	Synthesis and characterization of ligands	203
5.2.3	Synthesis and characterization of dinuclear Pt(II) complexes with phenyldiamine and cyclohexyldiamine bridges and two of their monomeric analogues	205
5.2.4	Kinetic measurements and computational details	207
5.2.4.1	<i>Preparation of aqueous solutions of Pt(II) complexes</i>	207
5.2.4.2	<i>Preparation of nucleophiles solutions for kinetic analyses</i>	208
5.2.4.3	<i>Instrumentation and spectrophotometric measurements</i>	209
5.2.4.4	<i>Computational calculations</i>	209
<b>5.3</b>	<b>Results and Discussion</b>	<b>210</b>
5.3.1	$pK_a$ measurements of the aqua Pt(II) complexes	210
5.3.2	Computational calculations	214
5.3.3	Kinetic measurements	222
<b>5.4</b>	<b>Conclusions</b>	<b>235</b>
<b>5.5</b>	<b>References</b>	<b>236</b>
<b>5.6</b>	<b>Supplementary information</b>	<b>239</b>

---

<b>5.7</b>	<b>Commentary notes</b>	<b>254</b>
5.7.1	X-rays diffraction analysis of ligand <b>L6</b> .	<b>256</b>
5.7.2	Comment on the crystal structure of ligand <b>L4</b>	<b>256</b>
5.7.3	References to the commentary notes	<b>257</b>
 <b>Appendices</b>		 <b>258</b>
<b>Appendix A</b>		<b>258</b>
<b>Paper A1</b>	D. Jaganyi, <b>A. Mambanda</b> and O. Q. Munro, A tripodal tris(thiophene) derivative of hexahydropyrimidine and its ladder-like extended structure' <i>Acta Cryst.</i> , 2007, <b>E63</b> , o2388–o2390.	<b>259</b>
<b>Paper A2</b>	<b>A. Mambanda</b> , D. Jaganyi, and O. Q. Munro, One-dimensional C-H...N hydrogen-bonded polymers in flexible tetrapyrindyl systems, <i>Acta Cryst.</i> , 2007, <b>C63</b> , o676-o680.	<b>262</b>
<b>Paper A3</b>	<b>A. Mambanda</b> , D. Jaganyi and K. Stewart, <i>N,N</i> -bis(2-pyridylmethyl)- <i>tert</i> -butylamine, <i>Acta Cryst.</i> , 2009, <b>E65</b> , o402.	<b>268</b>
<b>Appendix B</b>		<b>273</b>
<b>Appendix C</b>		<b>283</b>
<b>Appendix D</b>		<b>301</b>

---

## Acknowledgements.

My profound gratitude goes to my supervisor, Professor D. Jaganyi, for the guidance on the laboratory work, fruitful discussions, helpful comments and unreserved advice on the writing of this thesis.

I would like to thank Professor O. Q. Munro for his assistance with the X-ray diffraction analyses of the ligands, his advice, comments and encouragements to report on their structural data.

I am indebted to Dr. D. Reddy for the unreserved mentorship.

I would like to acknowledge the following people and institutions:

Prof. Dr. Rudi van Eldik and Ms Stephanie Hochreuther, at the Institute of Inorganic Chemistry, University of Erlangen-Nürnberg, Germany, for the assistance with High-pressure measurements, CHN analysis and their fruitful discussions on the work reported in Chapter Three.

The National Research Foundation of South Africa and University of KwaZulu-Natal for financial assistance.

The academic staff members in the School of Chemistry (Pietermaritzburg Campus). Many thanks go to Dr. S. Spankie and Dr. M. Low for their assistance on my arrival in South Africa and their continued encouragements.

Mr. Craig Grimmer, for NMR spectral acquisition, assistance in running the kinetic experiments by NMR spectroscopy and his advice sought thereof.

Dr. F. Khan for the acquisition of MS spectra.

The technical staff: Messers. H. Desai and S. Ball for the procurements, Messers P. Forder and C. Mortlock for the glassblowing services and repairing of broken pieces, Ms F. Zuma for the technical assistance in the laboratory and her warm friendship, Messers. R. Somaru, F. Shaik and M. Makatini for technical assistance and the 'Team' from the Mechanical workshop for maintenance of the Stopped-flow analyzer and the vacuum pumps.

My colleagues in the Inorganic/Physical Research Group: P. O. Ongoma and U. Chathuri for the fruitful discussions in the Laboratory and for offering a brotherhood platform, Mrs. K-L Barry for her unreserved advice in the laboratory and Kate Gillam and Aishath Shaira for the fruitful discussions in the laboratory.

My spouse and family for the love and support. Lastly, I would like to praise the Almighty for His Love and Grace.

---

## Abstract

The influence on the reactivity of both the length as well as the structural nature of diamine bridges linking dinuclear Pt(II) complexes with homotopic bis(2-pyridylmethyl)amine headgroups has been investigated. For this purpose, three sets of square-planar Pt(II) complexes sharing a common non-labile bis(2-pyridylmethyl)amine chelate were synthesized and characterized by various spectroscopic methods. The substitution of the coordinated aqua ligands by three thiourea nucleophiles of different steric demands was studied in acidic aqueous medium under pseudo first-order conditions. The reactions were studied as a function of concentration, temperature and in some cases under an applied pressure using the standard stopped-flow technique and UV-visible spectrophotometry. Their thermodynamic properties were investigated by studying the acid-base equilibria of the coordinated aqua ligands using a spectrophotometric titration method. DFT Quantum mechanical calculations were also performed to determine their geometry-optimized structures and energies of the frontier molecular orbitals.

The first set of Pt(II) complexes comprise dinuclears, all bridged by a flexible  $\alpha,\omega$ -alkyldiamines. The second set of complexes is Pt(II) amphiphilic mononuclear analogues of the former set, formed intuitively by excising off one of the Pt(II) chelate headgroups. The last set of complexes comprises Pt(II) dinuclear complexes which are structurally related to the first set, but are linked by relatively rigid linkers, which are made up of either phenyldiamine or diaminocyclohexane fragments. In two of the complexes, a single methylene spacer ( $\text{CH}_2$ ) group is incorporated between the rigid moieties of the diamine bridge so as to elongate the average distances separating their Pt(II) atoms as well as to modulate the rigidity of the complexes. For comparison purposes, two monomeric analogues bearing the phenyl and cyclohexyl appended groups, respectively, were studied and reported together with these complexes.

In general, the substitution reactions of the coordinated aqua ligands of all the Pt(II) complexes by the three sulfur donor nucleophiles (Nu) proceed via a two-step reaction pathway. The first step, whose rate constant is denoted in subsequent text as  $k_{2(1)}^{\text{st}}$ , involves the substitution of the aqua ligands. The second step, induced by the coordination of the strong labilizing thiourea nucleophiles and whose rate constant is denoted in the text as  $k_{2(2)}^{\text{nd}}$ , is ascribed to the dechelation of the one of the *cis*-coordinated pyridyl units. Thus, the

---

substitution of the aqua ligands and the subsequent dechelation of the pyridyl units, can be expressed as  $k_{\text{obs}(1^{\text{st}}/2^{\text{nd}})} = k_{2(1^{\text{st}}/2^{\text{nd}})}[\text{Nu}]$  for all the reactions. Negative entropy of activation, negative volume of activation (in cases where measurements were carried out) and second-order kinetics for the substitution reactions all support an associative mode of activation.

The substitution reactivity of all the dinuclear complexes is influenced to a greater extent by the steric influences conferred by the bridge as well as a weak electronic effect. The steric influences are mutual, axially exerted and seemingly unique to the square-planar terdentate chelate headgroups. The steric influences depend strictly on length of the diamine (*i.e.*, the average distances separating the Pt centres of the dinuclears) as well as molecular symmetries and shapes of the complexes. The molecular symmetries and hence the shapes of the complexes depend on the parity of the connecting bonds in the diamine (whether even or not). If the connecting bonds of the bridges are even,  $C_{2h}$  structures and hence slip-up molecular geometry are preferred. Their overlap geometries cause mutual and axial steric influences on the Pt(II) square-planar chelates which retard substitutional reactivity when the bridge is short. When odd, bowl-shaped complexes of the  $C_{2v}$  point group symmetry are preferred in which the axial steric influences are absent at their Pt(II) chelates. In addition their bowl geometry causes an entrapment of the incoming nucleophiles, causing unusually high reactivity when compared to their even-bridged counterpart.

For both molecular symmetries ( $C_{2h}$  or  $C_{2v}$ ), the reactivity of the dinuclear complex depends on the average distances separating the Pt(II) centres of the dinuclears. In the former type of complexes, when the average distances separating their Pt(II) centres are long, the axial steric influences at each Pt(II) chelate due to their  $C_{2h}$  overlap geometry is weakened, leading to enhanced reactivity as the chain length is increased. In the latter type of complexes, this weakens the ‘entrapment’ effect of their bowl-shaped geometry, resulting in a steady decrease in reactivity when the chain length of the linker is increased. In addition rigidity and planarity within the backbone of the diamine bridge has been found to distort the bowl cavity causing weakening of the ‘entrapment effect’ resulting in the lower rates than expected.

The chain length as well as the structural make-up of the linker also determines the amount of electron density donated inductively from the linker to the Pt ions as well as the effective nuclear charge at each Pt(II) centre due to charge addition. These are two opposing

---

factors which also influence the rate of substitution in these complexes to some extent. The inductive effect as well as the presence of a domineering steric influence in the  $C_{2h}$  overlap geometry was verified by studying the reactivity of the analogous amphiphilic Pt(II) complexes.

---

## List of Abbreviations

---

<b>A</b>	associative mechanism
AgClO <sub>4</sub>	silver perchlorate
AgSO <sub>3</sub> CF <sub>3</sub>	silver trifluoromethanesulfonate
B3LYP	Becke-Perdev-Parr model. A local density functional model which improves on the local density by accounting explicitly for the non-uniformity in the electron density.
<b>bpma</b>	[Pt(H <sub>2</sub> O) <i>N,N</i> -bis(2-pyridylmethyl)](CF <sub>3</sub> SO <sub>3</sub> ) <sub>2</sub> .
<b>bpba</b>	[Pt(H <sub>2</sub> O) <i>N,N</i> -bis(2-pyridylmethyl)butylamine)](CF <sub>3</sub> SO <sub>3</sub> ) <sub>2</sub> .
<b>bpcHna</b>	[Pt(H <sub>2</sub> O) <i>N,N</i> -bis(2-pyridylmethyl)cyclohexylamine)](CF <sub>3</sub> SO <sub>3</sub> ) <sub>2</sub>
<b>bpda</b>	[Pt(H <sub>2</sub> O) <i>N,N</i> -bis(2-pyridylmethyl)decylamine)](CF <sub>3</sub> SO <sub>3</sub> ) <sub>2</sub> .
<b>bpea</b>	[Pt(H <sub>2</sub> O) <i>N,N</i> -bis(2-pyridylmethyl)ethylamine)](CF <sub>3</sub> SO <sub>3</sub> ) <sub>2</sub> .
<b>bpha</b>	[Pt(H <sub>2</sub> O) <i>N,N</i> -bis(2-pyridylmethyl)hexylamine)](CF <sub>3</sub> SO <sub>3</sub> ) <sub>2</sub> .
<b>pppa</b>	[Pt(H <sub>2</sub> O) <i>N,N</i> -bis(2-pyridylmethyl)propylamine)](CF <sub>3</sub> SO <sub>3</sub> ) <sub>2</sub> .
<b>bpPha</b>	[Pt(H <sub>2</sub> O) <i>N,N</i> -bis(2-pyridylmethyl)phenylamine)](CF <sub>3</sub> SO <sub>3</sub> ) <sub>2</sub> .
<b>bptba</b>	[Pt(H <sub>2</sub> O) <i>N,N</i> -bis(2-pyridylmethyl) <i>tert</i> -butylamine)](CF <sub>3</sub> SO <sub>3</sub> ) <sub>2</sub> .
<b>But</b>	[{Pt(H <sub>2</sub> O)} <sub>2</sub> <i>N,N,N',N'</i> -tetrakis(2-pyridylmethyl)-1,4-butanediamine)](CF <sub>3</sub> SO <sub>3</sub> ) <sub>4</sub> .
CF <sub>3</sub> SO <sub>3</sub> H	trifluoromethanesulfonic acid.
<b>cHn</b>	[{Pt(H <sub>2</sub> O)} <sub>2</sub> ( <i>N,N,N',N'</i> -tetrakis(2-pyridylmethyl)- <i>trans</i> -1,4-cyclohexyldiamine)](CF <sub>3</sub> SO <sub>3</sub> ) <sub>4</sub> .
CN	commentary notes
D	dissociative mechanism
<b>dcHnm</b>	[{Pt(H <sub>2</sub> O)} <sub>2</sub> ( <i>N,N,N',N'</i> -tetrakis(2-pyridylmethyl)-4,4'-methylenediaminocyclohexane)](CF <sub>3</sub> SO <sub>3</sub> ) <sub>4</sub> .
<b>Dec</b>	[{Pt(H <sub>2</sub> O)} <sub>2</sub> ( <i>N,N,N',N'</i> -tetrakis(2-pyridylmethyl)-1,10-decanediamine)](CF <sub>3</sub> SO <sub>3</sub> ) <sub>4</sub> .
δ/ ppm	chemical shift in parts per million
Δ <i>H</i> <sup>‡</sup>	enthalpy of activation
Δ <i>S</i> <sup>‡</sup>	entropy of activation
Δ <i>V</i> <sup>‡</sup>	volume of activation
DFT	density functional theory
dien	diethylenetriamine
DMF	dimethyl formamide
dmtu	<i>N, N'</i> -dimethylthiourea.
DNA	deoxyribose nucleic acid
<b>dPhm</b>	[{Pt(H <sub>2</sub> O)} <sub>2</sub> ( <i>N,N,N',N'</i> -tetrakis(2-pyridylmethyl)-4,4'-methylenediphenylamine)](CF <sub>3</sub> SO <sub>3</sub> ) <sub>4</sub>
<b>En</b>	[{Pt(H <sub>2</sub> O)} <sub>2</sub> ( <i>N,N,N',N'</i> -tetrakis(2-pyridylmethyl)-1,2-ethanediamine)](CF <sub>3</sub> SO <sub>3</sub> ) <sub>4</sub> .
GMP	Guanosine monophosphate
<b>Hex</b>	[{Pt(H <sub>2</sub> O)} <sub>2</sub> ( <i>N,N,N',N'</i> -tetrakis(2-pyridylmethyl)-1,6-hexanediamine)](CF <sub>3</sub> SO <sub>3</sub> ) <sub>4</sub> .
HOMO	highest occupied molecular orbital.
<i>k</i> <sub>2(1<sup>st</sup>/2<sup>nd</sup>)</sub>	second-order rate constants for the first and second substitution steps.
<i>k</i> <sub>-2</sub>	first-order rate constant for the backward reaction step.
<i>k</i> <sub>obs(1<sup>st</sup>/2<sup>nd</sup>)</sub>	observed pseudo first-order rate constants for the first and second reaction steps.
LFER	linear free energy relationship.
LUMO	lowest unoccupied molecular orbital.
I	interchange mechanism

---

---

IR	infrared
$\lambda$	wavelength
LACVP+**	pseudopotentials which include not only the valence <i>s</i> - and <i>p</i> -type orbitals but also the highest set of core orbitals, and in which the non-hydrogen and hydrogens atoms are supplemented by <i>d</i> - and <i>p</i> -type Gaussian functions, respectively.
LiSO <sub>3</sub> CF <sub>3</sub>	lithium trifluoromethanesulfonate
M	mole per litre
MO	molecular orbital
<b>mPh</b>	[[Pt(H <sub>2</sub> O)] <sub>2</sub> ( <i>N,N,N',N'</i> -tetrakis(2-pyridylmethyl)-1,3-phenyldiamine)](CF <sub>3</sub> SO <sub>3</sub> ) <sub>4</sub> .
NMR	Nuclear magnetic resonance
Nu	nucleophile
<i>o</i> -	ortho position of a functional group.
<i>para</i> -	forth position from a functional group on benzene ring
Ph	phenyl ligand
Phen	1,10-phenathrene
<b>pPh</b>	[[Pt(H <sub>2</sub> O)] <sub>2</sub> ( <i>N,N,N,N'</i> -tetrakis(2-pyridylmethyl)-1,4-phenyldiamine)](CF <sub>3</sub> SO <sub>3</sub> ) <sub>4</sub> .
<b>Prop</b>	[[Pt(H <sub>2</sub> O)] <sub>2</sub> ( <i>N,N,N,N'</i> -tetrakis(2-pyridylmethyl)-1,3-propanediamine)](CF <sub>3</sub> SO <sub>3</sub> ) <sub>4</sub> .
<b>Oct</b>	[[Pt(H <sub>2</sub> O)] <sub>2</sub> ( <i>N,N,N,N'</i> -tetrakis(2-pyridylmethyl)-1,8-octatenediamine)](CF <sub>3</sub> SO <sub>3</sub> ) <sub>4</sub> .
SI	supporting information
terpy	2,2':6',2''-terpyridine
tu	thiourea
tmtu	<i>N, N, N', N'</i> -tetramethylthiourea
TOF MS-ES <sup>+</sup>	A time-of-flight mass spectrometer with an electron spray source operated in the positive ion mode.
<i>X</i>	leaving group

---

---

## List of Figures and Schemes

---

<b>Figure 1.1</b>	Structures of cisplatin and its analogues of mononuclear Pt(II) complexes.	<b>2</b>
<b>Figure 1.2</b>	Equilibria processes attained by cisplatin in the cytosol and its complex formation of 1,2-intrastrand d(GpG)-Pt crosslinks on DNA.	<b>5</b>
<b>Figure 1.3</b>	Depiction of the major adducts which can be formed when cisplatin interacts with DNA.	<b>6</b>
<b>Figure 1.4</b>	Schematic diagrams showing the mechanism of action of cisplatin and its competing bio-transformational routes.	<b>8</b>
<b>Figure 1.5</b>	Schematic illustration of how sulfur containing compounds are thought to act as potential drug reserving agents in platinum chemotherapy.	<b>10</b>
<b>Figure 1.6</b>	Postulated scheme illustrating the mismatch repair of 1,2-(GpG)-Pt intrastrand crosslinks of cisplatin.	<b>11</b>
<b>Figure 1.7</b>	Active platinum(II) compounds containing: aromatic, isopropyl and iminoether carrier ligands.	<b>16</b>
<b>Figure 1.8</b>	Structures of cationic dinuclear platinum complexes bridged by flexible $\alpha,\omega$ -alkyldiamines.	<b>20</b>
<b>Figure 1.9</b>	Multinuclear complexes with capabilities of forming non-covalent interactions (hydrogen bonding and electrostatic interactions) with genomic DNA.	<b>23</b>
<b>Figure 1.10</b>	Multinuclear platinum complexes with rigid aromatic linkers.	<b>26</b>
<b>Figure 1.11</b>	Di-/trinuclear bridged platinum(II) complexes with a dipyrazolymethane (dpzm) bridging linkers.	<b>27</b>
<b>Figure 1.12</b>	Rigid platinum(II) complexes with isomeric azines and azoles bridging ligands.	<b>30</b>
<b>Figure 2.1</b>	Structures of ZD0473 and its unhindered 3-picoline isomeric analogue.	<b>41</b>
<b>Figure 2.2</b>	Chemical structure of BBR3464.	<b>42</b>
<b>Figure 2.3</b>	Molecular orbital representation of the bonding in $[\text{PtCl}_4]^{2-}$ , illustrating the relative energies of the molecular orbitals.	<b>44</b>
<b>Figure 2.4</b>	An illustration of the different mechanisms of substitution at a square-planar metal centre as proposed by Langford-Gray.	<b>45</b>
<b>Figure 2.5</b>	Energy profiles for the associative mechanism of substitution.	<b>46</b>
<b>Figure 2.6</b>	Typical stacked plots of the pseudo first-order rate constants, $k_{\text{obs}}$ versus the concentration of incoming nucleophiles.	<b>51</b>
<b>Figure 2.7</b>	A depiction of the dual reaction pathway for an associatively-activated substitution reaction at a Pt(II) metal centre.	<b>52</b>

---

<b>Figure 2.8</b>	A typical plot of the dependence of observed rate constant (as $\ln k_{\text{obs}}$ ) on the pressure for the reaction between a Pt(II) complex ( <b>Oct</b> ) and thiourea nucleophile recorded at 320 nm.	<b>56</b>
<b>Figure 2.9</b>	Schematic diagram of a UV-Visible spectrophotometer.	<b>59</b>
<b>Figure 2.10</b>	Schematic diagram of a stopped-flow reaction analyzer.	<b>61</b>
<b>Figure 2.11</b>	A typical kinetic trace acquired on a stopped-flow reaction analyzer showing a perfect fit to a single exponential.	<b>62</b>
<b>Figure 2.12</b>	Influence of the ligand <i>cis</i> to the leaving group, on the mechanism of substitution of square-planar Pt(II) complexes.	<b>63</b>
<b>Figure 2.13</b>	Plots of the pseudo first-order rate constants, $k_{\text{obs}}$ , versus the concentration of the entering nucleophiles, $[Y]$ , at the <i>trans</i> -[Pt( <i>py</i> ) <sub>2</sub> Cl <sub>2</sub> ] substrate.	<b>66</b>
<b>Figure 2.14</b>	Schematic diagram showing the effect of the electrostatic interactions on the bond strength of the leaving group.	<b>70</b>
<b>Figure 2.15</b>	Schematic representation of the $\sigma$ - <i>trans</i> effect due to a stabilization of the trigonal bipyramidal intermediate.	<b>72</b>
<b>Figure 2.16</b>	Schematic representation of $\pi$ -back bonding of a strong acceptor ligand.	<b>73</b>
<b>Scheme 3.1</b>	Synthetic scheme followed for the synthesis of dinuclear platinum(II) complexes.	<b>86</b>
<b>Figure 3.1</b>	Chemical structures of the $[\{\text{Pt}(\text{H}_2\text{O})\}_2(N,N,N',N'\text{-tetrakis}(2\text{-pyridylmethyl})\text{-}\alpha,\omega\text{-alkyldiamines})](\text{CF}_3\text{SO}_3)_4$ complexes.	<b>89</b>
<b>Figure 3.2</b>	UV-visible spectrum for the titration of 0.1 mM <b>En</b> with NaOH, pH range 2-9.	<b>92</b>
<b>Figure 3.3</b>	Aerial view showing the angles of inclination, $\alpha$ , in the DFT calculated slip-up sandwich structures of <b>En</b> and <b>Dec</b> and the hinge angle, $\beta$ , of the bowl structure of <b>Prop</b> .	<b>99</b>
<b>Figure 3.4</b>	<sup>1</sup> H NMR (500 MHz) spectra array of <b>bpma-Cl</b> (showing only the aromatic region) acquired during its reaction with two equivalents of thiourea (tu) in DMF- <i>d</i> <sub>7</sub> at 298 K.	<b>102</b>
<b>Figure 3.5</b>	A typical plot of the changes in absorbance observed within the 275-400 nm wavelength range for the dechelation of the pyridyl units in <b>En</b> by tu at 298 K, pH = 2.0.	<b>106</b>
<b>Figures 3.6(a;b)</b>	Concentration dependence of (a) $k_{\text{obs. (1}^{\text{st}})}$ , s <sup>-1</sup> , for the simultaneous displacement of the aqua ligands and (b) $k_{\text{obs. (2}^{\text{nd}})}$ , s <sup>-1</sup> , for the dechelation of the pyridyl units in <b>En</b> by a series of thiourea nucleophiles.	<b>105</b>
<b>Figures 3.7(a;b)</b>	Temperature dependence of (a) $k_{2(1^{\text{st}})}$ , M <sup>-1</sup> s <sup>-1</sup> , for the simultaneous displacement of the first aqua ligand and (b) $k_{2(2^{\text{nd}})}$ , M <sup>-1</sup> s <sup>-1</sup> , for the dechelation of the pyridyl units in <b>En</b> by a series of thiourea nucleophiles.	<b>110</b>
<b>Figure SI 3.1</b>	UV-visible spectra for the titration of 0.1 mM <b>Oct</b> with NaOH, pH range 2-9, T = 298 K.	<b>130</b>

<b>Figure SI 3.2a</b>	A typical kinetic trace for the two-steps reaction between <b>bpma</b> (0.1 mM) and tu (3 mM) recorded at 276 nm, T = 298 K, pH = 2.0.	131
<b>Figure SI 3.2b</b>	<sup>1</sup> H NMR spectral array of <b>Dec-Cl</b> (showing only the aromatic region) acquired during its reaction with three equivalents of thiourea (tu) in DMF- <i>d</i> 7	132
<b>Scheme SI 3.2c</b>	Proposed mechanism of substitution of the aqua leaving groups in the chelated Pt(II) dinuclear complexes and <b>bpma</b> .	133
<b>Figure SI 3.2d</b>	Kinetic trace at 324 nm for the first reaction step between <b>Dec</b> (0.11 mM) and dmtu (3.3 mM) at 298 K, pH = 2.0.	133
<b>Figure SI 3.3a</b>	Concentration dependence of $k_{\text{obs.}(1^{\text{st}})}$ , s <sup>-1</sup> , for the simultaneous displacement of the aqua ligands in <b>Prop</b> by a series of thiourea nucleophiles.	134
<b>Figure SI 3.3b</b>	Concentration dependence of $k_{\text{obs.}(2^{\text{nd}})}$ , s <sup>-1</sup> , for the dechelation of the pyridyl units in <b>Prop</b> by a series of thiourea nucleophiles.	134
<b>Figure SI 3.3c</b>	Concentration dependence of $k_{\text{obs.}(1^{\text{st}})}$ , s <sup>-1</sup> , for the simultaneous displacement of the aqua ligands in <b>Oct</b> by thiourea nucleophiles.	135
<b>Figure SI 3.3d</b>	Concentration dependence of $k_{\text{obs.}(2^{\text{nd}})}$ , s <sup>-1</sup> , for the dechelation of the pyridyl units in <b>Oct</b> by thiourea nucleophiles.	135
<b>Figure SI 3.3e</b>	Plots of concentration dependence of $k_{\text{obs}(1^{\text{st}})}$ , s <sup>-1</sup> , for the simultaneous displacement of the aqua ligands in <b>En</b> , <b>Prop</b> , <b>But</b> and <b>Hex</b> by iodide nucleophile.	136
<b>Figure SI 3.3f</b>	Plots of concentration dependence of $k_{2(2^{\text{nd}})}$ , s <sup>-1</sup> , for the simultaneous displacement of the aqua ligands in <b>En</b> , <b>Prop</b> , <b>But</b> and <b>Hex</b> by iodide.	136
<b>Figure SI 3.4a</b>	Dependence of $k_{\text{obs.}}$ (repeated twice) on the on the pressure of the reaction mixture recorded at 320 nm for the simultaneous displacement of the aqua ligands in a reaction between <b>Prop</b> and tu.	137
<b>Figure SI 3.4b</b>	Dependence of $k_{\text{obs.}}$ (repeated twice) on the on the pressure of reaction mixture recorded at 320 nm for the simultaneous displacement of the aqua ligands in a reaction between <b>Oct</b> and tu.	137
<b>Scheme CN 3.1</b>	Synthetic scheme for the novel bis-(2-thienylmethyl)hexahydropyrimidine derivative.	139
<b>Figure 4.1</b>	Structures of the Pt(II) amphiphiles with <i>N,N</i> -bis(2-pyridylmethyl)alkylamine head groups.	149
<b>Figure 4.2</b>	UV-visible spectra for the titration of 0.1 mM <b>bpha</b> with NaOH, pH range 2-9, T = 298 K. Inset is the titration curve at 267 nm.	153
<b>Figure 4.3</b>	<sup>1</sup> H NMR (500 MHz) spectral array of <b>bpma-Cl</b> (showing only the aromatic region) acquired during its reaction with two equivalents of thiourea (tu) in DMF- <i>d</i> 7 at 298 K.	165
<b>Figure 4.4</b>	The general reaction scheme for the reactions between the complexes and the thiourea nucleophiles at a pH of 2.0.	167
<b>Figure 4.5</b>	A typical plot showing the two well-separated kinetic steps for reaction between <b>bppa</b> (0.1 mM) and dmtu (3 mM) recorded at 284 nm.	168

<b>Figure 4.6a</b>	Concentration dependence of $k_{\text{obs.}(2^{\text{nd}})}$ , $\text{s}^{-1}$ , for the dechelation of the pyridyl units in <b>bpba</b> by a series of thiourea nucleophiles.	<b>169</b>
<b>Figure 4.6b</b>	Concentration dependence of $k_{\text{obs.}(2^{\text{nd}})}$ , $\text{s}^{-1}$ , for the dechelation of the pyridyl units in <b>bpba</b> by a series of thiourea nucleophiles.	<b>169</b>
<b>Figure SI 4.1a</b>	Low resolution ESI mass spectrum of <b>L5</b> .	<b>188</b>
<b>Figure SI 4.1b</b>	$^1\text{H}$ Spectrum of $[\text{Pt}(\text{DMF})\text{N},\text{N}\text{-bis}(2\text{-pyridylmethyl})\text{propylamine}](\text{SO}_3\text{CF}_3)_2$ .	<b>189</b>
<b>Figure SI 4.1c</b>	$^{13}\text{C}$ Spectrum of $[\text{Pt}(\text{DMF})\text{N},\text{N}\text{-bis}(2\text{-pyridylmethyl})\text{propylamine}](\text{SO}_3\text{CF}_3)_2$ .	<b>190</b>
<b>Figure SI 4.1d</b>	$^{195}\text{Pt}$ Spectrum of $[\text{Pt}(\text{DMF})\text{N},\text{N}\text{-bis}(2\text{-pyridylmethyl})\text{propylamine}](\text{SO}_3\text{CF}_3)_2$ .	<b>191</b>
<b>Figure SI 4.2</b>	UV-visible spectra for the titration of 0.1 mM <b>bpea</b> with NaOH, pH range 2 - 9, T = 298 K. Insert is the titration curve at 267 nm.	<b>192</b>
<b>Figure SI 4.3a</b>	Stopped flow kinetic trace at 335 nm for the first reaction step between <b>bpba</b> (0.11 mM) and tmtu (3.3 mM) at 298 K, pH = 2.0	<b>193</b>
<b>Figure SI 4.3b</b>	Concentration dependence of $k_{\text{obs.}(1^{\text{st}})}$ , $\text{s}^{-1}$ , for the simultaneous displacement of the first aqua ligand in <b>bptba</b> by thiourea nucleophiles.	<b>194</b>
<b>Figure SI 4.3c</b>	Concentration dependence of $k_{\text{obs.}(1^{\text{st}})}$ , $\text{s}^{-1}$ , for the dechelation of the pyridyl units in <b>bptba</b> by thiourea nucleophiles.	<b>195</b>
<b>Figure SI 4.3d</b>	Temperature dependence of $k_{2(1^{\text{st}})}$ , $\text{M}^{-1}\text{s}^{-1}$ , for the simultaneous displacement of the first aqua ligand in <b>bptba</b> by thiourea nucleophiles.	<b>196</b>
<b>Figure SI 4.3e</b>	Temperature dependence of $k_{2(2^{\text{nd}})}$ , $\text{M}^{-1}\text{s}^{-1}$ , for the dechelation of the pyridyl units in <b>bptba</b> by thiourea, pH = 2.0.	<b>196</b>
<b>Figure 5.1</b>	Structures of the dinuclear Pt(II) complexes and their respective mononuclear analogues synthesized in this study.	<b>208</b>
<b>Figure 5.2</b>	UV-visible spectra for the titration of 0.11 mM <b>dcHnm</b> with NaOH, pH range 2 -9, T = 298 K. Insert is the titration curve at 268 nm.	<b>210</b>
<b>Figure 5.3</b>	Kinetic trace at 335 nm for the first reaction step between <b>dPhm</b> (0.11 mM) and dmtu (6.6 mM) at 298 K.	<b>223</b>
<b>Figure 5.4a</b>	Concentration dependence of $k_{\text{obs}(1^{\text{st}})}$ , $\text{s}^{-1}$ , for the simultaneous displacement of the aqua ligands in <b>cHn</b> by thiourea nucleophiles.	<b>224</b>
<b>Figure 5.4b</b>	Concentration dependence of $k_{\text{obs}(2^{\text{nd}})}$ , $\text{s}^{-1}$ , for the dechelation of the pyridyl units in <b>cHn</b> by nucleophiles.	<b>225</b>
<b>Figure 5.5a</b>	Temperature dependence of $k_{2(1^{\text{st}})}$ , $\text{M}^{-1}\text{s}^{-1}$ , for the simultaneous displacement of the first aqua ligand in <b>cHn</b> by thiourea nucleophiles.	<b>232</b>
<b>Figure 5.5b</b>	Temperature dependence of $k_{2(2^{\text{nd}})}$ , $\text{M}^{-1}\text{s}^{-1}$ , for the dechelation of the pyridyl units in <b>cHn</b> by thiourea nucleophiles.	<b>233</b>

<b>Figure SI 5.1a</b>	Mass spectrum (TOF-MS <sup>+</sup> ) for <i>N,N,N',N'</i> -tetrakis(2-pyridylmethyl)-4,4'-methylenediphenylamine ( <b>L6</b> ).	246
<b>Figure SI 5.1b</b>	Mass spectrum (TOF-MS <sup>+</sup> ) for <i>N,N,N',N'</i> -tetrakis(2-pyridylmethyl)-4,4'-methylenediaminocyclohexane ( <b>L7</b> ).	247
<b>Figure SI 5.2</b>	UV-visible spectra for the titration of 0.1 mM <b>bpPha</b> with NaOH, pH range 2-9.	248
<b>Figure SI 5.3</b>	A typical kinetic trace showing the two-steps reaction between <b>bpcHna</b> (0.1 mM) and tu (3 mM) recorded at 284 nm, T = 298 K, pH = 2.0.	249
<b>Figure SI 5.4a</b>	Concentration dependence of $k_{\text{obs},(1)}^{\text{st}}$ , s <sup>-1</sup> , for the simultaneous displacement of the aqua ligands in <b>bpcHna</b> by thiourea nucleophiles, pH = 2.0, T = 298 K.	250
<b>Figure SI 5.4b</b>	Concentration dependence of $k_{\text{obs},(2)}^{\text{nd}}$ , s <sup>-1</sup> , for the dechelation of the pyridyl units in <b>bpcHna</b> by thiourea, pH = 2.0, T = 298 K.	251
<b>Figure SI 5.5a</b>	Temperature dependence of $k_{2(1)}^{\text{st}}$ , M <sup>-1</sup> s <sup>-1</sup> , for the simultaneous displacement of the first aqua ligand in <b>bpcHna</b> by thiourea nucleophiles, pH = 2.0.	252
<b>Figure SI 5.5b</b>	Temperature dependence of $k_{2(2)}^{\text{nd}}$ , M <sup>-1</sup> s <sup>-1</sup> , for the dechelation of the pyridyl units in <b>bpcHna</b> by thiourea, pH = 2.0.	253

---

## List of Tables

---

<b>Table 2.1</b>	Effect of solvent on the rate of chloride exchange from <i>trans</i> -[Pt( <i>py</i> ) <sub>2</sub> Cl <sub>2</sub> ].	<b>68</b>
<b>Table 2.2</b>	Rate constants and activation parameters for the substitution of the coordinated chloride by I <sup>-</sup> in [Pd(II)(R <sub>n</sub> dien)Cl] <sup>+</sup> (n = 0, 3-5) in aqueous solution at 25.0 °C.	<b>75</b>
<b>Table 3.1</b>	Summary of pK <sub>a</sub> data obtained for the deprotonation of Pt-bound aqua ligands. (within pH range 2-9), using NaOH as titrant.	<b>93</b>
<b>Table 3.2</b>	Density functional theoretical (DFT) minimum energy structures, HOMO and LUMO frontier molecular orbitals for <b>bpma</b> , <b>En</b> , <b>Prop</b> and <b>Dec</b> .	<b>95</b>
<b>Table 3.3</b>	Summary of the calculated structural data at the DFT Level of Theory for the complexes with bis(2-pyridylmethyl)amine chelates.	<b>97</b>
<b>Table 3.4</b>	Summary of the rate constants for the simultaneous displacement of aqua ligands and the dechelation of the pyridyl units by neutral nucleophiles in <b>bpma</b> and a range of dinuclear complexes with bis(2-pyridylmethyl) chelate headgroups.	<b>107</b>
<b>Table 3.5</b>	Summary of the activation parameters for the simultaneous displacement of aqua ligands and the dechelation of the pyridyl units by neutral nucleophiles in <b>bpma</b> and a range of dinuclear Pt(II) complexes with a bis(2-pyridylmethyl) chelate headgroups.	<b>111</b>
<b>Table SI 3.1</b>	Summary of the wavelengths (nm) used for monitoring the reactions between a series of Pt(II) complexes with bis(2-pyridylmethyl) chelates and thiourea nucleophiles.	<b>122</b>
<b>Table SI 3.2</b>	Density functional theoretical (DFT) minimum energy structures, HOMO and LUMO frontier molecular orbitals for <b>Pen</b> and <b>Hep</b> .	<b>123</b>
<b>Table SI 3.3</b>	Electrostatic potential surface mapping of the dinuclear Pt(II) complexes bridged by flexible diamine linkers.	<b>124</b>
<b>Table SI 3.4a</b>	Average observed rate constants, $k_{\text{obs.}(1^{\text{st}})}, \text{s}^{-1}$ , for the simultaneous displacement of the aqua ligands in <b>Prop</b> thiourea nucleophiles.	<b>124</b>
<b>Table SI 3.4b</b>	Average observed rate constants, $k_{\text{obs.}(2^{\text{nd}})}, \text{s}^{-1}$ , for the dechelation of the pyridyl units in <b>Prop</b> by thiourea nucleophiles.	<b>124</b>
<b>Table SI 3.4c</b>	Average observed rate constants, $k_{\text{obs.}(1^{\text{st}})}, \text{s}^{-1}$ , for the simultaneous displacement of the aqua ligands in <b>Oct</b> by thiourea nucleophiles.	<b>125</b>
<b>Table SI 3.4d</b>	Average observed rate constants, $k_{\text{obs.}(2^{\text{nd}})}, \text{s}^{-1}$ , for the dechelation of the pyridyl units in <b>Oct</b> by thiourea nucleophiles.	<b>125</b>
<b>Table SI 3.5a</b>	Temperature dependence of $k_{2(1^{\text{st}})}, \text{M}^{-1}\text{s}^{-1}$ , for the simultaneous displacement of the aqua ligands in <b>Prop</b> by thiourea nucleophiles.	<b>125</b>
<b>Table SI 3.5b</b>	Temperature dependence of $k_{2(2^{\text{nd}})}, \text{M}^{-1}\text{s}^{-1}$ , for the dechelation of the pyridyl units in <b>Prop</b> by thiourea nucleophiles.	<b>126</b>

---

<b>Table SI 3.5c</b>	Temperature dependence of $k_{2(1^{st})}$ , $M^{-1} s^{-1}$ , for the simultaneous displacement of the aqua ligands in <b>Oct</b> by thiourea nucleophiles.	126
<b>Table SI 3.5d</b>	Temperature dependence of $k_{2(2^{nd})}$ , $M^{-1} s^{-1}$ , for the dechelation of the pyridyl units in <b>Oct</b> by thiourea nucleophiles.	126
<b>Table SI 3.6a</b>	Average observed rate constants, $k_{obs.(1^{st})}$ , $s^{-1}$ , for the simultaneous displacement of the aqua ligands in <b>En</b> by thiourea nucleophiles.	127
<b>Table SI 3.6b</b>	Average observed rate constants, $k_{obs.(2^{nd})}$ , $s^{-1}$ , for the dechelation of the pyridyl units in <b>En</b> by thiourea nucleophiles.	127
<b>Table SI 3.6c</b>	Temperature dependence of $k_{2(1^{st})}$ , $M^{-1} s^{-1}$ , for the simultaneous displacement of the aqua ligands in <b>En</b> by thiourea nucleophiles.	127
<b>Table SI 3.6d</b>	Temperature dependence of $k_{2(2^{nd})}$ , $M^{-1} s^{-1}$ , for the dechelation of the pyridyl units in <b>En</b> by thiourea nucleophiles.	128
<b>Table SI 3.7a</b>	Average observed rate constants, $k_{obs.(1^{st})}$ , $s^{-1}$ , for the simultaneous displacement of the aqua ligands in <b>Hex</b> by thiourea nucleophiles.	128
<b>Table SI 3.7b</b>	Average observed rate constants, $k_{obs.(2^{nd})}$ , $s^{-1}$ , for the dechelation of the pyridyl units in <b>Hex</b> by thiourea nucleophiles.	128
<b>Table SI 3.7c</b>	Temperature dependence of $k_{2(1^{st})}$ , $M^{-1} s^{-1}$ , for the simultaneous displacement of the aqua ligands in <b>Hex</b> by thiourea nucleophiles.	129
<b>Table SI 3.7d</b>	Temperature dependence of $k_{2(2^{nd})}$ , $M^{-1} s^{-1}$ , for the dechelation of the pyridyl units in <b>Hex</b> by thiourea nucleophiles.	129
<b>Table CN 3.1</b>	Molecular structures of three of the ligands showing the $C_2$ symmetry and a common inversion symmetry in <b>L2</b> , <b>L3</b> and <b>L6</b> .	138
<b>Table 4.1</b>	The $pK_a$ values for the deprotonation of Pt-bound aqua ligand in amphiphilic Pt(II) with bis(2-pyridylmethyl)amine chelate headgroups.	154
<b>Table 4.2a</b>	Summary of calculated DFT data for the amphiphilic Pt(II) complexes.	157
<b>Table 4.2b</b>	Extract of the calculated DFT data of the amphiphiles and the analogous dinuclears	158
<b>Table 4.2c</b>	DFT optimized structures, frontier molecular orbitals for amphiphilic Pt(II) complexes.	159
<b>Table 4.3a</b>	Summary of the second-order rate constants for the substitution reactions of thiourea and amphiphilic Pt(II) complexes.	170
<b>Table 4.3b</b>	Summary of the second-order rate constants for the substitution reactions by thiourea for amphiphilic and their analogous dinuclear Pt(II) complexes.	173
<b>Table 4.3b</b>	Summary of the activation parameters for the reactions of thiourea nucleophiles and amphiphilic Pt(II) complexes.	175

<b>Table SI 4.1</b>	Summary of the wavelengths (nm) used for monitoring the reactions between a series of Pt(II) mononuclear complexes with bis(2-pyridylmethyl) chelates and thiourea nucleophiles.	<b>181</b>
<b>Table SI 4.2a</b>	A comparative illustration of the DFT <sup>42</sup> minimum energy structures of the amphiphiles and their analogous dinuclear complexes.	<b>182</b>
<b>Table SI 4.2b</b>	Electrostatic potential surface mapping of the amphiphilic Pt(II) complexes.	<b>183</b>
<b>Table SI 4.3</b>	Geometry optimized structure of the <b>bpma-2tu</b> showing the decoordinates and dangling 2-pyridylmethyl arm.	<b>184</b>
<b>Table SI 4.4a</b>	Average observed rate constants, $k_{\text{obs.}(1)}^{\text{st}}$ , $\text{s}^{-1}$ , for the simultaneous displacement of the aqua ligands in <b>bptba</b> by thiourea nucleophiles, pH = 2.0, T = 298 K.	<b>184</b>
<b>Table SI 4.4b</b>	Average observed rate constants, $k_{\text{obs.}(2)}^{\text{nd}}$ , $\text{s}^{-1}$ , for the dechelation of the pyridyl units in <b>bptba</b> by thiourea nucleophiles.	<b>184</b>
<b>Table SI 4.4c</b>	Temperature dependence of $k_{2(1)}^{\text{st}}$ , $\text{M}^{-1} \text{s}^{-1}$ , for the simultaneous displacement of the aqua ligands in <b>bptba</b> by thiourea nucleophiles.	<b>184</b>
<b>Table SI 4.4d</b>	Temperature dependence of $k_{2(2)}^{\text{nd}}$ , $\text{M}^{-1} \text{s}^{-1}$ , for the dechelation of the pyridyl units in <b>bptba</b> by thiourea.	<b>185</b>
<b>Table SI 4.5a</b>	Average observed rate constants, $k_{\text{obs.}(1)}^{\text{st}}$ , $\text{s}^{-1}$ , for the simultaneous displacement of the aqua ligands in <b>bpea</b> by thiourea nucleophiles.	<b>185</b>
<b>Table SI 4.5b</b>	Average observed rate constants, $k_{\text{obs.}(2)}^{\text{nd}}$ , $\text{s}^{-1}$ , for the dechelation of the pyridyl units in <b>bpea</b> by thiourea nucleophiles.	<b>185</b>
<b>Table SI 4.5c</b>	Temperature dependence of $k_{2(1)}^{\text{st}}$ , $\text{M}^{-1} \text{s}^{-1}$ , for the simultaneous displacement of the aqua ligands in <b>bpea</b> by thiourea nucleophiles.	<b>185</b>
<b>Table SI 4.5d</b>	Temperature dependence of $k_{2(2)}^{\text{nd}}$ , $\text{M}^{-1} \text{s}^{-1}$ , for the dechelation of the pyridyl units in <b>bpea</b> by thiourea nucleophiles.	<b>193</b>
<b>Table SI 4.6a</b>	Average observed rate constants, $k_{\text{obs.}(1)}^{\text{st}}$ , $\text{s}^{-1}$ , for the simultaneous displacement of the aqua ligands in <b>bppa</b> by thiourea nucleophiles.	<b>186</b>
<b>Table SI 4.6b</b>	Average observed rate constants, $k_{\text{obs.}(2)}^{\text{nd}}$ , $\text{s}^{-1}$ , for the dechelation of the pyridyl units in <b>bppa</b> by thiourea nucleophiles.	<b>186</b>
<b>Table SI 4.6c</b>	Temperature dependence of $k_{2(1)}^{\text{st}}$ , $\text{M}^{-1} \text{s}^{-1}$ , for the simultaneous displacement of the aqua ligands in <b>bppa</b> by thiourea nucleophiles.	<b>186</b>
<b>Table SI 4.6d</b>	Temperature dependence of $k_{2(2)}^{\text{nd}}$ , $\text{M}^{-1} \text{s}^{-1}$ , for the dechelation of the pyridyl units in <b>bppa</b> by thiourea.	<b>187</b>
<b>Table CN 4.1</b>	Crystal plate and the molecular structure of <i>N,N</i> -bis(-pyridylmethyl) <i>tert</i> -butylamine ( <b>L3</b> ).	<b>197</b>
<b>Table CN 4.2</b>	Crystal data and structural refinement parameters for <b>L3</b> at 293 K.	<b>198</b>

<b>Table 5.1</b>	Summary of $pK_a$ data obtained for the deprotonation of Pt-bound aqua ligands (within pH range 2-9), using NaOH as titrant.	<b>212</b>
<b>Table 5.2a</b>	Density functional theoretical (DFT) minimum energy structures, HOMO and LUMO frontier molecular orbitals for dinuclear complexes with aromatic diamine and diaminocyclohexane bridging fragments.	<b>215</b>
<b>Table 5.2b</b>	Summary of DFT computational data for the dinuclear Pt(II) complexes and their mononuclear analogues.	<b>219</b>
<b>Table 5.3</b>	Summary of the rate constants for the simultaneous substitution of aqua ligands and the dechelation of one of the pyridyl units by thiourea nucleophiles in bis(2-pyridylmethyl)amine chelated dinuclear complexes with aromatic bridges and their monomeric analogue.	<b>226</b>
<b>Table 5.4a</b>	Summary of the activation parameters for the simultaneous displacement of aqua ligands and the dechelation of one of the pyridyl units by thiourea nucleophiles in bis(2-pyridylmethyl)amine chelated dinuclear complexes with aromatic bridges and their monomeric analogue.	<b>234</b>
<b>Table SI 5.1</b>	Summary of the wavelengths (nm) used for monitoring the reactions between a series of mononuclear and dinuclear complexes with cyclohexyl and phenyl groups.	<b>240</b>
<b>Table SI 5.2</b>	Electrostatic potential surface mapping of the dinuclear Pt(II) complexes bridged by rigid linkers and their mononuclear analogues.	<b>241</b>
<b>Table SI 5.3a</b>	Average observed rate constants, $k_{obs.(1)}^{st}$ , $s^{-1}$ , for the simultaneous displacement of the aqua ligands in <b>bpcHna</b> by thiourea nucleophiles.	<b>242</b>
<b>Table SI 5.3b</b>	Average observed rate constants, $k_{obs.(2)}^{nd}$ , $s^{-1}$ , for the dechelation of the pyridyl units in <b>bpcHna</b> by thiourea nucleophiles, pH = 2.0	<b>242</b>
<b>Table SI 5.3c</b>	Temperature dependence of $k_{2(1)}^{st}$ , $M^{-1} s^{-1}$ , for the simultaneous displacement of the aqua ligands in <b>bpcHna</b> by thiourea nucleophiles, pH = 2.0, T = 298 K	<b>242</b>
<b>Table SI 5.3d</b>	Temperature dependence of $k_{2(2)}^{nd}$ , $M^{-1} s^{-1}$ , for the dechelation of the pyridyl units in <b>bpcHna</b> by thiourea nucleophiles.	<b>243</b>
<b>Table SI 5.4a</b>	Average observed rate constants, $k_{obs.(1)}^{st}$ , $s^{-1}$ , for the simultaneous displacement of the aqua ligands in <b>dcHnm</b> by thiourea nucleophiles, pH = 2.0, T = 298 K.	<b>243</b>
<b>Table SI 5.4b</b>	Average observed rate constants, $k_{obs.(2)}^{nd}$ , $s^{-1}$ , for the dechelation of the pyridyl units in <b>dcHnm</b> by thiourea nucleophiles, pH = 2.0, T = 298 K.	<b>243</b>
<b>Table SI 5.4c</b>	Temperature dependence of $k_{2(1)}^{st}$ , $M^{-1} s^{-1}$ , for the simultaneous displacement of the aqua ligands in <b>dcHnm</b> by thiourea nucleophiles.	<b>244</b>
<b>Table SI 5.4d</b>	Temperature dependence of $k_{2(2)}^{nd}$ , $M^{-1} s^{-1}$ , for the dechelation of the pyridyl units in <b>dcHnm</b> by thiourea nucleophiles.	<b>244</b>
<b>Table SI 5.5a</b>	Average observed rate constants, $k_{obs.(1)}^{st}$ , $s^{-1}$ , for the simultaneous displacement of the aqua ligands in <b>pPh</b> by thiourea nucleophiles.	<b>244</b>

---

<b>Table SI 5.5b</b>	Average observed rate constants, $k_{\text{obs.}(2^{\text{nd}})}$ , $\text{s}^{-1}$ , for the dechelation of the pyridyl units in <b>pPh</b> by thiourea nucleophiles.	<b>245</b>
<b>Table SI 5.5c</b>	Temperature dependence of $k_{2(1^{\text{st}})}$ , $\text{M}^{-1} \text{s}^{-1}$ , for the simultaneous displacement of the aqua ligands in <b>pPh</b> by thiourea nucleophiles.	<b>245</b>
<b>Table SI 5.5d</b>	Temperature dependence of $k_{2(2^{\text{nd}})}$ , $\text{M}^{-1} \text{s}^{-1}$ , for the dechelation of the pyridyl units in <b>pPh</b> by thiourea nucleophiles.	<b>245</b>
<b>Table CN 5.1a</b>	Summary of the crystal and lattice structure ligand <b>L6</b> .	<b>255</b>
<b>Table CN 5.1b</b>	A summary of the structural data of ligand <b>L6</b> .	<b>256</b>

---

---

## Publications and conferences contributions

### Publications

Some of the ligands used to synthesize the platinum(II) complexes have been published as structural papers 1-3 and part of the work reported in Chapter Three has been published in *Dalton Transactions*.

1. **A. Mambanda**, D. Jaganyi and K. Stewart, *N,N*-bis(2-pyridylmethyl)-*tert*-butylamine, *Acta Cryst.*, 2009, **E65**, o402.
2. D. Jaganyi, **A. Mambanda** and O. Q. Munro, A tripodal tris(thiophene) derivative of hexahydropyrimidine and its ladder-like extended structure' *Acta Cryst.*, 2007, **E63**, o2388-o2390.
3. **A. Mambanda**, D. Jaganyi, and O. Q. Munro, One-dimensional C-H...N hydrogen-bonded polymers in flexible tetrapyridyl systems, *Acta Cryst.*, 2007, **C63**, o676-o680.
4. **A. Mambanda**, D. Jaganyi, S. Hochreuther and R. van Eldik, Tuning the reactivity of chelated dinuclear Pt(II) complexes through a flexible diamine linker. A detailed kinetic and mechanistic study, *Dalton Trans.*, 2010, **39**, 3995-3608.

### Oral presentations

South Africa Chemical Institute (SACI) Research Colloquium meeting, Durban University of Technology, 9 April 2008, entitled: *Tuning the reactivity of chelated dinuclear Pt(II) complexes through a flexible linker. A detailed kinetic and mechanistic study.*

Kenya Chemical Society (KCS) and EAEC/Theoretical Chemistry conference in Mombasa, Kenya from 5<sup>th</sup> to 9<sup>th</sup> of October 2009, entitled: *Tuning the reactivity of chelated dinuclear Pt(II) complexes through a flexible linker. A detailed kinetic and mechanistic study.*

Inorganic Reactions Mechanism Group (IRMG) Meeting, Kloster Banz, Germany, 7-10<sup>th</sup> January 2010 entitled: *Detailed kinetic & thermodynamic studies on the reactivity of chelated dinuclear Platinum(II) complexes.*

### Poster presentations

South Africa Chemical Institute (SACI) Research Colloquium meeting, University of KwaZulu-Natal, Westville Campus, 23 August 2008, entitled: *Kinetic study of chelated dinuclear Pt(II) complexes with diaminobenzene and diaminocyclohexane bridges.*

39<sup>th</sup> Convention of South Africa Chemical Institute, University of Stellenbosch, South Africa, 30 November to 5 December 2008, entitled: *Kinetics study of Pt(II) amphiphiles derived from a bis(2-pyridylmethyl)amine chelate headgroup.*

---

# Chapter One

## Use of Platinum complexes as anticancer pharmaceuticals.

### 1.0 Mononuclear Pt(II) complexes

#### 1.0.1 Introduction

Cancer is a condition caused by abnormalities in the genetic material of some transformed cells.<sup>1a,b</sup> Such abnormalities are known as malignant neoplasms. The malignant neoplasms may be due to the effects of carcinogens such as tobacco smoke, chemicals or ultraviolet B-type of radiation. The abnormalities affect two classes of genes *viz.*, cancer promoting and tumour suppressing oncogenes.<sup>1a,c</sup> The cancer promoting genes when activated, give rises to new properties in affected cells such as hyperactive growth and division, protection against programmed cell death, ill-recognition of normal tissue boundaries and the ability to become established in diverse tissue environments.<sup>1d</sup> This is accompanied by the inactivation of the tumour suppressor genes. When this happens, the result is loss of normal tissue functions in cells such as regular DNA transcription and replication, control over the cell cycle, normal orientations and adhesion within tissues and critical interactions for protective functions by the immune system. As a result, cancerous cells display one or more of the following: (i) uncontrolled growth, (ii) invasion of adjacent tissues and (iii) metastatic migration to other locations through the blood and the lymph systems.<sup>1a-b,2</sup>

Most malignant tumours can be treated and cured depending on their type, location and growth progression. Currently, cancer can be treated by surgery, chemotherapy, radiotherapy or a combination of the listed strategies.<sup>3</sup> Modern oncological research on anticancer metallopharms is now focused and geared on coming up with improved anti-cancer agents that target only abnormalities in tumour cell lines at a molecular level with minimum damage to normal healthy cells.<sup>4</sup> Inorganic metal complexes have evolved to become one of the most promising groups of anti-cancer therapeutics, with the  $d^8$  Pt(II) being the leading metal ion.<sup>5</sup> The prototypical example of the metal-based anti-proliferation cancer drug is *cis-*

## *Pt(II) based anticancer drugs*

diaminedichloroplatinum(II), (1), also known as cisplatin. The structures of cisplatin and its other successful analogues in the clinic which will be made reference to in this chapter are presented in Figure 1.1.

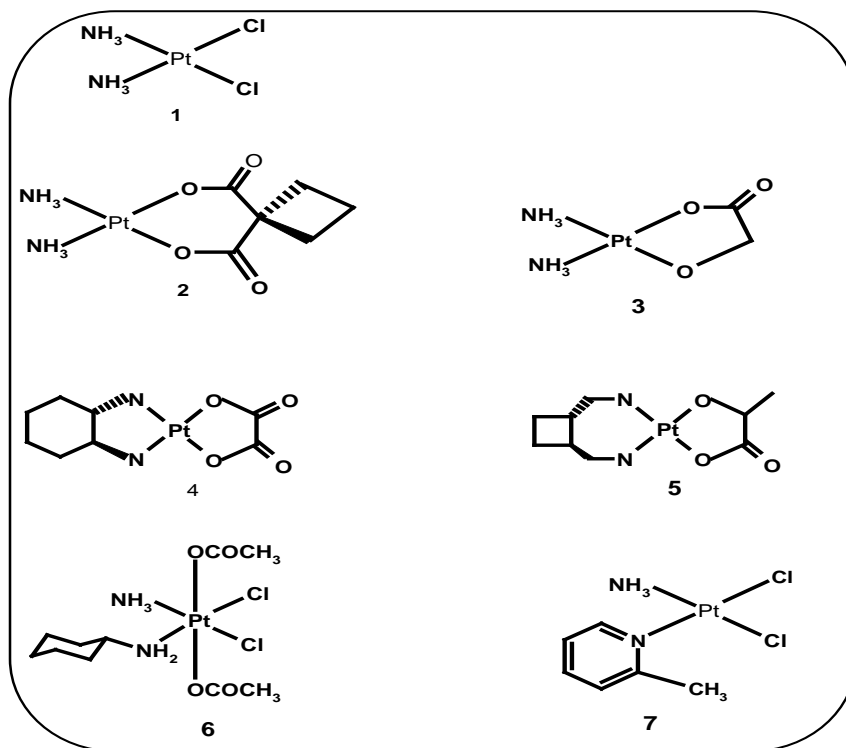


**Figure 1.1** Structures of cisplatin and its analogues of mononuclear Pt(II) complexes.

Cisplatin is one of the most widely used metal-based anticancer drugs, first approved for clinical use in 1978.<sup>6</sup> Currently it is used in the first-line treatment of several kinds of tumours such as cancers of the testicles, ovaries, bladder, head, neck, esophagus and lungs.<sup>2,4,5,7</sup> Its cure rate in testicular and ovarian cancers<sup>8</sup> is high (exceeding 90 %) particularly in tumours diagnosed in their early stages. It is also used in combination therapy with other antitumour drugs, such as arabinofurasylocytosine<sup>9a</sup>, 5-fluorouracil<sup>9b</sup>, bleomycin<sup>9c</sup> and paclitaxel.<sup>9c</sup> The mechanisms of action of non-metal based co-drugs are different but complementary to that of cisplatin. Some act by inhibiting mitosis (plant alkaloids), subverting pathways in DNA synthesis (antimetabolites) or produces adverse effects which are cytotoxic (antitumour antibiotics).<sup>2</sup>

## *Pt(II) based anticancer drugs*

---

Despite its unparalleled success against a number of malignancies, treatment to cisplatin is hampered by severe side-effects and drug resistance.<sup>3</sup> The toxicity is thought to be related to the binding of enzymes and protein residues to the platinum metal centre.<sup>4</sup> As a result, symptomatic malfunctions due to organelle damage, such as nephrotoxicity, neurotoxicity, ototoxicity, myelosuppression, nausea and vomiting have been reported in patients undergoing cisplatin treatment.<sup>10</sup> In many cases, these side-effects limit the dosage that can be administered in the clinic. Various drug-dosing protocol strategies have been advanced to minimize the problems of toxicity. These include clinical interventions such as intravenous hydration along with the use of diuretics, use of antiemetics such as serotonin receptors<sup>11,12</sup> as well as co-administration of the drug with chemo-protective agents.<sup>13,3</sup> The latter co-agents are salts or small biomolecules that contain sulfur donor atoms. Besides the problem of toxicity, several other tumour cell lines display intrinsic resistance to its treatment or may become refractory. Refractory tumours develop resistance after an initial response to treatment by the drug.<sup>3,6</sup> In addition, low saline solubility is a major inconvenient to its clinical use.

However, its early remarkable success in the clinic strengthened by the information gathered between its chance discovery in 1971 by Rosenberg<sup>14</sup> and its clinical approval in 1978 fueled extensive research to develop other new drugs of better efficacy and reduced toxicity. The information gathered then, formed the basis for the rationale design of new drug candidates that were expected to offer predictable pharmacokinetics and cytotoxicity properties. Thus, these new drug candidates were expected to display one or more of the following characteristics (i) be effective in a wider range of tumours, (ii) display higher cytotoxic potency (iii) and should have reduced side-effects in the clinic.<sup>4</sup>

As part of the roadmap to chartering the search for new platinum based anticancer drug, some classical guiding rules had been laid, all from the structure-activity relationships studies of Cleare and Hoeschele in 1973.<sup>16</sup> By then, it was established that for the platinum complexes to be antitumour active, the complexes would have to be neutral, would have a *cis*-square-planar geometry about the platinum(II) centre, of the general form *cis*-[Pt(*Am*)<sub>2</sub>X<sub>2</sub>], where (*Am*)<sub>2</sub> are either two monodentate or bidentate carrier amine ligands. The carrier ligands should bear at least one NH functional group, necessary for hydrogen bonding interactions with DNA. In the case of cisplatin, the hydrogen bonding occurs between the amine ligands

## *Pt(II) based anticancer drugs*

---

and the O6 of the guanines and the O5' of the phosphate groups of the DNA nucleobases. The ligands,  $X_2$  were normally a bidentate or two monodentate anionic leaving groups of moderate coordination strength (such as  $Cl^-$ ,  $SO_4^{2-}$  or the dicarboxylate). In the case of octahedral Pt(IV) complexes, an additional requirement was that the good leaving groups had to occupy axial positions. This would essentially make the Pt(IV) complexes the prodrugs of cisplatin analogue via reductive elimination. Thus, the ultimate milestone of these efforts was a rapid growth in the number of antitumour active Pt(II) complexes, the majority of which were essentially structural congeners of the parent drug, cisplatin. Despite the guiding rules in the design of the new drugs, only a handful of the compounds were eventually approved for clinical trials. Of those, carboplatin (**2**), nedaplatin (**3**), oxaliplatin (**4**) and lobaplatin (**5**)<sup>17</sup> (Figure 1.1) are the most successful candidates in the clinic.

Since most of these complexes were in fact structural analogues of the parent drug cisplatin, they inherited either some of the drawbacks of cisplatin or did not show any superior activity when compared to that of cisplatin. However, some of these follow-up drugs exhibited promising clinical efficacy. They showed remarkable activity in cisplatin resistant sub-lines in addition to having relatively lower side effects. Their structures and general mode of action are discussed in detail in section 1.0.4.

### **1.0.2 Mechanism of action of cisplatin.**

Cisplatin is commonly administered by intravenous injection at 100-200 mg  $d^{-1}$  for up to five consecutive days.<sup>9c</sup> It is believed to enter the cells mainly through passive diffusion.<sup>6a,18</sup> However, it has been reported in some recent studies that copper transporters, CTR1 sites, are in fact involved in its cellular uptake.<sup>19</sup> Although the cellular distribution of cisplatin and its exact mode of action with cellular material are not well understood, its interaction with the target DNA is now widely accepted to be responsible for its ant-cancer activity.<sup>20</sup> Experimental evidence<sup>21</sup> affirms that platinum drugs accumulate rapidly in the nucleoli of the cells, where they react with the highly concentrated double-stranded DNA. In transit, a relative high concentration of chloride ions in the extra-cellular fluids (~100 mM), keeps the drug in its neutral state.<sup>13,18</sup> However, on crossing the cell membrane, one or both chloride ligands are displaced by the aqua ligands to afford reactive cationic species. The first aquation reaction is

## *Pt(II) based anticancer drugs*

relatively rapid and is promoted by the low concentration ( $\sim 4$  mM) of the chloride in the cytosol. A depiction of some of the various equilibria attained in the cytosol before the ultimate complex formation reaction between cisplatin and its target sites on the nucleophilic DNA is shown in Figure 1.2. However, under physiological conditions, some of the drug may also be inactivated into its hydroxo species. A two-step ligand exchange (*viz.*, monofunctional binding followed by subsequent closure to form the bifunctional adducts) then occurs between the labile aqua ligands of the reactive form of the drug and the nucleobases of the DNA to afford bifunctional adducts, formed between the *cis*-Pt(NH<sub>3</sub>)<sub>2</sub> units and two adjacent bases located mainly on the same strand.<sup>6</sup> The rate determining step for each of the two binding events is thought to be the hydrolysis of the chloride ligands.<sup>22</sup> The mechanistic pathways summarizing the antitumour action of cisplatin is shown below in Figure 1.2.

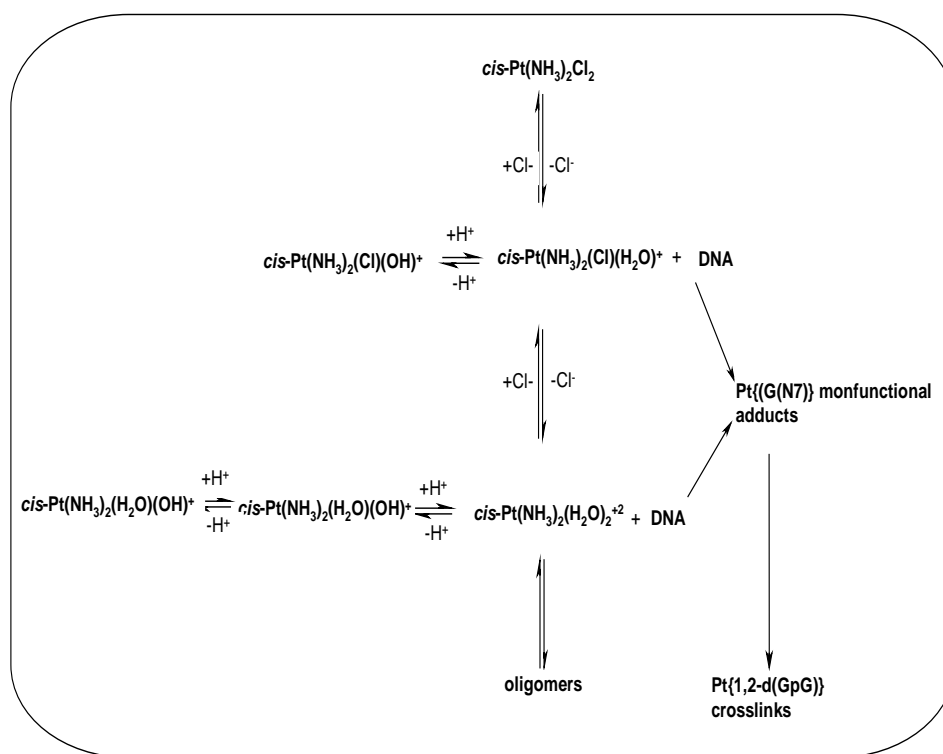


**Figure 1.2** Equilibria processes attained by cisplatin in the cytosol and its complex formation of 1,2-intrastrand d(GpG)-Pt crosslinks on DNA.<sup>5b,c</sup>

Mechanistic studies<sup>2,4,13</sup> have singled out the guanine-N7 atoms on adjacent nucleobases (guanine or to a less extent adenine) as the frequent sites for platination leading to metal chelates or crosslink adducts. *In vitro* experiments have shown that 1,2-intrastrand

## *Pt(II) based anticancer drugs*

d(GpG)-Pt crosslinks are the major products (70%), followed by 1,2-intrastrand d(ApG)-Pt (25%) and 1,3-d(AXG)-Pt (5-10%) crosslinks, respectively.<sup>23a,b</sup> Monofunctional adducts and protein-DNA crosslinks of cisplatin are however less common. Figure 1.3<sup>2</sup>, is an illustration of the different kinds of adducts that can be formed by the interaction of cisplatin with DNA.

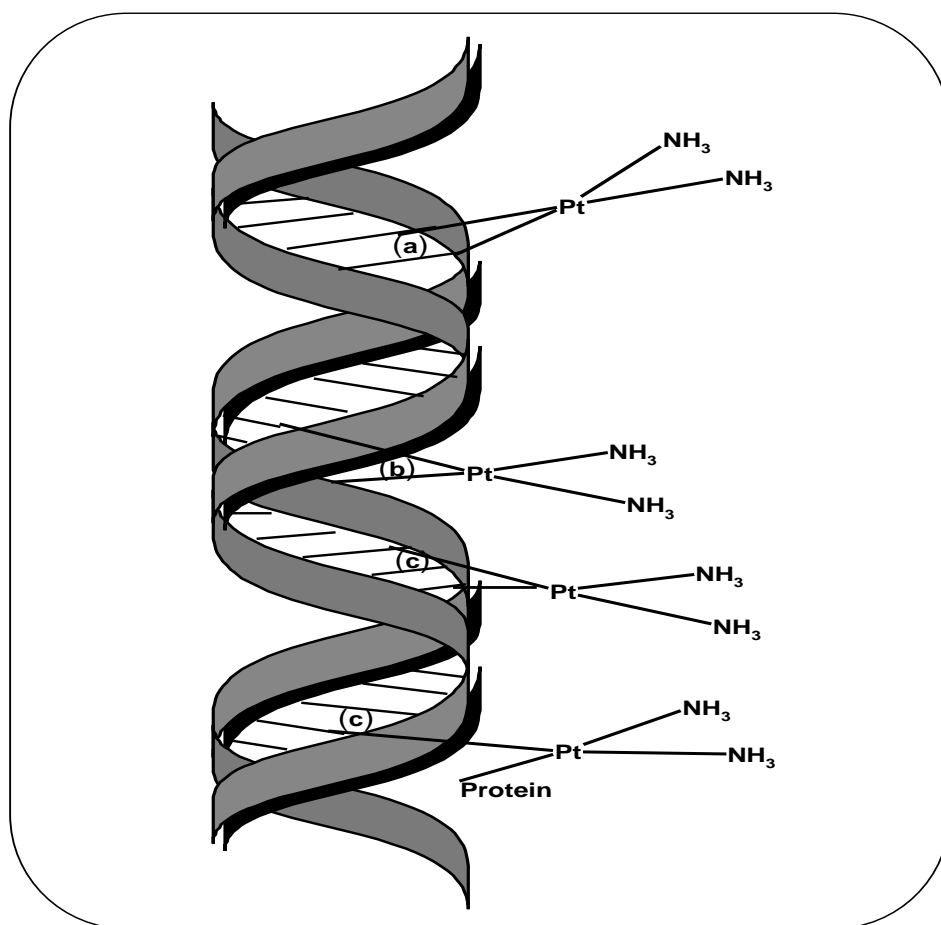


**Figure 1.3** Depiction of the major adducts which can be formed when cisplatin interacts with DNA.<sup>2</sup>  
(a) 1,2-intrastrand cross link; (b) interstrand crosslink; (c) 1,3-intrastrand crosslink and  
(d) protein-DNA crosslink.

In the 1,2-intrastrand d(GpG)-Pt crosslink, the platinum atom is located in the major groove of the helical strand of DNA. The effect of crosslinking at the guanine-N7 sites of two adjacent bases in a *cis*-orientation is to bend the double strand DNA, forming a kink<sup>23c,13a</sup> of about 45°-70°, towards the site of platination, resulting in partial unwinding and loss of helical stability. In perspective, the tertiary structure of the normal B-DNA is distorted by the 1,2-

## *Pt(II) based anticancer drugs*

---

intrastrand crosslinks. This conformational distortion of DNA changes the normal interactions of DNA with cellular proteins leading to either repair of the damage, by cutting out the Pt and re-synthesizing at the open sites or no repair triggering cell killing in a programmed protocol.<sup>6a,24a,b</sup> Specifically, the kinking elicits response from multiple signal pathways involving the *p53*, *Bcl-2* family, caspases, cyclins, CDKs, *pRb*, PKC and many other protein complexes that make-up the DNA-damage processing machinery.<sup>5b,c</sup> The processing of lesions may subsequently interfere with normal DNA transcription or replication.

Of the DNA-damage processing machinery, the high mobility group (HMG) proteins constitute the earliest mode of response agents to DNA damage by recognizing and binding to the site of platination.<sup>2</sup> Lippard and coworkers<sup>24c</sup> have reported a crystal structure of the DNA-binding domain of the HMG bound to platinated DNA. The crystal structure reveals a phenylalanine amino acid residue docked into the cavity created by the bending (kinking), forming face-to-face  $\pi$ - $\pi$  interactions with one platinated guanine and a face-to-edge (CH.. $\pi$ ) interactions with the other. The binding of the HMG and docking of its amino acid residue serves as a shield against proficient repair of the DNA lesions by the nuclear excision repair (NER) machinery.<sup>25</sup>

Although the consequences of the crosslinks and how they lead to cell death is not fully understood,<sup>20a</sup> the lesions are known to block the progression of DNA polymerase<sup>20b,c</sup> along the strands at the GpG-Pt damaged sites. This is believed to induce perturbations in the cell life cycle, eliciting a G2-phase arrest to repairing of DNA damage. Failure to repair lesions successfully triggers an abortive attempt at mitosis which results in cell death by apoptotic pathway (*vide supra*).<sup>6a,24a,b,26</sup> Apoptosis is a genetically controlled mechanism that ensures a regulated renewal of cells through a programmed death cycle during embryonic development and normal cellular homeostasis under various stimuli. It involves the concerted actions of a number of intracellular signaling pathways, including members of the caspase family of cysteine proteases, stored in most cells as zymogenes or procaspases,<sup>1a</sup> which are mainly responsible for distinguishing this process from other forms of cell death. It is characterized by three major phases.<sup>20,5c</sup> In the initial phase, a stimulus is received and is followed by a necessary response. This establishes an 'effector phase' in which decisions to allow cellular life or terminate it are coordinated. Finally, cellular repairs, DNA cleavage or auto digestion of

## *Pt(II) based anticancer drugs*

some proteins can take place in the 'execution phase'. On the other hand, cell life can be terminated also through processes such as autophagy, oncosis and necrosis, all characterized by the release of enzymes from damaged lysosomes that can digest and denature cellular proteins on depletion of ATP/NAD<sup>+</sup>.<sup>1a,20</sup> It happens in an uncontrollable fashion characterized by cell swelling and loss of homeostatic control.

The scheme of events summarizing the mechanisms of action and other biotransformational routes leading to the development of resistance (are discussed in section 1.0.3) is illustrated in Figure 1.4.

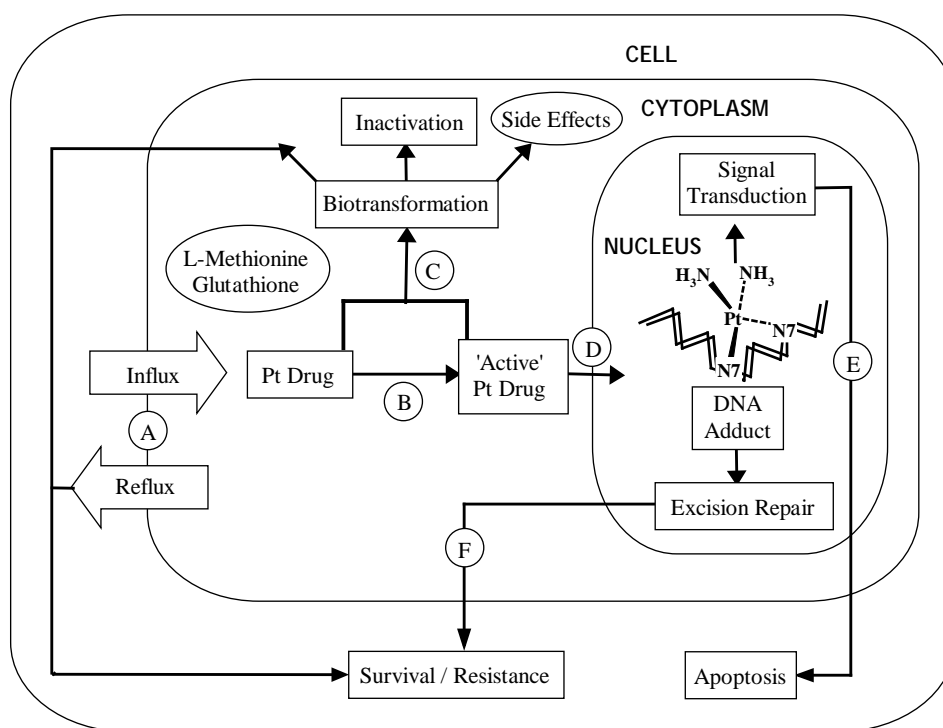


**Figure 1.4** Schematic diagram showing the mechanism of action of cisplatin and its competing bio-transformational routes. Adapted from N. K. Summa, PhD Thesis 'Thermodynamic and kinetic studies on biotransformation reactions of medical relevant mono- and polynuclear Pt(II) complexes' 2006, Institute für Anorganische und Analytische Chemie der Friedrich-Alexander-Universität Erlangen-Nürnberg, Germany.

As illustrated in Figure 1.4, the efficacy of cisplatin as a cytotoxic agent is dependent upon its bioavailability at the target site which in turn is dependent upon its net uptake (A) and the degree of detoxification (C) by other platinophilic agents, particularly S-containing nucleophiles. The latter causes drug inactivation, leading to resistance and toxic side-effects. Once it enters the cells, cisplatin is slowly hydrolyzed (B) to form the more reactive aqua species which are prone to other

## *Pt(II) based anticancer drugs*

---

bio-transformational pathways routed via C. In the nucleus, the drug platinates (D) DNA mainly at the N7 atoms of the guanine nucleobases to form DNA-Pt damage adducts. The DNA-Pt adducts may be recognized by different cellular sensors, prompting different cellular processes. This may lead to either inefficient recognition or unsuccessful repair mechanisms (E) resulting in apoptosis or the Pt-DNA adducts are efficiently repaired (F) and the cell survives. Enhanced or altered repair may lead to resistance of the drug.

### **1.0.3 Mechanism of cisplatin resistance.**

Resistance of cancers to cisplatin chemotherapy can be intrinsic or refractory. Intrinsic resistance is failure by tumourous cells to respond to the inhibitory effects of the drug. It is closely related to the drug's bio-transformational pathways that compete for the bioavailability of the drug at its target, DNA. Some tumours become refractory to continued use of the drug as a result of acquired mechanisms of resistance. If two or more drugs exhibit similar inhibitory profiles, then cross resistance may develop between them. The following are thought to be the underlying mechanisms responsible for manifestations of tumour resistance to cisplatin chemotherapy via the multi-drug resistance associated protein complexes (MRP):<sup>5b,13,27a</sup>

- (i) reduced drug uptake,
- (ii) increased detoxification by plasma proteins ( in the extracellular bio-domain) and sulfur containing biomolecules such as glutathione or metallothionein (intracellular bio-domain),
- (iii) increased repair of platinum-DNA adducts,
- (iv) increased tolerance to platinum-DNA adducts.

A reduced net uptake of cisplatin hampers the drug from reaching its intracellular target, DNA. It is an important factor to intrinsic resistance. In the cytosol, the reactive forms of the drug can be deactivated by other platinophiles such as glutathione, and metallothionein.<sup>27a</sup> Glutathione (glutamylcysteinylglycine) is an abundant thiol (0.5-10 mM) in mammalian cells, chiefly responsible for the control of lipid peroxidation. However, it readily reacts with platinum species thereby conferring a competitive pathway that can deplete intracellular concentration of the drug to level insufficient to inhibit tumour growth.<sup>3,6</sup> Metallothionein, a cysteine-rich protein responsible for the detoxification of heavy metals such as  $Pb^{2+}$  and  $Cd^{2+}$ , and methionine protein residues can also deactivate the drug in a similar way. The deactivated

## *Pt(II) based anticancer drugs*

(sulfur-coordinated forms of cisplatin) are then excreted as conjugates coupled to the multi-drug resistance proteins (MRP).<sup>5b,2,27a</sup> through the Golgi gateway. However, some authors<sup>13a</sup> have suggested that some sulfur containing biomolecules especially the thioethers<sup>27b,c</sup> and other platinumophiles<sup>27d</sup> can potentially play a positive role in drug delivery by acting as drug reservoirs and chemo-protectors, respectively. Thus, several sulfur containing compounds such as diethyldithiocarbamate (ddtc), sodium thiosulphate (sts), thiourea (tu) and mercaptomethane sulfonate (mesna) have been put forward for co-administration with platinum drugs.<sup>27d</sup> Shown in Figure 1.5 are the possible mechanistic pathways in which thioethers are thought to act as drug reservoir on of platinum chemotherapy.<sup>27b,c</sup>

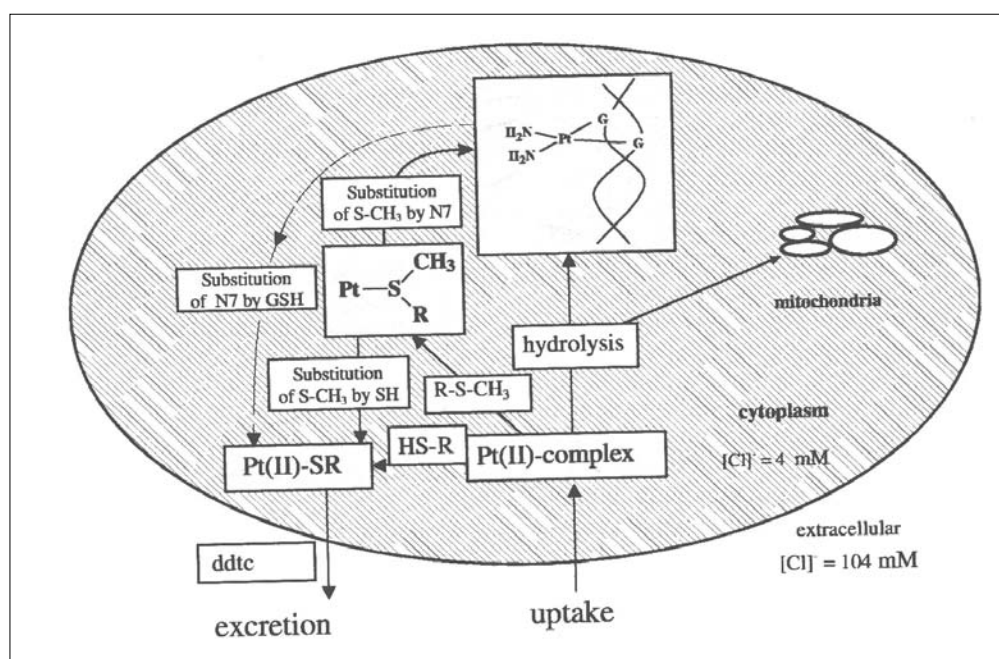


**Figure 1.5** Schematic illustration of how sulfur containing compounds are thought to act as potential drug reserving agents in platinum chemotherapy.<sup>27b,c</sup>

Besides reduced drug uptake and detoxification, intracellular concentration of the drug can also be depleted through increased efflux.

Another mechanism that contributes to cisplatin resistance is increased repair of DNA conformational damage by the nucleotide repair proteins (NER).<sup>28</sup> The NER protein complex recognizes DNA damage; excise the damaged segments off as 27-29 base pair oligonucleotides, prompting gap filling by DNA polymerase.<sup>5</sup> The more efficient the repair

## *Pt(II) based anticancer drugs*

machinery turns out to be, the more resistance the tumour cells become to the inhibitory effect of the drug. Reports on increased levels of NER in cell panels resistant to cisplatin treatment have come out from literature.<sup>3</sup>

Closely related to acquired resistance, is increased tolerance of the drug by the tumour cells. Drug tolerance is a multi-faceted manifestation of all the post-binding defense-elicited functions necessary for cell survival in a background of DNA conformational damage.<sup>20</sup> In one function, replication in DNA can proceed without excision by NER proteins and gap-filling by DNA polymerase. Another function is embodied in the mismatch (MMR) repair machinery, which mediates in futile cycles of base-pair repairs, leading to apoptotic pathways. A summary of the important functions closely related to acquired resistance is illustrated below in Figure 1.6. However, loss in the repairing proficiency by this complex as occurring often in insensitive tumorous cells leads to resistance through drug tolerance.<sup>2,5b</sup>

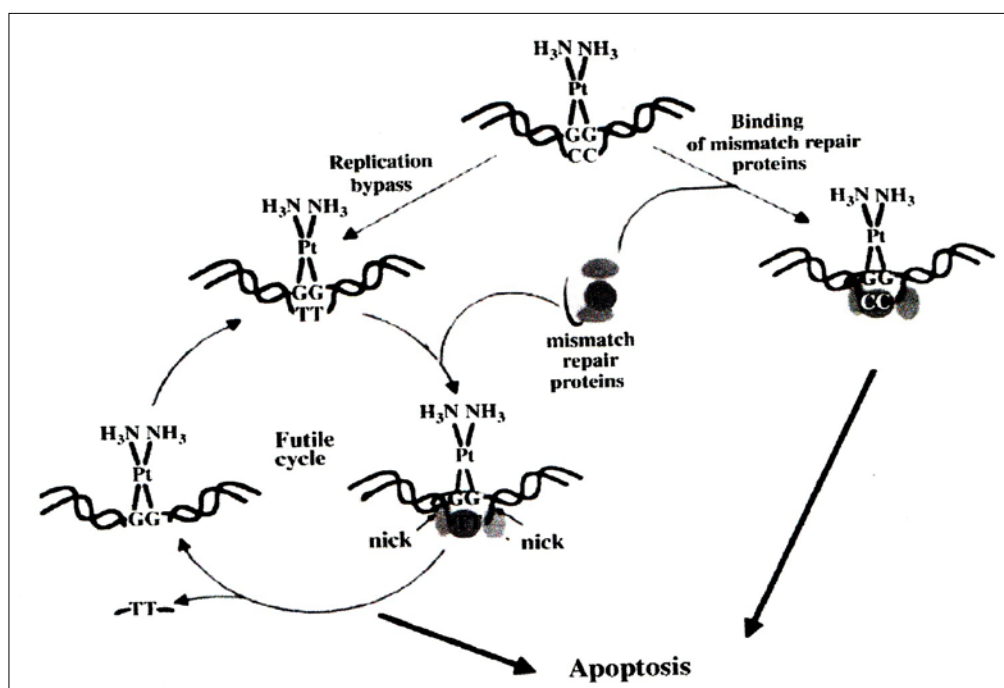


**Figure 1.6** Postulated scheme illustrating the mismatch repair of 1,2-(GpG)-Pt intrastrand crosslinks of cisplatin.<sup>5b</sup>

Just like the high mobility group proteins (HMG), MMR proteins complex can recognize the damaged lesions of DNA and attempt to correct any mismatches in base-pairing which may

## *Pt(II) based anticancer drugs*

---

have been induced by the 1,2-(GpG)-Pt intrastrand adducts. Mello *et al.*<sup>28</sup> have demonstrated that the human mismatch repair protein, (Hmsh2), binds specifically to DNA lesions and displays selectivity for the lesions induced by antitumour platinum compounds. However, this protein complex is incapable of repairing the Pt-DNA lesions. In sensitive tumour cell lines, the MMR complex normally initiates futile cycles to repairing of DNA-damaged adducts which signal apoptotic events as illustrated in Figure 6. Loss of proficiency in this complex as commonly occurring in tumourous cells can cause increased tolerance of the drug by blocking the futile cycles to repairing of the damage and the subsequent programmed death cycles.<sup>20</sup> Apoptotic malfunctions caused by mutant genes like the *p53* proteins sequence can also lead to tolerance of DNA lesions.<sup>20</sup>

### **1.0.4 The follow-up generations of cisplatin.**

Although the guiding rules of Cleare and Hoeschele<sup>16</sup> are now known not to be the universal pre-requisites for antitumour activity, they were useful in the development of several follow-up drug candidates that entered clinical evaluation. The candidates can be grouped into three major categories, *viz.*, drugs designed to address the problems of (i) toxicity, (ii) resistance and (iii) inconvenience of drug administration by parental means.

#### *1.0.4.1 Mononuclear platinum drugs with reduced toxic side effects.*

This group is exemplified by *cis*-diammine-1,1'-cyclobutanedicarboxylatoplatinum(II), carboplatin, **2**, and *cis*-diammine-glycolatoplatinum(II), nedaplatin, **3**, (Figure 1.1). The labile chloride groups in cisplatin are replaced by the bidentate (1,1'-cyclobutanedicarboxylate and glycolate, respectively) ligands.<sup>5c</sup> Since the carrier and active fragment, *cis*-[Pt(*Am*)<sub>2</sub>], was maintained in this category of drugs, it is not surprising that these complexes display similar antitumour activity profiles to that of cisplatin since they induce and form the same kind of lesions on DNA. However, the bidentate leaving groups confer good aqueous solubility and moderate hydrolytic kinetics.<sup>13</sup> This is important in two ways. Firstly, it improves the stability of the drugs by enhancing their circulation lifetime in the body. Lower reactivity of the drugs reduces their toxicity by decelerating the rate of competitive binding to plasma proteins and the ubiquitous glutathione and other platinum deactivating biomolecules. The lower reactivity also allows that a higher dose (as a higher as 2000 mg d<sup>-1</sup> for carboplatin) can be administered. As

## *Pt(II) based anticancer drugs*

---

a result carboplatin is now widely used for the treatment of ovarian cancer and exhibit reduced side effects.<sup>29</sup> It proves markedly less toxic to the kidneys and the nervous system causing less deleterious effects when compared to cisplatin.<sup>5b</sup> Unlike cisplatin, carboplatin is quickly extruded from the erythrocytes. Its activity though, is comparable to cisplatin in several cell lines.

Nedaplatin is approved for clinical use only in Japan.<sup>5</sup> Its activity and pharmacokinetics resemble that of carboplatin and can only be administered in the body through bolus infusion. However, both complexes suffer from cross resistance to cisplatin. The population of tumours treated by these two follow-up drugs is quite similar to that of cisplatin, making cisplatin the routine drug of choice except in cases where side effects prohibit its use.

### *1.0.4.2 Mononuclear platinum drugs designed to overcome cisplatin resistance.*

The most successful member of this group is oxalato(*trans-R,R*-1,2-diaminocyclohexane)platinum(II) also known as oxaliplatin (**4**, Figure 1.1). It has an advantage that it is active against a population of cancers that is different from those of cisplatin and can overcome cisplatin resistance in some tumours.<sup>30</sup> It is currently registered in many countries in Europe, Asia, USA and Latin America for first-line therapy of metastatic colorectal<sup>31</sup> cancer, a type of tumour that is insensitive to both cisplatin and carboplatin treatment. It can also be used in combination regimen with 5-fluorouracil and folic acid.<sup>31</sup> Like cisplatin and carboplatin, oxaliplatin forms 1,2-d(GpG)-Pt crosslinks, replacing the monodentate ammine ligands of cisplatin by a sterically demanding 1,2-diamminocyclohexane (dach) ligand. This, changes the active fragment in its crosslink adducts to a *cis*-Pt(dach)<sub>2</sub> chelate. The geometric constraint imposed on the DNA strands by the *cis*-Pt(dach)<sub>2</sub> can be the source of difference between the activity of oxaliplatin and that of cisplatin.<sup>32</sup> The bulky dach carrier ligand seems to have little influence on the interaction of the platinum centre with DNA, but has an overriding hindrance to the cellular machinery responsive to the processing functions of DNA lesions.<sup>3</sup> It is believed to play a role in hindering the binding of certain specific damage repair proteins such as the nucleotide excision repair (NER) at the lesion sites.<sup>2</sup> This act as a shield to the DNA damage adducts thus enhancing the probabilities of apoptotic pathways. This drug and two other tailored drugs *viz.*, carboplatin and nedaplatin,

## *Pt(II) based anticancer drugs*

---

share a common incorporated bidentate leaving group essential for modulating toxicity through slow ligand exchange reactions with plasma proteins. Thus, oxaliplatin lacks nephrotoxicity and exhibit milder hematological toxicity.<sup>33</sup> However, sensory neuropathy and gastrointestinal side effects are the dose limiting factors. To minimize side effects, liposomal-formulated Pt(dach)<sub>2</sub> complexes (L-NDDP and TRK-710)<sup>2</sup> have been prepared and are currently under clinical evaluation. They were designed to improve drug accumulation in tumour cell lines through efficient vascular permeability and retention. However, their tumour spectral profiles are not expected to be any different from that of oxaliplatin.

### 1.0.4.3 Orally administrable complexes.

The general problems of poor saline solubility (cisplatin and carboplatin) and poor pharmacostability<sup>3</sup> leading to limited bioavailability (oxaliplatin) make oral administration of clinical Pt drugs impractical. Currently, intravenous injection and infusion are the only plausible administration procedures for their clinical use. These parental methods are both inconvenient and costly to outpatients. To address these challenges, a new class of novel platinum(IV) complexes with an octahedral geometry was developed. For their general structures, two amine groups and two chloride groups, occupy the equatorial square planar as occurring in cisplatin while two readily leaving groups (acetates or hydroxo, *vide supra*) are in the axial *trans* positions.<sup>2</sup> The most notable member of this class of compounds is *trans*-bis-(acetato)aminedichloro(cyclohexylamine)platinum(IV), (JM216, **6**, Figure 1.1) also known as sastraplatin which is under phase III clinical trials in Europe and USA for treatment of ovarian and lung cancers.<sup>34</sup> This complex is regarded as a prodrug of cisplatin. It is thought to undergo reduction to yield cisplatin-like species.<sup>2,5</sup> It is highly soluble (0.3 mg mL<sup>-1</sup> in saline buffer) in aqueous solution and is moderately lipophilic, making its bioavailability by oral means possible. It exhibits better activity than cisplatin in several cisplatin sensitive and resistant cell lines in addition to having low nephrotoxicity and neurotoxicity.<sup>35</sup> Myelosuppression is the dose limiting factor.

Another highly promising drug admissible by oral means is *cis*-aminodichloro(2-methylpyridine)platinum(II) (Figure 1.1, **7**) also referred to as ZD0473, a drug candidate undergoing phase II clinical trials.<sup>3</sup> It is the first drug to display good oral availability and

## *Pt(II) based anticancer drugs*

---

antitumour activity. Its crystal data reveals that the pyridine ring is tilted by 102.7° with respect to the PtN<sub>2</sub>Cl<sub>2</sub> square-plane, placing the 2-methyl group directly over the platinum coordination plane.<sup>36</sup> This introduces some steric hindrance to any axial approach by oncoming nucleophiles on one side of the coordination square-plane. In the same manner, this axial hindrance is helpful in retarding *in vivo* cellular detoxifying reactions by the ubiquitous glutathione molecules and other cellular platinophiles, a feature closely linked to its ability to circumvent cisplatin resistance. Indeed, the rates of hydrolysis of ZD0473 were found to be lower than those of cisplatin and its analogous derivative, with a 3-methylpyridine carrier ligand.<sup>36</sup> Its reactivity towards thiourea, pyridine, methionine and GMP nucleophiles were also found to be less than that of cisplatin and its derivative containing the unsubstituted pyridine carrier ligand.<sup>37a</sup> It exhibits remarkably low resistance factors than cisplatin in two pairs of cisplatin-sensitive and resistance cell lines representing different mechanisms of resistance.<sup>37b</sup>

### 1.0.4.4 Active *trans*-platinum complexes.

The structure-activity relationship rules of Cleare and Hoeschele<sup>16</sup> were developed from the early studies that had previously mooted that *trans*-diamminedichloroplatinum(II), transplatin and its other *trans*-congeners lacked antitumour activity.<sup>38</sup> However, it later became clear that the rules were not entirely universal. Certain categories of *trans*-Pt(II) complexes turned out to have both *in vitro* and *in vivo* antitumour activities comparable to that of cisplatin. It is now known that the inactivity of transplatin lies in its kinetic instability (fast ligand kinetics) and consequent susceptibility to deactivation.<sup>38</sup> Unlike transplatin, all of congeners that turned out to be active, contained a communal planar ligand in their coordination spheres which are sterically hindered. The hindering ligands are thought to reduce the reactivity of *trans*-platinum complexes; thereby slowing down inactivation by cellular components through ligand exchange reactions.<sup>2</sup> This facilitates their interactions with the ultimate target nucleophilic site, DNA. The bulky ligands also induce similar DNA conformational damage to those caused by the 1,2-intrastrand crosslinks of cisplatin in their prevalent 1,3-interstrand adducts due to limited rotations within the crosslinks. The most notable subclasses of *trans*-platinum complexes which have shown remarkable *in vitro* antitumour activity include (i) *trans*-Pt(II) complexes bearing some planar aromatic ligand<sup>39</sup> such as pyridine, *N*-

## Pt(II) based anticancer drugs

methylimidazole, benzothiazole, thiazole, isoquinoline or quinoline (**8-12**); (ii) *trans*-Pt(II) complexes carrying an alkylamine (**13-14**)<sup>40</sup> and (iii) *trans*-Pt(II) complexes carrying an iminoether (**15**).<sup>41</sup> Their general structures are presented below in Figure 1.7.

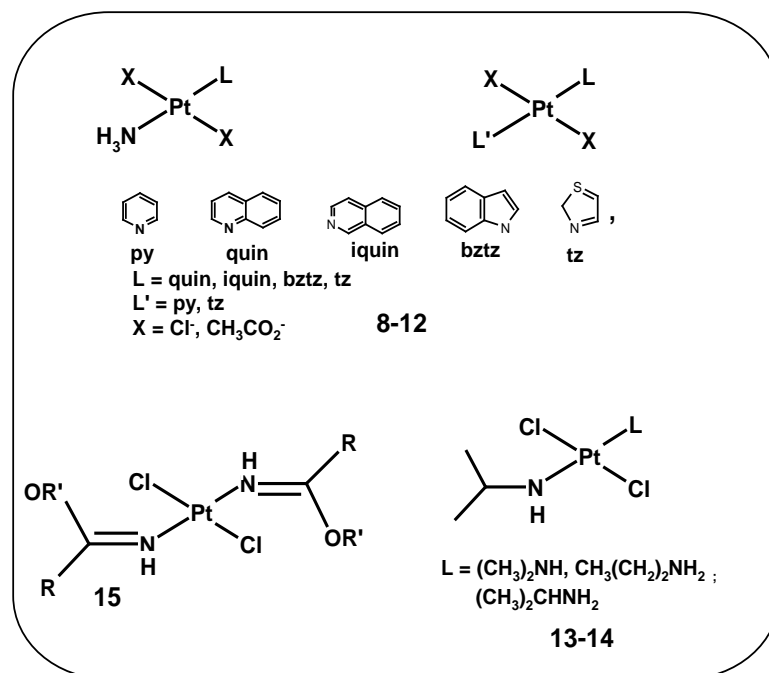


**Figure 1.7** Active platinum(II) compounds<sup>5b,c,39c</sup> containing: aromatic (*topmost left*), isopropyl (*right*) and iminoether carrier ligands (*lower left*). Planar ligands = Pyridine (py); quinoline (quin); isoquinoline (iquin), benzothiazole (bztz) or thiazole (tz).

The planar aromatic complexes (**8-12**, Figure 1.7) were found to exhibit good antitumour activity in cell panels resistant to cisplatin.<sup>39b</sup> The bulky planar groups are thought to exert slow ligand substitution kinetics thereby lowering inactivation by platinum scavenging biomolecules such as glutathione that are ubiquitous in the cytosol.<sup>39b,42</sup> In addition, the complexes display comparable cytotoxicity to their *cis*-analogues in cisplatin-sensitive cells.<sup>42</sup> In this series, the quinoline derivative exhibits superior reactivity.<sup>43</sup> Experimental and theoretical calculations suggested the formation of *quasi*-bifunctional adducts between the quinoline ligand and the DNA backbone, which provides additional interactions with the DNA. The DNA-platinum monofunctional adduct formed initially through the chloride ligand exchange, directs the *trans*-configured quinoline carrier ligand into a convenient position for

## *Pt(II) based anticancer drugs*

---

effective formation of intercalative *quasi* non-covalent-crosslink adducts with the nearest neighbouring nucleobase.<sup>43</sup>

The iminoether complexes, **15**, of the general structure given in Figure 1.7, have a planar geometry and fragments that introduce steric hindrance to the ligand exchange reactions.<sup>41b</sup> Binding to DNA is slower compared to both cisplatin and transplatin, reaching the same levels of platination only over a longer period of time. They preferably form monofunctional adducts that are stable in the presence of strong sulfur biomolecules.<sup>41c</sup> These *trans* configured iminoether complexes have antitumour activity comparable to that of cisplatin and are remarkably active against cisplatin resistant sub-cell lines.<sup>44</sup>

Very recently, a series of *trans*-[Pt(II)(piperazine) $X_2$ ] complexes were reported that displayed remarkable cytotoxicity against cisplatin resistant ovarian cancer cells.<sup>45</sup> These cationic complexes have good aqueous properties and bind more rapidly to DNA than cisplatin. Replacement of one of the piperazine ligand by  $NH_3$ , 4-picoline, butylamine produces compounds that induce similar conformational changes to that of transplatin in calf thymus DNA.<sup>46</sup> Petonja *et al.*<sup>47</sup> have recently reported on the kinetics and *in vitro* cytotoxicities of some new asymmetric *trans*-Pt(II) complexes of the general formula *trans*-[Pt(II)(azole)(*i*Pram)], where *i*Pram = isopropylamine and the azoles are pyrazole; 1-methyl pyrazole and 1-methylimidazole. These new agents overcome resistance against human ovarian carcinoma cell lines, A2780R, known to be insensitive to cisplatin,

In general, all active *trans*-platinum complexes are believed to form DNA lesions that are inherently different from those of their *cis*-counterparts.<sup>5b</sup> They predominantly form monofunctional DNA adducts<sup>48a</sup> as well as some interstrand DNA crosslinks<sup>48b</sup> instead of the 1,2-intrastrand crosslinks preferred in cisplatin reactions. Their interactions with DNA at a molecular level and hence their activity profiles are therefore markedly different from those of their analogous *cis*-agents. Despite their encouraging efficacy, none of these compounds has been advanced for clinic trials.

# *Pt(II) based anticancer drugs*

---

## **1.1 Multinuclear Pt(II) complexes**

### **1.1.1 Introduction**

The clinical use of cisplatin and its mononuclear analogues is hampered by several challenges as outlined in the previous sections of this chapter (*vide supra*). The most compelling problems are toxicity, tumour resistance (intrinsic and acquired) and an anti-cancer proliferation activity limited only to a narrow range of tumours.<sup>49</sup> A review on the efficacy of cisplatin and its subsequent generations of mononuclear platinum complexes<sup>2,3,49</sup> reveals that the mechanisms responsible for the problems of cisplatin-like antitumour platinum agents are complex and multi-factory (*vide supra*). For example, toxicity is closely related to the kinetic control of its ligand exchange reactions<sup>13b</sup> with non-target cellular proteins. Reactions between cisplatin-like drugs and plasma proteins are thought to cause toxicity and an induction of drastic side effects. Poor drug uptake and accumulation in tumour cells constitutes to natural resistance in tumour cells. Some tumours may develop refractory cellular responses prompted by increased tolerance to DNA damage, easy recognition of DNA damage and efficient repairs by cellular machinery. All forms of tumour resistances delineate the activity of the drugs only to a narrow range of tumours. Since the type of DNA conformational lesions induced by all bifunctional mononuclear agents is similar {1,2-d(GpG)-Pt intrastrand} and thus elicit a common cellular processing response pathway, it becomes evident that the downstream problems emanating from their use are commonly the same.

To overcome drug toxicity and resistance, a new class of Pt(II) anti-tumour complexes with improved drug targeting properties and a radical DNA binding mechanism, were needed, respectively.<sup>5b</sup> To try and minimize reactions causing toxic side effects, various drug targeting strategies (through selective accumulation and activation in tumour cells) such as enhanced permeability and retention effect;<sup>50</sup> liposomal delivery;<sup>51</sup> polymer conjugation<sup>52</sup> and low active biomolecular carrier mediated drug delivery<sup>53</sup> have been explored. Intensive research in this area is ongoing and more research is still needed before such strategies can be fully exploited to mitigate the problem of toxicity in healthy cells.

However, protracted pursuance of an avenue leading to DNA binding mechanisms which are radically different<sup>48a,54</sup> from that of cisplatin and its analogues paved way to novel multinuclear platinum complexes whose development was pioneered by Farrell and

## *Pt(II) based anticancer drugs*

---

coworkers.<sup>55</sup> The design crafted into these complexes has not only the potential to circumvent easy recognition of their DNA damage adducts and ultimate repair by cellular proteins but increased cytotoxic activity.

Multinuclear platinum complexes contain at least two or more platinum atoms connected together by a bridging linker. The linking bridge ensures that at least two terminus platinum centres are available for binding with the purine nucleobases of DNA.<sup>56</sup> Moreover, structural differences based on the linking bridge, the terminal carrier ligand around the platinum atoms as well as changing the number of enjoined platinum atoms offer many design possibilities for their synthesis. These numerous possibilities have potential to result in multinuclear platinum complexes of multitudinally different intrinsic properties. For example, in cases where the linking ligand is maintained the same, geometric isomers are conceivable, differing in the mutual positions of the leaving groups (in complexes with bifunctional terminus) or the positions of the leaving groups relative to the linking alkyldiamine ligand (in complexes with monofunctional terminus).

A convenient notation to name these isomeric multinuclear bearing alkyldiamine linkers has been developed by Farrell and coworkers<sup>54</sup> and will be adopted hereafter. In this notation, the numbers denote the number of leaving (chloride, anionic) groups on each platinum chloride. *Trans* or *cis* refer to the mutual geometry of the leaving groups (in the case of bifunctional platinum metal centre) or the geometry of the leaving groups relative to the linking alkyldiamine ligands (for mono-functional complexes). For example, 1,1-*trans,trans* refers to a monofunctional dinuclear platinum complex assumed to be linked by an alkyldiamine ligand. For complexes bearing other linking ligands, an inclusion of the name of the bridging ligand is necessary for complete specification.

### **1.1.2 Multinuclear Pt(II) complexes bridged by flexible diamines.**

The terminus platinum atoms for the first reported multinuclear complexes were linked by a flexible alkyldiamine chain,<sup>54</sup> enabling formation of unique long range DNA adducts between the reactive termini and the purine nucleobases in each DNA strand (*vide supra*). Functionally, formation of 1,2-d(GpG)-Pt intrastrands as well as long range interstrand cross links,<sup>57</sup> between the termini platinum centres and DNA are conceivable, depending on the

## *Pt(II) based anticancer drugs*

structural nature of the bridge, the length of the bridge, the number of the leaving groups at each terminus centre and their relative geometries around the terminal platinum centre. More importantly, long range interstrand DNA adducts,<sup>58</sup> mechanistically found to be formed on DNA in relatively high abundance by these complexes, are known to be insensitive to repair by cellular extracts.<sup>59</sup> Thus, these multinuclear complexes have potential not only to display superior antitumour activity, but to circumvent cisplatin resistance as they are less susceptible to DNA damage repair.

The first reported multinuclear complexes containing two platinum centres were based on a cisplatin-like (2,2-*cis,cis*, **16a**) and a transplatin-like (2,2-*trans,trans*, **16b**)<sup>54a,b</sup> termini structures and were bifunctional at each metal centre. Their structures together with their isomeric monofunctional counterparts which can be synthesized starting from transplatin (1,1-*trans,trans*, **17a**) and cisplatin (1,1-*cis,cis*, **17b**)<sup>60</sup> are presented in Figure 1.8. The terminus carrier ligand structures of the monofunctional dinuclear complexes are similar to Hollis's cationic complexes<sup>61</sup> at each Pt terminal centre and their details are discussed in section 1.1.2.

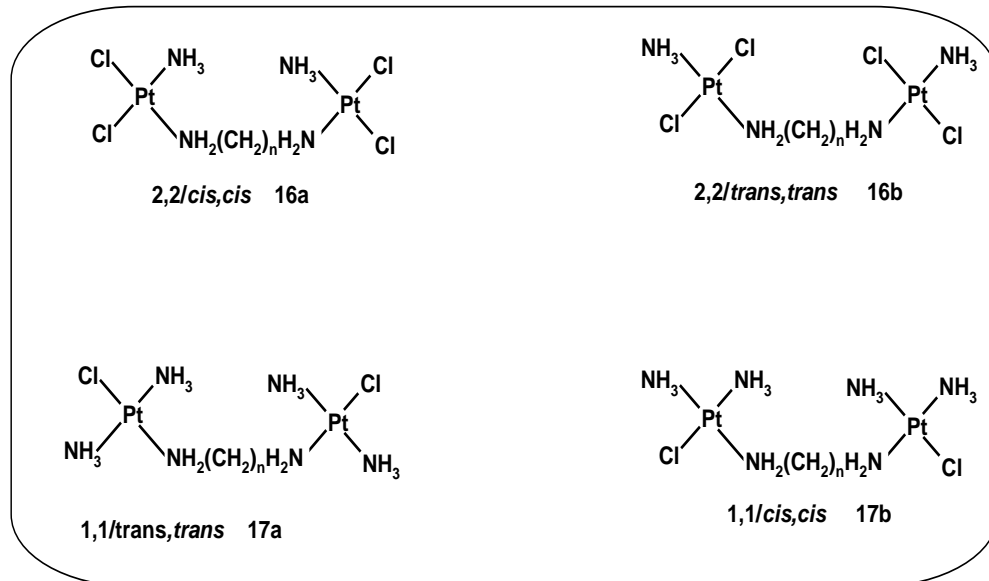


**Figure 1.8** Structures of cationic dinuclear platinum complexes bridged by flexible alkyldiamines.<sup>54</sup>

Dinuclear complexes with bifunctional platinum termini (2,2-*trans,trans*) and 2,2-*cis,cis*) meet the requirements of a neutral Pt terminus centre, having a square-planar geometry

## *Pt(II) based anticancer drugs*

---

which contain two *trans*- or *cis*-chloro leaving groups with at least one amino group.<sup>56</sup> Thus, in addition to forming a high percentage of long range interstrand cross linked adducts with DNA<sup>58</sup>, the 2,2-*cis,cis* isomers are capable of forming also 1,2 d(GpG)-Pt intrastrand adducts at each cisplatin-like terminus.<sup>55</sup> Replacement of the *cis*-chlorido groups with a malonate ligand results in a complex with improved salinity solubility and exhibits good anti-proliferation activity in resistant cancer cell lines.<sup>62</sup>

Monofunctional dinuclear complexes *viz.*, 1,1-*trans,trans* (**17a**) and 1,1-*cis,cis* (**17b**), represent the most dramatic examples of a subclass of dinuclear platinum compounds that break the traditional design rules for classical platinum complexes.<sup>16</sup> These complexes have not only one anionic leaving group at each terminus but are cationic.<sup>63</sup> They show better salinity properties and remarkable accumulation<sup>64</sup> in various tumour cell lines, leading to tissue concentration levels comparable and in some cases higher than cisplatin. The high positive charge on these complexes stabilizes their non-covalent binding to polyanionic DNA. Elsewhere, it has been reported<sup>65</sup> that the hydrolysis products of cisplatin are actually involved in hydrogen bonding and electrostatic pre-associative interactions with polyanionic DNA. These pre-association mechanisms of cisplatin are crucial for subsequent covalent binding of the drug to DNA. It is also expected that electrostatic interactions caused by these cationic multinuclear platinum complexes will proliferate, leading to efficient binding on the DNA due to their higher positive charges.

Both isomeric forms of monofunctional dinuclear complexes (the 1,1-*trans,trans* and 1,1-*cis,cis*) have antitumour activity that is better than or comparable to cisplatin in sensitive cells. However their activity in cisplatin resistant sublines is markedly different. The 1,1/*trans,trans* isomers overcome cross resistance while the 1,1-*cis,cis* isomers do not.<sup>66</sup> It is believed that geometric constraints force the 1,1-*cis,cis* isomers to form only a subset of adducts induced on DNA by their 1,1-*trans,trans* isomeric counterparts.

Despite violating the classical structure-activity relationships of Cleare and Hoeschele<sup>16</sup> in a rather dramatic way, these cationic dinuclear complexes have been shown to display remarkable *in vitro* activity in cisplatin-resistant cell lines in addition to being active against a broad spectrum of tumours. However, the 1,1-*trans,trans* complexes bind to DNA more rapidly<sup>67,68</sup> and form a significantly higher percentage of DNA interstrand crosslinks<sup>69a</sup> than

## *Pt(II) based anticancer drugs*

---

their 1,1-*cis,cis* isomeric counterparts. In addition, only the 1,1-*trans,trans* isomers are capable of forming intrastrand crosslinks possibly due to some steric overplay in the 1,1-*cis,cis* counterparts.<sup>68,69b</sup> In general, the 1,1-*trans,trans* isomers are more cytotoxic than their 1,1-*cis,cis* counterparts.<sup>66</sup> However, recent mechanistic studies<sup>70,71</sup> have shown that the former isomers are more prone to degradation by strong sulfur containing nucleophiles via liberation of the alkyldiamine linker. Thus, their cellular accumulation is expected to be compromised by the thiols such as glutathione known to be ubiquitous in the cytosol. Moreover, rapid ligand kinetics can potentially exacerbate the problem of toxicity.

Fortunately, drug delivery propositions aimed at addressing these shortcomings have been put forward. In one of the most promising propositions, encapsulation of some flexible 1,1-*trans,trans* multinuclear platinum complexes using some rate impeding cucurbituril portals has been reported.<sup>72a</sup> In a reaction between a cucurbit[6]uril encapsulated-1,1-*trans,trans*, n=8, complex and biogenic nucleophiles (namely glutathione and cysteine) it was demonstrated using <sup>1</sup>H NMR spectroscopy that encapsulation of the *trans* dinuclear complexes can lead to reduced reactivity with these strong nucleophiles. In contrast to all reactions of glutathione and cysteine with nude 1,1-*trans,trans* complexes as previously reported,<sup>70,71</sup> no evidence of any linker degradation was reported when an encapsulation portal was employed for the complex. Thus, cucurbit[6]uril encapsulation is a promising drug delivery strategy with a huge potential to impede drug depletion by competing cellular platinophiles of similar nucleophilicity to the sulfur containing nucleophiles used in the study. This does not only lead to enhanced antitumour activity but to reduced drug toxicity due to slackened ligand exchange reactions between the drug and plasma proteins. The cucurbituril portals are thought to offer a cushioning manifold for reactive termini of the multinuclear platinum complexes through a folding matrimony of the flexible linker piece inside their cavity.<sup>72b</sup>

In contrast to their mononuclear counterparts, multinuclear complexes are generally known to induce transition of the normal right handed B-DNA helix into the Z-DNA helix<sup>73,74</sup> which is believed to help escape from DNA damage recognition by proteins and the repair machinery. The escape is thought to be crucial in overcoming cisplatin resistance. More significantly for all multinuclear enjoined by straight chain alkyldiamine linkers, a pattern between their antitumour activity and the length of the dinuclear complexes have been



## *Pt(II) based anticancer drugs*

---

polyanionic DNA by the multinuclear masterpiece drug. This compound is active against pancreatic, lung, and melanoma cancers and is currently in Phase II clinical trials.<sup>54b</sup> BBR3464 is therefore capable of rapidly binding to DNA forming various long range intra-/interstrand crosslinks, with the latter comprising the majority of the adducts. The DNA interstrand crosslinks formed by this agent has been shown to distort the helical conformation of DNA weakly and are therefore ill-recognized by damaged-DNA binding proteins including the HMG and RPA.<sup>78</sup> Thus, the diversified nature of the DNA crosslinks of this agent is more likely to be responsible for its remarkable cytotoxicity.

Preclinical studies<sup>66</sup> using several human tumour cells and tumour xenographs with intrinsic cisplatin resistance has demonstrated that BBR3464 has cytotoxicity potency at concentration 20-fold lower than cisplatin in both cell panels. Tumour cells with mutant *p53* genes, which are usually insensitive to treatment by platinum drugs, are also hypersensitive to this agent, suggesting an induction to apoptosis through bypassing the *p53* mediated pathways.<sup>66,76</sup> The tumour suppressor protein *p53* is a potent mediator of cellular responses against genotoxic assaults.<sup>66b</sup> This unprecedented efficacy in cells with mutant *p53* genes builds hope that this agent can potentially inhibit tumour growth in over 60 % of cases of cancers where mutant *p53* status has been indicated.<sup>78</sup>

In a related effort, Farrell and coworkers<sup>79</sup> have synthesized an octa-cationic cousin of BBR3464 in which the terminal chloride ligands of BBR3464 were replaced by the protonated hexylamime ( $-(\text{CH}_2)_6\text{NH}_3^+$ ) groups. This compound display unprecedented long range bis-threading non-covalent interacting capabilities. The structure of the termini Pt centre allows the complex to interact only in a non-covalent manner with the nucleobases of DNA (hydrogen bonding and electrostatic interactions), wherein two of its *cis* amine groups are involved in hydrogen bonding with an oxygen atom of the phosphate backbone. This agent has encouraging *in vitro* and *in vivo* activities.

A variation to this strategy incorporating natural occurring and protonated polyamines, (Figure 1.9, (19-20)) as linking ligands has been advanced and pursued.<sup>80,54</sup> The polyamines, through their cationic quaternary amines, provide sites for a stronger pre-association with genomic DNA through hydrogen bonding and electrostatic interactions. Besides stabilizing the long-range crosslinks formed by these complexes, pre-association is thought to increase the

## *Pt(II) based anticancer drugs*

---

local concentration of the drugs, thus increasing the probability of binding at these sites *vide supra*.<sup>81</sup> Just like BBR3464, these compounds are highly cytotoxic, particularly in cisplatin-resistance cell lines.<sup>81,82</sup>

As was the problem with several mononuclear platinum complexes, the remarkable efficacy of multinuclear platinum complexes was found to be tainted by acute toxicity, prohibiting any further clinical tests on some of these potential drug candidates.<sup>83,84,18</sup> To address this problem, Farrell and coworkers<sup>85</sup> have recently unveiled a new strategy to minimize toxicity of the parent polyamines bridged complexes. Using a 1,1-*trans,trans*-spermidine, they demonstrated that acetylation protection of the quaternary nitrogen atoms of the linker in these multinuclear Pt complexes has potential to deliver the drug to the targeted tissues in a form which is less toxic and better tolerated by the host. Hydrolysis of the formed amide (*in vitro*) can be induced within the 6-8 pH range, resulting in the release of the underivatized form of the drug. Besides, the amine protection of 1,1-*trans,trans*-spermidine, shields the prodrug from binding to deactivating plasma proteins without an accompanying compromise on its antitumour activity.<sup>85</sup>

### **1.1.3 Multinuclear Pt(II) bridged by rigid linkers.**

Meanwhile, a number of other linking ligands have been used to develop related dinuclear platinum complexes.<sup>55c</sup> These include aromatic bridges with or without atomic or molecular tandem spacers (*viz.*, isomeric phenyldiamine;<sup>86</sup> mesitylene;<sup>87</sup> 4,4'-dipyridyl(sulfide/selenide);<sup>88</sup> 4,4'-dipyrazolylmethane;<sup>89a</sup> 4,4'-methylenediaminobenzene;<sup>89b</sup> isomeric azines;<sup>90</sup> isomeric azoles<sup>91</sup> and hydrazine<sup>92</sup> to mention just a few.

An appealing design of a novel trinuclear complex, endowed with a bridge of modulated rigidity comes from the mesitylene ligand. The structure of the complex (**21**) is shown in Figure 1.10.<sup>87a,b</sup>

## Pt(II) based anticancer drugs

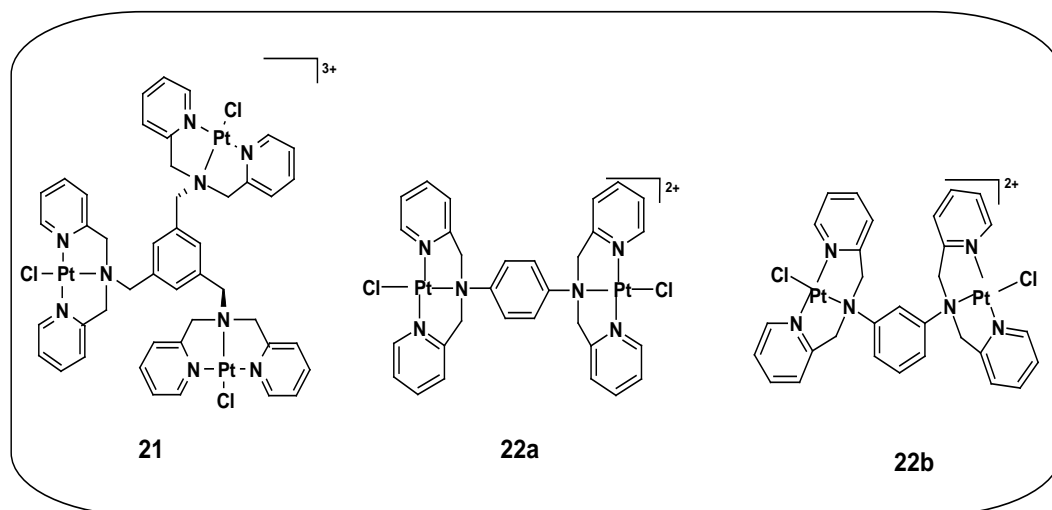


**Figure 1.10** Multinuclear platinum complexes with rigid aromatic linkers<sup>86, 87</sup>

The mesitylene ligand offers rigidity as well as planarity on its core phenyl ring. Incorporation of this ligand to link three *N,N'*-bis(2-pyridylmethyl)amine Pt(II) chelates at the three terminus platinum centres gives a trinuclear complex of moderate rigidity. In perspective, a three dimensional architecture endowed with a pseudo  $C_3$  rotational symmetry about the central mesitylene ring is formed by its three chelated square-planar termini. The trinuclear, **21**, has a stronger binding affinity for DNA and exhibits more cytotoxic potency against P-388 and A-549 cell lines than cisplatin. The average distance between the reactive termini and the modulated flexibility crafted in by the enjoining  $\text{CH}_2$  groups of the mesitylenes, confer reasonable chances for the formation of both intrastrand and interstrand DNA adducts. Unlike other mono-functional multinuclear complexes with monodentate ligands around the platinum centres, this complex reacts with glutathione with no evidence of cleavage of its enjoining linker.<sup>87b</sup> Chelation is a likely factor impeding linker liberation upon binding of biogenic thiols.

Related dinuclear complexes with isomeric phenyldiamine rigid linkers (**22a** and **22b**, Figure 1.10) utilizing the same chelate carrier ligand system at each platinum centre have been reported in a mechanistic study by Hofmann *et al.*<sup>86</sup> However, their binding affinities to DNA as well as their cytotoxic activities have not been tested. From within the domain of rigid linkers, other cyclic alkyldiamines such as 1,4-diaminocyclohexane and its rigidity-modulated analogue, 4,4'-methylenediaminocyclohexane provide other possible structural bridging motifs

## *Pt(II) based anticancer drugs*

for building up a series of complexes affording a holistic understanding of factors underlying the structural-activity relationships in dinuclear platinum complexes.

Another intriguing set of dinuclear platinum complexes of modulated-rigidity comes from the early studies of Broomhead *et al.*<sup>93</sup> In these complexes, two cisplatin-like centres were enjoined by one or two 4,4'-dipyrazoymethane (dpzm) bridging linkers. Disappointingly, these complexes were found to have inferior antitumour activity<sup>93</sup> when compared to cisplatin. Discouragingly, they also showed poor aqueous solubility, possibly due to their considerable lipophilicity and were not further considered for clinical tests. Wheate *et al.*<sup>89a</sup> extended this work by utilizing a single 4,4'-dipyrazoymethane bridge to enjoin two or three platinum centres of 1,1-*trans,trans* geometry at their terminal centres. The dpzm moiety offers a bridging ligand system of moderate rigidity, stemmed from the enjoined pyrazoyl ligands that are linked up by an incorporated CH<sub>2</sub> spacer. These novel dinuclear and trinuclear complexes (**23-24**) are the true analogues of the 1,1-*trans,trans*, n = 6 and BBR3464, respectively and their structures are shown in Figure 1.11.

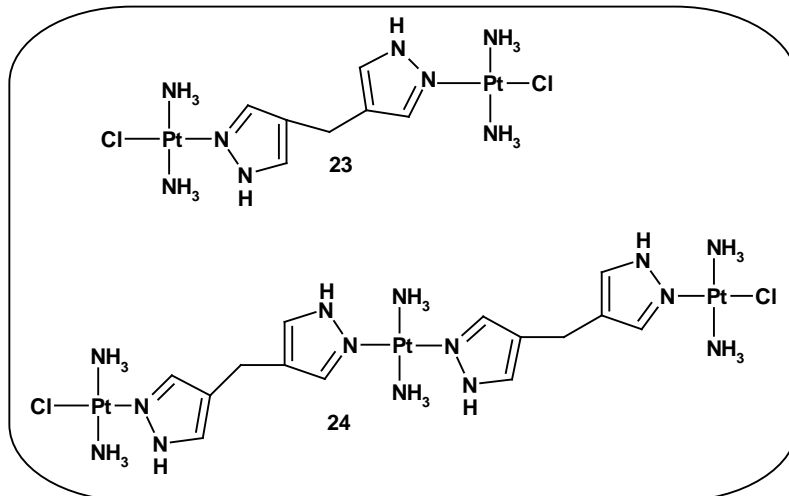


**Figure 1.11** Di-/trinuclear bridged platinum(II) complexes with a dipyrazoymethane (dpzm) bridging linkers.<sup>89a</sup>

The dipyrazoymethane bridged complexes showed a higher propensity to form long range interstrand with DNA than 1,2-*intra*strand formed by cisplatin at nanomolar (nM) concentration range. Despite maintaining their activity in L1210, L1210/DPP resistant sublines and human ovarian carcinoma 2008, the dpzm linked complexes displayed inferior antitumour

## *Pt(II) based anticancer drugs*

---

activity when compared to their aliphatic-bridged counterparts.<sup>89a</sup> Given the structural similarity in the coordination spheres of these two sets of complexes, the results suggest that increased rigidity in the bridging linker might lead to a reduction in cytotoxicity. Other similar complexes granting this modulated rigidity via their linking ligands are the 4,4'-dipyridyl(sulfide/-selenide)<sup>88</sup> and 4,4'-methylenediaminobenzene.<sup>89b</sup> They all have shown promising *in vitro* as well as *in vivo* antitumour activities.

Although it is not fully understood as to how the nature of the linking ligand (the structural features that controls rigidity/ flexibility of the linking ligand) affect activity in the 1,1-*trans,trans* analogues, it has been shown at least for the 1,1-*cis,cis* counterparts that steric influence originating from the linker<sup>89b</sup> is a crucial factor controlling the kinetics of the ligand exchange process. Ligand exchange reactions are believed to be the gateway to formation of potent DNA conformational lesions in tumour cells leading to subsequent slower processing by the cellular machinery.<sup>18</sup> A comparison of the reactions between 1,1/*cis,cis* (alkyldiamine, n = 6) and 1,1/*cis,cis* (4,4'-dipyridylsulfide) with glutathione suggests that steric hindrance of the phenyl rings of the latter complex is likely to impede deactivation by strong sulfur containing molecules.<sup>88</sup>

The prototypically rigid monofunctional dinuclear complexes (**25-29**) come from the studies of Kalayda *et al.*<sup>90</sup> The structures of the complexes are depicted in Figure 1.12.

## Pt(II) based anticancer drugs

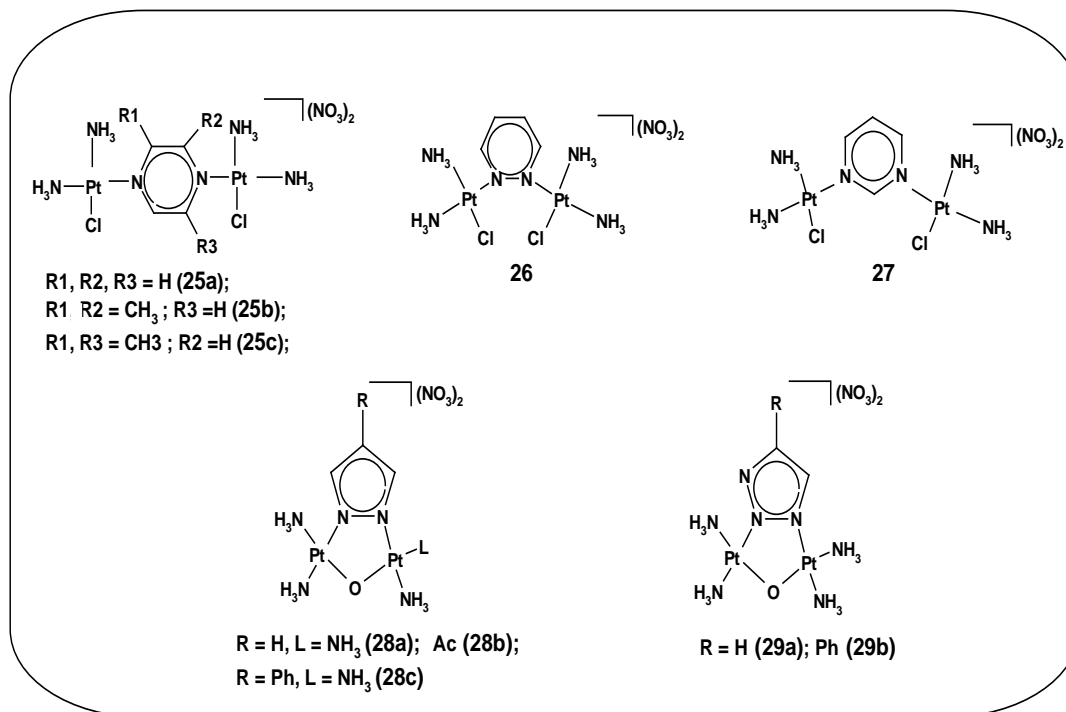


**Figure 1.12** Rigid platinum(II) complexes with isomeric azines and isomeric azoles bridging ligands.<sup>90</sup>

In the study of Kalayda,<sup>90a</sup> isomeric azines were utilized to link platinum centres bearing monodentate amine carrier ligands in a 1,1-*cis,cis* fashion. For the series (**25a-c**, Figure 1.12), the unsubstituted azines were shown to exhibit superior cytotoxicities in L1210 murine leukemia cell lines. The pyrazine-linked complex (**25a**) in particular displayed the highest antitumour activity. Unlike the dpzm-bridged complexes, (**23-24**)<sup>86</sup> and the claim implied thereof that rigidity of the bridge may lead to their poor cytotoxicities, the isomeric azine-bridged series have been found to exhibit good anticancer activity, more so in cisplatin resistance cells.<sup>90c</sup> Compared to cisplatin, their antitumour activities were observed to be generally comparable in several human tumour cell lines.<sup>90a</sup> Unlike BBR3464 and other 1,1-*trans,trans* analogues, their 1,1-*cis,cis* geometry is expected to be less susceptible to linker cleavage by reactions with sulfur bio-nucleophiles.

In a variation approach to Kalayda's rigid 1,1-*cis,cis* series, Komeda *et al.*<sup>91</sup> developed some pyrazole-linked complexes (**28-29**, Figure 1.12). In these complexes, the  $\mu$ -oxo ligand is incorporated as both a bridging and leaving group. The average distance between the reactive

## *Pt(II) based anticancer drugs*

---

termini for the complexes is comparable to the distance separating sequential nucleobases in a normal B-type DNA helical strand. This was evidenced from the solved crystal structure of [*cis*-Pt(9-EtG)<sub>2</sub>]<sub>2</sub>(μ-OH)(μ-pyrazolate)], EtG = 9-ethylguanine, a model nucleobase.<sup>91a,c</sup> The orientation of the model nucleobases in the crystal structure is similar to the normal configuration of the nucleobases in a normal B-type DNA. These complexes were therefore designed to mimic cisplatin's mode of binding in which 1,2 d(GpG)-Pt crosslinks are formed. Unlike cisplatin though, their rigidity were hoped to confer minimal conformational deformation in which the DNA helix structure would remain relatively undisturbed.<sup>91b</sup> In this way, the conformational changes induced by the agents may escape recognition by DNA repair proteins. This is beneficial, more so in resistant cell lines. Indeed, these complexes exhibit better cytotoxicity than cisplatin in several human tumour cell lines including MCF7, EVSA-T (breast cancer), WIDR (colon cancer) IGROV (ovarian cancer) M19 (melanoma), A498 (renal) and H226 (non small lung cancer).<sup>91b, d</sup>

# *Pt(II) based anticancer drugs*

---

## 1.2 Aims of the study

Most multinuclear platinum complexes seem to exhibit cytotoxicity comparable to and in some cases better than that of cisplatin, especially for polynuclear complexes of monofunctionality. Of special interest are the 1,1-*trans,trans* and 1,1-*cis,cis* cationic complexes linked by flexible alkydiamine ligands which have been established to have remarkable antitumour activity in cisplatin resistant cells. The former complexes are endowed with superior cytotoxicities and the ability to circumvent cisplatin resistance. This is attributed to their ability to form long range intra- / and inter-strand hairpin crosslinks on nuclear DNA and induction of B- to Z-DNA transitions.<sup>94</sup> However, *trans*-labilization of their leaving groups induced by the coordination of strong sulfur biomolecules has been reported to degrade these complexes resulting in the loss of the alkydiamine linker.<sup>70a,71</sup> The observed degradation products can be modeled by reactions of the dinuclear complexes with sulfur containing nucleophiles.<sup>70b</sup> On the one hand, the 1,1/*cis,cis* complexes are relatively less potent. However, they are less prone to linker loss though labilization by coordinated sulfur nucleophiles.<sup>95</sup> Rigid bridging linkers are yet to be fully explored to gain an adequate understanding on how rigidity affects cytotoxicity.

Reedijk<sup>7b,13</sup> underscores that a full understanding of the underlying kinetics is crucial in the design of new targeted drugs with improved antitumour activities. The reactivity of the drugs can determine the extent of drug reaching the target sites as well as the extent of side reactions, its circulation lifetime and more importantly the antitumour activity of the drug in the target sites just to mention a few. Therefore, kinetic and mechanistic study of the substitution reactions of a set of platinum complexes with appropriate model nucleophiles has become part of the protracted search<sup>96</sup> for the Pt therapeutic drug of improved efficacy.

As part of this wide-cast search for future drugs of improved efficacy, it was undertaken to study the thermodynamic as well as the kinetic properties of three sets of inter-related complexes designed to offer an in-depth understanding of the role of the diamine bridging linkers on the reactivity of chelated dinuclear Pt complexes with archetypical bis(2-pyridylmethyl)amine headgroups. This work seek to gain an instructive understanding of the role of the specific structural properties defining the diamine bridge on the reactivities of the Pt centres of the resultant dinuclear complexes and other multinuclear which are already known to

## *Pt(II) based anticancer drugs*

---

have a superior antitumour activity. This is demonstrated in the encouraging trial clinical results of BBR3464, a trinuclear, designed by Farrell<sup>54-60</sup> and coworkers.

To achieve this, two sets of dinuclear complexes, one bearing flexible  $\alpha,\omega$ -alkyldiamines of variable chain length and another bridged by either phenyldiamine or diaminocyclohexane fragments were synthesized and their substitution reactions with three thiourea nucleophiles carried out in aqueous lithium triflate medium at pH 2. The chosen thiourea nucleophiles of varying steric size are good models for reactions involving sulfur-containing nucleophiles which commonly take place in biological tissues and are therefore available for competition reactions with Pt based drugs. These nucleophiles are also known to have good aqueous solubility, are neutral and of high nucleophilicity.<sup>97</sup>

A third set of complexes that were studied, comprises mononuclear analogues of the dinuclear complexes in which the bridging moiety has been turned into a dangling pendant. It was expected that reactivity data from this study would be useful in gaining a full understanding of the general role of the diamine (*i.e.*, the chain length of the alkyldiamine bridge as well as the change in the chemical structures to other groups such as the moderate rigid diaminocyclohexane and phenyldiamine groups) on the general reactivity of the dinuclear complexes. Excision of one of the chelate headgroups of the studied dinuclear to form their respective mononuclear complexes bearing dangling alkylamine; phenylamine and cyclohexylamine pendants practically exclude other factors that mask a full understanding of the intrinsic role of the diamine bridge through a composite contribution towards the control of reactivity at the Pt centres of complexes. Specifically, possible factors such as in-space charge addition, electronic effects and steric influences due to the linker which can potentially complicate the assignment of which of these factors actually control reactivity in the multinuclear complexes is eliminated. A deeper understanding of this nature is crucial in the design of targeted Pt drugs of predictable pharmacokinetic behaviour and targeting specific tissue and hence of high efficacy.

## *Pt(II) based anticancer drugs*

---

### 1.3 References

- 1 (a) M. Pan and C. Ho, *Chem. Soc. Rev.*, 2008, **37**, 2558; (b) <http://www.diseasedatabase.com/dd28843.htm> viewed on 2/11/2008; (c) S. B. Howell, *Cancer Cells*, 1990, **2**, 35; (d) H. Grunicke, W. Doppler and W. Helliger, *Arch Gerschwulstforsch*, 1999, **99**, 2711.
- 2 Y. Ho, S. F. Au-Yeung and K. W. To, *Med. Res. Rev.*, 2003, **23**, 633.
- 3 M. Glanski, M. A. Jakupec and B. K. Keppler, *Curr. Med. Chem.*, 2005, **12**, 225.
- 4 I. Kostava, *Recent Patents on Drug Discovery*, 2006, **1**, 1.
- 5 (a) M. J. Hannon, *Pure Appl. Chem.*, 2007, **79**, 2243; (b) L. M. Pasetto, M. A. D'Andrea, A. A. Brandes, E. Rossi, S. Monfardini, *Critic. Rev. Onco. / Hemat.*, 2006, 59; (c) C. J. Jones and J. Thornback, *Medicinal Applications of Coordination Chemistry*, RSC Publishing, Cambridge, UK, 2007, pp. 218-257
- 6 (a) E. R. Jameison, S. J. Lippard, *Chem. Rev.* 1999, 2467; (b) K. R. Barnes and S. J. Lippard, In *Metal ion in Biological systems*, A. Sigel, Ed., Marcel Dekker, New York, 2004, **42**, 143.
- 7 (a) S. M. Cohen and S. J. Lippard, *Prog. Nucleic acid Res. Mol. Bol.*, 2001, **67**, 93. (b) J. Reedijk, *Eur. J. Inorg.*, 2009, 1312.
- 8 (a) R. F. Ozols and S. D. Williams, *Curr. Probl. Cancer*, 1989, **13**, 287; (b) R. F. Ozols, *Curr. Probl. Cancer*, 1992, **6**, 879.
- 9 (a) L. J. Swinnen, D. M. Barnes, S. G. Fisher, K. S. Albain, R. I. Fisher and L. C. Erickson, *Cancer Res.*, 1989, **49**, 1383; (b) T. Esak, S. Nakano, T. Tatsumoto, M. Kurokka-Migita, K. Mitsugi, M. N. Nakamura, Y. Niko, *Cancer Res.*, 1992, **52**, 6501. (c) L. Kelland, *Nat. Rev. Cancer*, 2007, **7**, 573.
- 10 (a) G. J. Bosl and R. J. Motzer, *New Engl. J. Med.*, 1997, **337**, 242; (b) H. M. Keys, B. N. Bundy, F. B. Stehman, L. I. Muderspach, W. E. Chafe, C. L. Suggs, J. L. Walkker and D. N. Gersell, *New Engl. J. Med.*, 1999, **340**, 1154.
- 11 D. Hayes, E. Cvitkovic, R. Golbey, E. Schneiner, H. I. Krakoff, *Proc. Am. Assoc. Cancer Res.*, 1976, **17**, 169.
- 12 L. Z. Cubeddu, I. S. Horrmann, N. T. Fuenmayor, A. L. Finn, *New Engl. J. Med.*, 1996, **322**, 810.
- 13 (a) J. Reedijk, *Chem. Rev.*, 1999, **99**, 2499; (b) J. Reedijk, *PNAS.*, 2003, **100**, 3611. (c) J. H. J. den Hartog, C. Altona, J. H. van Boom, G. A. van der Marel, C. A. G. Haasnoot, J. Reedijk, *J. Biomol. Struct. Dyn.*, 1985, **2**, 1137. (d) J. H. J. den Hartog, C. Altona J. H. van

## *Pt(II) based anticancer drugs*

---

- Boom, G. A. van der Marel, C. A. G. Haasnoot, J. Reedijk, *J. Am. Chem. Soc.* 1984, **106**, 1528.
- 14 B. Rosenberg, L. van Camp, J. E. Trosko and V. H. Mansour, *Nature*, 1969, **222**, 385.
- 15 I. Otto and R. Gust, *Phar. unsever Zeit.*, 2006, **35**, 124.
- 16 (a) M. J. Cleare and J. D. Hoeschele, *Plat. Met. Rev.*, 1973a, **17**, 2. (b) M. J. Cleare and J. D. Hoeschele, *Bioinorg. Chem.*, 1973b, **77**, 187.
- 17 M. A. Fertes, C. Alonso and J. M. Pérez, *Chem. Rev.*, 2003, **4**, 889.
- 18 J. A. Rice, D. M. Crothers, A. L. Pinto and S. J. Lippard, *Proc. Natl. Acad. Sci. USA*, 1988, **85**, 4188.
- 19 D. P. Lin, T. Okuda, A. Holzer and. Herskowitz, *Proc. J. Natl. Acad. Sci., USA*, 2002, **99**, 14298.
- 20 (a) Y. Jung and S. J. Lippard, *Chem. Rev.*, 2007, 1387. (b) S. Cruet-Hennequart, M. T. Glynn, L. S. Murillo, S. Coyne, M. P. Carty, *DNA Repair*, 2008, **7**, 582. (c) Y. Jung, S. J. Lippard, *J. Biol. Chem.*, 2006, **281**, 1361.
- 21 B. A. Jensen, P. Wielaard, G. V. Kalayda, M. Ferrari, C. Molenaar, J. H. Tanke, J. Bouwer and J. Reedijk, *J. Inorg. Chem.*, 2003, **21**, 227.
- 22 D. P. Bancroft, C. A. Lepre and S. J. Lippard, *J. Chem. Soc.*, 1990, **112**, 6860.
- 23 (a) M. Kartalou, J. and M Essigman, *Mutat. Res.*, 2001, **478**, 1; (b) A. M. J. Fichtinger-Schepman, J. L. van der Veer, J. H. J. den Hartog, P. H. M. Lohnman and J. Reedijk, *Biochem.*, 1985, **24**, 707.
- 24 (a) M. J. Allday, G. J. Inman, D. H. Crawford and N. P. Farrell, *EMBO J.*, 1995, **14**, 4994; (b). G. Wang, E. Reed and Q. Lid, *Onco. Rep.*, 2004, **12(5)**, 955; (c) U. M. Ohndorf, M. A. Rould, Q. He, C. O. Pabo and S. J. Lippard, *Nature*, 1999, **399**, 708.
- 25 (a) S. J. Brown, P. J. Kellet and S. J. Lippard, *Science*, 1993, **261**, 603; (b) J. C. Huang, D. B. Zamble, J. T. Reardon and S. J. Lippard, A. Sancar, *Proc. J. Natl. Acad. Sci. USA*, 1994, **91**, 10394.
- 26 (a) T. W. Sorenson, M. Eastman, *Cancer Res.*, 1988, **48**, 4484; (b) M. Eastman, In *Cisplatin: Chemistry and biochemistry of a leading anticancer drug*, 1999, B. Lippert, Ed. Wiley VCH, Weinheim, 111.
- 27 (a) C. H. Versantvoort, H. J. Broxterman, T. R. Badrij, J. Scheper and P. R. Twentyman, *J. Cancer*, 1995, **72**, 82; (b) J. Teuben, M. Rodriguez. I. Zubiri and J. Reedijk, *J. Chem.*

## *Pt(II) based anticancer drugs*

---

- Soc., Dalton Trans.*, 2000, 369; (c) D. Petrović, B. Stojimirović, B. Petrović, Z. M. Bugarčić and Z. D. Bugarčić, *Bioorg. & Med. Chem.*, 2007, **15**, 4203; (d) K. Lemma S. K. C. Elmroth and Elding, *J. Chem. Soc., Dalton Trans.*, 2002, 1288.
- 28 J. A. Mello, S. Acharya, R. Fishel, J. M. Essigmann, *Chem. Biol.*, 1996, 579.
- 29 J. C. Ruckdeschel, *Semin. Oncol.*, 1994, **21**, 114.
- 30 T. Tashiro, T. Kawada and Y. Sakurai, *Biomed. Pharmacother.*, 1989, **43**, 251.
- 31 E. Raymond, S. G. Chaney, A. Taama, *Ann. Oncol.*, 1998, **9**, 1098.
- 32 (a) O. Rixe, W. Ortuzer and M. Alvarez, *Biochem. Pharmacol.*, 1996, **24** 1855; (b) W. Ortuzer, K. Paul and O. Rixe, *Proc. Am. Assoc. Cancer Res.*, 1994, **35**, 332.
- 33 M. Boisdron-Celle, A. Lebouil, P. Allain and E. Gamelin, *Bull. Cancer*, 1998, **88**, 14-19.
- 34 X. Anon, *Drug Res. Dev.*, 2002, **3(1)**, 67.
- 35 E. Fokkema, H. J. Groen, M. N. Helder, E. G. Vries and C. Meijer, *Biochem. Pharmacol.*, 2002, **63**, 1989.
- 36 Y. Chen, Z. Guo, S. Parsons and P. J. Sadler, *Chem. Eur. J.*, 1998, **4**, 672.
- 37 (a) J. F. Holford, F. I. Raynaud, B. A. Murrer, K. Grimaldi, J. A. Hartley, M. J. Abrams and L. R. Kelland, *Anti-Cancer Drug Des.*, 1998a, **13**, 118; (b) J. F. Holford, S. Y. Sharp, B. A. Murrer, M. Abrams and L. R. Kelland, *Br. J. Cancer*, 1998b, **77**, 366.
- 38 (a) N. Farrell, *Met. Ions Biol. Syst.*, 1996, **32**, 603. (b) N. Farrell, *Eur. J. Inorg.*, 2009, 1293.
- 39 (a) N. Farrell, L. D. Kelland, J. D. Roberts and M. van Beusichem, *Cancer Res.*, 1992, **52**, 5065; (b) N. Farrell, T. T. Ha, J. P. Souchard, F. L. Wimmer, S. Cross and N. P. Johnson, *J. Med. Chem.*, 1992, **32**, 2240. (c) S. M. Aris and N. Farrell, *Eur. J. Inorg.*, 2009, 1293.
- 40 (a) R. Prokop, J. Kasparková and O. Nováková, *Biochem. Pharmacol.*, 2004, **67**, 1097; (b) E. I. Montero, S. Diaz, A. M. Gonzalez-Vadillo, J. M. Perez, C. Alonso, and C. Navarro-Ranninger, *J. Med. Chem.*, 1999, **36**, 4264; (c) J. M. Perez, A. M. Gonzalez, A. Alvarez-Valdes, C. Alonso, C. Navarro-Ranninger, *J. Inorg. Biochem.*, 1999, **77**, 37.
- 41 (a) M. Coluccia, A. Nassi, F. Loseto, A. Boccarelli, M. A. Mariggio, D. Giordano, F. P. Intini, P. Caputo and G. Natale, *J. Med. Chem.* 1992, **36**, 510; (b) M. Coluccia, A. Boccarelli, M. A. Mariggio, D. Giordano, F. P. Intini, P. Caputo and G. Natale, *Chem. Biol. Interac.*, 1995, **98**, 251; (c) G. Natale, M. Coluccia, *Coord. Chem.*, 2001, **216**, 384.

## *Pt(II) based anticancer drugs*

---

- 42 M. van Beusichem and N. Farrell, *Inorg. Chem.*, 1992, **31**, 634.
- 43 A. ZÁKOVSKÁ, O. NOVÁKOVÁ, Z. BALCAROVÁ, U. BIERBACH, N. FARRELL and V. BRABEC, *Eur. J. Biochem.*, 1998, **254**, 547.
- 44 K. J. Mellish, C. F. Barnard, B. A. Murrer, L. R. Kelland, *Int. J. Cancer*, 1995, **62(6)**, 717.
- 45 Y. Najajreh, J. M. Perez, C. Alonso, C. Navarro-Ranninger and D. Gibson, *J. Med. Chem.*, 2002, **45**, 5189.
- 46 P. A. Nguewa, M. A. Fuertes and S. Iborra, *J. Inorg. Biochem.*, 2005, **99**, 727.
- 47 E. Petonja, A. Gallipolli, S. van Zutphen, S. Komeda, D. Reddy, D. Jaganyi, M. Lutz, D. M. Tooke, A. L. Spek, C. Navarro-Ranninger and J. Reedijk, *J. Inorg. Biochem.*, 2006, **100**, 1955.
- 48 (a) Brabec, K. Neplechová, J. Kasparková and N. Farrell, *J. Bio. Inorg. Chem.*, 2000, **5**, 364; (b) J. M. Perez, M. A. Fuertes, C. Alonso and C. Navarro-Ranninger, *Crit. Rev. Oncol. Hematol.*, 2000, **35**, 109.
- 49 E. Wong and C. M. Giandomenico, *Chem. Rev.*, 1999, **99**, 2451.
- 50 H. Maeda, J. Wu, T. Sawa, Y. Matsumura and K. Hori, *J. Contr. Release*, 2000, **65**, 271.
- 51 M. D. Demario, N. J. Vogelzang, L. Janisch, M. Tonda, M. A. Amentea, L. Pendyala and M. J. Ratain, *Pro. Am. Soc. Clin. Oncol.*, 1998, 17.
- 52 R. Duncan, S. Gac-Breton, R. Keane, R. Musula, Y. N. Sat, R. Satchi and F. Searle, *J. Contr. Release*, 2001, **74**, 135.
- 53 S. Slaby, M. Glanski, S. W. Metzger and B. K. Keppler, *Contrib. Onco.*, 2000, **54**, 201.
- 54 (a) N. Farrell, *Comments Inorg. Chem.*, 1995, **16 (6)**, 373; (b) V. Brabec, *Prog Nucl. Acid Res. Mol. Biol.*, 2002, **71**, 1; (c) N. Farrell, *Metal Ions Bio.*, 2004, **41**, 252; (d) S. W. Johnson, K. V. Ferry and T. C. Hamilton, *Drug Res. Updates*, 1998, **1**, 243.
- 55 (a) N. Farrell, S. G. de Almeida and K. A. Skova, *J. Am. Soc.* 1988, **110**, 5018; (b) N. Farrell, Y. Qu, *Inorg. Chem.*, 1989, **28**, 3416; (c) N. J. Wheate and J. G. Collins, *Coord. Chem. Rev.*, 2003, 133.
- 56 J. D. Roberts, B. van Houten, Y. Qu and N. Farrell, *Nucleic Acids Res.*, 1989, **17**, 47.
- 57 A. Hegmans, S. J. Berner-Price, M. S. Davies, D. S. Thomas, A. S. Humphreys and N. Farrell, *J. Am. Soc.*, 2004, **126**, 48076.

## *Pt(II) based anticancer drugs*

---

- 58 Y. Qu, L. Feng, B. van Houten, N. Farrell and Y. Qu, *Biochemistry*, 1990, **29**, 9522.
- 59 J. Kasparková, J. Zehnulova, N. Farrell and V. Brabec, *J. Bio. Inorg. Chem.*, 2002, 277, 48076.
- 60 N. Farrell, Y. Qu and M. P. Hacker, *J. Med. Chem.*, 1990, **33**, 2179.
- 61 L. S. Hollis, *J. Med. Chem.*, 1989, **32(1)**, 128.
- 62 A. J. Kracker, J. D. Hoeschele, W. L. Elliot, H. D. Hollis, A. Showwalter, A. D. Sereel, N. Farrell, Y. Qu and M. P. Hacker, *J. Med. Chem.*, 1992, **35**, 4526.
- 63 N. Farrell, Y. Qu, U. Bierback, M. Valsecchi and E. Menta, In: *Cisplatin Chemistry and biochemistry of a leading anticancer drug*, 1999, B. Lippert Ed, Verlag Helvetica Chemica Acta, Zurich, Wiley-VCH, Weinheim, 479.
- 64 P. Perego, C. Caserini, L. Gatti, N. Carenini, S. Colangelo, I. Romanelli, R. Supino, D. Viano, R. Leone, S. Spinelli, G. Pezzoni, C. Manzotti, N. Farrell and F. Zunino, *J. Inorg. Biochem.*, 1999, **77**, 59.
- 65 Y. Wang, N. Farrell and J. D. Burgess, *J. Am. Chem. Soc.*, 2001, **123**, 5576.
- 66 (a) C. Manzotti, G. Pratesi, E. Menta, R. Di, E. Cavalletti, H. H. Fiebig, R. L. Kelland, D. Polizzi, G. Pezzoni, R. Supino, N. Farrell and F. Zunino, *Cli. Cancer Res.*, 2000, **6**, 2626; (b) F. Janas, N. Albrechtsen, I. Dornreiter, L. Wiesmuller, F. Grosse and W. Deppert, *Cell Mol. Life Sci.*, 1999, **55**, 12.
- 67 J. W. Cox, S. Berners-Price, M. S. Davies, Y. Qu, and N. Farrell, *J. Am. Chem. Soc.*, 2001, **123**, 1316.
- 68 K. J. Mellish, Y. Qu and N. Scarsdale, *Nucleic Acid Res.*, 1997, **25**, 1265.
- 69 (a) Y. Zou, B. van Houten and N. Farrell, *Biochem.*, 1994, **33**, 5404; (b) Y. Qu, M. J. Bloemink, K. J. Mellish, H. Rauter, K. A. Smeds and N. Farrell, *NATO Adv. Sci. Innov. Ser.*, 1997, **26**, 435.
- 70 (a) M. E. Oehlsen, Y. Qu and N. Farrell, *Inorg. Chem.*, 2003, **42**, 5498; (b) V. Vacchina, L. Torti, C. Allievi and R. Lobinski, *J. Anal. At. Spectrom.*, 2003, **18**, 884.
- 71 N. Summa, J. Maigut, R. Puchta and R. van Eldik, *Inorg. Chem.*, 2007, **46**, 2094.
- 72 (a) D. Bali, P. Dali, A. J. Coe, A. Ii, J. Day and N. G. Collins, *J. Chem. Soc. Dalton Trans.*, 2006, 5337; (b) N. G. Collins, R. I. Taleb, A. M. Kruse-Heuer, R. I. Cook S. Wang, V. J. Higgins and J. Aldrich-Wright, *J. Chem. Soc. Dalton Trans.*, 2007, 5055.

## *Pt(II) based anticancer drugs*

---

- 73 (a) A. Johnson, Y. Qu, B. van Houten and N. Farrell, *Nucl. Acids Res.*, 1992, **20**, 1697; (b) N. Farrell, T. G. Appleton, Y. Qu, J. D. Roberts, A. P. Soares Fontes, K. A. Skov, P. Wu and Y. Zou, *Biochem.*, 1995, **43**, 15480.
- 74 P. K. Wu, M. Kharatishvili, Y. Qu and N. Farrell *J. Inorg. Biochem.*, 1996, **63**, 9.
- 75 J. Jensen, J. van der Zwan, H. den Dulk, J. Brouwer and J. Reedijk, *J. Med. Chem.*, 2001, **44**, 245.
- 76 (a) N. Farrell and Y. Qu, In *Platinum based Drugs in Cancer Therapy*, 2000, L. R. Kelland, Farrell Eds, Humana Press: Totowa, NJ, 321; (b) N. Farrell and S. Spinelli, In *Uses of Inorganic chemistry in medicine*, 1999, N. Farrell Ed., Royal Society of Chemistry, Cambridge, UK, 124.
- 77 (a) P. Perego, C. Caserini, L. Gatti, N. Carenini, S. Romanelli, R. Supino, D. Colangelo, I. Viano, R. Leone, S. Spinelli, G. Pezzoni, C. Manzotti, N. Farrell and F. Zunino, *Mol. Pharmacol.*, 1999, **55**, 528; (b) C. Manzotti, G. Pratesi, E. Menta, R. Di Domenico, E. Cavalletti, H. H. Fiebig, L. R. Kelland, N. Farrell, D. Polizzi, R. Supino, G. Pezzoni and F. Zunino, *Clin. Cancer Res.*, 2000, **6** (7), 2626.
- 78 (a) V. Brabec and J. Kasparková, *J. Drug Res. Updates*, 2002, **8**, 131.
- 79 (a) A. L. Harris, X. H. Yang, A. Hegmans, L. Povirk, J. J. Ryan, L. Kelland and N. P. Farrell, *Inorg. Chem.*, 2005, **44**, 9598; (b) A. L. Harris, J. J. Ryan and N. P. Farrell, *Mol. Pharm.*, 2006, **69**, 666.
- 80 J. D. Roberts, J. Peroutka, G. Beggiolin, C. Manzotti, L. Piazzoni and N. Farrell, *J. Inorg. Biochem.*, 1999, **77**, 47.
- 81 (a) H. Rauter, R. Didomenico, E. Menta, E. Oliva, Q. Yu and N. Farrell, *Inorg. Chem.*, 1997, **36**, 3919; (b) N. Farrell, In *Polynuclear Platinum Drugs, Metals Ions in Biological Systems*, 2004, A. Sigel and H. Sigel Eds. Marcel Dekker, Inc, New York, 41, 252.
- 82 J. D. Roberts, A. P. Soares Fontes, K. A. Skov, P. Wu and Y. Zou, *Biochem.*, 1995, **43**, 15480.
- 83 P. P. Calvert, M. S. Highley, A. N. Hughes, E. R. Plummer, A. S. Azzabi, M. G. Camboni, E. Verdi, A. Bernareggi, M. Zucchetti and A. M. Robnison, *Clin. Cancer Res.*, 1999, **5**, 3796.
- 84 S. Christina, C. Giuseppe, G. Luca, F. Peccatori, G. Gicomo, Z. Massimo, A. Rochi, M. Claudio, I. Paolo, B. Alberto, C. Garbriella and M. Silva, *Clin. Cancer Res.*, 1999, **5**, 3853.
- 85 A. Hegmans, J. Kasparkova, O. Vrana, L. R. Kelland, V. Brabec and N. P. Farrell, *J. Med. Chem.*, 2008, **51**, 2254.

## *Pt(II) based anticancer drugs*

---

- 86 A. Hoffmann and R. Van Eldik, *J. Chem. Soc. Dalton Trans.*, 2003, 2979.
- 87 (a) Y. Zhao, W. He, P. Shi J. Zhu, L. Qia, L. Lin and Z. Guo, *J. Chem. Soc., Dalton Trans.*, 2006, 2617; (b) X. Wang and Z. J Guo, *J. Chem. Soc., Dalton Trans.*, 2008, 1521.
- 88 G. Zhao, H. Lin, S. Zhu, H. Sun and Y. Chen, *Anti-Cancer Drug Des.*, 1998, **13**, 769.
- 89 (a) N. J. Wheate, C. Cullinane, L. K. Webster and J. G. Collins, *Anti-Cancer Drug Des.*, 2001, **16**, 91; (b) D. M. Fan, X. L. Yang, X. Y. Wang, J. F. Mao, J. Ding, L. P. Lin and Z. J. Guo, *JBIC, J. Biol. Inorg. Chem.*, 2007, **12**, 677.
- 90 (a) G. V. Kalayda, S. Komeda, K. Ekeda, T. Sato M. Chikuma and J. Reedijk., *J. Eur. Inorg. Chem.*, 2003, **46**, 4347; (b) S. Komeda, G. V. Kalayda, M. Lutz, A. L. Spek, M. Chikuma and J. Reedijk, *Inorg. Chem.*, 2003, **46**, 1210; (c) S. Komeda, G. V. Kalayda, M. Lutz, A. L. Spek, T. Sato, M. Chikuma and J. Reedijk., *J. Med. Chem.*, 2003, **46**, 1210.
- 91 (a) S. Komeda, H. Ohishi, H. Harikawa, K. Sakaguchi, A. L. Spek, M. Chikuma and J. Reedijk, *J. Chem. Soc., Dalton Trans.*, 1999, **39**, 2959; (b) S. Komeda, M. Lutz, A. L. Spek, M. Chikuma and J. Reedijk, *Inorg. Chem.*, 2000, **39**, 4230; (c) S Komeda, *PhD Thesis*, Leiden University, Netherlands; (d) S. Komeda, M. Lutz, A. L. Spek, Y. Yamanaka, T. Sato, M. Chikuma and J. Reedijk, *J. Am. Chem. Soc.*, 2002, **124**, 4738.
- 92 (a) L. Nguyen, J. Kolzeka and C. Bois, *Inorg. Chim. Acta.*, 1991, **190**, 217; (b) J. Kolzeka, E. Segal and C. Bois, *J. Inorg. Biochem.*, 1992, **47**, 67.
- 93 (a) J. A. Broomhead, L. M. Rendina and M. Sterns, *Inorg. Chem.*, 1991, 31, 1880; (b) A. Broomhead, L. M. Rendina and L. K. Webster, *J. Inorg. Biochem.*, 1993, **49**, 221; (c) J. A. Broomhead and M. J. Lynch, *J. Inorg. Chim. Acta.*, 1995, **240**, 13.
- 94 P. K Wu, M. Kharatishvill, Y. Qu and N. Farrell, *J. Inorg. Biochem.*, 1992, **643**, 9.
- 95 J. W. Williams, Y. Qu, H. Bulluss. E. Alvorado and N. Farrell, *Inorg. Chem.*, 2007, **46**, 5820.
- 96 D. Jaganyi, K. De Boer, J. Gertenbach, J. Perils, *Inte. J. Chem. Kinetics*, 2008, 809.
- 97 (a) N. Summa, J. Maigut, W. Schiessl, R. Puchta, N. van Eikema-Hommes and R. van Eldik, *Inorg. Chem.*, 2006, **45** (7), 2948

## Chapter Two

**A review on the theoretical aspects on the ligand substitution reactions of square-planar Pt(II) complexes focusing on the general role of the non-leaving ligand backbone.**

### **2.0 Theoretical aspects of ligand substitution reaction at a Pt(II)square-planar centre.**

#### **2.0.1 Introduction**

The rationale design of new platinum-based anticancer pharmaceuticals is undoubtedly underpinned on an intimate understanding of the kinetics underlying the interactions of the drugs with its target material (now widely believed to be genomic DNA) and other deactivating extracellular bio-competing materials *viz.*, plasma proteins (cysteine and metallomethionine residues) and enzymatic receptors and some intracellular sulphur bio-regulating molecules such as glutathione.<sup>1a,b</sup>

A comparison down the Group 10 triad elements, reveals that the majority of the complexes that are antitumour active are derived mainly from the platinum(II) metal ion.<sup>1c</sup> It is thought that the wide-span antitumour activity exhibited by the majority of the  $d^8$  Pt(II) metal complexes is derived from their moderate ligand exchange rates which are comparable to the rates of cell division processes in most biological tissues.<sup>1d</sup> Unlike their analogous complexes derived from Ni(II) or Pd(II) metal ions or from other  $d^8$  metal ions such Rd(I); Ir(I) or Ru(III), which are generally inactive<sup>2,1c</sup> and characterised by rapid ligand exchange kinetics, platinum(II) complexes are thermodynamically stable and display moderate to slow reactivity (moderate kinetic lability) in their ligand substitution reactions.<sup>1b,d</sup> Analogous complexes of the isoelectronic Au(III) ion are antitumour active but are generally thermodynamically unstable. As a result of this, research on platinum pharmaceuticals has placed the kinetics of the ligand exchange reactions on the centre stage in the rationale designing of current and future platinum drugs with improved therapeutic efficacy.<sup>1c</sup>

Central to this role, has been the careful control of the rate of ligand exchange at a Pt(II) metal centre (and hence the reactivity of the complexes) while maintaining the right geometry around the metal centre. This has been achieved through a systematic control of the

## Ligand substitution reactions of Pt(II) complexes

steric, electronic and/or hydrogen-bonding properties of the complexes. A good example to emerge out of this kind of approach is *cis*-aminodichloro(2-methylpyridine)platinum(II), also known as ZD0473, a drug candidate currently undergoing phase II clinical trials.<sup>3</sup> The drug can be conveniently administered by oral means and has an activity comparable to cisplatin. The structure of ZD0473 and its inactive 3-picoline isomeric analogue is shown in Figure 2.1.

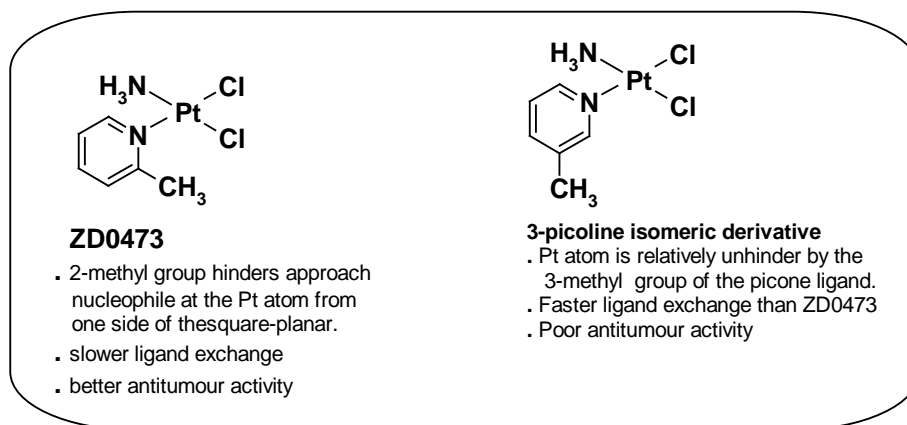


**Figure 2.1** Structures of ZD0473 and its unhindered and inactive 3-picoline isomeric analogue.

Its crystal data reveals that the pyridine ring is tilted by 102.7° with respect to the PtN<sub>2</sub>Cl<sub>2</sub> square-plane, placing the *ortho*-methyl group directly over the platinum coordination plane.<sup>4</sup> This introduces some steric hindrance to any axial approach by oncoming nucleophiles on one side of its square-coordination plane. However, this retardation in the rate of its ligand substitution reactions is considered essential for slowing down other *in vivo* reactions in which competing strong sulphur bio-nucleophiles such as glutathione and sulphur containing proteins would rapidly sequester the drug before it reaches its destination, a factor closely linked to its ability to circumvent cisplatin resistance. Indeed, the rates of hydrolysis of ZD0473 were found to be lower than those of cisplatin and its unhindered and analogous derivative, containing a 3-methylpyridyl carrier ligand.<sup>4</sup> Its reactivity towards thiourea, pyridine, methionine and GMP nucleophiles was found to be less than cisplatin and its analogous derivative containing the unsubstituted pyridine carrier ligand.<sup>5a</sup> It exhibits remarkably low resistance factors than cisplatin in several pairs of cisplatin-sensitive and resistance cell lines.<sup>5b</sup>

Apart from controlling the antitumour activity, the kinetics of the ligand exchange reactions of platinum complexes is also important in controlling other side-reactions that mediate toxicity.<sup>1</sup> Data from literature regarding the structure-activity relationships (reported in Chapter One, section 1.0.4), reiterates that the kinetic data initially gathered on the ligand

# Ligand substitution reactions of Pt(II) complexes

exchange reactions of cisplatin was momentous in the rational design of the subsequent generations of mononuclear platinum drugs showing reduced side effects, smaller cisplatin cross-resistance factors or in some cases providing complementary roles to cisplatin. Notable examples include carboplatin, nedaplatin and oxaliplatin.<sup>6</sup>

Similar approaches have been pursued in the rationale design of multinuclear complexes. For example, in the cationic multinuclear Pt(II) complexes such as BBR3464, hydrogen bonding and electrostatic interactions have been exploited for the indirect kinetic control of the ligand exchange reactions between genomic DNA and the reactive centres.<sup>7</sup> The chemical structure of BBR3464 is shown in Figure 2.2.

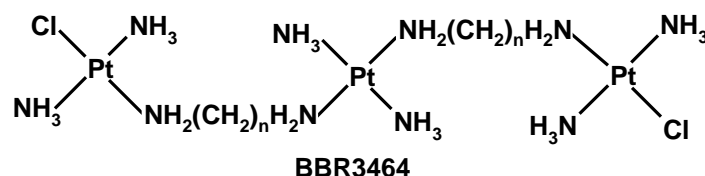


**Figure 2.2** Chemical structure of BBR3464<sup>7</sup>

Since the antitumour activity of platinum drugs is closely related to their substitutional reactivity, a brief summary of the relevant theoretical aspects covering the possible mechanisms of substitution in  $d^8$  metal complexes, the modern techniques for reliable measurement of the kinetic data for the ligand substitution reactions will be undertaken. This will be followed by a focused but comprehensive review on the general role of the non-leaving ligand backbone around Pt(II) metal centres, focussing on some selected examples on how an accurate control of reactivity of the metal complexes has been exploited for rational design of targeted drug candidates of improved efficacy.

## **2.0.2 Chemical bonding in square-planar $d^8$ Pt(II) metal complexes.**

Platinum is a Group 10 metal element which exists mainly in the 0, +1, +2, and +4 oxidation states spawning a diverse range of organometallic and coordination compounds.<sup>8</sup> The majority of its compounds are of square-planar and octahedral coordinative geometries. These complexes display excellent thermodynamic stability and moderate ligand substitution kinetics. This makes platinum and its compounds valuable in many industrial applications. Apart from platinum's widespread traditional use in areas such as alloying, catalysis of important organometallic transformations, its application window has been widened to other areas such as photoluminescence and chemotherapy. Its use in chemotherapy in particular was stimulated

## Ligand substitution reactions of Pt(II) complexes

by the serendipitous discovery of *cis*-diaminedichloroplatinum(II), also known as cisplatin by Rosenberg in the late 1960s.<sup>8</sup>

The  $d^8$  Pt(II) ion forms stable mononuclear and multinuclear coordinative compounds with anionic as well as neutral donor ligands. The non-labile ligand can be monodentate or multidentate. Its square-planar compounds therefore display one or more of the following characteristics: a higher propensity to undergo nucleophilic attack at the vacant  $p_z$  orbital {due to its coordinative unsaturation, which leads to formation of stable  $d^{10}$  Pt(0) complexes (in oxidative addition reactions) as well as undergoing ligand substitution reactions which are associatively-activated in the majority of cases}; a greater tendency to undergo reductive elimination reactions wherein electrons are lost from the filled  $d_z^2$  orbital in which stable  $d^6$  Pt(IV) complexes are formed) as well as the formation of strong  $\pi$ - $\sigma$ -bonds especially with softer ligands such as those containing sulphur and phosphorous donor atoms.

Although most of the known complexes of platinum are square-planar or octahedral, the former group of compounds form the majority and are more prominent in photophysical as well as therapeutic applications. At the central  $d^8$  Pt(II) ion in a square-planar complex, there are nine valence atomic orbitals available for coordinative bonding, *viz.*, the five  $5d$ , a  $6s$  and three  $6p$  orbitals.<sup>9</sup> Of these atomic orbitals, only the  $6s$ ,  $5d_{x^2-y^2}$ ,  $6p_x$  and  $6p_y$  are of the right symmetry for  $\sigma$ -overlap with the atomic orbitals of ligands approaching from *trans* directions. The  $5d_z^2$  atomic orbital is orthogonal to the other  $\sigma$ -bonding atomic orbitals and its capacity to participate in an in-plane  $\sigma$ -overlap is insignificant, the *trans*-directing hybrid atomic orbitals formed from the linear combination of these four atomic orbitals at the metal ion ( $dsp^2$ ) have predominantly an  $s$  character.

On the one hand, the  $d_{xy}$ ,  $d_{xz}$ ,  $d_{yz}$  and  $p_z$  orbitals are of the right symmetry for forming  $\pi$ -bonds with orbitals of equivalent symmetry on the ligands. If the overlap between the  $d_{xy}$  orbital and the  $\pi$ -orbitals of appropriate energy of the ligands to form a  $\pi$ -molecular orbital is considered to be in-plane, then the  $d_{xz}$  and  $d_{yz}$  orbitals can each interact with two  $\pi$ -ligand orbitals on the ligands approaching from directions that are mutually orthogonal. The 16 electrons are accommodated in these nine orbitals thus leaving a vacant  $p_z$  orbital for interactions with axially approaching ligands (nucleophiles) in a nucleophilic substitution reaction.

As shown in the molecular orbital (MO) diagram<sup>9</sup> of  $[\text{PtCl}_4]^{2-}$  (Figure 2.3), the most stable molecular orbitals are the  $\sigma$ -bonding type, resulting from the overlap of the hybrid

## Ligand substitution reactions of Pt(II) complexes

atomic orbitals derived from a linear combination of the  $d_{x^2-y^2}$ ,  $p_x$ ,  $p_y$  and  $d_z^2$  orbitals of the Pt(II) metal ion and appropriate  $\sigma$ -type orbitals of the ligands. Next on the energy scale are the  $\pi$ -bonding molecular orbitals, which are derived from a sideways overlap of the  $d_{xy}$ ,  $d_{xz}$ ,  $d_{yz}$ ,  $p_x$  and  $p_z$  metal atomic orbitals of the Pt(II) metal ion and the atomic orbitals of appropriate symmetry on the ligands. The anti-bonding molecular orbitals are represented next and are a result of the combination of the metal's  $dsp^2$  hybrid orbitals with  $\sigma$ ,  $\pi$  ligand orbitals in an anti fashion. The MOs that are used for the coordinative bonding  $[\text{PtCl}_4]^{2-}$  and their relative energies are presented in Figure 2.3.

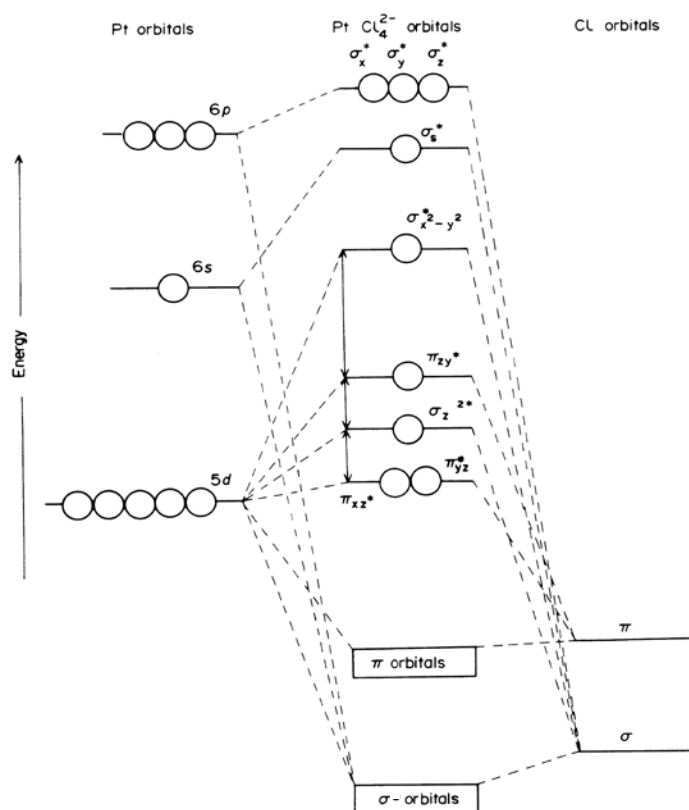


**Figure 2.3** Molecular orbital representation of the bonding in  $[\text{PtCl}_4]^{2-}$ , illustrating the relative energies of the molecular orbitals.<sup>9</sup>

From the above MO diagram of  $[\text{PtCl}_4]^{2-}$ , one can reckon that any nucleophilic substitution reactions involving the displacement of any of the coordinated ligand at the Pt metal centre by an incoming ligand will proceed preferably via an associatively activated route because of the availability of an axially low-lying energy and vacant  $p_z$  orbital on the metal centre which can receive electron density from on coming nucleophiles.<sup>8,10</sup> If the ligand exchange process is a simple substitution process, the reaction proceed to form product with no

# Ligand substitution reactions of Pt(II) complexes

overall change in the oxidation state of the metal centre. However, since bonds are made and broken along the reaction coordinate in a concerted manner, the coordination number of the metal ion is temporally changed.<sup>8</sup> The temporal change in the coordination number reflects the overall effect of several synchronized changes occurring within the electronic distributions along the reaction coordinates of the activated complex caused by the concerted bond making (with the incoming nucleophiles) and breaking processes (with the leaving group) at the central metal atom. If the lifetimes of the species formed along the reaction coordinate is fairly long, the existence of the intermediate species can be confirmed by indirect spectroscopic methods.

## 2.0.3 Mechanism labels at a square-planar geometry.

According to Langford and Gray,<sup>11</sup> ligand substitution reaction mechanisms of transition metal complexes comprise the following major categories namely: (i) Associative (**A**), (ii) Dissociative (**D**) and (iii) Interchange (**I**). The potential energies characterizing each of the categories are presented in Figure 2.4.

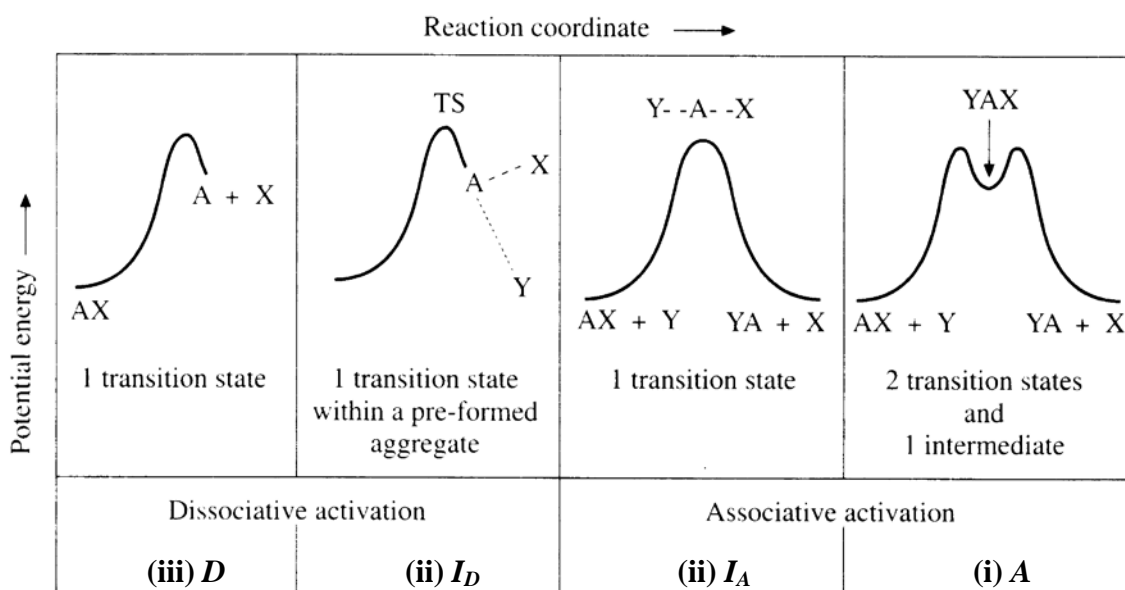


**Figure 2.4** An illustration of the potential energy profiles for the different mechanisms of substitution at a square-planar metal centre as proposed by Langford-Gray.<sup>9</sup>

The **A** mechanism proceeds via two transition states, involving an intermediate whose coordination number has increased by one, while a **D** mechanism proceeds via one transition state leading to an intermediate whose coordination number has decreased by one. In both mechanisms, the intermediate species should survive several molecular collisions before forming the final product. In this classification, the existence of intermediate(s) can be inferred

## Ligand substitution reactions of Pt(II) complexes

by methods such as the theoretical quantum chemical calculations or in rare occasions by experimental evidence. The presence of minimum stationary points along the potential energy surface (PES) as depicted in Figure 2.4 and further elaborated in Figure 2.5 signifies the presence of finite intermediates along the reaction coordinate.

The most compelling pieces of experimental evidence for the existence of such intermediate species has come from structural determinations by X-rays diffraction analysis of some serendipitously isolated intermediates with well defined penta-valent trigonal bipyramid coordinate geometries.<sup>8</sup> In such instances, the detected structural changes offer direct evidence that the intermediate is formed from the reactants in an associatively activated fashion, from where the leaving group is eventually substituted to form the final product in a relatively facile manner. On the potential energy surface (PES), the intermediate spots as a minimum turning point between two energy maxima, defining the two transition states. The lifetime of the intermediate is gauged by the depth of the minimum point. The potential energies at the two maxima, *i.e.*, one corresponding to the bond making (early transition state) and another to the bond breaking process (late transition state) can be symmetric or asymmetric (Figure 2.5). This depends on the relative energies for the synchronized processes leading to the formation and breaking of bonds in the activated complex.

If no stationary points can be detected on the PES then an interchange (**I**) mechanism is assumed to operate. In this intermediary mechanism label, formation of the bond between the entering ligand and the metal centre is in concert with weakening of the bond to the coordinated leaving group. The defining characteristics of each mechanism label assuming a square-planar geometry is summarized below.

- (i) Associative (**A**): In a limiting associative (**A**) mechanism, a nucleophile (*Y*) or a solvent molecule (*S*) enter the coordination sphere of the metal complex  $L_3MX$ , where *X* is a leaving group and *L* is a carrier ligand leading to intermediates,  $L_3MXY$  or  $L_3MXS$ , with an increased coordination number from which the leaving group, *X*, is lost in a subsequent step (Figure 3.5). In the early transition state, the bond between the metal centre and the incoming ligand, *Y*, is largely established whilst the bond between the metal centre and the leaving ligand is essentially weakened. Thus, the rate determining step is the making of bond between the incoming ligand, *Y*, and the metal complex. In a non-coordinating medium, the observed rate of approach to equilibrium in the presence of an excess concentration of *Y* is therefore dependent on the nature of the nucleophile, *Y*.<sup>11</sup> Thus; the rate of

# Ligand substitution reactions of Pt(II) complexes

substitution depends strongly on the nature of the incoming ligand, since it participates in the early transition state. The details of the possible potential energy profile in an associative mechanistic pathway are shown in Figure 2.5.

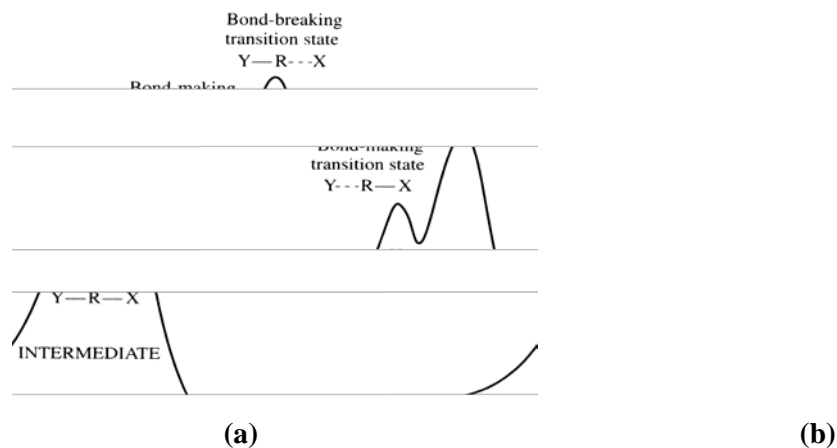


**Figure 2.5** Potential energy profiles<sup>9</sup> for the substitution process which is associative, **A**. Case (a) formation of the final product from the activated complex depends more on the rate at which the bond between the metal centre and the leaving group is broken. (b) Formation of the final product from the activated complex depends more on the rate at which a new bond between the incoming group and the metal centre is formed.

- (ii) **Dissociative (D)**: This is a substitutional pathway that involves an intermediate of decreased coordination number. In a dissociatively activated mechanism, reactants pass through a single transition state to form a 14-electron (T-shaped) intermediate that must be able to survive several molecular collisions before reacting with *Y* to form the product. In the transition state from which the intermediate forms, the bond between the metal ion and the leaving group is virtually broken while that of the incoming ligand has not been formed. Thus, the intermediate does not have any residual influence from the departed ligand, on its ability to discriminate other ligands within its secondary shell assemblage. The rate of approach to equilibrium in the presence of an excess concentration of *Y* is therefore only dependent on the nature of the leaving group, *X*, and independent of nature of the incoming *Y* nucleophiles.<sup>11</sup> Thus, the rate-determining step is the breaking of the bond between the metal centre and the leaving group.
- (iii) **Interchange (I)**: Between the limiting **A** and **D** mechanisms there exists a continuum of mechanisms characterized by the existence of a single activated complex in which the entering and the leaving ligands make various contributions to the

## Ligand substitution reactions of Pt(II) complexes

energetics of the transition state.<sup>11</sup> The mechanisms range from the associative interchange,  $I_a$ , a mechanistic pathway in which bond making is more prominent within the structure of the activated complex, through an interchange,  $I$ , where both bond making and breaking are in concert through to the dissociative interchange,  $I_d$ , where bond breaking is more dominant. No discernible intermediates are presumed within the structure of the activated complex for an interchange mechanism, and their general mechanistic features are similar to a typical  $S_N2$  reaction on a carbon atom.<sup>12</sup>

This classification system is however characterized by several challenges. Firstly, diagnosis of mechanistic pathways is based solely on qualitative criteria, *i.e.*, whether the substitutional reaction is sensitivity or insensitivity to the nature of the entering ligand. Secondly, the detection of intermediates is a very demanding task. Further, whenever they exist, the intermediates are very short lived and present in extremely low concentrations. In most cases, evidence for their existence requires use of indirect methods.

Merbach<sup>13</sup> proposed a more refined classification of mechanisms for ligand substitution reactions. The assignment of the mechanism labels was shifted to other measurable parameters that depended on the mode of activation. To date, the parameters that are used for assigning mechanisms in ligand substitution reaction are determined from experiments in which the observed rates of reactions are measured as either the pressure or temperature of a reacting mixture is varied. This is done in accordance to the principles based on the Van't Hoff equation and the Transition-state theory, respectively. The latter theory was developed in the late 1930s by Eyring, Evans and Polanyi.<sup>14</sup> In both approaches, the mode of activation of the reaction is assumed to be thermal.

From the results of the dependence of rate constants on temperature and pressure changes, one can estimate the activation parameters, *viz.*, the activation enthalpy ( $\Delta H^\ddagger$ ), activation entropy ( $\Delta S^\ddagger$ ) and the activation volume ( $\Delta V^\ddagger$ ), respectively.<sup>15</sup> The value of  $\Delta H^\ddagger$  is a good estimate of the energy barrier necessary to activate reactants to the transition state. The degree of disorder in the microscopic states of the transition state and its compactness relative to the reactants can be inferred from the  $\Delta S^\ddagger$  and  $\Delta V^\ddagger$  values, respectively. The relative magnitudes of these activation parameters are useful supplements in the assignment of mechanism labels.<sup>16</sup> If the values of  $\Delta V^\ddagger$  and  $\Delta S^\ddagger$  are both negative, and are accompanied by low enthalpies of activation values ( $\Delta H^\ddagger$ ), then the reaction is said to be associatively

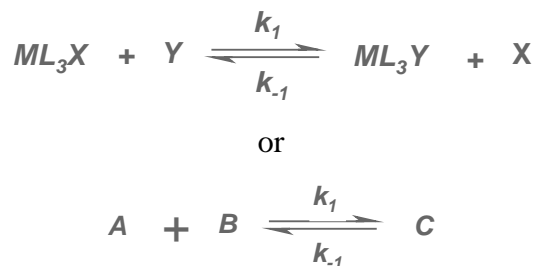
# Ligand substitution reactions of Pt(II) complexes

activated.<sup>12</sup> On the other hand, if the values of  $\Delta V^\ddagger$  and  $\Delta S^\ddagger$  are both positive (and large) and accompanied by large and positive enthalpy of activation values ( $\Delta H^\ddagger$ ), then the reaction is said to be dissociatively activated.<sup>15</sup> For an interchange mechanism, *I*, the values of activation parameters are relatively small and closer to zero. The details of the theories and relevant experimental procedures which are followed in order to measure these activation parameters in the laboratory will be given in Section 2.1.2 of this chapter.

## 2.1. Measurements of kinetic parameters for ligand substitution reactions.

### 2.1.1 Measurement of the rate constants.

Because of the bimolecular nature of all associatively-activated substitution reactions at a square-planar geometry, a common course of their reactions can be represented by either of the equations given below. In the latter equation, *A* represents the metal complex,  $ML_3X$ , while *B* represents the nucleophile, *Y*. Often, in ligand substitution reactions, this type of reaction does not reach completion, but instead attain an equilibrium position. Thus, this reaction scheme can be depicted as shown below by,



The forward elementary reaction step is second-order, while the reverse reaction step is first-order. Thus, the kinetics of the reaction assumes mixed order behaviour. Because of the complexity of the reaction, the forward ligand substitution process can be studied conveniently under pseudo first-order conditions. Practically, this is met by providing an excess-fold in the initial concentration of one of the reactants, e.g. *B* (the nucleophile) over that of *A* (metal complex), such that  $[B]_0 \gg [A]_0$ .

The overall rate of this reaction can be expressed as,

$$\frac{-d[A]}{dt} = \frac{-d[B]}{dt} = \frac{d[C]}{dt} = k_1[A]_t[B]_t - k_{-1}[C]_t \quad \mathbf{I}$$

Applying the mass balance on the reactants,

$$[A]_t = [A]_0 - [C]_t$$

## Ligand substitution reactions of Pt(II) complexes

$$[B]_t = [B]_0 - [C]_t,$$

thus, at equilibrium,  $[A]_{eq} = [A]_t - [C]_{eq}$  **2a**

$$[B]_{eq} = [B]_0 - [C]_{eq}. \quad \mathbf{2b}$$

Since at equilibrium, the net rate of reaction equals zero, equation (eqn.) **1** can be

written as: 
$$\frac{-d[A]}{dt} = k_1[A]_{eq}[B]_{eq} - k_{-1}[C]_{eq} = 0.$$

$$\Rightarrow k_1[A]_{eq}[B]_{eq} = k_{-1}[C]_{eq}. \quad \mathbf{3}$$

Substituting for an expression of  $[C]_{eq}$  (as written in eqn. **2a**) in eqn. **3**,

$$k_1[A]_{eq}[B]_{eq} = k_{-1}\{[A]_0 - [A]_{eq}\}$$

$$\Rightarrow k_{-1}[A]_0 = k_1[A]_{eq}[B]_{eq} + k_{-1}\{[A]_{eq}\}. \quad \mathbf{4}$$

Substituting  $[C]_t = [A]_t - [A]_0$  in eqn. **1** and replacing the term  $k_{-1}[A]_0$  as given in eqn. **4**, simplifies eqn. **1** to,

$$\frac{-d[A]}{dt} = k_1[A]_t[B]_t - k_1[A]_{eq}[B]_{eq} - k_{-1}[A]_{eq} - k_{-1}[A]_t. \quad \mathbf{1a}$$

Noting that  $[B]_0 \gg [A]_0$  and substituting  $[B]_{eq}$  and  $[B]_t$  as expressed in eqn. **2b** and its corresponding mass balance equation, respectively, and approximating that  $k_1[A]_t[A]_0 \approx k_1[A]_{eq}[B]_t$ ;  $k_1[A]_t^2 \approx k_1[A]_{eq}^2$  simplifies eqn. **1a** to:

$$\frac{-d[A]}{dt} = k_1[A]_t[B]_0 - k_1[A]_{eq}[B]_0 - k_{-1}[A]_{eq} - k_{-1}[A]_t,$$

$$= \{k_1[B]_0 + k_{-1}\}([B]_{eq} - k_{-1}[B]_t). \quad \mathbf{1b}$$

Separating variables and integrating eqn. **1b** gives:

$$\int_{[A]_0}^{[A]_t} \frac{d[A]}{([A]_t - [A]_{eq})} = -\{k_{-1} + k_1[B]_0\} \int_0^t dt,$$

which results in:  $\ln \left( \frac{[A]_t - [A]_{eq}}{[A]_0 - [A]_{eq}} \right) = -\{k_{-1} + k_1[B]_0\}t$  **1c**

$$= -k_{obs}.t, \text{ where,}$$

$$\text{where, } k_{obs} = (k_{-1} + k_1[B]_0).$$

# Ligand substitution reactions of Pt(II) complexes

or

$$k_{obs} = k_{-1} + k_1 [nu] \quad 5$$

From eqn. 5, a plot of  $k_{obs}$  versus the initial concentration of the nucleophile,  $[B]_0$ , is linear with a slope equal to the second-order rate constant,  $k_1$ , and an intercept value equal to the first-order rate constant,  $k_{-1}$ . Typical stacked plots are shown in Figure 2.6.

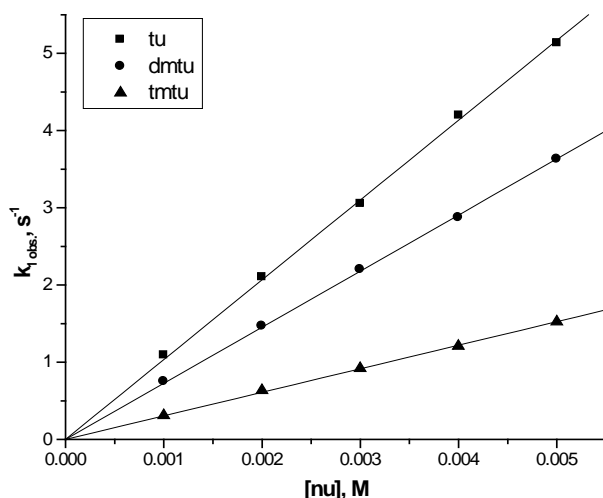


**Figure 2.6** Typical plots of the pseudo first-order rate constants,  $k_{obs}$  versus the concentration of the incoming nucleophiles (three sulphur donor nucleophiles) for the substitution reaction of a mononuclear Pt(II) complex at 298 K in a non-coordinating aqueous solvent.

The second-order rate constant,  $k_1$ , represents the rate of the direct nucleophilic attack on the metal centre by the entering nucleophile ( $B$ ). Most of the associatively-activated reactions follow a course of reaction represented by the reaction scheme shown above and therefore exhibit a two-term rate law as expressed in eqn. 5.

The two possible mechanistic pathways for the substitution at a Pt(II) metal centre as implied by the two-term rate law is summarized in Figure 2.7. The  $k_{-1}$  term usually signifies the existence of a back reaction. In the absence of a parallel elementary step involving the solvent attack, the ratio of ( $k_1/k_{-1}$ ) can be considered to be a good estimate of the thermodynamic equilibrium constant,  $K$ , for the reversible reaction involving elementary steps of mixed molecularity. However, as shown in Figure 2.7, the  $k_{-1}$  term can also be an indication of the existence of an alternative and parallel solvolysis pathway involving a direct attack of the metal centre by the nucleophile (as measured by the  $k_1$ ). This happens when the solvent medium actively participates in the substitutional process. In such cases, the  $k_{-1}$  pathway involves two sequential elementary steps, viz., the slow and rate-determining step involving the

## Ligand substitution reactions of Pt(II) complexes

formation of the solvento-coordinated intermediate followed by its rapid displacement by the incoming nucleophiles. This solvolysis pathway follows first-order kinetics and is therefore independent

of the concentration of nucleophile (B).

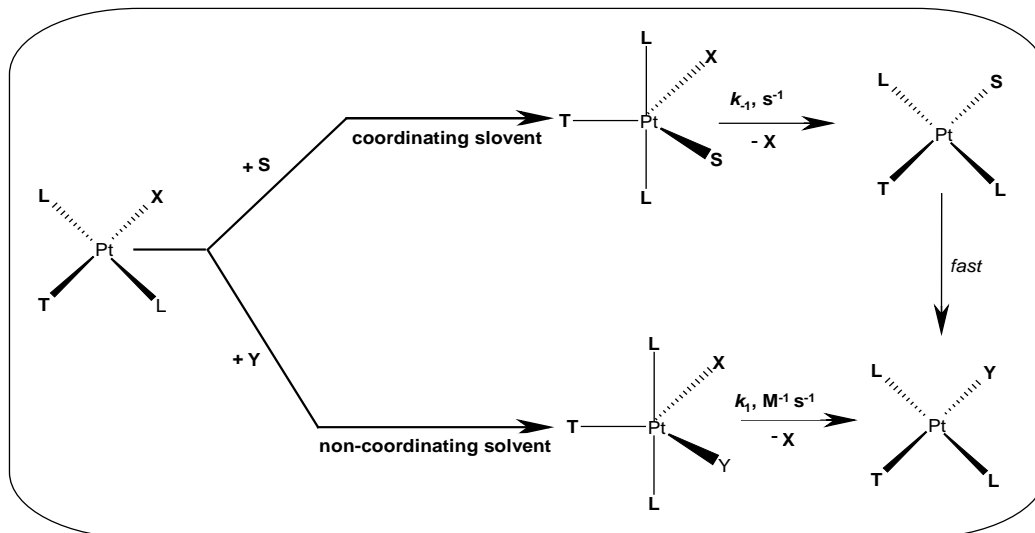


**Figure 2.7** A depiction of dual reaction pathway for an associatively-activated substitution reaction at a Pt(II) metal centre.<sup>8</sup>

As depicted in Figure 2.7, the second-order rate constant,  $k_1$ , for the bimolecular substitution of the leaving group at the metal is dependent on the concentration of the incoming nucleophile. Thus, under pseudo first-order conditions and in cases where non-coordinating solvents are used such that the parallel solvolysis pathway is assumed to be non-existent, the value of  $k_1$  can be calculated directly from eqn. 5. This is done by measuring the dependence

# Ligand substitution reactions of Pt(II) complexes

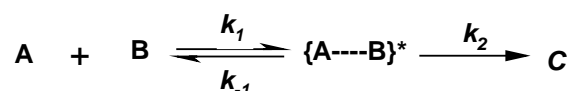
of observed (pseudo) first-order rate constants,  $k_{obs}$ , on the initial concentration of nucleophile  $[B]_0$  which is normally provided in at least ten-fold excess of the metal complex  $[A]$  in a 1:1 complex formation reaction. The value of the second-order rate constant is calculated from the slope of a plot exemplified in Figure 2.6 and its magnitude is a direct measure of the reactivity of the complex towards the nucleophile. If a non-zero  $y$ -intercept plot is obtained from this concentration dependence study (Figure 2.6), then a back reaction in which the nucleophile,  $B$ , is being substituted from the metal centre or a parallel solvolysis pathway can be assumed. Thus, a plot which passes through zero signifies that the forward reaction is irreversible.

## 2.1.2 Measurement of the activation parameters.

### 2.1.2.1 Measurement of enthalpy of activation ( $\Delta H^\ddagger$ ) and entropy of activation ( $\Delta S^\ddagger$ ).

Apart from measuring the values of the rate constants of the reactions, there is need to unravel the mechanistic pathway underlying ligand substitution reactions. One way to achieve this is to experimentally test how the rate of reaction depends on concentration (testing a derived rate-law) using a knowledge base constructed from a proposed theoretical model describing fully the mechanistic pathway underlying the reaction. Another approach and one frequently adopted to supplement data from the former approach,<sup>12</sup> is to measure the activation parameters for the reaction. For inorganic reaction mechanisms, the relative magnitudes of these parameters are used for assigning mechanism labels. As already pointed out, their measurements are carried out as stipulated in the Transition State theory<sup>14</sup> and the Van't Hoff equation. Practically, the activation parameters are determined from experiments in which the dependence of the observed (pseudo) first-order rate constants is measured as the temperature or pressure of the reaction mixture is systematically varied. The activation parameters together with the rate law (an experimentally verified expression on how the rate constant fit in a proposed theoretical kinetic model) obtained thereof constitute a complete description of the kinetic behaviour of that particular reaction system.

According to the Transition State Theory, a reaction between  $A$  (the metal complex) and  $B$  (the nucleophile) attains a pre-equilibrium<sup>17</sup> with its activated complex  $\{A\cdots B\}^*$ , before it converts to  $C$  (the substituted product) and the mechanism can be written as:



Thus, the rate of reaction can be written as:

# Ligand substitution reactions of Pt(II) complexes

$$-\frac{d[A]}{dt} = k_2[A\dots B]^* \quad 6$$

From the pre-equilibrium,  $K^\ddagger = \frac{[A\dots B]_{eq}^*}{[A]_{eq}[B]_{eq}}$ ,

$$\Rightarrow [A\dots B]^* = [A]_{eq}[B]_{eq} K^\ddagger \quad 7$$

Substituting for  $[A\dots B]^*$  (eqn 7) in eqn. 6 thus,

$$-\frac{d[A]}{dt} = \frac{k_b T}{h} K^\ddagger [A]_{eq} [B]_{eq} \quad 6a$$

where  $k_b$  = Boltzmann's constant ( $1.38 \times 10^{-23} \text{ J K}^{-1}$ )  
 $h$  = Planck's constant ( $6.626 \times 10^{-34} \text{ J s}^{-1}$ ).

$$-\frac{d[A]}{dt} \equiv k_2[A]_t[B]_t \quad 6b$$

Comparing eqns. 6a and 6b,

$$k_2 = \frac{k_b T}{h} K^\ddagger \quad 8$$

But  $K^\ddagger$  is related to the free energy of activation,  $\Delta G^\ddagger$  by

$$RT \ln K^\ddagger = \Delta G^\ddagger = \Delta H^\ddagger - T\Delta S^\ddagger$$

$$\Rightarrow K^\ddagger = e^{-\left(\frac{\Delta G^\ddagger}{RT}\right)}$$

$$K^\ddagger = e^{\left(\frac{\Delta S^\ddagger}{RT}\right)} e^{-\left(\frac{\Delta H^\ddagger}{RT}\right)} \quad 9$$

Substituting for  $K^\ddagger$  (as expressed in eqn. 4) in eqn. 3 yields:

$$k_2 = \frac{k_b T}{h} e^{-\left(\frac{\Delta G^\ddagger}{RT}\right)} = \frac{k_b T}{h} e^{-\left(\frac{\Delta H^\ddagger}{RT}\right)} e^{\left(\frac{\Delta S^\ddagger}{RT}\right)} \quad 8a$$

Rearranging eqn. 3a and taking natural logarithms of both sides,

$$\ln\left(\frac{k_2}{T}\right) = -\frac{\Delta H^\ddagger}{RT} + \left(23.8 + \frac{\Delta S^\ddagger}{R}\right) \quad 10$$

From eqn. 10, a plot of  $\ln\left(\frac{k_2}{T}\right)$  versus  $\frac{1}{T}$  gives a slope and y-intercept equal to  $-\frac{\Delta H^\ddagger}{R}$  and  $\left(23.8 + \frac{\Delta S^\ddagger}{R}\right)$  from which the enthalpy of activation ( $\Delta H^\ddagger$ ) and the entropy of activation ( $\Delta S^\ddagger$ ) can be calculated, respectively. This plot is known as the Eyring plot.<sup>14,17</sup> The Eyring plot is a representation of how the measured rate constant depends on the temperature of a reaction system. The relative magnitudes of the two activation parameters determined from the plot are

## Ligand substitution reactions of Pt(II) complexes

useful supplementary criteria through which ligand substitution reaction mechanisms may be assigned. In an associatively-activated substitution reaction, the relative magnitude of the  $\Delta H^\ddagger$  values tend to be small while their values of  $\Delta S^\ddagger$  are usually negative when compared to those for dissociatively activated reactions whose values of  $\Delta H^\ddagger$  and  $\Delta S^\ddagger$  are usually large and positive.<sup>8</sup> However, in cases where the assignment is made solely on the basis of these activation parameters then, kinetic data from several different nucleophiles may be necessary before reliable conclusions can be drawn for that substitution reaction. While the values of  $\Delta H^\ddagger$  determined from the slope are reasonably more reliable, large relative errors are endemic to the determination of  $\Delta S^\ddagger$  values, as the data is calculated from values extrapolated to infinite temperatures.<sup>15,16</sup>

A more powerful and often a more reliable parameter in assigning mechanism is the activation volume,  $\Delta V^\ddagger$ . It can be determined from a series of experiments in which one measures the observed rate constants,  $k_{obs}$ , as the pressure which is applied on a reaction mixture is varied.<sup>15</sup> However, for meaningful diagnosis, it is still crucial to include the values of the two activation parameters, *i.e.*,  $\Delta V^\ddagger$  and  $\Delta S^\ddagger$ , for the purposes of making conclusive mechanism assignment.

### 2.1.2.2 Measurement of the activation volume ( $\Delta V^\ddagger$ )

The activation volume for a reaction is determined from dependence of the logarithm of the observed rate constants on the pressure applied to the reacting system.<sup>15</sup> The principle on which its measurement in the laboratory is stemmed will be outlined below. From the thermodynamic equation,

$$dG = VdP - SdT, \quad 11$$

the partial derivative of the change in the free energy of a reaction,  $\Delta G$ , with respect to the applied pressure for a reaction carried under isothermal conditions, can be written as,

$$\left(\frac{\partial(\Delta G)}{\partial P}\right)_T = \Delta V^0, \quad 12$$

where  $\Delta V^0$  is the difference in the partial molar volumes between the products and the reactants.

Since  $\Delta G = -RT \ln K$ , then *eqn. 12* can be expressed as

$$\Rightarrow \left(\frac{\partial(-RT \ln K)}{\partial P}\right)_T = \Delta V^0 \quad 12a$$

## Ligand substitution reactions of Pt(II) complexes

$$\Rightarrow \left( \frac{\partial(\ln K)}{\partial P} \right)_T^0 = -\frac{\Delta V^0}{RT} \quad 12b$$

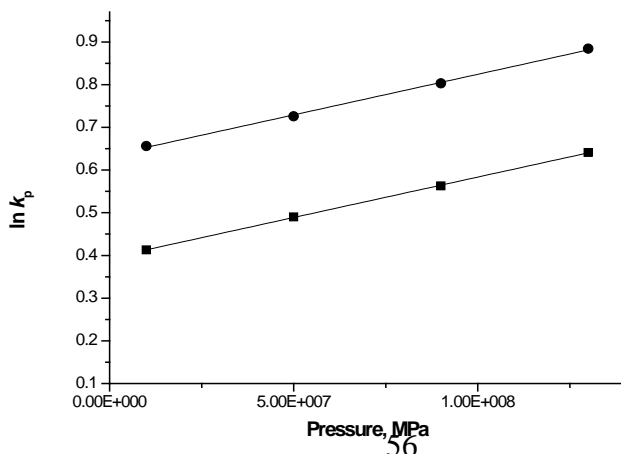
$$\Rightarrow \left( \frac{\partial \left( \ln \left( \frac{k_1}{k_{-1}} \right) \right)}{\partial P} \right)_T^0 = -\frac{\Delta V^0}{RT} \quad 12c$$

$$\Rightarrow \frac{\partial(\ln k_1)}{\partial P} = \left( -\frac{\Delta V^0}{RT} + \frac{\partial \ln k_{-1}}{\partial P} \right) = -\frac{\Delta V^\ddagger}{RT} \quad 12d$$

where,  $\Delta V^\ddagger$  is the volume of activation and is equal to the difference in the partial molar volumes between the transition state and the reactants and is considered independent of the applied pressure. Taking integrals of both sides of eqn. 12d within an applied pressure range of  $P = 0$  to  $P = P$  yields,

$$\ln k_1 = \ln(k_1)_0 - \frac{\Delta V^\ddagger}{RT} P \quad 13$$

Thus from eqn. 13, a plot of  $\ln k_1$  against the applied pressure is linear with a slope equal to  $-\frac{\Delta V^\ddagger}{RT}$ , from which the activation volume,  $\Delta V^\ddagger$ , can be directly evaluated. A typical plot is depicted in Figure 2.8. The error associated with its determination is relatively small. Because the activation volumes for ligand substitution reactions are intrinsically small (presenting small coefficients in eqn. 13), high applied pressures are needed (several MPa) to have an appreciable effect on the rate of reaction. Fortunately, equipment for monitoring reactions in solution spectrophotometrically and with capabilities of maintaining an applied pressure of up to 200 MPa on the reaction compartment have been developed for accurate determination of activation volumes ( $\Delta V^\ddagger$ ) data.<sup>18</sup>



# Ligand substitution reactions of Pt(II) complexes

**Figure 2.8** Dependence of  $\ln k_{\text{obs}}$  (repeated twice) on pressure for the reaction mixture between a Pt(II) complex (**Oct**) and a thiourea nucleophile recorded at 320 nm for the displacement of the aqua ligands.

The values of the measured activation volumes,  $\Delta V^\ddagger$ , comprise two components, *viz.*, the intrinsic activation volumes ( $\Delta V_{\text{int.}}^\ddagger$ ) and the electrostriction activation volumes ( $\Delta V_{\text{el.}}^\ddagger$ ).<sup>19</sup> The latter is founded in the restrictions effected on the activated complex by the reigning charge distributions of the activated complex and is usually small. In practice,  $\Delta V^\ddagger \approx \Delta V_{\text{int.}}^\ddagger$ . The  $V_{\text{el.}}^\ddagger$  component becomes important only in reactions proceeding with a net change in the overall charge between reactants and products. Thus, for reactions that proceed with no change in the overall charge, the volume of activation data can provide a more reliable indicator of the type of mechanism followed by the reaction even in the absence of a full knowledge of the rate law.

On the basis of the pressure dependence studies alone, an associatively activated process is indicated by an acceleration of the rate of reaction when the pressure applied on the reacting mixture is increased.<sup>15</sup> Thus, an increase in the pressure applied to a reaction system causes the observed rate constant ( $k_{\text{obs}}$ ) to increase such that  $\Delta V^\ddagger$  is negative in *eqn. 13*, implying a mechanistic pathway proceeding via a contracted transition state involving a greater degree of bond making. The negative volume, thus corresponds to the decrease in volume effectively equal to the partial molar volume of the entering ligand as it is lost from the inner-shell ligand assemblage on forming the penta-coordinated transition state.<sup>18</sup> Conversely, a dissociatively-activated process is indicated when an increase in the applied pressure causes a deceleration in the observed rate of reaction such that  $\Delta V^\ddagger$  is positive. This positive volume corresponds to the liberation of the leaving group into the inner-shell ligand assemblage leading to the formation of the tri-coordinated transition state. This leads to a more expanded transition state resulting from a dominant bond breaking process.

## **2.1.3 Instrumentation for studying the kinetics of ligand substitution reactions of Pt(II) complexes.**

### *2.1.3.1 General experimental considerations for chemical kinetics of substitution reactions.*

## *Ligand substitution reactions of Pt(II) complexes*

An essential stage of all chemical kinetics experiments involves an accurate recording of the concentration of either reactants or products as a function of time. The recorded concentration-time resolved data is then fitted to an appropriate theoretical kinetic model from which the rate law can be deduced. The experiments should be designed in a manner that enables a sound testing for the suitability of the theoretical kinetic model defining the proposed mechanism. The kinetic model which is tested is formulated after considering all the theoretical kinetic aspects that approximate a best description of the proposed mechanism for the reaction.

If all reactions proceeded at conventionally slow rates, they could easily be studied by mixing the reagents and then determining their real time-resolved concentration profiles using suitable conventional techniques. Where moderately slow-to-very fast rates of reactions are anticipated, a property of the reaction mixture known to vary directly with the concentration of reacting species or the product is conveniently chosen to monitor the observed rates of reaction instead. Examples of such properties of a system which are usually used to follow the progress of reactions include the optical absorbance, luminescence, electrical conductivity and optical rotation just to mention a few. Methods which employ any of the properties are called physical methods.

An outdated but still useful approach to the acquisition of kinetic data is to sample out the reaction mixture at predefined times during the progression of the reaction. This is referred to as intermittent sampling and is only useful for very slow reactions with a half-life in excess of several minutes. The samples are quenched immediately they are withdrawn out. This is accomplished through addition of a chemical reagent, changing the pH or temperature of the reaction mixture.<sup>20</sup> However, the applicability of such classical and conventional physical methods to the study of fast reactions can result in serious errors.<sup>21</sup> One has to reckon that an accurate acquisition of the data during the initial stages of a fast reaction is almost impossible since a minimum mixing time of reagents in excess of 20 s is needed for manual initiation. Acquiring sufficient kinetic data points to match the rapid changes that occur at the initial stages of the reactions by intermittent sampling presents another challenge. However, the data acquisition problem can be improved if the kinetic data is acquired continuously during the course of the reaction.

Ligand substitution at a square-planar Pt(II) centre is characterised by moderately slow to very fast reactions. For this reason, the study of ligand substitution reactions requires modern spectrometers, which have the capabilities of acquiring data continuously. Thus, if the

# Ligand substitution reactions of Pt(II) complexes

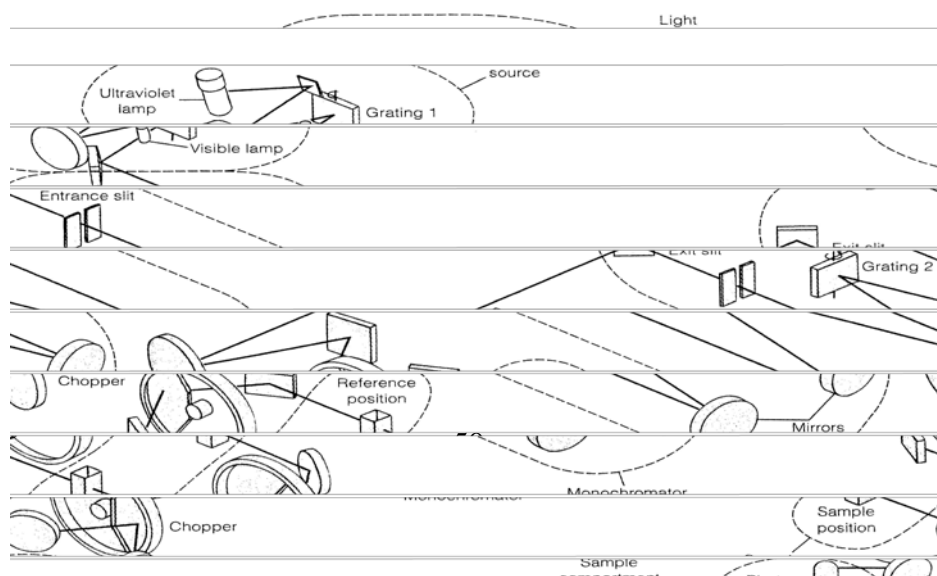
kinetics is moderately slow, manual mixing of reactants, coupled to a continuous data acquisition by a spectroscopic technique can provide credible kinetic data for the substitution reactions. This approach is still quite relevant to studying the kinetics of slow ligand substitution reactions of Pt(II) metal complexes, wherein spectroscopic techniques such as nuclear magnetic resonance (NMR), UV-visible, infrared spectroscopy are used for data acquisition.

For very fast reactions however, techniques which have fast mixing and fast data acquisition capabilities, enough to match the rapid changes that occur especially in the initial stages of the reaction are needed. One such class of specialized techniques meeting these requirements are the flow techniques developed from the pioneer work of Hartridge and Roughton.<sup>22</sup> Thus, two of the spectroscopic techniques mentioned above *viz.*, UV-visible spectroscopy (typically suited for studying the kinetics of slow reactions) and stopped-flow (suited for fast reactions) will be described in detail shortly.

## 2.1.3.2 UV-visible Spectrophotometer.

UV-visible spectrophotometry is a sensitive technique that can detect samples of low concentrations in the sub-micromolar range. If a compound has  $\pi$ -electrons or a non-bonding electron pair it can undergo electronic transitions originating from its highest occupied molecular orbital (HOMO) to the lowest unoccupied molecular orbital (LUMO) upon absorbing light in the ultraviolet and visible regions, causing absorption bands in the spectra. An instrument for acquiring such spectra is called the UV-visible absorption spectrophotometer.

As depicted in Figure 2.9, the instrument comprises two sources of radiation spanning the visible and ultraviolet range, the sample holding compartment, the monochromator, the detecting system and the output-readout device.



## Ligand substitution reactions of Pt(II) complexes

**Figure 2.9** Schematic diagram of a UV-Visible spectrophotometer.<sup>23</sup>

In order to acquire kinetic data in replicates during the experimental runs, the spectrometers are equipped with a special module for selectively driving the holding cell compartments to the path of source radiation. Thermostating of the reaction mixture either through an external or internal temperature control device is necessary for credible kinetic results. A special cuvette design called a tandem cuvette should be used for initiating the kinetic reactions. It has two compartments that allow one to pre-equilibrate the reactants at the required temperature before manually mixing them to initiate the reaction.

The spectrophotometer measures the amount of light transmitted after irradiating a beam of light (in the visible or ultraviolet) through a sample column of an optical path length equivalent to 1 cm. The optical transmittance,  $T$ , is related to the concentration of the species under study by the Beer's law.<sup>23</sup>

$$A = \epsilon Cl$$

where,  $A$ , is the optical absorbance and is numerically equal to negative logarithm of transmittance ( $-\log T$ ),  $\epsilon$  is the molar absorptivity of the absorbing medium,  $C$  is the molar concentration of the absorbing species and  $l$  is the path length of the absorbing medium in cm. Thus, by measuring the optical absorbance of the reaction mixture at predefined times or in a continuous manner, the concentration-time-resolved spectrum of the system can be determined from the Beer's law. Often, the absorbance-time resolved data is used directly to evaluate the observed rate constants.

For accurate results, the absorbance-time resolved data is acquired at a predetermined wavelength at which a significant change in the absorbance occurs with time. Thus, before an appropriate monitoring technique can be chosen for the kinetics experiment, a trial experiment to establish the most suitable wavelengths at which the reaction is to be monitored and for estimating the timescale of the reaction should be conducted. The scanning facility on most modern UV-visible absorption spectrophotometers is useful for this end.

# Ligand substitution reactions of Pt(II) complexes

Apart from its convenient use in the monitoring the kinetics of conventionally slow reactions, UV-visible absorption spectroscopy is also used for performing spectrophotometric titrations. Specifically, these titrations are performed to determine important thermodynamic data such as the binding mechanism of the DNA nucleobases and for the accurate determination of the  $pK_a$  values of the coordinated protic ligands especially the aqua ligands, useful for gaining an in-depth understanding of the underlying mechanistic pathways. In the latter case, the aqua complex is titrated with a suitable base and the resultant changes monitored spectrophotometrically. The  $pK_a$  values of the coordinated aqua ligand is a useful piece of thermodynamic data for probing the general electrophilicity of the central metal atoms especially in those complexes with strong  $\pi$ -acceptor carrier ligands.<sup>24</sup>

The direct proportionality between a measurable physical parameters and concentration of the reaction system as exemplified by the Beer-Lambert law allows one to derive directly the rate-law in terms of the measurable physical parameter. For instance, where a reaction follows first-order kinetics, the integrated rate-law can be expressed in terms of the concentration or optical absorbance by:

$$\ln\left(\frac{C_0}{C_t}\right) = \ln\left(\frac{A_0 - A_\infty}{A_t - A_\infty}\right) = k_1 t$$

where  $[A]_0$ ,  $[A]_\infty$  and  $[A]_t$  are the initial absorbance, the absorbance at the end of the reaction and the absorbance at any given time, respectively. Thus, as already stated the absorbance-time resolved data can be used to evaluate directly the pseudo first-order rate constant,  $k_{obs}$ . The data is then fitted to a standard single exponential equation using a non-linear least-squares procedure from which the pseudo first-order rate constant,  $k_{obs}$ , for the reaction can be evaluated.

### 2.1.3.3 Flow Methods

Flow techniques are one of the techniques which have adequate design capabilities for rapid mixing of reactants and prompt acquisition of sufficient kinetic data in the initial stages of a fast reaction.<sup>20</sup> In one form of their design, reactants are rapidly mixed and allowed to flow continuously<sup>25</sup> along the length of a reaction loop to form a continuous stream. The concentration-time resolved spectrum is obtained by measuring the concentration of the reactants or products at various positions of the loop at a predetermined wavelength. A

## Ligand substitution reactions of Pt(II) complexes

variation to this design is the stopped-flow technique. The technique is schematically illustrated in Figure 2.10.

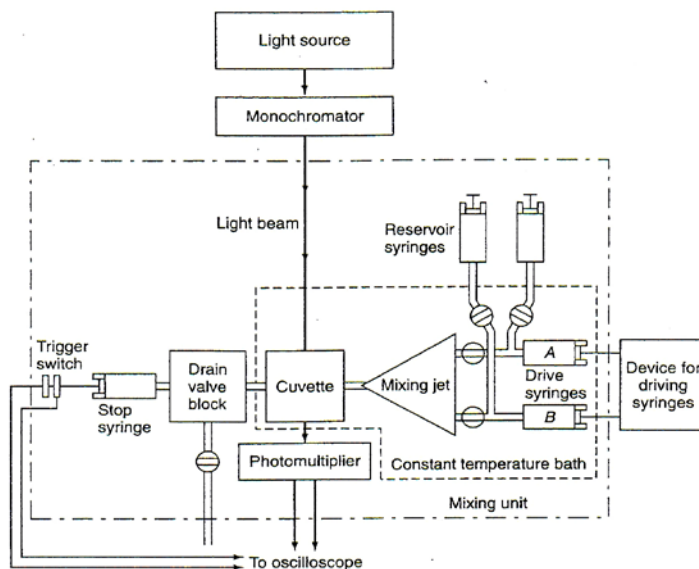


**Figure 2.10** Schematic diagram of a stopped-flow reaction analyzer.<sup>21</sup>

As shown in Figure 2.10, the reaction analyzer consists of the drive syringes, *A* and *B*, which are filled through separate valves from the reservoir syringes, containing the individual reactants. The drive syringes are usually thermostated through a water bath encasement. Once filled, the solutions are allowed to equilibrate at the specified temperature. The reactants are charged into the reaction chamber by a compressed gas-driven piston (800 kPa) in such a manner that allows ultra rapid mixing (within 1 ms) of the two reactants as their streams impinge on one another on the entrance of the reaction chamber. The impinging of the reactants also serves as a trigger to the data acquisition device, which may be an oscilloscope or a digital sensitizer. Thus, the reacting species is static (stopped-flow)<sup>20</sup> during the acquisition of the kinetic data. UV-visible spectrophotometry is the most commonly used detector for the reaction analyzer. Once the reactants impinge on each other in the observation chamber, the data acquisition system is prompted to record the absorbance-time resolved kinetic trace at a set wavelength. The kinetic traces are then processed and the observed (pseudo) first-order rate constants evaluated by an online computer program. A typical single exponential kinetic trace acquired on a stopped-flow reaction analyzer is shown in Figure 2.11.

# Ligand substitution reactions of Pt(II) complexes

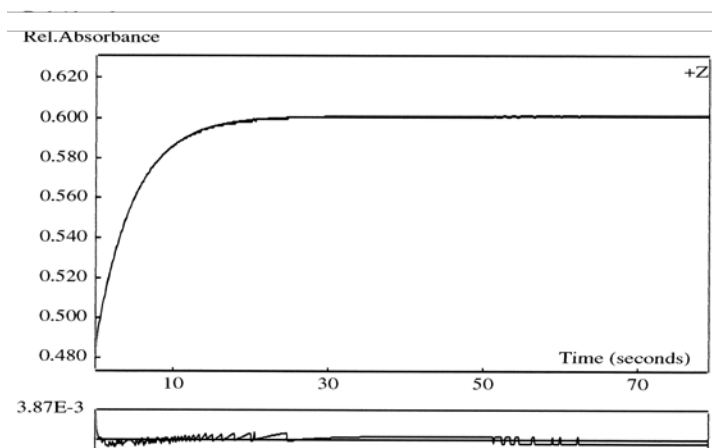


**Figure 2.11** A typical kinetic trace acquired on a stopped-flow reaction analyzer showing a perfect fit to a single exponential for the reaction between  $[\text{Pt}\{(o\text{-CF}_3\text{-Ph})\text{Ph-bipy}\}\text{Cl}]$  ( $5.285 \times 10^{-5}\text{M}$ ) and thiourea ( $1.664 \times 10^{-3}\text{M}$ ) in methanol,  $\lambda = 348\text{ nm}$ ,  $I = 0.1\text{M}$  ( $\text{LiClO}_4$ ) and  $T = 298\text{K}$ .

## 2.2 General considerations for substitution reactions of Pt(II) complexes.

### 2.2.1 Associative activation at a Pt(II) metal centre.

A vast majority of ligand substitution reactions at a square-planar geometry occurs mainly through an associative mode of activation.<sup>11,8</sup> Square-planar complexes have 16 electrons in their valence shells and are therefore coordinatively unsaturated. As a result of this, formation of an associatively-activated 18-electron transition state intermediate is favoured on energetic grounds. In an associatively-activated substitution process, the coordination number of the metal centre increases from four to five along the reaction coordinates, leading to a trigonal bipyramidal transition state. In its early transition state, the two groups that were *cis* to the leaving group occupy axial positions while the *trans* ligand, the leaving and incoming groups all share the equatorial positions of the trigonal bipyramid (penta-coordinate) intermediate. The incoming ligand occupies the coordination position that was vacated by the leaving ligand in the substituted product. Thus, the course of substitution proceeds with stereochemical retention of the coordinated ligands.<sup>26,8</sup>

However, reports in literature exist in which some of the ligand substitution reactions proceed via a dissociatively activated pathway.<sup>27</sup> This has been reported in square-planar complexes in which the platinum metal atom is bonded to two strong  $\sigma$ -donor ligands such as  $\text{CH}_3$  or Ph ligands, which are positioned *cis* to thioether leaving groups. In organometallics,

## Ligand substitution reactions of Pt(II) complexes

such coordinatively unsaturated 14-electron intermediates are useful sythons,<sup>27a</sup> in catalytic cycles, affording a range of valuable organic compounds.

In one mechanistic study,<sup>27b</sup> involving complexes of the type,  $[cis\text{-Pt}(\text{Ph})(L)\text{SR}_2]$ , (i)  $L = \text{Ph}$  or  $\text{CH}_3$ ; (ii)  $L = \text{CO}$  and the reference complex,  $L = \text{Cl}^-$ , it was demonstrated that a change in one of the *cis* ligand,  $L$ , from a strong  $\sigma$ -bonding ligand such  $\text{CH}_3$  or  $\text{Ph}$  in (i) to either a CO {a strong  $\pi$ -acceptor ligand such as CO in (ii)} or  $\text{Cl}^-$  weak  $\sigma$ -donor (the reference complex) causes a mechanistic changer-over from a dissociative to an associative. Three of the studied complexes are shown in Figure 2.12.

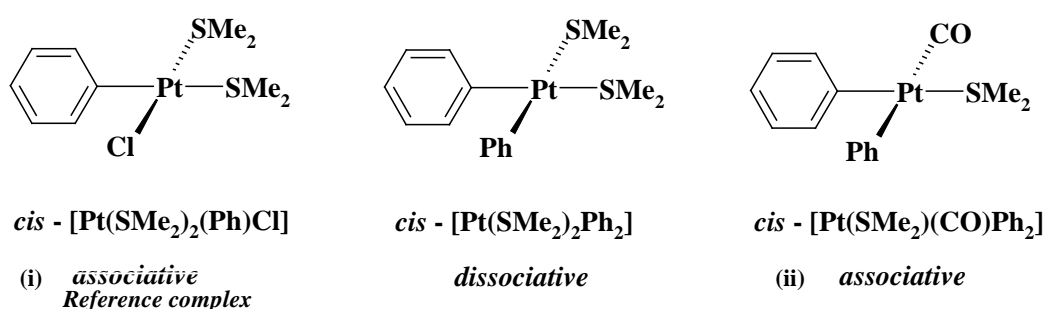


**Figure 2.12** Influence of the strong  $\sigma$ -bonding ligand *cis* to the leaving group on the mechanism of substitution of square-planar Pt(II) complexes.

The geometry of the ligands in case (i) resulted in increased bond weakening in the Pt-S bond of the thioether leaving groups (as a result of the high *trans*-influence of the two strong  $\sigma$ -bonding ligands) and an increase in electron density at the metal centre, thus preventing a facile approach of the incoming nucleophiles as a result of the stabilization of the transition state in the coordinatively unsaturated 14-electron intermediate by the two strong  $\sigma$ -bonded ligands. However, when one of the strong  $\sigma$ -bonding ligands is replaced by a good  $\pi$ -acceptor ligand such as CO {as in case (ii)} which is efficient in delocalizing excess electron density brought in by incoming ligands away from the metal centre, the penta-coordinated transition state is stabilized instead, switching the activation back to an associative mode.

In a reaction involving a related complex,<sup>27c</sup> wherein the two strong  $\sigma$ -bonding ligands (dissociative activators) were replaced by a strong  $\pi$ -acceptor 2,2'-biphenyl dianion, the presumed electron density relief at the Pt(II) metal centre was not adequate to switch the mechanism from a dissociative to an associative mode. The 2,2'-biphenyl dianion provides two strong  $\sigma$ -bonding carbon donors necessary to activate a dissociative pathway. Its in-plane cyclometalated geometry was expected also to stabilize the penta-coordinated intermediate through  $\pi$ -back bonding into its extended  $\pi$ -conjugated framework as a result of increased electrophilicity at the metal centre.

# Ligand substitution reactions of Pt(II) complexes

Apart from the work of Romeo and co-workers,<sup>27</sup> not so many examples are known of substitution reactions at a square-planar Pt(II) metal centre which proceed via a dissociatively activated pathway. Thus, in the remaining sections of this chapter, only pertinent aspects controlling the general reactivity of associatively activated reactions will be concentrated on.

## 2.2.2 Nature of the entering and leaving groups.

As discussed in *section 2.1.1*, the second-order rate constant ( $k_1$ ) in the two-term rate law (*Eqn. 5*) is strongly dependent on the nature of the entering ligand. This dependence of the rates of substitution on the nature of the entering ligand is a useful diagnostic tool for assigning associatively-activated mechanisms (*vide supra*).

The entering ligand is called a nucleophile. A nucleophile,  $Y$ , uses its lone pair of electrons to attack an electron-deficient atom (Pt in this case) other than a proton. Nucleophilicity is a measure of how readily the nucleophile is able to attack such an atom. It is measured by the second-order rate constant,  $k_1$ , for the substitution process.<sup>8,11</sup> For nucleophiles with the same donor atoms, nucleophilicity bears a direct relationship with the basicity of nucleophile, a measure of how strongly the donor atom shares its electron with the proton.<sup>28</sup> In such instances, strong bases are better nucleophiles, while weak bases are poor nucleophiles leading to a linear correction between reactivity (as measured by the second-order rate constant) and the basicity of the incoming nucleophile. For the same reason, it is easier to displace a leaving group that has a lower basicity and hence lower nucleophilicity constant since some bond breaking is involved in its activated state.

The direct relationship between the basicity and nucleophilicity is maintained if nucleophilic groups bearing different donor atoms all of comparable atomic sizes are being compared. For example, since the change in atomic sizes of elements across the Period Table is generally moderate while their basicity decreases to a significant extent, the nucleophilicity of their ligands therefore decreases across the Period. For the first row elements the  $\text{CH}_3^-$  becomes a better nucleophile than  $\text{F}^-$  in most nucleophilic substitution reactions occurring at Pt(II) metal centre. Pitteri *et al.*<sup>29</sup> have demonstrated that reactivity of several Pt(II) tridentate complexes depends both on the basicity of incoming nitrogen ligands<sup>29a,b</sup> as well as leaving nitrogen groups<sup>29c</sup> as controlled by the  $\text{p}K_a$  values of their conjugates.

However, when the sizes of the donor atoms are markedly different, and the reactions occur in a non-gaseous solvent, then the relationship between nucleophilicity and basicity depends on the nature of the solvent. In protic solvents (hydrogen bond donors) the direct

## Ligand substitution reactions of Pt(II) complexes

relationship is inverted<sup>28</sup> due to the presence of ion-dipole interactions between the nucleophile and the protic solvents. However, in aprotic solvents nucleophilicity remain directly related to basicity.

Using the reaction,



a comprehensive study initiated to rank the nucleophile on nucleophilic scale at Pt(II) metal centre was conducted using *trans*-[Pt(II)(py)<sub>2</sub>Cl<sub>2</sub>] as the reference substrate. The rates of substitution was measured using incoming ligands spanning a wide range of nucleophilicities in a methanolic medium.<sup>8,11,17b</sup> The nucleophilicity constant,  $n^{\circ}_{\text{Pt}}$ , of an incoming ligand as measured at this reference substrate is defined as the logarithm number of the second-order rate constant normalized to the value measured for methanol at 30 °C. Thus,  $n^{\circ}_{\text{Pt}}$  can be expressed as  $\log(k_Y/k^{\circ}_s)$ , where  $k_Y$  is the second-order rate constant for the substitution by the entering ligand,  $k^{\circ}_s$  is the second-order rate constant for the attack by the methanol solvent and is equal to  $\{k_s/[\text{MeOH}]\}$ . The equation simplifies to  $n^{\circ}_{\text{Pt}} = n_{\text{Pt}} + 1.39$ , when the concentration of pure methanol is assumed to be 24.3 M at 30 °C. An example of the stacked plots of the observed first-order rate constants,  $k_{\text{obs}}$ , versus the concentration of the various in-coming nucleophiles [Y] is shown in Figure 2.13.

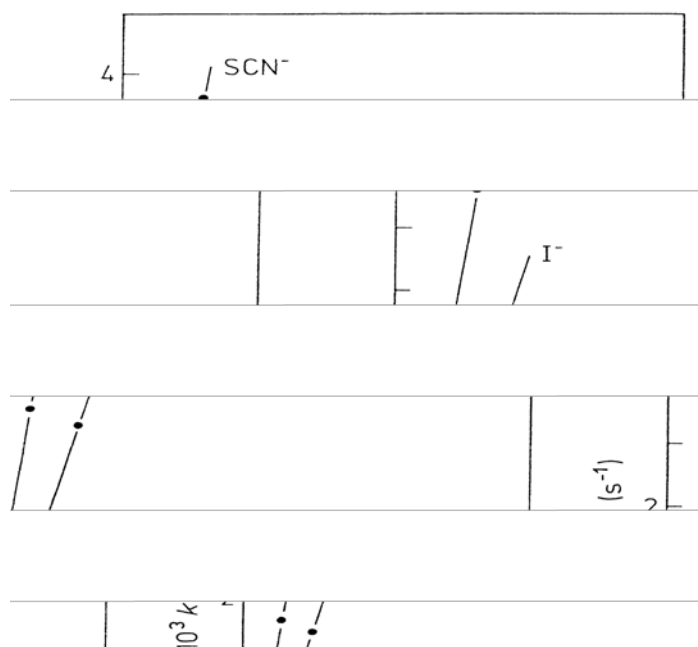


**Figure 2.13** Plots of the pseudo first-order rate constants,  $k_{\text{obs}}$ , versus the concentration of the entering nucleophiles, [Y], at the *trans*-[Pt(py)<sub>2</sub>Cl<sub>2</sub>] substrate by a series of nucleophiles in methanol at 30.0 °C.

## Ligand substitution reactions of Pt(II) complexes

Nucleophilicity constants collated from several studies<sup>30</sup> using the *trans*-[Pt(II)(*py*)<sub>2</sub>Cl<sub>2</sub>] as a substrate, ranks the reactivity of the nucleophiles in the approximate order: methanol < F<sup>-</sup> < H<sub>2</sub>O < OH<sup>-</sup> ~ Cl<sup>-</sup> ~ NH<sub>3</sub> ~ Me<sub>2</sub>SO < NO<sub>2</sub><sup>-</sup> ~ C<sub>5</sub>H<sub>5</sub>N ~ PhNH<sub>2</sub> ~ Ph<sub>2</sub>S < imidazole ~ (PhCH<sub>2</sub>)<sub>2</sub>S < NH<sub>2</sub>NH<sub>2</sub> ~ NH<sub>2</sub>OH < Br<sup>-</sup> ~ PhSH < Et<sub>2</sub>S ~ (Et<sub>2</sub>N)<sub>3</sub>P ~ thiourea < N<sub>3</sub><sup>-</sup> < I<sup>-</sup> < Me<sub>2</sub>Se ~ SCN<sup>-</sup> < SO<sub>3</sub><sup>2-</sup> Ph<sub>3</sub>As ~ CN<sup>-</sup> < S<sub>2</sub>O<sub>3</sub><sup>2-</sup> ~ Et<sub>3</sub>As < R<sub>3</sub>P. Thus, the trialkylphosphine reagents are the best nucleophiles so far at this substrate. The trend in the reactivity of some nucleophiles reflects their basicities (especially in cases where the sizes of the donor atoms are the same). An exception to this trend is noticed in some stronger nucleophiles endowed with both strong  $\sigma$ -donor and  $\pi$ -acceptor abilities such as thiourea, thiocyanate and azide. This can be confirmed from the reactions involving these nucleophiles with other Pt(II) substrates, in which their  $\pi$ -acceptor ligand framework is used to transfer electron density away from the metal centre.<sup>31</sup> Such ligands are called biphilic nucleophiles.

Thus, when the same experiments are repeated using substrates other than *trans*-[Pt(II)(*py*)<sub>2</sub>Cl<sub>2</sub>] under the same experimental conditions, then an opportunity to measure the discriminating abilities of different substrates for a range of nucleophiles is opened. If the value of  $\log k_Y$ , where  $k_Y$  is the measured second-order rate constant for an incoming nucleophile,  $Y$ , is plotted against the calculated  $n^\circ_{\text{Pt}}$  values, a free energy linear relationship<sup>32</sup>:

$$\log k_Y = S \cdot n^\circ_{\text{Pt}} + C, \text{ is obtained.}$$

where,  $S$  is the nucleophilic discrimination factor, and  $C$  is the intrinsic reactivity. The slope of the above linear plot,  $S$ , is an estimate of the nucleophilic discrimination ability of the complex for the nucleophiles.<sup>8,11</sup> It reflects also the electrophilicity and steric properties at the site of substitution felt by incoming nucleophiles. A value of  $S$  equal to 1 is assigned for the reference complex, *trans*-[Pt(*py*)<sub>2</sub>Cl<sub>2</sub>], while a value of  $S > 1$ , indicates increased reactivity of the complex toward the range of nucleophiles used relative to the reference complex. The intercept,  $C$ , estimates the reactivity the poorest nucleophilic reagent at this substrate. Complexes with high  $C$  values are less discriminating in their reactions with different nucleophiles and consequently have a small  $S$  value.

Apart from basicity, polarizability of the nucleophile is another critical factor known to affect the rates of substitutions at a square-planar geometry. In ligand substitution reactions, high nucleophilicity constants at several Pt(II) substrates are usually quoted for readily polarizable incoming ligands such as the iodide and the sulfur containing nucleophiles.<sup>33a</sup> This

# Ligand substitution reactions of Pt(II) complexes

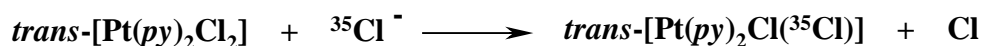
happens as result of the relatively large size of the Pt atom (its softness) and hence the marked diffusivity<sup>33b</sup> of its valence orbitals. The Pt(II) metal ion therefore forms stronger covalent bonds with softer (easily polarizable due to a high diffusivities of its valence orbitals) incoming ligands. As a result, ligands which are highly polarizable substitute the leaving groups more rapidly at the square-planar Pt(II) metal centres.

Another important intrinsic factor which controls the ability of the incoming nucleophile to donate its lone pair of electrons to the metal centre is its steric bulkiness, a kind of steric effect that depends on the size of the donor atom or other substituents adjacent to it. Bulky ligands which have substituents likely to cause steric blocking of the donor atom are retarded in their approach to the metal centre. This results in lower rates of substitution at the metal centre. Since the *trans* non-labile, the entering and leaving groups occupy the equatorial trigonal plane in the trigonal bipyramid transition state, a bulky incoming ligand will slow down the formation of the activated complex thus, destabilizing its state relative to ground state due to increased steric repulsions. As a result of this, associatively-activated reactions are very sensitive to the steric demands of the incoming ligands since the reactions proceed via common transition state with an increased coordination number.<sup>11</sup> This mechanistic test is useful for confirming associatively-activated reaction at  $d^8$  square-planar Pt(II) metal complexes.<sup>8,11,17</sup> Indeed, this has been used to confirm associatively-activated mechanisms in square-planar Pt(II) complexes in numerous studies.<sup>34</sup>

### 2.2.3 Effect of solvent.

The established two-term rate law<sup>8</sup> for associatively-activated substitution reactions at  $d^8$  square-planar Pt(II) complexes includes a term that is independent of the entering nucleophile which is usually ascribed to a parallel solvolysis pathway. The solvent pathway involves a direct participation of the solvent through a direct displacement of the leaving ligand. The rate of substitution is therefore expected to increase with an increase in the coordination ability of the solvent.

For the ligand substitution reaction between *trans*-[Pt(*py*)<sub>2</sub>Cl<sub>2</sub>] and radio-labelled <sup>36</sup>Cl<sup>-</sup>,



the results indicated that the reaction proceed predominantly through a solvolytic pathway when highly coordinating solvent were used. In such instances, the magnitude of measured value of  $k_{-1}$  (measuring the parallel solvolytic pathway) was found to be greater than the product of

# Ligand substitution reactions of Pt(II) complexes

$k_1[\text{Cl}^-]^{35a}$ . The values of  $k_{-1}$  were found to increase in the order of the strength of the solvent in the order  $\text{ROH} < \text{H}_2\text{O} \sim \text{CH}_3\text{NO}_2 < \text{DMSO}$ . On the one hand, poor coordinating solvents such as benzene, carbon tetrachloride and sterically hindered alcohols contributed little to the overall rates of reactions. The second-order rate constant,  $k_1$ , for the direct ligand exchange process in such solvents were found to be higher in non-polar solvents such as carbon tetrachloride than in polar solvents such as dimethylformamide due to the poor solvating abilities of the non-polar solvents. The measured results are summarized in Table 2.2.

Coordinating Solvent	$k_{-1}, 10^{-5} \text{ s}^{-1}$	Non-coordinating Solvent	$k_1, \text{M}^{-1} \text{ s}^{-1}$
DMSO	380	$\text{CCl}_4$	$10^4$
$\text{H}_2\text{O}$	3.5	$\text{C}_6\text{H}_6$	$10^2$
EtOH	1.4	<i>i</i> -BuOH	$10^{-1}$
MeOH	0.4	$\text{Me}_2\text{C}(\text{O})$	$10^{-2}$

**Table 2.1** Effect of solvent on the rate of chloride exchange from *trans*-[Pt(py)<sub>2</sub>Cl<sub>2</sub>].<sup>35a</sup>

Similar results have been reported by Romeo *et al.*<sup>35b</sup> Linear free energy relationships between various common parameters that are used to describe the Lewis acidity of the solvent (such as the acceptor numbers; Taft'  $\alpha$ ; Dimroth-Reichard's  $E_T$  parameters) and reactivity (as measured by the  $k_1$  term) were found. They concluded that the observed rate constants depended strongly on the solvation of the anionic incoming nucleophile.

## 2.2.4 Nature of the other coordinated groups.

A particular feature of the ligand substitution at square-planar Pt(II) complexes is the important role placed on the carrier ligand (non-labile ligand framework) in controlling the general reactivity of the metal centre. Both the *trans*- and *cis*-carrier ligands affect the rate of substitution at the central metal all be it in a different way. The effect on the reactivity is more prominent from non-labile ligands that are positioned *trans* to the leaving group. This effect which is caused by a non-labile ligand on the rate of substitution of another ligand positioned *trans* to itself is known as the *trans*-effect.<sup>8,11,17</sup> A strong *trans*-ligand (one which is high in the *trans*-effect series) promotes rapid substitution of the ligand in the position *trans* to itself than it does on the ligand that is *cis*-positioned.<sup>8</sup> The *trans*-effect is therefore purely kinetic. Thus, the relative stabilities of both the ground state and the activated transition state are relevant in

## Ligand substitution reactions of Pt(II) complexes

determining its overall magnitude, as they both affect the size of activation barrier necessary to activate the reactants to the transition state.

Closely related, but characteristically distinct to the *trans*-effect is the *trans*-influence. This is the effect of the *trans*-ligand on the ground state properties of the complexes.<sup>8,11</sup> This is an equilibrium phenomenon. A ligand with a strong *trans*-influence affect the equilibrium state properties of the ligand *trans* to itself by weakening the bond between the metal and that ligand.<sup>36</sup> This ligand normally has a large  $\sigma$ -inductive donor capacity and weak  $\pi$ -acceptor ability. Data in support of this comes from theoretical calculations<sup>9</sup> of the  $\sigma$ -overlap integrals between several  $\sigma$ -donor ligands and the Pt(II) metal ion, wherein the integral values were found to decrease in the order  $\text{Si} > \text{H} \sim \text{C} \sim \text{P} > \text{Cl} > \text{N} > \text{O} > \text{F}$ . The ranking correlates well with the decreasing order in the size of the Pt(II)-X bond length, where X is the leaving group positioned *trans* to the  $\sigma$ -donor ligand. Experimental measurements have also demonstrated that the strength of the bond between the leaving group and the metal ion, is elongated (X-rays diffraction analysis). The labilized bond resonates at lower vibrational frequencies (infrared data). Changes indicative of this labilization can be observed in the chemical shifts of the resonances due to leaving ligand in the NMR spectral data of the complex. All these experimental data purports to an equilibrium state wherein the strength of the bond between the leaving ligand and metal centre is compromised (reduced) when a strong *trans*-influence ligand is coordinated to the metal centre. The weakening of the M-X bond promotes high rates of substitution at a planar-square Pt(II) centre.<sup>2</sup>

The *trans*-influence and the *trans*-effect have been explained using several theories, two of the most prominent of which are the polarisation theory and the  $\pi$ -bonding Theory.<sup>8</sup> The molecular orbital theory was later espoused by Langford and Gray<sup>9</sup> to unify the two. It is now known that the *trans*-effect and the *trans*-influence can be fully described by invoking both the  $\sigma$ -inductive as well as  $\pi$ -acceptor abilities of the activating *trans*-ligand. As such, the two aspects should be considered separately in order to fully account for their contributions to the two effects on reactivity of platinum complexes.

In the electrostatic polarization theory of Grinberg<sup>37</sup>, the primary charge carried by the central metal ion in [*trans*-Pt(II)L<sub>2</sub>TX] (where T = a *trans* non-labile group; X = leaving group) induces a primary dipole in the *trans*-ligand which in turn induces a secondary dipole in the metal ion. The orientation of the secondary dipole on the metal is such as to repel the negative charge in the leaving group thereby lengthening and weakening the bond.<sup>38</sup> Thus, the

## Ligand substitution reactions of Pt(II) complexes

magnitude of this effect is expected to correlate positively with the polarizability of both the *trans*-director ligand as well as the metal centre, a correlation that is observed in some of the ligands in the *trans*-effect series. Figure 2.14 is a simplified depiction of the effect of the electrostatic interactions between the *trans* ligand and the central metal ion and its ultimate effect on the bond strength of the leaving group

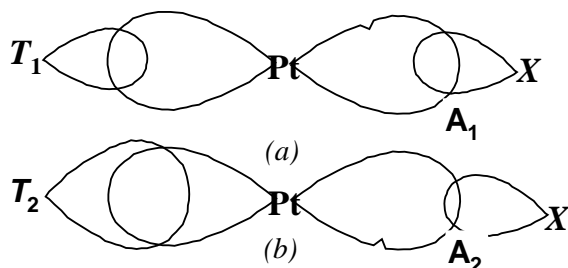


**Figure 2.14** Schematic diagram showing the effect of the electrostatic interactions on the bond strength and the overlap parameter,  $A$ .  $A_1 > A_2$ , if as in case (b) a *trans* ligands,  $T_2$  stronger than  $T_1$  case (a) is *trans* to the leaving group  $X$ , leading to weaker Pt-X bond strengths in case (b).

However, this electrostatic treatment could not account as to why reactivity was not responsive to this polarization effect as would be expected on the basis of the charge carried by the *trans*-ligand,  $T$ . It also did not correlate well in complexes with characteristically shorter Pt- $T$  bonds, wherein it was expected to be relatively high. To fully predict the effect of the *trans*-ligand on reactivity, the covalence character of the bond between the *trans*-ligand and the metal had to be included. Thus, the Polarization theory was satisfactory in as far as only accounting for the equilibrium ground state properties of the Pt(II) complexes and their consequent effects on reactivity. In other word, only the contributions from the *trans*-influence could be accounted satisfactorily for by this theory.

Later on, when the molecular orbital (MO) theory was applied, Langford and Gray<sup>9</sup> were able to explain the large *trans*-effect displayed by the strong  $\sigma$ -bonding ligands. Invoking the MO theory, they noted that of the four valence atomic orbitals on the metal (*viz.*,  $d_{x^2-y^2}$ ,  $s$ ,  $p_x$  and  $p_y$ ) which are involved in the formation of a square-planar complex, only the  $p_x$  atomic orbital is of the right symmetry for forming a  $\sigma$ -bonding molecular framework possessing *trans*-directional properties. Thus, in this MO arrangement, the *trans*-ligand,  $T$ , and the leaving group share the same  $\sigma_x$  molecular orbital derived from the overlap of  $p_x$  at the metal centre for bonding. Thus, when strong  $\sigma$ -bonding ligands such as  $H^-$  and  $CH_3^-$  are in the *trans*-position, they contribute a great deal of electron density into the shared  $\sigma_x$  molecular orbital of the metal. This will repel the electrons of the ligand in the *trans*-position such that its bonding to

## Ligand substitution reactions of Pt(II) complexes

the metal centre is weakened. This is in agreement with the predictions from the Polarization Theory. This leads to an increased rate of replacement of this group regardless of the mechanism of substitution.

Langford and Gray<sup>9</sup> reckoned that since there are more orbitals available for the  $\sigma$ -bonding framework in the trigonal plane of the activated complex than in the square-planar complex, the formation of the penta-coordinated transition state is more stabilized. In the square-planar complex, the *trans*-ligand and the leaving group share only one  $p_x$  orbital at the metal centre along the  $x$ -axis availing a theoretical covalency character of 0.5 in the bonds. On adding the entering ligand axially, the leaving ligand, X, move out of the square-plane away from the direction of approach of the incoming ligand, resulting in the trigonal bipyramidal transition state in which the *trans*-ligand, the leaving and entering groups share the equatorial trigonal plane. This is illustrated in Figure 2.15 below.

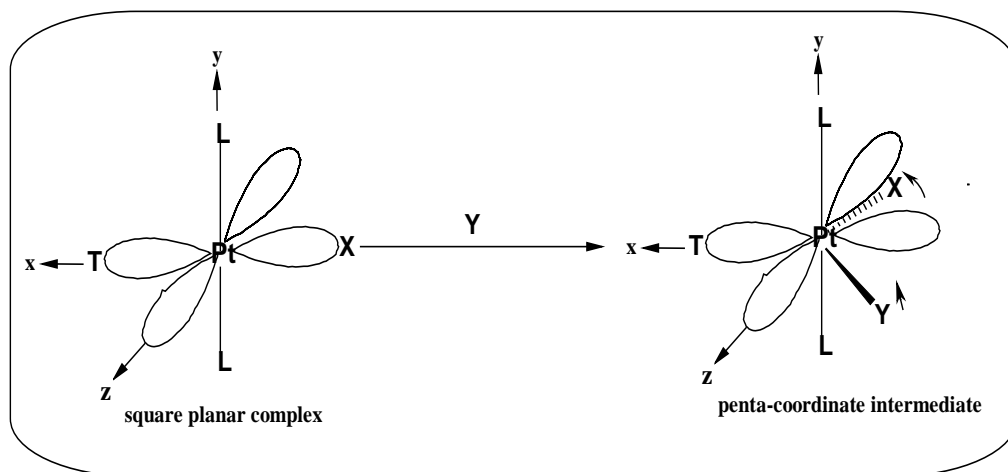


**Figure 2.15** An illustration of the  $\sigma$ -*trans* effect due to a stabilization of the trigonal bipyramidal intermediate. Only one  $p$  orbitals is available for  $\sigma$ -bonding to two ligands in the reactant whereas two  $p$  orbitals are suitable for  $\sigma$ -bonding of three ligands in the transition state.<sup>9</sup>

In this equatorial plane, two  $p$  orbitals ( $p_x$ ,  $p_z$ ) are now available for bonding to the three ligands bringing in a theoretical bonding covalency of 0.67 in the transition state. Thus, strong  $\sigma$ -bonding ligands will have a stronger  $\sigma$ -bonding framework resulting from their efficient utilization of the extra  $p$ -orbital thereby stabilizing the energy of the transition state

## Ligand substitution reactions of Pt(II) complexes

relative to the ground state. This results in higher rates of substitution at the metal centres. This kind of contribution to the *trans*-effect is called the  $\sigma$ -*trans* effect.

To account for the contribution of the multiple-bond character of the bond between the metal centre and the *trans*-effector ligand (Pt-*T*) towards activating reactivity of the metal centre, the  $\pi$ -bonding theory was invoked.<sup>9,11,38</sup> It is noted that of the five vacant antibonding molecular orbitals ( $\pi_{xy}^*$ ;  $\pi_{xz}^*$ ;  $\pi_{yz}^*$ ;  $\sigma_z^{*2}$  and  $\sigma_{x^2-y^2}^{*2}$ ) available and centred at the metal centre of square-planar geometry, only three ( $\pi_{xy}^*$ ;  $\pi_{xz}^*$ ;  $\pi_{yz}^*$ ) have the proper symmetry and energy for  $\pi$ -interactions with the orbitals from the *trans* ligand, *T*, and the leaving group, *X*. However, on forming the transition state with the incoming group, the molecular orbitals increases to four (including the ( $\sigma_{x^2-y^2}^*$ ), all available for  $\pi$ -interactions with the *trans*-ligand, the entering, and the leaving groups on the trigonal plane. Thus, the trigonal bipyramid transition state will be stabilized more by a *trans*-ligand possessing empty low lying  $\pi$ -orbitals since their interaction with the filled *d*-orbitals on the metal centre delocalizes the excess electron density away from the metal centre thereby lowering the energy of the activated complex. The net effect of a good  $\pi$ -acceptor ligand occupying a *trans*-position is to lower the activation energy of the substitution reaction.<sup>38</sup> Thus, the strong  $\pi$ -acceptor ligand stabilises the trigonal bipyramid transition relative to the ground state by withdrawing the  $\pi$ -electron density of the metal into their own empty  $\pi^*$ -orbitals as shown in Figure 2.16 below. This will enhance the addition of the incoming ligand leading to a rapid reaction. This effect is called the  $\pi$ -*trans* effect.

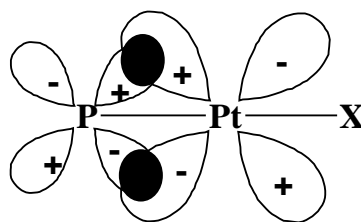
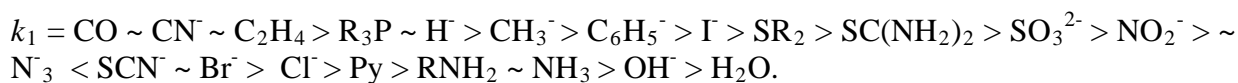


**Figure 2.16** Schematic representation of  $\pi$ -back bonding of a strong acceptor ligand.<sup>38</sup> Because more orbitals are available for delocalization of charge away from the metal centre in the transition state than in the ground state, this bonding scheme stabilises the transition state more than it does in square-planar ground state. If *L* and *X* are in the *xy*- plane, then the orbitals shown are derived from the  $d_{xz}$  or  $d_{xy}$ .

From the extensive studies carried out on the effect of the *trans*-ligand on the substitutional reactivity at a Pt(II) square-planar coordination plane, using various incoming

## Ligand substitution reactions of Pt(II) complexes

ligands, the overall qualitative order of the *trans* effect series as ranked in order of the measured second-order rate constants,  $k_1$ , was found to be:



As outlined above, the molecular orbital theory, MO, proved useful in harmonising the two underlying theories. It is noteworthy that there exist ligands such as thiourea or the iodide anion, which display a dual character in their activation of the ligand *trans* to their positions by utilizing both their  $\sigma$ - and  $\pi$ - molecular orbital frameworks for bonding during ligand substitutional reactions.

Apart from the *trans*-effect, the non-labile ligands can affect the rate of substitution through their steric features. Steric effects are space-filling effects.<sup>28</sup> These effects fall into two major categories, namely steric bulky and steric hindrance. The former transmit repulsive strain between atoms or a group of atoms caused by a mutual repulsion in their electron densities when they are brought into a close-up proximity. When this happens around a central atom or site of reaction, these atoms are considered overcrowded round it. The magnitude of this kind of steric effect is directly proportional to the spatial size (a volume effect) of the substituent causing it. If on the one hand, a substituent or part of it causes a blockade in the approach of one reactant toward a site of reaction, an effect called steric hindrance is operational at the site of reaction. This group is said to be shielding the site of reaction from a direct attack by an incoming reactant. This type of steric effect depends not only on its spatial size (as measured by its volume) but also on its relative spatial orientation or configuration with respect to the targeted site of reaction. This is especially critical in  $d^8$  square-planar metal complexes, where the geometry of the vacant orbitals on the metal centre requires that the nucleophile approach the central metal centre axially. The presence of axially configured substituents on the non-labile ligands usually shields the  $d^8$  metal centre from attack by incoming nucleophile resulting in retarded rates of substitution.

If the steric features are maintained constant at a square-planar geometry, the magnitude of the steric effects at the reaction site depend also on the positions of steric imposing substituents relative to the leaving group.<sup>39</sup> While increasing the steric features of the non-labile ligands in a square-planar complex is generally known to decrease the rate of substitution, the retardation effect is more prominent if the steric imparting groups are located in a *cis*-position than in the *trans*-position relative to the leaving group.<sup>8</sup> This effect was studied<sup>39</sup> in a series of complexes of the form [*cis*-/*trans*-Pt(PEt<sub>3</sub>)<sub>2</sub>(R)X] (*R* = phenyl, *o*-tolyl,

## Ligand substitution reactions of Pt(II) complexes

mesityl;  $X = \text{MeOH}, \text{Cl}^-, \text{Br}^-$ ). When the *trans*-isomer was used as a substrate, substitution of the chloro species by thiourea, demonstrated that the presence of one or two *ortho*-methyl groups on the phenyl rings imparts a deceleration in the rate of substitution by only two orders of magnitude from the substituent having the largest steric features (mesityl) to the unsubstituted phenyl ring. When the experiments were repeated using the *cis*-isomer, a greater decrease in the rate, spanning five-orders of magnitude was observed from the most sterically hindered (with a mesityl substituent) to the least hindered complex (one with an unsubstituted phenyl ring). It was concluded that, steric hindrance from a substituent in the *cis*-position to the leaving group has a significantly larger effect on the rate of substitution than in the *trans*-position at a square-planar geometry. In the transition state of the *cis*-isomer, the steric imparting mesityl group, occupy an axial position leading to increased repulsions between its *ortho*-methyl substituents, the entering and leaving groups. In the case of the *trans*-isomer, the same group is in an equatorial position and consequently the repulsions between its *ortho*-methyl groups, the entering and leaving group are reduced and the rate of retardation in the substitutions is less affected.<sup>17b</sup> This kind of retardation has been used as a drug design tool in the synthesis of drugs with reduced toxicity and improved efficacy as demonstrated in the efficacy of ZD0473, a Pt(II) drug undergoing clinical trials (section 2.0.1).<sup>3,4</sup>

Steric effects transmitted by both the bulkiness of non-labile ligands as well as hindrance to the approach of the ligand are demonstrated in several studies<sup>40</sup> involving a series of cationic complexes with a diethylenetriamine (dien) non-labile ligand backbone. The ligand backbone was substituted by different steric-imparting groups to give a series of complexes of the form:  $[\text{Pd(II)}-; \text{Pt(II)}-LX]$ , where  $L = (1,4,7-R_3\text{dien}); (1,1,7,7-R_4\text{dien}); (1,1,4,7,7-R_5\text{dien})$ ,  $R = \text{Me}, \text{Et}$ ;  $X = \text{Cl}^-, \text{Br}^-, \text{I}^-, \text{py}, \text{NH}_3, \text{CO}_3^{2-}, \text{C}_2\text{O}_4^{2-}, \text{H}_2\text{O}$ . Results in Table 2.3 indicates that substitution of the leaving ligands by various nucleophiles increases as the number as well as the size of the substituents,  $R$ , resulted in a corresponding decrease in the rate of substitution at the Pd(II)-; Pt(II) metal centres. Congestion on the metal centre (increasing the size of  $R$  groups) as well as the hindering to the direct approach of the nucleophile (the  $R$  group occupying axial spatial positions in the transition state) contributed toward the total steric effects about the metal centres.

**Table 2.2** Rate constants and activation parameters for the substitution of the coordinated chloride by  $\text{I}^-$  in  $[\text{Pd(II)}\{(\text{R}_n\text{dien})\}\text{Cl}]^+$  ( $n = 0, 3-5$ ) in aqueous solution at 25.0 °C.<sup>40</sup>

$\text{R}_n\text{dien}$	$k_1, \text{s}^{-1}$	$\Delta H^\ddagger, \text{kJ mol}^{-1}$	$\Delta S^\ddagger, \text{J K}^{-1} \text{mol}^{-1}$	$\Delta V^\ddagger, \text{cm}^3 \text{mol}^{-1}$
-------------------------	----------------------	---	--	--

## *Ligand substitution reactions of Pt(II) complexes*

dien	44	43	-69	-10.0
1,4,7-Et <sub>3</sub> dien	10	41	-86	-10.8
1,1,7,7-Et <sub>4</sub> dien	2.2 x 10 <sup>-3</sup>	66	-74	-14.9
1,1,4,7,7-Me <sub>5</sub> dien	0.28 x 10 <sup>-4</sup>	50	-88	-10.9
1,1,4,7,7-Et <sub>5</sub> dien	7.2 x 10 <sup>-4</sup>	59	-106	-12.8

In general the presence of steric demanding ligands on the square-plane decreases the rate of replacement of the leaving group since the five-coordinate intermediate species, usually formed during the ligand substitution is not readily formed.<sup>41</sup>

In analysing steric effects at a square-planar geometry, it is necessary to consider the steric configurations of the substituents both in the transition state as well as in the ground-state so as to accurately predict their relative contributions to the steric effects at the central metal ion in both states. In most cases, the presence of bulky groups around the central metal ion is assumed to lead to a congested transition state which causes retardation in the rate of substitution. However, some studies<sup>42</sup> have suggested that if the ground-state steric effects are dominant relative to the transition state, then an unusual acceleration in the rate of substitution in an associatively-activated reaction may take precedence. It is argued that the labilization of the co-ligand and leaving group become a necessary relief mechanism for the build-up in the pertinent repulsive forces associated with such a crowded metal centre. According to this hypothesis and depending on the geometry of the bulky groups relative to the leaving group, it is conceived that steric effects will reach a point where a mechanistic change over from an associatively-activated pathway to a dissociatively-activated pathway can be triggered. A change-over in mechanism of this nature is rare and is only likely to take place when two bulky groups occupy the *cis*-positions relative to the leaving group<sup>17b</sup>.

Other than steric effects, basicity of the *cis*-donor atoms has been shown to control reactivity as well. A simple control of the basicity of the amine ligands *cis*-to the leaving group was found to affect the reactivity in a significant way, with the least basic groups producing the most reactive complexes. For the same reason a replacement of one of the *cis*-pyridyl unit with a phenyl (a strong  $\sigma$ -donor atom) in Pt(N-N-N)Cl where N-N-N is a terpyridine ligand, resulted in decrease in reactivity of the complex by a factor of about 16 when tu is the incoming nucleophile.<sup>43</sup>

Despite all that is known about factors that control the rates of substitutions of mononuclear complexes with square-planar geometries, not much the same can be said for

# Ligand substitution reactions of Pt(II) complexes

multinuclear complexes. Central to this challenge, is the need to resolve the structural complexity of the linking bridging moieties of the multinuclear Pt(II) complexes in order to gain a better understanding of the specific role served by the bridging linker in the control of the reactivity of the metal centres. What is known though is that the bridging linker confers special structural properties on the metal complexes such as structural flexibility (as in an alkanediamine<sup>44-45</sup> linker) and structural rigidity (as in azines,<sup>46</sup> azoles<sup>47</sup> and the dipyrazolylmethane<sup>48</sup>) apart from serving as the linking structural entity between the Pt(II) centres. This has sparked an interest to embark on a comprehensive study seeking to gain a better understanding of how the subtle changes in their structural make-up (such as changing the length of their aliphatic chain as well as changing the structural moieties forming the diamine bridge) affect the ligand substitution reactions of dinuclear Pt(II) complexes. The details of the aims of work are as outlined at the end of Chapter One.

## 2.3 References

- 1 (a) J. Reedijk, *Chem. Rev.* 1999, **99**, 2499; (b) J. Reedijk, *PNAS*. 2003, **100**, 3611; (c) J. Reedijk, *Eur. J. Inorg. Chem.*, 2009, 1303; (d) N. De Barrios, G. González, A. Grandas, M. Martinez and V. Moreno, *Inorganic Reaction Mechanisms*, 1999, **1**, 205.
- 2 D. S. Gill, In *Platinum Coordination Complexes in Cancer Chemotherapy*, M. P. Hacker, E. B. Douple, I. H. Krakoff Eds., Martinus Nijhoff Publishing, Boston MA, 1984, 267.
- 3 E. Wong, C. M. Giandomenico, *Chem. Rev.*, 1999, **99**, 2451.
- 4 Y. Chen, Z. Guo, S. Parsons, P. J. Sadler, *Chem. Eur. J.* 1998, **4**, 672.
- 5 (a) J. F. Holford, F. I. Raynaud, B. A. Murrer, K. Grimaldi, J. A. Hartley, M. J. Abrams, L. R. Kelland, *Anti-Cancer Drug Des.*, 1998a, **13**, 118; (b) J. F. Holford, S. Y. Sharp, B. A. Murrer, M. Abrams, L. R. Kelland, *Br. J. Cancer*, 1998b, **77**, 366.
- 6 Y. Zhao, W. He, P. Shi J. Zhu, L. Qia, L. Lin, Z. Guo, *J. Chem. Soc.; Dalton Trans.* 2006, 2617.
- 7 (a) Q. Liu, Y. Qu, R. van Antwerpen, N. Farrell, *Biochemistry*, 2006, **45**, 4248; (b) N. Farrell, Y. Qu, M.P. Hacker, *J. Med. Chem.*, 1990, **33**, 2179; (c) L. R. Kelland, B. A. Murrer, G. Abel, C. M. Giandomenica, P. Mistry, K. R. Harrap, *Cancer Res.* **52**, 1992, 822; (d) P. Perego, L. Gatti, C. Caserini, R. Supino, D. Colangelo, R. Leone, *J. Inorg. Biochem.*, 1999, **77** 59; (e) M. S. Davies, J. W. Cox, S. J. Berners-Price, Y. Qu, N. Farrell, *J. Am. Chem. Soc.*, 2001 **123**, 1316-1326.

## Ligand substitution reactions of Pt(II) complexes

- 8 (a) M. L. Tobe and J. Burgess, *Inorganic Reaction Mechanisms*, Addison Wisely, Longman, Ltd., Essex, 1999, pp. 30-33; 70-112.
- 9 F. Basolo and R. G. Pearson, *Mechanism of Inorganic Reactions*, 2<sup>nd</sup> Ed., Wiley, New York 1967, pp. 80-115
- 10 J. D. Atwood, *Inorganic and Organometallic Reaction Mechanisms*, 2<sup>nd</sup> Ed., Wiley-VCH, NY, 1997, pp. 43-61.
- 11 C. H. Langford, H. B. Gray, *Ligand Substitution Dynamics*, 1965, Benjamin, New York.
- 12 D. T. Richens, *Chem. Rev.* 2005, **105**, 1961.
- 13 A. E. Merbach, *Pure Appl. Chem.*, 1982, 54, 217.
- 14 (a) M. G. Evans, M. Polanyi, *Trans. Faraday Soc.*, 1935, 31, 875; (b) Laidler, J. H. Meiser, *Physical Chemistry*, 3<sup>rd</sup> Ed. Houghton, Mufflin, New York, 1999, pp. 394-5.
- 15 M. Kotowski, D. A. Palmer, H. Kelm, *Inorg. Chem.*, 1979, **18(9)**, 2555.
- 16 L. Helm, and A. E. Merbach, *J. Chem. Soc. Dalton Trans.*, 2002, 633.
- 17 (a) S. R. Logan, *Fundamentals of Chemical Kinetics*, Longman, Essex, 1996, pp. 1-27; (b) R. B. Jordan, *Reaction Mechanisms of Inorganic and Organometallic Systems*, Oxford University Press, New York, 1991, pp. 1-16;
- 18 R. van Eldik, W. Gaede, S. Wieland, J. Kraft, M. Spitzer, D. A. Palmer, *Rev. Sci. Instrum.*, 1993, **64**, 1355.
- 19 F. P. Rotzinger, *Chem. Rev.*, 2005, **105**, 2003.
- 20 R. G. Wilkins, *Kinetics and Mechanism of Reactions at Transition Metal Complexes*, 2<sup>nd</sup> Ed., VCH, Weinheim, 1991, pp. 199-201, 232-242.
- 21 K. J. Laidler, J. H., Meiser, *Physical Chemistry*, 3<sup>rd</sup> Ed., Houghton Mifflin, Boston, 1999, pp. 378-381.
- 22 (a) H. Hartridge, F. J. W. Roughton, *Proc. R. Soc.*, London, 1923, **A104**, 376; (b) J. W. Moore, R. G. Pearson, *Kinetics and Mechanism*, 3<sup>rd</sup> Ed., John Wiley & Sons, New York, 1981, 12-36.
- 23 (a) D. C. Harris, *Quantitative Chemical Analysis*, 4<sup>th</sup> Ed., W. H. Freeman & Co., New York, 1995, pp. 480-417; (b) D. A. Skoog, D. M. West, J. R. Holler, *Fundamentals in Analytical Chemistry*, 7<sup>th</sup> Ed., Hartcourt College Publishers, Fort Worth, 1997, pp 510-530.
- 24 (a) D. Jaganyi, A. Hofmann and R. van Eldik, *Angew. Chem. Int. Ed.*, 2001, **40**, 1680; (b)

## *Ligand substitution reactions of Pt(II) complexes*

---

- A. Hofmann, D. Jaganyi, O. Q. Munro, G. Liehr and R. van Eldik, *Inorg. Chem.*, 2003, **42**, 1688.
- 25 K. A. Connors, *Chemical Kinetics: The Study of Reaction Rates in Solution*, Wiley-VCH, New York, 1990, pp.1-22, 57-68, 177-180.
- 26 F. A. Cotton, G. Wilkinson, P. L. Gaus, *Basic Inorganic Chemistry*, 3<sup>rd</sup> Ed. Wiley & Sons, 1995, pp. 200-205
- 27 (a) A. Marrone, N. Re and R. Romeo, *Organometallics*, 2008, **27**, 2215; (b) M. R. Plutino, L. M. Scolaro, R. Romeo, Grassi, *Inorg. Chem.*, 1992, **31**, 4383; (c) M. R. Plutino, L. M. Scolaro, R. Romeo, Grassi, *Inorg. Chem.*, 2000, **39**, 2712; (d) Alibrandi, G. Bruno, S. Lanza, D. Minniti, R. Romeo, M. L. Tobe, *Inorg. Chem.*, 1987, **26**, 185; (e) Lanza, D. Minniti, L. P. Moore, J. Sachindis, R. Romeo and M. L. Tobe, *Inorg. Chem.*, 1984, **23**, 4428; (f) G. D. Minniti, G. Alibrandi, M. L. Tobe, R. Romeo, *Inorg. Chem.*, 1987, **26**, 3956.
- 28 P. Y. Bruice, *Organic Chemistry*, 2<sup>nd</sup> Ed., Prentice Hall, 1998, pp. 363-366.
- 29 (a) M. Bellicini, L. Cattalini, G. Marangoni, B. Pitteri, *J. Chem. Soc. Dalton Trans.*, 1994, 1805; (b) B. Pitteri, G. Marangoni, F. V. Viscutim, L. Cattalini and T. Bobbo, *Polyhedron*, 1998, **17** (4) 475; (c) B. Pitteri, M. Bortoluzzi, *Polyhedron*, 2008, **27**, 2259.
- 30 (a) R. G. Pearson, H. Sobel, J. Songstad, *J. Am. Chem. Soc.*, 1968, **90**, 319; (b) L. Cattalini, M. Bonivento, G. Michelon, M. L. Tobe, A. T. Treadgold, *Gazz. Chim. Ital.*, 1988, **118**, 725; (c) T. Hoover, P. Zipp, *Inorg. Chim. Acta.*, 1982, **63**, 9. (d) J. R. Gaylor, C. V. Senoff, *Can. J. Chem.*, 1971, **49**, 2390; (e) U. Belluco, M. Martelli, A. Orio, *Inorg. Chem.*, 1966, **5**, 582.
- 31 B. Pitteri, M. Bortoluzzi and G Marangoni, *Transition Met. Chem.*, 2005, **30**, 1008.
- 32 U. Belluco, L. Cattalini, F. Basolo, R. G. Pearson and A. Turco, *J. Am. Chem. Soc.*, 1965, **87**, 241.
- 33 (a) K. F. Purcell, I. Kotz, *Inorganic Chemistry*, Holt-Saunders, 1977, pp. 694-755. (b) S. M. Owen and A. T. Bruker, *A Guide to Modern Inorganic Chemistry*, Longman Scientific & Technical, Essex, England, 1991, pp. 193-194
- 34 (a) M. Bellicini, L. Cattalini, G. Marangoni and B. Pitteri, *J. Chem. Soc. Dalton Trans.*, 1994, 1805; (b) B. Pitteri, G. Marangoni and L. Cattalini, *J. Chem. Soc Dalton Trans.*, 1994, 3539; (c) B. Pitteri, G. Marangoni, F. V. Viscutim, L. Cattalini and T. Bobbo, *Polyhedron*, 1998, **17**, 475.
- 35 (a) R. G. Pearson, H. B. Gray and F. Basolo, *J. Am. Chem. Soc.*, 1960, **82**, 787. (b) R. Romeo, G. Arena, L. M. Scolaro and M. R. Plutino, *Inorg. Chim. Acta*, 1995, **240**, 81.
- 36 (a) A. Pidcock, R. E. Richards and L. M. Venanzi, *J. Chem. Soc. (A)*, 1966, 1707; (b) T. G. Appleton, H. C. Clark and L. E. Manzer, *Coord. Chem. Rev.*, 1973, **10**, 335.

## Ligand substitution reactions of Pt(II) complexes

- 37 (a) A. Grinberg, *Acta Physicochim. SSSR*, 1935, **3**, 573; (b) A. A. Grinberg, *Ann. Inst. Platine SSSR*, 1927, **5**, 109.
- 38 J. D. Atwood, *Inorganic and Organometallic Reaction Mechanisms*, 2<sup>nd</sup> Ed., Wiley-VCH Inc., NY, 1997, pp. 43-61.
- 39 (a) F. Basolo, J. Chatt, H. B. Gray, R. G. Pearson and B. L. Shaw, *J. Chem. Soc.*, 1961, 2207; (b) G. Faroare, V. Ricevuto, R. Romeo and M. Trozzi, *J. Chem. Soc. (A)*, 1971, 1877; (c) R. Romeo, M. L. Tobe and M. Trozzi, *Inorg. Chim. Acta.*, 1974, **11**, 231; (d) R. Romeo, D. Minniti and M. Trozzi, *Inorg. Chim. Acta.*, 1975, **14**, L15; (e) R. Romeo, D. Minniti and M. Trozzi, *Inorg. Chem.*, 1976, **15**, 1134. (f) R. Romeo, *Inorg. Chem.*, 1978, **17**, 2040; (g) R. van Eldik, D. A. Palmer and H. Kelm, *Inorg. Chem.*, 1978, **18**, 572.
- 40 (a) J. B. Goddard and F. Basolo, *Inorg. Chem.*, 1968, **7**, 2456; (b) M. Kotowski and R. van Eldik, *Inorg. Chem.*, 1986, **25**, 3896; (c) J. J. Pienaar, M. Kotowski and R. van Eldik, *Inorg. Chem.*, 1989, **28**, 373; (d) J. Berger, M. Kotowski, R. van Eldik, U. Frey, L. Helm and A. E. Merbach, *Inorg. Chem.*, 1989, **28**, 3759.
- 41 G. Natale, M. Coluccia, *Coord. Chem. Rev.*, 2001, **216**, 384.
- 42 (a) F. Basolo, H. B. Gray, R.G. Pearson, *J. Amer. Chem. Soc.* 1960, **82**, 4200; (b) R. G. Pearson, *Inorg. Chem. Soc.* 1988, **27**, 734
- 43 D. Jaganyi, D. Reddy, J. A. Gertenbach, O. Q. Munro and R. van Eldik, *J. Chem. Soc., Dalton Trans.*, **2004**, 299.
- 44 N. Farrell, S. G. De Almeida and K. A. Skov, *J. Am. Chem. Soc.*, 1988, **110**, 5018.
- 45 N. Farrell, *Comments Inorg. Chem.*, 1995, **16(6)**, 373.
- 46 (a) S. Komeda, G. V. Kalayda, M. Lutz, A. L. Spek, T. Sato, M. Chikuma and J. Reedijk, *J. Med. Chem.*, 2003, **46**, 1210; (b) G. V. Kalayda, S. Komeda, K. Ekedo, T. Sato, M. Chikuma and J. Reedijk, *J. Eur. Inorg. Chem.*, 2003, 4347.
- 47 (a) S. Komeda, M. Lutz, A. L. Spek, M. Chikuma and J. Reedijk, *Inorg. Chem.*, 2000, **39**, 4230; (b) S. Komeda, M. Lutz, A. L. Spek, Y. Yamanaka, T. Sato, M. Chikuma and J. Reedijk, *J. Am. Chem. Soc.*, 2002, **124**, 4738.
- 48 S. L. Woodhouse and L.M. Rendina, *Chem. Commun.*, 2001, 2464; (b) N. J. Wheate, C. Cullinane, L. K. Webster and J. G. Collins, *Anti-Cancer Drug Design*, 2001, 1691.

## Chapter Three

*Extra supplementary data linked to this work is attached to the Appendix.*

### **Tuning the reactivity of chelated dinuclear Pt(II) complexes through a flexible diamine linker. A detailed kinetic and mechanistic study.**

#### **3.0 Abstract**

The rate of displacement of the aqua ligands by three neutral nucleophiles (Nu) of different steric demands, namely thiourea (tu), *N,N'*-dimethylthiourea (dmtu) and *N,N,N',N'*-tetramethylthiourea (tmtu) and an anionic nucleophile (I) in complexes of the form  $[\{\text{Pt}(\text{H}_2\text{O})\}_2(\text{N,N,N',N'}\text{-tetrakis}(2\text{-pyridylmethyl})\text{-N}(\text{CH}_2)_n\text{N})(\text{CF}_3\text{SO}_3)_4, n = 2$  (**En**); 3 (**Prop**); 4 (**But**); 6 (**Hex**); 8 (**Oct**) and 10 (**Dec**), was studied under pseudo first-order conditions as a function of concentration, temperature and pressure using stopped-flow techniques and UV-visible spectrophotometry. The pseudo first-order rate constants,  $k_{\text{obs}(1^{\text{st}}/2^{\text{nd}})}$ , for the simultaneous substitution of the aqua ligands and the proposed subsequent dechelation of the pyridyl units, respectively, agreed well to the rate law:  $k_{\text{obs}(1^{\text{st}}/2^{\text{nd}})} = k_{2(1^{\text{st}}/2^{\text{nd}})}[\text{Nu}]$ . High negative activation entropies, negative volumes of activation and second-order kinetics for the displacement reactions all support an associative mode of activation. Except for **Prop**, the rate of the simultaneous substitution of the aqua ligands in the complexes was found to increase as the chain length of the linker increases from **En** to **Hex**, beyond which any further increase in chain length is not accompanied by a further increase in reactivity. The reactivity trend of the even-bridged complexes with  $C_{2h}$  symmetry is ascribed to a concomitant decrease in axial steric influences imposed on one side of the square-planar picolyl chelates by the other as the chain length increases. Based on the model structures of the complexes, this kind of steric imposition occurs only in complexes with an even number of  $\text{CH}_2$  groups within the linker. The **Prop** complex, having a  $C_{2v}$  symmetry showed exceptional high reactivity towards the nucleophiles. A cage effect, evolving from its bowl-shaped molecular structure, is proposed to explain this high reactivity. The order of reactivity of the nucleophiles increased in the order  $\text{I} \gg \text{tu} \approx \text{dmtu} > \text{tmtu}$ , in line with the strong electrostatic interactions between the highly

# *Pt(II) complexes with $\alpha,\omega$ -alkyldiamine bridges*

---

polarizable iodide nucleophile and the Pt centers, steric retardation effects in the case of tmtu and dominating positive inductive effects for the dmtu nucleophile.

## **3.1 Introduction**

The interaction of platinum based drugs with DNA is now widely accepted as the mechanism responsible for their anti-cancer activity.<sup>1-4</sup> Multinuclear Pt(II) complexes synthesized first by Farrell and his group,<sup>5-8</sup> can form a wide variety of DNA adducts through their diversified structural properties. Specifically, the length of the diamine linker is known to control the relative amounts of interstrand/ intrastrand DNA crosslinks that can be formed by the complexes.<sup>6</sup> This confers them with a wide span of activities relative to the most successful mononuclear anti-cancer drugs, *viz.*, cisplatin, carboplatin and oxaliplatin.

The most successful representative of this class of complexes is BBR3464, [ $\mu$ -*trans*-Pt(NH<sub>3</sub>)<sub>2</sub>{*trans*-PtCl(NH<sub>3</sub>)<sub>2</sub>NH<sub>2</sub>(CH<sub>2</sub>)<sub>6</sub>NH<sub>2</sub>}<sub>2</sub>](NO<sub>3</sub>)<sub>4</sub>, a trinuclear complex with monodentate amine ligands around the Pt centers. It shows remarkable cytotoxicity against pancreatic, lung and melanoma cancers and has already entered phase two of the clinical trials.<sup>9</sup> It has a therapeutic index that is comparable to cisplatin and shows a remarkable lack of resistance in cisplatin-insensitive cell lines.<sup>10</sup> However, it has emerged from the results of recent studies,<sup>7,11,12</sup> that BBR3464 and its analogues, which have monodentate amine ligands around the platinum centers and leaving groups of *trans* geometry to the alkanediamine linker, can be degraded *in vitro* via liberation of the alkanediamine bridge. This happens when strong *trans*-effect ligands like the sulfur containing bio-molecules, whose *in vivo* prevalence is quite notable, substitute the leaving groups on the Pt centers.

Besides this, data in literature lacks coherence in terms of how the bridging diamine linker controls the reactivity of the Pt centers in multinuclear complexes. Recent studies have shown a general increase in reactivity of some  $\alpha,\omega$ -alkanediamine-bridged dinuclear Pt(II) complexes with monodentate<sup>13</sup> amines and bis(2-pyridylmethyl)amine<sup>14</sup> carrier ligands around the Pt centers. This happens when the chain length of the  $\alpha,\omega$ -alkanediamine, a measure of the average distance between their coordination spheres, is reduced.<sup>14</sup> The increase in reactivity was ascribed to an increase in charge addition of the Pt atoms caused by a combination of increased electrostatic interactions with concomitant reduction in the  $\sigma$ -donor capacity towards

## *Pt(II) complexes with $\alpha,\omega$ -alkyldiamine bridges*

---

each Pt atom. In three separate kinetic studies, van Eldik and co-workers<sup>14a-c</sup> studied the substitution of aqua ligands in alkanediamine-bridged dinuclear complexes with a bis(2-pyridylmethyl)amine chelate framework around each Pt atom using anionic<sup>14a,b</sup> and biologically relevant<sup>14c</sup> nucleophiles. In all cases, they reported a similar trend in reactivity as reported by Jaganyi *et al.*<sup>13</sup> for the dinuclear complexes with monodentate amine ligands around the Pt(II) centers. The interactions or lack of it, occurring between the two Pt(II) centers, were found to correlate with the average Pt-Pt distance between them, becoming weaker as the alkanediamine chain length increases. Interestingly, the combined results of the three studies,<sup>14a-c</sup> clearly indicate that complexes bearing alkanediamine bridges with an odd number of CH<sub>2</sub> groups (n = 3, 5, 7) have a superior reactivity gradient per unit increase in CH<sub>2</sub> groups when compared to complexes bridged by an even number of CH<sub>2</sub> groups. This trend has not been fully understood.

More so, a substitution mechanism in which the second observed step is in fact a ring-opening process has been proposed for the decane-bridged complex, in which one of the *cis*-positioned pyridyl arms of the picolyl unit is decoordinated from the Pt(II) centers. This is well supported by <sup>195</sup>Pt NMR data.<sup>14c</sup> However, should this be happening as proposed, it may imply that all the other complexes would necessarily undergo dechelation in their second observed steps bearing in mind reactivity had been reported to increase inversely with chain length according to two of the previous studies. Even though the linkers of the complexes were not completely liberated from the Pt atoms as reported for complexes studied by Summa *et al.*,<sup>11</sup> the results imply that the bis(2-pyridylmethyl)amine chelate core carrier ligand, is partially prone to *cis*-substitutional labilization via dechelation of the picolyl arms by the strong sulfur nucleophiles. However, data available in literature<sup>15,16a</sup> from other studies for the reactions between the sulfur containing nucleophiles and chelated Pt(II) complexes clearly shows that chelation can mitigate the problem of labilization of the *trans*-donor atoms by incoming sulfur containing molecules. In addition, increased chelation at a monomeric Pt(II) center has been shown to enhance reactivity<sup>16b,c</sup> apart from conferring thermodynamic stability.<sup>16d</sup>

One of the many challenges limiting an adequate understanding of the role of the bridging linker on the reactivity of multinuclear Pt(II) complexes is its concomitant structural complexity. The linker serves as an integral part of the core backbone of the carrier ligand

# *Pt(II) complexes with $\alpha,\omega$ -alkyldiamine bridges*

---

framework around each Pt(II) center as well as being the linking structural entity between the Pt(II) centers. It also confers special structural properties on the metal complexes such as structural flexibility (as in an alkanediamine<sup>5-6</sup> linker) and structural rigidity (as in azines,<sup>17</sup> azoles<sup>18</sup> and the dipyrazolylmethane<sup>19</sup>). To gain a full understanding of possible factors controlling reactivity at square-planar Pt(II) centers in multinuclear complexes, one has to perform a systematic study in which all the other structural features within the series of complexes under study are kept constant while the feature of interest is varied.

This work reports on the influence of the bridging alkanediamine linker in dinuclear Pt(II) complexes with a bis(picoyl)amine chelate backbone. The picoyl  $\pi$ -acceptor fragments do not have an ‘electronic linkage’<sup>20</sup> between them since their combined  $\pi$ -conjugation framework is not extended. To accomplish these objectives, six complexes of the type,  $[\{\text{Pt}(\text{H}_2\text{O})\}_2(N,N,N',N'\text{-tetrakis}(2\text{-pyridylmethyl})\text{-N}(\text{CH}_2)_n\text{N})(\text{CF}_3\text{SO}_3)_4]$ ,  $n = 2$  (**En**); 3 (**Prop**); 4 (**But**); 6 (**Hex**); 8 (**Oct**) and 10 (**Dec**) were synthesized. All except **Prop** have even numbers of  $\text{CH}_2$  groups in their alkanediamine bridge. The monomeric analogue to these complexes,  $[\text{Pt}(\text{H}_2\text{O})(N,N\text{-bis}(2\text{-pyridylmethyl})\text{amine})(\text{CF}_3\text{SO}_3)_2]$ , (**bpma**) was also studied under the same experimental conditions.

## **3.2 Experimental**

### **3.2.1 Preparation of ligands**

Ligands **L1** to **L6**, were synthesized following the literature method of Sato *et al.*<sup>21</sup> These were namely,  $N,N,N',N'$ -tetrakis(2-pyridylmethyl)-1,2-ethanediamine (**L1**);  $N,N,N',N'$ -tetrakis(2-pyridylmethyl)-1,3-propanediamine (**L2**);  $N,N,N',N'$ -tetrakis(2-pyridylmethyl)-1,4-butanediamine (**L3**);  $N,N,N',N'$ -tetrakis(2-pyridylmethyl)-1,6-hexanediamine (**L4**);  $N,N,N',N'$ -tetrakis(2-pyridylmethyl)-1,8-octanediamine (**L5**) and  $N,N,N',N'$ -tetrakis(2-pyridylmethyl)-1,10-decanediamine (**L6**).

Colorless crystals (X-ray quality) in the case of **L1**, **L2**, **L3** and **L6** were obtained from solutions of ethanol by slow evaporation of the solvent over several days. For the full structural report of **L2-L4** refer to section 3.7 (Commentary notes) and Appendix A, Paper A2. The other ligands were collected as microcrystalline powders from a suspension of the oils in ethanol. The identity and purity of the compounds was further confirmed by <sup>1</sup>H NMR, <sup>13</sup>C NMR, TOF

## *Pt(II) complexes with $\alpha,\omega$ -alkyldiamine bridges*

---

MS-ES<sup>+</sup> micro analysis and Infrared (IR). The IR spectra of the ligands showed common characteristic peaks at the following frequencies cm<sup>-1</sup>: 2937 (broad, medium, C<sub>sp</sub><sup>3</sup>-H stretch); 1589 (sharp and strong, C<sub>sp</sub><sup>2</sup>=N stretch, pyridyl rings).

**(L1)** Yield: 985 mg (77 %). <sup>1</sup>H NMR (500 MHz, CD<sub>3</sub>OD)  $\delta$  / ppm: 8.39 (td, 4H); 7.72 (td, 4H); 7.52 (d, 4H); 7.25 (td, 4H); 3.31 (m, 4H); 2.69 (s, 8H). IR (KBr, 4000-400 cm<sup>-1</sup>)  $\bar{\nu}$ : 2958-2854 (alkyl C-H stretch); 1589 (C=N, pyridyl). *Anal. Calc. for C<sub>26</sub>H<sub>28</sub>N<sub>6</sub>*: C, 73.56; H, 6.65; N, 19.79. *Found*: C, 73.22; H, 6.72; N, 19.72. MS-ES<sup>+</sup>, m/e: 425.2194 (M + 1)<sup>+</sup>; 447.2259 (M + Na)<sup>+</sup>; 471.3126 (M + 2Na)<sup>+</sup>.

**(L2)** Yield: 833 mg (64 %). <sup>1</sup>H NMR (500 MHz, D<sub>2</sub>O spiked with DCl)  $\delta$  / ppm: 8.60(d, 4H); 8.38 (t, 4H); 7.94 (d, 4H); 7.82 (t, 4H), 4.20 (s, 8H), 2.50 (t, 4H); 1.71(m, 2H). <sup>13</sup>C NMR (125 MHz, D<sub>2</sub>O spiked with DCl)  $\delta$  / ppm: 23.0; 52.5; 55.0; 127.1; 128.0; 128.0; 145.0; 148.0; 154.0. IR (KBr, 4000-400 cm<sup>-1</sup>)  $\bar{\nu}$ : 2958-2854 (alkyl C-H stretch); 1589 (C=N, pyridyl). *Anal. Calc. for C<sub>27</sub>H<sub>30</sub>N<sub>6</sub>*: C, 73.94; H, 6.89; N, 19.17; *Found*: C, 74.08; H, 6.96; N, 19.17. MS-ES<sup>+</sup> m/e: 439.2453 (M + 1)<sup>+</sup>; 461.2428 (M + Na)<sup>+</sup>.

**(L3)** Yield: 1367 mg (67 %). <sup>1</sup>H NMR (500 MHz, CD<sub>3</sub>OD)  $\delta$  / ppm: 8.41 (d, 4H); 7.77 (td, 4H); 7.58 (d, 4H); 7.26 (tt, 4H); 3.31 (m, 8H); 2.45 (s, br, 4H); 1.49 (m, 4H). IR (KBr, 4000-400 cm<sup>-1</sup>)  $\bar{\nu}$ : 2958-2854 (alkyl C-H stretch); 1589 (C=N, pyridyl). *Found: Anal. Calc. for C<sub>28</sub>H<sub>32</sub>N<sub>6</sub>*: C, 74.30; H, 7.13; N, 18.57; *Found*: C, 74.30; H, 7.13; N, 18.53. MS-ES<sup>+</sup>, m/e: 453.2199 (M + 1)<sup>+</sup>; 475.2120 (M + Na)<sup>+</sup>.

**(L4)** Yield: 604 mg (28 %). <sup>1</sup>H NMR (500 MHz, D<sub>2</sub>O)  $\delta$  / ppm: 8.30 (d, 4H); 7.68 (t, 4H); 7.30 (d, 4H); 7.20 (t, 4H); 3.70 (s, br, 4H); 3.40 (m, 8H); 2.00 (s, 4H). IR (KBr, 4000-400 cm<sup>-1</sup>)  $\bar{\nu}$ : 2958-2854 (alkyl C-H stretch); 1589 (C=N, pyridyl). *Anal. Calc. for C<sub>30</sub>H<sub>36</sub>N<sub>6</sub>*: C, 74.96; H, 7.55; N, 17.49; *Found*: C, 74.96; H, 7.52; N, 17.92. m/e: 481.9523 (M + 1)<sup>+</sup>.

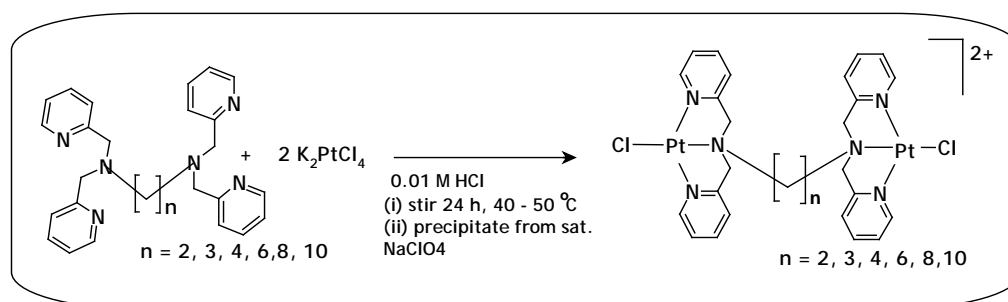
**(L5)** Yield: 996 mg (44 %). <sup>1</sup>H NMR (500 MHz, D<sub>2</sub>O spiked with DCl)  $\delta$  / ppm: 8.50 (d, 4H); 8.26 (t, 4H); 7.82 (d, 4H); 7.70 (t, 4H), 4.15 (s, 8H), 2.45 (t, 4H); 1.20 (m, 4H); 0.85 (m, 8H). <sup>13</sup>C NMR (125 MHz, D<sub>2</sub>O spiked with DCl)  $\delta$  / ppm: 25.0; 26.2; 28.4; 54.8; 55.3; 127.1; 128.0; 142.0; 146.0; 154.2. IR (KBr, 4000-400 cm<sup>-1</sup>)  $\bar{\nu}$ : 2958-2854 (alkyl C-H stretch); (C=N, pyridyl). *Anal. Calc. for C<sub>32</sub>H<sub>40</sub>N<sub>6</sub>*: C, 75.56; H, 7.92; N, 16.52; *Found*: C, 75.80; H, 8.02; N, 16.73. MS-ES<sup>+</sup>, m/e: 509.2449 (M + 1)<sup>+</sup>; 510.2950 (M + 2)<sup>+</sup>; 531.2671 (M + Na)<sup>+</sup>.

# Pt(II) complexes with $\alpha,\omega$ -alkyldiamine bridges

(L6) Yield: 859 mg (35 %).  $^1\text{H}$  NMR (500 MHz,  $\text{D}_2\text{O}$  spiked with DCl)  $\delta$  / ppm: 8.49 (d, 4H); 8.26 (t, 4H); 7.82 (d, 4H); 7.70 (t, 4H), 4.15 (s, 8H), 2.45 (t, 4H); 1.20 (m, 4H); 0.85 (m, 12H).  $^{13}\text{C}$  NMR (125 MHz,  $\text{D}_2\text{O}$  spiked with DCl)  $\delta$  / ppm: 25.0; 26.2; 28.4; 28.5; 54.8; 55.5; 127.1; 128.0; 142.0; 146.0; 154.0. IR (KBr, 4000-400  $\text{cm}^{-1}$ )  $\bar{\nu}$ : 2958-2854 (alkyl C-H stretch); 1589 (C=N, pyridyl). *Anal. Calc.* for  $\text{C}_{34}\text{H}_{44}\text{N}_6$ : C, 76.08; H, 8.26; N, 15.56; *Found*: C, 75.95; H, 8.33; N, 15.54.

## 3.2.2 Synthesis of Pt(II) complexes.

The dinuclear Pt(II) complexes (**1** to **6**), and the mononuclear Pt(II) complex (**7**), listed below were synthesized starting from ligand **L1** to **L6** and *N,N*-bis(2-pyridylmethyl)amine, respectively, following a literature procedure reported by Hofmann *et al.*<sup>14a</sup> The procedure is summarized in Scheme 3a.



**Scheme 3.1** Synthetic scheme followed for the synthesis of dinuclear platinum(II) complexes.

Complexes synthesized and used for this kinetic study were  $[\{\text{Pt}(\text{Cl})\}_2(\text{N},\text{N},\text{N}',\text{N}'\text{-tetrakis}(2\text{-pyridylmethyl})\text{-}1,2\text{-ethanediamine})](\text{ClO}_4)_2$  (**1**);  $[\{\text{Pt}(\text{Cl})\}_2(\text{N},\text{N},\text{N}',\text{N}'\text{-tetrakis}(2\text{-pyridylmethyl})\text{-}1,3\text{-propanediamine})](\text{ClO}_4)_2$  (**2**);  $[\{\text{Pt}(\text{Cl})\}_2(\text{N},\text{N},\text{N}',\text{N}'\text{-tetrakis}(2\text{-pyridylmethyl})\text{-}1,4\text{-butanediamine})](\text{ClO}_4)_2$  (**3**);  $[\{\text{Pt}(\text{Cl})\}_2(\text{N},\text{N},\text{N}',\text{N}'\text{-tetrakis}(2\text{-pyridylmethyl})\text{-}1,6\text{-hexanediamine})](\text{ClO}_4)_2$  (**4**);  $[\{\text{Pt}(\text{Cl})\}_2(\text{N},\text{N},\text{N}',\text{N}'\text{-tetrakis}(2\text{-pyridylmethyl})\text{-}1,8\text{-octanediamine})](\text{ClO}_4)_2$ , (**5**);  $[\{\text{Pt}(\text{Cl})\}_2(\text{N},\text{N},\text{N}',\text{N}'\text{-tetrakis}(2\text{-pyridylmethyl})\text{-}1,10\text{-decanediamine})](\text{ClO}_4)_2$  (**6**) and  $[\text{Pt}(\text{Cl})(\text{N},\text{N}\text{-bis}(2\text{-pyridylmethyl})\text{amine})](\text{ClO}_4)$  (**7**).

## *Pt(II) complexes with $\alpha,\omega$ -alkyldiamine bridges*

---

Their purity was confirmed by  $^1\text{H}$  NMR,  $^{195}\text{Pt}$  NMR, micro analysis and infrared (IR). The IR spectra of all the complexes showed common characteristic peaks in the ranges 320-340  $\text{cm}^{-1}$  (weak) and 1090-1100  $\text{cm}^{-1}$  (broad, strong). These are due to Pt-Cl and Cl-O (perchlorate counter ion) vibrational stretches, respectively. The latter vibrational peaks confirm the cationic nature of the complexes.

(1) Yield: 153.6 mg (59 %).  $^1\text{H}$  NMR (500 MHz, DMF- $d_7$ )  $\delta$  / ppm: 8.78 (d, 4H); 8.33 (td, 4H); 7.77 (t, 8H); 7.72(d, 4H); 5.45 (d, 4H); 5.08 (d, 4H).  $^{195}\text{Pt}$  NMR (107 MHz, DMF- $d_7$ )  $\delta$  / ppm: -2339.3. IR (KBr, 4000-300  $\text{cm}^{-1}$ )  $\bar{\nu}$ : 2958-2854 (alkyl C-H stretch); 1589 (C=N, pyridyl); 1090-1100 (perchlorate counter ion); 324-330 Pt-Cl stretch). *Anal. Calc. for*  $\text{Pt}_2\text{C}_{26}\text{H}_{28}\text{N}_6\text{Cl}_4\text{O}_8$ : C, 28.79; H, 2.60; N, 7.75; *Found*: C, 28.73; H, 2.72; N, 7.90.

(2) Yield: 187.2 mg (71 %).  $^1\text{H}$  NMR (500 MHz, DMF- $d_7$ )  $\delta$  / ppm: 8.71 (dd, 4H); 8.35 (td, 4H); 7.76 (d, 8H); 5.40 (d, 4H); 4.98 (d, 4H); 3.20 (m, 4H); 2.30 (m, 4H).  $^{195}\text{Pt}$  NMR (107 MHz, DMF- $d_7$ )  $\delta$  / ppm: -2344.8. IR (KBr, 4000-300  $\text{cm}^{-1}$ )  $\bar{\nu}$ : 2958-2854 (alkyl C-H stretch); 1589 (C=N, pyridyl); 1090-1100 (perchlorate counter ion); 324-330 (Pt-Cl stretch). *Anal. Calc. for*  $\text{Pt}_2\text{C}_{27}\text{H}_{30}\text{N}_6\text{Cl}_4\text{O}_8$ : C, 29.51; H, 2.75; N, 7.65; *Found*: C, 29.12; H, 2.95; N, 7.48.

(3) Yield: 213.6 mg (81 %).  $^1\text{H}$  NMR (500 MHz, DMF- $d_7$ )  $\delta$  / ppm: 8.85 (d, 4H); 8.34 (td,4H);7.81 (d, 4H); 7.75 (t, 4H); 5.40 (d, 4H); 4.90 (d, 4H); 3.55 (s(br), 4H); 2.15 (s (br), 4H).  $^{195}\text{Pt}$  NMR (107 MHz, DMF- $d_7$ )  $\delta$  / ppm: -2348.8. IR (KBr, 4000-300  $\text{cm}^{-1}$ )  $\bar{\nu}$ : 2958-2854 (alkyl C-H stretch); 1589 C=N, (pyridyl); 1090-1100 (perchlorate counter ion); 324-330 Pt-Cl stretch). *Anal. Calc. for*  $\text{Pt}_2\text{C}_{28}\text{H}_{30}\text{N}_6\text{Cl}_4\text{O}_8$ : C, 30.22; H, 2.89; N, 7.55; *Found*: C, 30.38; H, 2.93; N, 7.50.

(4) Yield: 211.3 mg (77 %).  $^1\text{H}$  NMR (500 MHz, DMF- $d_7$ )  $\delta$  / ppm: 9.00 (d, 4H); 8.40 (td,4H);7.90 (d, 4H); 7.80 (t, 4H); 5.40 (d, 4H); 5.00 (d, 4H); 3.15 (s(br), 4H); 1.60 (s (br), 4H); 1.10 (s (br), 4H).  $^{195}\text{Pt}$  NMR (107 MHz, DMF- $d_7$ )  $\delta$  / ppm: -2347.0. IR (KBr, 4000-300  $\text{cm}^{-1}$ )  $\bar{\nu}$ : 2958-2854 (alkyl C-H stretch); 1589 C=N, (pyridyl); 1090-1100 (perchlorate counter ion); 324-330 (Pt-Cl stretch). *Anal. Calc. for*  $\text{Pt}_2\text{C}_{30}\text{H}_{36}\text{N}_6\text{Cl}_4\text{O}_8$ : C, 31.58; H, 3.18; N, 7.36; *Found*: C, 31.14; H, 3.11; N, 7.22.

## *Pt(II) complexes with $\alpha,\omega$ -alkyldiamine bridges*

---

(5) Yield: 230.0 mg (82 %).  $^1\text{H}$  NMR (500 MHz, DMF- $d_7$ )  $\delta$  / ppm: 9.05 (d, 4H); 8.40 (td, 4H); 7.92 (d, 4H); 7.80 (t, 4H); 5.45 (d, 4H); 5.12 (d, 4H); 3.20 (s(br), 4H); 1.60 (s (br), 4H); 1.10 (s (br), 8H).  $^{195}\text{Pt}$  NMR (107 MHz, DMF- $d_7$ )  $\delta$  / ppm: -2345.6. IR (KBr, 4000-300  $\text{cm}^{-1}$ )  $\bar{\nu}$ : 2958-2854 (alkyl C-H stretch); (1589 (C=N, pyridyl); 1090-1100 (perchlorate counter ion); 324-330 (Pt-Cl stretch). *Anal. Calc. for*  $\text{Pt}_2\text{C}_{32}\text{H}_{40}\text{N}_6\text{Cl}_4\text{O}_8$ : C, 32.88; H, 3.44; N, 7.19; *Found*: C, 32.41; H, 3.38; N, 7.22.

(6) Yield: 273 mg (95 %).  $^1\text{H}$  NMR (500 MHz, DMF- $d_7$ )  $\delta$  / ppm: 9.05 (d, 4H); 8.40 (td, 4H); 7.94 (d, 4H); 7.79 (t, 4H); 5.45 (d, 4H); 5.10 (d, 4H); 3.20 (s (br), 4H); 2.15 (s, 4H); 1.65 (s (br), 4H); 1.10 (s (br), 8H).  $^{195}\text{Pt}$  NMR (107 MHz, DMF- $d_7$ )  $\delta$  / ppm: -2346.9. IR (KBr, 4000-300  $\text{cm}^{-1}$ )  $\bar{\nu}$ : 2958-2854 (alkyl C-H stretch); 1589 (C=N, pyridyl); 1090-1100 (perchlorate counter ion); 324-330 (Pt-Cl stretch). *Anal. Calc. for*  $\text{Pt}_2\text{C}_{34}\text{H}_{44}\text{N}_6\text{Cl}_4\text{O}_8$ : C, 34.12; H, 3.70; N, 7.02; *Found*: C, 34.12; H, 3.79; N, 6.93.

(7) Yield: 228.4 mg (90 %).  $^1\text{H}$  NMR (400 MHz, DMF- $d_7$ )  $\delta$  / ppm: 9.05 (d, 2H); 8.50 (t, 2H); 8.05 (d, 2H); 7.79 (t, 2H); 5.3 (d,d, 2H); 5.10 (d,d 2H).  $^{13}\text{C}$  NMR (125 MHz,  $\text{CDCl}_3$ )  $\delta$  / ppm: 60; 123.0; 126.0; 142.0; 149.0; 168.  $^{195}\text{Pt}$  NMR (107 MHz, DMF- $d_7$ )  $\delta$  / ppm: -2340. IR (KBr, 4000-300  $\text{cm}^{-1}$ )  $\bar{\nu}$ : 2958-2854 (alkyl C-H stretch); 1589 (C=N, pyridyl); 1090-1100 (perchlorate counter ion); 324-330 (Pt-Cl stretch). *Anal. Calc. for*  $\text{PtC}_{12}\text{H}_{13}\text{N}_3\text{Cl}_2\text{O}_4$ : C, 27.23; H, 2.48; N, 7.94; *Found*: C, 27.43; H, 2.52; N, 8.03.

### **3.2.3 Preparation of Pt(II) aqua complexes and nucleophiles solutions.**

The kinetic solutions namely,  $[\{\text{Pt}(\text{H}_2\text{O})\}_2(N,N,N',N'$ -tetrakis(2-pyridylmethyl)-1,2-ethanediamine)] $(\text{CF}_3\text{SO}_3)_4$ , **En**;  $[\{\text{Pt}(\text{H}_2\text{O})\}_2(N,N,N',N'$ -tetrakis(2-pyridylmethyl)-1,3-propanediamine)] $(\text{CF}_3\text{SO}_3)_4$ , **Prop**;  $[\{\text{Pt}(\text{H}_2\text{O})\}_2(N,N,N',N'$ -tetrakis(2-pyridylmethyl)-1,4-butanediamine)] $(\text{CF}_3\text{SO}_3)_4$ , **But**;  $[\{\text{Pt}(\text{H}_2\text{O})\}_2(N,N,N',N'$ -tetrakis(2-pyridylmethyl)-1,6-hexanediamine)] $(\text{CF}_3\text{SO}_3)_4$ , **Hex**;  $[\{\text{Pt}(\text{H}_2\text{O})\}_2(N,N,N',N'$ -tetrakis(2-pyridylmethyl)-1,8-octanediamine)] $(\text{CF}_3\text{SO}_3)_4$ , **Oct**;  $[\{\text{Pt}(\text{H}_2\text{O})\}_2(N,N,N',N'$ -tetrakis(2-pyridylmethyl)-1,10-decanediamine)] $(\text{CF}_3\text{SO}_3)_4$ , **Dec** and  $[\text{Pt}(\text{H}_2\text{O})(N,N$ -bis(2-pyridylmethyl)amine)] $(\text{CF}_3\text{SO}_3)_2$ , **bpma** were prepared following a literature procedure of Bugarčić *et al.*<sup>22</sup> The chemical structures of the dinuclears are shown in Figure 3.1 below.

## Pt(II) complexes with $\alpha,\omega$ -alkyldiamine bridges

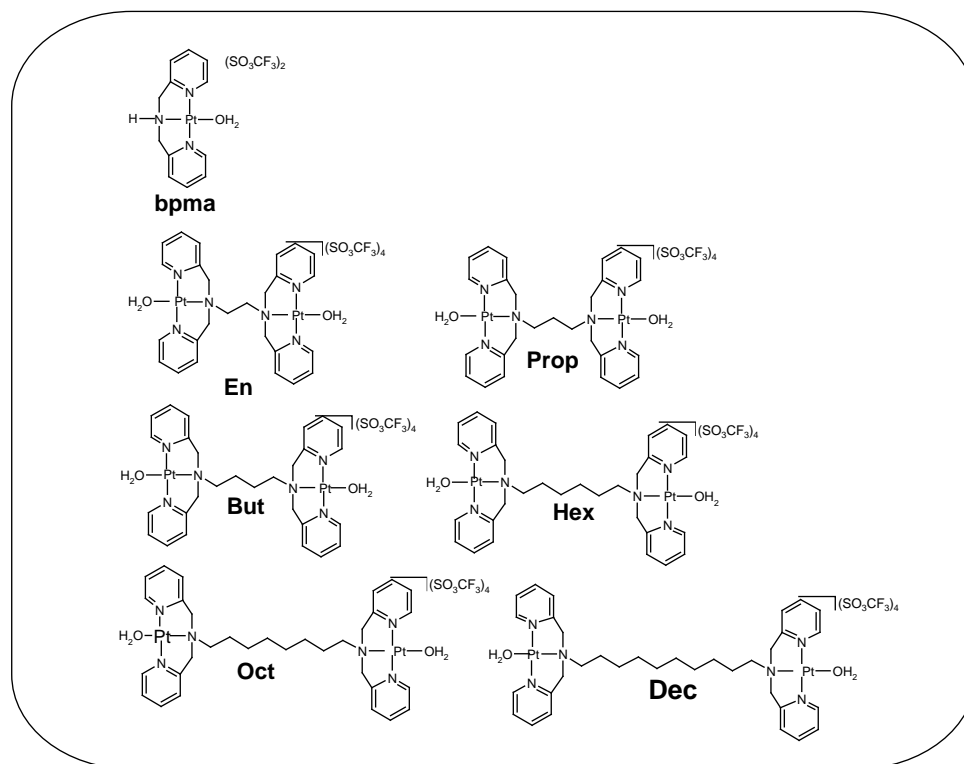


**Figure 3.1** Chemical structures of the  $[\{Pt(H_2O)\}_2(N,N,N',N'$ -tetrakis(2-pyridylmethyl)- $\alpha,\omega$ -alkyldiamines)](CF<sub>3</sub>SO<sub>3</sub>)<sub>4</sub> complexes.

To a suspension of about 0.5 mmol of the  $[\{Pt(Cl)\}_2(N,N,N',N'$ -tetrakis{(2-pyridylmethyl)-N(CH<sub>2</sub>)<sub>n</sub>N-}(ClO<sub>4</sub>)<sub>2</sub>, n = 2, 3, 4, 6, 8 and 10, in a 50 ml solution of 0.001 M CF<sub>3</sub>SO<sub>3</sub>H was added AgSO<sub>3</sub>CF<sub>3</sub> (1.99 mol. equivalents of the complex) dissolved in 0.01 M CF<sub>3</sub>SO<sub>3</sub>H (10 mL) and the mixture left to stir for 24 h at 50 °C in the dark. The silver chloride precipitate that formed was removed by filtering the mixture through a 0.45  $\mu$ m nylon membrane filter (Millipore) and the resultant filtrate was made up to the 100 mL volume mark with a 0.01 M CF<sub>3</sub>SO<sub>3</sub>H solution whose ionic strength had been adjusted to 0.02 M with LiSO<sub>3</sub>CF<sub>3</sub>. For the preparation of the **bpma** solution, the same procedure was followed using a 0.98 mol. equivalent of AgSO<sub>3</sub>CF<sub>3</sub>. Similarly, solutions of the nucleophiles, *viz.*, thiourea (tu), *N,N'*-dimethylthiourea (dmtu) and *N,N,N',N'*-tetramethylthiourea (tmtu) and iodide (I<sup>-</sup>) were prepared by dissolving known amounts of the nucleophiles in a 0.01 M CF<sub>3</sub>SO<sub>3</sub>H solution whose ionic strength had been adjusted to 0.02 M (LiSO<sub>3</sub>CF<sub>3</sub>).

## *Pt(II) complexes with $\alpha,\omega$ -alkyldiamine bridges*

---

### **3.2.4 Instrumentation and spectrophotometric measurements.**

Either a Bruker Avance DPX 500 or DPX 400 NMR spectrometer was used to follow the reactions of **bpma-Cl**, **Prop-Cl** and **Dec-Cl** with tu as well as to confirm the identity and purity of both the ligands and complexes. The kinetic experiments were initiated by mixing the chloride derivatives of the respective complexes with two (**bpma-Cl**) or three equivalents (dinuclear complexes) in an NMR tube at 25 °C. Elementary compositions of the ligands and complexes were determined on a Carlo Erba Elemental Analyzer 1106. Infrared spectra of all the compounds were recorded in the range 4000-300 cm<sup>-1</sup> on a Spectrum One FT-IR as KBr pellets. UV-visible spectra and kinetic measurements of slow reactions were recorded on a Cary 100 Bio UV-visible spectrophotometer with a cell compartment thermostated by a Varian Peltier temperature controller having an accuracy of  $\pm 0.05$  °C. The pH measurements were recorded on a Jenway 4330 pH meter with a combined Jenway glass microelectrode that had been calibrated with standard buffer solutions of pH 4.0, 7.0 and 10.0 (Merck). The KCl solution in the reference electrode was replaced with a 3 M NaCl electrolyte to prevent precipitation of KClO<sub>4</sub> during use.<sup>23,20a</sup> Kinetic measurements of fast reactions were monitored using an Applied Photophysics SX.18 MV (v4.33) stopped-flow reaction analyzer coupled to an online data acquisition system. The temperature of the instrument was controlled to within  $\pm 0.1$  °C.

### **3.2.5 Determination of $pK_a$ of aqua Pt(II) complexes.**

All pH measurements were made separately outside the stock solution. Small vials were used for sampling out aliquots (3 ml) of the aqua complex. After pH measurements, the complex was discarded to avoid its *in situ* precipitation as a chloro-derivative. The solution was titrated with NaOH within the pH range of 2 - 9. An example of the spectral changes recorded during the titration is shown for **En** in Figure 1. To avoid dilution effects due to addition of titrant, a large volume (250 mL) of metal complex was used for titration and small granules of crushed pellets were used within the pH range of 2 - 3. The NaOH solutions of decreasing concentrations were used in a manner that ensured that as many evenly distributed points were collected on the rising or falling sections of the titration curve. After each addition of titrant, the solution was stirred before its pH and respective spectrum were recorded. The

## *Pt(II) complexes with $\alpha,\omega$ -alkyldiamine bridges*

---

sample aliquots from each absorbance measurement were returned back to the stock solution after use. On addition of solutions of decreasing concentrations of  $\text{CF}_3\text{SO}_3\text{H}$  as titrant, the reversibility of the titration reaction was observed with the baseline remaining intact.

### **3.2.6 Kinetic measurements.**

All substitution reactions were performed under pseudo first-order conditions. The nucleophiles were provided in concentrations of at least a 20-fold excess over that of the dinuclear Pt(II) complexes in all reactions. This afforded at least a 10-fold excess concentration of the nucleophiles at each Pt center which is considered sufficient to force the reactions to go to completion. Similarly for **bpma**, a 10-fold excess of concentration of nucleophiles over that of the metal complex was provided. A pH of 2.0 and an ionic strength of 0.02 M were maintained throughout the kinetic runs. All the wavelengths at which kinetic measurements were performed were predetermined spectrophotometrically by monitoring the change in absorbance of the mixture of the complex and the nucleophile as a function of time. These are summarized as ESI in Table SI 3.1.

The temperature dependence of the observed rate constants for all reactions was studied within the range 15-35 °C. Kinetic measurements at elevated pressure (1-130 MPa) were performed on an in-house constructed high pressure stopped-flow instrument.<sup>24</sup> Only the first and faster reaction step involving reactions of all the dinuclear complexes with tu and tmtu nucleophiles was studied.

### **3.2.7 Computational details.**

Density functional theoretical (DFT)<sup>25</sup> calculations were performed with the Spartan '04 for Windows quantum chemical package<sup>26</sup> using the B3LYP,<sup>27</sup> a three parameter hybrid functional method, utilizing the LACVP+\*\*<sup>28</sup> pseudo-potentials basis set. The dinuclear complexes and the monomeric **bpma** were all modeled as cations of a total charge of +4 and +2, respectively. In addition to the synthesized complexes, the calculations were extended to include two other dinuclear complexes bridged by alkyldiamine linkers with five- (**Pen**) and seven- $\text{CH}_2$  groups (**Hep**).

# *Pt(II) complexes with $\alpha,\omega$ -alkyldiamine bridges*

## 3.3 Results.

### 3.3.1 Acid-base equilibria of the aqua Pt(II) complexes.

Figure 3.2 shows a typical example of the spectral changes observed during the titration of the **En** complex with NaOH. All spectra recorded in each titration passes through three isosbestic points (see also Figure SI 3.1, ESI, for **Oct**). The  $pK_a$  values for the complexes were determined from the titration traces taken at specific wavelengths from their repetitive spectra acquired during the pH changes. A representative spectral plot is shown as an inset in Figure 3.2. In the acidic range, the spectra of all the dinuclear complexes are characterized by a sharp maximum absorption band centred on 267 nm.

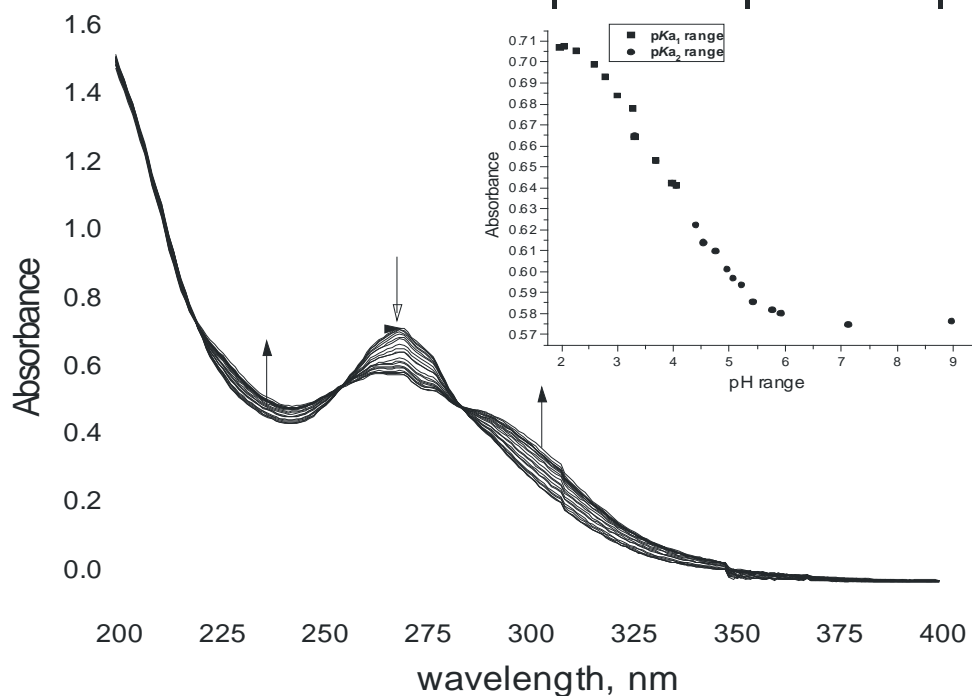


**Figure 3.2** UV-visible spectrum for the titration of 0.1 mM **En** with NaOH, pH range 2 - 9, T 298 K. Inset the titration curve at 268 nm.

The absorption peaks of all the complexes are similar in shape and comparable to those reported<sup>29</sup> for the mononuclear complex, [Pt(H<sub>2</sub>O)bis(2-pyridylmethyl)amine](CF<sub>3</sub>SO<sub>3</sub>)<sub>2</sub>, (**bpma**) under similar prevailing conditions. On titration with NaOH the peaks in the 266-268

## *Pt(II) complexes with $\alpha,\omega$ -alkyldiamine bridges*

nm range gradually decrease while the shoulders in the 276-278 nm range grow slightly in size. An additional broader shoulder peak appear in the range 300-305 nm during the course of the titration, as more and more of the hydroxo species of the complexes are formed.

The data was fitted to a standard equation for measuring two  $pK_a$  values using the Origin 7.5<sup>®30</sup> software. The titration data for all dinuclear complexes except for **Dec** fitted better to the equation describing two  $pK_a$  values. The data obtained including the value for **bpma**<sup>31a</sup> is presented in Table 3.1.

**Table 3.1** Summary of  $pK_a$  data obtained for the deprotonation of Pt-bound aqua ligands (within pH range 2 - 9), using NaOH as titrant.

		<b>En</b>	<b>Prop</b>	<b>But</b>	<b>Hex</b>	<b>Oct</b>	<b>Dec</b>
<b><math>pK_{a1}</math></b>	5.49 <sup>‡</sup>	3.31 ± 0.19	3.95 ± 0.10	4.07 ± 0.05	4.64 ± 0.17	4.23 ± 0.11	4.53 ± 0.07
<b><math>pK_{a2}</math></b>		4.31 ± 0.29	6.30 ± 0.04	5.26 ± 0.06	5.68 ± 0.07	5.59 ± 0.11	-

The titration data for the complexes were fitted to equation,  $y = a + (b-a)/(1+2.718^{((x-pK_{a1})/m)+(c-b)/(1+2.718^{((x-pK_{a2})/n))})$ , for measuring two  $pK_a$  values or the Boltzmann equation,  $y = A_2 + (A_1-A_2)/(1 + \exp((x-x_0)/dx))$ , for measuring one  $pK_a$  value using the Origin 7.5<sup>®</sup> program. <sup>‡</sup>Data quoted from Ref. 30.

Data in Table 3.1 shows that when the  $pK_a$  value of **bpma** is taken as the reference, the first  $pK_a$  values of all the dinuclear complexes are at least one pH unit lower than that of **bpma**. While the first  $pK_a$  values for complexes with longer bridges, viz., **Hex**, **Oct** and **Dec** are statistically constant, it is noted that the first  $pK_a$  values increases proportionally from 3.31 to 4.64 as the chain length of the linker is increased from **En** to **Hex** with the exception of **Prop**. It is also noted that the deprotonation of the second aqua ligand to form the hydroxo/hydroxo species occurs at higher pH values than that of the first.

### **3.3.2 Computational calculations.**

In order to gain an in-depth understanding of the structural as well as the electronic differences that exist in the complexes under study, we performed computational calculations and representative geometry-optimized structure for the **bpma**; **En**; **Prop** and **Dec** complexes and an extract of the calculated data is presented in Tables 3.2 and 3.3, respectively. The minimum energy structures of the included odd-bridged complexes (**Pen** and **Hep**) are

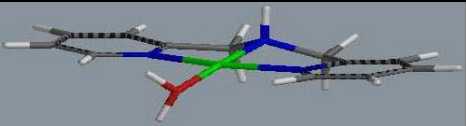
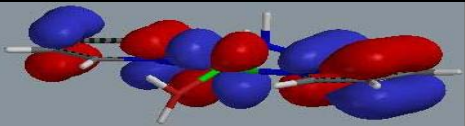
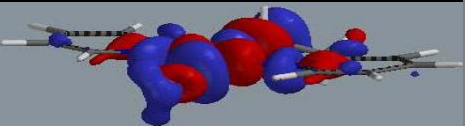
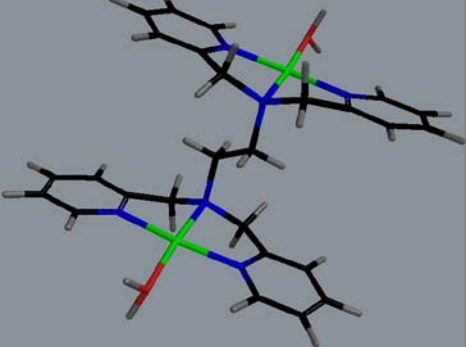
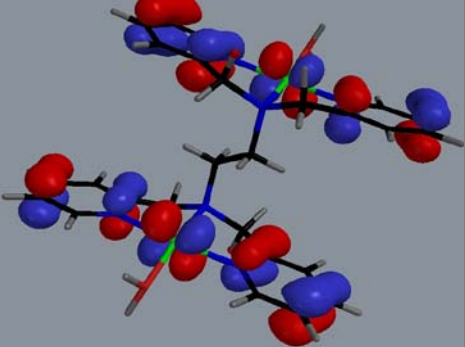
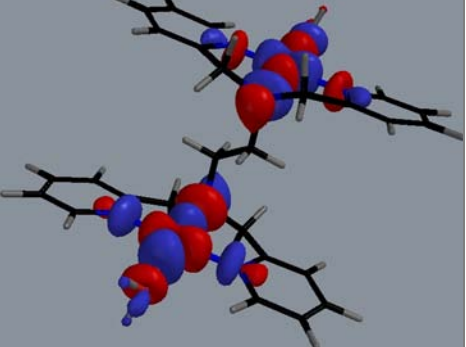
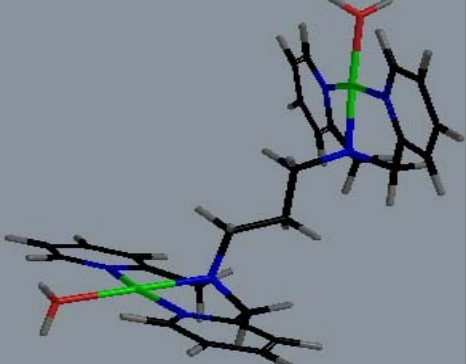
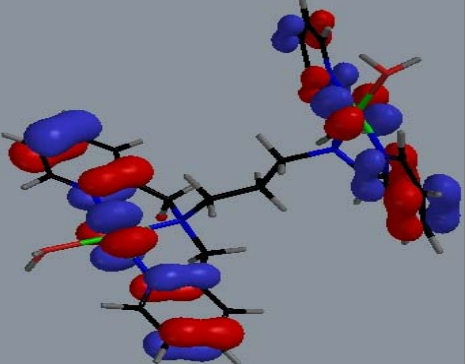
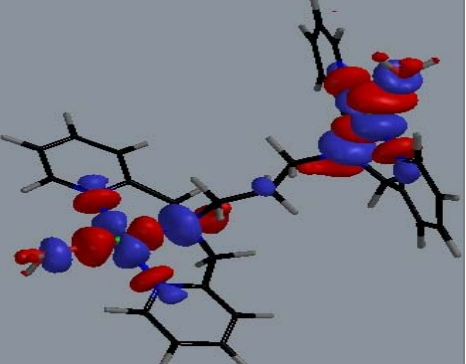
## *Pt(II) complexes with $\alpha,\omega$ -alkyldiamine bridges*

---

provided as ESI in Table SI 3.6. The mappings of the electron density on the electrostatic potential surfaces for the complexes are shown in Table SI 3.7.

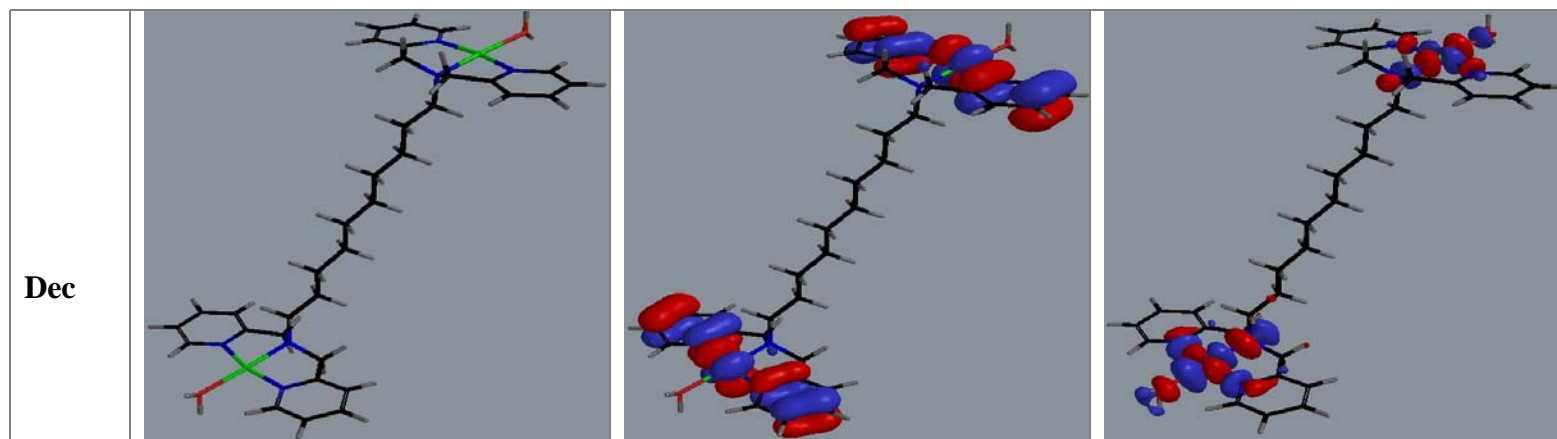
## *Pt(II) complexes with $\alpha,\omega$ -alkyldiamine bridges*

**Table 3.2** Density functional theoretical (DFT)<sup>25</sup> minimum energy structures, HOMO and LUMO frontier molecular orbitals for **bpma**, **En**, **Prop** and **Dec**. The calculations were performed with the Spartan '04 for Windows quantum chemical package<sup>26</sup> using the B3LYP hybrid functional method<sup>27</sup> utilizing the LACVP+\*\*<sup>28</sup> pseudopotentials basis set.

	Structure	HOMO Map	LUMO Map
<b>bpma</b>			
<b>En</b>			
<b>Prop</b>			

## *Pt(II) complexes with $\alpha,\omega$ -alkyldiamine bridges*

---



## *Pt(II) complexes with $\alpha,\omega$ -alkyldiamine bridges*

**Table 3.3** Summary of the calculated structural data at the DFT<sup>25</sup> Level of Theory for the complexes with bis(2-pyridylmethyl)amine chelates.

Property	bpma	En	Prop	But	Pen	Hex	Hep	Oct	Dec
<b>Bond lengths, Å</b>									
Pt-OH <sub>2</sub>	2.151	2.140	2.141	2.143	2.149	2.149	1.214	2.155	2.157
Pt-N <sub>trans</sub>	2.012	2.052	2.057	2.054	2.049	2.049	2.043	2.045	2.042
<b>Separation distance, Å</b>									
Pt <sub>1 coord. plane</sub> - Pt <sub>2 coord. plane</sub> <sup>†</sup>		3.63		4.28		5.84		7.39	9.16
<b>Bond angles, °</b>									
N <sub>cis</sub> -Pt-N <sub>cis</sub>	165.75	166.31	167.03	167.07	166.93	166.95	166.81	166.95	166.73
Pt <sub>1</sub> -N <sub>1 trans</sub> -N <sub>2 trans</sub>		105.80	137.85	134.50	142.9	135.76	148.4	136.51	135.37
$\beta$			124.0		139.8		160.8		
Elevation angle of bridge, $\alpha$ <sup>‡</sup>		74.20		45.50		44.24		43.49	44.57
Inclination angle of aqua ligands	10.69	19.50	14.85	16.74	13.85	16.11	13.37	15.36	14.85
<b>Energy gap, eV.</b>									
$\Delta E_{\text{LUMO-HOMO}}$	5.23	5.00	4.99	5.07	5.12	5.14	5.18	5.18	5.19
<b>Natural charges</b>									
Pt <sub>(1/2)</sub>	1.218	1.220	1.223	1.222	1.218	1.217	1.214	1.213	1.211
<b>Point group symmetry of the complex</b>	<i>C</i> <sub>2v</sub>	<i>C</i> <sub>2h</sub>	<i>C</i> <sub>2h</sub>						

<sup>†</sup> $\alpha$  is the supplementary angle to the angle {Pt1-N1<sub>trans</sub>-N2<sub>trans</sub>} in complexes with *C*<sub>2h</sub> symmetry. The projected separation distance between the first coordination plane and the second (Pt<sub>1 coord. plane</sub> - Pt<sub>2 coord. plane</sub>)<sup>†</sup> was calculated using  $\alpha$  and the length of the linker (N<sub>1 trans</sub>-N<sub>2 trans</sub>) as depicted in structures of **En** and **Dec** in Figure 3.3 while the angle  $\beta$ , subtended by the overlooking faces of the chelate was estimated as illustrated for the structure of **Prop** in the same Figure.

## *Pt(II) complexes with $\alpha,\omega$ -alkyldiamine bridges*

---

The model structures in Table 3.2 reveals that when the number of CH<sub>2</sub> groups in the linker is even, the structures adopt the C<sub>2h</sub> point group symmetry, whereas a C<sub>2v</sub> symmetry is preferred for **Prop** and its two other analogues with an odd number of carbon atoms in the diamine bridge (**Pen** and **Hep**, Table SI 3.5, ESI). The pertinent angles to the structural metrics of the complexes are depicted in Figure 3.3 for **En**, **Prop** and **Dec**.

The geometry about the Pt atoms is slightly distorted square-planar.<sup>31b</sup> The coordinated aqua ligands in **En** are 19.5° out of plane, while the aqua ligand in the **bpma** complex is tilted by only 10.69°, a value which compares well to a measured value of 10.51° for [Pt(*N,N*-bis(2-pyridylmethyl)amine)(H<sub>2</sub>O)]ClO<sub>4</sub>·2H<sub>2</sub>O, retrieved from the Cambridge Crystallographic database.<sup>31b</sup> However, on extending the length of the linker to **Dec** the angling decreases to 14.85°. Due to some moderate flexibility introduced by the methylene carbons of the picolyl units in the chelate framework, overcrowding around the Pt atom is averted by assuming an out-tipped conformation of the tertiary nitrogen atoms relative to the plane containing the atoms of Pt and picolyl units. This causes the angling down of the terminal aqua ligands. The increase in the angling out of the aqua ligands of all the dinuclear complexes when compared to **bpma**, is a clear sign that the PtN<sub>3</sub> coordination plane is under steric strain on one of its sides, which originate from the bridging linker. The magnitude of this strain depends on the angle of inclination,  $\alpha$ , as well as the length of the linker, decreasing from the vertically inclined shorter linker in **En** (74.2°) to the less inclined linker of **Dec** (44.6°). These inclination angles are referenced to the mean plane containing the Pt(II) atom and the atoms of the picolyl units as illustrated in the DFT calculated structures of **En** and **Dec** in Figure 3.3. A similar angle for the complexes with odd numbers of CH<sub>2</sub> groups in the linker (**Prop**, **Pen**, and **Hep**) could not be determined because of the shape of the structures they adopted.

## *Pt(II) complexes with $\alpha,\omega$ -alkyldiamine bridges*

---

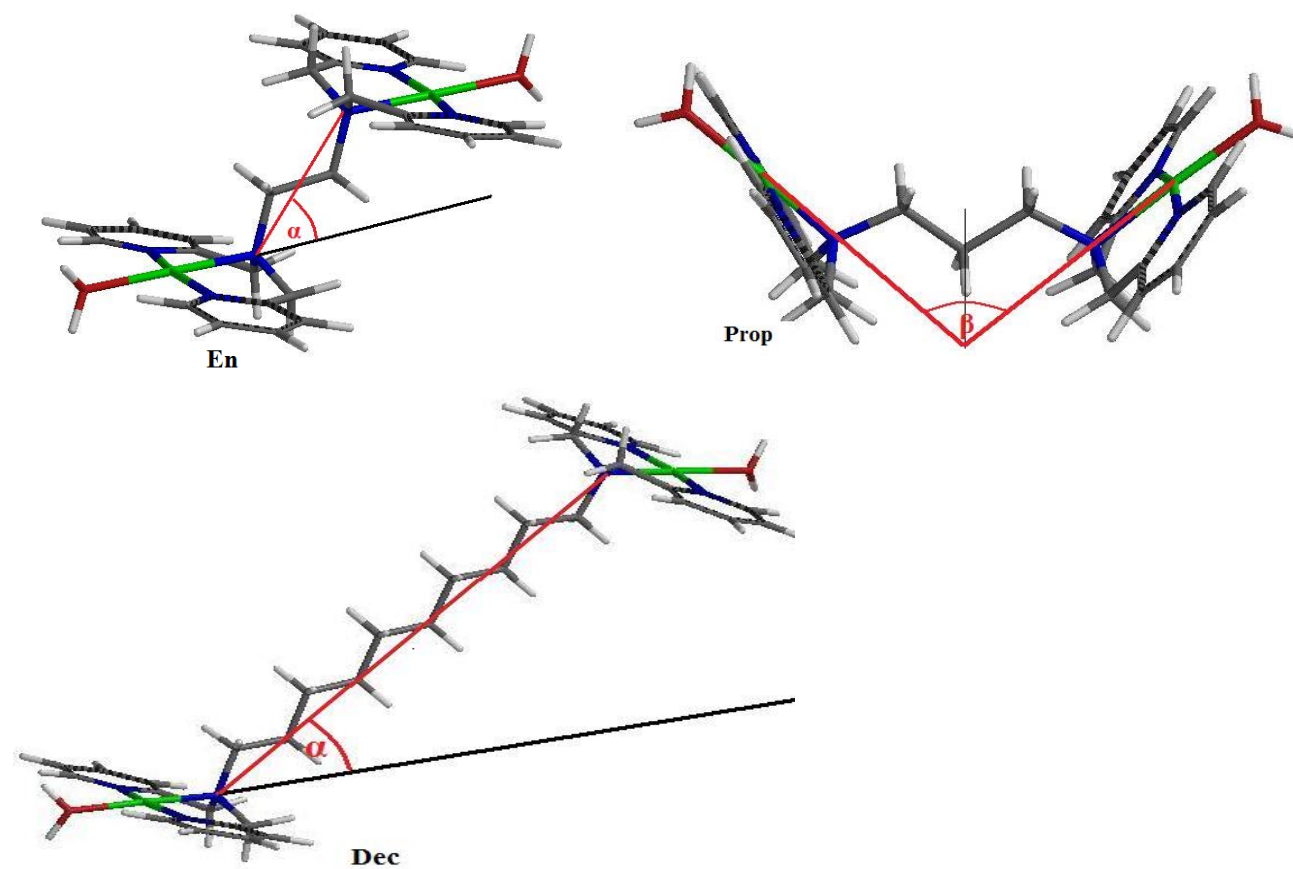


**Figure 3.3** Aerial view showing the angles of inclination,  $\alpha$ , in the DFT calculated slip-up sandwich structures of **En** and **Dec** and the hinge angle,  $\beta$ , of the bowl structure of **Prop**.

## *Pt(II) complexes with $\alpha,\omega$ -alkyldiamine bridges*

---

The mappings of the frontier orbitals (Table 3.2) are similar for all the complexes. The HOMO orbitals are concentrated on the pyridyl  $\pi$ -acceptor carrier ligands and shared with the Pt(II) metal ions. However, the LUMO is centred primarily on the metal center and the donor atoms of the chelating ligands. Both frontier orbitals have no electron density mapping within the linker piece. The similarity in the locations of the HOMO orbitals in these complexes is consistent with an effective  $\pi$ -back donation of electron density from the metal center into the two pyridyl units of the chelate due to their strong  $\pi$ -acceptability.<sup>20</sup> However, a general increase in the energy gap  $\Delta E_{(\text{HOMO-LUMO})}$ , of the frontier orbitals is observed as the chain length is increased. It is also noted that the Pt atoms in all dinuclear complexes carry symmetrical non-bonding orbital (NBO) charges suggesting that the metal centers are in the same electronic environment. However, the variation of the calculated charges with chain length is not linear as would be predicted on the basis of  $\sigma$ -inductive effects due to the linker towards the Pt atoms.

### **3. 3. 3 Kinetic measurements.**

The substitution of the aqua ligands in dinuclear Pt(II) complexes with bis(2-pyridylmethyl)amine chelates and in the monomeric analogue, **bpma**, by the thiourea nucleophiles and iodide occurs through two well separated steps, *viz.*, the simultaneous substitution of the coordinated aqua ligands and the dechelation of the *cis*-pyridyl ligands, as reported in previous studies<sup>14a-c</sup> for the former complexes.

Two observations stimulated this generalization. Firstly, it can be noted that the substitution of the coordinated aqua ligands in **Dec** can be fitted to two separate exponential functions despite the deprotonation equilibria showing a single  $\text{p}K_{\text{a}}$  value. This anomaly had been observed before,<sup>14b</sup> where the substitution of aqua ligands in **Dec** by a chloride anion could be fitted both to a single as well as a double exponential fit. However, using <sup>195</sup>Pt NMR and thiourea as the nucleophile, clear cut evidence of dechelation of the pyridyl units was confirmed,<sup>14c</sup> suggesting that the substitution of the coordinated aqua ligands on the Pt metal centers in **Dec**, occurs simultaneously. Thus, the second step observed in the former studies<sup>14b,c</sup> and confirmed in this study for this complex, can only be reasonably ascribed to the dechelation of one of the coordinated pyridyl ligands by the incoming nucleophiles.

## *Pt(II) complexes with $\alpha,\omega$ -alkyldiamine bridges*

---

Secondly, a second substitution step for the reaction between monomeric **bpma** and the thiourea nucleophiles which slowly reached equilibrium was observed. A representative of the time-resolved kinetic trace showing the two separate substitution steps is shown in Figure SI 3.2a (ESI) for the reaction between **bpma** (0.1 mM) and tu (3 mM). In all reported ligand substitution reactions for this complex using sulfur containing nucleophiles<sup>20,23,30,32a,33</sup> as well as anionic sulfur nucleophiles<sup>14a,32b,33</sup> as entering groups, nothing was mentioned about this second and slower substitution step. Thus, these two anomalous observations are in line with a mechanism consistent with ring opening as the second and slower observed step in both the **bpma** and **Dec** complexes.

To further confirm this, we studied the substitution reactions of three of the complexes, *viz.*, **bpma-Cl**, **Prop-Cl** and **Dec-Cl**, using <sup>1</sup>H NMR spectroscopy. An array of the <sup>1</sup>H NMR spectra (showing only the aromatic resonances) for the reaction between **bpma-Cl** and two equivalents of tu (in DMF-*d*7) is shown in Figure 3.4.

# Pt(II) complexes with $\alpha,\omega$ -alkyldiamine bridges

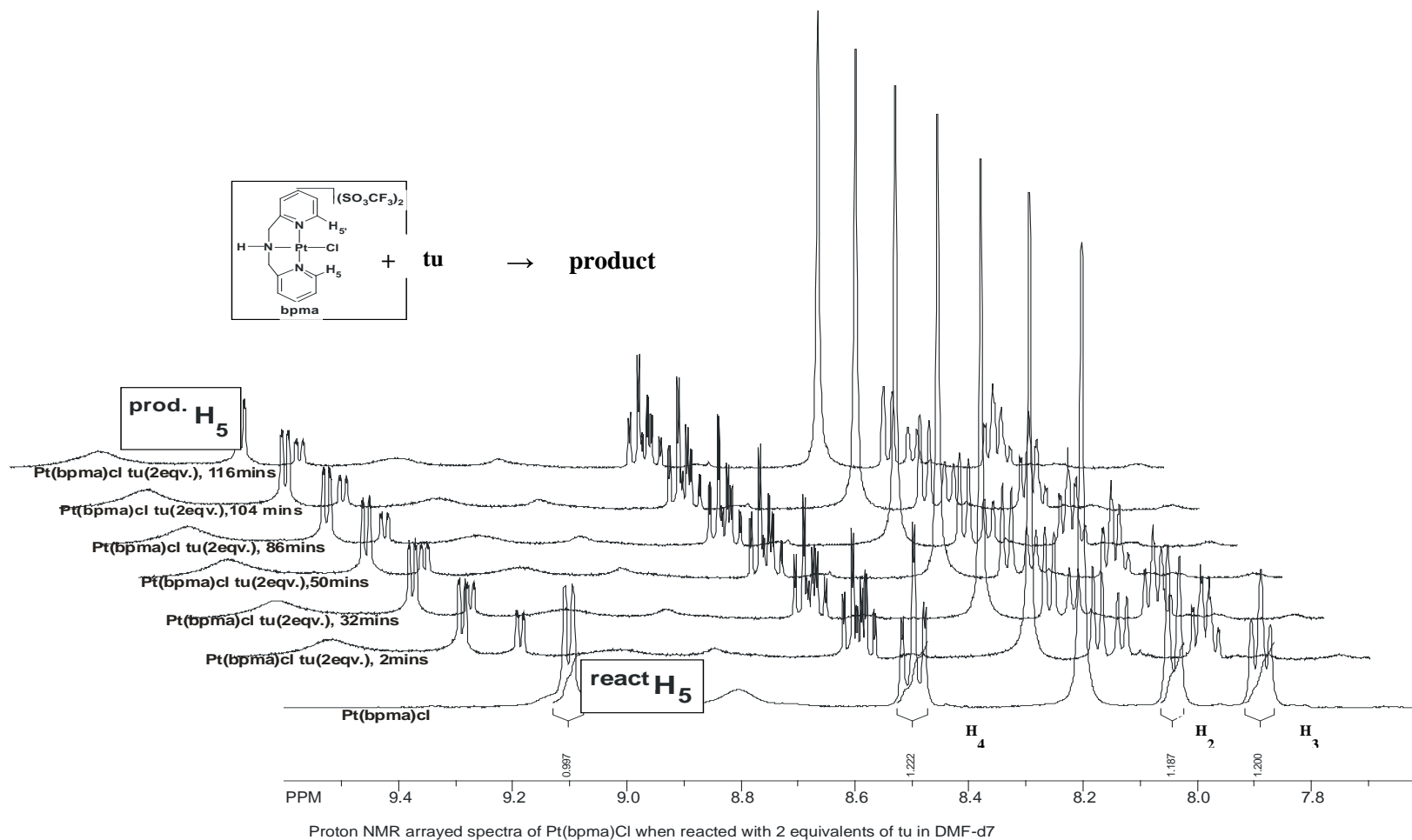


**Figure 3.4**  $^1\text{H}$  NMR (500 MHz) spectra array of **bpma-Cl** (showing only the aromatic region) acquired during its reaction with two equivalents of thiourea (tu) in DMF- $d_7$  at 298 K. The doublet at  $\delta = 9.12$  ppm corresponds to substituted product.

## *Pt(II) complexes with $\alpha,\omega$ -alkyldiamine bridges*

---

In all experiments involving the three complexes, a new set of resonances shifted downfield and integrating to an approximate ratio of to 2:1 (intermediate product : reactant) upon mixing the complexes with at least two equivalents of thiourea is observed for the H<sub>5</sub>/H<sub>5'</sub> protons on the pyridine rings. The adopted numbering system for the pyridyl protons used to monitor the progress of the reaction is shown in the structure of the **bpma Cl** complex as an inset in Figure 3.4. A distinctive shift in the chemical shift of the H<sub>5</sub> protons relative to the other three ring protons upon coordination of tu at the metal center is due to their close proximity to the N donor atom of the rings. As a result and can be noted in the spectral arrays of the reaction of **bpma**, the electronic environments of the other pyridyl protons are not affected to a great extent by the coordination of thiourea. Thus, the H<sub>5</sub> resonances were chosen to monitor the kinetic progression of the reaction.

The H<sub>5</sub> resonances of the **bpma-Cl** complex, labeled <sup>react.</sup>H<sub>5</sub>, which appear at  $\delta = 9.06$  ppm are shifted downfield to  $\delta = 9.12$  ppm in the tu-substituted derivative, labeled <sup>prod.</sup>H<sub>5</sub> in Figure 3.4. During the reaction, the <sup>prod.</sup>H<sub>5</sub> resonances of the intermediate product formed on the onset further grew while <sup>react.</sup>H<sub>5</sub> decreased accordingly. Since the first step which involves the substitution of the chlorido ligands is fast and complete in less than 20 s for all these complexes, it cannot be monitored by the NMR technique due to the limitations in the slow manual mixing of the reactants. Thus, it can be assumed that the subsequent changes in the arrays are certainly due to another step which is evidently observed in **bpma-Cl** as well, a mononuclear analogue with one leaving group. From the spectral arrays of the other complexes, again only two sets of H<sub>5</sub> resonances are observed upon mixing the dinuclear complexes with three equivalents of tu. No extra sets of resonances, in support of a stepwise second substitution were observed during the progression of the reactions with tu for up to three hours. In principle, the spectral arrays of **Prop-Cl** and **Dec-Cl** show the same pattern of substitution as observed in **bpma-Cl**. The spectral array for the reaction between **Dec-Cl** and three equivalents of tu is presented in Figure SI 3.2b (ESI).

If all the facts are added together, they clearly reiterate that the substitution of the chloride or aqua ligands in the dinuclear complexes occurs simultaneously irrespective of the length of the linker or the symmetry of the complexes. Based on the NMR study of **bpma-Cl**, it is reasonable to conclude that the ring opening is endemic to the bis(2-pyridylmethyl)amine

## *Pt(II) complexes with $\alpha,\omega$ -alkyldiamine bridges*

---

carrier ligand core despite the carrier ligand forming five-membered chelated rings which are known to be thermodynamically stable.<sup>34</sup> It is unlikely that the chain length of the diamine linker and hence the average distance separating the Pt centers causes this. It can therefore be assumed that the second and slower subsequent steps as observed in all the other dinuclear complexes bearing this carrier ligand as well as **bpma** are in fact the dechelation of the pyridyl units. The general reaction pathway for the substitution of the coordinated aqua ligands and the induced ring opening of the chelate ligand by the strong labilizing thiourea nucleophiles can therefore be represented by Figure SI 3.2c (ESI). Another observation in support of this is the second substitution step of all the reactions which is invariably 100 times slower when compared to the first. Relative to the first step, the rate constants for the second step depend weakly on the variation in the length of the alkanediamine linkers.

The two substitution steps were followed separately on the stopped-flow reaction analyzer. The first step is fast and complete within 50 s for. The second substitution step for the reactions between all nucleophiles and the least reactive complexes, *viz.*, **En** and **But**, were also repeated using UV-visible spectroscopy and followed for more than four half-lives of the second and slower substitution step to offer a comparison with the results from the stopped-flow analyzer. An example of kinetic trace recorded on a UV-visible spectrophotometer for the analysis of the dechelation and slower substitution step for the reaction between **En** (0.1 mM) and tu (6 mM) at 298 K, pH = 2.0, I = 0.02 M {CF<sub>3</sub>SO<sub>3</sub>H, adjusted with Li(SO<sub>3</sub>CF<sub>3</sub>)} is shown in Figure 3.5.

## *Pt(II) complexes with $\alpha,\omega$ -alkyldiamine bridges*

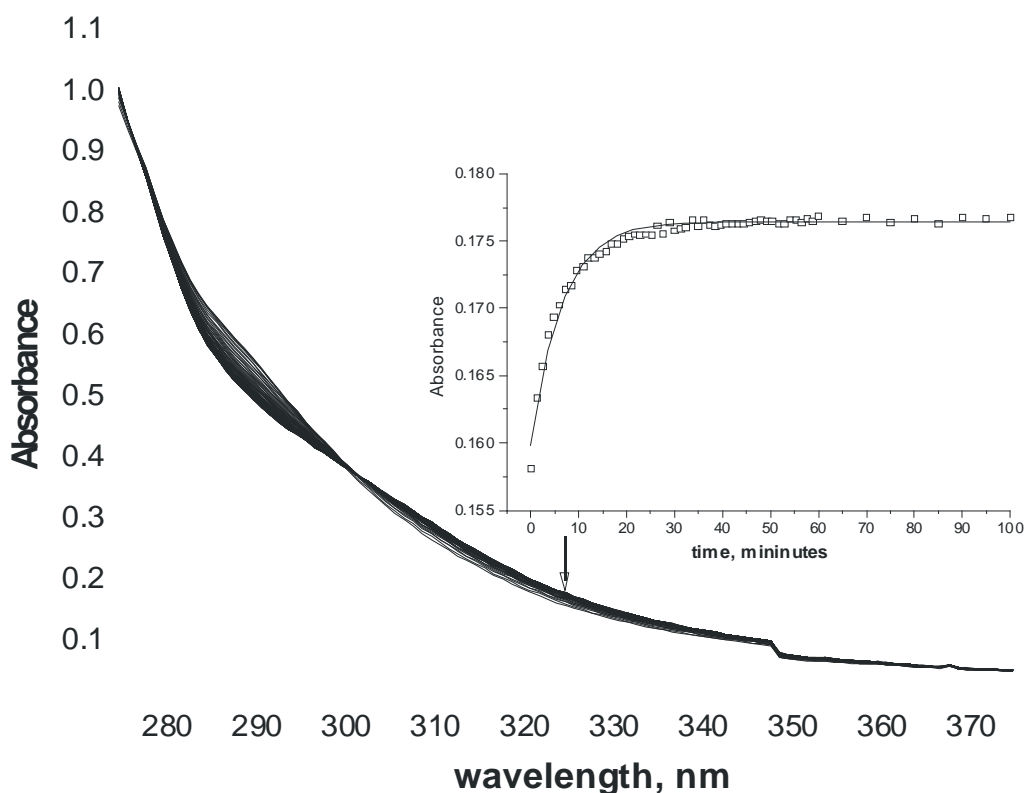


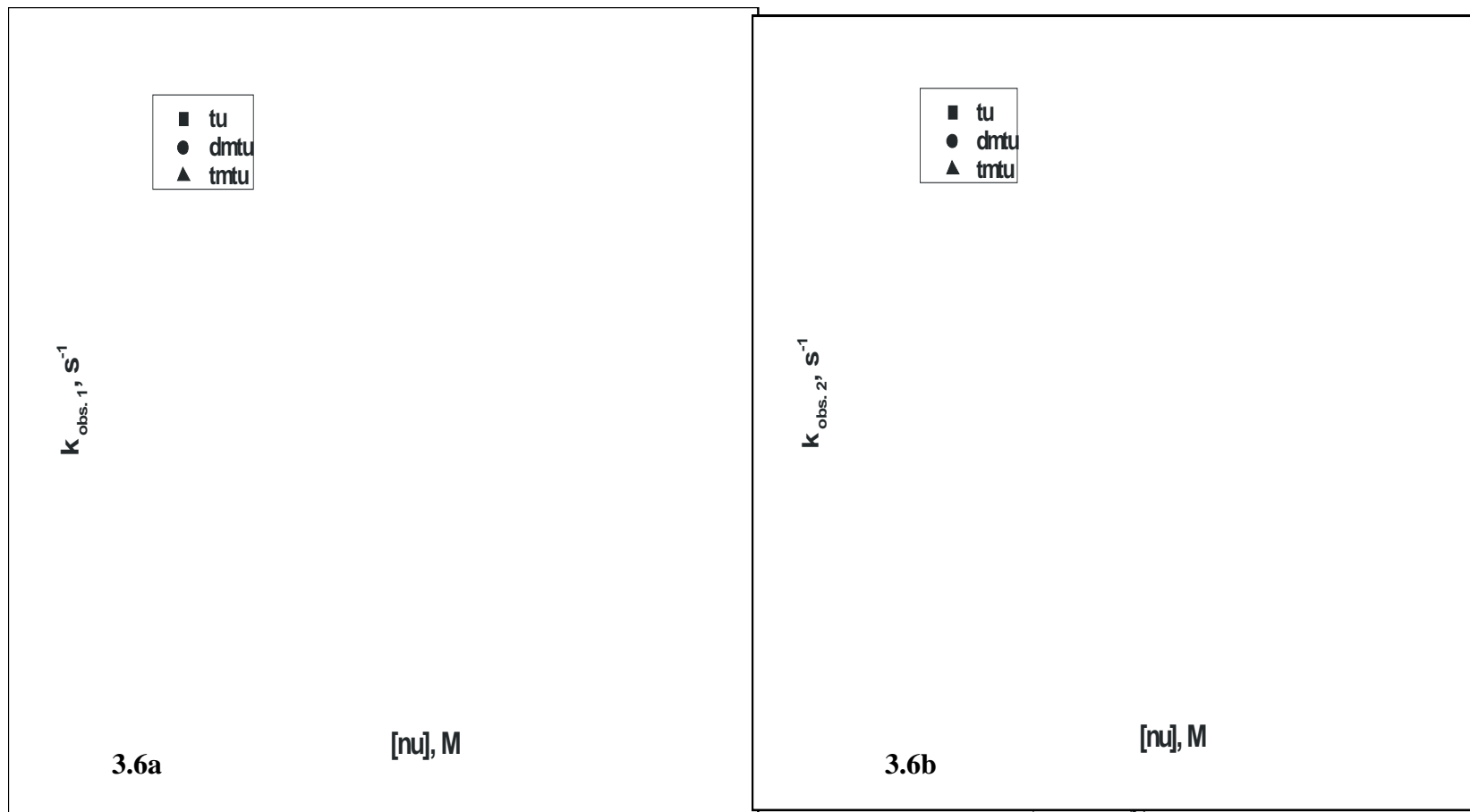
**Figure 3.5** A typical plot of the changes in absorbance observed within the 275-400 nm wavelength range for the dechelation of the pyridyl units in **En** by tu at 298 K, pH = 2.0, I = 0.02 M {CF<sub>3</sub>SO<sub>3</sub>H, adjusted with Li(SO<sub>3</sub>CF<sub>3</sub>)}, ([tu] maintained at a 60-fold excess over [complex]).

Inset: Kinetic trace taken at 325 nm.

The pseudo first-order rate constants,  $k_{\text{obs}(1/2)^{\text{st nd}}}$ , calculated from such kinetic traces were plotted against the concentration of the entering nucleophiles using the Origin 7.5<sup>®29</sup> software. Examples of plots of the observed pseudo first-order rate constants,  $k_{\text{obs}(1/2)^{\text{st nd}}}$ , against concentration of the nucleophiles for the two reaction steps is shown in Figures 3.6a and 3.6b for **En**. The slopes of the plots gave the second order rate constants  $k_{2(1/2)^{\text{st nd}}}$ , and their values are summarized in Table 3.4 for all the studied complexes.

## *Pt(II) complexes with $\alpha,\omega$ -alkyldiamine bridges*

## *Pt(II) complexes with $\alpha,\omega$ -alkyldiamine bridges*



**Figures 3.6a & 3.6b** Concentration dependence of (a)  $k_{\text{obs. (1)}^{\text{st}}}, \text{ s}^{-1}$ , for the simultaneous displacement of the aqua ligands and (b)  $k_{\text{obs. (2)}^{\text{nd}}}, \text{ s}^{-1}$ , for the dechelation of the pyridyl units in **En** by thiourea nucleophiles, pH = 2.0, T = 298 K, I = 0.02 M {0.01 M  $\text{CF}_3\text{SO}_3\text{H}$ , adjusted with  $\text{Li}(\text{SO}_3\text{CF}_3)$ }.

## *Pt(II) complexes with $\alpha,\omega$ -alkyldiamine bridges*

**Table 3.4** Summary of the rate constants for the simultaneous displacement of aqua ligands and the dechelation of the pyridyl units by neutral nucleophiles in **bpma** and a range of dinuclear complexes with bis(2-pyridylmethyl chelate headgroups).

Complex	nu	Second order rate constant, $M^{-1} s^{-1}$	
		$k_{2/1}^{st}$	$k_{2/2}^{nd}$
<b>bpma</b>	<b>tu</b>	$409 \pm 2$	$4.95 \pm 0.06$
	<b>dmtu</b>	$394 \pm 1$	$4.05 \pm 0.07$
	<b>tmtu</b>	$190 \pm 0.5$	$2.16 \pm 0.06$
<b>En</b>	<b>tu</b>	$151 \pm 1$	$0.81 \pm 0.02$
	<b>dmtu</b>	$92 \pm 1$	$0.53 \pm 0.01$
	<b>tmtu</b>	$23 \pm 1$	$0.51 \pm 0.01$
	<b>I-</b>	$(7.9 \pm 0.1) \times 10^3$	$(0.7 \pm 0.02) \times 10^3$
<b>Prop</b>	<b>tu</b>	$1033 \pm 7$	$4.53 \pm 0.07$
	<b>dmtu</b>	$727 \pm 3$	$4.78 \pm 0.10$
	<b>tmtu</b>	$305 \pm 2$	$3.13 \pm 0.05$
	<b>I-</b>	$(29.1 \pm 0.8) \times 10^3$	$(6.6 \pm 0.2) \times 10^3$
<b>But</b>	<b>tu</b>	$315 \pm 1$	$1.16 \pm 0.01$
	<b>dmtu</b>	$346 \pm 2$	$1.04 \pm 0.01$
	<b>tmtu</b>	$130 \pm 1$	$0.50 \pm 0.01$
	<b>I-</b>	$(14.1 \pm 0.7) \times 10^3$	$(4.5 \pm 0.1) \times 10^3$
<b>Hex</b>	<b>tu</b>	$579 \pm 2$	$5.30 \pm 0.03$
	<b>dmtu</b>	$606 \pm 4$	$5.86 \pm 0.07$
	<b>tmtu</b>	$182 \pm 1$	$1.23 \pm 0.01$
	<b>I-</b>	$(11.4 \pm 0.3) \times 10^3$	$(5.8 \pm 0.2) \times 10^3$
<b>Oct</b>	<b>tu</b>	$572 \pm 3$	$6.24 \pm 0.04$
	<b>dmtu</b>	$539 \pm 5$	$5.38 \pm 0.05$
	<b>tmtu</b>	$206 \pm 2$	$2.76 \pm 0.02$
<b>Dec</b>	<b>tu</b>	$641 \pm 3$	$6.49 \pm 0.15$
	<b>dmtu</b>	$632 \pm 5$	$2.49 \pm 0.02$
	<b>tmtu</b>	$198 \pm 2$	$1.83 \pm 0.01$

Both substitution steps for all the complexes gave excellent linear fits passing through the origin indicating that the backward reactions are insignificant or absent. Thus, the mechanism of the substitution of the aqua ligands by the thiourea nucleophiles in these dinuclear complexes for both steps is as proposed in an earlier study by van Eldik and co-workers,<sup>14c</sup> and can thus be represented by Figure SI 2c (ESI). The rate law can be expressed as in equation (1).

## *Pt(II) complexes with $\alpha,\omega$ -alkyldiamine bridges*

---

$$k_{\text{obs}(1^{\text{st}}/2^{\text{nd}})} = k_{2(1^{\text{st}}/2^{\text{nd}})}[\text{Nu}] \quad 3.1$$

The dechelation substitution step in **bpma**, however, gave a slight intercept when the observed first-order rate constant,  $k_{\text{obs}(2^{\text{nd}})}$ , was plotted against the concentration of the entering nucleophiles. Re-chelation of the pyridyl units at a pH of 2.0 can be ruled out since the N atoms of the pyridyl unit are protonated.<sup>14c</sup> The intercept is likely to be the slow aquation of the *cis*-coordinated thioureas which is assisted by steric repulsions from the dangling ends of the picolyl units.

A general look at the results in Table 3.4 shows that the simultaneous displacement of the aqua ligands as well as the subsequent dechelation of the pyridyl units is enhanced on increasing the chain length from **En** to **Dec**. An exception is **Prop**, which shows unusual high reactivity towards all the nucleophiles surpassing even **Dec**. This increase in the rate of substitution is, however, marginal for the dechelation step. The other trend that is general across all the complexes is that the substitution of the aqua ligands is about 100 times faster than the dechelation of the picolyl units as already stated. A detailed analysis of the substitution of the coordinated aqua ligands by these nucleophiles in the complexes reveals that the order of substitutional reactivity is **En** < **But** < **bpma** < **Hex**  $\approx$  **Oct**  $\approx$  **Dec** < **Prop**. Using **En**'s rate constant as the common value, the ratios of the rate of substitution of the aqua ligands of **En**, **But**, **Hex**, **Oct** and **Dec** by tu is 1: 2.1: 3.8: 3.8: 4.2, respectively. Thus, on extending the chain length of the bridge beyond **Hex**, the reactivity does not change significantly. The leveling effect of the reactivity and hence the similarity in the kinetic behaviour of the dinuclear complexes which are linked by flexible bridges of longer chain lengths ( $n = 8; 10$ ) has been reported<sup>14d</sup> in a related study involving two *cis*-bridged dinuclear Pt(II) bearing [Pt(DACH), DACH = (1*R*,2*R*)-(-)-1,2-diaminocyclohexane] non-labile chelate ligands.

However, on changing the structural nature of the incoming nucleophile from tu to tmtu, the trend remains almost the same, but the reactivity gradient along the series is markedly lower than that of tu or dmtu. It is also noted that the rate of substitution of the aqua ligand of **bpma** by tmtu is comparable to that of the dinuclear complexes of longer chain length (**Hex**, **Oct** and **Dec**). This is despite an increase in  $\sigma$ -inductive donation<sup>14d</sup> towards each of their Pt

## *Pt(II) complexes with $\alpha,\omega$ -alkyldiamine bridges*

---

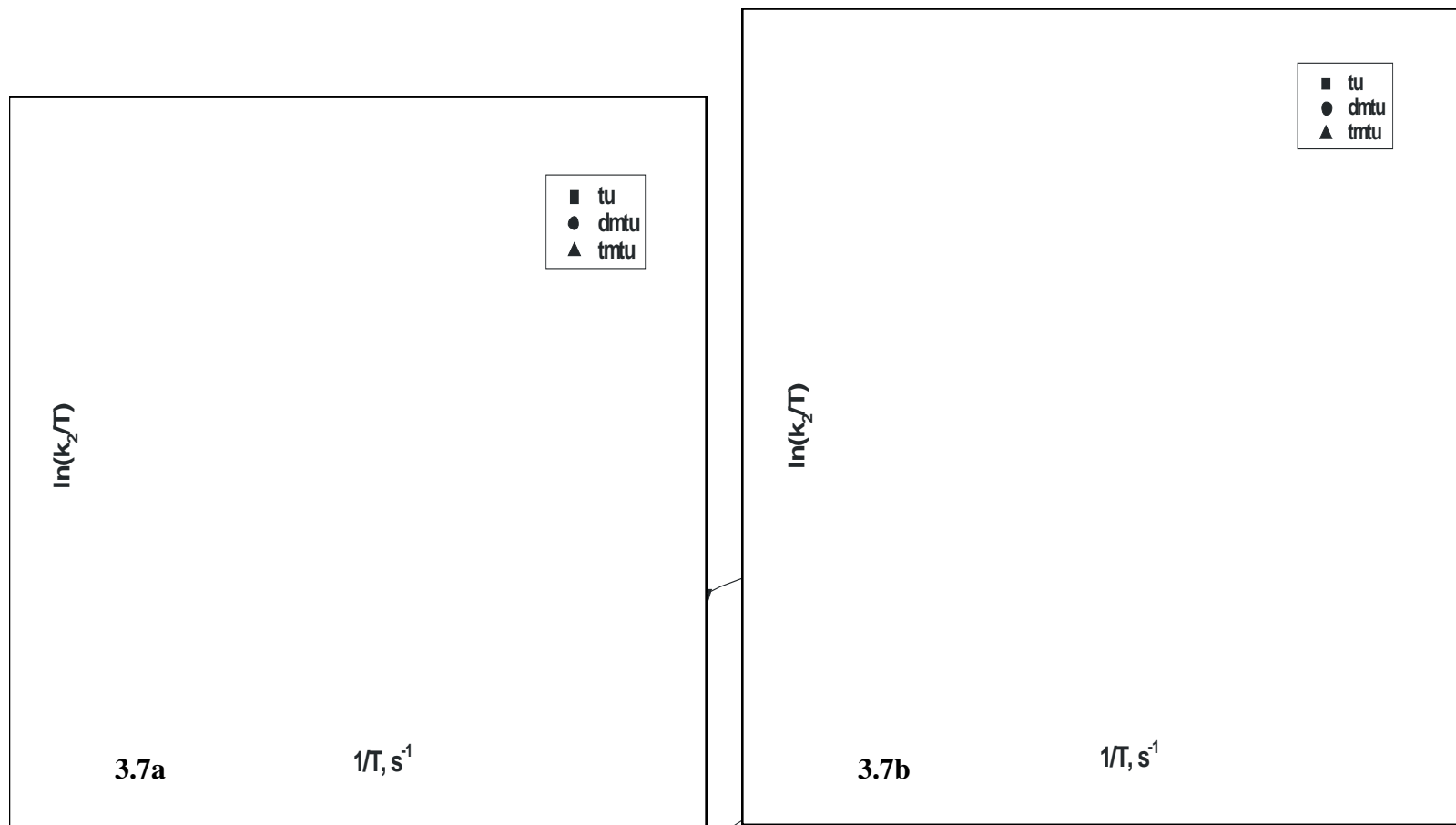
atoms and a higher charge of +4. This poor sensitivity toward changes in the electronic properties along the series by the bulky tmtu nucleophile is indicative of the presence of steric effects along the series of complexes.

Results in Table 3.4 further reveals that the rates of the simultaneous displacement of the aqua ligands in the **En** and **But** complexes are in fact lower than that in **bpma**. For example, despite an increase in the overall charge of +4 in **En**, the **bpma** complex reacts faster by factors of about 2.7 (tu), 4.3 (dmtu) and 8.3 (tmtu) than the former.

The order of reactivity of the thiourea nucleophiles at the Pt centers increases in the order  $tu \approx dmtu > tmtu$  and is in line with steric retardation in the case of tmtu and a dominating positive inductive effect in the case of dmtu. To test the reactivity trend observed for these complexes with the neutral nucleophiles, an ionic nucleophile ( $I^-$ ) was also used. Plots demonstrating a linear dependence of the rate constant on both the iodide concentration and the temperature are given as supporting information, Figures SI 3e and 3f, respectively. The calculated kinetic data from these plots is presented in Tables 3.4 and 3.5, respectively. The order of reactivity for the complexes with the iodide (**En** < **But**  $\approx$  **Hex** < **Prop**) remain similar to that already observed for the neutral thiourea nucleophiles. Again, we notice the ‘entrapment effect’ of the **Prop** complex, a structural phenomenon which as already explained, leads to its exceptional higher reactivity with the anionic iodide nucleophile.

The dependence of the two observed pseudo first-order rate constants,  $k_{obs(1^{st}/2^{nd})}$ , on temperature and pressure (for the first substitution step with tu and tmtu) resulted in the activation parameters ( $\Delta H^\ddagger_{(1^{st}/2^{nd})}$ ,  $\Delta S^\ddagger_{(1^{st}/2^{nd})}$ ) and  $\Delta V^\ddagger_{(1^{st})}$ , respectively. Typical Eyring plots for the two steps are shown in Figures 3.7a & 3.7b, respectively and the resultant activation enthalpy and entropy activation values are summarized in Table 3.5. Exemplary pressure dependence plots are provided for the reactions between **Prop** and **Oct** with tu in Figures SI 3.4a and 3.4b (ESI), respectively and the calculated values of  $\Delta V^\ddagger_{(1^{st})}$  are also presented in Table 3.5.

## *Pt(II) complexes with $\alpha,\omega$ -alkyldiamine bridges*



**Figures 3.7a & 3.7b** Temperature dependence of (a)  $k_{2(1^{st})}, M^{-1} s^{-1}$ , for the simultaneous displacement of the first aqua ligand and (b)  $k_{2(2^{nd})}, M^{-1} s^{-1}$ , for the dechelation of the pyridyl units in **En** by thiourea nucleophiles, pH = 2.0, I = 0.02 M (0.01 M  $CF_3SO_3H$ , adjusted with  $Li(SO_3CF_3)$ ).

## *Pt(II) complexes with $\alpha,\omega$ -alkyldiamine bridges*

**Table 3.5** Summary of the activation parameters for the simultaneous displacement of aqua ligands and the dechelation of the pyridyl units by thiourea nucleophiles in **bpma** and a range of dinuclear Pt(II) complexes with bis(2-pyridylmethyl)amine chelate headgroups (-- not determined).

Complex	nu	Activation enthalpy kJ mol <sup>-1</sup>		Activation entropy J mol <sup>-1</sup> K <sup>-1</sup>		Activation volume cm <sup>3</sup> mol <sup>-1</sup>
		$\Delta H^\ddagger_1$	$\Delta H^\ddagger_2$	$\Delta S^\ddagger_1$	$\Delta S^\ddagger_2$	$\Delta V^\ddagger_1$
bpma	tu	41.1 ± 0.9	46.1 ± 0.3	-57 ± 3	-79 ± 1	--
	dmtu	37.2 ± 0.9	52.0 ± 1.2	-71 ± 3	-59 ± 4	--
	tmtu	43.3 ± 1.1	59.3 ± 1.0	-57 ± 3	-37 ± 3	--
En	tu	40.9 ± 1.2	25.5 ± 0.7	-66 ± 4	-157 ± 2	-4.0 ± 0.2
	dmtu	48.8 ± 2.0	36.0 ± 1.1	-64 ± 6	-130 ± 4	--
	tmtu	43.3 ± 1.2	53.4 ± 1.5	-105 ± 4	-76 ± 4	-4.6 ± 0.2
	I	45.0 ± 1.0	38.4 ± 1.3	-21 ± 3	-50 ± 4	--
Prop	tu	24.3 ± 0.7	20.7 ± 0.5	-106 ± 2	-161 ± 2	-5.5 ± 0.3
	dmtu	34.3 ± 0.7	27.5 ± 0.6	-75 ± 2	-137 ± 2	--
	tmtu	39.4 ± 0.4	41.1 ± 2.0	-64 ± 1	-97 ± 6	-13.2 ± 0.2
	I	24.7 ± 0.7	29.8 ± 0.8	-71 ± 2	-65 ± 3	--
But	tu	37.0 ± 0.8	32.5 ± 1.0	-73 ± 3	-135 ± 3	-4.0 ± 0.2
	dmtu	40.4 ± 1.0	29.7 ± 0.5	-61 ± 3	-161 ± 2	--
	tmtu	41.6 ± 0.7	42.4 ± 1.0	-65 ± 2	-153 ± 3	-8.9 ± 0.3
	I	17.5 ± 0.4	28.5 ± 0.2	-108 ± 1	-81 ± 1	--
Hex	tu	34.3 ± 0.7	38.9 ± 1.0	-77 ± 2	-101 ± 3	-3.1 ± 0.1
	dmtu	43.0 ± 1.0	42.5 ± 2.0	-47 ± 3	-88 ± 6	--
	tmtu	47.2 ± 0.6	27.2 ± 0.6	-42 ± 2	-147 ± 2	-9.3 ± 0.2
	I	25.7 ± 0.7	15.8 ± 0.7	-81 ± 2	-122 ± 2	--
Oct	tu	30.5 ± 0.6	24.5 ± 0.5	-90 ± 2	-148 ± 2	-4.7 ± 0.1
	dmtu	32.2 ± 0.3	27.5 ± 0.6	-84 ± 1	-138 ± 2	--
	tmtu	46.7 ± 0.1	48.2 ± 0.9	-46 ± 3	-80 ± 3	-8.5 ± 0.2
Dec	tu	34.0 ± 0.8	28.9 ± 1.1	-78 ± 2	-122 ± 3	-4.6 ± 0.1
	dmtu	36.7 ± 1.0	32.5 ± 1.2	-69 ± 3	-127 ± 4	--
	tmtu	53.6 ± 1.0	36.9 ± 0.9	-42 ± 3	-114 ± 3	-12.7 ± 0.4

# *Pt(II) complexes with $\alpha,\omega$ -alkyldiamine bridges*

---

## 3.4 Discussion

### 3.4.1 Hydrolysis of complexes

The general increase in the basicity of the complexes as the length of the linker is increased is as a result of an increase in the  $\sigma$ -induction<sup>14d</sup> to the Pt center due to the linker. This results in a decrease in the positive charge on the Pt atoms. This deduction is supported by the shortening of the Pt-N bond lengths as the length of the linker increases as shown in Table 3 and is reflected on the calculated NBO charges. The static ground effect of this is to weaken the Pt-O bond of the coordinated aqua through the *trans* influence, leading to an increase in basicity as the chain length is increased. This is supported by the Pt-OH<sub>2</sub> bond lengths which increase with increasing chain length of the linker (Table 3.3). Thus, the length of the alkyldiamine linker reduces the charge addition between the two Pt centers and increases the  $\sigma$ -inductive effects<sup>14d</sup>, two factors that control the net effective charge carried by the Pt centers. In the case of the **Dec** complex, the charge addition to each Pt center is almost absent such that each center can be assumed to act independently. It can therefore be concluded that in this series of dinuclear complexes, the acidity of the coordinated aqua ligand is in fact controlled by the effective charge on the Pt atoms, which depends on the length of the linker to some point.

The higher pH values recorded for the deprotonation of the second aqua ligand to form the hydroxo/hydroxo species indicates a general reduction in the overall charge on the first Pt atom on forming the hydroxo species.<sup>14a</sup> Like in the first deprotonation step, both effects depend on the chain length of the bridge up to a point. What is noted is that the  $pK_{a2}$  values for the deprotonation of the second coordinated aqua ligands in **Hex**, **Oct** and **Dec** approximate that of **bpma**. The observation that these three complexes have approximately equal  $pK_{a2}$  values is similar to the trend observed in their  $pK_{a1}$  values, signifying that the effect of the chain length has a limit, after which it has no influence on the net effective charge of the Pt centers. The overall deprotonation of the coordinated aqua ligands clearly follows a two-step process. Despite this, and as shall be discussed later, the substitution of the coordinated ligands by the thiourea nucleophiles is however not stepwise and does not follow the trend of the deprotonation of the coordinated aqua ligands.

## *Pt(II) complexes with $\alpha,\omega$ -alkyldiamine bridges*

---

### 3.4.2 Kinetics

A look at the rate constants for the simultaneous displacement of the coordinated aqua ligands by the thiourea nucleophiles shows that the symmetry architectures of the alkanediamine linker control the substitution process. We previously reported<sup>35</sup> on the crystal structures of two of the metal-free analogues of these metal complexes, *viz.*, the ligands bridged by 1,3-propanediamine and 1,4-butanediamine chains. The number of CH<sub>2</sub> groups within the linker was found to play a pivotal role in the overall symmetry adopted by the ligands and also in their supramolecular chemistry. Thus, a crystallographic inversion symmetry of the metal-free ligands bearing an even number of CH<sub>2</sub> groups, confers a C<sub>2h</sub> symmetry to the complexes upon their coordination to Pt(II) atoms, while a two-fold rotational symmetry of the free ligands bridged by linkers with an odd number of CH<sub>2</sub> groups as exemplified by the structures of **Prop**, **Pen** and **Hep** favors formation of dinuclear complexes with a C<sub>2v</sub> symmetry (Tables 3.2 and SI 3.5). A consequent of this coordination requirement along the two square-planar chelates is to place the two Pt(II) centers into highly symmetrical environments upon their coordination to the bis(2-pyridylmethyl)amine chelates such that they can not be differentiated by the highly reactive sulfur nucleophiles. This symmetrical environment on the planes of the Pt atoms is supported by the calculated NBO charges on the Pt atoms (Table 3.3) which reveal a symmetrical charge distribution on the Pt atoms in all the dinuclear complexes. A result is the simultaneous substitution of the aqua ligands, a process that happens without undue dependence on the distance separating the Pt(II) centres in the complexes. This is despite a slight increase in the acidity of the protons of the aqua ligands brought about by an increased charge addition on decreasing the length of the linker.

Based on the *in vacuo* minimum energy structures of Table 3.2, also depicted in Figure 3.3, and notwithstanding conformation variability of the complexes, it is reasonable to assume that the symmetry of the complexes and the angles of elevation caused by the alkanediamine linker, including its electronic effects have an important bearing on the overall reactivity in these complexes. A look at the DFT calculated structures in Table 3.2 reveals that in the even-bridged complexes, the adopted C<sub>2h</sub> point group symmetry places the Pt coordination spheres into two roughly parallel planes as depicted in Figure 3.3. Viewed along the axis perpendicular to their mean planes containing the Pt atoms and the picolyl units, the bis(2-

## *Pt(II) complexes with $\alpha,\omega$ -alkyldiamine bridges*

---

pyridylmethyl)amine chelates are located in mutually slip-up positions. The alkyldiamine linker lies at an inclination angle,  $\alpha$ , that is inversely dependent on the length of the bridge. Relative to the plane containing one of the bis(2-pyridylmethyl)amine chelates, the linker projects the other chelate head at an angle which decreases sharply from 74.2° in **En** to 44.6° in **Dec** as documented in Table 3.3. When the chain length of the linker is increased, this has an effect of both increasing the projected distance locating the mean planes containing the chelates as well as their degree of mutual slip-up. In perspective, the chelates in **En** show a marked degree of aerial overlap and are separated by an elevation distance of only 3.63 Å, while those in **Dec** are well separated by as much as 9.16 Å (for an illustration refer also Figure 3.3). Since this slip-up of coordination spheres occurs in one of the directions of approach of the nucleophile, it becomes evident that for complexes with a  $C_{2h}$  point group symmetry, the length of the linker controls the extent of steric disposition mutually imposed on one side of the Pt square-planar coordination sphere. This happens on the same side bearing the inclined linker. When the chain length is short, this imposes a stronger aerial steric influence on the same side of the metal chelate in the direction of the axially incoming nucleophile. Thus, from a view taken perpendicular to the planes containing the square-planar chelates in **En** and other complexes of shorter bridges, it is observed that one of the sides bearing the linking bridge at each Pt center is markedly blocked by the other metal chelate headgroup from a direct attack by the nucleophile as compared to **Dec** and other analogues of longer chain length. This kind of imposed steric hindrance is likely to be the dominant factor accounting for the difference in reactivity in the complexes.

Our results also suggest that this kind of steric influence controlled by the symmetry dictated by the linker piece is more important in the complexes bridged by an alkanediamine of shorter chain length. The steric influences decrease proportionally as the chain length is increased from **En** to **Hex**. This causes a proportional increase in reactivity from **En** up to **Hex**. Beyond **Hex**, any further increase in chain length does not result in significant changes in the elevation angles of the linker bridges and its projected effects on the reactivity of the complexes. As a result of this, the reactivity of **Hex**, **Oct** and **Dec** for the simultaneous displacement of the aqua ligands by the thioureas remains high and comparable to each other.

## *Pt(II) complexes with $\alpha,\omega$ -alkyldiamine bridges*

---

In the absence of this kind of steric imposition, as is the case for **Prop** where the Pt coordination spheres are near-orthogonal, other factors become more important in controlling reactivity of the Pt centers. As shown in Figure 3.3, the calculated structure of **Prop** has two Pt atoms lying almost in near-orthogonal planes with no meaningful mutual shielding as a result of its  $C_{2v}$  symmetry. It is possible that the  $C_{2v}$  symmetry of **Prop** which draws the shape of the complex into a bowl-like cage,<sup>36</sup> can mediate in the entrapment of incoming nucleophiles aided by solvent molecules through the well known cage effect.<sup>37</sup> In keeping with the principles of the collision theory, this can increase the frequency of collisions between the Pt atoms and the entrapped nucleophiles within the overlooking faces of the bowl-shaped enclave. The result is a dramatic increase in the collision fraction, leading to more fruitful collisions. Conceivably, nucleophile-metal complex encounter pairs confined in a caged cleft can acquire sufficient energy to surmount the energy barrier. It thus stabilizes the transition state relative to the ground state. This stabilization is likely to depend on the depth of the cage.

To infer on the depth of the cleft,  $\beta$ , a hinge angle, formed by the mean planes of the overlooking square-planar faces of the **Prop** as shown in its calculated structure in Figure 3.3, such that its bisector passes through the central carbon of its propanediamine linker was calculated. The angle comes to  $124^\circ$ . This acute ‘bowling’ angle creates a cage of significant projected depth, enough to entrap axially approaching nucleophiles. Solvent molecules aid the entrapment process. Thus, deep and narrow bowled cages will increase the frequency of collisions. This is a likely explanation of the unusual high reactivity of **Prop** confirmed in this study and first observed by van Eldik and his group.<sup>14a</sup> When the rate constant for **Prop** determined in this study is combined to the rate constants for **Pen** and **Hep** from a previous study<sup>14c</sup> for *tu* as the entering nucleophile, a trend opposite to that recorded for the even-bridged complexes is observed. The second-order rate constant,  $k_{2(1^{st})}$ , increases monotonically from **Hep** ( $577 \pm 5 \text{ M}^{-1} \text{ s}^{-1}$ )<sup>14c</sup> through **Pen** ( $765 \pm 10 \text{ M}^{-1} \text{ s}^{-1}$ )<sup>14c</sup> to **Prop** ( $1033 \pm 7 \text{ M}^{-1} \text{ s}^{-1}$ ) in line with an increase in the entrapment effect as the basal width of the bowl is shortened. From this data, it is also clear that tuning the reactivity of dinuclear complexes with bis(2-pyridylmethethyl)amine chelate headgroups via varying the chain length of their alkanediamine linker will be more pronounced in the odd-bridged complexes than in their

## *Pt(II) complexes with $\alpha,\omega$ -alkyldiamine bridges*

---

related even-bridged analogues due to a combination of the absence of steric dispositions and the profound entrapment effect of their cage structures.

The deceleration in the rate of substitution in going from the monomeric **bpma** to the **En** and **But** dinuclear complexes is in support of the presence of axially imposed steric influences on their Pt coordination spheres conferred as a result of their shorter and markedly inclined linkers. As the length of the linker is increased to **Hex**, this steric imposition is further decreased. At the same time, an increase in the number of CH<sub>2</sub> groups along the series causes an increase in electron density in the linker and hence the  $\sigma$ -inductive effect<sup>14d</sup> towards each Pt center. This, together with a higher charge of +4 causes a marginal increase in the reactivity of **Hex** compared to **bpma**. However, any further decrease in steric imposition along the series beyond **Hex** is not accompanied by additional reactivity advantage over **bpma** as would be expected on the basis of a higher charge of +4 and a steady increase in the positive  $\sigma$ -inductive effects<sup>14d</sup> of the CH<sub>2</sub> groups towards the metal centers. Thus, an increase in the number of CH<sub>2</sub> groups from six in **Hex** to ten in **Dec** causes only a marginal increase in reactivity of about 1.6 (tu and dmtu) and 1.04 (tmtu). This is in spite of a slight elongation and weakening of the Pt-OH<sub>2</sub> bond (Table 3.3) as the chain length increases from **En** to **Dec**. It seems likely that this factor plays a subdued role in controlling reactivity in this series of complexes.

A common observation in the reactivity of these complexes is a second substitution step that proceed at an invariably slowly rate at about two order of magnitude lower than for the simultaneous displacement of the aqua ligands. This step is less sensitivity to the structural changes emanating from the linking diamino bridge. The behaviour is consistent with a substitution step involving the dechelation of one of the pyridyl units of the non-labile bis(2-pyridylmethethyl)amine chelate ligand as proposed in a previous study.<sup>14c</sup> It can possibly be due to the increased constraints poised on the incoming nucleophiles as they displace the coordinated pyridyl ligand at an already hindered Pt centre in the transition state.

The trend in the magnitude of the second-order rate constants (Table 3.4) for the substitution of the aqua ligands by the four nucleophiles (tu, dmtu, tmtu and I<sup>-</sup>) is similar to that reported for **bpma** by Jaganyi *et al.*<sup>20a,33a</sup> These values show that the iodide nucleophile reacts about 50 times faster than the most reactive neutral nucleophiles (tu and dmtu). This reactivity difference can be explained on the basis of the strong electrostatic attraction forces between the

## *Pt(II) complexes with $\alpha,\omega$ -alkyldiamine bridges*

---

anionic iodide nucleophile and the dicationic headgroups aided by the highly polarizability of this nucleophile. It is well documented that soft (polarizable) nucleophiles favour soft substrates like the Pt(II) ion resulting in superior reactivity.

The results of Table 3.5 shows that the activation entropies ( $\Delta S^\ddagger_{(1^{st}/2^{nd})}$ ) are large and negative while the activation enthalpies ( $\Delta H^\ddagger_{(1^{st}/2^{nd})}$ ) are low and positive. All this is in full support of an associative mechanism well known for  $d^8$  square planar metal complexes.<sup>38-41</sup> The acceleration of the reactions by pressure and hence the negative volumes of activation ( $\Delta V^\ddagger_{(1^{st})}$ ) measured in this study further support this mode of activation. Of note, are the large and more negative values for the volumes of activation measured for the reactions between **Prop** and the studied nucleophiles (tu and tmtu). It is an indication that the first reaction step for **Prop** proceeds via a more compact transition state when compared to other complexes. This is consistent with the proposed cage effect as discussed before. The collapse in volume in the transition state is mediated by the constraints of the entrapment effect and is therefore more negative when compared to the values of the other complexes.

### 3.5 Conclusions

This study has demonstrated that the symmetry elements of the dinuclear complexes with bis(2-pyridylmethyl)amine chelate headgroups as well as the length of the  $\alpha,\omega$ -alkanediamine linker can tune the reactivity of the complexes to some extent. For complexes with  $C_{2h}$  symmetry, their reactivity increases with increasing chain length of the  $\alpha,\omega$ -alkanediamine bridges to some point beyond which it levels off. This is attributed to the unblocking of axial steric impositions on one face of the Pt(II) square-planar coordination sphere conferred by the coordination sphere of the other Pt center in their  $C_{2h}$  slip-up sandwich molecular structures. This kind of mutual steric imposition reaches its limit of influence on reactivity in the **Hex** complex. When the complexes are bridged by an  $\alpha,\omega$ -alkanediamine linker bearing an odd number of carbon atoms as in the case of **Prop**, a cage effect evolving from the adopted bowl-shaped molecular structures controls reactivity. As a result of this, a significant entrapment effect on incoming nucleophiles take place inside the cavity of the bowl, more so in the acute-angled bowl of **Prop** causing an unusually high reactivity in this complex when compared to the rest of the complexes.

## *Pt(II) complexes with $\alpha,\omega$ -alkyldiamine bridges*

---

An observed second substitution step, confirmed by  $^1\text{H}$  NMR spectroscopy for the reaction between the monomeric and monofunctional **bpma** and tu, indicates that all the subsequent reaction steps which are observed in the analogous homotopic dinuclear complexes with common bis(2-pyridylmethyl)amine chelate headgroups are in fact the dechelations of one of one of their *cis*-coordinated pyridyl units. Given the high nucleophilicity of the sulfur bearing thiourea nucleophiles at the Pt metal centers, it is no surprise why the thermodynamically stable bis(2-pyridylmethyl)amine chelate system is partially labilized and thus undergoes dechelation. However, no evidence of degradation of the crucial  $\alpha,\omega$ -alkanediamine linker was observed for all dinuclear complexes.

### 3.6 References

- 1 E. Wong and C. M. Giandomenico, *Chem. Rev.*, 1999, **99**, 2451.
- 2 N. J. Wheate and J. G. Collins, *Coord. Chem. Rev.*, 2003, 133.
- 3 J. Reedijk, *Chem. Rev.*, 1999, **99**, 2499.
- 4 E. R. Jamieson and S. J. Lippard, *Chem. Rev.*, 1999, **99**, 2467.
- 5 N. Farrell, S. G. De Almeida and K. A. Skov, *J. Am. Chem. Soc.*, 1988, **110**, 5018.
- 6 N. Farrell, *Comments Inorg. Chem.*, 1995, **16(6)**, 373.
- 7 M. E. Oehlsen, Y. Qu, N. Farrell, *Inorg. Chem.*, 2003, **42**, 5498.
- 8 (a) N. Farrell, in *Platinum-based Drugs in cancer Therapy*, 2000, L. R. Kelland, N. Farrell, (Ed.), Human Press, Totowa 321; (b) T. D. McGregor, Z. Balcarova, Y. Qu, M. C. Tran, R. Zaludova, V. Brabec and N. Farrell, *J. Biol. Inorg. Chem.*, 1999, **77**, 43.
- 9 V. Brabec and J. Kasparková, *J. Drug Resistance Updates*, 2002, **8**, 131.
- 10 J. Kasparková, O. Vraná, N. Farrell and V. Brabec, *J. Biol. Inorg. Chem.*, 2004, **98**, 1560.
- 11 N. Summa, J. Maignut, R. Puchta and R. van Eldik, *Inorg. Chem.*, 2007, **46**, 2094.
- 12 V. Vacchina, L. Torte, C. Allievi and R. Lobeinski, *J. Anal. Atomic Spectrom.*, 2003, **18**, 884.
- 13 D. Jaganyi, V. M. Munisamy and D. Reddy, *Int. J. of Chem. Kinet.*, 2006, **38**, 202.

## *Pt(II) complexes with $\alpha,\omega$ -alkyldiamine bridges*

---

- 14 (a) A. Hofmann and R. van Eldik, *J. Chem. Soc., Dalton Trans.*, 2003, 2979; (b) H. Ertürk, A. Hofmann, R. Puchta and R. van Eldik, *Dalton Trans.*, 2007, 2295; (c) H. Ertürk, J. Maigut, R. Puchta and R. van Eldik, *Dalton Trans.*, 2008, 2759. (d) H. Ertürk, R. Puchta and R. van Eldik, *Eur. J. Inorg. Chem.*, 2009, 1334.
- 15 J. W. Williams, Y. Qu, H. Bulluss, E. Alvorado and N. Farrell, *Inorg. Chem.*, 2007, **46**, 5820.
- 16 (a) N. Summa, J. Maigut, W. Schiessl, R. Puchta, N. van Eikema-Hommes and R. van Eldik, *Inorg. Chem.*, 2006, **45** (7), 2948; (b) D. Reddy and D. Jaganyi, *Transition Met. Chem.*, 2006, **31**, 792; (c) M. Schmülling, A. D. Ryabov and R. van Eldik, *J. Chem. Soc. Dalton Trans.*, 1996, 1471; (d) M. J. Carter and J. K. Beattie, *Inorg. Chem.*, 1970, 1233.
- 17 (a) S. Komeda, G. V. Kalayda, M. Lutz, A. L. Spek, T. Sato, M. Chikuma and J. Reedijk, *J. Med. Chem.*, 2003, **46**, 1210; (b) G. V. Kalayda, S. Komeda, K. Ekeda, T. Sato, M. Chikuma and J. Reedijk, *J. Eur. Inorg. Chem.*, 2003, 4347.
- 18 (a) S. Komeda, M. Lutz, A. L. Spek, M. Chikuma and J. Reedijk, *Inorg. Chem.*, 2000, **39**, 4230; (b) S. Komeda, M. Lutz, A. L. Spek, Y. Yamanaka, T. Sato, M. Chikuma and J. Reedijk, *J. Am. Chem. Soc.*, 2002, **124**, 4738.
- 19 S. L. Woodhouse and L.M. Rendina, *Chem. Commun.*, 2001, 2464; (b) N. J. Wheate, C. Cullinane, L. K. Webster and J. G. Collins, *Anti-Cancer Drug Design*, 2001, 1691.
- 20 (a) D. Jaganyi, A. Hofmann and R. van Eldik, *Angew. Chem. Int. Ed.*, 2001, **40**, 1680; (b) Z. D. Bugarčić, G. Liehr and R. van Eldik, *J. Chem. Soc., Dalton Trans.*, 2002, 951.
- 21 A. Sato, Y. Mori, and T. Lida, *Synthesis*, 1992, 539.
- 22 Z. D. Bugarčić, B. V. Petrović and R. Jelić, *Transition Met. Chem.*, 2001, **26**, 668.
- 23 A. Hofmann, D. Jaganyi, O. Q. Munro, G. Liehr and R. van Eldik, *Inorg. Chem.*, 2003, **42**, 1688.
- 24 R. van Eldik, W. Gaede, S. Wieland, J. Kraft, M. Spitzer and D. A. Palmer, *Rev. Sci. Instrum.*, 1993, **64**, 1355.
- 25 (a) R. A. Friesner, *Chem. Phys. Lett.*, 1985, **116**, 539; (b) R. A. Friesner, *Annual Rev. Chem. Phys.*, 1991, **42**, 341.
- 26 (a) Spartan 04, Wavefunction, Inc., 18401 von Karman Avenue, Suite 370, Irvine, CA, 92612, USA; Q-Chem, Inc, The Design Center, suite 690, 5001, Baum Blvd., Pittsburgh, 15213, USA, 2004. <http://www.wavefun.com/>; (b) K. Kong, C. A. White, A. I. Krylov, C. D. Sherrill, R. D. Adamson, T. R. Furlani, M. S. Lee, A. M. Lee, S. R. Gwaltney, T. R. Adams, C. Ochsenfeld, A. T. B. Gilbert, G. S. Kedziora, V. A. Rassolov, D. R. Maurice, N.

## *Pt(II) complexes with $\alpha,\omega$ -alkyldiamine bridges*

---

- Nair, Y. Shao, N. A. Besley, P. E. Maslen, J. P. Dombroski, H. Daschel, W. Zhang, P. P. Korambath, J. Baker, E. F. C. Byrd, T. van Voorhuis, M. Oumi, S. Hirata, C. P. Hsu, N. Ishikawa, J. Florian, A. Warshel, B. G. Johnson, P. M. W. Gill and B. G. Pople, *J. Computational Chem.*, 2000, **21**, 1532.
- 27 (a) A. D. Becke, *J. Chem. Phys.*, 1993, **98**, 5648; (b) C. Lee, W. Yang and R. G. Parr, *Phys. Rev.*, 1998, **B37**, 785.
- 28 (a) P. C. Hariharan and J. A. Pople, *J. A. Chem. Phys. Lett.* 1972, **16**, 217; (b) P. J. Hay and W. R. Wadt, *J. A. Chem. Phys. Lett.*, 1985, **82**, 299.
- 29 B. Pitteri, G. Annibale, G. Marangoni, V. Bertilasi and V. Ferretti, *Polyhedron*, 2002, **21**, 2283.
- 30 Origin7.5™ SRO, v7.5714 (B5714), Origin Lab Corporation, Northampton, One, Northampton, MA, 01060, USA, 2003.
- 31 (a) D. Jaganyi and F. Tiba, *Transition Met. Chem.*, 2003, **28**, 803. (b) ConQuest v1.9, 2006, Cambridge Crystallographic Data Centre, 12 Union Road, Cambridge, CB21EZ, United Kingdom,.
- 32 (a) C. F. Weber and R. van Eldik, *Eur. J. Inorg. chem.*, 2005, 4755; (b) B. Pitteri, M. Bortoluzzi and G Marangoni, *Transition Met. Chem.*, 2005, **30**, 1008.
- 33 (a) D. Jaganyi, F. Tiba, O. Q. Munro, B. Petrović and Z. D. Bugarčić, *Dalton Trans.*, 2006, 2943; (b) Z. D. Bugarčić, G. Liehr and R. van Eldik, *Dalton Trans.*, 2001, 951.
- 34 S. M. Owen and A. T. Bruker, *A Guide to Modern Inorganic Chemistry*, Longman Scientific & Technical, Essex, England, 1991, pp. 193-194.
- 35 A. Mambanda, D. Jaganyi and O. Q Munro, *Acta Cryst.*, 2007, **C63**, o676.
- 36 U. Fekl and R. van Eldik, *Inorg. Chem.*, 2001, **40**, 3247
- 37 P. W. Atkins, *Physical Chemistry*, 6<sup>th</sup> Ed., Oxford University Press, Oxford, 1998, pp. 825-827.
- 38 M. L. Tobe and J. Burgess, *Inorganic Reaction Mechanisms*, Addison Wisey, Longman Ltd., Essex, 1999, pp. 30-33; 70-112.
- 39 J. D. Atwood, *Inorganic and Organometallic Reaction Mechanisms*, 2<sup>nd</sup> Ed., Wiley-VCH, NY, 1997, pp. 43-61.
- 40 R. G. Wilkins, *Kinetics and Mechanism of Reactions of Transition Metal Complexes*, 2<sup>nd</sup> Ed., VCH, Weinheim, 1991, pp. 199-201.

## *Pt(II) complexes with $\alpha,\omega$ -alkyldiamine bridges*

---

41 F. Basolo and R. G. Pearson, *Mechanism of Inorganic Reactions*, 2<sup>nd</sup> Ed., Wiley, New York, 1967, pp. 80-115.

### **3.7 Supporting Information.**

A summary of wavelengths used for kinetics; spectral changes for a titration of **Oct** with NaOH, a kinetic trace showing the two reaction steps for a reaction mixture of tu (3 mM) and **bpma**; <sup>1</sup>H NMR spectral arrays (aromatic protons only) for the reaction between tu and **Dec**; exemplary Tables of data and the respective plots showing the dependence of  $k_{\text{obs.}(1^{st}/2^{nd})}$  on concentration of nucleophiles, temperature and pressure of the system for some selected complexes and the model structures for **Pen** and **Hep** accompany the work reported in this Chapter as supporting information (SI).

## *Pt(II) complexes with $\alpha,\omega$ -alkyldiamine bridges*

---

**Table SI 3.1** Summary of the wavelengths (nm) used for monitoring the reactions between a series of Pt(II) complexes with bis(2-pyridylmethyl) chelates and thiourea nucleophiles.

<b>Complex</b>	<b>nu</b>	<b>Wavelength (<math>\lambda</math>), nm</b>
<b>En</b>	tu	325
	dmtu	327
	tmtu	330
	I <sup>-</sup>	308
<b>Prop</b>	tu	318
	dmtu	324
	tmtu	318
	I <sup>-</sup>	318
<b>But</b>	tu	315
	dmtu	325
	tmtu	327
	I <sup>-</sup>	310
<b>Hex</b>	tu	315
	dmtu	324
	tmtu	330
	I <sup>-</sup>	300
<b>Oct</b>	tu	312
	dmtu	324
	tmtu	327
<b>Dec</b>	tu	330
	dmtu	324
	tmtu	335
<b>bpma</b>	tu	276
	dmtu	276
	tmtu	300

## *Pt(II) complexes with $\alpha,\omega$ -alkyldiamine bridges*

---

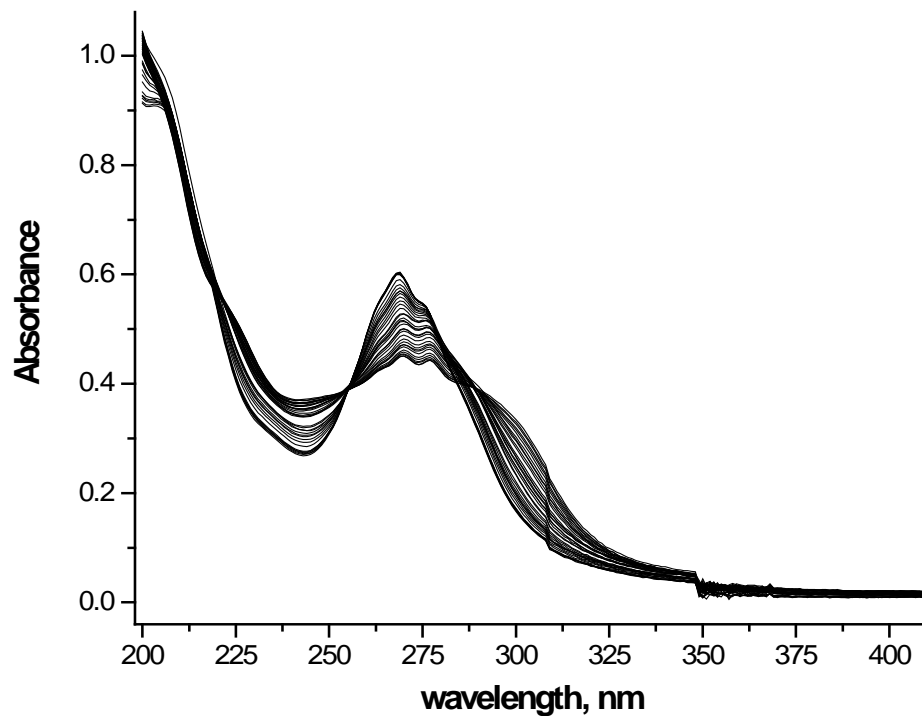


**Figure SI 3.1** UV-visible spectra for the titration of 0.1 mM Oct with NaOH, pH range 2-9, T= 298 K.

## *Pt(II) complexes with $\alpha,\omega$ -alkyldiamine bridges*

---

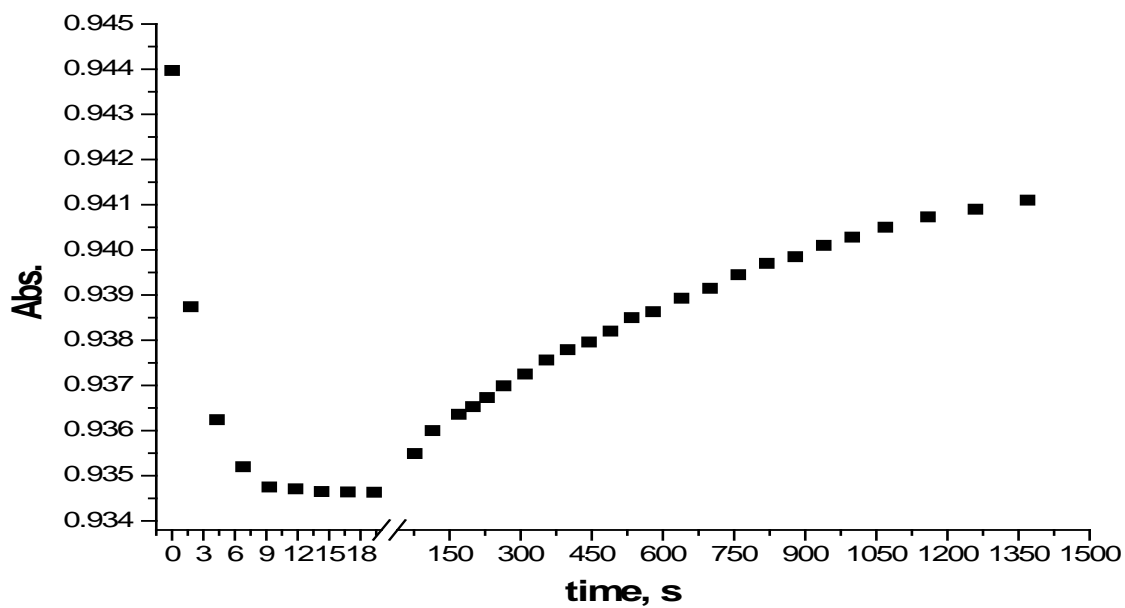


**Figure SI 3.2a** A typical kinetic trace for the two-steps reaction between **bpma** (0.1 mM) and **tu** (3 mM) recorded at 276 nm, T = 298 K, pH = 2.0, I = 0.02 M {CF<sub>3</sub>SO<sub>3</sub>H, adjusted with Li(SO<sub>3</sub>CF<sub>3</sub>)}.

# *Pt(II) complexes with $\alpha,\omega$ -alkyldiamine bridges*

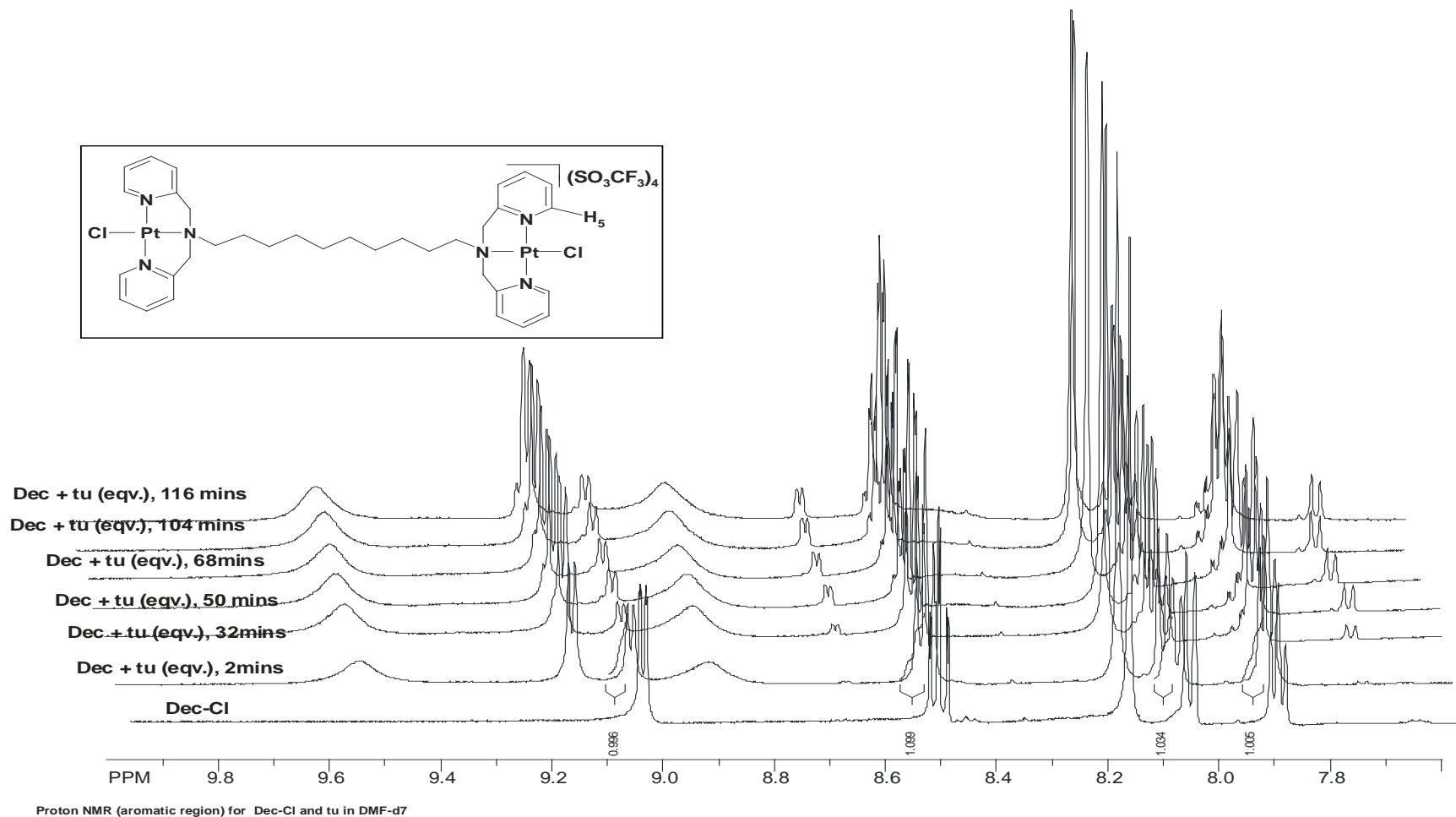


**Figure SI 3.2b**  $^1\text{H}$  NMR spectral array of **Dec-Cl** (showing only the aromatic region) acquired during its reaction with three equivalents of thiourea (tu) in DMF- $d_7$ .

## Pt(II) complexes with $\alpha,\omega$ -alkyldiamine bridges

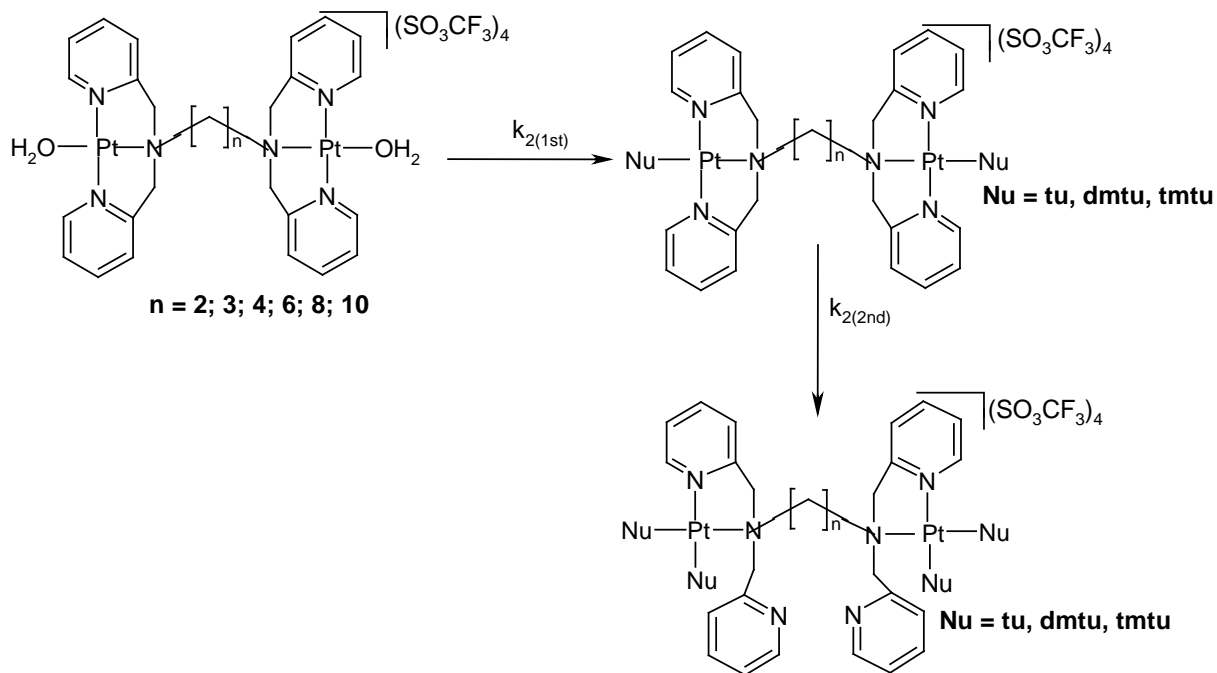


**Figure SI 3.2c** Proposed <sup>14c</sup> mechanism of substitution of the aqua leaving groups in the related Pt(II) dinuclear complexes and **bpma**.

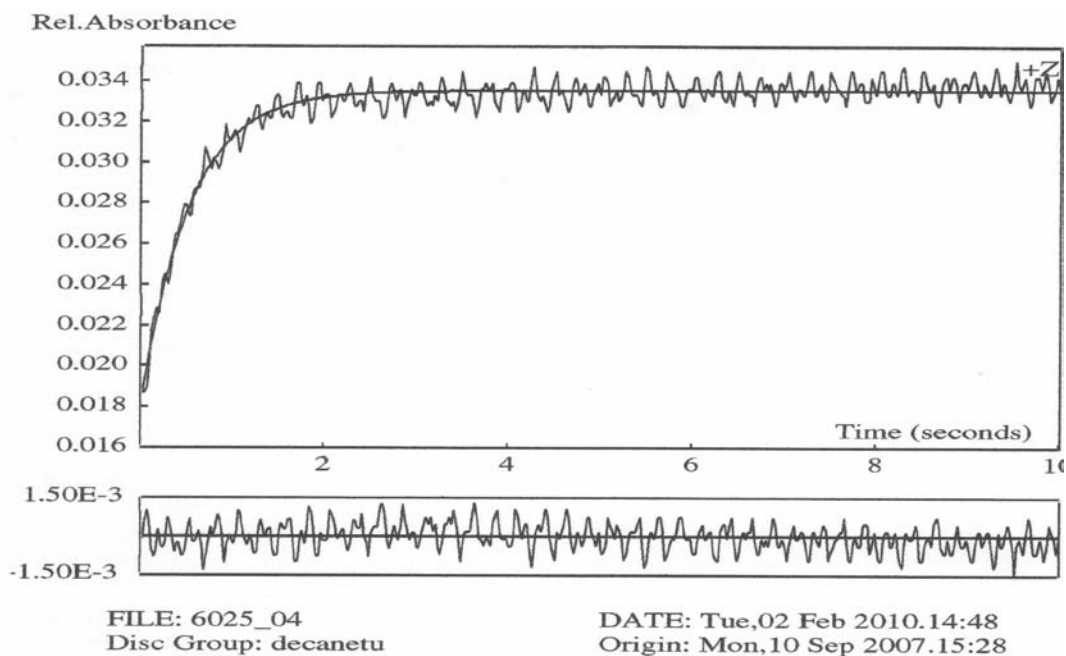


**Figure SI 3.2d** Kinetic trace at 324 nm for the first reaction step between **Dec** (0.11 mM) and **dmtu** (6.6 mM) at 298 K, pH = 2.0, I = 0.02 M {CF<sub>3</sub>SO<sub>3</sub>H, adjusted with Li(SO<sub>3</sub>CF<sub>3</sub>)}.

## Pt(II) complexes with $\alpha,\omega$ -alkyldiamine bridges

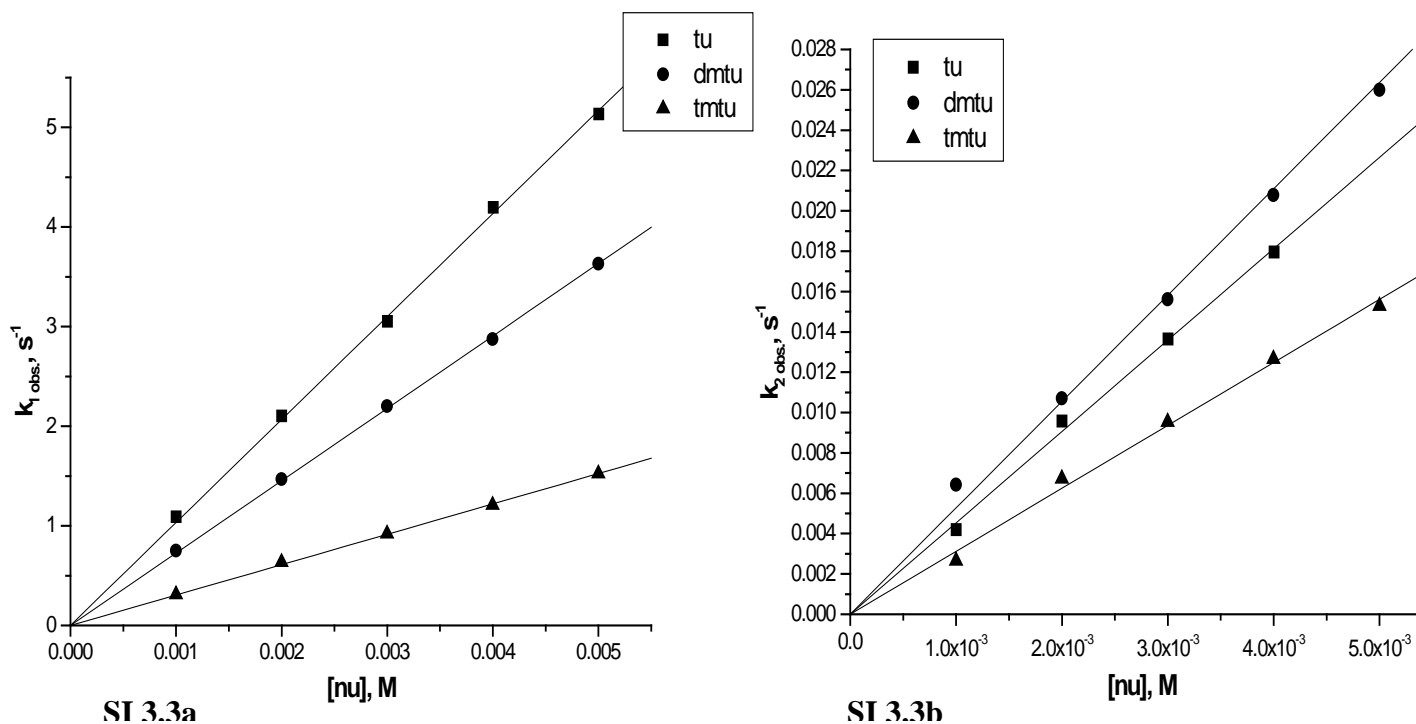


**Figure SI 3.3a** Concentration dependence of  $k_{\text{obs},(1)}^{\text{st}}, \text{s}^{-1}$ , for the simultaneous displacement of the aqua ligands in **Prop** by a series of thiourea nucleophiles, pH = 2.0, T = 298 K, I = 0.02 M {0.01 M  $\text{CF}_3\text{SO}_3\text{H}$ , adjusted with  $\text{Li}(\text{SO}_3\text{CF}_3)$ }.

**Figure SI 3.3b** Concentration dependence of  $k_{\text{obs},(2)}^{\text{nd}}, \text{s}^{-1}$ , for the dechelation of the pyridyl units in **Prop** by a series of thiourea nucleophiles, pH = 2.0, T = 298 K, I = 0.02 M {0.01 M  $\text{CF}_3\text{SO}_3\text{H}$ , adjusted with  $\text{Li}(\text{SO}_3\text{CF}_3)$ }.

## Pt(II) complexes with $\alpha,\omega$ -alkyldiamine bridges

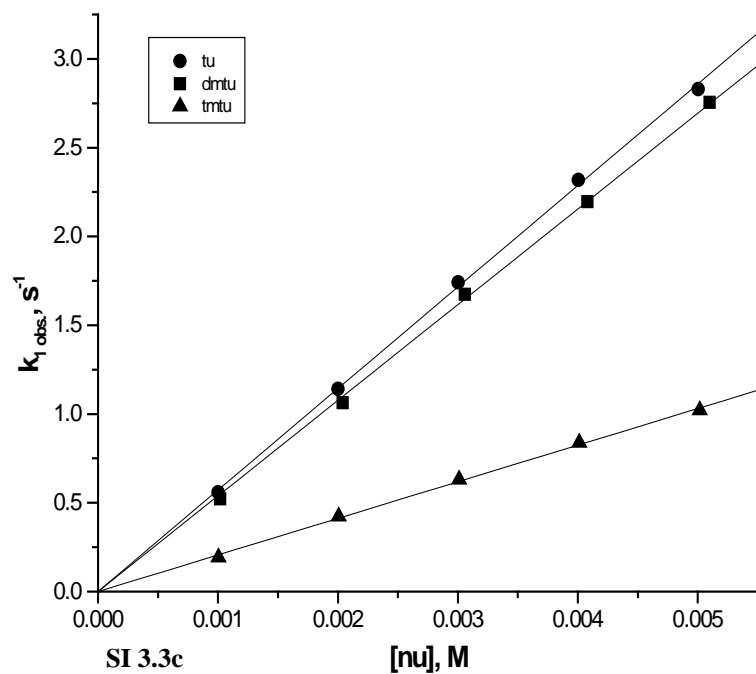


**Figure SI 3.3c** Concentration dependence of  $k_{\text{obs. (1st)}}$ , s<sup>-1</sup>, for the simultaneous displacement of the aqua ligands in **Oct** by thiourea nucleophiles, pH = 2.0, T = 298 K, I = 0.02 M {0.01 M CF<sub>3</sub>SO<sub>3</sub>H, adjusted with Li(SO<sub>3</sub>CF<sub>3</sub>)}.

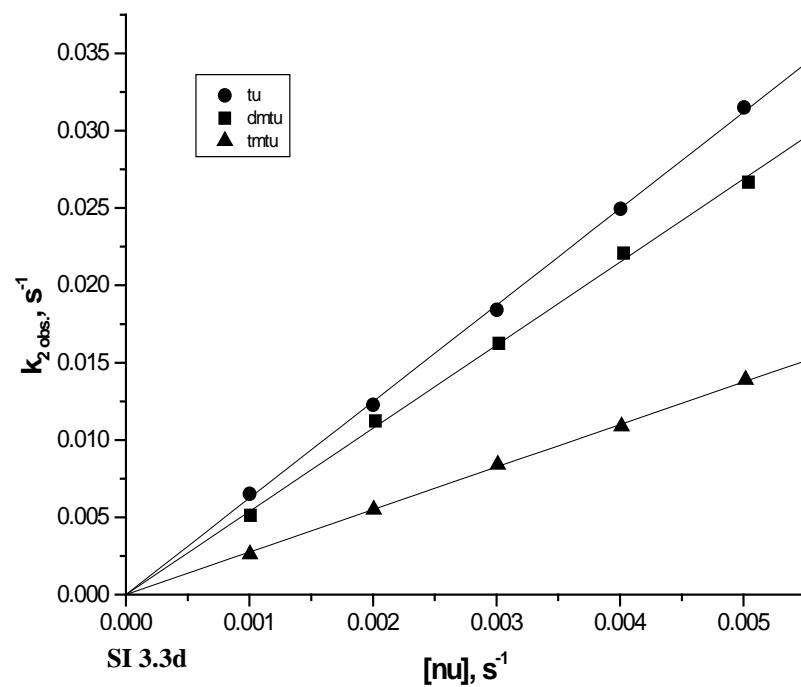


**Figure SI 3.3d** Concentration dependence of  $k_{\text{obs. (2nd)}}$ , s<sup>-1</sup>, for the dechelation of the pyridyl units in **Oct** by thiourea nucleophiles, pH = 2.0, T = 298 K, I = 0.02 M {0.01 M CF<sub>3</sub>SO<sub>3</sub>H, adjusted with Li(SO<sub>3</sub>CF<sub>3</sub>)}.

## Pt(II) complexes with $\alpha,\omega$ -alkyldiamine bridges

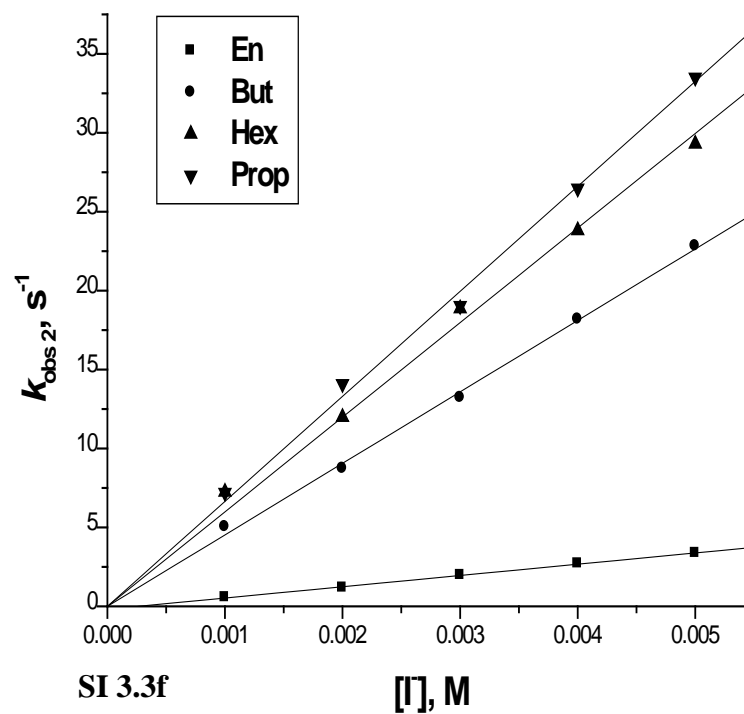
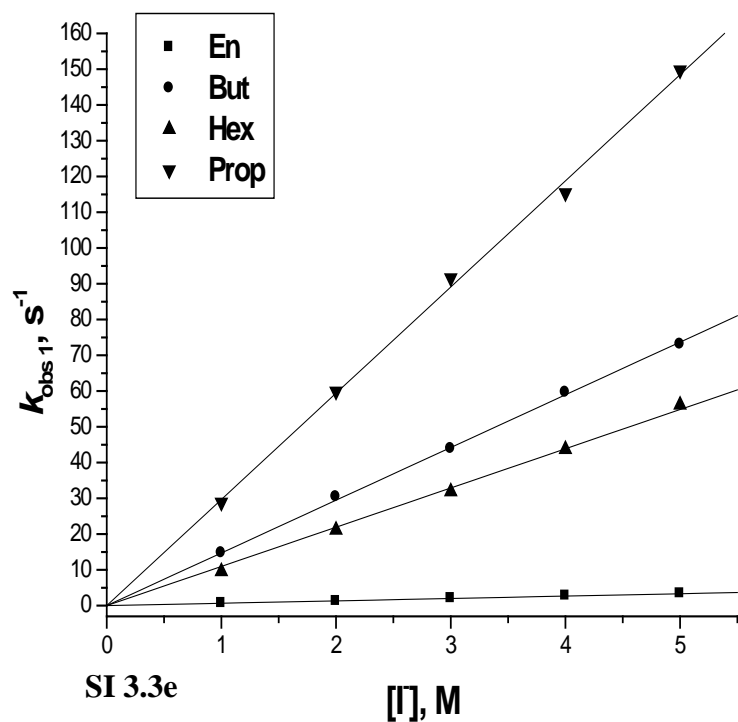


**Figure SI 3.3e** Plots of concentration dependence of  $k_{\text{obs}(1^{\text{st}})}$ , s<sup>-1</sup>, for the simultaneous displacement of the aqua ligands in **En**, **Prop**, **But** and **Hex** by iodide, pH = 2.0, T = 298 K, I = 0.02 M {0.01 M CF<sub>3</sub>SO<sub>3</sub>H, adjusted with Li(SO<sub>3</sub>CF<sub>3</sub>)}.

**Figure SI 3.3f** Plots of concentration dependence of  $k_{\text{obs}(2^{\text{nd}})}$ , s<sup>-1</sup>, for the simultaneous displacement of the aqua ligands in **En**, **Prop**, **But** and **Hex** by iodide, pH = 2.0, T = 298 K, I = 0.02 M {0.01 M CF<sub>3</sub>SO<sub>3</sub>H, adjusted with Li(SO<sub>3</sub>CF<sub>3</sub>)}.

## *Pt(II) complexes with $\alpha,\omega$ -alkyldiamine bridges*

**Table SI 3.2a.** Average observed rate constants,  $k_{\text{obs.}(1)^{\text{st}}}$ ,  $\text{s}^{-1}$ , for the simultaneous displacement of the aqua ligands in **Prop** thiourea nucleophiles, pH = 2.0, T = 298 K, I = 0.02 M {0.01 M  $\text{CF}_3\text{SO}_3\text{H}$ , adjusted with  $\text{Li}(\text{SO}_3\text{CF}_3)$ }.

nucleophiles					
tu ( $\lambda = 318 \text{ nm}$ )		dmtu ( $\lambda = 324 \text{ nm}$ )		tmtu ( $\lambda = 318 \text{ nm}$ )	
Conc., M	$k_{\text{obs.}, \text{s}^{-1}}$	Conc., M	$k_{\text{obs.}, \text{s}^{-1}}$	Conc., M	$k_{\text{obs.}, \text{s}^{-1}}$
0.001	1.091	9.996E-4	0.7499	0.001	0.3084
0.002	2.104	0.002	1.47	0.002	0.6344
0.003	3.051	0.003	2.201	0.003	0.918
0.004	4.197	0.004	2.874	0.004	1.208
0.005	5.135	0.005	3.633	0.005	1.522

**Table SI 3.2b** Average observed rate constants,  $k_{\text{obs.}(2)^{\text{nd}}}$ ,  $\text{s}^{-1}$ , for the dechelation of the pyridyl units in **Prop** by thiourea nucleophiles, pH = 2.0, T = 298 K, I = 0.02 M {0.01 M  $\text{CF}_3\text{SO}_3\text{H}$ , adjusted with  $\text{Li}(\text{SO}_3\text{CF}_3)$ }.

nucleophiles					
tu		dmtu		tmtu	
Conc., M	$k_{\text{obs.}, \text{s}^{-1}}$	Conc., M	$k_{\text{obs.}, \text{s}^{-1}}$	Conc., M	$k_{\text{obs.}, \text{s}^{-1}}$
0.001	0.0042	0.001	0.0064	0.001	0.0026
0.002	0.0096	0.002	0.0107	0.002	0.0067
0.003	0.0136	0.003	0.0156	0.003	0.0095
0.004	0.0180	0.004	0.0208	0.004	0.0126
		0.005	0.0260	0.005	0.0155

**Table SI 3.2c** Average observed rate constants,  $k_{\text{obs.}(1)^{\text{st}}}$ ,  $\text{s}^{-1}$ , for the simultaneous displacement of the aqua ligands in **Oct** by thiourea nucleophiles, pH = 2.0, T = 298 K, I = 0.02 M {0.01 M  $\text{CF}_3\text{SO}_3\text{H}$ , with  $\text{Li}(\text{SO}_3\text{CF}_3)$ }.

nucleophiles					
tu ( $\lambda = 312 \text{ nm}$ )		dmtu ( $\lambda = 324 \text{ nm}$ )		tmtu ( $\lambda = 327 \text{ nm}$ )	
Conc., M	$k_{\text{obs.}, \text{s}^{-1}}$	Conc., M	$k_{\text{obs.}, \text{s}^{-1}}$	Conc., M	$k_{\text{obs.}, \text{s}^{-1}}$
0.001	0.559	0.00102	0.522	0.00100	0.191
0.002	1.142	0.00204	1.064	0.00201	0.422
0.003	1.741	0.00306	1.673	0.00301	0.629
0.004	2.318	0.00408	2.195	0.00401	0.838
0.005	2.829	0.00510	2.755	0.00501	1.020

## *Pt(II) complexes with $\alpha,\omega$ -alkyldiamine bridges*

**Table SI 3.2d** Average observed rate constants,  $k_{\text{obs. (2}^{\text{nd}})}$ ,  $\text{s}^{-1}$ , for the dechelation of the pyridyl units in **Oct** by thiourea nucleophiles,  $\text{pH} = 2.0$ ,  $T = 298 \text{ K}$ ,  $I = 0.02 \text{ M}$   $\{0.01 \text{ M CF}_3\text{SO}_3\text{H}$ , adjusted with  $\text{Li}(\text{SO}_3\text{CF}_3)\}$ .

nucleophiles					
tu		dmtu		tmtu	
Conc., M	$k_{\text{obs.}}, \text{s}^{-1}$	Conc., M	$k_{\text{obs.}}, \text{s}^{-1}$	Conc., M	$k_{\text{obs.}}, \text{s}^{-1}$
0.001	0.0065	0.00101	0.0051	0.00100	0.0026
0.002	0.0123	0.00202	0.0112	0.00201	0.0055
0.003	0.0184	0.00302	0.0162	0.00301	0.0084
0.004	0.0249	0.00403	0.0221	0.00401	0.0109
0.005	0.0315	0.00504	0.0267	0.00501	0.0139

**Table SI 3.3a** Temperature dependence of  $k_{2(1^{\text{st}})}$ ,  $\text{M}^{-1}\text{s}^{-1}$ , for the simultaneous displacement of the aqua ligands in **Prop** by thiourea nucleophiles ( $[\text{nu}]$  at 60-fold excess over  $[\text{metal complex}]$ ),  $\text{pH} = 2.0$ ,  $I = 0.02 \text{ M}$  (0.01 M  $\text{CF}_3\text{SO}_3\text{H}$ , adjusted with  $\text{Li}(\text{SO}_3\text{CF}_3)$ ).

nucleophiles					
tu		dmtu		tmtu	
$1/T, \text{K}^{-1}$	$\ln(k_2/T)$	$1/T, \text{K}^{-1}$	$\ln(k_2/T)$	$1/T, \text{K}^{-1}$	$\ln(k_2/T)$
		0.00325	1.353	0.00325	0.669
0.0033	1.397	0.00330	1.164	0.00330	0.409
0.00335	1.243	0.00335	0.904	0.00335	0.145
0.00341	1.060	0.00341	0.672	0.00341	-0.108
0.00347	0.899	0.00347	0.436	0.00347	-0.408

**Table SI 3.3b** Temperature dependence of  $k_{2(2^{\text{nd}})}$ ,  $\text{M}^{-1}\text{s}^{-1}$ , for the dechelation of the pyridyl units in **Prop** by thiourea nucleophiles ( $[\text{nu}]$  at 60 fold excess of  $[\text{metal complex}]$ ),  $\text{pH} = 2.0$ ,  $I = 0.02 \text{ M}$  (0.01 M  $\text{CF}_3\text{SO}_3\text{H}$ , adjusted with  $\text{Li}(\text{SO}_3\text{CF}_3)$ ).

nucleophiles					
tu		dmtu		tmtu	
$1/T, \text{K}^{-1}$	$\ln(k_2/T)$	$1/T, \text{K}^{-1}$	$\ln(k_2/T)$	$1/T, \text{K}^{-1}$	$\ln(k_2/T)$
				0.00325	-3.942
0.0033	-3.778	0.0033	3.594	0.0033	-4.143
0.00335	-3.919	0.00335	3.771	0.00335	-4.420
0.00341	-4.072	0.00341	3.976	0.00341	-4.750
0.00347	-4.204	0.00347	4.159	0.00347	-5.020

## *Pt(II) complexes with $\alpha,\omega$ -alkyldiamine bridges*

**Table SI 3.3c** Temperature dependence of  $k_{2(1^{st})}$ ,  $M^{-1} s^{-1}$ , for the simultaneous displacement of the aqua ligands in **Oct** by thiourea nucleophiles ([nu] at 60-fold excess over [metal complex]), pH = 2.0, I = 0.02 M (0.01 M  $CF_3SO_3H$ , adjusted with  $Li(SO_3CF_3)$ ).

nucleophiles					
tu		dmtu		tmtu	
$1/T, K^{-1}$	$\ln(k_2/T)$	$1/T, K^{-1}$	$\ln(k_2/T)$	$1/T, K^{-1}$	$\ln(k_2/T)$
0.00325	1.099	0.00325	1.090	0.00325	0.074
0.00330	0.883	0.00330	0.890	0.00330	-0.183
0.00335	0.692	0.00335	0.711	0.00335	-0.505
0.00341	0.482	0.00341	0.472	0.00341	-0.853
0.00347	0.261	0.00347	0.237	0.00347	-1.175

**Table SI 3.3d** Temperature dependence of  $k_{2(2^{nd})}$ ,  $M^{-1} s^{-1}$ , for the dechelation of the pyridyl units in **Oct** by thiourea nucleophiles ([nu] at 60 fold excess of [metal complex]), pH = 2.0, I = 0.02 M (0.01 M  $CF_3SO_3H$ , adjusted with  $Li(SO_3CF_3)$ ).

nucleophiles					
tu		dmtu		tmtu	
$(1/T), K^{-1}$	$\ln(k_2/T)$	$(1/T), K^{-1}$	$\ln(k_2/T)$	$(1/T), K^{-1}$	$\ln(k_2/T)$
0.00325	-3.495	0.00325	-3.514	0.00325	-4.096
0.00330	-3.660	0.00330	-3.694	0.00330	-4.378
0.00335	-3.804	0.00335	-3.874	0.00335	-4.671
0.00341	-3.976	0.00341	-4.051	0.00341	-5.033
0.00347	-4.166	0.00347	-4.267	0.00347	-5.354

**Table SI 3.4a** Average observed rate constants,  $k_{obs.(1^{st})}$ ,  $s^{-1}$ , for the simultaneous displacement of the aqua ligands in **En** by thiourea nucleophiles, pH = 2.0, T = 298 K, I = 0.02 M {0.01 M  $CF_3SO_3H$ , adjusted with  $Li(SO_3CF_3)$ }.

nucleophiles					
tu ( $\lambda = 325nm$ )		dmtu ( $\lambda = 327 nm$ )		tmtu ( $\lambda = 330nm$ )	
Conc., M	$k_{obs.}, s^{-1}$	Conc., M	$k_{obs.}, s^{-1}$	Conc., M	$k_{obs.}, s^{-1}$
0.00101	0.151	0.001	0.0940	0.00101	0.0223
0.00201	0.287	0.002	0.1906	0.00201	0.0456
0.00301	0.452	0.003	0.2793	0.00301	0.0669
0.00402	0.618	0.004	0.3614	0.00402	0.0879
0.00503	0.749	0.005	0.4581	0.00503	0.1138

## *Pt(II) complexes with $\alpha,\omega$ -alkyldiamine bridges*

**Table SI 3.4b** Average observed rate constants,  $k_{\text{obs. (2}^{\text{nd}})}$ ,  $\text{s}^{-1}$ , for the dechelation of the pyridyl units in **En** by thiourea nucleophiles,  $\text{pH} = 2.0$ ,  $T = 298 \text{ K}$ ,  $I = 0.02 \text{ M}$   $\{0.01 \text{ M CF}_3\text{SO}_3\text{H}$ , adjusted with  $\text{Li}(\text{SO}_3\text{CF}_3)\}$ .

nucleophiles					
tu		dmtu		tmtu	
Conc., M	$k_{\text{obs.}, \text{s}^{-1}}$	Conc., M	$k_{\text{obs.}, \text{s}^{-1}}$	Conc., M	$k_{\text{obs.}, \text{s}^{-1}}$
0.001	0.00080	0.001	0.00057	0.00101	0.00048
0.002	0.00154	0.002	0.00113	0.00201	0.00099
0.00301	0.00249	0.003	0.00165	0.00301	0.00148
0.00401	0.00326	0.004	0.00205	0.00402	0.00205
0.00501	0.00395	0.005	0.00264	0.00503	0.00259

**Table SI 3.4c** Temperature dependence of  $k_{2(1^{\text{st}})}$ ,  $\text{M}^{-1} \text{s}^{-1}$ , for the simultaneous displacement of the aqua ligands in **En** by thiourea nucleophiles ( $[\text{nu}]$  at 60-fold excess over [metal complex]),  $\text{pH} = 2.0$ ,  $I = 0.02 \text{ M}$  (0.01 M  $\text{CF}_3\text{SO}_3\text{H}$ , adjusted with  $\text{Li}(\text{SO}_3\text{CF}_3)$ ).

nucleophiles					
tu		dmtu		tmtu	
$1/T., \text{K}^{-1}$	$\ln(k_2/T)$	$1/T., \text{K}^{-1}$	$\ln(k_2/T)$	$1/T., \text{K}^{-1}$	$\ln(k_2/T)$
0.00325	-0.142			0.00325	-2.281
0.00330	-0.408	0.00330	-0.881	0.00330	-2.455
0.00335	-0.685	0.00335	-1.177	0.00335	-2.748
0.00341	-1.008	0.00341	-1.425	0.00341	-2.962
0.00347	-1.230	0.00347	-1.783	0.00347	-3.189

**Table SI 3.4d** Temperature dependence of  $k_{2(2^{\text{nd}})}$ ,  $\text{M}^{-1} \text{s}^{-1}$ , for the dechelation of the pyridyl units in **En** by thiourea nucleophiles ( $[\text{nu}]$  at 60 fold excess of [metal complex]),  $\text{pH} = 2.0$ ,  $I = 0.02 \text{ M}$  (0.01 M  $\text{CF}_3\text{SO}_3\text{H}$ , adjusted with  $\text{Li}(\text{SO}_3\text{CF}_3)$ ).

nucleophiles					
tu		dmtu		tmtu	
$(1/T), \text{K}^{-1}$	$\ln(k_2/T)$	$(1/T), \text{K}^{-1}$	$\ln(k_2/T)$	$(1/T), \text{K}^{-1}$	$\ln(k_2/T)$
0.00325	-4.989	0.00325	-5.854	0.00325	-6.204
0.00330	-5.171	0.00330	-6.098	0.00330	-6.565
0.00335	-5.339	0.00335	-6.306	0.00335	-6.904
0.00341	-5.487	0.00341	-6.547	0.00341	-7.322
0.00347	-5.697	0.00347	-6.849	0.00347	-7.743

## *Pt(II) complexes with $\alpha,\omega$ -alkyldiamine bridges*

**Table SI 3.5a** Average observed rate constants,  $k_{\text{obs.}(1^{\text{st}})}$ ,  $\text{s}^{-1}$ , for the simultaneous displacement of the aqua ligands in **Hex** by thiourea nucleophiles,  $\text{pH} = 2.0$ ,  $T = 298 \text{ K}$ ,  $I = 0.02 \text{ M}$   $\{0.01 \text{ M CF}_3\text{SO}_3\text{H}$ , adjusted with  $\text{Li}(\text{SO}_3\text{CF}_3)\}$ .

nucleophiles					
tu ( $\lambda = 315 \text{ nm}$ )		dmtu ( $\lambda = 324 \text{ nm}$ )		tmtu ( $\lambda = 330 \text{ nm}$ )	
Conc., M	$k_{\text{obs.}, \text{s}^{-1}}$	Conc., M	$k_{\text{obs.}, \text{s}^{-1}}$	Conc., M	$k_{\text{obs.}, \text{s}^{-1}}$
0.00100	0.561	0.001	0.561	0.00100	0.171
0.00201	1.160	0.002	1.196	0.00201	0.367
0.00301	1.743	0.003	1.810	0.00301	0.542
0.00401	2.347	0.004	2.447	0.00401	0.737
0.00502	2.889	0.005	3.021	0.00502	0.912

**Table SI 3.5b** Average observed rate constants,  $k_{\text{obs.}(2^{\text{nd}})}$ ,  $\text{s}^{-1}$ , for the dechelation of the pyridyl units in **Hex** by thiourea nucleophiles,  $\text{pH} = 2.0$ ,  $T = 298 \text{ K}$ ,  $I = 0.02 \text{ M}$   $\{0.01 \text{ M CF}_3\text{SO}_3\text{H}$ , adjusted with  $\text{Li}(\text{SO}_3\text{CF}_3)\}$ .

nucleophiles					
tu		dmtu		tmtu	
Conc., M	$k_{\text{obs.}, \text{s}^{-1}}$	Conc., M	$k_{\text{obs.}, \text{s}^{-1}}$	Conc., M	$k_{\text{obs.}, \text{s}^{-1}}$
0.00100	0.0053	0.001	0.0058	0.00100	0.00127
0.00201	0.0109	0.002	0.0112	0.00201	0.00245
0.00301	0.0162	0.003	0.0172	0.00301	0.00364
0.00401	0.0212	0.004	0.0235	0.00401	0.00489
0.00502	0.0264	0.005	0.0298	0.00502	0.00619

**Table SI 3.5c** Temperature dependence of  $k_{2(1^{\text{st}})}$ ,  $\text{M}^{-1} \text{s}^{-1}$ , for the simultaneous displacement of the aqua ligands in **Hex** by thiourea nucleophiles ( $[\text{nu}]$  at 60-fold excess over  $[\text{metal complex}]$ ),  $\text{pH} = 2.0$ ,  $I = 0.02 \text{ M}$   $(0.01 \text{ M CF}_3\text{SO}_3\text{H}$ , adjusted with  $\text{Li}(\text{SO}_3\text{CF}_3)$ ).

nucleophiles					
tu		dmtu		tmtu	
$1/T, \text{K}^{-1}$	$\ln(k_2/T)$	$1/T, \text{K}^{-1}$	$\ln(k_2/T)$	$1/T, \text{K}^{-1}$	$\ln(k_2/T)$
0.00325	1.099	0.00325	1.314	0.00325	0.115
0.00330	0.910	0.00330	1.005	0.00330	-0.200
0.00335	0.661	0.00335	0.706	0.00335	-0.504
0.00341	0.432	0.00341	0.419	0.00341	-0.825
0.00347	0.179	0.00347	0.146	0.00347	-1.190

## *Pt(II) complexes with $\alpha,\omega$ -alkyldiamine bridges*

---

**Table SI 3.5d** Temperature dependence of  $k_2$  ( $2^{\text{nd}}$ ),  $\text{M}^{-1} \text{s}^{-1}$ , for the dechelation of the pyridyl units in **Hex** by thiourea nucleophiles ([nu] at 60 fold excess of [metal complex]), pH = 2.0, I = 0.02 M (0.01 M  $\text{CF}_3\text{SO}_3\text{H}$ , adjusted with  $\text{Li}(\text{SO}_3\text{CF}_3)$ ).

nucleophiles					
tu		dmtu		tmtu	
1/T, $\text{K}^{-1}$	$\ln(k_2/T)$	1/T, $\text{K}^{-1}$	$\ln(k_2/T)$	1/T, $\text{K}^{-1}$	$\ln(k_2/T)$
0.00325	-3.480			0.00325	-4.508
0.00330	-4.014	0.00330	-4.132	0.00330	-4.686
0.00335	-4.872	0.00335	-4.399	0.00335	-4.872
0.00341	-4.291	0.00341	-4.132	0.00341	-5.042
0.00347	-4.511	0.00347	-4.555	0.00347	-5.256

## *Pt(II) complexes with $\alpha,\omega$ -alkyldiamine bridges*

---

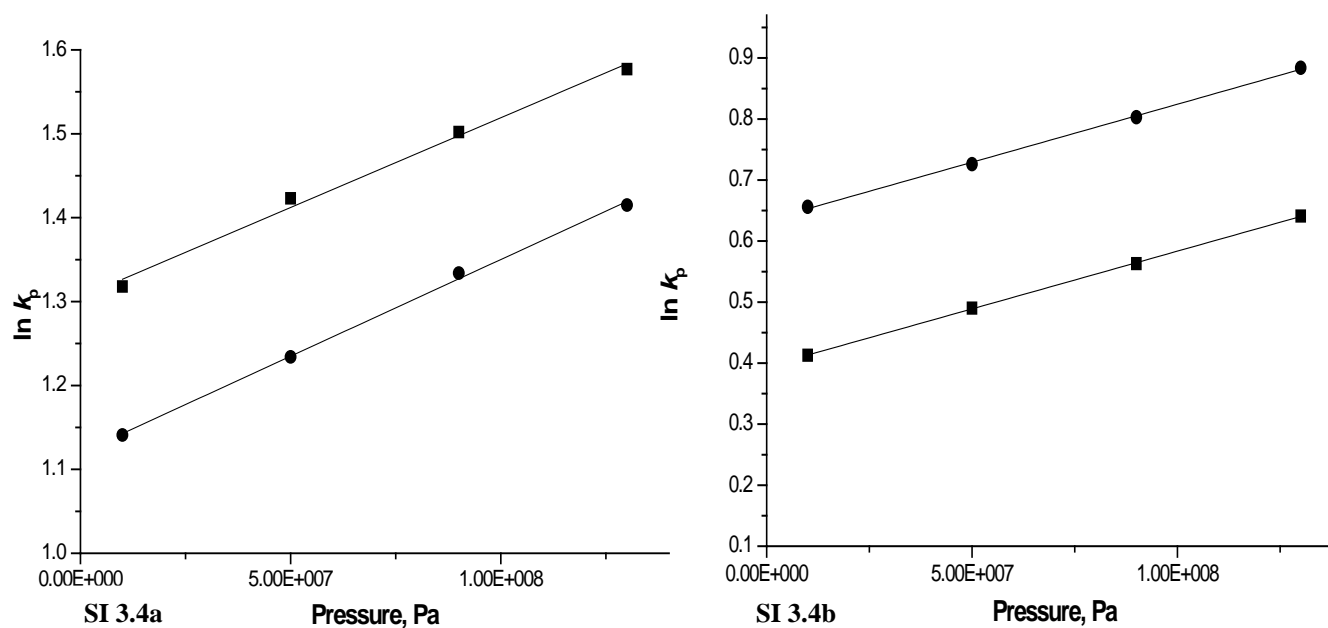
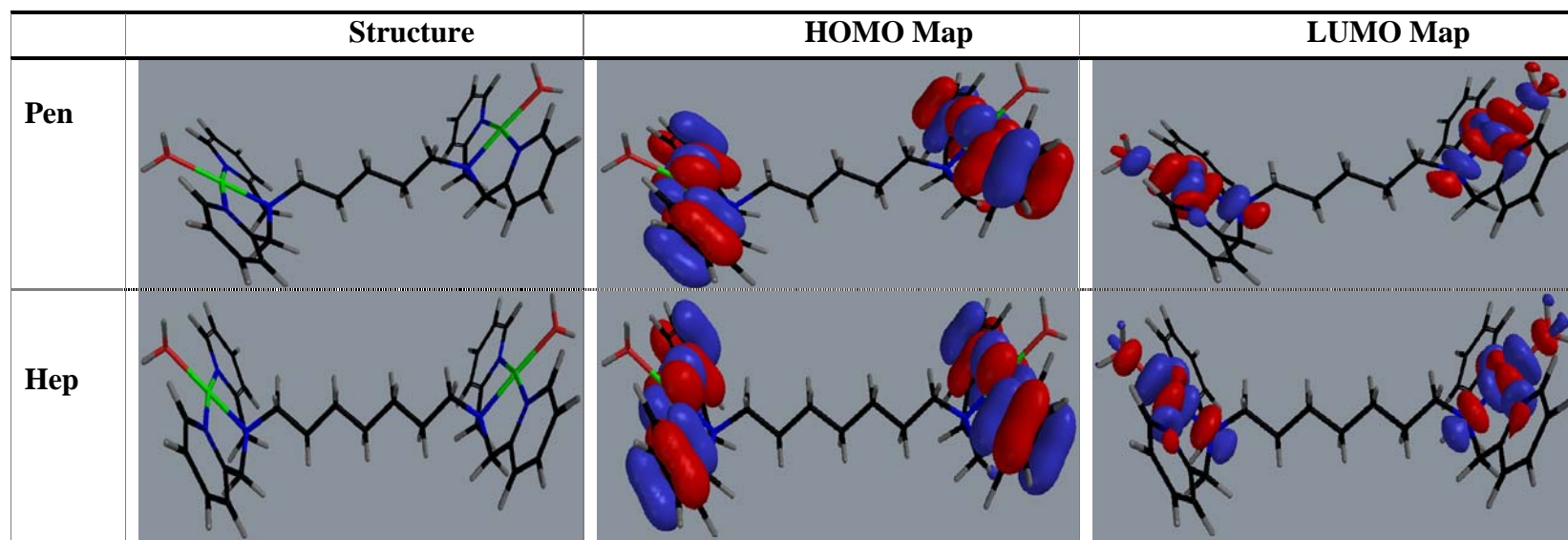


**Figure SI 3.4a** Dependence of  $k_{\text{obs}}$ . (repeated twice) on the on the pressure of the reaction mixture recorded at 320 nm for the simultaneous displacement of the aqua ligands in a reaction between **Prop** and tu, ([tu] maintained at a 60-fold excess concentration over the complex). at 298 K, pH = 2.0, I = 0.02 M {CF<sub>3</sub>SO<sub>3</sub>H, adjusted with Li(SO<sub>3</sub>CF<sub>3</sub>)}

**Figure SI 3.4b** Dependence of  $k_{\text{obs}}$ . (repeated twice) on the on the pressure of the reaction mixture recorded at 320 nm for the simultaneous displacement of the aqua ligands in a reaction between **Oct** and tu, ([tu] maintained at a 60-fold excess concentration over the complex) at 298 K, pH = 2.0, I = 0.02 M {CF<sub>3</sub>SO<sub>3</sub>H, adjusted with Li(SO<sub>3</sub>CF<sub>3</sub>)}

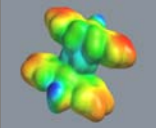
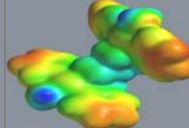
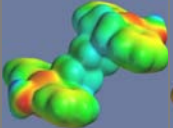
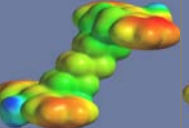
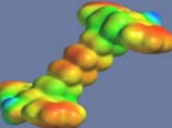
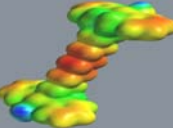
## *Pt(II) complexes with $\alpha,\omega$ -alkyldiamine bridges*

**Table SI 3.6** Density functional theoretical (DFT)<sup>26</sup> minimum energy structures, HOMO and LUMO frontier molecular orbitals for **Pen** and **Hep**. The calculations were performed with the Spartan '04 for Windows quantum chemical package<sup>27</sup> using the B3LYP hybrid functional method<sup>28</sup> and the LACVP+\*\*<sup>29</sup> pseudopotentials basis set.



## *Pt(II) complexes with $\alpha,\omega$ -alkyldiamine bridges*

**Table SI 3.6** Electrostatic potential surface mappings (EPS) of the dinuclear Pt(II) complexes bridged by flexible alkyldiamine linkers.

Complex	En	Prop	But	Hex	Oct	Dec
EPS						

### 3.8 Commentary notes (CN) to section 3.2.1

#### 3.8.1 X-rays diffraction analysis of ligands L2; L3 and L6.

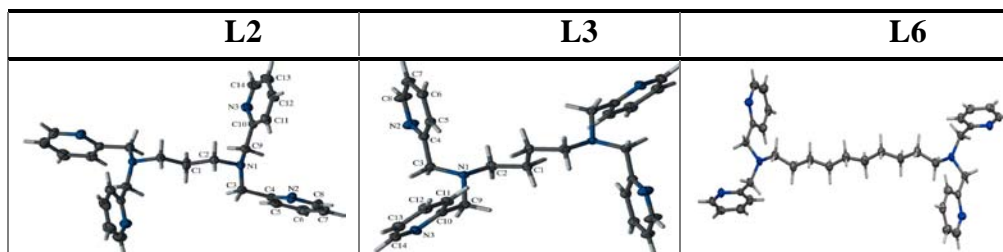
As alluded to in the main paper, colourless crystals {X-ray quality in the case of **L1** ( $n = 2$ ); **L2** ( $n = 3$ ) and **L3** ( $n = 4$ )} were yielded from a suspension of their oils or powder in ethanol. This was achieved through slow evaporation of the ethanol solvent over several days. The crystal structure of **L1** has been solved before while **L6** ( $n=10$ ) gave a poor diffraction pattern.

Only the crystal structures of ligands **L2** and **L3** were successfully solved by single crystal X-rays diffraction analysis and their structures are shown in Table CN1. The molecular structure of ligand **L3** was determined on an Oxford Diffraction Xcalibur2 CCD diffractometer. Data collection was by the *CrystAlis CCD* program while cell refinement and data reduction were done using the *CrystAlis RED* suite of programs.<sup>1</sup> Crystal structures were solved and refined by the SHELXL97<sup>2</sup> software while the *Orterp*<sup>3</sup> and *WinGX*<sup>4</sup> were used for all molecular graphics. Full details on the crystal structures and their intriguing supramolecular chemistry are reported in a published paper attached in the Appendix A:

Mambanda, D. Jaganyi, and O. Q Munro, One-dimensional C-H...N hydrogen-bonded polymers in flexible tetrapyridyl systems, *Acta Cryst.*, 2007, **C63**, o676–o680.

# Pt(II) complexes with $\alpha,\omega$ -alkyldiamine bridges

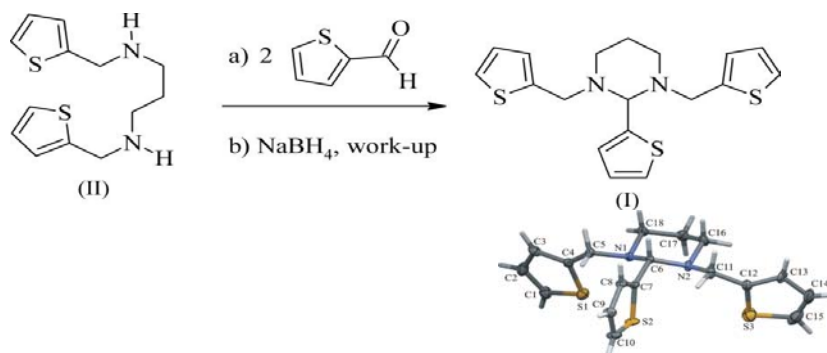
**Table CN 3.1** Molecular structures of three of the ligands showing the  $C_2$  symmetry and a common inversion symmetry in **L2**, **L3** and **L6**.



*N,N,N',N'*-tetrakis(2-pyridylmethyl)-1,3-propanediamine (**L2**); *N,N,N',N'*-tetrakis(2-pyridylmethyl)-1,4-butanediamine (**L3**); and *N,N,N',N'*-tetrakis(2-pyridylmethyl)-1,10-decanediamine (**L6**).

## 3.8.2 Comment on the crystal structures of ligands **L2**; **L3** and **L6**.

In our earlier efforts aimed at extending this work to afford similar hexadentate ligands with bis-(2-thienylmethyl)amine (SNS) using a published method<sup>21</sup> as shown in scheme CN 3.1 below, we ended up synthesizing new cyclic compounds namely the bis-(2-thienyl)methylimidazolidine derivative and the bis-(2-thienyl)methylhexahydropyrimidine derivative (whose molecular structure shown in scheme CN 3.1), when 1,2-ethanediamine and 1,3-propanediamine were used as the starting materials, respectively. A competitive intramolecular Mannich cyclization<sup>5</sup> of the intermediate reduction product (II), prevented the nucleophilic substitution at one of the amine N atom by the incoming and 2-thiynlcarbaldehyde molecule which would have afforded the targeted SNS hexadentate ligands. However, with a careful amine protection procedure using reagents such as Boc at one terminal of the diamine, the hexadendates can still be accessed for future investigation on the role of changing the donor atom on the reactivity of the complexes.



## *Pt(II) complexes with $\alpha,\omega$ -alkyldiamine bridges*

---

**Scheme CN 3.1** Synthetic scheme for the novel bis-(2-thienylmethyl)hexahydropyrimidine derivative.

Interestingly, both the imidazolidine and hexahydropyrimidine core ring systems are known to impart analgesic as well as antipyretic properties which are depended on the functional groups attached to the ring cores. An evaluation of the activities of these new compounds for this purpose is of interest since the synthesis of the compounds is straight forward and readily afforded in pure crystalline forms.

Single crystals of both the imidazolidine and the hexahydropyrimidine derivatives were obtained and analyzed by X-rays diffraction. Only the molecular structure of the latter could be solved fully. Its molecular structure is shown in Scheme CN 3.1 and the full details of its crystal structure are reported in an article:

D. Jaganyi, A. Mambanda and O. Q. Munro, A tripodal tris(thiophene) derivative of hexahydropyrimidine and its ladder-like extended structure' *Acta Cryst.*, 2007, **E63**, o2388–o2390.

### **3.8.3 References to the commentary notes.**

- 1 Oxford Diffraction, *CrysAlis CCD* and *CrysAlis RED*, Versions 1.171.29.9 (Release 23-03-2006 CrysAlis 171. Net), 2006, Oxford Diffraction Ltd., Abingdon, Oxfordshire, England.
- 2 G. M. Sheldrick, *SHELXS97* and *SHELXL97*, 1997, University of Göttingen, Germany.
- 3 L. J. Farrugia, *J. Appl. Cryst.*, 1997, **30**, 565.
- 4 L. J. Farrugia, *J. Appl. Cryst.*, 1999, **32**, 837.
- 5 Tse Lok Ho, *Tandem Organic reactions*, Wiley.com, Chapter 6, 101.

## Chapter Four

*Extra supplementary data linked to this work is attached to the Appendix.*

### **Kinetics study of Pt(II) amphiphiles derived from a bis(2-pyridylmethyl)amine chelate headgroup.**

#### **4.0 Abstract**

The substitution of aqua ligands of mononuclear Pt(II) complexes of the general form  $[\text{Pt}(\text{H}_2\text{O})(N,N\text{-bis}(2\text{-pyridylmethyl})\text{-N}(\text{CH}_2)_n\text{-CH}_3; \text{-NC}(\text{CH}_3)_3; \text{-NH})(\text{CF}_3\text{SO}_3)_2]$ ,  $n = 1$  (**bpea**); 2 (**bppa**); 3 (**bpba**); 5 (**bpha**), 9 (**bpda**)  $\text{-NC}(\text{CH}_3)_3$  (**bpbta**) and  $\text{-NH}$  (**bpma**) by thiourea nucleophiles was investigated under pseudo first-order conditions as a function of concentration and temperature using the stopped-flow technique and UV-visible spectroscopy. The substitution reactions occur via two separate reaction steps, each fitting to a single exponential curve. The mode of activation for both steps remains associative in nature and the observed rate constants can be fitted to the equation  $k_{\text{obs}}(1^{st}/2^{nd}) = k_2(1^{st}/2^{nd})[\text{Nu}]$ . The relative magnitude of the measured second-order rate constants for the substitution of the aqua ligands by the thiourea nucleophiles reflects the structural differences that exist between the complexes when alkyl groups of different chain lengths and structures are appended on the *trans*-N donor atom of the bis(2-pyridylmethyl)amine headgroup. In general, appending an alkyl hydrocarbon group on the *trans*-N donor atom of this chelate headgroup increases the rate of substitution of the aqua leaving group due to the stronger *trans*-influence of its alkylamine donor group. Primary alkyl pendants increase reactivity only to a moderate extent. However, when a *tert*-butyl group is appended on the same position, reactivity increases by a factor of about two. The increase in reactivity demonstrated in this complex, whose alkyl tail is branched on the  $\alpha$ -carbon, reiterates the inductive nature of the flow of electron density from the tailing groups towards the Pt(II) metal centres in the complexes. Since the primary alkyl-pendants become the structural linkers in the related flexible multi-topic Pt(II) complexes bridged by alkyldiamines, the reactivity trend of the studied complexes demonstrate that the electronic effect of the alkyldiamine bridge on the overall reactivity of their analogous dinuclear Pt(II) complexes is weak. It gets further weakened by other factors such as the steric features within the bridge and the native electronic effects within the donor chelate headgroups when the linker is short. A comparison of the reactivity data of these Pt amphiphiles with the  $\alpha,\omega$ -alkyldiamine-bridged

# Mononuclear Pt(II) complex with alkyl pendants

dinuclear complexes reported in Chapter Three reveals that the primary role of the flexible bridge on the reactivity of the latter complexes is to effect a structural constraint which has a profound bearing on the reactivity of the two Pt centres when the linker is short. The average distance separating the Pt centres and the adopted symmetries of the dinuclear complexes are two operational constraints due to the linker, proven to have an indirect influence on the reactivity of the Pt centres, since they directly control the amount of steric impositions as well as the electrostatic charge addition at each Pt chelate headgroup. However, a weak electronic effect, due to the linker, exists in the dinuclear complexes. This is evidenced from the slight increase in the reactivity of analogous amphiphiles of this study when the chain lengths of their pendants are increased.

## 4.1 Introduction

Mononuclear Pt(II)/Pd(II) complexes of tridentate ligands such as diethylenetriamine (dien)<sup>1-5</sup>, bis(2-pyridylmethyl)amine<sup>6-10</sup> and 2,2':6',2''-terpyridine (terpy)<sup>11-24</sup> have provided some of the most useful coordination compounds for studying the kinetics of substitution reactions at a square-planar geometry. Through their terdentate coordination, these ligands afford model four-coordinate chelated Pd(II)/Pt(II) complexes that are thermodynamically stable.<sup>7</sup> These square-planar substrates have a single leaving group, which simplifies the course of their substitution reactions known to proceed via an associative mechanism in the majority of cases.<sup>25</sup>

In much the same way some simple monodentate Pt(II) complexes were used to establish the role of the *trans*-effect in early ligand substitution reactions of planar-coordination complexes by Werner and Chernayev,<sup>26</sup> square-planar Pd(II)/Pt(II) complexes of these three terdentate ligands were useful in understanding the general role of the non-carrier chelate ligand system on the substitutional reactivity of their metal complexes.<sup>1-24</sup> It is now established that structural as well as electronic properties of the non-labile chelate ligands control the rate of substitution on their square-planar chelates.<sup>1-24</sup> In addition, the non-labile ligand system around the central metal ion can also exert in-lieu control of other physical properties of the complexes such as solubility, polarity and acidity thereby potentially influencing the mechanistic course of the substitution reactions.

Data in literature categorically shows that the lability of the leaving groups in chelated mononuclear complexes is influenced mainly by the bite angle, steric features<sup>1-3,25a</sup> as well as

## Mononuclear Pt(II) complex with alkyl pendants

the  $\sigma/\pi$ -structural features of the chelate ligand and its ancillary groups.<sup>1-24</sup> Rigid ligands form smaller bite angles at the central metal ions, causing steric strain within the chelate framework which leads to increased lability in the co-leaving groups.<sup>25b</sup> The presence of steric groups on the non-labile ligand backbone usually causes a steric retardation on the metal centre due to either congestion or direct hindrance to the approach of the nucleophiles.<sup>1-3,20,25</sup> This retardation effect is more pronounced when the steric ligands have a *cis*-geometry to the leaving group. Strong *trans*-labilizing groups cause a ground state destabilization of the *trans*-bond through a  $\sigma$ -effect and a transition state stabilization via the  $\pi$ -effect leading in both cases to increased reactivity.<sup>12-14</sup> On the contrary, a *cis*  $\sigma$ -donation towards the metal centre retards the rate of substitution.<sup>23</sup> Further to this, any withdrawal of excess electron density from the metal centre whether by  $\pi$ -resonance<sup>23b</sup> or by inductive means, leads to a general increase in the rate of substitution through stabilization of the transition state. Delocalization of charge from the metal centre by  $\pi$ -resonance depends on the extent of  $\pi$ -conjugation within the carrier ligand backbone, more so when the ligand is coordinated to a softer metal ion such as Pt(II).<sup>21-22</sup> As a result of this, complexes of the general form,  $[\text{Pt}(\text{terpy})\text{X}]^+$ ,  $\text{X} =$  mono anionic leaving ligand, are three to five orders of magnitude more reactive than  $[\text{Pt}(\text{dien})\text{X}]^+$ .<sup>12-14</sup>

The role of the ancillary groups on the  $\pi$ -effect of the terpy ligand in monofunctional complexes of the form:  $[\text{Pt}(4'\text{-}R\text{-terpy})\text{X}]^+$ ,  $R = \text{H}; \text{Ph}; \text{Ph}(\text{o-CH}_3); \text{Ph}(\text{o-Cl})$  or  $\text{Ph}(\text{o-CH}_3)$ , where Ph = phenyl group, has been studied in detail.<sup>23,24</sup> Introduction of electron-donating ancillary groups on the terpy ring system decreases the rate of substitution, while electron-withdrawing groups cause the opposite effect. For example, when three *tert*-butyl groups<sup>24a</sup> are appended on the *para* positions of the three rings of the terpy or when groups such as Ph<sup>23</sup> or  $\text{Ph}(\text{o-CH}_3)$ <sup>23,24b</sup> are attached on the *para* position of the central ring of the terpy ligand, a general decrease in lability of the leaving groups is observed relative to the parent terpy complex. The opposite is observed when electron withdrawing groups such as  $\text{Ph}(\text{o-CF}_3)$ <sup>23,24b</sup> or  $\text{Ph}(\text{o-Cl})\text{Ph}$ <sup>24b</sup> are appended on the same position. The ancillary groups influence the rate of substitution by controlling the extent of  $\pi$ -back donation of electron density from the metal centres into the terpy ring system.<sup>12-14,23a,24</sup>

However, in the absence of an extended  $\pi$ -conjugation in the chelate framework, as in the cases of Pt(II) complexes of the dien<sup>1-5</sup> and the bis(2-pyridylmethyl)amine ligands,<sup>6-10</sup> appending ancillary groups on the *trans*-position of the non-labile chelate ligand may assume a different role on the reactivity of their metal centres. Firstly, a decrease in the extended  $\pi$ -conjugation of the metal complexes occurs as a result of a proportional reduction in the

## Mononuclear Pt(II) complex with alkyl pendants

aromaticity of the chelate frameworks of the bis(2-pyridylmethyl)amine and the dien ligands when both are referenced to the planar framework of the terpy ligand. On a relative basis, this leads to metal chelates with reduced planarity and increased conformational flexibility, which may increase axial steric overlap felt at the central metal atoms. More importantly, the well understood  $\sigma$ -*trans* effect becomes more dominant over the  $\pi$ -effect.<sup>25</sup> When electron donating ancillary groups are appended on the *trans* donor atoms, a general increase in reactivity is expected through an increased ground state labilization at the *trans*-leaving groups. Electron withdrawing groups are expected to cause an opposite effect.

Appending functional groups at the *trans*-donor atom in chelated Pt(II) square-planar complexes is appealing in two ways. Firstly, if alkyl hydrocarbon chains or fluorinated alkyl chains are attached to the *trans*-donor N atom of some non-labile chelate headgroup such as the bis(2-pyridylmethyl)amine, amphiphilic ligands are formed whose coordination to the Pt(II) metal centre results in metallosurfactants with chelated headgroups.<sup>27-29</sup> The amphiphilic structures of the ligands thus, lend their interfacial surfactants properties, bringing in tailor-made structural organization in the molecules of the metal complexes at the different media interfaces.<sup>30</sup> This behaviour can be exploited in biological systems to increase the affinity of anti-tumour active Pt(II) compounds at the aqueous/phospholipid interface of plasma membrane and thus facilitating their efficient entry into the cell.<sup>31-33</sup> Since the metallosurfactants are formed from chelated amphiphile such as the bis(2-pyridylmethyl)alkylamine, the problem of loss of the appended group through *trans*-labilization induced by the coordination of strong sulfur containing coligands as recently reported for some structurally related dinuclear complexes is minimized.<sup>34</sup>

A recent study<sup>31</sup> has shown that increasing the lipophilicity of some platinum(II) amphiphilic complexes indeed enhances their rate of cellular uptake. Consequently, the cytotoxic activities of the monodentate Pt(II) complexes derived from *N*-alkylamine amphiphiles were found to increase as the chain length of the hydrophobic alkyl tail was extended. Secondly, dinuclear and multinuclear complexes of Farrell's design<sup>35-38</sup> are conceptually structured by attaching a second Pt(II) headgroup at the tailing end of the pendant of the amphiphilic alkylamine Pt(II) complexes. The alkylamine pendant is converted into a flexible diamine linking bridge in the resultant dinuclear complexes. Thus, a sound understanding of how appended groups such as the alkyl hydrocarbons at the *trans*-donor atoms of mononuclear Pt(II) amphiphiles affect their reactivity, is relevant in separating out the distinctive roles of the bridging groups such as the alkyldiamine, phenyldiamine or

# Mononuclear Pt(II) complex with alkyl pendants

diaminocyclohexane on the general reactivity of the related multinuclear complexes in which they become bridges. This retro-analysis of the role of bridging systems in multinuclear complexes is necessary because in these complexes, the role of the bridge on reactivity becomes multifaceted. The bridge serves as an integral component of the non-labile ligand as well as being the linking structural entity enjoining the Pt(II) centres. This shrouds its role on reactivity with nested complexity emanating from its steric features, symmetry requirements as well as its electronic properties. In dinuclear complexes with chelate headgroups such as the bis(2-pyridylmethyl)amine, it is quite possible that the structural features of the core linking groups can control the reigning symmetry elements within the molecular structure of complexes, thereby determining the steric influences at the Pt(II) centres due to the bridging groups.

As part of the study aimed at increasing an understanding of the underlying role of the flexible diamine bridging systems on the reactivity of dinuclear complexes with archetypal bis(2-pyridylmethyl)amine chelate headgroups, the substitution reactions of a series of six mononuclear complexes of the general form,  $[\text{Pt}(\text{H}_2\text{O})(N,N\text{-bis}(2\text{-pyridylmethyl})\text{-N}(\text{CH}_2)_n\text{-CH}_3; \text{-NC}(\text{CH}_3)_3; \text{-NH})(\text{CF}_3\text{SO}_3)_2]$ ,  $n = 1$  (**bpea**); 2 (**bppa**); 3 (**bpba**); 5 (**bpha**); 9 (**bpda**);  $\text{-NC}(\text{CH}_3)_3$  (**bpbta**) and  $\text{-NH}$  (**bpma**) with thiourea nucleophiles were investigated. In these platinum(II) amphiphilic complexes, the length of the alkyl tail appended on *trans*-N donor atom of the bis(2-pyridylmethyl)amine ligand is systematically increased. It was expected that the reactivity data from this study can be useful in gaining a full understanding of the intrinsic role of the alkyldiamine bridge on the general reactivity of related homotopic dinuclear complexes with bis(2-pyridylmethyl)amine headgroups.

## 4.2 Experimental

### 4.2.1 Preparation of ligands

Ligands, namely, *N,N*-bis(2-pyridylmethyl)ethylamine (**L1**); *N,N*-bis(2-pyridylmethyl)propylamine (**L2**); *N,N*-bis(2-pyridylmethyl)butylamine (**L3**); *N,N*-bis(2-pyridylmethyl)*tert*-butylamine (**L4**); *N,N*-bis(2-pyridylmethyl)hexylamine (**L5**) and *N,N*-bis(2-pyridylmethyl)decylamine (**L6**) were synthesized for this investigation. The ligands, **L1-L3**, **L5-L6** were all prepared using a method previously described in literature.<sup>39a,b</sup> For the synthesis of **L4**, this method was slightly modified as described by Mok *et al.*<sup>39c</sup>

## Mononuclear Pt(II) complex with alkyl pendants

This procedure yielded oil products (**L1**, **L3**, **L5-L6**) of sufficient purity for use in the platinum coordination. The purity of the ligands was confirmed by  $^1\text{H}$  NMR,  $^{13}\text{C}$  NMR, MS-ES<sup>+</sup> and elementary analysis (for non-oils). A typical mass spectrum of the ligands is given as supporting information in Figure SI 4.1a for ligand **L5**. Two of the ligands *viz.*, **L2** and **L4** yielded colourless crystals from slow evaporation of their oils. The structure of **L4** was successfully solved by X-rays diffraction analysis.<sup>40</sup>

**(L1)** Yield: 1.93 g, yellow oil (71 %).  $^1\text{H}$  NMR (400 MHz,  $\text{CDCl}_3$ )  $\delta$  / ppm: 8.41 (d, 2H); 7.60 (t, 2H); 7.35 (d, 2H); 7.20 (t, 2H); 3.75 (s, 4H); 2.58 (q, 2H); 1.10 (t, 3H).  $^{13}\text{C}$  NMR (125 MHz,  $\text{CDCl}_3$ )  $\delta$  / ppm: 12.0; 45.2; 60.0; 122.0; 123.0; 136.0; 149.0; 160. TOF MS-ES<sup>+</sup>, m/e: 228.1712, (M +1)<sup>+</sup>.

**(L2)** Yield: 1.84 g, colourless crystal blocks (63 %).  $^1\text{H}$  NMR (400 MHz,  $\text{CDCl}_3$ )  $\delta$  / ppm: 8.48 (d, 2H); 7.70 (t, 2H); 7.60 (d, 2H); 7.18 (t, 2H); 3.80 (s, 4H); 2.58 (t, 2H); 1.58 (m, 2H); 0.90 (t, 3H).  $^{13}\text{C}$  NMR (125 MHz,  $\text{CDCl}_3$ )  $\delta$  / ppm: 4; 20.0; 56.5; 62.0; 122.0; 123.0; 136.0; 149.0; 160. *Anal. Calc. for*  $\text{C}_{15}\text{H}_{19}\text{N}_3$ : C, 74.65; H, 7.93; N, 17.41; *Found*: C, 74.86; H, 8.02; N, 17.38. TOF MS-ES<sup>+</sup>, m/e: 242.1657, (M +1)<sup>+</sup>.

**(L3)** Yield: 1.82 g, yellow oil (60 %) bright.  $^1\text{H}$  NMR (400 MHz,  $\text{CDCl}_3$ )  $\delta$  / ppm: 8.41 (d, 2H); 7.38 (t, 2H); 7.36 (d, 2H); 7.0 (t, 2H); 3.78 (s, 4H); 2.50 (t, 2H); 1.45 (m, 2H) 1.22 (m, 2H); 0.79 (t, 3H).  $^{13}\text{C}$  NMR (125 MHz,  $\text{CDCl}_3$ )  $\delta$  / ppm: 8; 21.0; 29; 54.2; 62.0; 122.0; 123.0; 136.0; 149.0; 160. TOF MS-ES<sup>+</sup>, m/e: 256.1814, (M +1)<sup>+</sup>.

**(L4)** Yield: 1.73 g, colourless crystal blocks (60 %).  $^1\text{H}$  NMR (400 MHz,  $\text{CDCl}_3$ )  $\delta$  / ppm: 8.40(d, 2H); 7.60 (t, 2H); 7.45 (d, 2H); 7.05 (t, 2H); 3.98 (s, 4H); 1.18 (s, 9H).  $^{13}\text{C}$  NMR (125 MHz,  $\text{CDCl}_3$ )  $\delta$  / ppm: 27.0; 57.0; 122.0; 123.0; 136.0; 148.0; 160. *Anal. Calc. for*  $\text{C}_{16}\text{H}_{21}\text{N}_3$ : C, 75.26; H, 8.29; N, 16.46; *Found*: C, 75.19; H, 8.27; N, 16.37. TOF MS-ES<sup>+</sup>, m/e: 256.1806, (M +1)<sup>+</sup>.

**(L5)** Yield: 2.05 g, bright yellow oil (60 %).  $^1\text{H}$  NMR (400 MHz,  $\text{CDCl}_3$ )  $\delta$  / ppm: 8.42 (d, 2H); 7.48 (t, 2H); 7.60 (d, 2H); 7.0 (t, 2H); 3.70 (s, 4H); 2.48 (t, 2H); 1.42 (m, 2H); 1.18 (m, 6H); 0.78 (t, 3H).  $^{13}\text{C}$  NMR (125 MHz,  $\text{CDCl}_3$ )  $\delta$  / ppm: 8.5; 22.5; 27.0; 32.0; 55.0; 60.0; 74.0; 122.0; 123.0; 137.0; 149.0; 160. TOF MS-ES<sup>+</sup>, m/e: 284.2127, (M +1)<sup>+</sup>.

**(L6)** Yield: 3.19 g bright yellow oil (71 %).  $^1\text{H}$  NMR (400 MHz,  $\text{CDCl}_3$ )  $\delta$  / ppm: 8.40 (d, 2H); 7.45 (t, 2H); 7.60 (d, 2H); 7.0 (t, 2H); 3.35 (s, 4H); 2.45 (m, 2H); 1.40 (m, 2H); 1.20 (m, 14H); 0.8 (t, 3H).  $^{13}\text{C}$

## Mononuclear Pt(II) complex with alkyl pendants

NMR (125 MHz, CDCl<sub>3</sub>)  $\delta$  / ppm: 14; 22.5; 27.5; 30.0; 30.2; 33.0; 49.0; 55.2; 60.0; 122.0; 123.0; 134.0; 148.0; 161, TOF MS-ES<sup>+</sup>, m/e: 340.5019, (M + 1)<sup>+</sup>.

### 4.2.2. Synthesis of Pt(II) complexes.

Complexes (**1** and **2-7**), were synthesized starting from *N,N*-bis(2-pyridylmethyl)amine and ligands **L1** to **L6**, respectively, following a literature procedure reported by Hofmann *et al.*<sup>41a</sup> for analogous dinuclear complexes. These were namely, [Pt(Cl)(*N,N*-bis(2-pyridylmethyl)amine)](ClO<sub>4</sub>) (**1**); [Pt(Cl)(*N,N*-bis(2-pyridylmethyl)ethylamine)](ClO<sub>4</sub>) (**2**); [Pt(Cl)(*N,N*-bis(2-pyridylmethyl)propylamine)](ClO<sub>4</sub>) (**3**); [Pt(Cl)(*N,N*-bis(2-pyridylmethyl)butylamine)](ClO<sub>4</sub>) (**4**); [Pt(Cl)(*N,N*-bis(2-pyridylmethyl)*tert*-butylamine)](ClO<sub>4</sub>) (**5**); [Pt(Cl)(*N,N*-bis(2-pyridylmethyl)hexylamine)](ClO<sub>4</sub>) (**6**) and [Pt(Cl)(*N,N*-bis(2-pyridylmethyl)decylamine)](ClO<sub>4</sub>) (**7**).

Their purity was confirmed by <sup>1</sup>H NMR, <sup>13</sup>C NMR, <sup>195</sup>Pt NMR, micro analysis and infrared (IR). Exemplary NMR spectra of the complexes are given as supporting information in Figures SI 4.1b-d. The IR spectra of all the complexes showed common characteristic peaks in the ranges 320-340 cm<sup>-1</sup> (weak) and 1090-1100 cm<sup>-1</sup> (broad, strong). These are due to vibrational stretches of the Pt-Cl bond and Cl-O bond (perchlorate counter ion),<sup>31</sup> respectively. The latter vibrational peak confirms the cationic nature of the complexes.

**(1)** Yield: 228.4 mg (90 %). <sup>1</sup>H NMR (400 MHz, DMF-d<sub>7</sub>)  $\delta$  / ppm: 9.05 (d, 2H); 8.50 (t, 2H); 8.05 (d, 2H); 7.79 (t, 2H); 5.3 (d,d, 2H); 5.10 (d,d 2H). <sup>13</sup>C NMR (125 MHz, CDCl<sub>3</sub>)  $\delta$  / ppm: 60; 123.0; 126.0; 142.0; 149.0; 168. <sup>195</sup>Pt NMR (107 MHz, DMF-d<sub>7</sub>)  $\delta$  / ppm: -2340. IR (KBr, 4000-300 cm<sup>-1</sup>)  $\bar{\nu}$ : 2958-2854 (alkyl C-H stretch); 1589 (C=N, pyridyl); 1090-1100 (perchlorate counter ion); 324-330 (Pt-Cl stretch). *Anal. Calc. for* PtC<sub>12</sub>H<sub>13</sub>N<sub>3</sub>Cl<sub>2</sub>O<sub>4</sub>: C, 27.23; H, 2.48; N, 7.94; *Found*: C, 27.43; H, 2.52; N, 8.03.

**(2)**. Yield: 240.8 mg (89 %). <sup>1</sup>H NMR (400 MHz, DMF-d<sub>7</sub>)  $\delta$  / ppm: 8.95 (d, 2H); 8.40 (t, 2H); 7.92 (d, 2H); 7.78 (t, 2H); 5.45 (d, 2H); 5.05 (d, 2H) 3.34 (q, 2H); 1.40 (t, 3H). <sup>13</sup>C NMR (125 MHz, DMF-d<sub>7</sub>)  $\delta$  / ppm: 16.0; 60; 68, 124.0; 126.0; 142.0; 149.0; 166. IR (KBr, 4000-300 cm<sup>-1</sup>)  $\bar{\nu}$ : 2958-2854 (alkyl C-H stretch); 1589 (C=N, pyridyl); 1090-1100 (perchlorate counter ion); 324-330 (Pt-Cl stretch). <sup>195</sup>Pt NMR (107 MHz, DMF-d<sub>7</sub>)  $\delta$  / ppm: -2365. *Anal. Calc. for* PtC<sub>14</sub>H<sub>17</sub>N<sub>3</sub>Cl<sub>2</sub>O<sub>4</sub>: C, 30.17; H, 3.07; N, 7.54; *Found*: C, 30.52; H, 3.05; N, 7.60.

## *Mononuclear Pt(II) complex with alkyl pendants*

---

(3). Yield: 228.4 mg (83 %).  $^1\text{H}$  NMR (400 MHz, DMF- $d_7$ )  $\delta$  / ppm: 8.98 (d, 2H); 8.59 (t, 2H); 8.10 (d, 2H); 7.86 (t, 2H); 5.65 (d, 2H); 5.20 (d, 2H); 3.38 (t, 2H); 1.85 (m, 2H) 1.40 (t, 3H).  $^{13}\text{C}$  NMR (125 MHz, DMF- $d_7$ )  $\delta$  / ppm: 10.0; 22.0; 66.0; 65; 124.0; 126.0; 142.0; 149.0; 166. IR (*KBr*, 4000-300  $\text{cm}^{-1}$ )  $\bar{\nu}$ : 2958-2854 (alkyl C-H stretch); 1589 (C=N, pyridyl); 1090-1100 (perchlorate counter ion); 324-330 (Pt-Cl stretch).  $^{195}\text{Pt}$  NMR (107 MHz, DMF- $d_7$ )  $\delta$  / ppm: -2350. *Anal. Calc. for*  $\text{PtC}_{15}\text{H}_{19}\text{N}_3\text{Cl}_2\text{O}_4$ : C, 31.56; H, 3.35; N, 7.36; *Found*: C, 31.47; H 3.36; N 7.27.

(4). Yield: 221.2 mg (78 %).  $^1\text{H}$  NMR (400 MHz, DMF- $d_7$ )  $\delta$  / ppm: 8.92 (d, 2H); 8.42 (t, 2H); 7.95 (d, 2H); 7.78 (t, 2H); 5.50 (d, 2H); 5.05 (d, 2H); 3.25 (t, 2H); 1.70 (m, 2H); (m, 2H); 1.33 (m, 2H); 0.79 (t, 3H).  $^{13}\text{C}$  NMR (125 MHz, DMF- $d_7$ )  $\delta$  / ppm: 13; 18.0; 30; 64; 68; 124.0; 126.0; 142.0; 149.0; 166. IR (*KBr*, 4000-300  $\text{cm}^{-1}$ )  $\bar{\nu}$ : 2958-2854 (alkyl C-H stretch); 1589 (C=N, pyridyl); 1090-1100 (perchlorate counter ion); 324-330 (Pt-Cl stretch).  $^{195}\text{Pt}$  NMR (107 MHz, DMF- $d_7$ )  $\delta$  / ppm: -2335. *Anal. Calc. for*  $\text{PtC}_{16}\text{H}_{21}\text{N}_3\text{Cl}_2\text{O}_4$ : C, 32.83; H, 3.62; N, 7.18; *Found*: C, 32.77; H, 3.58; N, 7.12.

(5). Yield: 153.5 mg (54 %).  $^1\text{H}$  NMR (400 MHz, DMF- $d_7$ )  $\delta$  / ppm: 8.92 (d, 2H); 8.42 (t, 2H); 8.95 (d, 2H); 7.78 (t, 2H); 5.40 (s, 4H); 1.32 (s, 9H).  $^{13}\text{C}$  NMR (125 MHz, DMF- $d_7$ )  $\delta$  / ppm: 27.0; 64.0; 71; 124.0; 126.0; 142.0; 149.0; 166. IR (*KBr*, 4000-300  $\text{cm}^{-1}$ )  $\bar{\nu}$ : 2958-2854 (alkyl C-H stretch); 1589 (C=N, pyridyl); 1090-1100 (perchlorate counter ion); 324-330 (Pt-Cl stretch).  $^{195}\text{Pt}$  NMR (107 MHz, DMF- $d_7$ )  $\delta$  / ppm: -2375. *Anal. Calc. for*  $\text{PtC}_{16}\text{H}_{21}\text{N}_3\text{Cl}_2\text{O}_4$ : C, 32.83; H, 3.62; N, 7.18; *Found*: C, 32.69; H, 3.55; N, 7.12.

(6). Yield: 247.8 mg (84 %).  $^1\text{H}$  NMR (400 MHz, DMF- $d_7$ )  $\delta$  / ppm: 9.05 (d, 2H); 8.59 (t, 2H); 8.15 (d, 2H); 7.88 (t, 2H); 5.65 (d, 2H); 5.20 (d, 2H); 3.40 (m, 2H); 1.80 (m, 2H); 1.4 (m, 2H); 1.35 (m, 4H); 1.14 (t, 3H).  $^{13}\text{C}$  NMR (125 MHz, DMF- $d_7$ )  $\delta$  / ppm: 13; 22.0; 26; 27; 32; 64; 68; 124.0; 126.0; 142.0; 149.0; 166. IR (*KBr*, 4000-300  $\text{cm}^{-1}$ )  $\bar{\nu}$ : 2958-2854 (alkyl C-H stretch); 1589 (C=N, pyridyl); 1090-1100 (perchlorate counter ion); 324-330 (Pt-Cl stretch).  $^{195}\text{Pt}$  NMR (107 MHz, DMF- $d_7$ )  $\delta$  / ppm: -2330. *Anal. Calc. for*  $\text{PtC}_{18}\text{H}_{25}\text{N}_3\text{Cl}_2\text{O}_4$ : C, 31.56; H, 3.35; N, 7.36; *Found*: C, 31.47; H 3.36; N 7.27.

(7). Yield: 268.3 mg (84 %).  $^1\text{H}$  NMR (500 MHz, DMF- $d_7$ )  $\delta$  / ppm: 9.06 (dd, 2H); 8.60 (td, 2H); 8.15 (d, 2H); 7.95 (t, 2H) 5.64 (d, 2H); 5.2 (d, 2H); 3.40 (m, 2H); 1.80 (m, 2H); 1.4 (m, 14H); 1.14 (t, 3H).  $^{13}\text{C}$  NMR (125 MHz, DMF- $d_7$ )  $\delta$  / ppm: 13; 22.0; 26; 27; 32; 64; 68; 75; 124.0; 126.0; 142.0; 149.0; 166. IR (*KBr*, 4000-300  $\text{cm}^{-1}$ )  $\bar{\nu}$ : 2958-2854 (alkyl C-H stretch); 1589 (C=N, pyridyl); 1090-1100 (perchlorate counter ion); 324-330 (Pt-Cl stretch).  $^{195}\text{Pt}$  NMR (107 MHz, DMF- $d_7$ )  $\delta$  / ppm: -2350. *Anal. Calc. for*  $\text{PtC}_{22}\text{H}_{33}\text{N}_3\text{Cl}_2\text{O}_4$ : C, 39.47; H, 4.97; N, 6.28; *Found*: C, 39.18; H, 4.94; N, 6.46.

# Mononuclear Pt(II) complex with alkyl pendants

## 4.2.3. Preparation of aqua Pt(II) complexes.

The aqueous solutions of the complexes were prepared following a literature procedure of Bugarčić *et al.*<sup>8a</sup> [Pt(H<sub>2</sub>O)(*N,N*-bis(2-pyridylmethyl)amine)](CF<sub>3</sub>SO<sub>3</sub>)<sub>2</sub> (**bpma**); [Pt(H<sub>2</sub>O)(*N,N*-bis(2-pyridylmethyl)ethylamine)](CF<sub>3</sub>SO<sub>3</sub>)<sub>2</sub> (**bpea**); [Pt(H<sub>2</sub>O)(*N,N*-bis(2-pyridylmethyl)propylamine)](CF<sub>3</sub>SO<sub>3</sub>)<sub>2</sub> (**bppa**); [Pt(H<sub>2</sub>O)(*N,N*-bis(2-pyridylmethyl)butylamine)](CF<sub>3</sub>SO<sub>3</sub>)<sub>2</sub> (**bpba**); [Pt(H<sub>2</sub>O)(*N,N*-bis(2-pyridylmethyl)*tert*-butylamine)](CF<sub>3</sub>SO<sub>3</sub>)<sub>2</sub> (**bpbta**); [Pt(H<sub>2</sub>O)(*N,N*-bis(2-pyridylmethyl)hexylamine)](CF<sub>3</sub>SO<sub>3</sub>)<sub>2</sub> (**bpha**); [Pt(H<sub>2</sub>O)(*N,N*-bis(2-pyridylmethyl)decylamine)](CF<sub>3</sub>SO<sub>3</sub>)<sub>2</sub> (**bpda**). Their structures are shown in Figure 4.1.

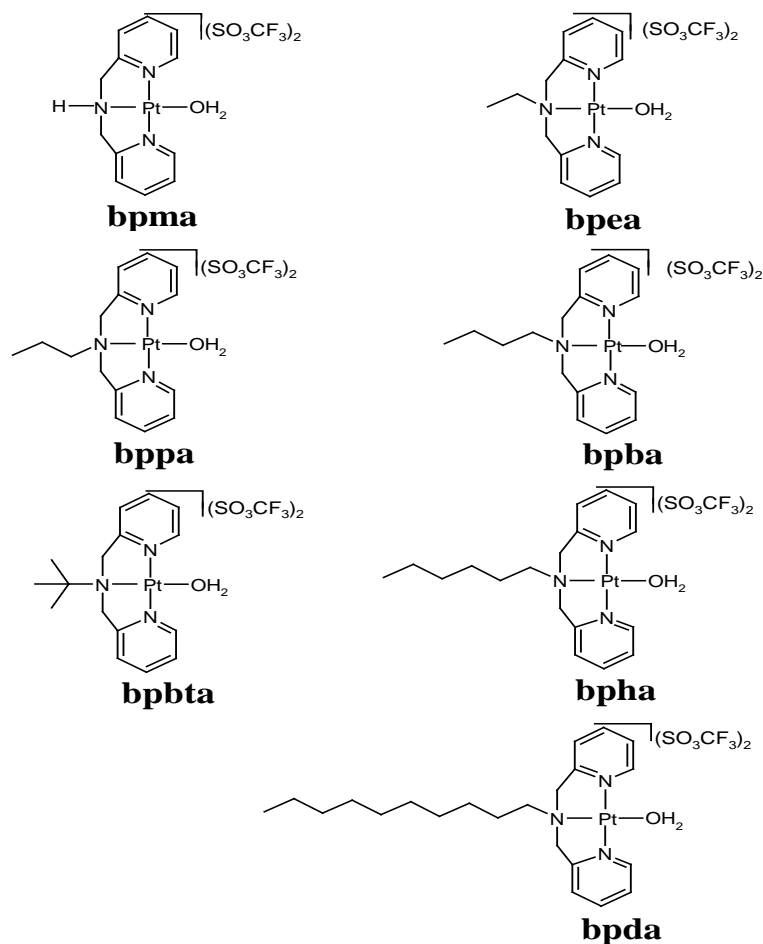


**Figure 4.1** Structures of the Pt(II) amphiphiles with *N,N*-bis(2-pyridylmethyl)alkylamine head groups.

To a suspension of [Pt(Cl)(*N,N*-bis(2-pyridylmethyl)alkylamine)](CF<sub>3</sub>SO<sub>3</sub>)<sub>2</sub> (0.5 mmol) layered in 50 mL solution of 0.001 M CF<sub>3</sub>SO<sub>3</sub>H was added AgSO<sub>3</sub>CF<sub>3</sub> (0.99 equivalents of the complex) dissolved in 0.01 M CF<sub>3</sub>SO<sub>3</sub>H (10 mL) and the mixture left to stir for 24 hours at

## Mononuclear Pt(II) complex with alkyl pendants

40-50 °C. The AgCl precipitate was removed by filtration through a 0.45 µm nylon membrane and the filtrate made up to volume (100 mL) with 0.01 M CF<sub>3</sub>SO<sub>3</sub>H which had been adjusted to an ionic strength of 0.02 M with LiSO<sub>3</sub>CF<sub>3</sub> to afford a stock concentration of approximately 0.5 mM of the complex. The 0.02 M ionic strength solution used for subsequent dilutions was prepared by dissolving 1.56 g of LiSO<sub>3</sub>CF<sub>3</sub> in 1 L of ultrapure water to which had been added 0.88 mL of concentrated CF<sub>3</sub>SO<sub>3</sub>H. This solution ensured a pH of 2 and a constant ionic strength of 0.02 M and was used for all dilutions of both the Pt(II) complex solutions as well as for dissolving nucleophiles for kinetics experiments. Solutions for the determination of the pK<sub>a</sub> values of the aqua complexes were prepared by diluting the metal complexes with ultra pure water and adjusting their pH to 2 with concentrated CF<sub>3</sub>SO<sub>3</sub>H to afford solutions with initial peak absorbencies of about 0.75.

### **4.2.4. Preparation of nucleophile solutions for kinetic analysis.**

Solutions of the nucleophiles *viz.*, thiourea (tu), *N,N'*-dimethylthiourea (dmtu) and *N,N,N',N'*-tetramethylthiourea (tmtu) were prepared by dissolving appropriate amounts of the nucleophiles in a 0.02 M ionic strength solution (0.01 M CF<sub>3</sub>SO<sub>3</sub>H adjusted with LiSO<sub>3</sub>CF<sub>3</sub>). The stock solution of each nucleophile of concentration approximately 50-fold in excess of the complex was then diluted with the 0.02 M ionic strength solution to afford serial concentrations of 40; 30; 20 and 10-fold in excess over that of the metal complex. These concentrations of the nucleophiles were chosen to maintain pseudo first-order conditions.

### **4.2.5. Physical measurements and instrumentation.**

#### **4.2.5.1 Spectrophotometric measurements.**

NMR spectra of ligands and complexes were acquired on a Bruker Avance DPX 400 while the NMR spectral array for the reaction between **bpma** and tu were acquired on a Bruker Avance DPX 500. Low resolution electron-spray ionization (ESI<sup>+</sup>) mass spectra of ligands were recorded on a TOF Micromass spectrometer. Elementary composition was determined on a Carlo Erba Elemental Analyzer 1106. An Oxford Diffraction Xcalibur2 CCD diffractometer was used to solve the crystal structure of **L4**.<sup>40</sup> Kinetics measurements of fast reactions were monitored using an SX.18 MV stopped-flow spectrophotometer (Applied Photophysics) coupled to an online data acquisition system. The temperature of the instrument was controlled to within ± 0.1 °C. Spectrophotometric pK<sub>a</sub> titrations, wavelength searching experiments and

## *Mononuclear Pt(II) complex with alkyl pendants*

---

kinetic measurements of slow reactions, were recorded on a Cary 100 Bio UV-visible spectrophotometer equipped with a Varian Peltier temperature thermostat with an accuracy of  $\pm 0.05$  °C. The pH measurements were recorded on a Jenway 4330 pH meter with a combined Jenway glass microelectrode that had been calibrated with standard buffer solutions of pH 4.0, 7.0 and 10.0 (Merck). The spectrophotometric titrations were carried out as previously described.<sup>7</sup> A typical titration spectrum is shown in Figure 4.2 and the  $pK_a$  values obtained thereof are tabled in Table 4.1.

### *4.2.5.2 Kinetic measurements*

Before each reaction could be studied, a trial experiment to establish the wavelength at which the kinetics could be studied was carried out by recording spectral changes resulting from mixing the complex and nucleophiles. The wavelengths chosen for studying the reactions are summarized in Table SI 4.1. Fast reactions were initiated by a pressure-driven cross-plunging technique in the chamber of the stop-flow reaction analyzer. For slow reactions, equal volumes of pre-equilibrated solutions of the complex and nucleophile were manually mixed in a Suprasil tandem cuvette (optical dimension = 2 x 0.44 cm). All kinetics reactions were studied as a function of concentration and temperature (15-35 °C) under pseudo first-order conditions. This was achieved by providing at least a 10-fold excess in the concentration of the nucleophiles over that of the metal complexes. This also forced the reactions to go to completion.<sup>41a</sup> A pH of 2.0 and an ionic strength of 0.02 M were maintained throughout the kinetic runs. The kinetic data is summarized in Tables 4.3a and 4.3b.

### *4.2.5.3 Computational details*

Density functional theoretical (DFT)<sup>42</sup> calculations were performed with the Spartan '04 for Windows quantum chemical package<sup>43</sup> using the B3LYP<sup>44</sup>, a three parameter hybrid functional method, utilizing the LACVP+\*\*<sup>45</sup> pseudopotentials basis set. The calculated structures and key geometrical data are summarized in Tables 4.2a and 4.2b.

## **4.3 Results and Discussion**

### **4.3.1 Synthesis and characterization**

In this study, six square-planar Pt(II) complexes were synthesized from their *N*-pendant bis(2-pyridylmethyl)alkylamine ligands which differed in the chain lengths and structures of their alkyl tails. The details of the spectroscopic data for the ligands as well as their complexes

## Mononuclear Pt(II) complex with alkyl pendants

are listed in the experimental sections 4.2.1 and 4.2.2, respectively. Ligands **L1**<sup>39b</sup> and **L4**<sup>39c</sup> and the **bpma** complex<sup>8a,9b,11</sup> have been prepared and described before and their data is in good agreement with that obtained from earlier preparations. An exemplary mass spectrum for the ligands is shown in Figure SI 4.1a (supporting information) for the hexyl-appended ligand used to synthesize the **bpha** complex. The elementary analysis and NMR data for the ligands and complexes support the proposed chemical structures.

Due to the poor solubility of the complexes in most common non-solvating solvents, DMF-*d*<sub>7</sub> was used to record their NMR spectra. Typical NMR spectra for the complexes are given as supporting information Figures SI 4.1b-1d for the **bppa-Cl** complex. The chemical shifts of the proton resonances of all complexes appear downfield relative to those of the free ligands, an indication that coordination at the Pt(II) metal centres has occurred. Like in the case of the reference complex, **bpma**, only four resonances appear in the aromatic regions of the spectra for all the complexes, implying that the pyridyl sets of protons are equivalent in solution due to the symmetrical coordination of the pyridyl rings at the metal centres. The methyl protons of the pendant aliphatic tails appear as a triplet signature in all the spectra. The three equivalent methyl groups of the **bptba** derivative appear as a singlet integrating to nine protons. The <sup>195</sup>Pt signals for all the complexes appear within the range: -2300 ppm to -2370 ppm, a range typical for the chelated Pt(NNN) planar-coordination spheres.<sup>46</sup> Their IR spectra show common vibration bands in the ranges: 320-340 cm<sup>-1</sup> and 1090-1100 cm<sup>-1</sup> for the vibrational stretches of the Pt-Cl bond<sup>12</sup> and O-Cl bond (perchlorate counter ion), respectively.<sup>47</sup>

### 4.3.2 Acid-base equilibria of the aqua Pt(II) complexes.

Before the complex could be studied kinetically, the acidities of the coordinated aqua ligands as a function of the chain length of the *N*-pendant alkyl groups were investigated. A typical plot of the UV-visible spectra acquired during the course of the titration of the complexes with NaOH is shown in Figure 4.2 for **bpha**. In the acidic range, the spectra of all the amphiphiles complexes are characterized by a sharp absorption maximum centred at 268 nm.

## Mononuclear Pt(II) complex with alkyl pendants

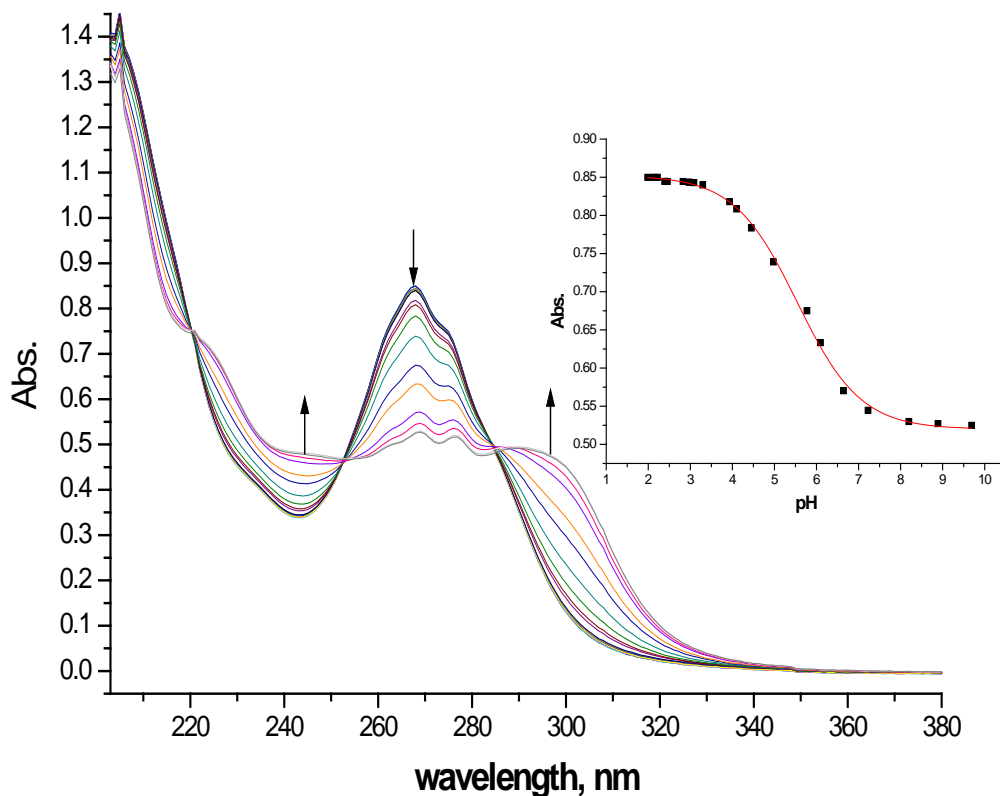


**Figure 4.2** UV-visible spectra for the titration of 0.1 mM **bpha** with NaOH, pH range 2-9, T = 298 K. Inset is the titration curve at 267 nm.

The absorption peaks of all the complexes are similar in shape and comparable to those reported in Chapter Three and for the mononuclear complex, [Pt(H<sub>2</sub>O)bis(2-pyridylmethyl)amine](CF<sub>3</sub>SO<sub>3</sub>)<sub>2</sub>, (**bpma**)<sup>18</sup> under similar prevailing conditions. The peaks in the 267-269 nm range gradually decrease while the shoulders in the 277-278 nm range grow slightly in size on addition of NaOH. An additional broader shoulder peak appear in the range 300-305 nm during the course of the titration, as more and more of the hydroxo species of the complexes are formed.

Shown as an inset (Figure 4.2) is a plot of the changes in the relative absorbance recorded at 267 nm during the course of the titration. When this data is fitted to the standard Boltzmann equation, the  $pK_a$  values for the deprotonation of the protons of the coordinated aqua ligands are obtained. The results are summarized in Table 4.1. Included for comparison purposes in Table 1 is the  $pK_a$  data of the analogous diplatinum complexes with flexible  $\alpha,\omega$ -alkyldiamine work which were reported in Chapter Three, section 3.3.1.

## Mononuclear Pt(II) complex with alkyl pendants

**Table 4.1** The  $pK_a$  values for the deprotonation of Pt-bound aqua ligand in amphiphilic and flexible Pt(II) dinuclear complexes with bis(2-pyridylmethyl)amine chelate headgroups.

Mononuclear	bpma	bpea	bppa	bpba	bptba	bpha	bpda
$pK_a^\ddagger$	$5.45 \pm 0.05$ $5.49 \pm 0.08^\dagger$	$5.45 \pm 0.05$	$5.47 \pm 0.03$	$5.48 \pm 0.05$	$5.64 \pm 0.17$	$5.48 \pm 0.15$	$5.52 \pm 0.02$
<b>Dinuclear*</b>		<b>En</b>	<b>Prop</b>	<b>But</b>		<b>Hex</b>	<b>Dec</b>
$pK_{a1}$		$3.31 \pm 0.19$	$3.95 \pm 0.10$	$4.07 \pm 0.05$		$4.64 \pm 0.17$	$4.53 \pm 0.03$
$pK_{a2}$		$4.31 \pm 0.29$	$6.30 \pm 0.04$	$5.26 \pm 0.06$		$5.68 \pm 0.07$	-

$^\ddagger$ The  $pK_a$  were determined by fitting the titration data to the Boltzmann equation,  $y = A_2 + (A_1 - A_2)/(1 + \exp((x - x_0)/dx))$  using Origin 7.5<sup>®</sup> program. The titration data for the dinuclear complexes were fitted to equation,  $y = a + (b - a)/(1 + 2.718^{((x - pK_{a1})/m)}) + (c - b)/(1 + 2.718^{((x - pK_{a2})/n)})$ , for measuring two  $pK_a$  values or the Boltzmann equation,  $y = A_2 + (A_1 - A_2)/(1 + \exp((x - x_0)/dx))$ , for measuring one  $pK_a$  value using the Origin 7.5<sup>®</sup> program.  $^\dagger$  Value reported in Ref. 6. \*Data extracted from Table 3.1, section 3.3.3, Chapter Three.

## Mononuclear Pt(II) complex with alkyl pendants

The  $pK_a$  values of the mononuclear Pt(II) complexes indicate that at a pH of 2.0 (0.01 M  $\text{CF}_3\text{SO}_3\text{H}$  solution), at which the kinetics of reactions were studied, all the complexes exist as their aqua forms. Acidification of their basic solutions, during the course of the titration lead to spectra which are identical to those recorded in the acidic pH range.

When compared to the  $pK_a$  value of the reference complex, **bpma** ( $pK_a = 5.45 \pm 0.05$ ) the value determined in this study and in two other previous studies<sup>6,22</sup> indicates that the basicity of the amphiphiles does not change significantly if one takes into account the error limits. An exception is the **bptba** complex where a  $pK_a$  value of  $5.64 \pm 0.17$  was recorded. The  $pK_a$  values of these amphiphilic complexes reveal that the contribution due to their primary alkyl tails to the basicity of the coordinated aqua ligands is relatively smaller or non-existent. However, when an alkyl group with a branched  $\alpha$ -carbon such as a *tert*-butyl hydrocarbon (**bptba**) is appended to the chelate headgroup, the deprotonation occurs at slightly higher pH value. One would have expected a general increase in the basicity of the coordinated aqua ligands with the increase in the chain length of the appended tail on the *trans*-N donor atom of the **bpma** chelate headgroup due to the increased donation of electron density by inductive effects<sup>47a</sup> from the tail groups. For the tertiary hydrocarbon groups which are known to be better  $\sigma$ -donors<sup>47b</sup> than their primary counterparts, the effect should have been even bigger. This is because being a strong  $\sigma$ -donor group, the *tert*-butyl should strengthen the bond between the Pt atom and the *trans*-N (Pt-N) thereby weakening the *trans* Pt-O bond of the aqua leaving group. This in turn should strengthen the O-H bonds of the coordinated aqua ligand resulting in the deprotonation occurring at higher pH values. This expectation was not observed, an indication that the donation due to the attached primary alkyl tail is weaker than the  $\pi$ -back bonding due to the pyridyl rings.

However, a comparison of the  $pK_a$  data for the complexes (Table 4.1) with that of the analogous dinuclear complexes (reported in Table 3.1, Chapter Three) reveals that the first deprotonation of the coordinated aqua ligand occurs at pH values that are about one unit lower, signifying the increase in the acidities of the coordinated aqua on attaching the second chelate headgroup on forming the dinuclear complexes. In addition, it is observed that the acidity of the dinuclear complexes having  $C_{2h}$  point group symmetry increases inversely with the chain length of the bridge. When one compares the  $pK_a$  data for the **bppa/Prop** pair, the  $C_{2v}$  symmetry of **Prop** which confers unique bowl structure seems to raise the  $pK_{a2}$  value ( $6.30 \pm 0.04$ ) more than it lowers the  $pK_{a1}$  relative to the  $pK_a$  data of **bppa**. Thus, the acidity of the diaqua platinum complexes reported in Chapter three, already known<sup>41b</sup> to correlate

## *Mononuclear Pt(II) complex with alkyl pendants*

positively with the effective charge of the Pt metal centres is controlled by in-space charge addition as already discussed in Chapter Three, section 3.3.2, since it has been shown that the electronic effect of the primary tail of the analogous amphiphiles is weak. This observation affirms what has been suggested by Hofmann *et al.*<sup>41a</sup>, that charge addition at the Pt centres of these chelated dinuclear is an important factor controlling their substitutional reactivity. This control is more important when the linker is short. The similarity between the  $pK_a$  values of the mononuclears (pH range:  $5.45 \pm 0.05$  -  $5.52 \pm 0.02$ ) and the  $pK_{a2}$  of the dinuclear platinum complexes (pH range:  $5.26 \pm 0.06$  -  $5.59 \pm 0.18$ ) signifies the stepwise nature of the deprotonation of the coordinated aqua ligand in the latter complexes. As shown in data of **Prop**<sup>41a,b</sup> and relative to its  $C_{2h}$  analogues, this stepwise deprotonation of the coordinated aqua ligands to form the aqua/hydroxo and the hydroxo/hydroxo depends also on the symmetry of the chelated complex which in turn is directly controlled by whether the number of carbon atoms in the flexible linker is even or odd.<sup>41b</sup>

### **4.3.3 Computational calculations**

In order to understand the role of the structural as well as the electronic differences that exist in the complexes, computational calculations were carried at the DFT<sup>42</sup> level of theory and an extract of the data as well as the geometry-optimized structure are presented in Tables 4.2a and 4.2c, respectively. To further the understanding of the role the linker plays<sup>41b</sup>, key computational data for the analogous dinuclear complexes already reported in Chapter Three (Tables 3.2 and 3.3) have been selected and incorporated into Table 4.2b for comparison with that of the complexes of the present study.

# Mononuclear Pt(II) complex with alkyl pendants

Table 4.2a Summary of DFT<sup>42</sup> calculated data for the amphiphilic Pt(II) complexes.

Property	bpma	bpea	bppa	bpba	bptba	bpha	bpda
<b>Bond lengths, Å</b>							
Pt-OH <sub>2</sub>	2.151	2.158	2.159	2.159	2.163	2.161	2.163
Pt-N <sub>trans</sub>	2.012	2.035	2.034	2.035	2.052	2.036	2.035
<b>Separation distance, Å</b>							
N <sub>1 trans</sub> -C <sub>methyl tail</sub>		2.596	3.929	5.158	1.605	7.71	12.86
Pt-H <sub>proxim</sub>	2.62	2.99	2.99	2.98	2.99	2.99	3.01
<b>Bond angles, °</b>							
N <sub>cis</sub> -Pt-N <sub>cis</sub>	165.8	166.6	166.4	166.4	166.9	166.5	166.4
Pt <sub>1</sub> -N <sub>1 trans</sub> -C <sub>methyl tail</sub>		130.1	127.0	138.95	115.7	139.2	139.5
Elevation angle of tail, α, ‡		49.9	53.0	41.05	64.3	40.8	40.5
Inclination angle of aqua ligands (relative to the coord. plane)	10.69	13.51	13.57	13.52	16.29	13.60	13.44
<b>Energy gap, eV</b>							
LUMO Energy, eV	-8.53	-8.62	-8.71	-8.54	-8.53	-8.51	-8.49
HOMO Energy, eV	-12.78	-13.86	-13.81	-13.78	-13.69	-12.75	-11.07
ΔE <sub>LUMO-HOMO</sub> ,	4.23	5.24	5.10	5.24	5.16	4.24	2.59
<b>Natural Charges Pt</b>							
	1.215	1.209	1.206	1.206	1.213	1.206	1.205
<b>Symmetry</b>							
	C <sub>2h</sub>						
<b>Dipole moment, D</b>							
	2.47	5.48	7.81	11.1	7.17	18.6	36.6

‡ α is angle {Pt1-N1<sub>trans</sub>-C<sub>methyl tail</sub>}.

# Mononuclear Pt(II) complex with alkyl pendants

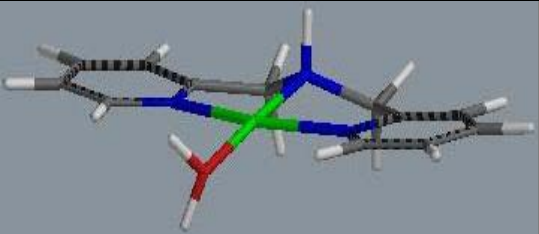
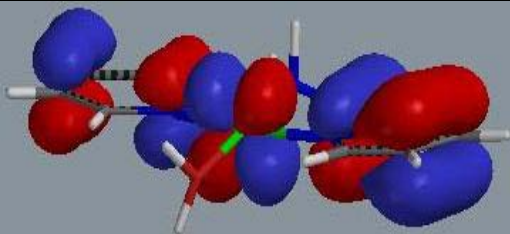
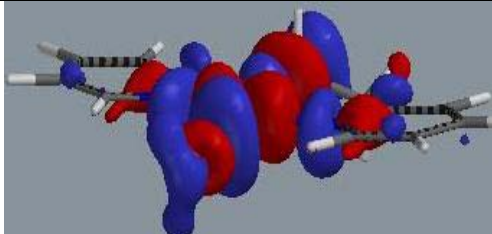
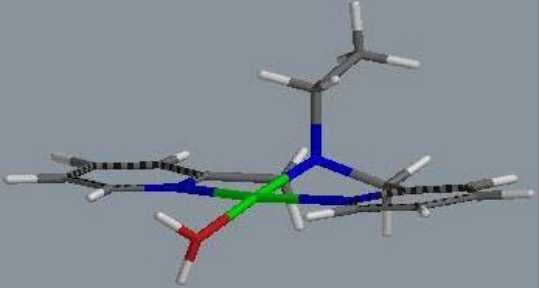
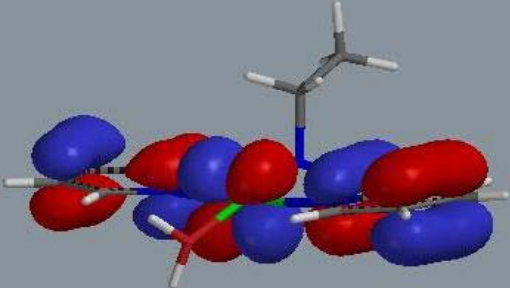
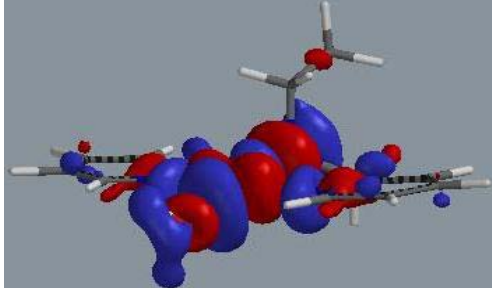
**Table 4.2b** A summary of DFT<sup>42</sup> computed data for the amphiphilic and the dinuclear Pt(II) complexes.

<b>Amphiphilic complex (n)<sup>#</sup></b>	<b>bpma (0)</b>	<b>bpea (2)</b>	<b>bppa (3)</b>	<b>bpba (4)</b>	<b>bptba (4)</b>	<b>bpha (6)</b>	<b>bpda (10)</b>
<b>Property</b>							
<b>Bond lengths, Å</b>							
Pt-OH <sub>2</sub>	2.151	2.158	2.159	2.159	2.163	2.161	2.163
Elevation angle, α <sup>‡</sup>		49.9	53.0	41.1	44.3	40.8	40.5
<b>Separation distance, Å</b>							
N <sub>1 trans</sub> -C <sub>methyl tail</sub>		2.60	3.93	5.16	1.61	7.71	12.9
ΔE <sub>LUMO-HOMO</sub> , eV	5.23	5.24	5.10	5.24	5.16	4.24	2.59
<b>Natural Charges: Pt</b>							
<b>Symmetry</b>	C <sub>2h</sub>	C <sub>2h</sub>	C <sub>2h</sub>				
<hr/>							
<b>Dinuclear* complex (n)<sup>#</sup></b>	<b>En (2)</b>	<b>Prop (3)</b>	<b>But (4)</b>	<b>Pen (5)</b>	<b>Hex (6)</b>	<b>Hep (7)</b>	<b>Dec (10)</b>
<b>Property</b>							
<b>Bond lengths, Å</b>							
Pt-OH <sub>2</sub>	2.140	2.141	2.143	2.149	2.149	1.214	2.157
Hinge Angle, β <sup>§</sup>		124	-	139.8	-	160.8	-
Elevation angle, α <sup>‡</sup>	74.4	-	45.5	-	44.2	-	44.6
<b>Energy gap, eV</b>							
ΔE <sub>LUMO-HOMO</sub> ,	5.00	4.99	5.07	5.12	5.14	5.14	5.19
<b>Separation distance, Å</b>							
Pt <sub>1 coord. plane</sub> - Pt <sub>2 coord. plane</sub>	3.63	-	4.24	-	5.84		9.16
<b>Natural Charges: Pt</b>	1.220	1.223	1.222	1.218	1.217	1.214	1.214
<b>Symmetry</b>	C <sub>2h</sub>	C <sub>2v</sub>	C <sub>2h</sub>	C <sub>2v</sub>	C <sub>2h</sub>	C <sub>2v</sub>	C <sub>2h</sub>

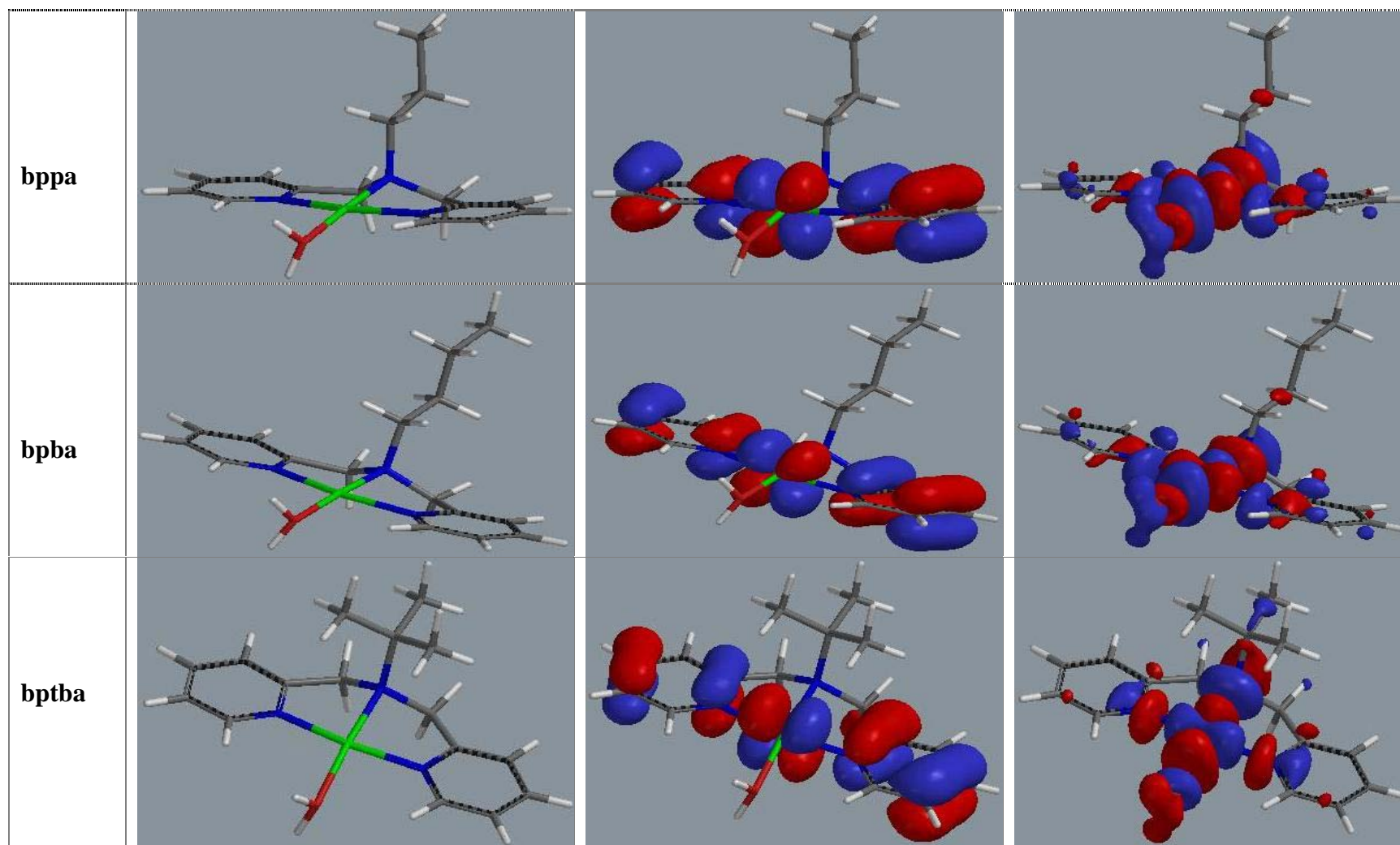
\*Data extracted from Table 3.2, section 3.3.3, Chapter Three. <sup>‡</sup>For amphiphilic complexes, α is the angle {Pt1-N1<sub>trans</sub>-C<sub>methyl tail</sub>}. <sup>†</sup>α is the supplementary angle to the angle {Pt1-N1<sub>trans</sub>-N2<sub>trans</sub>} in dinuclear complexes with C<sub>2h</sub> symmetry. <sup>§</sup>In the C<sub>2v</sub> symmetry of **Prop**, β, is the hinge angle made at the central carbon by the Pt atoms. <sup>#</sup>(n) is the number of carbon in the appended tail or the linking bridge.

## Mononuclear Pt(II) complex with alkyl pendants

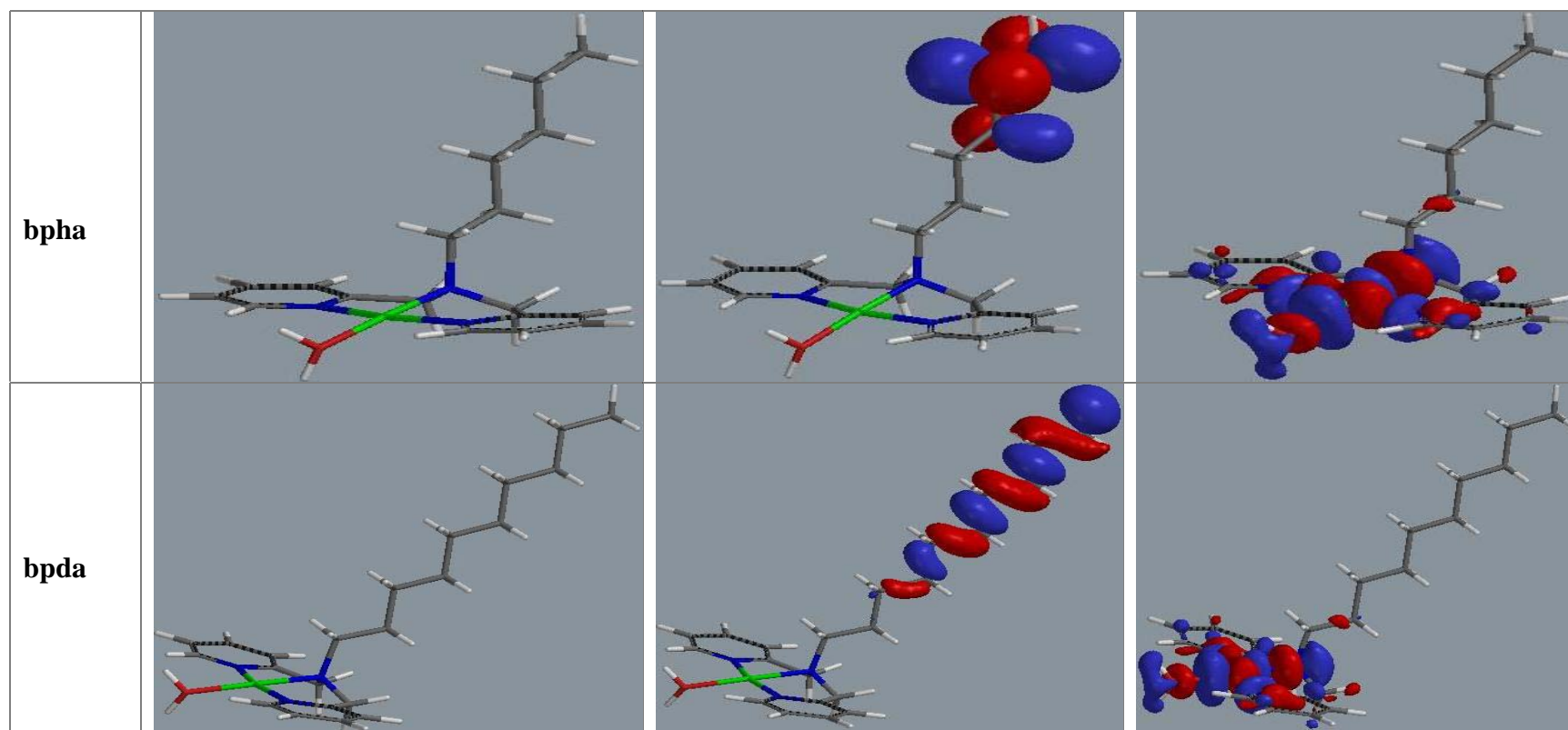
**Table 4.2c** Density functional theoretical (DFT)<sup>42</sup> minimum energy structures, HOMO and LUMO frontier molecular orbitals for amphiphilic Pt(II) complexes. The calculations were performed with the Spartan '04 for Windows quantum chemical package<sup>43</sup> using the B3LYP hybrid functional method<sup>44</sup> utilizing the LACVP+\*\*<sup>45</sup> pseudopotentials basis set.

Complex	Structure	HOMO Map	LUMO Map
bpma			
bpea			

## *Mononuclear Pt(II) complex with alkyl pendants*



## Mononuclear Pt(II) complex with alkyl pendants



## *Mononuclear Pt(II) complex with alkyl pendants*

---

The optimized structures in Table 4.2c reveal that all the amphiphilic complexes adopt a  $C_{2h}$  point-group symmetry in which the inclined and appended alkyl tails bisect the square-planes of their chelate headgroups. Unlike the structures of the mononuclear complexes, the adopted molecular structures of the dinuclears (Chapter Three, Table 3.2, Table SI 4.5a, supporting information) specifically depend on whether the number of carbon atoms in the bridge is even or odd, reflecting a constraining role due to the bridge. This constraint determines the average distance separating Pt atoms and thus, the magnitude of the electrostatic charge added at each Pt centre in the dinuclears.

Data in Table 4.2a shows a sharp increase in the dipole moment from **bpea** (5.48 D) to **bpda** (36.5 D) when the chain length of the pendant hydrocarbon tail is increased from an ethyl tail (2.60 Å) to a decyl tail (12.9 Å) indicating the amphiphilic character of the complexes as the hydrophobicity of the alkyl tails is increased. Another effect of increasing the chain length of the appended alkyl tails is noted in the calculated Pt-O bond lengths (Table 4.2a) which increase moderately and proportionally from **bpea** to **bpda**. When the calculated Pt-O bond lengths of the complexes with pendant groups are compared to **bpma**'s, the largest elongation of the bond (0.012 Å) is recorded in the **bptba**, an analogue with an  $\alpha$ -branched *tert*-butyl tail. This elongation of the coligand of **bptba** corroborates with its higher  $pK_a$  value, indicating that branching at the  $\alpha$ -carbon of the appended tail (**bptba**) is accompanied by a ground state weakening of the bond between the Pt(II) centre and the aqua leaving groups. The increase in the *trans*-influence of the appended alkylamine donor group when the chain length is extended is due to an increase in the  $\sigma$ -donation of electron density towards the Pt atom.

The mappings of the frontier orbitals (Table 4.2c) are all similar, with the only differences occurring in the location of the HOMO of the **bpha** and **bpda** complexes. For the rest of the complexes, the HOMO orbitals are located on the pyridyl  $\pi$ -acceptor carrier ligands and shared with the Pt atoms. The LUMO are centred primarily on the metal centres and the donor atoms of the chelating ligands. However, in the **bpha** and **bpda** complexes, the HOMO frontier orbitals are centred on the ligands and located primarily on the tip-ends of their appended groups. This is an indication that while the electron density increases with the increase in the chain length of the appended group (refer to Table SI 4.5a for the electrostatic potential surfaces of the complexes), its donation by inductive effects towards the Pt atom depends specifically on bond connectivity such that it becomes less effective as the number of connecting bonds counted away from the metal centre increases due to the changes in

## *Mononuclear Pt(II) complex with alkyl pendants*

---

chain length of the pendant. As will be discussed shortly, this will cause a leveling effect on the reactivity of the complexes.

From the data of Table 4.2a, a direct relationship is noticed between the chain length of the alkyl pendant tails and the HOMO-LUMO energy gaps which decrease as the chain length of the tails for the complexes is increased with the exception of **bppa**. The  $\sigma$ -donation of electron density, albeit moderate, towards the Pt(II) centres is also reflected in the increasingly raised energy levels of the HOMO orbitals as the chain length is increased. Unlike the amphiphiles, the HOMO frontier orbitals of the dinuclears (when data in Table 4.2c is compared to that from Table 3.2, section 3.2.2, Chapter Three) are located primarily at the bis(2-pyridyl)  $\pi$ -acceptor ligands irrespective of the chain length or the symmetry adopted by the dinuclear complexes. When a second Pt chelate is attached to the aliphatic pendant of the amphiphile, it stabilizes the energy of HOMO relative to that of the mononuclear (if data in Table 4.2a is compared to data of Table 3.3, section 3.2.2, Chapter Three) more so in complexes of shorter Pt, Pt distances where  $\sigma$ -donation due the bridge is relatively lower, signifying the decrease in inductive donation as the linker is shortened. It is also noted that the location of the frontier orbitals of the dinuclears are not affected by the number of carbon atoms of the linking bridge as it does for molecular symmetry. This is an indication that while the  $\sigma$ -inductive effect of the bridge is less important, the increase in the effective charge in the dinuclear, especially for short-bridged complexes stabilizes the energy of the frontier orbitals.

A comparison of the calculated charges on Pt atoms for complexes with *N*-pendant tails relative to **bpma**'s value indicates that the charges on the former complexes are generally lower and almost constant across the members of the homolog as a result of the positive inductive effects towards the metal centres from the appended groups. However, on bringing the second Pt chelate (Table 3.3, section 3.3.2, Chapter Three) the calculated NBO charges of Pt atoms decrease to a minimum before it levels-off as the chain length of the bridge is increased, reiterating the importance of electrostatic (in-space charge) addition in the control of the effective charge on the Pt centres of the dinuclears. As discussed in section 3.3.2 in Chapter Three, electrostatic charge addition in the dinuclears is dependent on other factors such as the length of the linker and the symmetry of the complex as determined by the number of carbon atoms of the flexible linker.

While the linker constrains the chelate headgroups to specific relative loci in the dinuclears with flexible bridges, it is the steric requirements and the electrostatic repulsions

## *Mononuclear Pt(II) complex with alkyl pendants*

---

that determine the ultimate geometry assumed by the dinuclear. This is revealed in the angle of inclination of the free rotating tail of the amphiphiles which is always lower than the relatively restrained bridging linker as the chelates headgroups assumes lowest energy configurations in which the two aforesaid factors are minimized.

### **4.3.4 Kinetics measurements.**

The substitution of the coordinated aqua ligands by the thiourea nucleophiles were studied as a function of concentration at 25 °C. Two reaction steps, taken to be the substitution of the aqua ligand and the subsequent dechelation of one of the coordinated pyridyl units<sup>41c-d</sup> were observed. This conclusion was reached after monitoring the reaction between **bpma-Cl** and tu (2 eqv.) by <sup>1</sup>H NMR spectroscopy. An array of the proton NMR spectra (showing the aromatic region only) which was recorded or reaction is shown in Figure 4.3.

# Mononuclear Pt(II) complex with alkyl pendants

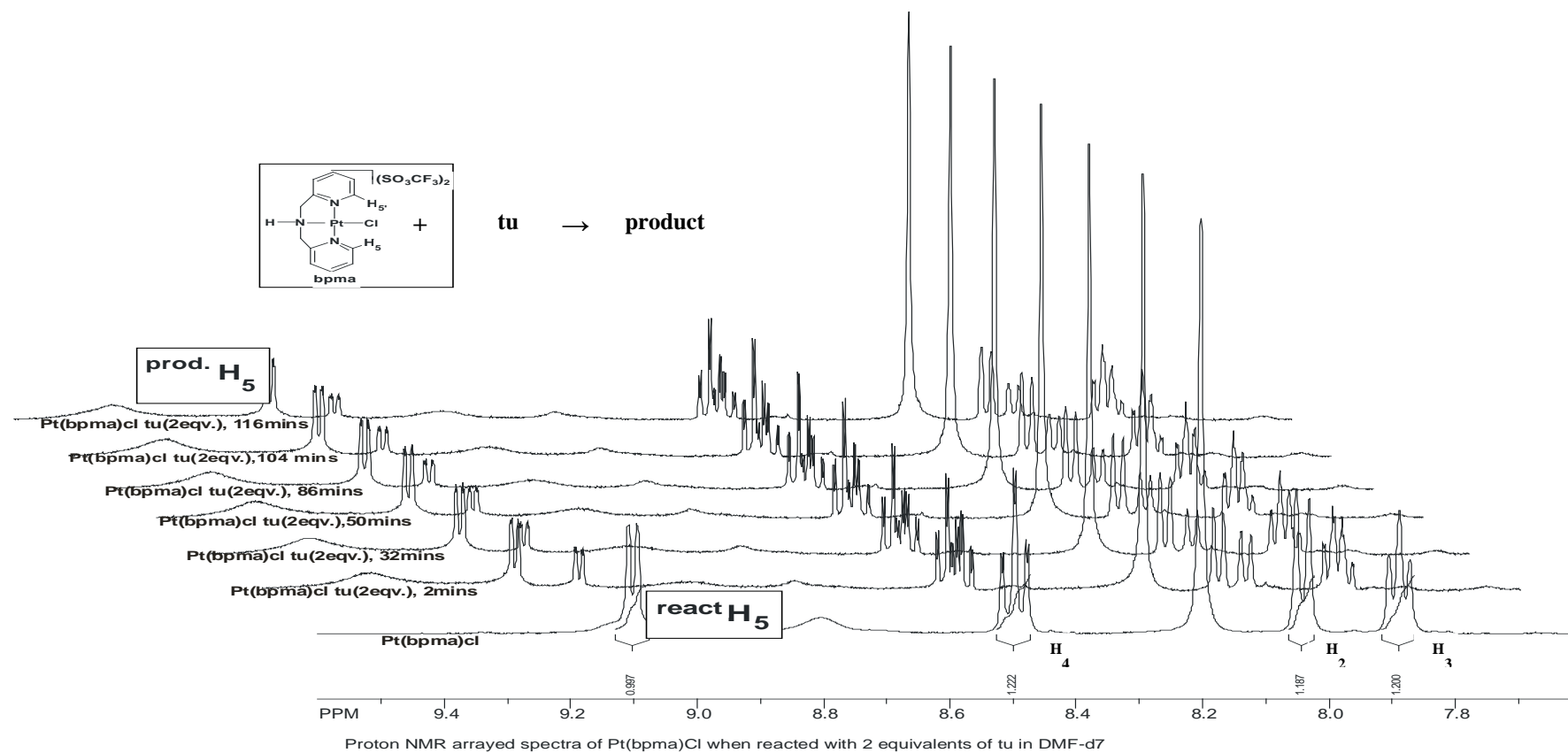


**Figure 4.3** <sup>1</sup>H NMR (500 MHz) spectra array of **bpma-Cl** (showing only the aromatic region) acquired during its reaction with two equivalents of thiourea (tu) in DMF-*d*<sub>7</sub> at 298 K. The doublet at  $\delta = 9.12$  ppm corresponds to substituted product.

## Mononuclear Pt(II) complex with alkyl pendants

As shown in Figure 4.3, a subsequent reaction step is observed in the spectral arrays of **bpma**. A new set of resonances which are shifted downfield at  $\delta = 9.12$  ppm and integrating to an approximate ratio of 2:1 (intermediate product: to the reactant) upon mixing the complexes with two equivalents of thiourea is observed for the H<sub>5</sub>/H<sub>5'</sub> protons of pyridine rings. The numbering system for the pyridyl protons used to monitor the progress of the reaction is shown on the structure of the **bpma-Cl** complex (Inset to Figure 4.3). Because of their distinctive chemical shifts relative to the other three ring protons, the H<sub>5</sub> protons were chosen to monitor the kinetic progression of the reaction. The H<sub>5</sub> resonances of the **bpma-Cl** complex, labeled <sup>react</sup>H<sub>5</sub>, which appear at  $\delta = 9.06$  ppm are shifted downfield to  $\delta = 9.12$  ppm in the tu-substituted derivative, labeled <sup>prod</sup>H<sub>5</sub> in Figure 4.3. During the course of the reaction, the <sup>prod</sup>H<sub>5</sub> resonances of the intermediate product which had formed instantly further grew while <sup>react</sup>H<sub>5</sub> resonances decreased accordingly. Since the first step which involves the substitution of the chloride ligand is fast and complete in less than 20 s for all these complexes, its evolution cannot be monitored by the NMR spectroscopy due to the limitations imposed by slow manual mixing of the reactants. Thus, it can be assumed that the subsequent changes in the intensities of the <sup>prod</sup>H<sub>5</sub> resonances as observed in the spectral array of this reaction are certainly due to a subsequent step which is evidently observed in this complex despite it having only one leaving group and an expected thermodynamic stability due to the chelate effect of the ligand system. Thus, the general course of substitution of the coordinated aqua coligands by the thiourea nucleophiles in all the complexes is as previously proposed<sup>41c-d</sup> and depicted in Figure 4.4. The structure of the final product (**bpma-tu<sub>2</sub>**) and its electrostatic potential map are depicted in Figure SI 4.6 (supporting information).

# Mononuclear Pt(II) complex with alkyl pendants

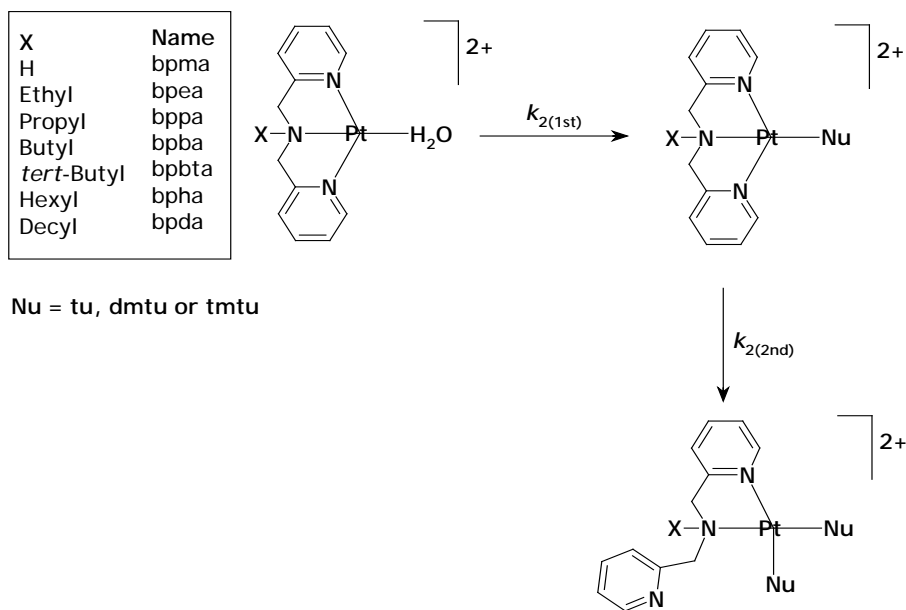


**Figure 4.4** The general reaction scheme for the reactions between the complexes and the thiourea nucleophiles at a pH of 2.0.

In all cases, the first substitution step is very fast. This step, as already stated and shown for the reaction of **bpma** and tu ( $^1\text{H}$  NMR experiment), is too fast to be observed on the timescales of  $^1\text{H}$  NMR or UV-visible spectroscopies. It was therefore studied on the stopped-flow technique while the subsequent and slower steps were studied by UV-visible spectroscopy. An example of the combined time-resolved kinetic traces showing the two substitution steps recorded when a 0.1 mM solution of **bppa** is reacted with 3 mM of dmtu is shown in Figure 4.5.

## Mononuclear Pt(II) complex with alkyl pendants

---

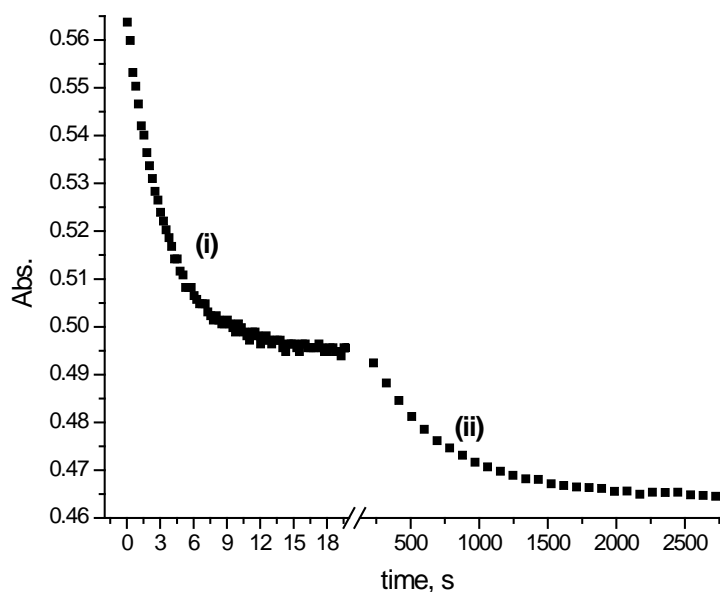


**Figure 4.5** Typical two well-separated kinetic traces for the two-steps reaction between **bpba** (0.1 mM) and dmtu (3 mM) recorded at 284 nm, T = 298 K, pH = 2.0, I = 0.02 M CF<sub>3</sub>SO<sub>3</sub>H, adjusted with Li(SO<sub>3</sub>CF<sub>3</sub>)}. Step (i): The substitution of the aqua studied by the stopped-flow technique. Step (ii)} The dechelation of one of the pyridyl units studied by V-visible spectroscopy.

Each of the two substitution steps are well separated and could be fitted perfectly to single-exponential models. The dependence of the observed first-order rate constants,  $k_{\text{obs}(1^{\text{st}}/2^{\text{nd}})}$ , on the concentration of the nucleophiles resulted in the second-order rate constants,  $k_{2(1^{\text{st}}/2^{\text{nd}})}$  and representative plots, demonstrating a good linear dependence of the observed rate constants on the concentration of the thiourea nucleophiles is shown in Figures 4.6a and 4.6b for **bpba**.

## Mononuclear Pt(II) complex with alkyl pendants

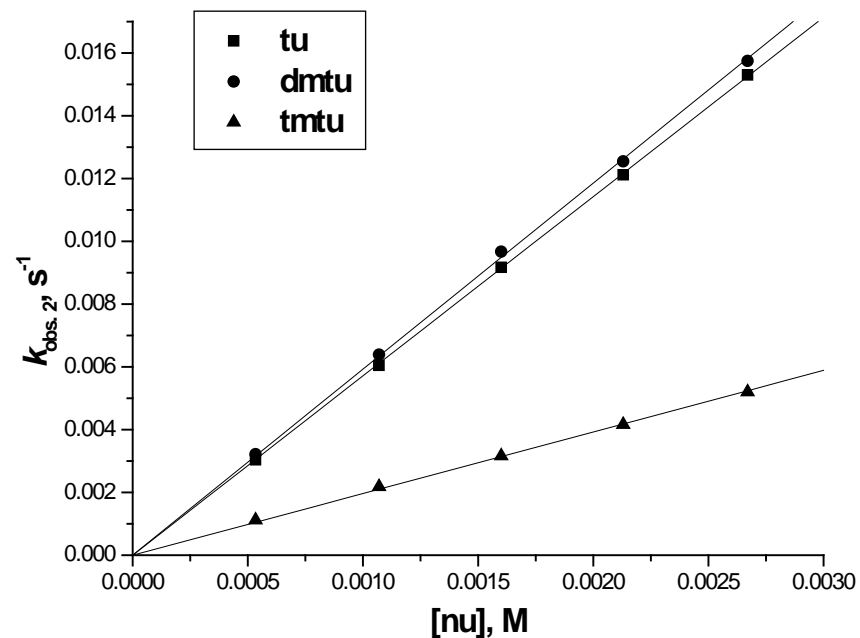
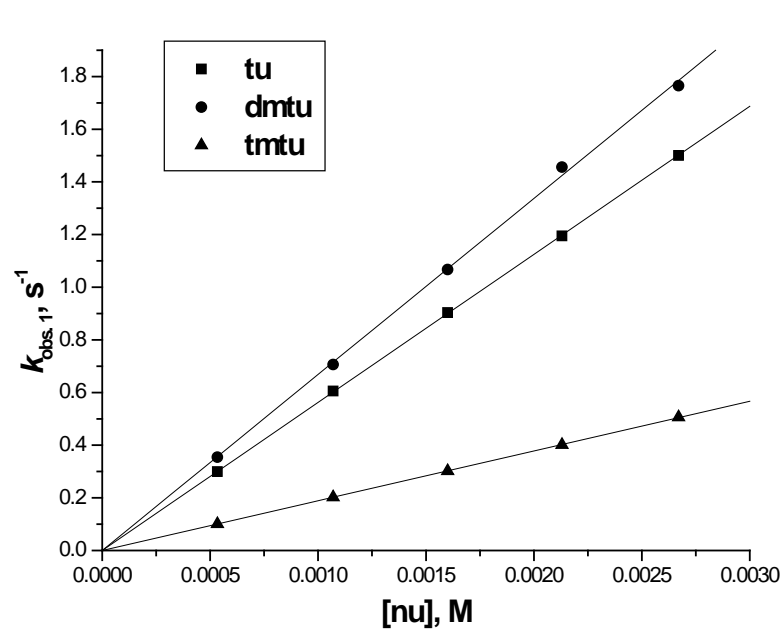


**Figure 4.6a** Concentration dependence of  $k_{\text{obs},1}^{\text{st}}$ , s<sup>-1</sup>, for the substitution of the aqua ligand in **bpba** by thiourea nucleophiles, pH = 2.0, T = 298 K, I = 0.02 M {0.01 M CF<sub>3</sub>SO<sub>3</sub>H, adjusted with Li(SO<sub>3</sub>CF<sub>3</sub>)}.

**Figure 4.6b** Concentration dependence of  $k_{\text{obs},2}^{\text{nd}}$ , s<sup>-1</sup>, for the dechelation of the pyridyl units in **bpba** by thiourea nucleophiles, pH = 2.0, T = 298 K, I = 0.02 M {0.01 M CF<sub>3</sub>SO<sub>3</sub>H, adjusted with Li(SO<sub>3</sub>CF<sub>3</sub>)}.

## *Mononuclear Pt(II) complex with alkyl pendants*

The rate constants resulting from the direct attack by the nucleophiles at 25 °C were obtained from the slopes of the concentration dependence plots and are summarized in Table 4.3a.

**Table 4.3a** Summary of the second-order rate constants for the displacement of aqua ligands and the dechelation of the pyridyl units by thiourea nucleophiles in amphiphilic Pt(II) complexes with a bis(2-pyridylmethyl) chelate headgroup.

Complexes	nu	Second order rate constant, M <sup>-1</sup> s <sup>-1</sup>	
		<i>k</i> <sub>2/1</sub> <sup>st</sup>	<i>k</i> <sub>2/2</sub> <sup>nd</sup>
<b>bpma</b>	<b>tu</b>	409 ± 2	4.95 ± 0.06
	<b>dmtu</b>	394 ± 1	4.05 ± 0.07
	<b>tmtu</b>	190 ± 0.5	2.16 ± 0.06
<b>bpea</b>	<b>tu</b>	500 ± 3	4.96 ± 0.07
	<b>dmtu</b>	615 ± 2	5.78 ± 0.04
	<b>tmtu</b>	217 ± 3	2.56 ± 0.02
<b>bppa</b>	<b>tu</b>	524 ± 4	4.64 ± 0.06
	<b>dmtu</b>	669 ± 1	5.79 ± 0.03
	<b>tmtu</b>	196 ± 0.7	2.46 ± 0.02
<b>bpba</b>	<b>tu</b>	561 ± 0.1	5.72 ± 0.02
	<b>dmtu</b>	670 ± 4	5.93 ± 0.03
	<b>tmtu</b>	189 ± 0.4	1.96 ± 0.02
<b>bptba</b>	<b>tu</b>	1001 ± 10	9.30 ± 0.03
	<b>dmtu</b>	991 ± 7	10.85 ± 0.07
	<b>tmtu</b>	382 ± 0.2	3.73 ± 0.03
<b>bpha</b>	<b>tu</b>	566 ± 3	4.24 ± 0.07
	<b>dmtu</b>	668 ± 4	5.94 ± 0.05
	<b>tmtu</b>	187 ± 0.3	2.04 ± 0.01
<b>bpda</b>	<b>tu</b>	669 ± 6	6.49 ± 0.15
	<b>dmtu</b>	701 ± 7	6.89 ± 0.02
	<b>tmtu</b>	216 ± 2	1.83 ± 0.01

The absence of intercepts in all the plots suggests that both steps are irreversible in nature. Thus, the rate equations for the two substitution steps in complex with alkyl pendants can be written as shown in equation 1:

$$k_{\text{obs. (1}^{\text{st}}/2^{\text{nd}})} = k_{\text{obs. (1}^{\text{st}}/2^{\text{nd}})}[\text{nu}] \quad 4.1$$

Data in Table 4.3a, indicate that when an alkyl functional group is attached to the *trans*-N donor atom of the bis(2-pyridylmethyl)amine chelate headgroup, the resultant metallosurfactant complex is more reactive towards the thiourea nucleophiles than **bpma**. When the rate constant for the substitution of the coordinated aqua in **bpma** is taken as a

## Mononuclear Pt(II) complex with alkyl pendants

reference value, the relative ratios of the substitution of the aqua ligands of **bpma**; **bpea**; **bppa**; **bpba**; **bptba**; **bpha** and **bpda** by tu is 1: 1.22: 1.28 :1.37: 2.45 :1.38 :1.63, respectively. A more or less similar trend is observed when dmtu is the incoming nucleophile. The calculated activation ratios of the bis(2-pyridylmethyl)amine headgroup due to the  $\sigma$ -induction<sup>23b</sup> from the appended alkyl tail bear a moderate dependence on the chain length of the appended alkyl tail. Reactivity increases only slightly and proportionally from **bpea** to **bpba**. Beyond the butyl tail, the effect of the tail group on the reactivity of the metal centre becomes roughly constant.

However, when the alkyl group is changed to a *tert*-butyl tail in **bptba**, reactivity increases by a factor of about 2.45 when both tu and dmtu are the incoming nucleophiles. Thus, by replacing two methylene hydrogens in **bpea** with two methyl groups to form the *tert*-butyl tail of **bptba**, the reactivity of the complex towards the nucleophiles doubles. Further to this, the isomeric **bpba**, which has a primary butyl group as a pendant, is less reactive by factor of 0.56 (tu) and 0.68 (dmtu) compared to **bptba**. This is because the *tert*-butyl is a better  $\sigma$ -donor<sup>47a</sup> than the straight chain alkyl group. As a result, it has a stronger *trans*-influence. Branching at the  $\alpha$ -carbon of its tail group increases the  $\sigma$ -donation of electron density towards the Pt atom relative to its isomeric analogue, **bpba** (which has an aliphatic tail), causing increased labilization at its *trans*-leaving group.

In general, the inductive effects of the appended alkyl tails increases the *trans*-influence of the alkylamine donor group leading to a general increase in reactivity of complexes relative to **bpma**. As stated before, and according to the Polarization theory,<sup>25</sup> this strengthens the Pt-N<sub>*trans*</sub> bond at the expense of the Pt-O bond of the aqua leaving group, resulting in ground state destabilization effects. This is confirmed in the DFT-calculated Pt-O bond lengths which increase proportionally along the series. A maximum elongation in this bond is recorded in the **pbtba** complex. The extent of bond weakening of the leaving group in this complex is reflected in its superior reactivity when compared to the rest of the complexes

It is also noted that while the electron density generally increases with the increase in the chain length of the tail, its  $\sigma$ -donation towards the metal centre decreases inversely with the number of connecting bonds within the chain, away from the N-donor atom. A balance between these two factors on the *trans*-influence of the tail reaches its maximum in the **bpba** complex, beyond which any further increase in electron density is countered by the ineffective  $\sigma$ -inductive effects towards the donor atoms. The *trans*-influence of the tail

## Mononuclear Pt(II) complex with alkyl pendants

reaches a maximum when  $n = 4$  where any further increase in the chain size (electron density and hence its  $\sigma$ -effect) is not matched by a proportional increase in labilization of the aqua leaving groups. As already stated, the HOMO orbitals of the complexes with longer alkyl tails *viz.*, **bpha** and **bpda** are peculiarly located on the alkyl tips of the ligands. As a result, any further increase in electron density resulting from additional methylene groups in the alkyl pendants longer than the butyl tail is not matched by further increases in lability of the leaving groups in the complexes, causing the leveling-off in reactivity.

The rate of dechelation of one of the *cis*-coordinated pyridyl rings is two orders of magnitude smaller when compared with the substitution of the aqua ligand. A similar pattern of substitution has been reported for the analogous dinuclear complexes.<sup>41</sup> The rate of ring opening of the chelate headgroups (measured by  $k_{(2^{nd})}$ ) is less responsive to changes occurring in the structure of pendant tail group of the complexes except for the **bptba** complex. This is consistent with a process in which the thermodynamically stable chelate structure is partially destroyed, wherein both an electronic effect as well as steric repulsions around the Pt(II) metal centre in the substituted products are at play.<sup>47</sup> Firstly, a facilitated attack (due to the strong *trans*-effect of the first coordinated tu) by a second thiourea molecule on the *trans*-positioned amine nitrogen of the chelate is unlikely because of the steric constraints<sup>41c-d</sup>. However, it can be noted that in the optimized structures of the complexes (Table 4.2c) the aqua coligand assumes a tipped-off configuration out of the NNN-square-plane, an indication of the existence of some steric strain with the chelate headgroup from the two bulky pyridyl rings. The release of the strain in the chelate through dechelation of one of the pyridyl arms and the strong affinity of the sulfur donor nucleophiles for the platinum metal centres are the likely driving forces for the ring opening process. This second reaction step, observed in all the mononuclear complexes reiterates that one of the coordinated *cis*-pyridyl units of the chelate headgroup can be substituted by the strong thiourea nucleophiles at the metal centres. Similar decoordination of a chelated ligand by strong nucleophiles has been observed before.<sup>48</sup>

Since the amphiphiles reported in this Chapter is formed intuitively by excising off one of their chelated Pt(II) headgroups of the dinuclears reported in Chapter Three, a comparison of their reactivity data with those of dinuclear complexes becomes necessary to gain a full understanding of the role of the bridging linker on the reactivity of the latter set of complexes. Any differences in the reactivity data between the two sets of complexes is due to the effects related to bridging or constraining the two chelated Pt(II) reactive centres by the

## Mononuclear Pt(II) complex with alkyl pendants

$\alpha,\omega$ -alkyldiamine linker. Thus, for the purpose of this comparison, data have been extracted from Table 3.4 in Chapter Three, and literature<sup>41c,d</sup> and is summarized in Table 4.3b.

**Table 4.3b** A comparison of the second-order rate constant for the substitution of the aqua ligands in Pt(II) amphiphiles and their analogous dinuclear complexes using tu as nucleophiles.

$k_{2/1}^{st}, M^{-1} s^{-1}$					
Amphiphilic Pt(II) complex # (n)	Symmetry		Dinuclear Pt(II) Complex # (n)	Symmetry	
<b>bpma (0)</b>		409 ± 2			
<b>bpea (2)</b>	$C_{2h}$	500 ± 3	<b>‡En (2)</b>	$C_{2h}$	151 ± 1
<b>bppa (3)</b>	$C_{2h}$	524 ± 4	<b>*Prop (3)</b>	$C_{2v}$	1033 ± 7
<b>bpba (4)</b>	$C_{2h}$	561 ± 1	<b>‡But (4)</b>	$C_{2h}$	315 ± 1
<b>bpbta (4)<sub>branched</sub></b>	$C_{2h}$	1001 ± 10			
			<b>*Pen (5)</b>	$C_{2v}$	765 ± 10
			<b>‡Hex (6)</b>	$C_{2h}$	579 ± 2
			<b>*Hep (7)</b>	$C_{2v}$	577 ± 5
<b>bpda (10)</b>	$C_{2h}$	669 ± 6	<b>‡Dec (10)</b>	$C_{2h}$	641 ± 3

<sup>‡</sup>Data extracted from Table 3.4, Chapter Three (or Ref. 41b) and <sup>\*</sup>Ref 41c-d. # (n) is the number of carbon in the appended tail or the linking bridge.

While the work reported in Chapter Three, addressed the effect of the chain length on reactivity of the Pt centres in detail, it could not answer a closely related question such as ‘What is the consequence of constraining two or more chelated Pt(II) centres through an alkyldiamine bridge on their general reactivities?’ This question can be answered better through comparing the reactivity data of the two sets of complexes since other masking factors such as charge addition and steric influences composited in the dinuclear complexes are eliminated in the amphiphiles. If one compares reactivity data for the mononuclear and dinuclear complexes in Tables 4.3b, the consequent of constraining two *N,N*-bis(2-pyridylmethyl)amine headgroups through a flexible linker becomes evident. When the bridge is short and has an even number of carbon atoms (*i.e.* the complex has a  $C_{2h}$  symmetry), the rates of substitutions of the leaving groups of the dinuclears<sup>41b</sup> by thiourea are significantly lower than their respective monomeric counterparts. For example, the aqua ligands in **bpea** are 3 times more labile than those of **En**, respectively. The reactivity factor decreases to about 1.7 (tu) between the **But** and the **bpba** complexes. When the same comparison is made between the mononuclears and their dinuclear analogues of longer tail/bridges ( $n > 6$ ) no reactivity difference is evident between them. But, when the number of carbon atoms in the bridge is

## Mononuclear Pt(II) complex with alkyl pendants

odd, as is the case for **Prop**, its monomeric analogue, **bppa**, is significantly less reactive by 50%.

The decrease in the rates of substitution of the aqua leaving group of the dinuclear complexes bridged by short linkers (**En** and **But**) relative to their amphiphilic analogues (**bpea** and **bpba**) indicates how the steric influences endemic in the  $C_{2h}$  symmetry of former complexes control reactivity of their Pt(II) centres resulting from the constraints imposed by the shorter chain lengths of their bridges. As already discussed, when one square-planar of the dinuclear complexes which imposes steric influences at the other chelate is excised off from the bridge, the resultant amphiphile has a higher substitutional reactivity towards the thiourea nucleophiles. This happens despite their (**bpea** and **bpba**) lower formal charges of +2 relative to the +4 of their dinuclear (**En** and **But**) counterparts. When the same comparison is extended to the **Hex/bpha** and **Dec/bpda** pairs of complexes, the reactivity advantage in the mononuclears over their dinuclears diminishes. In fact, there are no significant differences between the reactivities beyond **Hex** and the **bpha** complexes.

The differences in the reactivities between the two sets of complexes as the chain length of the tail/bridge is changed demonstrates the presence of dominating steric dispositions in the the  $C_{2h}$  symmetry of the even bridged dinuclears due to the overlap geometry of their Pt chelate headgroups. When the even bridges are short, the rates of substitutions are lower than their mononuclear analogues. When the length of the bridge is increased, the steric disposition by each square-planar chelate in their slip-up sandwich overlap geometry is reduced causing a concomitant increase in reactivity. The influence on reactivity due to the steric disposition reaches its limit in the **Hex/bpha** complexes. The reactivity trend observed in these dinuclear complexes is in line with the view that when the chain length of the bridge is increased, the enjoined Pt(II) centres become mutually independent from the influence from the other.<sup>9,41c</sup>

However, in the **Prop** complex, the mutual steric impositions observed in the other dinuclear complexes is absent because of its bowl structure. Its reactivity is higher than that of its monomeric analogue, **bppa**, an observation that suggest an 'entrapment effect' to the oncoming nucleophiles due to the bowl-shaped structure ( $C_{2v}$  symmetry) of dinuclear complex. When reactivity data of **Prop** is compared to that reported for **Pen** and **Hep** from the study of van Eldik and coworkers<sup>41c</sup> this 'entrapment effect' weakens due to the widening of the basal width of the bowl as the chain length is increased.

## Mononuclear Pt(II) complex with alkyl pendants

The reactions were also studied within the temperature range 15-35 °C, from which the activation parameters  $\{\Delta H^\ddagger_{(1/2)^{\text{st/nd}}}, \Delta S^\ddagger_{(1/2)^{\text{st/nd}}}\}$  for the two substitution steps could be determined. The activation data is summarized in Table 4.3c.

**Table 4.3c** Summary of the activation parameters for the displacement of aqua ligands and the dechelation of the pyridyl units by thiourea nucleophiles in amphiphilic Pt(II) complexes with a bis(2-pyridylmethyl) chelate headgroup.

Complex	nu	Activation enthalpy, kJ mol <sup>-1</sup>		Activation entropy, J mol <sup>-1</sup> K <sup>-1</sup>	
		$\Delta H^\ddagger_1$	$\Delta H^\ddagger_2$	$\Delta S^\ddagger_1$	$\Delta S^\ddagger_2$
bpma	tu	41.1 ± 0.9	46.1 ± 0.3	-57.3 ± 3.0	-78.8 ± 0.8
	dmtu	37.2 ± 0.9	52.0 ± 1.2	-70.7 ± 3.0	-59.2 ± 3.8
	tmtu	43.3 ± 1.1	59.3 ± 1.0	-56.6 ± 3.4	-37.5 ± 3.0
bpea	tu	35.0 ± 0.4	49.9 ± 1.3	-76.3 ± 1.2	-64.5 ± 3.8
	dmtu	35.5 ± 0.3	46.6 ± 0.5	-72.9 ± 1.1	-77.6 ± 1.6
	tmtu	46.1 ± 0.6	50.4 ± 0.9	-45.9 ± 1.8	-68.8 ± 1.1
bppa	tu	36.1 ± 1.1	49.7 ± 1.2	-72.5 ± 3.2	-65.1 ± 4.0
	dmtu	38.5 ± 0.1	50.7 ± 0.6	-62.1 ± 3.0	-60.7 ± 2.0
	tmtu	46.9 ± 1.5	54.2 ± 0.4	-44.0 ± 4.6	-55.2 ± 1.2
bpba	tu	40.2 ± 0.8	40.5 ± 1.3	-57.2 ± 2.6	-95.0 ± 4.0
	dmtu	33.7 ± 1.6	36.2 ± 1.3	-75.2 ± 4.8	-108.5 ± 4.2
	tmtu	47.3 ± 0.8	45.1 ± 1.2	-63.2 ± 2.5	-85.7 ± 3.6
bptba	tu	29.3 ± 0.7	46.6 ± 1.3	-89.8 ± 0.8	-68.5 ± 4.4
	dmtu	32.2 ± 0.3	48.8 ± 0.3	-84.4 ± 1.0	-61.3 ± 1.0
	tmtu	46.7 ± 0.1	49.4 ± 0.4	-85.6 ± 3.2	-68.8 ± 1.2
bpha	tu	42.5 ± 1.1	41.7 ± 0.8	-50.3 ± 3.2	-92.8 ± 2.5
	dmtu	36.9 ± 0.8	42.6 ± 0.8	-68.3 ± 3.0	-86.4 ± 2.4
	tmtu	43.8 ± 1.3	53.7 ± 0.7	-55.0 ± 4.0	-60.3 ± 2.3
bpda	tu	40.0 ± 0.8	40.5 ± 1.3	-48.8 ± 3.0	-95.0 ± 4.0
	dmtu	41.9 ± 0.9	36.2 ± 1.3	-70.7 ± 3.0	-108.5 ± 4.2
	tmtu	43.7 ± 0.7	45.1 ± 1.2	-54.1 ± 2.4	-85.7 ± 3.6

The activation enthalpy ( $\Delta H^\ddagger_{(1/2)^{\text{st/nd}}}$ ) values are low while the values of the activation entropies ( $\Delta S^\ddagger_{(1/2)^{\text{st/nd}}}$ ) are large and negative, indicating that the substitution mechanism in both steps is associative in nature.<sup>25</sup> In general, the activation enthalpies for the dechelation of one of the pyridyl units are slightly larger than for the simultaneous substitution of the aqua ligands, signifying the slowness of the former process.

# *Mononuclear Pt(II) complex with alkyl pendants*

---

## 5.4 Conclusion

In this study, we have shown that reactivity of Pt(II) complexes with a common bis(2-pyridylmethyl)amine headgroup can be systematically tuned by introducing alkyl hydrocarbon tail groups of different chain lengths and structures on the *trans*-N donor atoms of the chelate headgroup. The differences in the second-order rate constants for the substitution of their coordinated aqua ligands reflect the role of positive  $\sigma$ -inductive donation of electron density due to chain lengths of the appended alkyl tails on the reactivity of the metal centres in going from **bpea** to **bpda**. It is clear that appending an alkyl hydrocarbon group on the *trans*-N donor atom of the **bpma**, accelerate the rate of substitution of the aqua leaving group albeit to a moderate extent through a ground state destabilization of the Pt-O bond of the leaving group. However, when a tertiary alkyl group such as a *tert*-butyl is appended on the same position, reactivity increases by a factor of about two. The difference in the reactivity of this complex, whose alkyl tail is branched on its  $\alpha$ -carbon, when compared to its other members of the homologue, reiterates the inductive nature of the flow of electron density from the tailing groups towards the Pt metal centres in these complexes.

Since the alkyl pendants become the structural linkers in the multinuclear Pt(II) complexes bridged by flexible  $\alpha,\omega$ -alkyldiamine, the reactivity trend of the studied complexes demonstrates that the electronic effect of the alkyldiamine bridge on the overall reactivity of the multinuclear Pt(II) complexes in which they become bridges is weak. This gets further weakened by other factors such as the steric features within the bridge and also the native electronic effects around the Pt(II) chelate headgroups.

When the rates of substitution of the leaving groups of the amphiphiles by the thioureas are compared to their analogous dinuclears', it becomes evident that the linker assumes a constraining role on the reactivities of the Pt(II) chelate headgroups when the linker is short. The chain length of the flexible  $\alpha,\omega$ -alkyldiamine bridge determines both the average distance separating the chelated Pt headgroups as well as the symmetry (which specifically depends on the number of carbon atoms in the linker is even or not) of the resultant dinuclear complexes, two factors which are important in the control of their substitutional reactivity. The number (even or odd) carbon atoms constituting the aliphatic bridge determines the symmetry adopted by the complexes as well as the average distance separating the Pt centres, two factors which critically determine the amount of steric influences felt at the Pt centres. When two *N,N*-bis(2-pyridylmethyl)amine chelated Pt(II) square-planar chelates are constrained through a

## Mononuclear Pt(II) complex with alkyl pendants

flexible diamine linker bearing an even number of carbon atoms, mutual steric influences on each chelate are enacted as a result of the slip-up sandwich structures of the resultant complexes. The effects on the reactivity of the complexes by these steric impositions are dependant on the chain length of the linking alkyldiamine bridge. Thus, the steric influences decelerate the rate of substitution in complexes of shorter bridges more effectively and become less important as the length of the bridge is increased. This kind of influence on reactivity enacted by the constraints of the bridge is absent in the analogous amphiphilic mononuclears.

However, when the constraint between the chelated Pt(II) centres is by a bridge with an odd number of carbon atoms, the resultant bowl-shaped structures causes an 'entrapment effect' that increases reactivity relative to their monomeric counterparts as demonstrated in the reactivity of the **Prop/bppa** pair of complexes. The 'entrapment effect' is depended on the angle subtended by the edges of the bowl, becoming weaker as the length of the alkyldiamine bridge is increased.

While no evidence of loss of the appended alkyl groups of the linkers from these mononuclear complexes by the strong substituting thiourea nucleophiles was recorded, dechelation of the one of the pyridyl arm of the bis(2-pyridylmethyl)amine chelate headgroups was observed for the amphiphiles. However, the substitution process remained associative in nature as it for the dinuclear complexes.

### 4.5 References

- 1 F. Basolo, J. Chat, H. B. Gray, R. G. Pearson and B. L. Shaw *J. Chem. Soc.*, 1961, 2207.
- 2 (a) H. B. Gray, *J. Chem. Soc.*, 1962, 1548; (b) M. Schmülling, A. D. Ryabov and R. van Eldik, *J. Chem. Soc. Chem. Comm.*, 1992, 1609.
- 3 V. Deubel, *J. Am. Chem. Soc.*, 2002, **124**, 5834.
- 4 K. Lemma S. K. C. Elmroth and L. I. Elding, *J. Chem. Soc., Dalton Trans.*, 2002, 1288.
- 5 J. Teuben, M. Rodriguez. I. Zubiri and J. Reedijk, *J. Chem. Soc., Dalton Trans.*, 2000, 369.
- 6 D. Jaganyi and F. Tiba, *Transition Met. Chem.*, 2003, **28**, 803.
- 7 D. Jaganyi, F. Tiba, O. Q. Munro, B. Petrović and Z. D. Bugarčić, *J. Chem. Soc., Dalton Trans.*, 2006, 2943.

## *Mononuclear Pt(II) complex with alkyl pendants*

---

- 8 (a) Z. D. Bugarčić, G. Liehr and R. van Eldik, *J. Chem. Soc., Dalton Trans.*, 2002, 951; (b) Z. D. Bugarčić, G. Liehr and R. van Eldik, *J. Chem. Soc., Dalton Trans.*, 2001, 2825.
- 9 (a) B. Pitteri, G. Annibale, G. Marangoni, L. Cattalini, F. Visentin, V. Bertilasi and P. Gilli, *Polyhedron*, 2001, **20**, 869; (b) G. Annibale, M. Brandolisio and B. Pitteri, *Polyhedron*, 1995, **14**, 451.
- 10 Z. D. Bugarčić, S. T. Nandibewoor, M. S. Hamza, F. Heinmann and R. van Eldik, *J. Chem. Soc., Dalton Trans.*, 2006, 279.
- 11 B. Pitteri, E. I. J. Breet and R. van Eldik, *Inorg. Chim. Acta.*, 1983, **301**, 76.
- 12 R. J. Mureinik and M. Bidani, *Inorg. Chim. Acta.*, 1978, **29**, 37.
- 13 B. Pitteri, G. Marangoni L. Cattalini and T. Bobbo, *J. Chem. Soc., Dalton Trans.*, 1995, 3853.
- 14 R. Romeo, R. Plutino, L. M. Scolaro, S. Stoccoro and G. Minghetti, *Inorg. Chem.*, 2000, **39**, 4749.
- 15 G. Annibale, M. Brandolisio, Z. Bugarčić and L. Cattalini, *Transition Met. Chem.*, 1998, **23**, 715.
- 16 B. Pitteri, G. Marangoni, L. Cattalini and F. V. Visulim and T. Bobbo, *Polyhedron*, 1998, **17**, 475.
- 17 B. V. Petrović, M. I. Djuran and Z. D. Bugarčić, *Metal Based Drugs*, 1999, **6**, 355.
- 18 B. Pitteri, G. Annibale, G. Marangoni, V. Bertilasi and V. Ferretti, *Polyhedron*, 2002, **21**, 2283.
- 19 Z. D. Bugarčić, F. W. Heinmann and R. van Eldik, *J. Chem. Soc., Dalton Trans.*, 2004, 279.
- 20 T. Rau, and van Eldik, *Metal Ions in Biological systems*, A. Sigel and H. Sigel Eds. Marcel Dekker, New York, 1996, **32**, 339.
- 21 A. Hofmann, L. Dahlenburg and R. van Eldik, *Inorg. Chem.*, 2003, **42**, 6528.
- 22 A. Hofmann, D. Jaganyi, O. Q. Munro, G. Liehr and R. van Eldik, *Inorg. Chem.*, 2003, **42**, 1688.
- 23 (a) D. Jaganyi, D. Reddy, J. A. Gertenbach, O. Q. Munro and R. van Eldik, *J. Chem. Soc., Dalton Trans.*, 2004, 299; (b) H. Ertürk, R. Puchta and R. van Eldik, *Eur. J. Inorg. Chem.*, 2009, 1334.
- 24 (a) D. Reddy and D. Jaganyi, *Dalton Trans.*, 2008, 6724; (b) D. Jaganyi, K. de Boer, J.

## *Mononuclear Pt(II) complex with alkyl pendants*

---

Gertenbach, J. Perils, *Inte. J. Chem. Kinetics*, 2008, 809.

- 25 (a) F. Basolo and R.G. Pearson, *Mechanisms of Inorganic Reactions*, 2<sup>nd</sup> Ed., Wiley, New York 1967, pp. 80-115; (b) K. F. Purcell, I. Kotz, *Inorganic Chemistry*, Holt-Saunders, 1977, pp. 694-755; (c) M. L. Tobe and J. Burgess, *Inorganic Reaction Mechanisms*, Addison-Wesley, Longman, Ltd., Essex, 1999, pp. 30-33; 70-112.
- 26 (a) A. Z. Werner and I. Cheryaev, *Ann. Instr. Platne SSSR*, 1926, **4**, 261. (b) A. Z. Werner *Anorg. Allg. Chem.*, 1893, **3**, 367;
- 27 G. Ghirlanda, P. Scrimin, A. E. Kaifer and L. A. Echegoyen, *Langmuir*, 1996, **12**, 3695.
- 28 P. C. Griffiths, I. A. Fallis, T. Chuenpratoom and R. Watanesk, *Adv. Colloid Inter. Sci.*, 2006, **122**, 107.
- 29 F. L. Lesh, S. S. Hindo, M. J. Heeg, M. M. Allard, P. Jain, B. Pong, L. Hryhorczuk, C. N. Verani, *Eur. J. Inorg. Chem.*, 2009, 345.
- 30 U. Maran, H. Conley, M. Frank, A. M. Arif, A. M. Orendt, D. Britt, V. Hlady, R. Davis and P. J. Stang, *Langmuir*, 2008, **24**, 5400.
- 31 H. Silva, C. V. Barra, C. France da Costa, M. V. de Almeida, E. T. Cesar, J. N. Silveira, A. Garnier-Suillerot, F. C. S. De Paula, E. C. Pereira Maia, A. P. S. Fontes, *J. Inorg. Biochem.*, 2008, **201**, 767.
- 32 T. Kapp, A. Dullin and R. Gust, *J. Med. Chem.*, 2006, **49**, 1182.
- 33 S. Schreiner, S. V. P. Malheiros, E. De Paula, *Biochim. Biophys. Acta., Biomemb.*, 2000, **1506**, 210.
- 34 M. E. Oehlsen, Y. Qu, N. Farrell, *Inorg. Chem.*, 2003, **42**, 5498.
- 35 N. Farrell, S. G. de Almeida and K. A. Skova, *J. Am. Soc.*, 1988, **110**, 5018.
- 36 N. Farrell and Y. Qu, *Inorg. Chem.*, 1989, **28**, 3416.
- 37 N. Farrell, Y. Qu, U. Bierback, M. Valsecchi and E. Menta, In: *Cisplatin Chemistry and biochemistry of a leading anticancer drug*, 1999, B. Lippert Ed, Verlag Helvet. Chem. Acta, Zurich, Wiley-VCH, Weinheim, 479.
- 38 P. Perego, C. Caserini, L. Gatti, N. Carenini, S. Colangelo, I. Romanelli, R. Supino, D. Viano, R. Leone, S. Spinelli, G. Pezzoni, C. Manzotti, N. Farrell and F. Zunino, *J. Inorg. Biochem.*, 1999, **77**, 59.
- 39 (a) A. Sato, Y. Mori and T. Lida, *Synthesis*, 1992, 539; (b) S. Pal, M. K. Chan. and W. H. Armstrong, *J. Am. Chem. Soc.* 1992, **114**, 6398; (c) H. J. Mok, J. A. Davies, S. Pal, S. K. Mandal and W. H. Armstrong, *Inorg. Chim. Acta*, 1997, **263**, 385.
- 40 A. Mambanda, D. Jaganyi and K. Stewart, *Acta Cryst.*, 2009, **E65**, o402.

# *Mononuclear Pt(II) complex with alkyl pendants*

---

- 41 (a) A. Hofmann and R. van Eldik, *J. Chem. Soc., Dalton Trans.*, 2003, 2979. (b) A Mambanda, D. Jaganyi, S. Hochreuther<sup>b</sup> and R. van Eldik, A Mambanda, D. Jaganyi, S. Hochreuther<sup>b</sup> and R. van Eldik, *Dalton Trans.*, 2010, **39**, 1 (c) H. Ertürk, A. Hofmann, R. Puchta and R. van Eldik, *Dalton Trans.*, 2007, 2295; (d) H. Ertürk, J. Maigut, R. Puchta and R. van Eldik, *Dalton Trans.*, 2008, 2759.
- 42 (a) R. A. Friesner, *Chem. Phys. Lett.*, 1985, **116**, 539; (b) R. A. Friesner, *Annual Rev. Chem. Phys.*, 1991, **42**, 341.
- 43 (a) Spartan 04, Wavefunction, Inc., 18401 von Karman Avenue, Suite 370, Irvine, CA, 92612, USA; Q-Chem, Inc, The Design Center, suite 690, 5001, Baum Blvd., Pittsburgh, 15213, USA, 2004. <http://www.wavefun.com/>; (b) K. Kong, C. A. White, A. I. Krylov, C. D. Sherrill, R. D. Adamson, T. R. Furlani, M. S. Lee, A. M. Lee, S. R. Gwaltney, T. R. Adams, C. Ochsenfeld, A. T. B. Gilbert, G. S. Kedziora, V. A. Rassolov, D. R. Maurice, N. Nair, Y. Shao, N. A. Besley, P. E. Maslen, J. P. Dombroski, H. Daschel, W. Zhang, P. P. Korambath, J. Baker, E. F. C. Byrd, T. van Voorhuis, M. Oumi, S. Hirata, C. P. Hsu, N. Ishikawa, J. Florian, A. Warshel, B. G. Johnson, P. M. W. Gill and B. G. Pople, *J. Computational Chem.*, 2000, **21**, 1532.
- 44 (a) A. D. Becke, *J. Chem. Phys.*, 1993, **98**, 5648; (b) C. Lee, W. Yang and R. G. Parr, *Phys. Rev.*, 1998, **B37**, 785.
- 45 (a) P. C. Hariharan and J. A. Pople, *J. A. Chem. Phys. Lett.* 1972, **16**, 217; (b) P. J. Hay and W. R. Wadt, *J. A. Chem. Phys. Lett.*, 1985, **82**, 299.
- 46 H. Ertürk, J. Maigut, R. Puchta and R. van Eldik *J. Chem. Soc., Dalton Trans.*, 2008, 2759
- 47 (a) N. C. Baird and M. A. Whitehead, *Theoret. Chim. Acta, (Berl.)*, 1966, **6**, 167. (b) P. Y. Bruice, *Organic Chemistry*, 2<sup>nd</sup> Ed., Prentice Hall, 1998, pp. 363-366.
- 48 G. Annibale, L. Cattalini, G. Natile, *J. C. S. Dalton*, 1975, 188.

## **4.6 Supporting Information**

A summary of the wavelengths used for kinetics; exemplary mass spectra for ligands **L5**; NMR spectra for **bpba**; spectral changes for the titration of **bpea** with NaOH; exemplary Tables of data and the respective plots showing the dependence of  $k_{\text{obs.}(1^{\text{st}}/2^{\text{nd}})}$  on concentration of nucleophiles and temperature for some selected complexes (**bpba**, **bpea** and **bpba**); extract of the DFT calculated structures of the dinuclears of Chapter Three and the amphiphiles; electrostatic potential surfaces of the amphiphiles and the calculated

## *Mononuclear Pt(II) complex with alkyl pendants*

---

structure of **bpma-tu<sub>2</sub>** accompany the work reported in this Chapter as supporting information (SI).

**Table SI 4.1** Summary of the wavelengths (nm) used for monitoring the reactions between a series of Pt(II) mononuclear complexes with bis(2-pyridylmethyl)amine chelates and thiourea nucleophiles.

<b>Complex</b>	<b>nu</b>	<b>Wavelength (<math>\lambda</math>), nm</b>
<b>bpma</b>	tu	276
	dmtu	276
	tmtu	300
<b>bpea</b>	tu	276
	dmtu	276
	tmtu	330
<b>bppa</b>	tu	276
	dmtu	276
	tmtu	326
<b>bpba</b>	tu	283
	dmtu	286
	tmtu	325
<b>bpbta</b>	tu	288
	dmtu	286
	tmtu	320
<b>bpha</b>	tu	308
	dmtu	307
	tmtu	336
<b>bpda</b>	tu	300
	dmtu	305
	tmtu	300

# Mononuclear Pt(II) complex with alkyl pendants

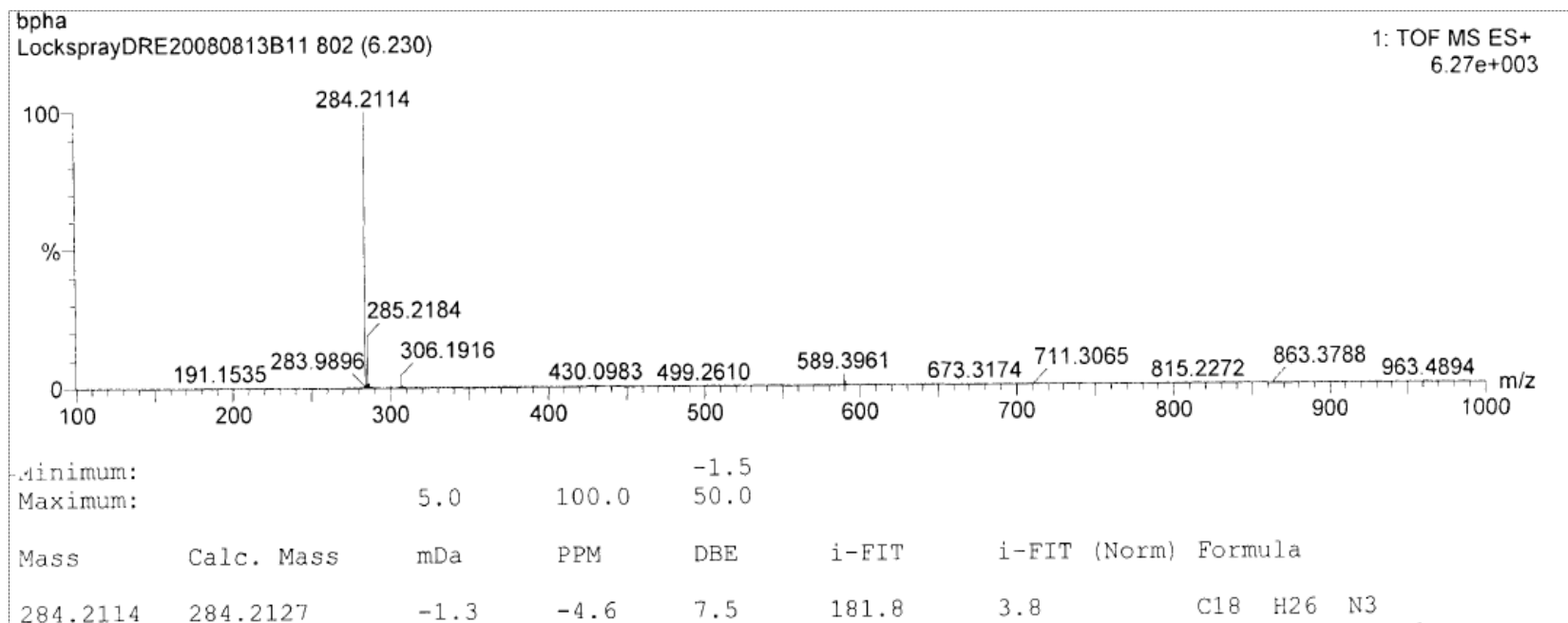


**Figure SI 4.1a** Low resolution ESI mass spectrum of *N,N*-bis(2-pyridylmethyl)hexylamine (**L5**).

# Mononuclear Pt(II) complex with alkyl pendants

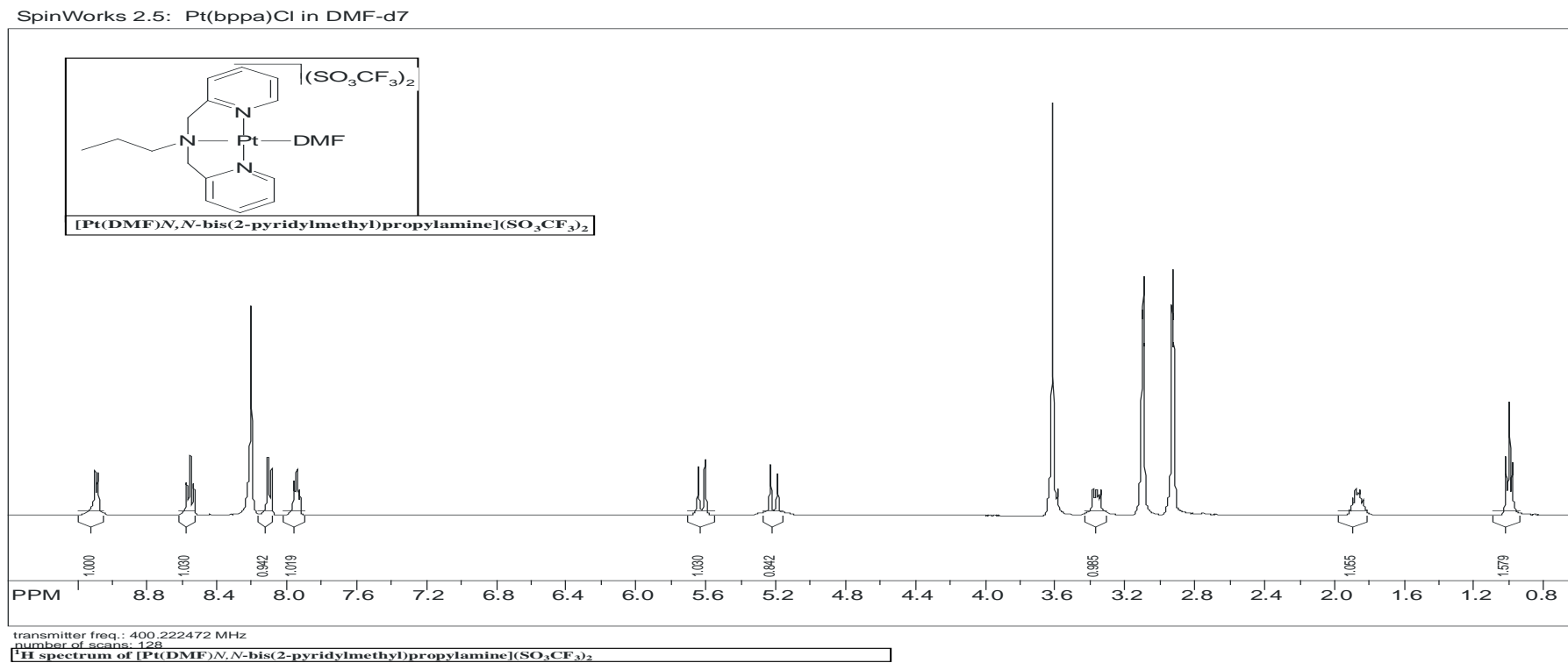


**Figure SI 4.1b** <sup>1</sup>H Spectrum of [Pt(DMF)N,N-bis(2-pyridylmethyl)propylamine](SO<sub>3</sub>CF<sub>3</sub>)<sub>2</sub>.

# Mononuclear Pt(II) complex with alkyl pendants

SpinWorks 2.5: Pt(bppa)Cl in DMF-d7

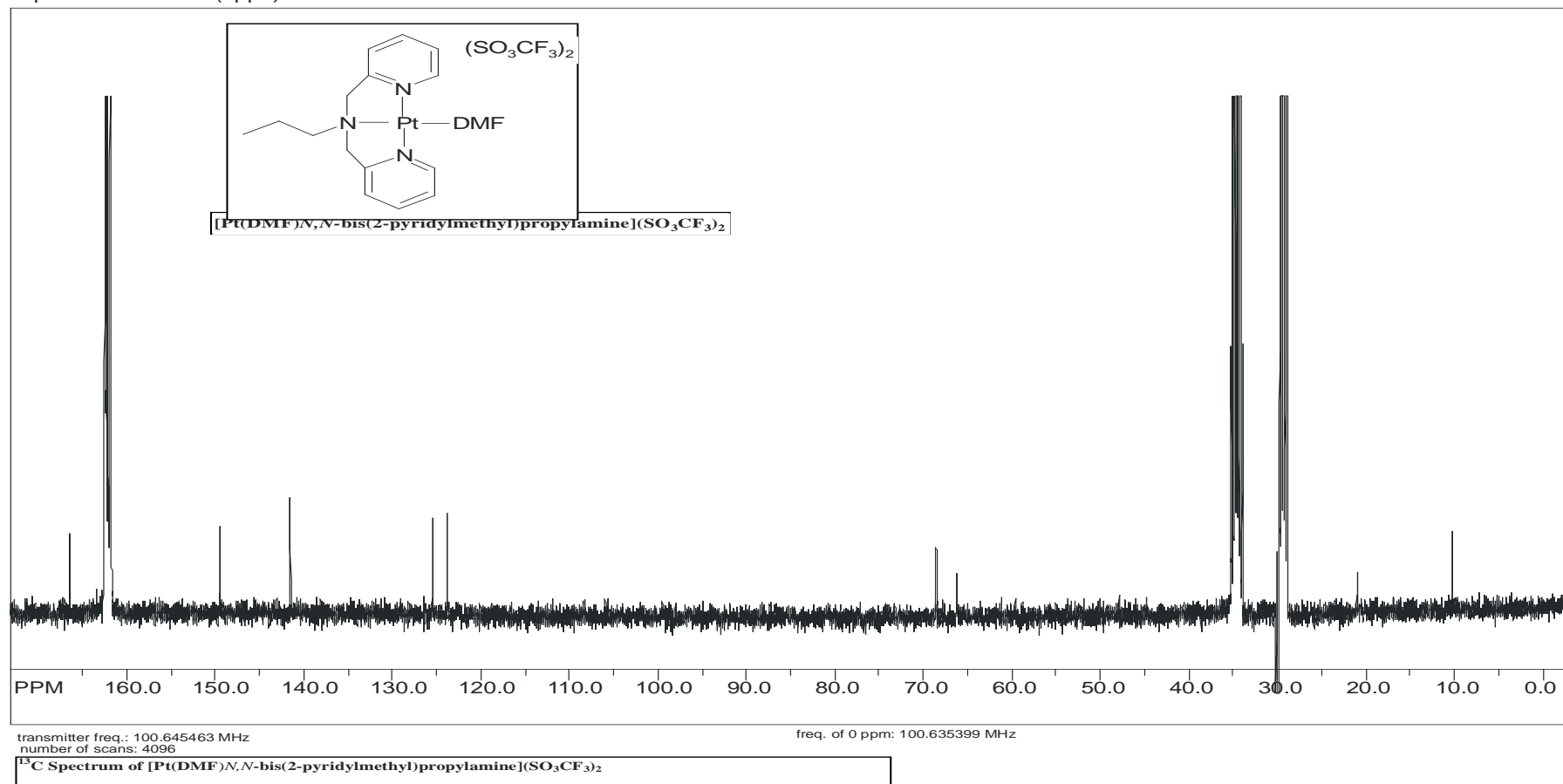
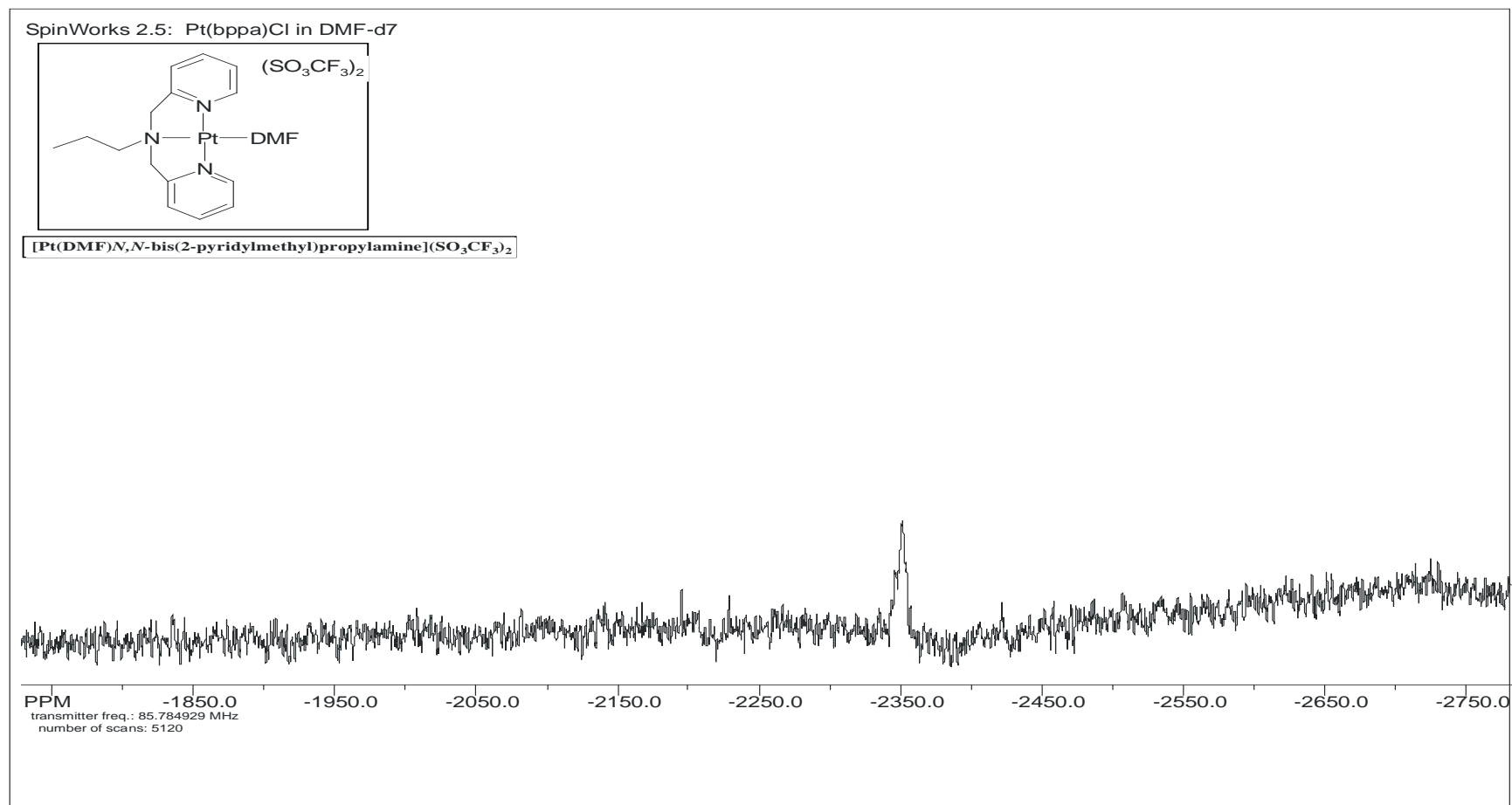


Figure SI 4.1c  $^{13}\text{C}$  Spectrum of  $[\text{Pt}(\text{DMF})\text{N},\text{N}\text{-bis}(2\text{-pyridylmethyl})\text{propylamine}](\text{SO}_3\text{CF}_3)_2$ .

## Mononuclear Pt(II) complex with alkyl pendants



**Figure SI 4.1d** <sup>195</sup>Pt Spectrum of [Pt(DMF)*N,N*-bis(2-pyridylmethyl)propylamine](SO<sub>3</sub>CF<sub>3</sub>)<sub>2</sub>.

## Mononuclear Pt(II) complex with alkyl pendants

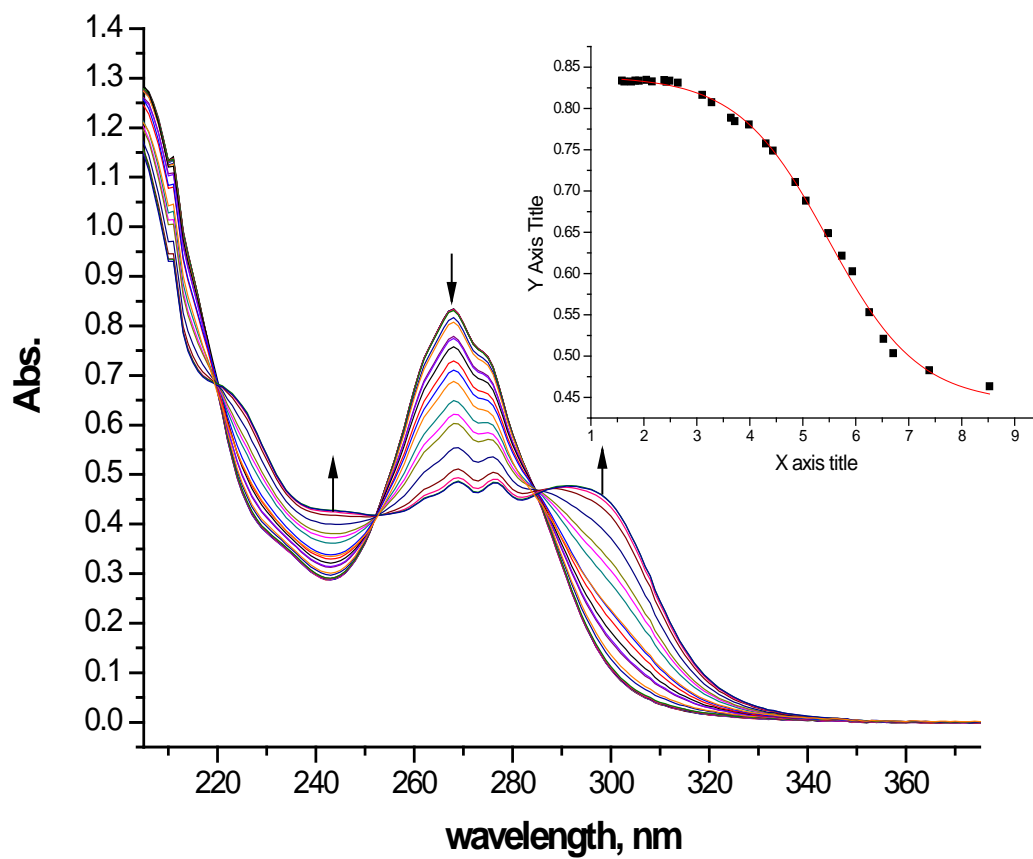


**Figure SI 4.2** UV-visible spectra for the titration of 0.1 mM **bpea** with NaOH, pH range 2 - 9, T = 298 K. Inset is the titration curve at 267 nm.

## Mononuclear Pt(II) complex with alkyl pendants

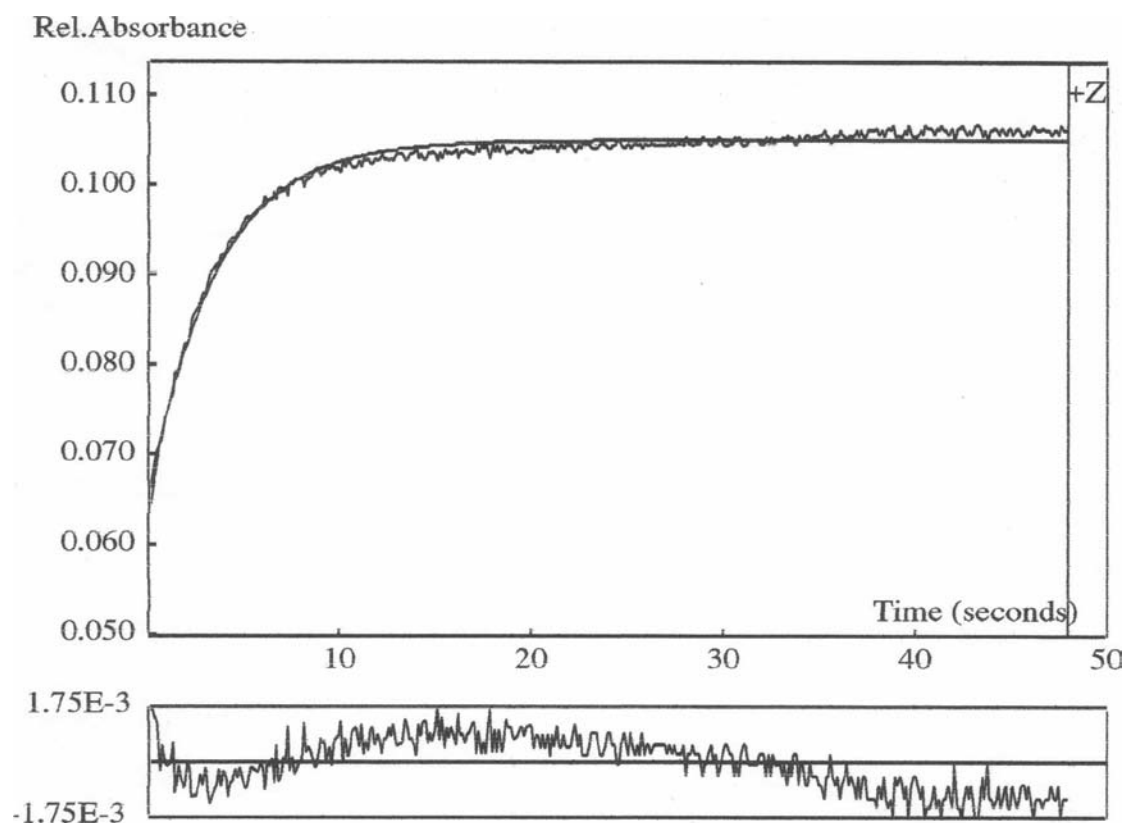


**Figure SI 4.3a** Stopped flow kinetic trace at 335 nm for the first reaction step between **bppa** (0.11 mM) and **tmtu** (3.3 mM) at 298 K, pH = 2.0, I = 0.02 M {CF<sub>3</sub>SO<sub>3</sub>H, adjusted with Li(SO<sub>3</sub>CF<sub>3</sub>)}.

**Table SI 4.2a** Average observed rate constants,  $k_{\text{obs},1}^{\text{st}}$ , s<sup>-1</sup>, for the simultaneous displacement of the aqua ligands of **bptba** by thiourea nucleophiles, pH = 2.0, T = 298 K, I = 0.02 M {0.01 M CF<sub>3</sub>SO<sub>3</sub>H, adjusted with Li(SO<sub>3</sub>CF<sub>3</sub>)}.

[tu], M	$k_{\text{obs},1}, \text{s}^{-1}$	[dmtu], M	$k_{\text{obs},1}, \text{s}^{-1}$	[tmtu], M	$k_{\text{obs},1}, \text{s}^{-1}$
5.34E-4	0.562	5.36E-4	0.5645	5.36E-4	0.1517
0.0011	1.117	0.00107	1.135	0.00107	0.3012
0.0016	1.619	0.00161	1.572	0.00161	0.4554
0.00213	2.166	0.00214	2.153	0.00214	0.6032
0.00267	2.633	0.00268	2.608	0.00268	0.7561

## Mononuclear Pt(II) complex with alkyl pendants

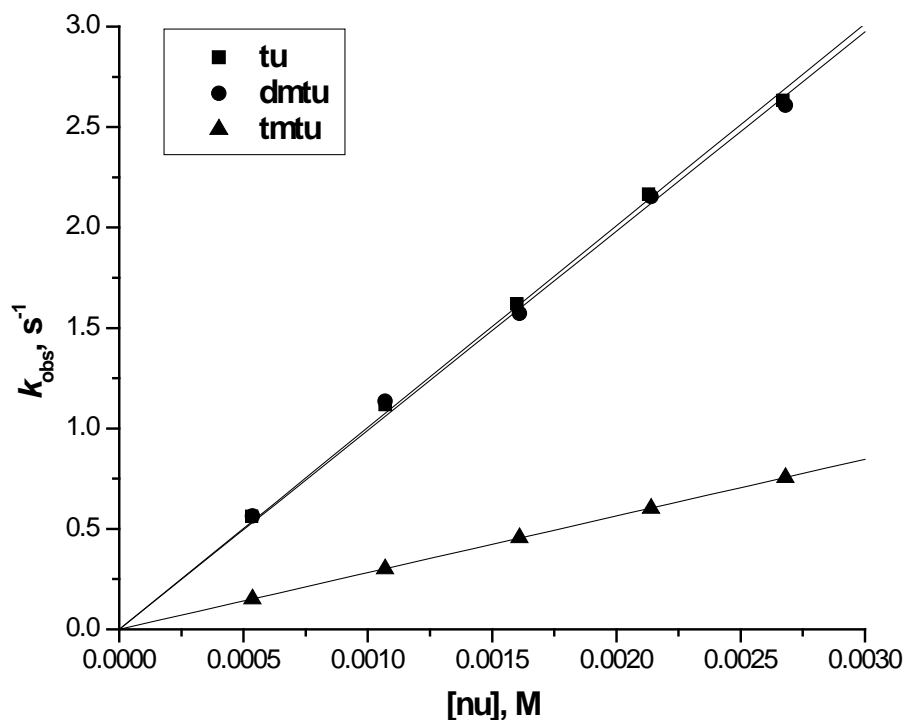


**Figure SI 4.3b** Concentration dependence of  $k_{\text{obs.}(1)}^{\text{st}}$ ,  $\text{s}^{-1}$ , for the substitution of the aqua ligand of **bptba** by thiourea nucleophiles,  $\text{pH} = 2.0$ ,  $T = 298 \text{ K}$ ,  $I = 0.02 \text{ M}$   $\{0.01 \text{ M CF}_3\text{SO}_3\text{H}$ , adjusted with  $\text{Li}(\text{SO}_3\text{CF}_3)\}$ .

**Table SI 4.2b** Average observed rate constants,  $k_{\text{obs.}(2)}^{\text{nd}}$ ,  $\text{s}^{-1}$ , for the dechelation of the pyridyl units of **bptba** by thiourea nucleophiles,  $\text{pH} = 2.0$ ,  $T = 298 \text{ K}$ ,  $I = 0.02 \text{ M}$   $\{0.01 \text{ M CF}_3\text{SO}_3\text{H}$ , adjusted with  $\text{Li}(\text{SO}_3\text{CF}_3)\}$ .

[tu], M	$k_{\text{obs } 2}, \text{s}^{-1}$	[dmtu], M	$k_{\text{obs } 2}, \text{s}^{-1}$	[tmtu], M	$k_{\text{obs } 2}, \text{s}^{-1}$
5.35E-4	0.00612	5.33E-4	0.00578	5.33E-4	0.0018
0.00107	0.0121	0.00107	0.0116	0.00107	0.00406
0.0016	0.01834	0.0016	0.0174	0.0016	0.00595
0.00214	0.02424	0.00213	0.02314	0.00213	0.00801
0.00267	0.0306	0.00267	0.0288	0.00267	0.00998

# Mononuclear Pt(II) complex with alkyl pendants

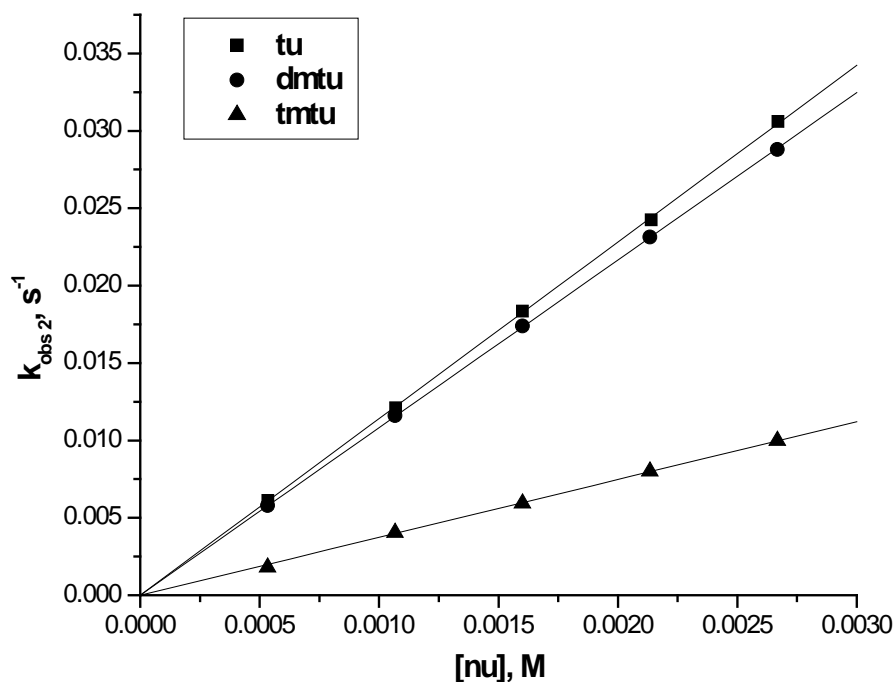


**Figure SI 4.3c** Concentration dependence of  $k_{obs(2^{nd})}$ , s<sup>-1</sup>, for the dechelation of the pyridyl units of **bptba** by thiourea nucleophiles, pH = 2.0, T = 298 K, I = 0.02 M {0.01 M CF<sub>3</sub>SO<sub>3</sub>H, adjusted with Li(SO<sub>3</sub>CF<sub>3</sub>)}.

**Table SI 4.2c** Temperature dependence of  $k_{2(1^{st})}$ , M<sup>-1</sup> s<sup>-1</sup>, for the simultaneous displacement of the aqua ligands of **bptba** by thiourea nucleophiles, pH = 2.0, I = 0.02 M 0.01M CF<sub>3</sub>SO<sub>3</sub>H, adjusted with Li(SO<sub>3</sub>CF<sub>3</sub>).

tu		dmtu		tmtu	
1/T, K <sup>-1</sup>	ln(k/T)	1/T, K <sup>-1</sup>	ln(k/T)	ln(k/T)	ln(k/T)
0.00325	1.541	0.00325	1.613	0.00325	0.2078
0.0033	1.337	0.0033	1.412	0.0033	-0.1072
0.00335	1.067	0.00335	1.1829	0.00335	-0.4222
0.00341	0.7764	0.00341	0.919	0.00341	-0.7307
0.00347	0.5587	0.00347	0.7219	0.00347	-1.035

# Mononuclear Pt(II) complex with alkyl pendants

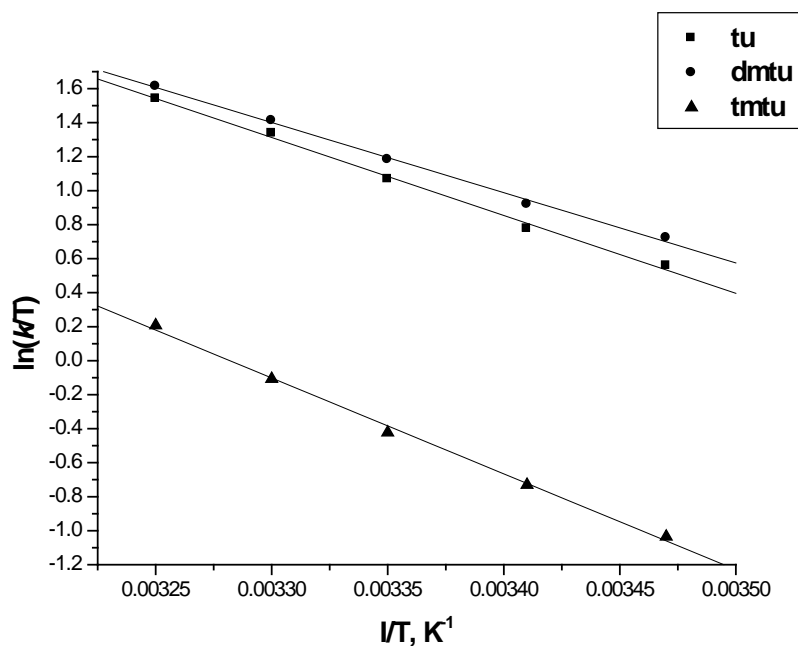


**Figure SI 4.3d** Temperature dependence of  $k_{2(1)^{st}}$ ,  $M^{-1} s^{-1}$ , for the simultaneous displacement of the first aqua ligand of **bptba** by thiourea nucleophiles, pH = 2.0, I = 0.02 M (0.01 M  $CF_3SO_3H$ , adjusted with  $Li(SO_3CF_3)$ ).

**Table SI 4.2d** Temperature dependence of  $k_{2(2)^{nd}}$ ,  $M^{-1} s^{-1}$ , for the dechelation of the pyridyl units of **bptba** by thiourea, pH = 2.0, I = 0.02 M (0.01 M  $CF_3SO_3H$ , adjusted with  $Li(SO_3CF_3)$ ).

tu		dmtu		tmtu	
1/T, K <sup>-1</sup>	ln(k/T)	1/T, K <sup>-1</sup>	ln(k/T)	1/T, K <sup>-1</sup>	ln(k/T)
0.00325	-2.33	0.00325	-2.63	0.00325	-3.79
0.0033	-2.594	0.0033	-2.924	0.0033	-4.072
0.00335	-2.896	0.00335	-3.226	0.00335	-4.382
0.00341	-3.281	0.00341	-3.581	0.00341	-4.74
0.00347	-3.62	0.00347	-3.92	0.00347	-5.09

# Mononuclear Pt(II) complex with alkyl pendants

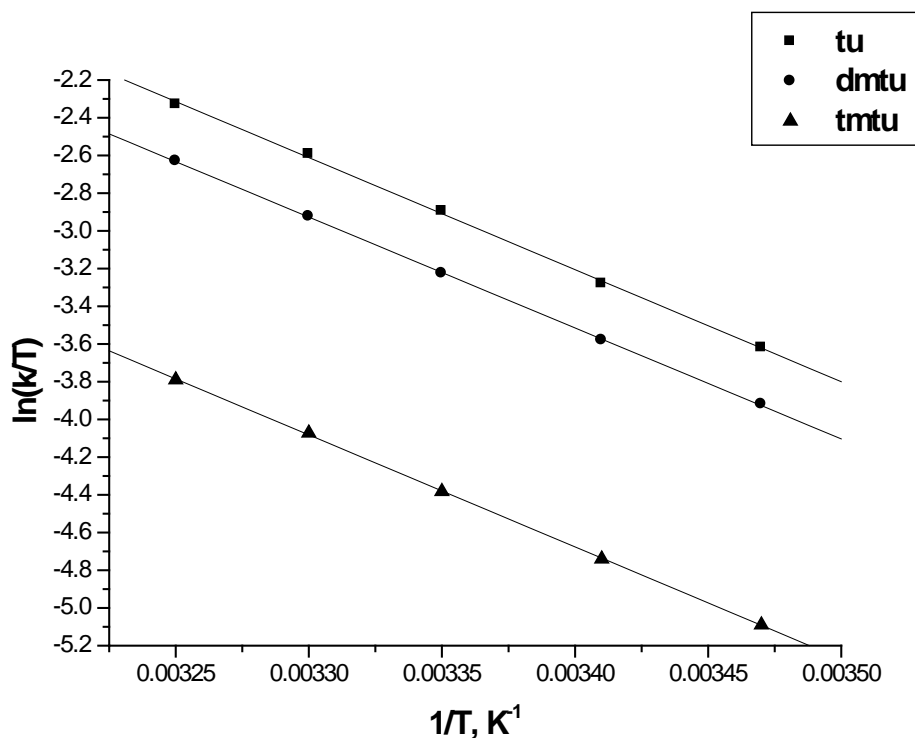


**Figure SI 4.3e** Temperature dependence of  $k_{2(2^{\text{nd}})}$ ,  $\text{M}^{-1} \text{s}^{-1}$ , for the dechelation of the pyridyl units of **bptba** by thiourea,  $\text{pH} = 2.0$ ,  $I = 0.02 \text{ M}$  ( $0.01 \text{ M CF}_3\text{SO}_3\text{H}$ , adjusted with  $\text{Li}(\text{SO}_3\text{CF}_3)$ ).

**Table SI 4.3a** Average observed rate constants,  $k_{\text{obs}(1^{\text{st}})}$ ,  $\text{s}^{-1}$ , for the simultaneous displacement of the aqua ligands of **bpea** by thiourea nucleophiles,  $\text{pH} = 2.0$ ,  $T = 298 \text{ K}$ ,  $I = 0.02 \text{ M}$  ( $0.01 \text{ M CF}_3\text{SO}_3\text{H}$ , adjusted with  $\text{Li}(\text{SO}_3\text{CF}_3)$ ).

[tu], M	$k_{\text{obs } 1}, \text{s}^{-1}$	[dmtu], M	$k_{\text{obs } 1}, \text{s}^{-1}$	[tmtu], M	$k_{\text{obs } 1}, \text{s}^{-1}$
5.35E-4	0.2719	5.346E-4	0.3313	5.34E-4	0.1169
0.00107	0.5449	0.00107	0.6673	0.00107	0.2323
0.0016	0.8151	0.0016	0.9914	0.0016	0.3477
0.00214	1.048	0.00214	1.318	0.00213	0.4615
0.00267	1.347	0.00267	1.638	0.00267	0.5792

**Table SI 4.3b** Average observed rate constants,  $k_{\text{obs}(2^{\text{nd}})}$ ,  $\text{s}^{-1}$ , for the dechelation of the pyridyl units of **bpea** by thiourea nucleophiles,  $\text{pH} = 2.0$ ,  $T = 298 \text{ K}$ ,  $I = 0.02 \text{ M}$  ( $0.01 \text{ M CF}_3\text{SO}_3\text{H}$ , adjusted with  $\text{Li}(\text{SO}_3\text{CF}_3)$ ).

[tu], M	$k_{\text{obs } 2}, \text{s}^{-1}$	[dmtu], M	$k_{\text{obs } 2}, \text{s}^{-1}$	[tmtu], M	$k_{\text{obs } 2}, \text{s}^{-1}$
5.33E-4	0.00254	5.334E-4	0.00303	5.33E-4	0.00144
0.00107	0.00514	0.00107	0.00638	0.00107	0.00273
0.0016	0.00758	0.0016	0.0091	0.0016	0.00399
0.00213	0.01054	0.00213	0.01242	0.00213	0.00551
0.00266	0.01357	0.00267	0.0153	0.00267	0.00687

# Mononuclear Pt(II) complex with alkyl pendants

**Table SI 4.3c** Temperature dependence of  $k_{2(1)^{st}}$ ,  $M^{-1} s^{-1}$ , for the simultaneous displacement of the aqua ligands of **bpea** by thiourea nucleophiles, pH = 2.0, I = 0.02 M (0.01 M  $CF_3SO_3H$ , adjusted with  $Li(SO_3CF_3)$ ).

tu		dmtu		tmtu	
1/T, $K^{-1}$	ln(k/T)	1/T, $K^{-1}$	ln(k/T)	1/T, $K^{-1}$	ln(k/T)
0.00325	0.9559	0.00325	1.155	0.00325	0.2492
0.0033	0.755	0.0033	0.9367	0.0033	-0.0284
0.00335	0.5278	0.00335	0.7203	0.00335	-0.3174
0.00341	0.2808	0.00341	0.4787	0.00341	-0.6556
0.00347	0.036	0.00347	0.2091	0.00347	-0.9644

**Table SI 4.3d** Temperature dependence of  $k_{2(2)^{nd}}$ ,  $M^{-1} s^{-1}$ , for the dechelation of the pyridyl units of **bpea** by thiourea, pH = 2.0, I = 0.02 M (0.01 M  $CF_3SO_3H$ , adjusted with  $Li(SO_3CF_3)$ ).

tu		dmtu		tmtu	
1/T, $K^{-1}$	ln(k/T)	1/T, $K^{-1}$	ln(k/T)	1/T, $K^{-1}$	ln(k/T)
0.00325	-3.447	0.00325	-3.351	0.00325	-4.163
0.0033	-3.775	0.0033	-3.648	0.0033	-4.46
0.00335	-4.054	0.00335	-3.913	0.00335	-4.763
0.00341	-4.45	0.00341	-4.244	0.00341	-5.14
0.00347	-4.761	0.00347	-4.563	0.00347	-5.489

**Table SI 4.4a** Average observed rate constants,  $k_{obs(1)^{st}}$ ,  $s^{-1}$ , for the simultaneous displacement of the aqua ligands of **bppa** by thiourea nucleophiles, pH = 2.0, T = 298 K, I = 0.02 M {0.01 M  $CF_3SO_3H$ , adjusted with  $Li(SO_3CF_3)$ }.

[tu], M	$k_{obs 1}, s^{-1}$	[dmtu], M	$k_{obs 1}, s^{-1}$	[tmtu], M	$k_{obs 1}, s^{-1}$
5.333E-4	0.2732	5.3369E-4	0.3549	5.3519E-4	0.1052
0.00107	0.5463	0.00107	0.7126	0.00107	0.209
0.0016	0.8153	0.0016	1.08	0.00161	0.3105
0.00213	1.134	0.00213	1.426	0.00214	0.4222
0.00266	1.418	0.00267	1.799	0.00268	0.526

**Table SI 4.4b** Average observed rate constants,  $k_{obs(2)^{nd}}$ ,  $s^{-1}$ , for the dechelation of the pyridyl units of **bppa** by thiourea nucleophiles, pH = 2.0, T = 298 K, I = 0.02 M {0.01 M  $CF_3SO_3H$ , adjusted with  $Li(SO_3CF_3)$ }.

[tu], M	$k_{obs 2}, s^{-1}$	[dmtu], M	$k_{obs 2}, s^{-1}$	[tmtu], M	$k_{obs 2}, s^{-1}$
5.333E-4	0.00254	5.333E-4	0.00306	5.3519E-4	0.00137
0.00107	0.00514	0.00107	0.00638	0.00107	0.00258
0.0016	0.00758	0.0016	0.00922	0.00161	0.0039
0.00213	0.01054	0.00213	0.0124	0.00214	0.00532
0.00266	0.01337	0.00266	0.0155	0.00268	0.00659

## Mononuclear Pt(II) complex with alkyl pendants

**Table SI 4.4c** Temperature dependence of  $k_{2(1^{st})}$ ,  $M^{-1} s^{-1}$ , for the simultaneous displacement of the aqua ligands of **bppa** by thiourea nucleophiles, pH = 2.0, I = 0.02 M (0.01 M  $CF_3SO_3H$ , adjusted with  $Li(SO_3CF_3)$ ).

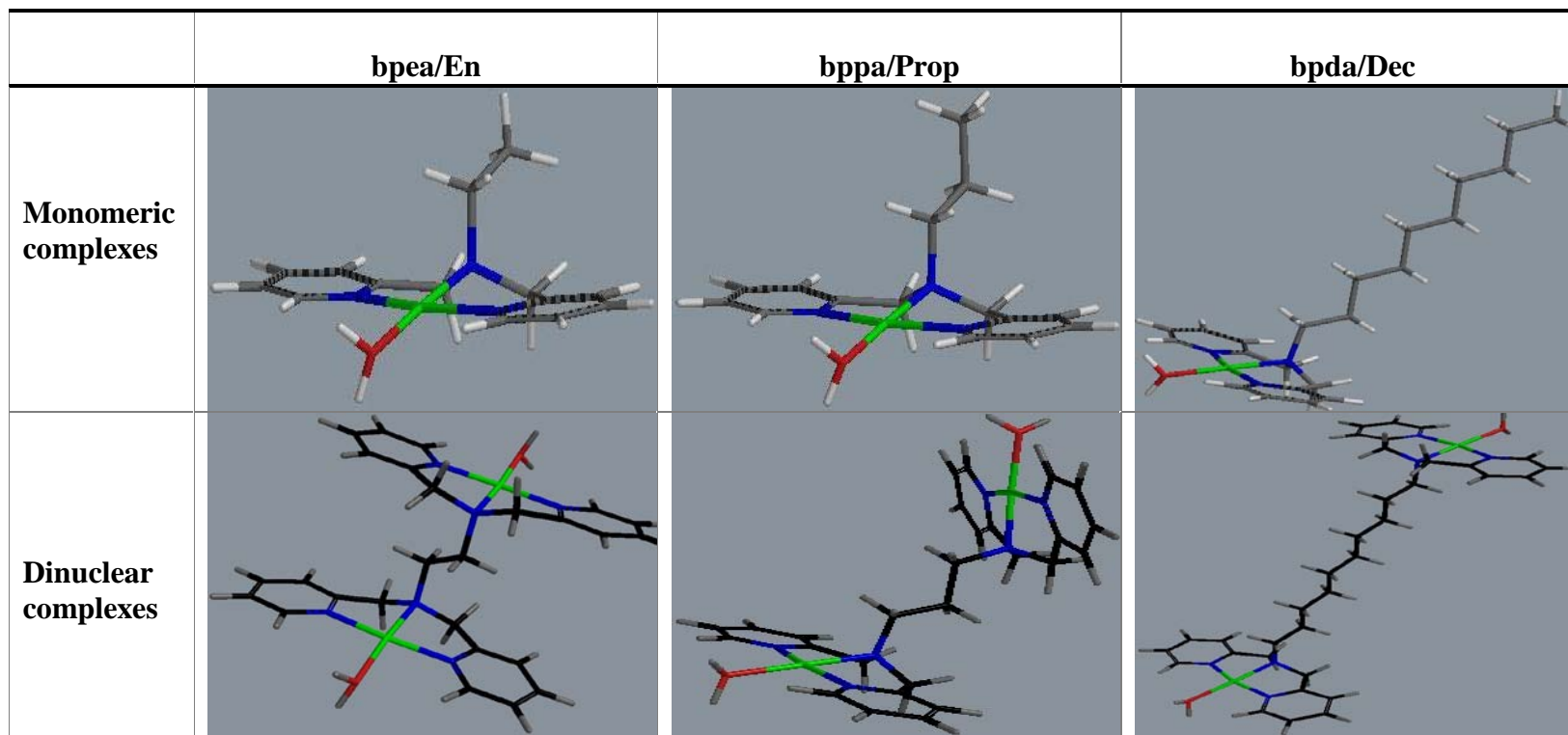
tu		dmtu		tmtu	
1/T, K <sup>-1</sup>	ln(k/T)	1/T, K <sup>-1</sup>	ln(k/T)	1/T, K <sup>-1</sup>	ln(k/T)
0.00325	0.9706	0.00325	1.155	0.00325	0.2078
0.0033	0.771	0.0033	0.9367	0.0033	-0.1072
0.00335	0.5761	0.00335	0.7203	0.00335	-0.4222
0.00341	0.3109	0.00341	0.4787	0.00341	-0.7307
0.00347	0.0109	0.00347	0.2091	0.00347	-1.035

**Table SI 4.4d** Temperature dependence of  $k_{2(2^{nd})}$ ,  $M^{-1} s^{-1}$ , for the dechelation of the pyridyl units of **bppa** by thiourea, pH = 2.0, I = 0.02 M (0.01 M  $CF_3SO_3H$ , adjusted with  $Li(SO_3CF_3)$ ).

tu		dmtu		tmtu	
1/T, K <sup>-1</sup>	ln(k/T)	1/T, K <sup>-1</sup>	ln(k/T)	1/T, K <sup>-1</sup>	ln(k/T)
0.00325	-3.531	0.00325	-3.321	0.00325	-4.062
0.0033	-3.835	0.0033	-3.633	0.0033	-4.39
0.00335	-4.143	0.00335	-3.948	0.00335	-4.73
0.00341	-4.53	0.00341	-4.318	0.00341	-5.109
0.00347	-4.836	0.00347	-4.658	0.00347	-5.497

# Mononuclear Pt(II) complex with alkyl pendants

Table SI 4.5a A comparative illustration of the DFT<sup>42</sup> minimum energy structures of amphiphiles and their analogous dinuclears.



## Mononuclear Pt(II) complex with alkyl pendants

---

Table SI 4.5b Electrostatic potential surface (EPS) mappings of the amphiphilic Pt(II) complexes.

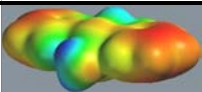
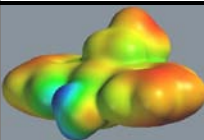
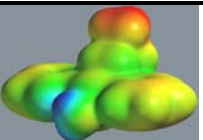
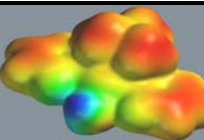
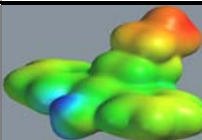
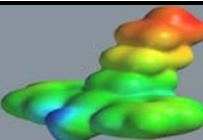
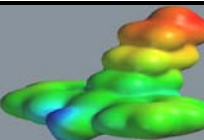
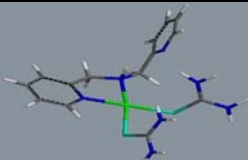
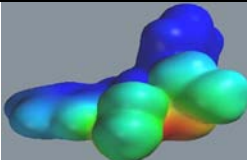
Complex	bpma	bpea	bppa	bptba	bpba	bpha	bpda
EPS							

Table SI 4.6 Geometry optimized structure of the **bpma-tu<sub>2</sub>** showing the dangling 2-(pyridylmethyl) arm.

Complex	Structure	EPS
bpma-2tu		

# Mononuclear Pt(II) complex with alkyl pendants

## 4.7 Commentary notes (CN) to section 4.2.1

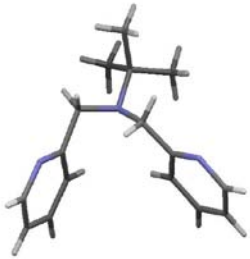
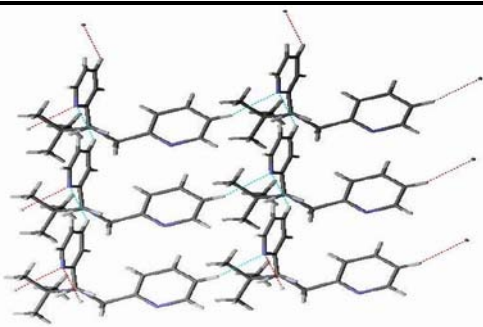
### 4.7.1 X-rays diffraction analysis of *N,N*-bis(2-pyridylmethyl)*tert*-butylamine (L4).

As alluded to in the main paper, colourless crystals (X-ray quality in the case of **L2** and **L4**) were yielded from a suspension of their oils in ethanol. This was achieved through slow evaporation of the ethanol solvent over several days. The crystal structure of **L4** was solved by X-rays diffraction while **L2** melted into an amorphous white solid. Table CN 4.1 shows the size of the crystal used for diffraction, an Orterp representation of the molecular structure of **L4** and how the molecules of the ligand pack in the solid state.

The molecular structure of ligand **L4** was determined on an Oxford Diffraction Xcalibur2 CCD diffractometer. Data collection was performed by the *CrystAlis CCD* program while cell refinement and data reduction were done using the *CrystAlis RED* suite of programs.<sup>1</sup> Crystal structures were solved and refined by the SHELXL97<sup>2</sup> software while the *Orterp*<sup>3</sup> and *WinGX*<sup>4</sup> were used for all molecular graphics. Full details on the crystal structures and their intriguing supramolecular chemistry are reported in the published paper in the Appendix A:

Mambanda, D. Jaganyi and K. Stewart, '*N,N*-Bis(2-pyridylmethyl)*tert*-butylamine.' *Acta Cryst.*, 2009, **E65**, o402.

**Table CN 4.1** Crystal plate and the molecular structure of *N,N*-bis(2-pyridylmethyl)*tert*-butylamine (**L4**).

Crystal	Molecular structure of L4	Crystal packing
		

# *Mononuclear Pt(II) complex with alkyl pendants*

**Table CN 4.2** Crystal data and structural refinement parameters for **L4** at 293 K.

Identification code	bptba_rt
Empirical formula	C <sub>8</sub> H <sub>10.50</sub> N <sub>1.50</sub>
Formula weight	127.68
Temperature	293(2) K
Wavelength	0.71073 Å
Crystal system, space group	Monoclinic , C c
Unit cell dimensions	a = 6.1808(3) Å; $\alpha$ = 90 deg. b = 17.9502(8) Å; $\beta$ = 100.239(4) deg. c = 13.7079(6) Å; $\gamma$ = 90 deg.
Volume	1496.62(12) Å <sup>3</sup>
Z, Calculated density	8, 1.133 Mg m <sup>-3</sup>
Absorption coefficient	0.068 mm <sup>-1</sup>
F(000)	552
Crystal size	0.4x0.5x0.5 mm
Theta range for data collection	4.07 to 31.89 deg.
Limiting indices	-8<h<7, -26<k<26, -18<l<20
Reflections collected / unique	7475 / 3310 [R <sub>(int)</sub> = 0.0116]
Completeness to $\theta = 25.00$	99.5 %
Refinement method	Full-matrix least-squares on F <sup>2</sup>
Data / restraints / parameters	3310 / 2 / 175
Goodness-of-fit on F <sup>2</sup>	1.030
Final R indices [I>2 $\sigma$ (I)]	R1 = 0.0416, wR <sup>2</sup> = 0.1113
R indices (all data)	R1 = 0.0506, wR <sup>2</sup> = 0.1160
Absolute structure parameter	1.0(19)

## **4.7.2** *References to the commentary notes.*

- 1 Oxford Diffraction, *CrysAlis CCD* and *CrysAlis RED*, Versions 1.171.29.9 (Release 23-03-2006 CrysAlis 171. Net), 2006, Oxford Diffraction Ltd., Abingdon, Oxfordshire, England.
- 2 G. M. Sheldrick, *SHELXS97* and *SHELXL97*, 1997, University of Göttingen, Germany.
- 3 L. J. Farrugia, *J. Appl. Cryst.*, 1997, **30**, 565.
- 4 L. J. Farrugia, *J. Appl. Cryst.*, 1999, **32**, 837.

## Chapter Five

*Extra supplementary data linked to this work is attached to the Appendix.*

### **Kinetic study of chelated dinuclear Pt(II) complexes with diaminobenzene and diaminocyclohexane bridges.**

#### **5.0 Abstract**

Substitution reactions of [Pt(H<sub>2</sub>O)*N,N*-bis(2-pyridylmethyl)phenylamine)](CF<sub>3</sub>SO<sub>3</sub>)<sub>2</sub>, **bpPha**; [Pt(H<sub>2</sub>O)]<sub>2</sub>(*N,N,N',N'*-tetrakis(2-pyridylmethyl)-1,3-phenyldiamine)](CF<sub>3</sub>SO<sub>3</sub>)<sub>4</sub>, **mPh**; [Pt(H<sub>2</sub>O)]<sub>2</sub>(*N,N,N',N'*-tetrakis(2-pyridylmethyl)-1,4-phenyldiamine)](CF<sub>3</sub>SO<sub>3</sub>)<sub>4</sub>, **pPh**; [Pt(H<sub>2</sub>O)]<sub>2</sub>(*N,N,N',N'*-tetrakis(2-pyridylmethyl)-4,4'-methylenediphenylamine)](CF<sub>3</sub>SO<sub>3</sub>)<sub>4</sub>, **dPhm**; [Pt(H<sub>2</sub>O)(*N,N*-bis(2-pyridylmethyl)cyclohexylamine)](CF<sub>3</sub>SO<sub>3</sub>)<sub>2</sub>, **bpcHna**; [Pt(H<sub>2</sub>O)]<sub>2</sub>(*N,N,N',N'*-tetrakis(2-pyridylmethyl)-*trans*-1,4-cyclohexyldiamine)](CF<sub>3</sub>SO<sub>3</sub>)<sub>4</sub>, **cHn** and [Pt(H<sub>2</sub>O)]<sub>2</sub>(*N,N,N',N'*-tetrakis(2-pyridylmethyl)-4,4'-methylenedicyclohexylamine)](CF<sub>3</sub>SO<sub>3</sub>)<sub>4</sub>, **dcHnm** with thiourea nucleophiles was studied in acidified (pH 2) 0.01 M LiCF<sub>3</sub>SO<sub>3</sub> aqueous medium under pseudo first-order conditions using stopped-flow and UV-visible spectrophotometric techniques. The rate of substitution of the aqua ligands by tu and dmtu nucleophiles decreases in the order: **bpPha** > **dPhm** ≈ **pPh** ≈ **mPh** and **bpcHna** > **dcHnm** > **cHn** for complexes containing the diaminobenzene and diaminocyclohexane fragments, respectively. The order of reactivity in both sets of complexes is controlled by the level of steric influences due to the linker felt at the bis(2-pyridylmethyl)amine chelated metal centres. The steric influences are relatively lower in the monomeric analogues. For the dinuclear analogues, the steric imposition at each chelate headgroup depends on the molecular structures of the complexes as controlled by the symmetry elements of the diamino linker as well as its length, measured by the average distance separating the Pt metal centres. High negative activation entropies and second-order kinetics for the ligand substitution reactions support an associative mode of activation.

# *Pt(II) complexes with rigid diamine bridges*

---

## **5.1 Introduction**

Multinuclear Pt(II) complexes represent a novel class of compounds that have shown great potential in cancer chemotherapy.<sup>1</sup> The most well known complexes are joined by structural linkers affording terminal platinum centres possessing one or two labile ligands. Their binding mechanisms to DNA are distinctively different<sup>2</sup> from those of classical drugs such as *cis*-diaminedichloroplatinum(II) (cisplatin) and its analogues leading to unique biological activities. Long range interstrand as well as intrastrand crosslinks on DNA are formed.<sup>3a</sup> These crosslinked adducts are less prone to repair by the various cellular proteins leading to enhanced cytotoxicity.<sup>3b-d</sup>

The nature of the structural linker joining the terminal platinum centres is an important feature controlling the ultimate types of adducts formed between the multinuclear complexes and the targeted nucleobasic sites on DNA as well as other competing bionucleophilic molecules.<sup>4</sup> For example, in BBR3464<sup>1,3b</sup> and other related trinuclear complexes, the structural linking moiety includes a central tetraamine coordinated Pt(II) atom, separated from the terminal platinum atoms by alkyldiamine linkers. The terminal Pt atoms are involved in covalent binding with the nucleobases of DNA. The role of the central coordination sphere is to provide additional positive charges and hydrogen bonding donor sites which enable fast cellular uptake due to the favourable electrostatic and dipolar interactions with polyanionic DNA.<sup>5</sup>

For dinuclear complexes, the electronic properties as well as the structural properties of the linker are thought to convey distinctive coordinative chemistries on the enjoined Pt centres. Dinuclear complexes bridged by aliphatic diamines of variable chain lengths<sup>6a-b</sup>, azines<sup>7</sup>, azoles<sup>8</sup>, 4,4'-dipyrazolylmethane<sup>9a</sup> and 4,4'-methylenedianiline<sup>9b</sup> structural groups have been reported. In these complexes, the nature and in particular the length of structural motifs linking the Pt(II) coordination spheres are thought to play a pivotal structural-directing role<sup>6a,9</sup> by introducing flexibility/rigidity of variable magnitude to the complexes. Such structural effects have potential to control the symmetry elements of the complexes as well as the distance separating their terminal coordinating centres, respectively. When the structural linker is an aliphatic diamine, relatively flexible complexes are afforded while an aromatic diamine or a diaminocycloalkane fragment within the bridge is expected to introduce some degree of rigidity in the multinuclear complexes<sup>6b</sup>. Recently, single methylene spacers incorporated within the 4,4'-dipyrazolylmethane<sup>9a</sup>, the 4,4'-methylenedianiline<sup>9b</sup> and the mesitylene<sup>10</sup>

## *Pt(II) complexes with rigid diamine bridges*

---

bridging linkers have been utilized to access multinuclear Pt(II) complexes of moderate flexibility.

A perusal of data in literature on cytotoxicities of complexes bridged by flexible alkyldiamines shows that their biological activities depend on the average distance separating the Pt(II) ions<sup>11,6</sup>, with the chain length equivalent to a 1,6-diaminohexane<sup>6a,b</sup> seeming to be the optimum separation distance for maximum activity. It is predictable that rational design of utility multinuclear drugs is going to be tailored around structural linkers of equivalent lengths.<sup>12</sup> Moreover, significant differences in *in vitro* cytotoxic activities of the dinuclear complexes can be noticed when a comparison is made between complexes of equivalent average Pt, Pt separation distances differing mainly in the chemical structures of their bridges.<sup>11b,10b,6b</sup>

A remarkable way of tuning the flexibility of multinuclear complexes is demonstrated in a trinuclear Pt(II) complex derived from the *N,N,N,N',N',N'',N'',N''*-hexakis(2-pyridylmethyl)-1,3,5-tris(aminomethyl)benzene ligand.<sup>10</sup> The central mesitylene bridge confers moderate rigidity to the complex, in which the three pronged *N,N*-bis(2-pyridylmethyl)amine Pt(II) chelates are spaced from the rigid benzene core by methylene spacers. In the nanomolar concentration range, this complex displays remarkably higher cytotoxicity against P-388 and A-549 tumour cell lines than cisplatin.<sup>10b</sup> In addition, its pseudo  $C_3$  rotational symmetry of the chelated Pt(II) centres about the central mesityl core affords a complex capable of forming variable intrastrand and interstrand DNA crosslinking adducts leading to different biological activities. No degradation of the mesitylene bridge was induced by glutathione (GSH), even after allowing the reaction mixture to age for up to 24 hours.<sup>10b</sup>

Despite all that is known about the effects of the structure of the bridging motifs on cytotoxicity, there is limited data to formulate structure-reactivity relationships between the nature of the bridging moieties of multinuclear platinum complexes and the lability of the leaving groups of the Pt centres. The kinetics studies of Hoffmann *et al.*<sup>13a</sup> and Jaganyi *et al.*<sup>13b</sup> have established that reactivity of dinuclears with flexible  $\alpha,\omega$ -alkyldiamine linkers is dependent on the average distance separating their Pt centres. However, the actual contribution of the bridge to the molecular mechanism of the substitution of the leaving groups remains elusive even for homologous dinuclears in which a simple structural attribute of the diamine bridge is varied while maintaining the same structural backbone of the linker. For example, the direct impact on reactivity of the complexes due to structural attributes of the bridge such as its steric and its electronic properties is not fully understood. Of particular need is a sound

## *Pt(II) complexes with rigid diamine bridges*

---

understanding of the restrictive roles of the bridging linker on the reactivity of the enjoined Pt centres. It has come out of the recent kinetic studies<sup>13a, 14a</sup> that the average distance separating the Pt centres is not the only critical factor controlling reactivity of the Pt metal centres bridged by the flexible diamines, but the molecular symmetry adopted by the complexes as well. A  $C_{2h}$  symmetry of the even-bridged complexes resulted in a general decrease in the rates of substitution of the leaving groups when the average distance separating the Pt centers was decreased, suggesting the presence of mutual and domineering steric imposition influences on the Pt square-planes due to the overlapping geometry of the Pt chelate headgroups. This was profound especially in complexes with shorter diamine bridges. An unusual high reactivity recorded for **Prop**,<sup>14a</sup> an analogue with a  $C_{2v}$  symmetry conferred by the odd number of carbon atoms in its bridge was explained on the basis of an 'entrapment effect' to the incoming nucleophiles due to the bowl molecular shape of this complex.<sup>14a</sup> The new proposal unveils a new thinking that the reactivity of the dinuclears can be controlled also through an elegant choice of the structural properties of the diamine bridge such as its rigidity, the extent of  $\pi$ -conjugation and  $\sigma$ -inductive effects within the backbone of the diamine bridge, steric imposing features and even its dipolar hydrogen interactions.

The reactivity of Pt drugs is known however to affect the biological activities in as many different ways. It can determine the extent of interactions with DNA, with a high rate of formation of DNA crosslinks leading to superior cytotoxicity.<sup>6,15</sup> Reactivity also controls the extent of side reactions with non-target cellular material. Rapid reactions with other cellular material have been linked to toxicity and intrinsic resistance.<sup>15b</sup> Moreover, it is already known for mononuclear Pt complexes, that the electronic as well as the steric properties of the immediate carrier ligand framework around the Pt(II) centres<sup>1,15</sup> do indeed affect reactivity. It is possible that any steric influences conveyed through the native symmetry elements of the linker as well as the electronic properties can be mirrored in the overall reactivity of the multinuclear platinum complexes.

In this study, a total of five dinuclear complexes as well as their two mononuclear analogues were synthesized and their ligand substitution reactions studied with thiourea nucleophiles in acidified (pH 2.0) lithium triflate  $\{\text{Li}(\text{CF}_3\text{SO}_3)\}$  aqueous medium. Three of the dinuclear complexes are linked by bridges bearing aromatic diamine moieties while the other two are linked by bridges containing the diaminocyclohexane moieties. This work seeks to extend our understanding on the role of the diamine bridge on the reactivity of the dinuclear

# *Pt(II) complexes with rigid diamine bridges*

---

complexes when variable structural rigidity as well planarity is introduced in the structural backbone of diamine bridges.

## **5.2 Experimental**

### **5.2.1 Materials and reagents.**

All synthetic reactions were performed under an inert atmosphere of nitrogen. All reagents were used as supplied. The diamines were procured from Fluka. 2-(pyridylmethyl)chloride.hydrochloride, sodium perchlorate monohydrate ( $\text{NaClO}_4 \cdot \text{H}_2\text{O}$ ), silver perchlorate ( $\text{AgClO}_4$ , 99.9%) and the thiourea nucleophiles were purchased from Aldrich. Potassium tetrachloroplatinate ( $\text{K}_2\text{PtCl}_4$ , 99.99%) was purchased from Strem Chemicals. Ultrapure water (Modulab System) was used for all aqueous reactions.

### **5.2.2 Preparation of ligands.**

The ligands synthesized for this investigation were namely, *N,N'*-bis(2-pyridylmethyl)phenylamine (**L1**); *N,N,N',N'*-tetrakis(2-pyridylmethyl)-1,3-phenyldiamine (**L2**); *N,N,N',N'*-tetrakis(2-pyridylmethyl)-1,4-phenyldiamine (**L3**); *N,N,N',N'*-tetrakis(2-pyridylmethyl)-4,4'-methylenediphenylamine (**L4**); *N,N*-bis(2-pyridylmethyl)cyclohexylamine (**L5**); *N,N,N',N'*-tetrakis(2-pyridylmethyl)-*trans*-1,4-cyclohexyldiamine (**L6**); *N,N,N',N'*-tetrakis(2-pyridylmethyl)-4,4'-methylenediaminocyclohexane (**L7**).

A procedure described by Karlin and coworkers<sup>16</sup> for the tris[(2-pyridyl)methyl]amine derivative was followed for the preparation of **L1**. To 6 mL of 20 % NaOH solution was added in a dropwise manner a chilled aqueous solution of 2-picolychloride hydrochloride (24 mmol in 1.5 mL of water) resulting in the release of the amine as a pink emulsion. While stirring, doubly distilled aniline (1.1 mL, 12 mmol) in 10 mL of dichloromethane was added in drops to the pink emulsion at room temperature. Over a period of 48 h, an additional 40 mL of 20 % NaOH was added in a dropwise manner. During the addition of NaOH, the pH of the reaction mixture was kept below 9.0 by adding only sufficient NaOH solution to maintain the colour of the reaction mixture pale orange. Further additions were resumed when the colour of the mixture appeared light green. At the end of the additions, the aqueous layers were washed five times with 20 ml portions of dichloromethane, the extracts concentrated, dried and purified as previously described Buchen *et al.*<sup>17a</sup>

## *Pt(II) complexes with rigid diamine bridges*

---

Ligand **L2** was prepared following the procedures of Schindler *et al.*<sup>17b</sup> while the procedure of Buchen *et al.*<sup>17a</sup> was used to prepare hexadentate ligands **L3** and **L4** with some minor modifications in their final purification steps. For the preparations of all the ligands with an aromatic core, it was necessary to elute the concentrated organic layers through a chromatographic column packed with 2 g of activated charcoal, 5 g neutral alumina and sodium sulphate using chloroform as a solvent to collect light yellow coloured solutions. On concentrating these solutions, an oil is yielded for **L1** while white to off-white fine powders were obtained from slow evaporation of their ethanol (**L2**) and ether (**L4**) solutions while **L3** precipitated out as beige flakes. Re-crystallization of the crude powders from their hot solutions {ethanol/acetone (19:1) mixture for **L2** and **L3**; and ether for **L4**} afforded their pure compounds.

The procedure of Sato *et al.*<sup>18</sup> was adapted for the synthesis of ligands **L5** to **L7** based on the report of Toftlund<sup>19</sup> described for the 1,2-diaminocyclohexane derivative.

All the synthesized ligands were characterized by micro analysis (except for **L1** which was yielded as an oil); NMR and TOF MS ES<sup>+</sup>. Exemplary mass spectra for **L6** and **L7** are shown in Figures SI 1a and 1b (supporting information), respectively. The crystal structure of **L6** was solved by X-Ray diffraction analysis and is discussed in the Commentary notes (CN), section 5.8. The crystal structure of ligand, **L6**, its packing pattern in the solid and other important crystal data are presented in Tables CN 5.1 and 5.2 (commentary notes).

**(L1)** Yield: 2507 mg (71 %), bright orange oil. <sup>1</sup>H NMR (400 MHz, CDCl<sub>3</sub>) δ / ppm: 8.58 (d, 2H); 7.7 (t, 2H); 7.65 (dt, 4H); 7.60 (t, 1H); 7.20 (m, 2H), 6.7 (m, 2H); 4.50 (s, 4H). <sup>13</sup>C NMR (100 MHz, CDCl<sub>3</sub>) δ / ppm 57.0; 113; 117; 122; 123; 129; 138; 147; 150; 165. IR (*KBr*, 4000-400 cm<sup>-1</sup>)  $\bar{\nu}$ : 2958-2854 (alkyl C-H stretch); 1589 (C=N, pyridyl). MS-ES<sup>+</sup>, m/e: 276.1501, (M + 1)<sup>+</sup>.

**(L2)** Yield: 1006 mg (35 %), off white powder. <sup>1</sup>H NMR (400 MHz, CDCl<sub>3</sub>) δ / ppm: 8.62 (d, 4H); 8.29 (t, 4H); 7.85 (d, 4H); 7.75 (t, 4H); 6.0 (m, 4H), 5.60 (s, 8H). <sup>13</sup>C NMR (100 MHz, CDCl<sub>3</sub>) δ / ppm: 59.0; 112, 113; 122.0; 123.0; 128.0; 136.5; 141.0; 150.0; 162.0. IR (*KBr*, 4000-400 cm<sup>-1</sup>)  $\bar{\nu}$ : 2958-2854 (alkyl C-H stretch); 1589 (C=N, pyridyl). *Anal. Calc. for* C<sub>30</sub>H<sub>28</sub>N<sub>6</sub>: C, 76.24; H, 5.97; N, 17.78; *Found*: C, 76.28; H, 5.97; N, 17.53. MS-ES<sup>+</sup> m/e: 473.2468 (M + 1)<sup>+</sup>

**(L3)** Yield: 1365 mg (48 %), beige flakes. <sup>1</sup>H NMR (400 MHz, CDCl<sub>3</sub>) δ / ppm: 8.65 (d, 4H); 8.29 (t, 4H); 7.85 (d, 4H); 7.75 (t, 4H), 6.0 (m, 4H) 5.60 (s, 8H). <sup>13</sup>C NMR (100 MHz, CDCl<sub>3</sub>) δ / ppm: 59.0;

## *Pt(II) complexes with rigid diamine bridges*

---

113; 122.0; 123.0; 136.5; 141.0; 150.0; 162.0. IR (*KBr*, 4000-400  $\text{cm}^{-1}$ )  $\bar{\nu}$ : 2958-2854 (alkyl C-H stretch); 1589 (C=N, pyridyl). *Anal. Calc.* for  $\text{C}_{30}\text{H}_{28}\text{N}_6$ : C, 76.24; H, 5.97; N, 17.78; *Found*: C, 76.26; H, 5.85; N, 17.86. MS-ES<sup>+</sup> m/e: 473.2454 (M + 1)<sup>+</sup>

**(L4)** Yield: 1123 mg (33 %), off-white powder. <sup>1</sup>H NMR (400 MHz,  $\text{CDCl}_3$ )  $\delta$  / ppm: 8.60 (d, 4H); 7.60 (t, 4H); 7.35 (d, 4H); 7.20 (t, 4H); 7.0 (m, 4H); 6.6 (m, 4H); 4.8 (s, 8H); 4.45 (s, 2H). <sup>13</sup>C NMR (100 MHz,  $\text{CDCl}_3$ )  $\delta$  / ppm: 41; 57; 112; 113; 122.0; 123.0; 128.0; 136.0; 150.0; 158.0. IR (*KBr*, 4000-400  $\text{cm}^{-1}$ )  $\bar{\nu}$ : 2958-2854 (alkyl C-H stretch); 1589 (C=N, pyridyl). *Anal. Calc.* for  $\text{C}_{37}\text{H}_{34}\text{N}_6$ : C, 78.97; H, 6.09; N, 14.95; *Found*: C, 78.55; H, 6.13; N, 14.62. MS-ES<sup>+</sup> m/e: 563.2923 (M + 1)<sup>+</sup>

**(L5)** Yield: 1342 mg (40 %), white powder. <sup>1</sup>H NMR (400 MHz,  $\text{CDCl}_3$ )  $\delta$  / ppm: 8.58 (d, 2H); 8.50-7.60 (m, 4H); 7.05 (t, 2H); 3.39 (s, 4H); 2.55 (m, 1H); 1.90 (d, 2H); 1.8 (m, 2H); 1.60 (d, 2H); 1.35 (m, 2H); 1.19 (m, 2H). <sup>13</sup>C NMR (100 MHz,  $\text{CDCl}_3$ )  $\delta$  / ppm: 27.0; 29; 57.0; 60.5; 122.0; 123.0; 136.0; 148.0; 161. IR (*KBr*, 4000-400  $\text{cm}^{-1}$ )  $\bar{\nu}$ : 2958-2854 (alkyl C-H stretch); 1589 C=N (pyridyl). MS-ES<sup>+</sup>, m/e: 282.2069, (M + 1)<sup>+</sup>. *Anal. Calc.* for  $\text{C}_{18}\text{H}_{23}\text{N}_3$ : C, 76.81; H, 8.24; N, 14.93; *Found*: C, 76.8; H, 8.18; N, 14.89.

**(L6)** Yield: 1276 mg (44 %), white powder. <sup>1</sup>H NMR (400 MHz,  $\text{CDCl}_3$ )  $\delta$  / ppm: 8.60 (t, 4H); 7.50-7.60 (m, 8H); 7.10 (t, 4H); 3.95 (s, 8H); 2.35 (m, 2H); 2.10 (m, 4H); 1.4 (m, 4H). <sup>13</sup>C NMR (100 MHz,  $\text{CDCl}_3$ )  $\delta$  / ppm: 27; 47; 56; 60; 122.0; 123.0; 136; 149.0; 158.0. IR (*KBr*, 4000-400  $\text{cm}^{-1}$ )  $\bar{\nu}$ : 2958-2854 (alkyl C-H stretch); 1589 (C=N, pyridyl). *Anal. Calc.* for  $\text{C}_{30}\text{H}_{34}\text{N}_6$ : C, 75.28; H, 7.16; N, 17.56; *Found*: C, 75.29; H, 7.10; N, 17.45. MS-ES<sup>+</sup> m/e: 479.2973 M + 1)<sup>+</sup>

**(L7)** Yield: 1519 mg (44 %), off-white powder. <sup>1</sup>H NMR (400 MHz,  $\text{CDCl}_3$ )  $\delta$  / ppm: 8.62 (t, 4H); 7.50-7.65 (m, 8H); 7.10 (t, 4H); 3.95 (s, 8H); 2.45 (t, 2H); 1.95 (d, 4H); 1.70 (m, 4H); 1.48 (q, 2H); 1.25 (m, 4H); 1.15 (t, 2H); 1.0 (m, 4H). <sup>13</sup>C NMR (100 MHz,  $\text{CDCl}_3$ )  $\delta$  / ppm: 28.0; 33.2; 34.0; 44.0; 57.5; 60.0; 122.0; 123.0; 136.5; 148.0; 162.0. IR (*KBr*, 4000-400  $\text{cm}^{-1}$ )  $\bar{\nu}$ : 2958-2854 (alkyl C-H stretch); 1589 (C=N, pyridyl). *Anal. Calc.* for  $\text{C}_{37}\text{H}_{46}\text{N}_6$ : C, 77.31; H, 8.07; N, 14.62; *Found*: C, 77.28; H, 8.26; N, 14.41. MS-ES<sup>+</sup> m/e: 575.3862 (M + 1)<sup>+</sup>.

### **5.2.3 Synthesis of Pt(II) complexes.**

The two mononuclear and the dinuclear Pt(II) complexes listed below (**1-7**) were synthesized starting from ligand **L1** to **L7**, following a literature procedure.<sup>19</sup> The complexes

## *Pt(II) complexes with rigid diamine bridges*

---

were characterized by NMR, IR and micro analysis. These were [Pt(Cl)(*N,N*-bis(2-pyridylmethyl)phenylamine)](ClO<sub>4</sub>) (**1**); [{"Pt(Cl)}<sub>2</sub>(*N,N,N',N'*-tetrakis(2-pyridylmethyl)-1,3-phenyldiamine)](ClO<sub>4</sub>)<sub>2</sub> (**2**); [{"Pt(Cl)}<sub>2</sub>(*N,N,N',N'*-tetrakis(2-pyridylmethyl)-1,4-phenyldiamine)](ClO<sub>4</sub>)<sub>2</sub> (**3**); [{"Pt(Cl)}<sub>2</sub>(*N,N,N',N'*-tetrakis(2-pyridylmethyl)-4,4'-methylenediphenylamine)](ClO<sub>4</sub>)<sub>2</sub> (**4**); [Pt(Cl)(*N,N*-bis(2-pyridylmethyl)cyclohexylamine)](ClO<sub>4</sub>) (**5**); [{"Pt(Cl)}<sub>2</sub>(*N,N,N',N'*-tetrakis(2-pyridylmethyl)-*trans*-1,4-cyclohexyldiamine)](ClO<sub>4</sub>)<sub>2</sub> (**6**); [{"Pt(Cl)}<sub>2</sub>(*N,N,N',N'*-tetrakis(2-pyridylmethyl)-4,4'-methylenediaminocyclohexane)](ClO<sub>4</sub>)<sub>2</sub> (**7**).

**1** Yield: 245.9 mg (56 %). <sup>1</sup>H NMR (400 MHz, DMF-*d*<sub>7</sub>) δ / ppm: 9.10 (d, 2H); 8.30-8.40 (t, d merged, 4H); 7.85 (d, 2H); 7.75 (m, 2H); 7.5 (m, 2H); 7.35 (m, 1H) 5.7 (d, 2H); 6.0 (d, 2H). <sup>13</sup>C NMR (100.6 MHz, DMF-*d*<sub>7</sub>) δ / ppm: 71.0; 124.0; 125.0; 127; 130; 136.0; 142; 149.5; 150; 166. <sup>195</sup>Pt NMR (107.2 MHz, DMF-*d*<sub>7</sub>) δ / ppm: -2300. IR (*KBr*, 4000-300 cm<sup>-1</sup>)  $\bar{\nu}$ : 2958-2854 (alkyl C-H stretch); (1589 (C=N, pyridyl); 1090-1100 (perchlorate counter ion); 324-330 (Pt-Cl stretch). *Anal. Calc. for* PtC<sub>18</sub>H<sub>17</sub>N<sub>3</sub>Cl<sub>2</sub>O<sub>4</sub>: C, 35.72; H, 2.83; N, 6.94; *Found*: C, 35.83; H, 2.79; N 6.92

**2** Yield: 190.0 mg (47 %). <sup>1</sup>H NMR (400 MHz, DMF-*d*<sub>7</sub>) δ / ppm: 8.95 (d, 4H); 8.25 (t,d, 6H); 7.85 (m, 4H); 7.75 (t, s (merged), 6H), 6.0 (d, 4H) 5.60 (d, 4H). <sup>13</sup>C NMR (125 MHz, DMF-*d*<sub>7</sub>) δ / ppm: 58.0; 113; 122.0; 123.0; 136.5; 141.0; 150.0; 162.0. <sup>195</sup>Pt NMR (107 MHz, DMF-*d*<sub>7</sub>) δ / ppm: -2312. IR (*KBr*, 4000-300 cm<sup>-1</sup>)  $\bar{\nu}$ : 2958-2854 (alkyl C-H stretch); 1589 (C=N, pyridyl); 1090-1100 (perchlorate counter ion); 324-330 (Pt-Cl stretch). *Anal. Calc. for* Pt<sub>2</sub>C<sub>30</sub>H<sub>28</sub>N<sub>6</sub>Cl<sub>4</sub>O<sub>8</sub>: C, 31.81; H, 2.49; N, 7.42 ; *Found*: C, 31.84; H, 2.47; N, 7.39.

**3** Yield: 215.6 mg (53 %). <sup>1</sup>H NMR (400 MHz, DMF-*d*<sub>7</sub>) δ / ppm: 9.02 (d, 4H); 8.55 (m, 8H); 8.25 (m, 4H); 7.95 (m, 4H), 6.0 (d, 4H) 5.60 (d, 4H). <sup>13</sup>C NMR (125 MHz, DMF-*d*<sub>7</sub>) δ / ppm: 59.0; 113; 122.0; 123.0; 136.5; 141.0; 150.0; 162.0. <sup>195</sup>Pt NMR (107 MHz, DMF-*d*<sub>7</sub>) δ / ppm: -2315. IR (*KBr*, 4000-300 cm<sup>-1</sup>)  $\bar{\nu}$ : 2958-2854 (alkyl C-H stretch); 1589 (C=N, pyridyl); 1090-1100 (perchlorate counter ion); 324-330 (Pt-Cl stretch). *Anal. Calc. for* Pt<sub>2</sub>C<sub>30</sub>H<sub>28</sub>N<sub>6</sub>Cl<sub>4</sub>O<sub>8</sub>: C, 31.81; H, 2.49; N, 7.42; *Found*: C, 31.79; H, 2.46; N, 7.32.

**4** Yield: 152.2 mg (34 %). <sup>1</sup>H NMR (400 MHz, DMF-*d*<sub>7</sub>) δ / ppm: 9.05 (d, 4H); 8.60 (t, 4H); 7.95 (d, 4H); 7.85 (t, 4H); 7.5 (m, 4H); 7.2 (m, 4H); 5.4 (d, 4H), 5.3 (d, 4H); 4.2 (s, 2H). <sup>13</sup>C NMR (100 MHz, CDCl<sub>3</sub>) δ / ppm: 41; 57; 112; 113; 122.0; 123.0; 128.0; 136.0; 150.0; 158.0. IR (*KBr*, 4000-300 cm<sup>-1</sup>)  $\bar{\nu}$ : 2958-2854 (alkyl C-H stretch); 1589 (C=N, pyridyl); 1090-1100 (perchlorate counter ion); 324-330

# *Pt(II) complexes with rigid diamine bridges*

---

(Pt-Cl stretch). *Anal. Calc. for Pt<sub>2</sub>C<sub>37</sub>H<sub>34</sub>N<sub>6</sub>Cl<sub>4</sub>O<sub>8</sub>*: C, 36.34; H, 2.80; N, 6.87; *Found*: C, 36.41; H, 2.80; N, 6.77.

**5** Yield: 207.8 mg (47 %). <sup>1</sup>H NMR (400 MHz, DMF-*d*<sub>7</sub>) δ / ppm: 9.05 (d, 2H); 8.40 (t, 2H); 7.95 (d, 2H); 7.80 (t, 2H); 5.45 (d, 2H); 5.35 (d, 2H); 3.05 (m, 1H); 2.35 (m, 2H); 1.7 (m, 2H) 1.2 (m, 6H). <sup>13</sup>C NMR (125 MHz, DMF-*d*<sub>7</sub>) δ / ppm: 24.5; 25.0; 30.0; 66.0; 73; 123.0; 126.0; 142.0; 149.0; 168. <sup>195</sup>Pt NMR (85 MHz, DMF-*d*<sub>7</sub>) δ / ppm: -2335. IR (*KBr*, 4000-300 cm<sup>-1</sup>)  $\bar{\nu}$ : 2958-2854 (alkyl C-H stretch); 1589 (C=N, pyridyl); 1090-1100 (perchlorate counter ion); 324-330 (Pt-Cl stretch). *Anal. Calc. for PtC<sub>18</sub>H<sub>23</sub>N<sub>3</sub>Cl<sub>2</sub>O<sub>4</sub>*: C, 35.36; H, 3.79; N, 6.94; *Found*: C, 35.36 ; H, 3.83; N, 6.92.

**6** Yield: 169.7 mg (41 %). <sup>1</sup>H NMR (400 MHz, DMF-*d*<sub>7</sub>) δ / ppm: 8.90 (d, 4H); 8.3 (t, 4H); 8.4 (d, 4H); 7.75 (t, 4H), 5.2 (d, 4H), 5.30 (d, 4H); 2.35 (m, 2H); 2.10 (m, 4H); 1.5 (m, 4H). <sup>13</sup>C NMR (125 MHz, DMF-*d*<sub>7</sub>) δ / ppm: 58; 60; 122.0; 123.0; 136; 149.0; 158.0. <sup>195</sup>Pt NMR (85 MHz, DMF-*d*<sub>7</sub>) δ / ppm: -2330. IR (*KBr*, 4000-300 cm<sup>-1</sup>)  $\bar{\nu}$ : 2958-2854 (alkyl C-H stretch); 1589 (C=N, pyridyl); 1090-1100 (perchlorate counter ion); 324-330 (Pt-Cl stretch). *Anal. Calc. for Pt<sub>2</sub>C<sub>30</sub>H<sub>34</sub>N<sub>6</sub>Cl<sub>4</sub>O<sub>8</sub>*: C, 31.64; H, 3.01; N, 7.38; *Found*: C, 31.63; H, 3.06; N, 7.36.

**7** Yield: 177.4 mg (40 %). <sup>1</sup>H NMR (400 MHz, DMF-*d*<sub>7</sub>) δ / ppm: 9.05 (d, 4H); 8.42 (t, 4H); 7.95 (d, 4H); 7.79 (t, 4H), 5.38 (d, 4H), 5.29 (d, 4H); 3.0 (m, 2H); 2.45 (m, 4H); 1.8 (m, 4H); 1.59 (m, 4H); 1.4 (m, 2H); 1.0 (m, 6H). <sup>13</sup>C NMR (100 MHz, DMF-*d*<sub>7</sub>) δ / ppm: 23.0; 52.5; 55.0; 127.1; 128.0; 128.0; 145.0; 148.0; 164.0. <sup>195</sup>Pt NMR (107 MHz, DMF-*d*<sub>7</sub>) δ / ppm: -2320. IR (*KBr*, 4000-300 cm<sup>-1</sup>)  $\bar{\nu}$ : 2958-2854 (alkyl C-H stretch); 1589 (C=N, (pyridyl)); 1090-1100 (perchlorate counter ion); 324-330 (Pt-Cl stretch). *Anal. Calc. for Pt<sub>2</sub>C<sub>37</sub>H<sub>46</sub>N<sub>6</sub>Cl<sub>4</sub>O<sub>8</sub>*: C, 35.99; H, 3.75; N, 6.81; *Found*: C, 35.90; H, 3.73; N, 6.64.

## **5.2.4 Kinetic measurements and computational details**

### **5.2.4.1 Preparation of aqueous solutions of Pt(II) complexes.**

The structures of the aqua derivatives of the complexes synthesized and used in the kinetics experiments are shown in Figure 4.1. The aqueous solutions of the complexes were prepared from their respective chloro derivatives following a literature procedure by Bugarčić *et al.*<sup>20</sup> The aqua complexes investigated were [Pt(H<sub>2</sub>O)(*N,N*-bis(2-pyridylmethyl)phenylamine)](CF<sub>3</sub>SO<sub>3</sub>)<sub>2</sub> (**bpPha**); [{Pt(H<sub>2</sub>O})<sub>2</sub>(*N,N,N',N'*-tetrakis(2-pyridylmethyl)-1,3-phenyldiamine)](CF<sub>3</sub>SO<sub>3</sub>)<sub>4</sub> (**mPh**); [{Pt(H<sub>2</sub>O})<sub>2</sub>(*N,N,N',N'*-tetrakis(2-pyridylmethyl)-1,4-phenyldiamine)](CF<sub>3</sub>SO<sub>3</sub>)<sub>4</sub> (**pPh**); [{Pt(H<sub>2</sub>O})<sub>2</sub>(*N,N,N',N'*-tetrakis(2-

## *Pt(II) complexes with rigid diamine bridges*

pyridylmethyl)-4,4'-methylenediphenylamine)](CF<sub>3</sub>SO<sub>3</sub>)<sub>4</sub>, (**dPhm**); [Pt(H<sub>2</sub>O)(*N,N*-bis(2-pyridylmethyl)cyclohexylamine)](CF<sub>3</sub>SO<sub>3</sub>)<sub>2</sub> (**bpcHna**); [{Pt(H<sub>2</sub>O)}<sub>2</sub>(*N,N,N',N'*-tetrakis(2-pyridylmethyl)-*trans*-1,4-cyclohexyldiamine)](CF<sub>3</sub>SO<sub>3</sub>)<sub>4</sub> (**cHn**); [{Pt(H<sub>2</sub>O)}<sub>2</sub>(*N,N,N',N'*-tetrakis(2-pyridylmethyl)-4,4'-methylenediaminocyclohexane)](CF<sub>3</sub>SO<sub>3</sub>)<sub>4</sub> (**dcHnm**).

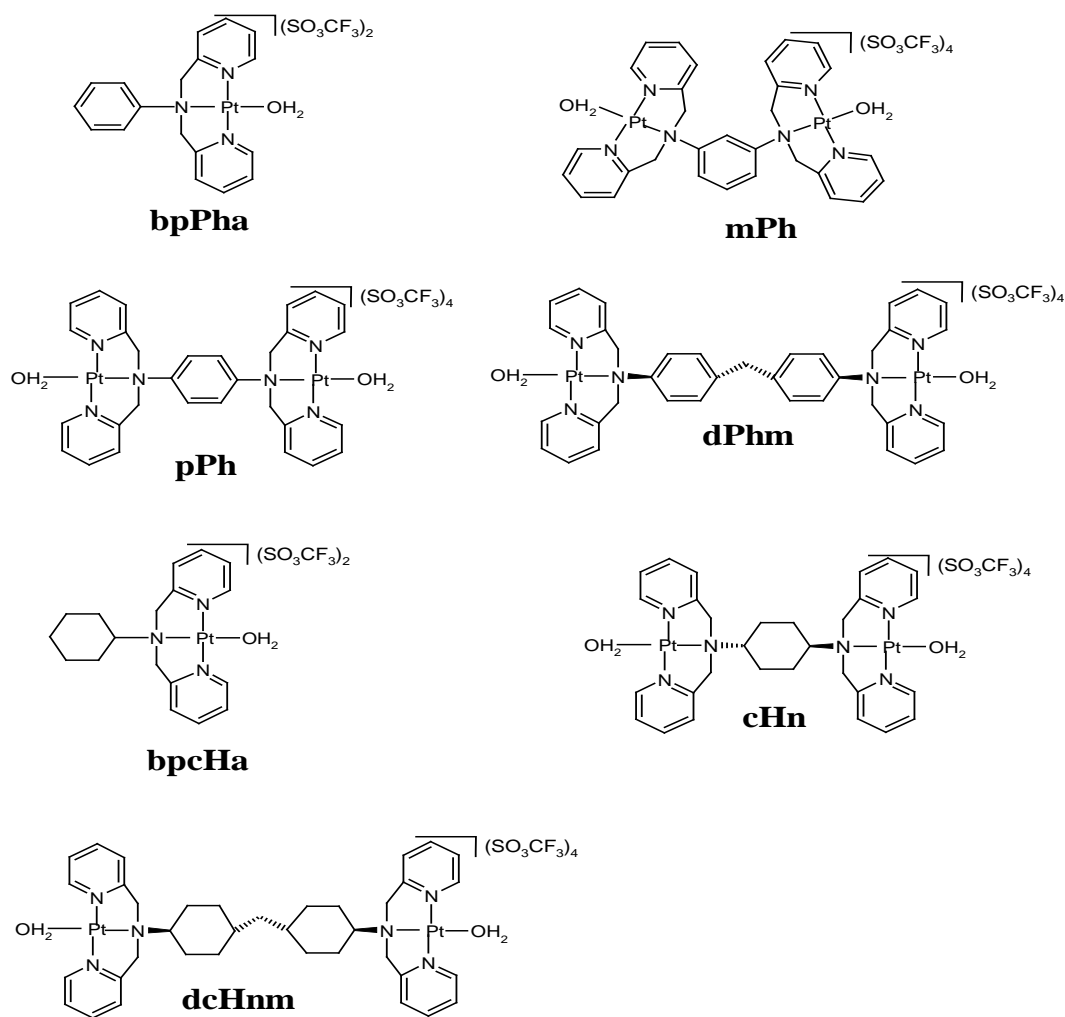


**Figure 5.1** Structures of dinuclear Pt(II) complexes and their respective mononuclear analogues synthesized in this study.

### 5.3.4.2 Preparation of nucleophile solutions for kinetic analyses.

Solutions of the nucleophiles *viz.* thiourea (tu), *N,N*-dimethylthiourea (dmu) and *N,N,N',N'*-tetramethylthiourea (tmtu) were prepared by dissolving appropriate amounts of the nucleophiles in a solution pH 2 whose ionic strength had been adjusted to 0.02 M using LiSO<sub>3</sub>CF<sub>3</sub>. The stock solution of each nucleophile, of concentration approximately equal to 100-fold over that of the dinuclear complexes or 50-fold over that of the monomeric complexes

## *Pt(II) complexes with rigid diamine bridges*

---

(**bpPha** and **bpcHna**), was diluted with a 0.02 M ionic strength solution to afford serial concentrations which are least 20-fold (for dinuclears) and 10-fold excess (mononuclears) over that of the metal complexes. These concentrations of the entering nucleophiles were chosen to maintain pseudo first-order conditions during the course of the experiments. This also forced the reactions to go to completion.

### *5.2.4.3 Instrumentation and spectrophotometric measurements.*

A Bruker Avance DPX 400 NMR spectrometer and a Carlo Erba Elemental Analyzer 1106 were used to confirm the identity and purity of both the ligands and complexes. Infrared spectra of all the compounds were recorded in the range 4000-300  $\text{cm}^{-1}$  on a Spectrum One FT-IR as KBr pellets. The mass spectral data of ligands were acquired by Micromass TOF MS operated in a positive ion mode. UV-visible spectra and kinetic measurements of slow reactions were recorded on a Cary 100 Bio UV-visible spectrophotometer with a cell compartment thermostated by a Varian Peltier temperature controller having an accuracy of  $\pm 0.05$   $^{\circ}\text{C}$ . The pH measurements were recorded on a Jenway 4330 pH meter with a combined Jenway glass microelectrode which had been calibrated with standard buffer solutions of pH 4.0, 7.0 and 10.0 (Merck). The KCl solution in the reference electrode was replaced with a 3 M NaCl electrolyte to prevent precipitation of  $\text{KClO}_4$  during use.<sup>13</sup> Kinetic measurements of fast reactions were monitored on an Applied Photophysics SX.18 MV (v4.33) stopped-flow reaction analyzer coupled to an online data acquisition system. The temperature of the instrument was controlled to within  $\pm 0.1$   $^{\circ}\text{C}$ .

### *5.2.4.4 Computational calculations.*

Density functional theoretical (DFT)<sup>21</sup> calculations were performed with the Spartan '04 for Windows quantum chemical package<sup>22</sup> using the B3LYP<sup>23</sup>, a three parameter hybrid functional method, utilizing the LACVP+\*\*<sup>24</sup> pseudopotentials basis set. The dinuclear and the monomeric complexes (**bpcHna** and **bpPha**) were all modeled as cations of a total charge of +4 and +2, respectively. Their geometry-optimized structures and key geometrical data from the calculations are summarized in Tables 5.2a and 5.2b.

# Pt(II) complexes with rigid diamine bridges

## 5.3 Results and Discussion

### 5.3.1 Acidity of the aqua Pt(II) complexes.

A typical plot of the UV-visible spectra acquired during the course of the titration of the complexes with NaOH is shown in Figure 5.2 for **dcHnm**. Shown as an inset in the Figure are the absorbance changes recorded at a wavelength of 268 nm as a function of pH.

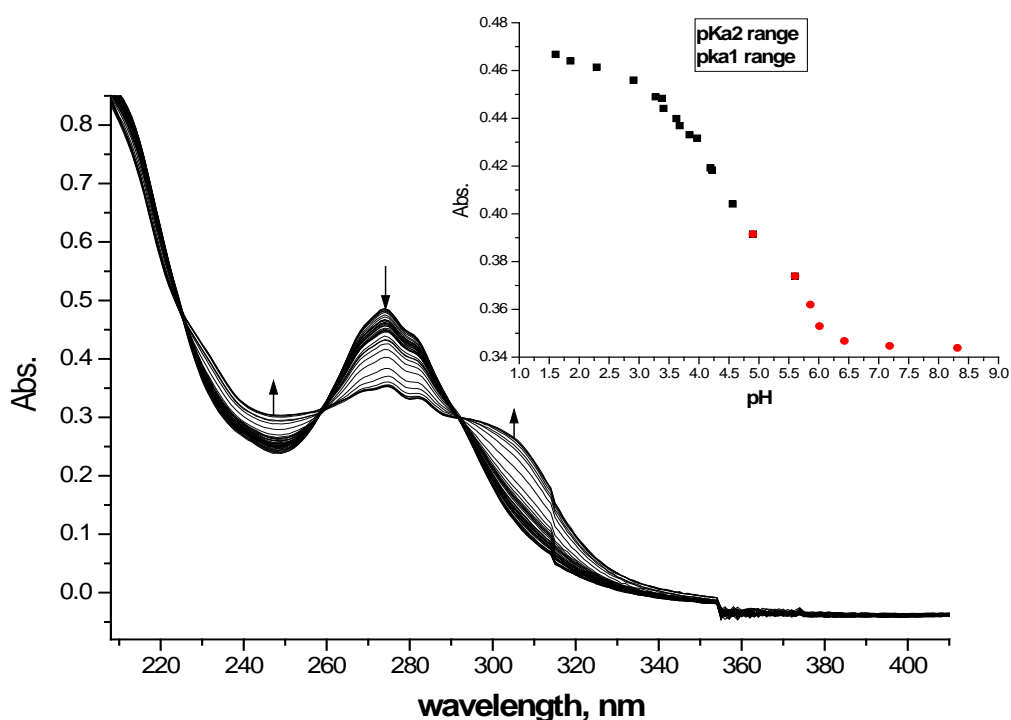


**Figure 5.2** UV-visible spectra for the titration of 0.11 mM **dcHnm** with NaOH, pH range 2 - 9, T = 298 K. Inset is the titration curve at 268 nm.

In the acidic range, the spectra of all the dinuclear complexes and the two mononuclear complexes are characterized by a sharp absorption band (refer also to Figure SI 5.2, supporting information for the titration spectra of **bpPha**). Their peaks maxima appear all within a narrow wavelength range of 267-270 nm and have red-shifted shoulders featuring within the 276-278 nm range. The absorption maxima for complexes bridged by phenyldiamines occur around 270 nm while the diaminocyclohexane-bridged complexes have their absorption maxima around 268 nm. The absorption peaks are similar in shape and comparable to those for the flexible  $\alpha,\omega$ -alkyldiamine-bridged dinuclears<sup>14a</sup>, the analogous amphiphiles reported in Chapter Four and that reported<sup>25</sup> for the mononuclear complex,  $[\text{Pt}(\text{H}_2\text{O})(N,N\text{-bis}(2-$

## *Pt(II) complexes with rigid diamine bridges*

---

pyridylmethyl)amine](CF<sub>3</sub>SO<sub>3</sub>)<sub>2</sub>] (**bpma**) under similar prevailing conditions. Addition of the titrant (NaOH) leads to immediate changes in the spectra. The peaks in the 267-270 nm range gradually decrease while the shoulders in the 276-278 nm range grow slightly in size. An additional broader shoulder peak shapes up in the range 300-305 nm during the course of the titration, as hydroxo species of the complexes are formed. When the titration data which is taken at a single wavelength within the 267-270 nm peaking range is fitted to the standard Boltzmann equation, the p*K*<sub>a</sub> values for the deprotonation of the protons of the coordinated aqua ligands are obtained. The results are summarized in Table 5.1.

## *Pt(II) complexes with rigid diamine bridges*

---

**Table 5.1** Summary of  $pK_a$  data obtained for the deprotonation of Pt-bound aqua ligands (within pH range 2-9), using NaOH as titrant.

	<b>bpma</b>	<b>bpPha</b>	<b>mPh</b>	<b>pPh</b>	<b>dPhm</b>	<b>bpcHna</b>	<b>cHn</b>	<b>dcHnm</b>
<b><math>pK_{a1}</math></b>	$5.49^* \pm 0.20$	$5.45 \pm 0.20$	$3.25 \pm 0.07$	$3.32 \pm 0.05$	$4.10 \pm 0.03$	$5.65 \pm 0.19$	$4.64 \pm 0.15$	$4.35 \pm 0.05$
<b><math>pK_{a2}</math></b>			$5.12 \pm 0.05$	$5.23 \pm 0.06$	$5.30 \pm 0.3$		$5.68 \pm 0.18$	$5.72 \pm 0.02$

The data from the titrations were fitted either to equation,  $y = a + (b-a)/(1+2.718^{((x-pK_{a1}/m)+(c-b)/(1+2.718^{((x-pK_{a2})/n))$ ), for measuring two  $pK_a$  values or the Boltzmann equation,  $y = A_2 + (A_1-A_2)/(1+\exp((x-x_0)/dx))$  for measuring one  $pK_a$  value using Origin 7.5<sup>®</sup> program \* Ref 30.

## *Pt(II) complexes with rigid diamine bridges*

---

The  $pK_a$  values indicate that at a pH of 2 (0.01 M  $CF_3SO_3H$  solution), at which the kinetics of reactions were studied, all the complexes exist as their aqua forms. To confirm the presence of the aqua species in solution, the titration was carried out with both NaOH and triflic acid with the reversibility of the spectra being observed.

The deprotonation of the aqua ligands of the dinuclear complexes occurred in a stepwise fashion. A look at the data in Table 5.1 shows that the deprotonation of the first aqua ligand of each dinuclear complex occurs at pH values that are about one unit lower than the values at which the second aqua ligands are deprotonated. The increase in the acidity of the coordinated aqua ligand when the chelate headgroups are joined together by diamine bridges to form the dinuclears has been observed before<sup>14a</sup> when  $pK_a$  data of the dinuclear complexes bridged by the flexible alkyldiamine bridges were compared to that of their analogous amphiphiles reported in Chapter Four. In the flexible dinuclears, electrostatic charge addition at the dicationic Pt atoms increased the acidity of the coordinated aqua ligands and the effect was more profound in complexes with short bridges. A similar effect can be seen in the  $pK_{a1}$  data of **mPh**, **pPh** and **cHn** wherein the introduction of rigidity and planarity through short aromatic diamine and diaminocycloalkane bridges resulted in deprotonation occurring at lower pH values when compared to their mononuclear analogues. The extent of acidification of the coordinated aqua ligands in the three dinuclear is however similar to that observed for dinuclears bearing flexible diamine bridges of shorter chain length (**Prop** and **En**)<sup>14a</sup> possibly due to efficient delocalization of charge within the aromatic diamine and comparable inductive effects in the cycloalkyldiamine bridge.

The  $pK_{a2}$  values for phenyldiamine-bridged ( $pK_{a2}$  range: 5.12-5.30) and the diaminocyclohexyl-bridged dinuclear complexes ( $pK_{a2}$  range: 5.68-5.72) are all comparable to the  $pK_a$  values of their respective mononuclear analogues **bpPha** (5.45) and **bpcHna** (5.65), indicating the stepwise nature of the deprotonation process in all the dinuclear complexes. A comparison of the  $pK_{a1}$  values of the deprotonation in complexes with methylene spacers in their bridges *viz.*, **dPhm** ( $4.10 \pm 0.03$ ) and **dcHnm** ( $4.35 \pm 0.05$ ) and their respective analogues with a single ring in their bridges *viz.*, **pPh** ( $3.32 \pm 0.05$ ) and **cHn**: ( $4.64 \pm 0.15$ ), reveals that the first  $pK_a$  values for the former type of complexes are slightly higher than for the latter complexes. As the average distance between the Pt atoms of the former complexes are increased through methylene spacing, a general increase in the basicity is observed as a result of less effective charge addition at each Pt atom. The trend in the results of the measured  $pK_a$  data for phenyl and the cyclohexyl-bridge sets of complexes is similar to one that has already

## *Pt(II) complexes with rigid diamine bridges*

---

been reported in a recent study by Eldik *et al.*,<sup>26</sup> in which the shorter and conjugated diamine bridge coordinated *cis* to the aqua leaving groups of the Pt(DACH) headgroups caused increased acidity of the coordinated aqua coligand leading to lower  $pK_a$  values. *Cis*- $\alpha,\omega$ -diaminoalkane bridged complexes ( $n = 8; 10$ ), on one hand recorded higher  $pK_a$  values due to the  $\sigma$ -donation of electron density of their aliphatic linkers towards each Pt atom.

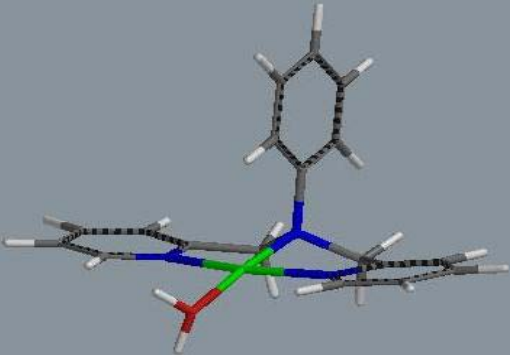
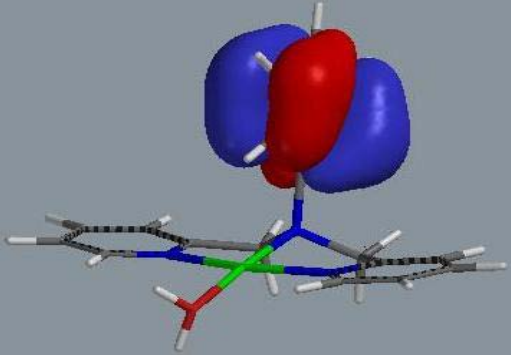
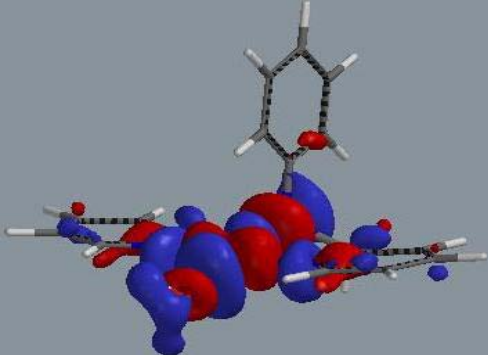
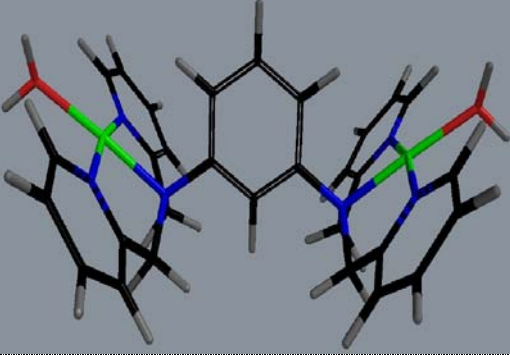
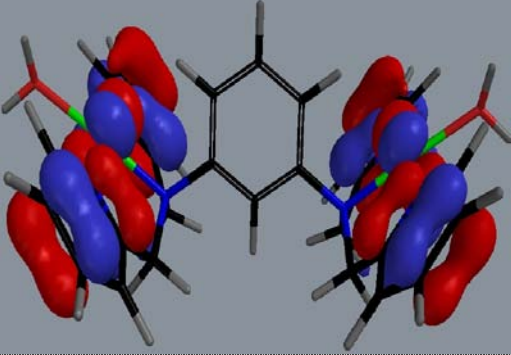
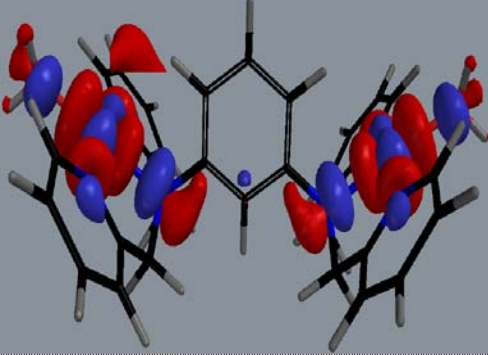
Another notable difference between the hydrolysis equilibria of these two sets of complexes, is that the aqua ligands of the phenyldiamine-bridged complexes are slightly more acidic ( $pK_{a1}$  range: 3.25-4.10) when compared to those for respective complexes bridged by diaminocyclohexane fragments ( $pK_{a1}$  range: 4.35-4.64). Phenyldiamines ( $sp^2$  carbon atoms) are known to be slightly poor  $\sigma$ -donors than cycloalkyldiamines ( $sp^3$  carbon atoms)<sup>27</sup> resulting in better electron density flow towards the Pt centres in the latter complexes, which makes their Pt centres less electrophilic. A lower electrophilicity of the Pt atoms due to positive inductive effects makes deprotonation difficult in the coordinated aqua ligands resulting in an increase in the basicity of the complex.<sup>28</sup> The magnitude of  $pK_a$  values of the analogous mononuclear complexes **bpcHna** and **bpPha** Table 5.1 reflects the relative magnitude of the  $\sigma$ -donation due to the pendants towards the Pt centres. A change in hybridization of the carbon atoms of the cyclohexyl pendant from  $sp^3$  to an  $sp^2$  in phenyl tail is accompanied by a decrease in the basicity of 0.1 of the coordinated aqua ligand in accordance with a decrease in the *trans*-influence in the latter pendant.<sup>27</sup> When the comparison is extended to **bpha** (Chapter Four, section 4.3.2, Table 4.1), an amphiphile with a hexyl ( $sp^3$  primary carbon), its  $pK_a$  ( $5.48 \pm 0.05$ ) is lower than that of **bpcHna** by the same margin. Since the cyclohexyl pendant is bonded to the *trans*-N donor atom of the chelate through a secondary alkyl group which is known<sup>27</sup> to be a better  $\sigma$ -donor than a primary alkyl substituent of the **bpha**, this further reaffirms that the basicity of the complexes is influenced by the donor capacity of the pendant which becomes the bridge in the respective dinuclears. Further the Pt-O bond lengths increase in the order **bpPha** < **bpha** < **bpcHna** due to the increasing strength in their *trans*-influence of their ancillary pendants as shown by the computational calculations in Tables 4.2b (Chapter 4, (**bpha**) and 5.2a (**bpPha** and **bpcHna**)).

### 5.3.2 Computational calculations

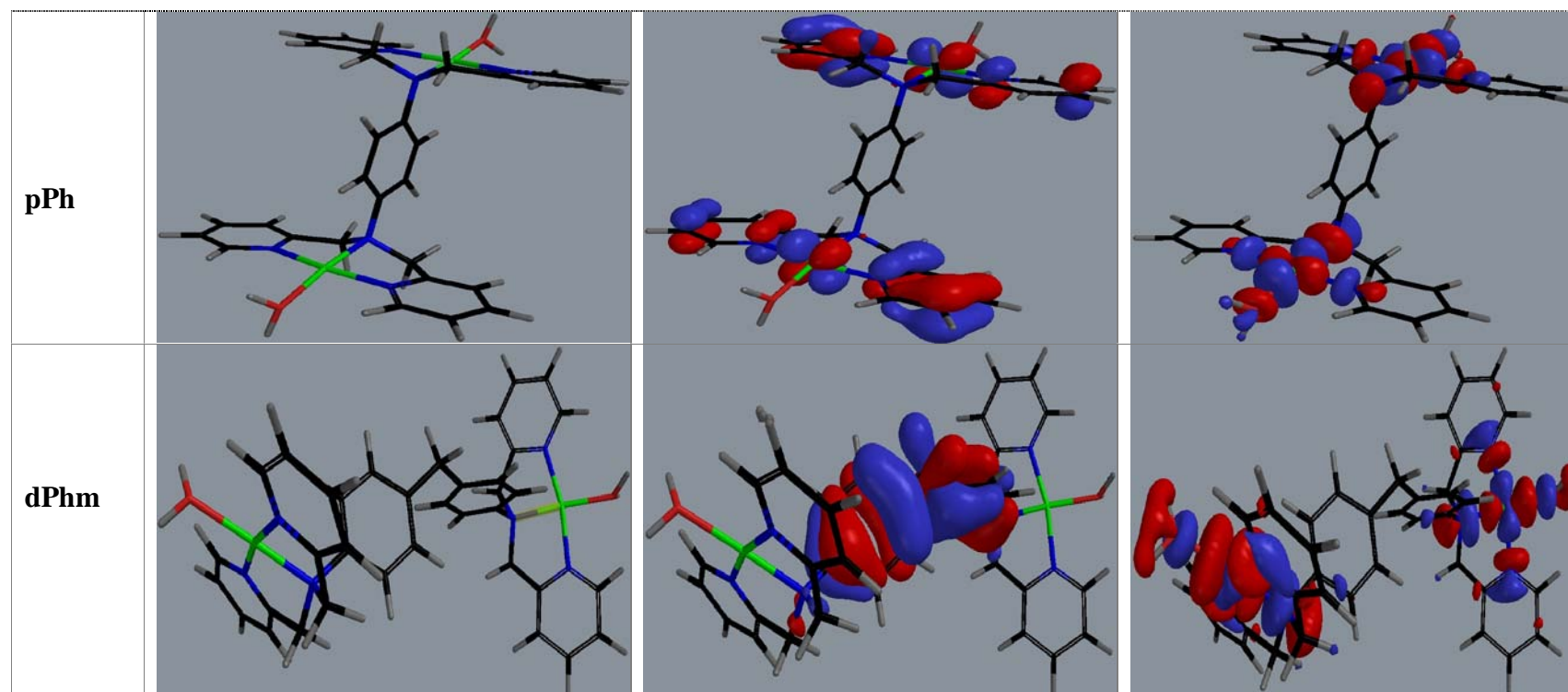
Table 5.2a shows the geometry-optimized structure and the location of the frontier molecular orbitals. Their electrostatic potential maps are given in Figure SI 5.5 (supporting information). An extract of the complexes' structural data from the calculations is summarized in Table 5.2b, respectively.

## *Pt(II) complexes with rigid diamine bridges*

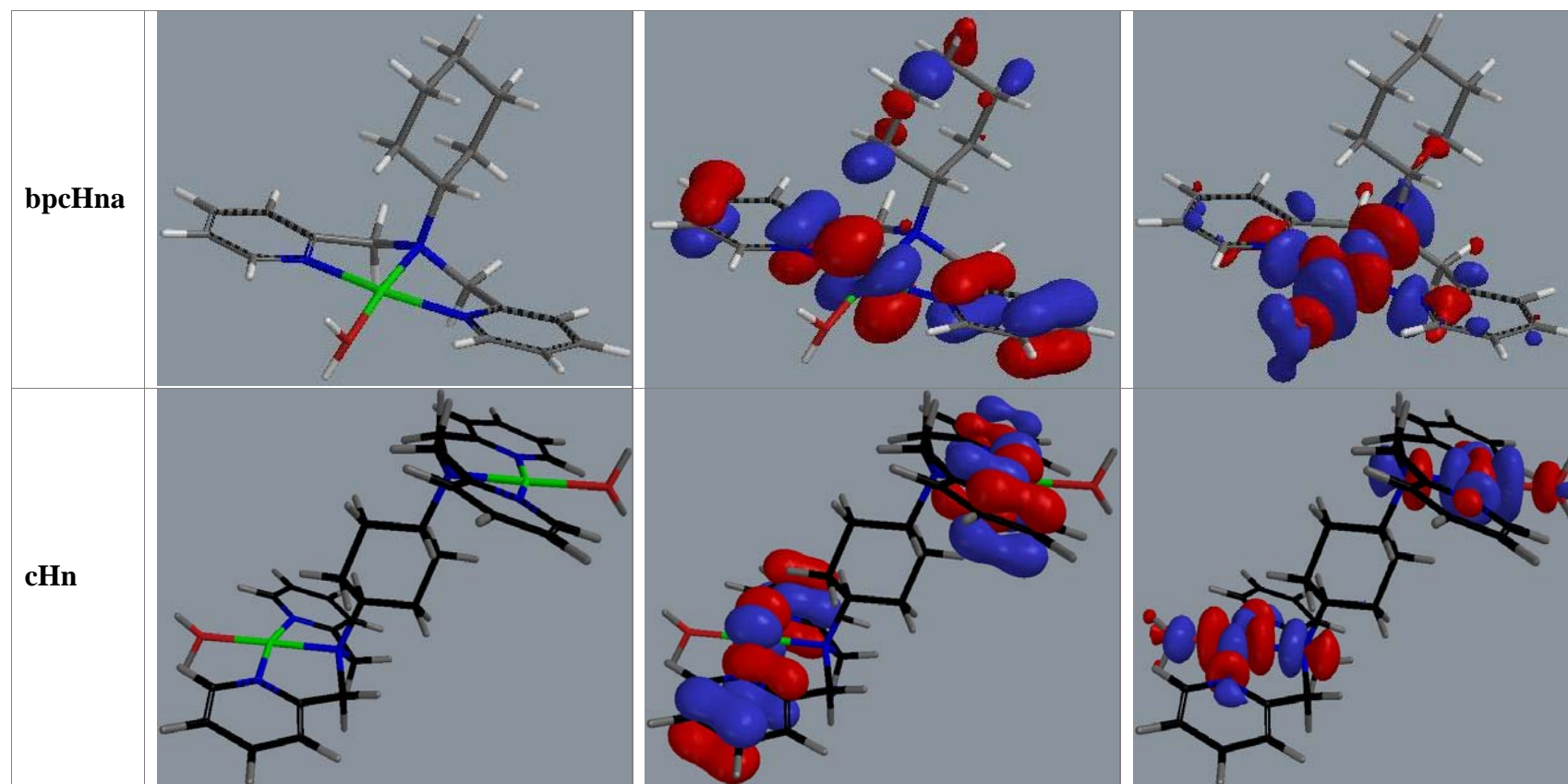
**Table 5.2a** Density functional theoretical (DFT)<sup>21</sup> minimum energy structures, HOMO and LUMO frontier molecular orbitals for dinuclear complexes with aromatic diamine and diaminocyclohexane bridging fragments. The calculations were performed with the Spartan '04 for Windows quantum chemical package<sup>22</sup> using the B3LYP hybrid functional method<sup>23</sup> utilizing the LACVP+\*\*<sup>24</sup> pseudopotentials basis set.

Complex	Structure	HOMO Map	LUMO Map
bpPha			
mPh			

## *Pt(II) complexes with rigid diamine bridges*

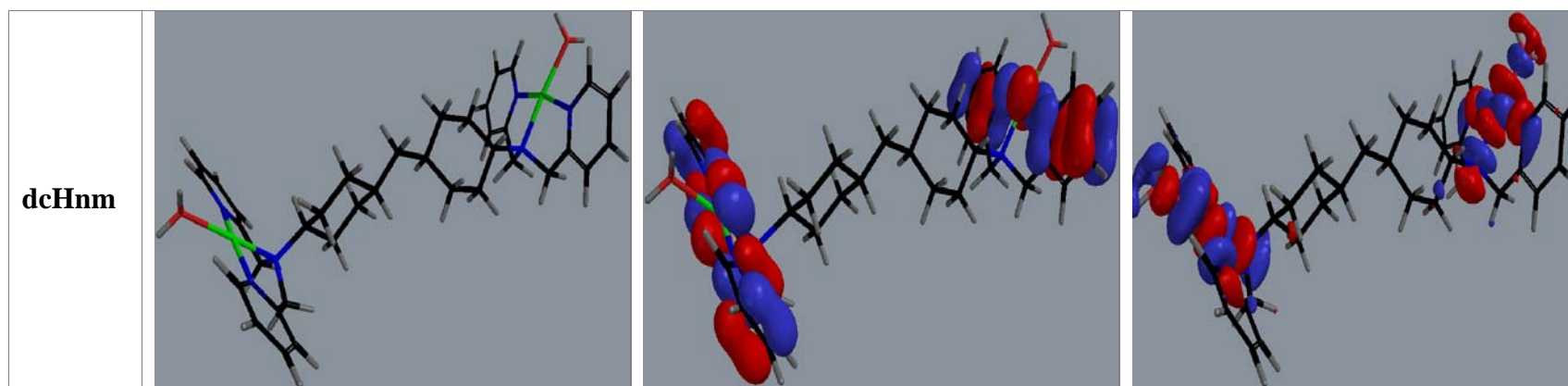


## *Pt(II) complexes with rigid diamine bridges*



## *Pt(II) complexes with rigid diamine bridges*

---



## Pt(II) complexes with rigid diamine bridges

**Table 5.2b** Summary of DFT<sup>21</sup> computational data for the dinuclear Pt(II) complexes and their mononuclear analogues.

Property	bpma	bpPha	mPh	pPh	dPhm	bpcHna	cHn	dcHnm
<b>Bond lengths, Å</b>								
Pt-OH <sub>2</sub>	2.151	2.155	2.140	2.140	2.143	2.164	2.144	2.156
Pt-N <sub>trans</sub>	2.012	2.048	2.052	2.64	2.054	2.046	2.062	2.052
<b>Separation distance, Å</b>								
N <sub>1 trans</sub> -N <sub>2 trans</sub>			3.950	5.234	6.536		5.99	11.30
Pt <sub>1 coord. plane</sub> - Pt <sub>2 coord. plane</sub> <sup>†</sup>			3.63	8.59	10.63		8.77	14.20
Pt-H <sub>proximal</sub>		2.62	2.65	2.72	2.76	2.79	2.87	2.79
<b>Bond angles, °</b>								
N <sub>cis</sub> -Pt-N <sub>cis</sub>	165.8	167.7	166.4	167.03	167.4	166.8	166.9	166.8
Pt <sub>1</sub> -N <sub>1 trans</sub> -N <sub>2 trans</sub>			105.80	118.5			119.2	38.98
N <sub>1 trans</sub> C <sub>bridge's central</sub> -N <sub>2 trans</sub>			125.5		134.5			143.1
Elevation angle of bridge/tail, α, <sup>‡</sup>		63.4		61.5	131.3	63.2	60.8	
Inclination angle of aqua ligands (relative to the coord. plane)		12.92	11.92	15.38	14.39	12.51	13.36	12.11
<b>Energy gap, eV</b>								
LUMO Energy, eV	-8.53	-8.53	-12.22	-18.78	-10.82	-11.09	-10.64	-10.32
HOMO Energy, eV	-12.78	-12.78	-17.15	-17.05	-15.33	-16.23	-15.82	-15.51
ΔE <sub>LUMO-HOMO</sub> ,	4.25	4.25	4.93	4.99	4.51	5.14	5.18	5.19
<b>Natural Charges</b>								
Pt <sub>1/2</sub>	1.215	1.215	1.231	1.226	1.221	1.203	1.220	1.215
<b>Symmetry</b>								
	C <sub>2h</sub>	C <sub>2h</sub>	C <sub>2v</sub>	C <sub>2h</sub>	C <sub>2v</sub> (distorted)	C <sub>2h</sub>	C <sub>2h</sub>	C <sub>2v</sub>

<sup>‡</sup>α is the supplementary angle to the angle {Pt1-N1<sub>trans</sub>-N2<sub>trans</sub>} in complexes with C<sub>2h</sub> symmetry. The projection of the first coordination plane relative second (Pt<sub>1 coord. plane</sub> - Pt<sub>2 coord. plane</sub>)<sup>†</sup> was calculated from α and the length of the linker (N<sub>1 trans</sub>-N<sub>2 trans</sub>).

## *Pt(II) complexes with rigid diamine bridges*

---

The calculated structures shown in Table 5.2a reveals that the shapes adopted by the dinuclear complexes, depends on the native symmetry elements within the bridging linker. One can reckon that  $\pi$ -back bonding between the filled orbitals on the Pt metal centres and the pyridyl  $\pi$ -acceptor ligands of the chelate headgroups is maximized if the pyridine rings maintain an in-plane coordination geometry about the square coordination plane.<sup>28</sup> It seems however, that chelation of the Pt atoms wherein an in-plane geometry of the pyridyl rings of the bis(2-pyridylmethyl)amine headgroups is maintained, creates structural constraints at the two square-coordination planes in these dinuclear complexes, which require reorganization within the linker piece to ensure maximum  $\pi$ -back bonding from the filled orbitals of the metal centres to the pyridyl acceptor units. This reorganization is mediated by the native symmetry elements within the linking fragment leading to symmetry-protracted molecular structures in which in-plane  $\pi$ -back bonding between the  $\pi$ -acceptor pyridyl units and the Pt atoms is least compromised.

Geometry-optimized structures in Table 5.2a reveals that the native symmetry elements operational in these complexes depend specifically on the number of carbon atoms,  $n$ , within a fragment constituting the shortest asymmetric connectivity between the N atoms of the diamine linker. In the cases of the phenyldiamine bridges, factors such as rigidity and planarity of the linking rings within the bridge appear also to mediate the structural directing-role of the symmetry elements. Thus, in the isomeric **mPh** and **pPh** complexes, wherein the N atoms of the phenyldiamine are linked by phenyl bridging fragments bearing three and four carbon atoms, respectively, different structures are calculated. A change from a 1,3- to 1,4-connectivity in the N atoms of the diamine causes a flip in the shape of the calculated structures from a bowl-shaped,  $C_{2v}$ , to a slip-up sandwich,  $C_{2h}$ , respectively. In these two isomeric complexes, the plane of the bridging phenyldiamine ring is also shared by Pt,  $N_{trans}$  and the O atoms. It therefore bisects the coordination plane containing the in-plane pyridyl ring atoms.

A general pattern can therefore be drawn between the number of carbon atoms,  $n$ , in an asymmetric and connective fragment of carbon atoms of the diamine bridge and the shape adopted by the *N,N*-bis(2-pyridylmethyl)amine chelated dinuclear Pt(II) complexes. If  $n$  is odd, the dinuclear complex is bowl or trough-shaped and falls in a  $C_{2v}$  point group while an even number of carbon atoms in the connecting fragment results in a slip-up sandwich structure of the  $C_{2h}$  point group. A similar relationship between the nature of the bridging linker and the adopted molecular structure is illustrated in the crystal structures of 3,6-bis{*trans*-

## *Pt(II) complexes with rigid diamine bridges*

---

Pt(PEt<sub>3</sub>)<sub>2</sub>(NO<sub>3</sub>)<sub>2</sub>}-9,10-bis(hexyloxy-; dodecyloxy-)phenanthrene,<sup>29</sup> two dinuclear Pt(II) complexes with a common phenanthrene bridge, where the three conjugated and angular rings of the bridge, forces bowl molecular structures in the complexes. Thus, the subtle differences in the symmetry elements of the bridges and hence the different molecular shapes of the dinuclear complexes as shown in their DFT<sup>21</sup>-optimized structures can control the rate of ligand substitution reactions at the square planar-chelates of these complexes. The molecular shapes of the complexes as controlled by the symmetry elements of linking bridge can confer ‘pre-orientation effects’<sup>30</sup> to approaching nucleophiles in their outer-sphere ligand assemblage shell. Pre-orientation of nucleophiles in the bowl-shaped structure can cause an entrapment effect<sup>31</sup> resulting in relatively lower activating energies, resulting in high reactivity. The structure directing role of the linker in these dinuclear open possibility of extra favourable pre-orientated non-bonding hydrophobic interactions with the DNA nucleobases similar to the electrostatic effects induced by the central tetraamine coordinated Pt moiety in BBR3464<sup>1,3b</sup>.

A slip-up structure of complexes such as **pPh** and **cHn** imposes mutual steric hindrance in the direction of approach of the nucleophile due to the shortness and rigidity of the linker which raises the activation barrier of the transition state resulting in lower rates of substitution. This observation is similar to previous findings<sup>14a</sup> for dinuclears bridged by flexible  $\alpha,\omega$ -alkyldiamines, where the lowest rates of substitution were recorded for **En**, a complex bridged by two carbons.

Using the same generalization, the structure adopted by **cHn** should be no different from that of **pPh**, since there are four carbon atoms connecting the N atoms in the *trans*-1,4-diaminocyclohexane linker fragment. Indeed, the preferred structure for **cHn** from the DFT<sup>21</sup> calculations is a slip-up sandwich. Unlike the structure of **pPh** though, the frame of the diaminocyclohexane ring of **cHn** lies at a slightly tilted angle to the bisector plane to the equatorial square-plane of the Pt chelates. Similar symmetry elements can also be noticed in the structures of the respective mononuclear complexes, *viz.*, **bpPha** and **bpcHna**.

The structure of the diamine bridge of **dPhm** can be viewed as formed through a tail-to-tail joining of the appended phenyl groups of two **bpPha** complexes through incorporation of a methylene spacer. The N atoms of its diamine linker are connected by a fragment comprising two phenyl rings and a methylene-carbon spacer, making a total of nine carbon atoms within the shortest asymmetric chain of carbon atoms making up the diamine bridge. On the basis of the generalization made above, the complex should be bowl-shaped and should have a C<sub>2v</sub> point-group symmetry. However, its calculated structure turns out to be a heavily distorted

## *Pt(II) complexes with rigid diamine bridges*

---

trough-shaped bowl, in which the Pt coordination planes are orientated in a twisted fashion relative to an ideal trough-shaped structure. The two enjoined aromatic rings lie in almost perpendicular planes. The distortion in its shape is a necessary reorganization extended beyond the linker framework, mediated by both the rigidity of the planar phenyl rings as well as the flexibility of the methylene carbon spacer. The sheer-twisted overlooking coordination planes of this distorted bowl-shaped structure make a hinge angle of  $135^\circ$  at the central carbon atom of the methylene spacer of the linker. Thus, the distorted bowl is relatively shallow in depth and has a wider basal separation distance. Thus, from these distorted structural features, no reactivity advantage over **pPh** can be expected.

As already explained for the structure of **dPhm** bridge, if a methylene spacer is incorporated to join two cyclohexyl pentants of the **bpcHna** complexes in a tail-to-tail fashion, a trough-shaped bowl is expected. This is found to be true from the DFT<sup>21</sup> calculations and indeed the structure of the **dcHnm** complex falls into a  $C_{2v}$  point group symmetry, derived from a string of nine carbon atoms connected to the N atoms of the diamine linker. The moderate flexibility of the diaminocyclohexane ring atoms allow the nine carbon atoms forming the linking fragments of the diamine bridge to connect in a helical fashion which orient the two enjoined cyclohexyl rings' frames into a screw-like twist. This helical conformation of the linker atoms seems to be the compensating structural reorganization necessary to avert the same kind of distortion observed in the calculated structure of the more rigid **dPhm** complex. Its overlooking coordination planes make a hinge angle of  $143^\circ$  at the carbon of the central methylene spacer. Thus, its cavity is relatively shallow in depth and has a wider basal separation distance.

As will be discussed shortly, the structural features of the diamino linkers and steric influences they cause at the Pt square-planes of these complexes appear to be the major factors controlling the reactivity of their substitution reactions with thiourea nucleophiles.

### **4.3.3 Kinetic measurements**

Spectral changes accompanying the reactions between the complexes and nucleophiles (tu, dmtu, tmtu) were recorded over the 200-600 nm wavelengths range to establish suitable wavelengths at which their kinetic measurements could be performed. The list of wavelengths chosen to monitor the substitution of the coordinated aqua ligands in these complexes is summarized in Table SI 5.1 (supplementary information). The trial experiments also showed that all reactions were characterized by two steps, a fast step fitting the timescale of the

## *Pt(II) complexes with rigid diamine bridges*

---

stopped-flow reaction analyzer and a slower second step that could be studied by UV-visible spectroscopy. These reaction steps are assumed to be the substitution of the coordinated aqua ligands followed by the displacement of one of the coordinated pyridyl units in the chelate framework.<sup>32</sup> For the dinuclear analogues, the substitution of the two aqua ligands occurs simultaneously.

Reactions were initiated by either a pressure-driven mixing technique in which equal volumes of the complex and the nucleophile were forced into the chamber of the stopped-flow instrument or by manually mixing of equal amounts of the reagents in a tandem cuvette on the UV-visible spectrophotometer. Each reaction step was followed spectrophotometrically for more than six half-lives. The data were fitted to a non-linear least-square procedure. A representative plot from the stopped-flow analyzer is shown in Figure 5.3 for the first step involving the reaction between **dPhm** (0.11 mM) and dmtu (6.6 mM).

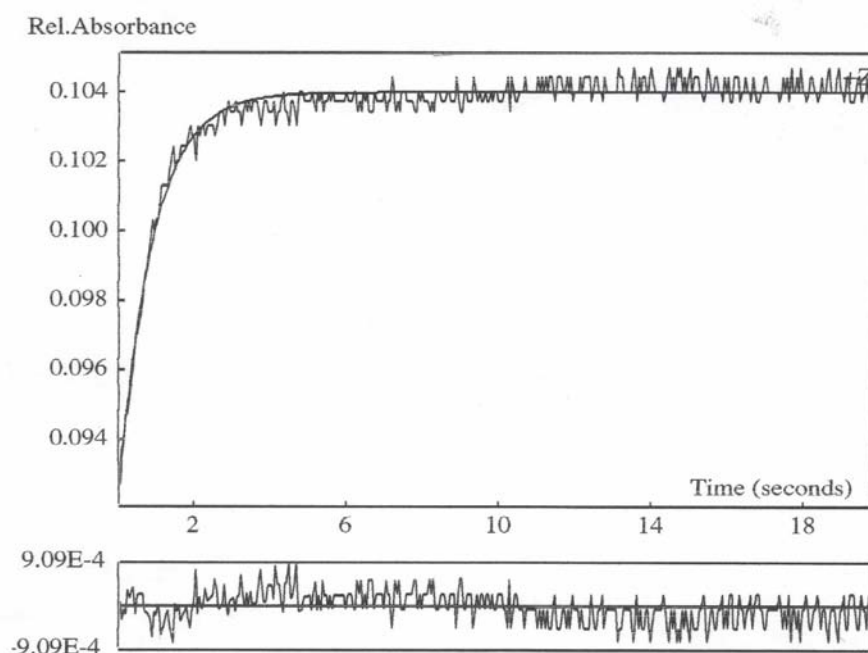


**Figure 5.3** A typical kinetic trace from the Stopped-flow acquired at 335 nm for the simultaneous substitution of the aqua between **dPhm** (0.11 mM) and dmtu (6.6 mM) at 298 K, pH = 2.0, I = 0.02 M {CF<sub>3</sub>SO<sub>3</sub>H, adjusted with Li(SO<sub>3</sub>CF<sub>3</sub>)}.

The kinetic data for the two steps fit perfectly to separate single exponentials. The pseudo first-order rate constants,  $k_{\text{obs.}(1/2)}$ , obtained were plotted against the concentration of the entering nucleophiles (Nu) using Origin 7.5<sup>®33</sup> software. The plots of the observed rate constants were found to be linearly related to the concentration of the entering nucleophiles (Nu) with

## *Pt(II) complexes with rigid diamine bridges*

negligible zero y-intercepts. Representative plots for the reactions between the **cHn** complex and the nucleophiles are shown in Figures 5.3a and 5.3b.

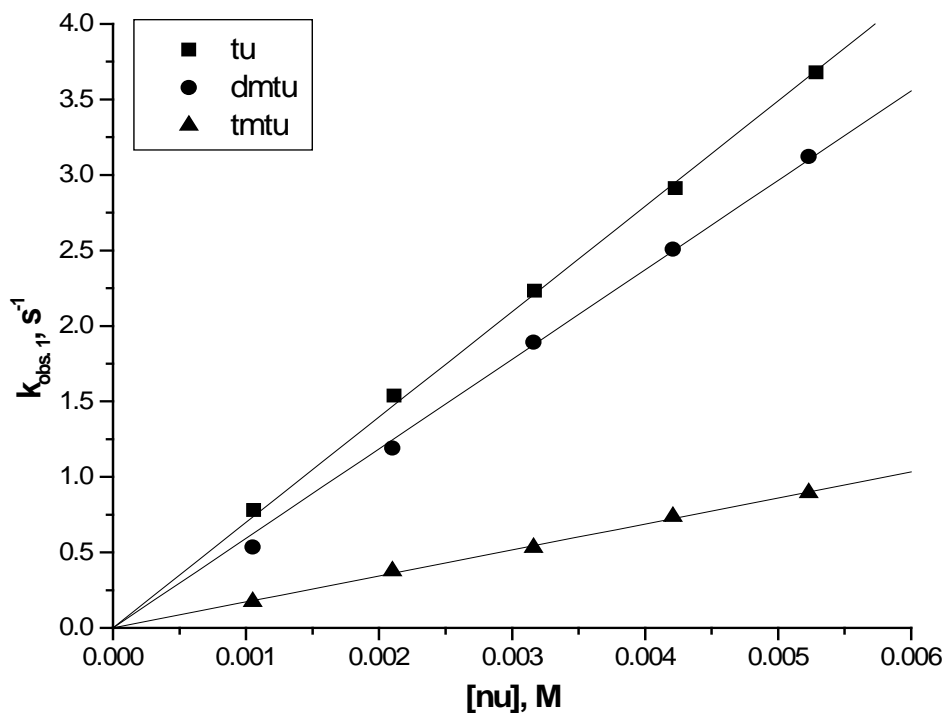


**Figure 5.4a** Concentration dependence of  $k_{obs(1)}^{st}$ ,  $s^{-1}$ , for the simultaneous displacement of the aqua ligands in **cHn** by thiourea nucleophiles, pH = 2.0, T = 298 K, I = 0.02 M {0.01 M  $CF_3SO_3H$ , adjusted with  $Li(SO_3CF_3)$ }.

## Pt(II) complexes with rigid diamine bridges

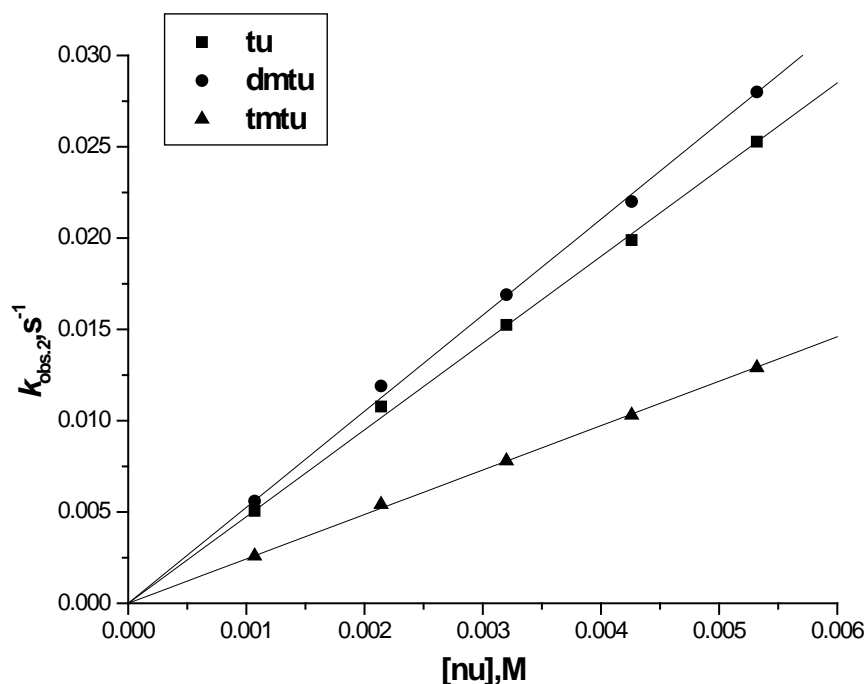


**Figure 5.4b** Concentration dependence of  $k_{obs(2)}^{nd}$ ,  $s^{-1}$ , for the dechelation of the pyridyl units in **cHn** by nucleophiles, pH = 2.0, T = 298 K, I = 0.02 M {0.01 M  $CF_3SO_3H$ , adjusted with  $Li(SO_3CF_3)$ }.

As previously proposed<sup>32,14a</sup>, the dependence of the observed pseudo first-order rate constants,  $k_{obs(1/2)}$ , on concentration of nucleophiles can be described by equation 1:

$$k_{obs(1/2)} = k_{2(1/2)}[Nu] \quad 5.1$$

where Nu = tu, dmtu, tmtu.

The values of the second-order rate constants,  $k_2$ , which resulted from the direct attack of the thiourea nucleophiles were obtained from the slopes of these plots at 25 °C and are summarized in Table 5.3 for complexes bridged by the phenyldiamine and diaminocyclohexane fragments, respectively. Included for comparison purposes in the same Table is the kinetic data of  $Pt(H_2O)(N,N\text{-bis}(2\text{-pyridylmethyl)amine})(CF_3SO_3)_2$  (**bpma**) and **bpha**. While the values of the rate constants of **bpma** determined in this study compares well with those from two previous studies,<sup>28,34</sup> a slower and second step due to the dechelation of one of the coordinated pyridyl units was observed in this study.

## Pt(II) complexes with rigid diamine bridges

**Table 5.3** Summary of the rate constants for the simultaneous substitution of aqua ligands and the dechelation of one of the pyridyl units by thiourea nucleophiles in bis(2-pyridylmethyl)amine chelated dinuclear complexes with aromatic bridges and their monomeric analogue.

Complex (Symmetry)	nu	Second order rate constant, $M^{-1} s^{-1}$	
		$k_{2/1}^{st}$	$k_{2/2}^{nd}$
<b>bpma</b>	<b>tu</b>	$409 \pm 2$	$4.95 \pm 0.06$
	<b>dmtu</b>	$394 \pm 1$	$4.05 \pm 0.07$
	<b>tmtu</b>	$190 \pm 0.5$	$2.16 \pm 0.06$
<b>bpPha</b> ( $C_{2h}$ )	<b>tu</b>	$702 \pm 3$	$6.32 \pm 0.1$
	<b>dmtu</b>	$940 \pm 3$	$6.35 \pm 0.09$
	<b>tmtu</b>	$223 \pm 2$	$3.32 \pm 0.02$
<b>mPh</b> ( $C_{2v}$ )	<b>tu</b>	$498 \pm 2$	$5.17 \pm 0.02$
	<b>dmtu</b>	$477 \pm 3$	$4.01 \pm 0.01$
	<b>tmtu</b>	$133 \pm 1$	$1.60 \pm 0.03$
<b>pPh</b> ( $C_{2h}$ )	<b>tu</b>	$487 \pm 4$	$4.21 \pm 0.02$
	<b>dmtu</b>	$569 \pm 3$	$4.81 \pm 0.06$
	<b>tmtu</b>	$253 \pm 1$	$2.28 \pm 0.02$
<b>dPhm</b> ( $C_{2v}$ ) <sub>distorted</sub>	<b>tu</b>	$555 \pm 4$	$4.65 \pm 0.02$
	<b>dmtu</b>	$490 \pm 5$	$4.84 \pm 0.04$
	<b>tmtu</b>	$295 \pm 2$	$2.64 \pm 0.02$
<b>bpha</b> <sup>§</sup> ( $C_{2h}$ )	<b>tu</b>	$566 \pm 3$	$4.24 \pm 0.07$
	<b>dmtu</b>	$668 \pm 4$	$5.94 \pm 0.05$
	<b>tmtu</b>	$187 \pm 0.3$	$2.04 \pm 0.01$
<b>bpcHna</b> ( $C_{2h}$ )	<b>tu</b>	$942 \pm 4$	$6.95 \pm 0.01$
	<b>dmtu</b>	$1031 \pm 6$	$9.56 \pm 0.02$
	<b>tmtu</b>	$209 \pm 1$	$2.18 \pm 0.05$
<b>cHn</b> ( $C_{2h}$ )	<b>tu</b>	$602 \pm 9$	$4.75 \pm 0.07$
	<b>dmtu</b>	$698 \pm 6$	$5.26 \pm 0.05$
	<b>tmtu</b>	$172 \pm 2$	$1.63 \pm 0.02$
<b>dcHnm</b> ( $C_{2v}$ )	<b>tu</b>	$774 \pm 3$	$7.76 \pm 0.07$
	<b>dmtu</b>	$937 \pm 3$	$8.69 \pm 0.09$
	<b>tmtu</b>	$211 \pm 2$	$2.43 \pm 0.05$

<sup>§</sup>Data extracted from Table 4.3a, Section 4.3.4, Chapter 4.

A comparison between the rate constants (Table 5.3a) for the substitution of the aqua ligands for the **bpPha** and **bpcHna** complexes (with appended rings) and **bpma** indicates that the former complexes are more reactive toward the thiourea nucleophiles. However, when compared to the reactivity of the amphiphiles reported in Chapter Four, it is noted that the influence on reactivity of the bis(2-pyridylmethyl)amine chelate headgroup due to the appended hydrocarbon rings (phenyl or cyclohexyl) of **bpPha** and **bpcHna** is stronger than

## *Pt(II) complexes with rigid diamine bridges*

---

from a primary alkyl tail of the amphiphiles and less than that due to tail appended through a tertiary  $\alpha$ -carbon (**bptba**). It follows that the effect of appending a phenyl or cyclohexyl ring to the *trans*-N donor atom of the bis(2-pyridylmethyl)amine chelate framework of **bpma**, is to increase the flow of electron density towards the Pt atom through  $\sigma$ -inductive effects from these cyclic groups.<sup>27</sup> Consequently, the Pt-N<sub>*trans*</sub> bond in the complexes should be shorter than that of **bpma**, resulting in higher rates of substitutions relative to **bpma**. Evidence in support of this comes from their calculated Pt-OH<sub>2</sub> bond lengths presented in Table 5.2b which are both longer than that of **bpma**.

The **bpcHna** show a slight reactive advantage over its phenyl analogue, **bpPha**. Since the only difference in these two complexes lies in the hybridization of their appended ring carbon atoms, the cyclohexyl ring clearly displays better  $\sigma$ -donor properties towards the N atom of the chelate framework than the phenyl ring. This is because the phenyl ring retains the electron density by delocalization through its  $\pi$ -framework, making it a slightly weaker  $\sigma$ -donor.<sup>27</sup> Consequently, the LUMO of **bpcHna** (11.09 eV.) is raised relative to that of **bpPha** (8.53 eV.) (refer to Table 5.2b) and the Pt-OH<sub>2</sub> (2.164 Å) of **bpcHna** is slightly longer than that of **bpPha** (2.155 Å).

If the comparison is extended to **bpha**, the effect of cyclizing a hexa carbon pendant is revealed if the rates of substitution of the aqua ligands are compared with those of **bpcHna**. Cyclization of the hexyl into cyclohexyl increases the rates in accordance with  $\sigma$ -donation which increase from **bpha** to **bpcHna**. The appended group in the **bpcHna** complex is bonded to the *trans*-N atom through a secondary carbon which is known to be a better  $\sigma$ -donor than a primary carbon, *vide supra*.<sup>27</sup> If the cyclohexyl functional pendant is regarded intuitively as formed through an intramolecular cyclization of the aliphatic hexyl pendant at its  $\alpha$ -carbon, then it is noted that this carbon is in fact receiving electron density by  $\sigma$ -inductive effects from two propyl-like fragments within its cyclic structure. Since reactivity is tuned on the basis of this structural difference occurring at its  $\alpha$ -carbon, it further reaffirms that the transfer of electronic charge towards the metal centre in these two functional groups is by inductive effects.

The order of substitution of the coordinated aqua ligands in these complexes by tu and dmtu nucleophiles is **bpcHna** > **bpha**  $\approx$  **bpPha** and reflects the strength in the *trans*-influence due to the inductive effects of the pendants. These effects decrease in the order of branching at the  $\alpha$ -carbon in the cyclic tail of **bpcHna** and the type of hybridization of the ring carbon atoms in the case of **bpPha**. For alkyl pendants with the same number of carbon

## *Pt(II) complexes with rigid diamine bridges*

---

atoms, reactivity of their complexes can be tuned through changing the structural nature as well as the hybridization of the carbon atoms.

However, when another **bpma** chelate headgroup is attached to phenyl and the cyclohexyl rings (to form the **pPh** and **cHn** dinuclear complexes respectively), it is noticed that the rate of the simultaneous substitution of the aqua ligands of the two dinuclear complexes are slightly lower than those of their respective mononuclear analogues and the calculated deceleration factors are of comparable magnitude. As shown in Table 5.2a, the symmetry elements ( $C_{2h}$ ) in the two sets of complexes are essentially the same with the only structural difference between them being the attachment of a second bis(2-pyridylmethyl)amine chelate headgroup, which confers an overall charge of +4 in the dinuclears. It becomes certain that the reduction in the rates of substitution of the aqua ligands of the dinuclears relative to that of mononuclear analogues is a result of a domineering steric influence that is felt at each Pt metal centres when two bis(2-pyridylmethyl)amine chelate headgroups are enjoined by a short and rigid ring bridge. The rigid and short phenyl or cyclohexyl bridge is inclined at an angle which is almost perpendicular to the equatorial square-planes such that the slipped-up coordination planes of their chelate-head groups mutually pose steric influence to the aerial approach of the nucleophiles on each Pt centre. It can be presumed that equal amounts of steric influences are felt by the Pt atoms of these two dinuclear complexes. A similar relation was observed between the  $\alpha,\omega$ -alkyldiamine bridge dinuclears of short chain length (**En** and **But**) and their analogous amphiphiles (**bpea** and **bpba**), respectively.

However, **cHn** is slightly more reactive than **pPh**. It becomes certain that the difference in the reactivity between **cHn** and **pPh** is a result of the difference in the  $\sigma$ -inductive contributions of each ring towards the N donor atom. The trend in the rate of substitution of the leaving group for both phenyl and the cyclohexyl-bridge sets of complexes corroborates well with what has already been reported in a recent study by Eldik *et al.*,<sup>26</sup> (vide supra) in which the shorter and conjugated but-1,3-diyne bridge increased the electrophilicity of the Pt metal atoms due to the bridge's efficient withdrawal of electron density from the metal atoms by  $\pi$ -resonance. Rigidity, a shorter Pt, Pt average distance and  $\pi$ -conjugation were cited as factors responsible for increased lability of the diaqua complexes. When the bridge was changed to saturated  $\alpha,\omega$ -diaminoalkanes ( $n = 8; 10$ ), which are longer and flexible, the electrophilicity of their Pt centres was curtailed as a result of better positive  $\sigma$ -inductive effect due to the  $\alpha,\omega$ -alkyldiamine linkers. This caused a reduction

## *Pt(II) complexes with rigid diamine bridges*

---

in the rates of substitutions of their aqua leaving groups when compared to the complex bearing the conjugated buta-1,3-diyne. However, for the dinuclear complexes reported in Chapter Three, a reduction in the reactivity is observed when the average Pt, Pt distance is short (**En** and **But**) due to a dominating steric effect brought about by the overlap geometry of the bis(2-pyridylmethyl)amine chelate headgroup.<sup>14a</sup>

When the reactivity of **pPh** is compared to its isomeric analogue, **mPh**, a similar retardation is observed for the isomers relative to **bpPha**, their common mononuclear analogue. This is despite the optimized molecular structures of these two isomeric complexes falling into two differently symmetry point groups, namely, the  $C_{2v}$  (bowl) and  $C_{2h}$  (slip-up sandwiches) point groups, respectively. As discussed before and proposed for the anomalous high reactivity of **Prop** from the previous work,<sup>14a</sup> the bowl-shaped **mPh** complex would be expected to exhibit a reactivity advantage over **pPh** due to the absence of the steric disposition on its equatorial coordination spheres coupled to an effective entrapment of the incoming nucleophiles that is mediated by the proposed cage effect.<sup>31</sup> However, from the optimized structure of **mPh** (Table 5.2a) and unlike that of **Prop**, the bowl cavity formed by the overlooking coordination faces of the chelate headgroups of **mPh** is blocked by the phenyl bridge which protrudes into the cavity of the bowl thereby preventing entrapment<sup>32,31</sup> effect to the nucleophiles. The steric hindrance to the approach of the incoming nucleophiles by the atoms of the phenyl bridge results in a poor localization effect to the incoming nucleophiles leading to a reduction in the rates of substitution. Thus, in these two complexes the magnitude of the steric effects mutually disposed on each equatorial coordination plane in **pPh** is of comparable magnitude to the steric hindrance of the protruding phenyl atoms in the **mPh** complex.

When the length of the bridge is extended to a diamine bridge comprising two rings (aniline or cyclohexylamine) connected back to back by a methylene spacer to form an asymmetric connecting fragment of nine carbon atoms in **dPhm** and **dcHnm**, the coordinated aqua ligands of the two dinuclears are not labilized to the same extent despite them falling in the same  $C_{2v}$  point group. As already stated the changes in the structures of the two bridges introduce limited flexibility (through the spacer) as well as large average separation distances of the Pt centres which forms the basal length of the bowl trough of these two complexes. However, the reactivity of **dPhm** does not differ significantly from that of **pPh** while that of **dcHnm** is increased relative to that of **cHn**. As pointed out earlier, the distortion in the trough structure of **dPhm**, coupled to the low-depth nature of its cavity reduces the entrapment<sup>31,30</sup> of

## *Pt(II) complexes with rigid diamine bridges*

---

the nucleophiles significantly at the twisted coordination planes of this complex leading to heavily distorted bowl trough structure. Thus, for this reason, no reactivity advantage over its homologous analogue, **pPh** is expected.

Unlike in the phenylamine-spaced bridge complexes, the effect of inserting a methylene carbon spacer between two cyclohexyl pendants of **bpcHna** units is relayed within the entire molecular structure of the **dcHnm** complex. An undistorted trough-shaped structure of **dcHnm** aides some form of entrapment<sup>31,30</sup> of incoming nucleophiles even though it might be relatively less effective due to the shallowness of the cavity of the trough. As expected for this molecular structure, a combination of some cage effect<sup>31</sup> and an increased separating distance in the Pt centres results the reactivity advantage. Thus, the methylene spacer enjoining two moderately flexible cyclohexyl rings has the role of not only increasing the average length of the diamine bridge but also of determining the symmetry elements within the entire diamino bridge necessary to maintain in an in-plane geometry at the *N,N*-bis(2-pyridylmethyl)amine Pt chelates. The slight better trough-bowl cavity of **dcHnm** results in high rates of substitution in this complex when compared to **dPhm**, a complex whose trough bowl is heavily distorted. Coupled to this, is the superior  $\sigma$ -inductive ability of cyclohexyl ring framework relative to the phenyl ring system occurring towards the *trans*-N donor atom of the chelates.<sup>27</sup>

A common observation in the reactivity of these complexes is a second substitution step which is less sensitivity to the structural changes emanating from the linking diamino bridge. This behaviour is consistent with a substitution step involving the dechelation of one of the pyridyl units of the non-labile chelate ligand as proposed in a previous study<sup>32</sup> and observed in the dinuclears of Chapter Three and the analogous amphiphiles of Chapter Four. The second substitution step, thus proceed at an invariably slowly rate, which is about two order of magnitude lower than for the simultaneous displacement of the aqua ligands. This is possibly due to the increased constraints in the transition states, poised on the incoming nucleophiles as they displace the coordinated pyridyl ligand at an already hindered Pt centre.<sup>35,36,30</sup> The presence of an unexpected second substitution in both of the monomeric complexes (**bpPha** and **bpcHna**) reaffirms the proposition of the dechelation of one of the *cis*-pyridyl units of the chelate ligand from the Pt(II) metal ion.<sup>32,14a</sup> Similar de-coordination of chelated amine ligands at a square-planar have been reported for Au(III),<sup>36</sup> Pt(II) and Pd(II) metal centres<sup>37</sup> by sulfur containing nucleophiles. The Pt metal centre in particular has a high propensity to form stable bonds with the soft sulfur nucleophilic base than the weaker amine ligands.<sup>39</sup>

## *Pt(II) complexes with rigid diamine bridges*

The reactivity of the nucleophiles reflects the steric effects in the case of tmtu characteristic of a mechanism involving bond making in the transition state. The rates of the simultaneous substitutions of the aqua in these complexes by tmtu are about three times lower than those of either tu or dmtu. This reactivity trend is in line with the steric size of this nucleophile relative to the other two. The presence of four methyl substituents adjacent to the sulfur donor atom of this nucleophile retards its rates of approach at the Pt metal centres, resulting in lower substitution rates. When compared to the reactions involving tu and dmtu, this nucleophile causes only a marginal change in reactivity when the structural features of the dinuclear complexes are changed across the two sets of complexes. As reported in other similar substitution reactions,<sup>40,34,28</sup> the nucleophilicity of dmtu was found to be comparable and in some cases superior to that of tu despite a slight increase in the steric bulkiness of this nucleophile. The  $\sigma$ -donation of electron density into the thiocarbonyl bond due to the two methyl groups of dmtu causes an increase in the basicity<sup>27b</sup> of the sulfur donor atom relative to tu's, resulting in competitive reactivity at the Pt centres in these complexes due to the positive inductive effect from the two methyl groups. The sensitivity of the substitution reactions to the steric sizes of these nucleophiles also confirms the associative nature of the activation process.<sup>39,30</sup> The observed trend is also true for the second substitution step that involves the dechelation of the coordinated pyridyl unit.

The dependence of the second-order rate constants on temperature were also studied in the range 15-35 °C. The thermal activation parameters for the substitution and the subsequent dechelation step ( $\Delta H_{(1/2)}^\ddagger$ ;  $\Delta S_{(1/2)}^\ddagger$ ) were calculated from the slopes and the intercepts of their Eyring plots,<sup>35</sup> respectively, as formulated in the equation 2,

$$\ln\left(\frac{k_2}{T}\right) = -\frac{\Delta H^\ddagger}{RT} + \left(23.8 + \frac{\Delta S^\ddagger}{R}\right). \quad 5.2$$

Exemplary Eyring plots are shown below in Figures 4.5a & 4.5b for the two reaction steps of **cHn** with nucleophiles.

## *Pt(II) complexes with rigid diamine bridges*

---

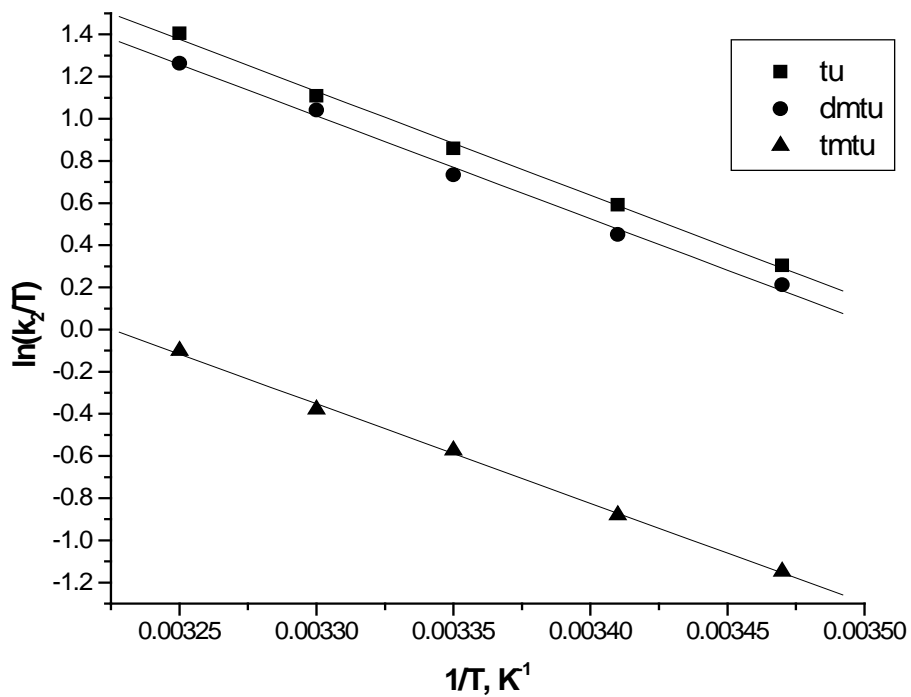


**Figure 5.5a** Temperature dependence of  $k_{2(1)^{st}}, M^{-1} s^{-1}$ , for the simultaneous displacement of the first aqua ligand in  $cHn$  by thiourea nucleophiles pH = 2.0, I = 0.02 M (0.01 M  $CF_3SO_3H$ , adjusted with  $Li(SO_3CF_3)$ ).

## *Pt(II) complexes with rigid diamine bridges*

---

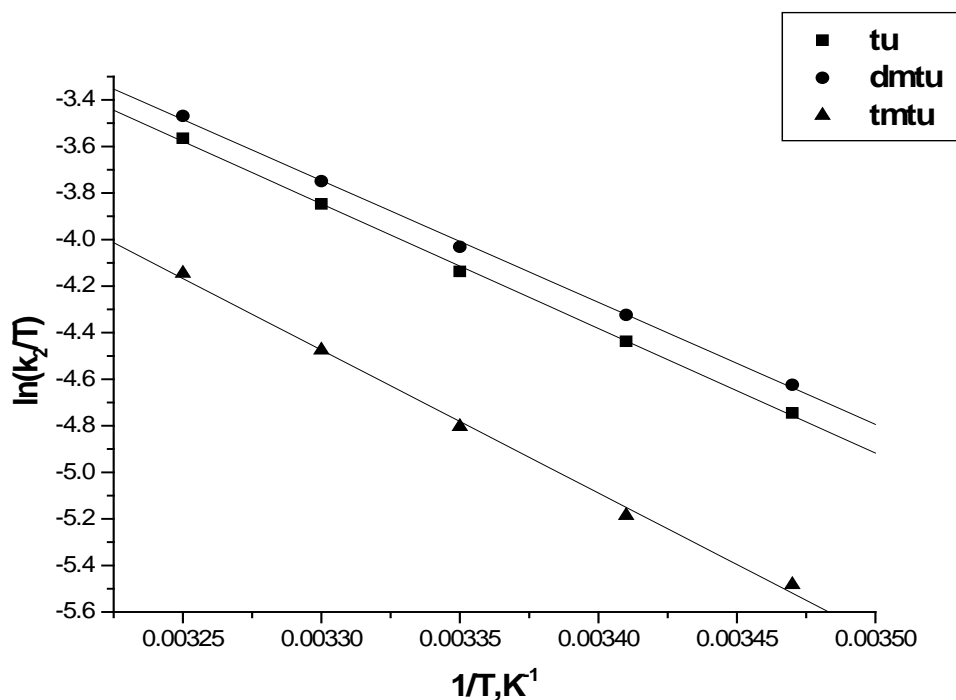


**Figure 5.5b** Temperature dependence of  $k_{2(2^{nd})}$ ,  $M^{-1} s^{-1}$ , for the dechelation of the pyridyl units in **cHn** by thiourea nucleophiles, pH = 2.0, I = 0.02 M (0.01 M  $CF_3SO_3H$ , adjusted with  $Li(SO_3CF_3)$ ).

The activation data from the plots are presented in Tables 5.4 for the phenyldiamine- and diaminocyclohexane-bridged complexes, respectively.

## *Pt(II) complexes with rigid diamine bridges*

**Table 5.4a** Summary of the activation parameters for the simultaneous displacement of aqua ligands and the dechelation of one of the pyridyl units by thiourea nucleophiles in bis(2-pyridylmethyl)amine chelated dinuclear complexes with aromatic bridges and their monomeric analogue.

Complexes	nu	Activation enthalpy, kJ mol <sup>-1</sup>		Activation entropy, J mol <sup>-1</sup> K <sup>-1</sup>	
		$\Delta H^\ddagger_1$	$\Delta H^\ddagger_2$	$\Delta S^\ddagger_1$	$\Delta S^\ddagger_2$
bpma	tu	41.1 ± 0.9	46.1 ± 0.3	-57.5 ± 3.0	-78.8 ± 0.8
	dmtu	37.2 ± 0.9	52.0 ± 1.2	-70.7 ± 3.0	-59.3 ± 3.8
	tmtu	43.3 ± 1.1	59.3 ± 1.0	-56.3 ± 3.4	-37.5 ± 3.0
bpPha	tu	37.8 ± 1.4	45.7 ± 1.3	-63.5 ± 4.3	-76.7 ± 4.0
	dmtu	32.5 ± 0.7	42.6 ± 0.8	-79.5 ± 2.3	-86.4 ± 2.4
	tmtu	41.6 ± 1.3	52.3 ± 1.1	-61.0 ± 3.8	-69.9 ± 3.3
mPh	tu	34.2 ± 0.8	31.9 ± 1.6	-78.3 ± 2.0	-123.6 ± 4.0
	dmtu	28.2 ± 0.2	42.1 ± 0.7	-98.4 ± 0.8	-88.6 ± 2.0
	tmtu	46.7 ± 1.3	54.6 ± 1.2	-73.7 ± 4.0	-61.6 ± 3.5
pPh	tu	31.9 ± 1.5	44.9 ± 0.5	-93.6 ± 4.0	-82.9 ± 1.7
	dmtu	34.7 ± 0.6	44.1 ± 0.3	-76.0 ± 2.0	-84.7 ± 1.1
	tmtu	52.6 ± 1.3	52.1 ± 1.4	-73.7 ± 4.0	-85.2 ± 4.2
dPhm	tu	38.1 ± 0.6	45.7 ± 0.9	-145.9 ± 2.0	-79.1 ± 3.0
	dmtu	36.9 ± 0.7	43.9 ± 0.9	-74.6 ± 2.0	-85.0 ± 3.0
	tmtu	42.1 ± 0.3	50.2 ± 0.4	-96.8 ± 1.0	-69.0 ± 1.4
bpha <sup>§</sup>	tu	42.5 ± 1.1	41.7 ± 0.8	-50.3 ± 3.2	-92.8 ± 2.5
	dmtu	36.9 ± 0.8	42.6 ± 0.8	-68.3 ± 3.0	-86.4 ± 2.4
	tmtu	43.8 ± 1.3	53.7 ± 0.7	-55.0 ± 4.0	-60.3 ± 2.3
bpcHna	tu	24.3 ± 0.7	42.5 ± 1.8	-106.0 ± 2.0	-85.8 ± 6.0
	dmtu	34.3 ± 0.7	5.0 ± 1.6	-75.2 ± 2.2	-76.5 ± 5.0
	tmtu	39.4 ± 0.4	53.7 ± 0.4	-64.5 ± 1.4	-58.7 ± 1.3
cHn	tu	31.9 ± 1.5	45.5 ± 0.8	-106.0 ± 2.0	-82.9 ± 2.6
	dmtu	40.6 ± 1.4	43.5 ± 0.9	-75.2 ± 2.2	-83.5 ± 2.8
	tmtu	39.1 ± 1.6	51.1 ± 0.6	-64.5 ± 1.6	-66.5 ± 5.0
dcHnm	tu	38.4 ± 0.8	44.0 ± 1.1	-61.2 ± 3.0	-80.6 ± 2.6
	dmtu	40.9 ± 2.0	40.9 ± 0.8	-57.2 ± 2.2	-90.2 ± 2.6
	tmtu	46.6 ± 1.6	53.4 ± 0.9	-64.5 ± 1.4	-54.9 ± 3.0

<sup>§</sup>Data extracted from Table 4.3c, Section 4.3.4, Chapter 4.

From the results of the temperature dependence of the second-order rate constants presented in Tables 5.4, all the values of the enthalpies of activation ( $\Delta H^\ddagger_{(1/2)}$ ) are small while the values of the activation entropies ( $\Delta S^\ddagger_{(1/2)}$ ) are large and negative. Thus, the mechanism of substitution for both steps remains associative in nature.<sup>39</sup> The activation enthalpies for the

## *Pt(II) complexes with rigid diamine bridges*

---

dechelation of one of the pyridyl units are slightly larger than for the simultaneous substitution of the aqua ligands, indicating the slower nature of the former process.

### 4.4 Conclusions

This study has shed some light on the role of the rigidity of the diamine linkers in the substitution reactions of chelated dinuclear complexes. It can therefore be concluded that the observed reactivity differences in the studied dinuclear complexes stems mainly from the extent of steric influences exerted on the Pt square-planar chelates atoms from the structural make-up of the linking bridge. These steric effects depend on the symmetry elements of the linker as well as on the average distance separating the Pt atoms of the dinuclear complexes, as determined by the average length of the diamino linker. In this study when the distance is short (**pPh** and **cHn**), the complexes are less reactive than their respective analogues (**dPhm** and **dcHnm**) whose Pt, Pt separation distances have been extended through incorporation of a methylene spacer between two of their respective ring fragments. However, by incorporating a methylene spacer between the two cyclohexylamine or phenylamine moieties of the diamine bridge, not only is the distance separating the Pt atoms of the latter complexes increased, but their molecular structures are architected into trough-shaped bowls whose symmetry elements are mediated by the extent of rigidity and planarity of the rings. Unlike the rigid 4,4'-methylenediphenylamine bridge of **dPhm** which causes a heavy distortion to its trough-shaped structure, the relatively flexible 4,4'-methylenediaminocyclohexane bridge allows a better  $C_{2v}$  trough-shaped structure in the **dcHnm** complex, leading to its enhanced reactivity over **dPhm** complex due to its better abilities to 'entrap' incoming nucleophiles in its cavity in the transition state.

Complexes bridged by diaminocyclohexane (**cHn** and **dcHnm**) or appended to a cyclohexylamine (**bpcHna**) fragments showed a slight reactivity advantage over those bridged by phenyldiamines (**pPh**; **mPh** and **dPhm**) or with an appended phenylamine (**bpPha**) group, indicating that the former types of bridges or pendants are better  $\sigma$ -donors<sup>27b</sup> towards the Pt atoms. The reactivity difference between the **pPh** and **cHn**, two isosteric complexes bridged by short and rigid bridges and having a common  $C_{2h}$  point group symmetry better demonstrate this point. Because of their similar metrics and symmetry, similar steric impositions due to their overlap geometry can be assumed at their Pt square-planes. The higher reactivity of **cHn**

## *Pt(II) complexes with rigid diamine bridges*

---

can only be attributed to the better  $\sigma$ -donor of the diaminocyclohexane bridge when compared to the phenyldiamine of **pPh** towards the Pt centres.

Although no evidence of liberation of the diamine linkers or amine pendants from the dinuclear and their mononuclear complexes by the strong substituting thiourea nucleophiles was recorded, a second step taken to be a partial ring opening of the bis(2-pyridylmethethyl)amine chelate headgroups was observed in all cases. The mode of activation remained associative in nature in all cases.

### 5.5 References

- 1 V. Brabec and J. Kasparková, *J. Drug Resistance Updates*, 2002, **8**, 131.
- 2 (a) M. J. Bloemink and J. Reedijk, In, *Metal ion Biological systems*, 1996, **32**, A. Sigel, H. Sigel Eds., Marcel Dekker, New York, 641; (b) M. Adams, R. P. A'Hern, A. H. Calvert, J. Carmichael, P. I. Clark, R. E and Coleman, *Br. J. Cancer*, **78**, 1998, 1404.
- 3 (a) J. Kasparková, J. Nováková, O. Vrána, N. Farrell and V. Brabec, *J. Biol. Inorg. Chem.*, 1999, **38**, 10997; (b) J. Kasparková, J. Zehnulova, N. Farrell and V. Brabec, *J. Bio. Inorg. Chem.*, 2002, **277**, 48076; (c) M. S. Ali, K. H. Whitmire, T. Toyomasi, Z. H. Siddik and A. R. Khokhar, *J. Inorg. Biochem.*, 1999, **77**, 231; (d) J. W Cox, S. J. Berners-Price, M. S. Davies, W. Barlage, Y. Qu and N. Farrell, *Inorg. Chem.*, 2000, **39**, 1710.
- 4 J. Kasparková, O. Vraná, N. Farrell and V. Brabec, *J. Biol. Inorg. Chem.*, 2004, **98**, 1560.
- 5 (a) Q. Liu, Y. Qu, R. van Antwerpen and N. Farrell, *Biochemistry*, 2006, **45**, 4248; (b) N. Farrell, Y. Qu and M. P. Hacker, *J. Med. Chem.*, 1990, **33**, 2179; (c) L. R. Kelland, B. A. Murrer, G. Abel, C. M. Giandomenica, P. Mistry and K. R. Harrap, *Cancer Res.*, 1992, **52**, 822; (d) P. Perego, L. Gatti, C. Caserini, R. Supino, D. Colangelo and R. Leone, *J. Inorg. Biochem.*, 1999, **77**, 59; (e) M. S. Davies, J. W. Cox, S. J. Berners-Price, Y. Qu and N. Farrell, *J. Am. Chem. Society*, 2001, **123**, 1316.
- 6 N. Farrell, *Comm. Inorg. Chem.*, 1995, **16(6)**, 373. (b) N. J. Wheate and J. G. Collins, *Coord. Chem. Rev.*, 2003, 133. (c) H. Silva, C. V. Barra, C. F. Da Costa, M. V. De Almeida, E. T. Cesar, J. N. Silveira, A. Garneir-Suillerot, F. C. F. de Paula, E. C. Pereira-Maia and A. P. S. Fontes, *J. Inorg. Biochem.*, 2008, **102**, 767.
- 7 S. Komeda, G. V. Kalayda, M. Lutz, A. L. Spek, T. Sato, M. Chikuma and J. Reedijk, *J. Med. Chem.*, 2003, **46**, 1210.
- 8 G. V. Kalayada, S. Komeda, K. Ekedda, T. Sato, M. Chikuma and J. Reedijk, *Inorg. Chem.*, 2003, 4347.
- 9 (a) N. J. Wheate, C. Cullinane, L. K. Webster and J. G. Collins, *Anti-Cancer Drug Des.*, 2001, **16**, 91; (b) D. M. Fan, X. L. Yang, X. Y. Wang, J. F. Mao, J. Ding, L. P. Lin and Z. J. Guo, *J. Biol. Inorg. Chem.*, 2007, **12**, 677.

## *Pt(II) complexes with rigid diamine bridges*

---

- 10 (a) Y. Zhao, W. He, P. Shi, J. Zhi, L. Qui, L. Lin and Z. Guo, *J. Chem. Soc., Dalton Trans.*, 2006, 2617; (b) X. Wang and Z. Guo, *J. Chem. Soc., Dalton Trans.*, 2007, 1521.
- 11 S. W. Johnson, K. V. Ferry and T. C. Hamilton, *Drug Resistance Update*, 1998, **1**, 243.
- 12 F. Huq, H. Daghriri, J. Q. Yu, H. Tayyern, P. Beale and M. Zhang, *Eur. J. Med. Chem.*, 2004, **39**, 947.
- 13 (a) A. Hofmann and R. van Eldik, *J. Chem. Soc., Dalton Trans.*, 2003, 2979. (b) D. Jaganyi, V. M. Munisamy and D. Reddy, *Int. J. of Chem. Kinet.*, 2006, **38**, 202.
- 14 (a) A Mambanda, D. Jaganyi, S. Hochreuther and R. van Eldik, *Dalton Trans.*, 2010, **39**, 1; (b) H. Ertürk, A. Hofmann, R. Puchta and R. van Eldik *J. Chem. Soc., Dalton Trans.*, 2007, 2295.
- 15 (a) J. Reedijk, *Chem. Rev.*, 1999, **99**, 2499; (b) J. Reedijk, *PNAS.*, 2003, **100**, 3611; (c) D. Petrović, B. Stojimirović, B. Petrović, Z. M. Bugarčić and Z. D. Bugarčić, *Bioorg. Med. Chem.*, 2007, **15**, 4203.
- 16 Z. Tyeklár, R. R. Jacobson, N. Wei, N. N. Murthy, J. Zubieta, K. D. Karlin, *J. Am. Chem. Soc.*, 1993, **115**, 2677.
- 17 (a) T. Buchen, A. Hazell, L. Jessen, C. J. McKenzie, L. P. Nielson, J. Z. Pedersen and D. Schollmeyer, *J. Chem. Soc., Dalton Trans.*, 1997, 2697; (b) S. Foxon, J. Xu, S. Turba, M. Leibold, F. Hampel, O. Walter, C. Wurtele, M. Holthausen and S. Schindler, *Eur. J. Inorg. Chem.*, 2007, 423.
- 18 A. Sato, Y. Mori and T. Lida, *Synthesis*, 1992, 539.
- 19 H. Toftlund and S. Yde-Andersen, *Acta Chem. Scand.*, 1981, **A35** (8), 575.
- 20 Z. D. Bugarčić, B. V. Petrović and R. Jelić, *Transition Met. Chem.*, 2001, **26**, 668.
- 21 (a) R. A. Friesner, *Chem. Phys. Lett.*, 1985, **116**, 539; (b) R. A. Friesner, *Annual Rev. Chem. Phys.*, 1991, **42**, 341.
- 22 (a) A. D. Becke, *J. Chem. Phys.*, 1993, **98**, 5648; (b) C. Lee, W. Yang and R. G. Parr, *Phys. Rev.*, 1998, **B37**, 785.
- 23 (a) Spartan 04, Wavefunction, Inc., 18401 von Karman Avenue, Suite 370, Irvine, CA, 92612, USA; Q-Chem, Inc, The Design Center, suite 690, 5001, Baum Blvd., Pittsburgh, 15213, USA, 2004. <http://www.wavefun.com/>; (b) K. Kong, C. A. White, A. I. Krylov, C. D. Sherrill, R. D. Adamson, T. R. Furlani, M. S. Lee, A. M. Lee, S. R. Gwaltney, T. R. Adams, C. Ochsenfeld, A. T. B. Gilbert, G. S. Kedziora, V. A. Rassolov, D. R. Maurice, N. Nair, Y. Shao, N. A. Besley, P. E. Maslen, J. P. Dombroski, H. Daschel, W. Zhang, P. P. Korambath, J. Baker, E. F. C. Byrd, T. van Voorhuis, M. Oumi, S. Hirata, C. P. Hsu, N. Ishikawa, J. Florian, A. Warshel, B. G. Johnson, P. M. W. Gill and B. G. Pople, *J. Computational Chem.*, 2000, **21**, 1532.

## *Pt(II) complexes with rigid diamine bridges*

---

- 24 (a) P. C. Hariharan and J. A. Polpe, *J. A. Chem. Phys. Lett.* 1972, **16**, 217; (b) P. J. Hay and W.R. Wadt, *J. A. Chem. Phys. Lett.*, 1985, **82**, 299.
- 25 (a) B. Pitteri, G. Annibale, G. Marangoni, V. Bertolasi and V. Ferretti, *Polyhedron*, 2002, **21**, 2283.
- 26 H. Ertürk, R. Puchta and R. van Eldik, *Eur. J. Inorg. Chem.*, 2009, 1334.
- 27 (a) A. Albert and E. P. Serjant, *Ionization constants of Acid and Bases*, 1962, Methuen, London. (b) P. Y. Bruice, *Organic Chemistry*, 2<sup>nd</sup> Ed., Prentice Hall, 1998, pp. 363-366. (c) M. Shmülling, D. M. Grove, G. van Koten, R. van Eldik, N. Veldman and A. L. Spek, *Oganometallics*, 1996, **15**, 1384
- 28 (a) D. Jaganyi, A. Hofmann and R. van Eldik, *Angew. Chem. Int. Ed.*, 2001, **40**, 680; (b) A. Hofmann, D. Jaganyi, O. Q. Munro, G. Liehr and R. van Eldik, *Inorg. Chem.*, 2003, **42**, 1688.
- 29 U. Maran, H. Conley, M. Frank, A. M. Arif, A. M. Orendt, D. Britt, V. Hlady, R. Davis and P. J. Stang, *Langmuir*, 2008, **24**, 5400.
- 30 R. J. Mureinik and W. Robb, *Inorg. Chim. Acta.*, 1971, **5(3)**, 333.
- 31 (a) P. W. Atkins, *Physical Chemistry*, 6<sup>th</sup> Ed., Oxford University Press, Oxford, 1998, pp. 825-827. (b) K. J. Laidler and J. H., Meiser, *Physical Chemistry*, 3<sup>rd</sup> Ed., Houghton Mifflin, Boston, 1999, pp. 465-466.
- 32 H. Ertürk, J. Maigut, R. Puchta and R. van Eldik, *J. Chem. Soc., Dalton Trans.*, 2008, 2759.
- 33 Origin<sup>7.5™</sup> SRO, v7.5714 (B5714), Origin Lab Corporation, Northampton, One, Northampton, MA, 01060, USA, 2003.
- 34 D. Jaganyi and F. Tiba, *Transition Met. Chem.*, 2003, **28**, 803.
- 35 J. H. Espenson, *Chemical Kinetics and Reaction Mechanism*, 2<sup>nd</sup> Ed., McGraw-Hill, New York, 1995, Chpt. 2 and 6.
- 36 G. Annibale, L. Cattalini, G. Natile, *J. C. S. Dalton*, 1975, 188.
- 37 (a) J. Tauben, M. Rodriguez, I. Zubiri and J. Reedijk, *J. Chem. Soc., Dalton Trans.*, 2000, 369; (b) E. L. M. Lempers and J. Reedijk, *Inorg. Chem*, 1990, **29**, 217; (c) T. G. Appleton, J. W. Connor, J. R. Hall, P. D. Prenzler, *Inorg. Chem.*, 1989, **28**, 2030; (d) E. W. Abel, S. K. Bhargava, K. G. Orrell, In *Progress in Inorganic Chemistry*, S. J. Lippard Ed., John Wiley, 1984, **32**, 1; (e) T. Rau, R. Alsfasser, A. Zahl, and R. Van Eldik, *Inorg. Chem.*, 1998, **37**, 4223.
- 38 (a) F. Basolo, H. B. Gray, R. G. Pearson, *J. Amer. Chem. Soc.*, 1960, **82**, 4200.
- 39 (a) M. L. Tobe and J. Burgess, *Inorganic Reaction Mechanisms*, Addison Wisey, Longman,

## *Pt(II) complexes with rigid diamine bridges*

---

*Ltd.*, Essex, 1999, pp. 30-33; 70-112.

- 40 (a) D. Jaganyi, F. Tiba, O. Q. Munro, B. Petrović and Z. D. Bugarčić, *Dalton Trans.*, 2006, 2943; (b) D. Jaganyi, K. De Boer, J. Gertenbach, J. Perils, *Inte. J. of Chem. Kinetics*, 2008, 809; (c) D. Reddy and D. Jaganyi, *Trans. Met. Chem.*, 2006, **31**, 792; (d) D. Jaganyi, D. Reddy, J. A. Gertenbach, O. Q. Munro and R. van Eldik, *Dalton Trans.*, 2004, 299.

### **5.6 Supplementary Information**

A summary of the wavelengths used for kinetics; exemplary mass spectra for ligands **L6** and **L7**, spectral changes for the titration of **bpPha** with NaOH; a kinetic trace showing the two reaction steps for a reaction mixture of tu (3 mM) and **bpcHna** (0.11 mM); exemplary Tables of data and the respective plots showing the dependence of  $k_{\text{obs.}(1/2^{\text{nd}})}$  on concentration of nucleophiles and temperature for some selected complexes (**bpcHna**, **dcHnm** and **pPh**), accompany the work reported in this Chapter as supporting information (SI).

**Table SI 5.1** Summary of the wavelengths (nm) used for monitoring the reactions between a series of Pt(II) complexes with bis(2-pyridylmethyl)amine chelates and thiourea nucleophiles.

## *Pt(II) complexes with rigid diamine bridges*

---

<b>Complex</b>	<b>nu</b>	<b>wavelength (<math>\lambda</math>), nm</b>
<b>bpPha</b>	tu	310
	dmtu	286
	tmtu	312
<b>mPh</b>	tu	312
	dmtu	325
	tmtu	335
<b>pPh</b>	tu	315
	dmtu	325
	tmtu	330
<b>dPhm</b>	tu	315
	dmtu	318
	tmtu	335
<b>bpcHna</b>	tu	283
	dmtu	284
	tmtu	315
<b>cHn</b>	tu	324
	dmtu	325
	tmtu	318
<b>dcHnm</b>	tu	325
	dmtu	325
	tmtu	327

## Pt(II) complexes with rigid diamine bridges

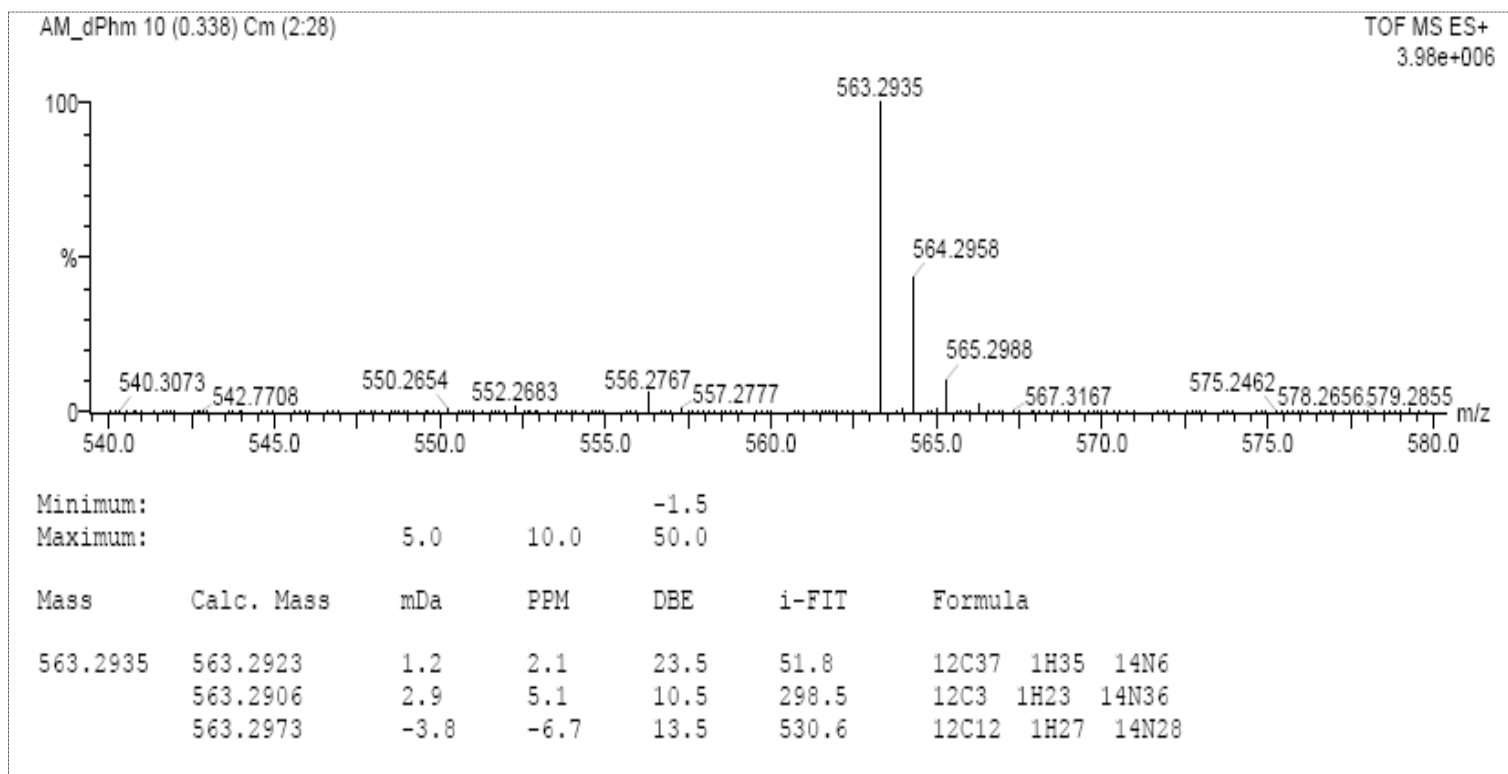


**Figure SI 5.1a** Mass spectrum (TOF-MS<sup>+</sup>) for *N,N,N',N'*-tetrakis(2-pyridylmethyl)-4,4'-methylenediphenylamine (**L6**).

## Pt(II) complexes with rigid diamine bridges

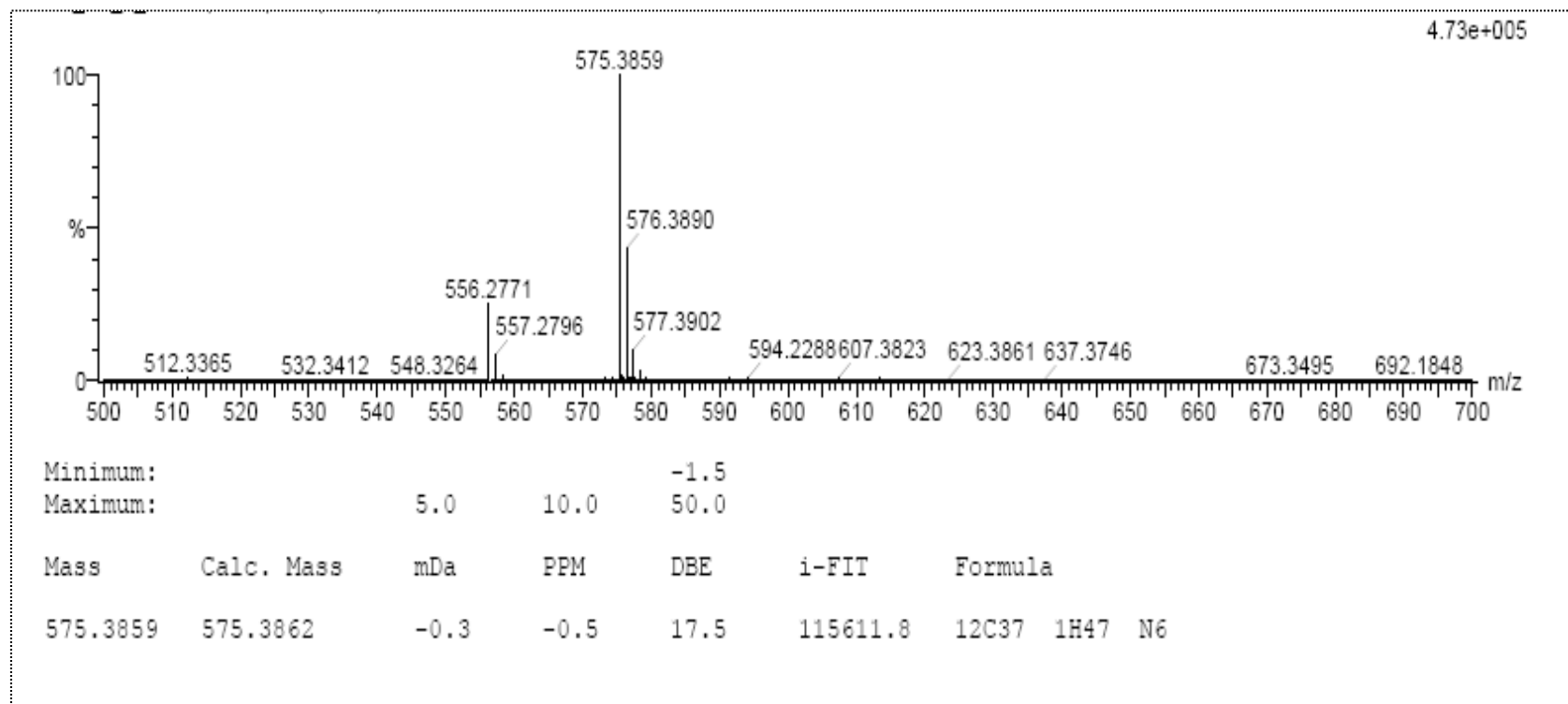


**Figure SI 5.1b** Mass spectrum (TOF-MS<sup>+</sup>) for *N,N,N',N'*-tetrakis(2-pyridylmethyl)-4,4'-methylenediaminocyclohexane (**L7**)

## *Pt(II) complexes with rigid diamine bridges*

---

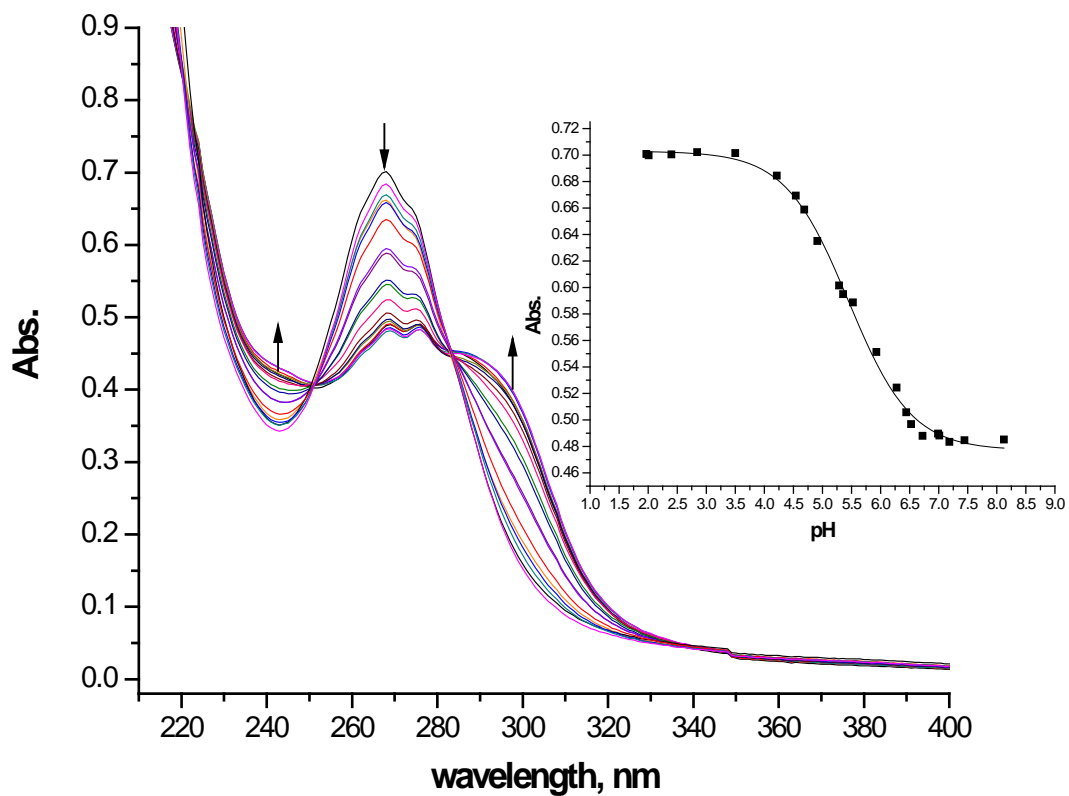


**Figure SI 5.2** UV-visible spectra for the titration of 0.1 mM **bpPha** with NaOH, pH range 2-9,  $T = 298$  K.

## *Pt(II) complexes with rigid diamine bridges*

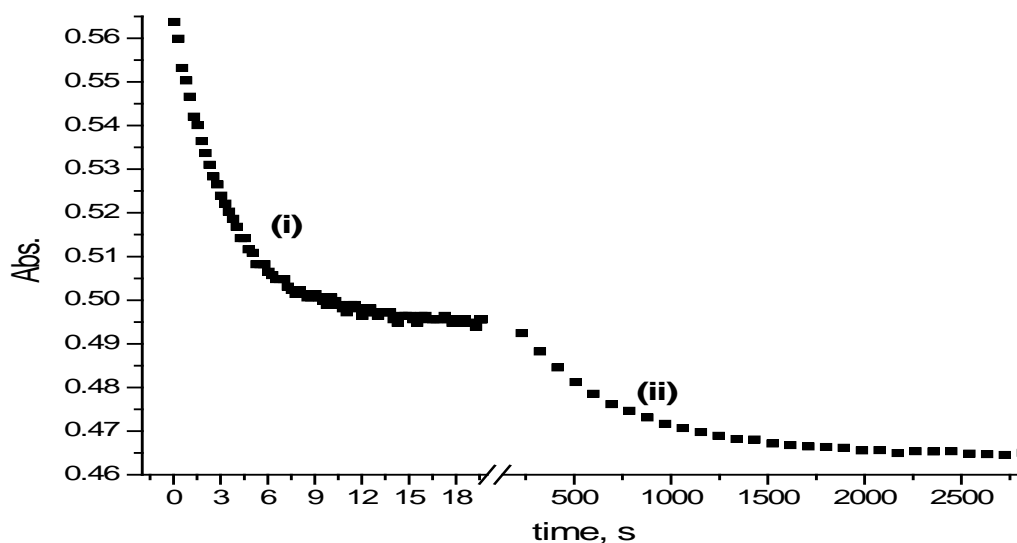


**Figure SI 5.3** A typical kinetic trace showing the two-steps reaction between **bpcHna** (0.1 mM) and **tu** (3 mM) recorded at 284 nm,  $T = 298$  K,  $\text{pH} = 2.0$ ,  $I = 0.02$  M  $\{\text{CF}_3\text{SO}_3\text{H}$ , adjusted with  $\text{Li}(\text{SO}_3\text{CF}_3)\}$ .

**Table SI 5.2a** Average observed rate constants,  $k_{\text{obs},(1^{\text{st}})}$ ,  $\text{s}^{-1}$ , for the simultaneous displacement of the aqua ligands in **bpcHna** by thiourea nucleophiles,  $\text{pH} = 2.0$ ,  $T = 298$  K,  $I = 0.02$  M  $\{0.01$  M  $\text{CF}_3\text{SO}_3\text{H}$ , adjusted with  $\text{Li}(\text{SO}_3\text{CF}_3)\}$ .

[tu], M	$k_{\text{obs}, 1}, \text{s}^{-1}$	[dmtu], M	$k_{\text{obs}, 1}, \text{s}^{-1}$	[tmtu], M	$k_{\text{obs}, 1}, \text{s}^{-1}$
5.33E-4	0.482	5.33E-4	0.525	5.34E-4	0.1166
0.0011	1.018	0.0011	1.081	0.0011	0.228
0.0016	1.525	0.0016	1.616	0.0016	0.334
0.0021	2.012	0.0021	2.194	0.0021	0.450
0.0027	2.496	0.0027	2.779	0.0027	0.551

## *Pt(II) complexes with rigid diamine bridges*

**Table SI 5.2b** Average observed rate constants,  $k_{\text{obs.}(2^{\text{nd}})}, \text{s}^{-1}$ , for the dechelation of the pyridyl units in **bpcHna** by thiourea nucleophiles, pH = 2.0, T = 298 K, I = 0.02 M {0.01 M  $\text{CF}_3\text{SO}_3\text{H}$ , adjusted with  $\text{Li}(\text{SO}_3\text{CF}_3)$ }.

[tu], M	$k_{\text{obs } 2}, \text{s}^{-1}$	[dmtu], M	$k_{\text{obs } 2}, \text{s}^{-1}$	[tmtu], M	$k_{\text{obs } 2}, \text{s}^{-1}$
5.33E-4	0.00409	5.3E-4	0.0048	5.33E-4	0.00128
0.0011	0.00794	0.0011	0.0095	0.0011	0.00216
0.0016	0.01064	0.0016	0.0147	0.0016	0.00374
0.0021	0.01464	0.0021	0.0198	0.0021	0.0046
0.0027	0.01864	0.0027	0.0266	0.0027	0.00573

**Table SI 5.2c** Temperature dependence of  $k_{2(1^{\text{st}})}, \text{M}^{-1} \text{s}^{-1}$ , for the simultaneous displacement of the aqua ligands in **bpcHna** by thiourea nucleophiles, pH = 2.0, I = 0.02 M (0.01 M  $\text{CF}_3\text{SO}_3\text{H}$ , adjusted with  $\text{Li}(\text{SO}_3\text{CF}_3)$ ).

tu		dmtu		tmtu	
1/T, K <sup>-1</sup>	ln(k/T)	1/T, K <sup>-1</sup>	ln(k/T)	1/T, K <sup>-1</sup>	ln(k/T)
0.00325	1.654	0.00325	1.758	0.00325	0.1939
0.0033	1.412	0.0033	1.502	0.0033	-0.07
0.00335	1.204	0.00335	1.253	0.00335	-0.368
0.00341	0.9062	0.00341	0.9781	0.00341	-0.608
0.00347	0.6515	0.00347	0.6894	0.00347	-0.974

**Table SI 5.2d** Temperature dependence of  $k_{2(2^{\text{nd}})}, \text{M}^{-1} \text{s}^{-1}$ , for the dechelation of the pyridyl units in **bpcHna** by thiourea nucleophiles, pH = 2.0, I = 0.02 M (0.01 M  $\text{CF}_3\text{SO}_3\text{H}$ , adjusted with  $\text{Li}(\text{SO}_3\text{CF}_3)$ ).

tu		dmtu		tmtu	
1/T, K <sup>-1</sup>	ln(k/T)	1/T, K <sup>-1</sup>	ln(k/T)	1/T, K <sup>-1</sup>	ln(k/T)
0.00325	-3.142	0.00325	-3.013	0.00325	-4.258
0.0033	-3.364	0.0033	-3.294	0.0033	-4.563
0.00335	-3.658	0.00335	-3.498	0.00335	-4.898
0.00341	-4.002	0.00341	-.858	0.00341	-5.281
0.00347	-4.231	0.00347	-4.217	0.00347	-5.675

## *Pt(II) complexes with rigid diamine bridges*

---

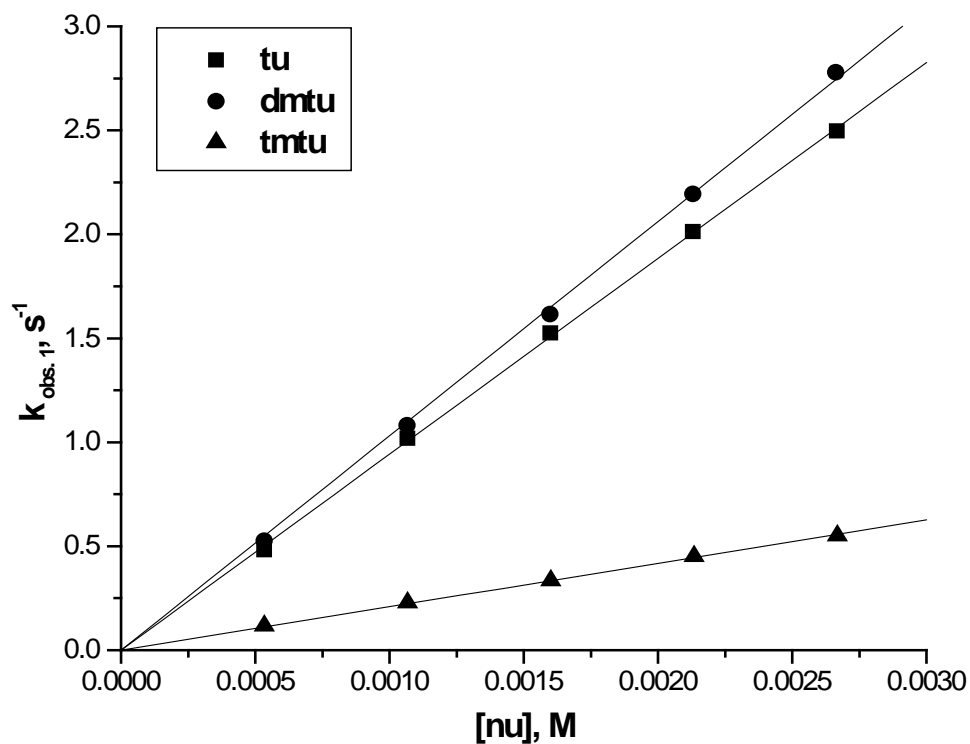


**Figure SI 5.4a** Concentration dependence of  $k_{\text{obs.}(1)}^{\text{st}}$ ,  $\text{s}^{-1}$ , for the simultaneous displacement of the aqua ligands in **bpcHna** by thiourea nucleophiles, pH = 2.0, T = 298 K, I = 0.02 M {0.01 M  $\text{CF}_3\text{SO}_3\text{H}$ , adjusted with  $\text{Li}(\text{SO}_3\text{CF}_3)$ }.

## *Pt(II) complexes with rigid diamine bridges*

---

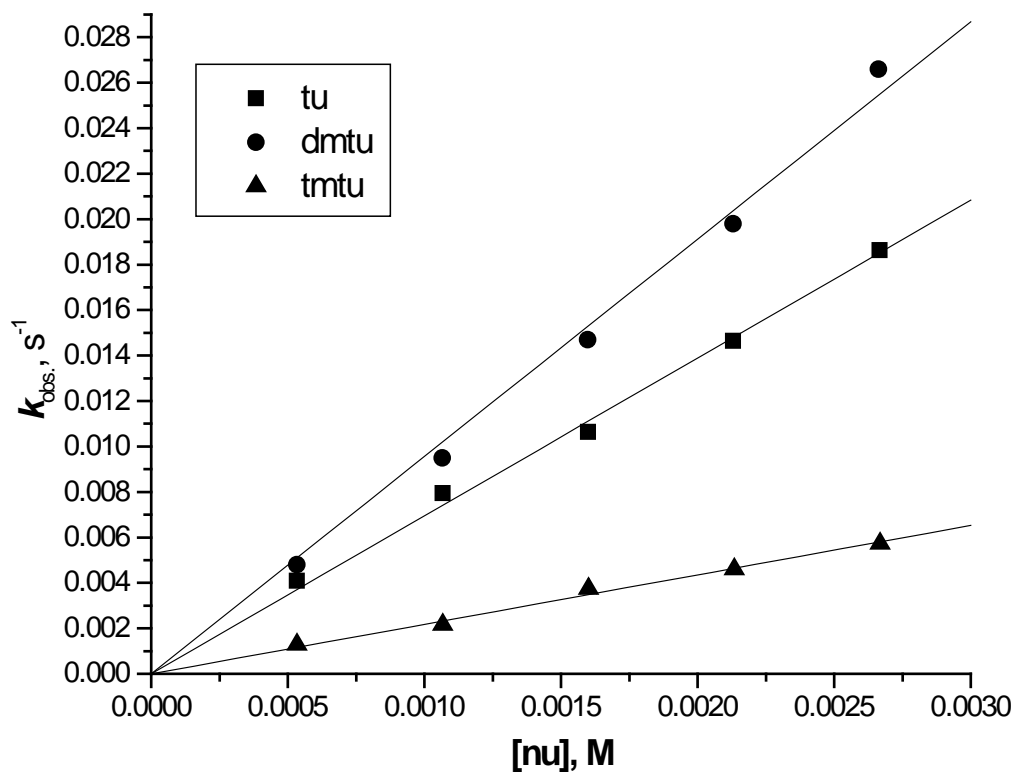


**Figure SI 5.4b** Concentration dependence of  $k_{\text{obs.}(2^{\text{nd}})}$ , s<sup>-1</sup>, for the dechelation of the pyridyl units in **bpcHna** by thiourea, pH = 2.0, T = 298 K, I = 0.02 M {0.01 M CF<sub>3</sub>SO<sub>3</sub>H, adjusted with Li(SO<sub>3</sub>CF<sub>3</sub>)}.

## *Pt(II) complexes with rigid diamine bridges*

---

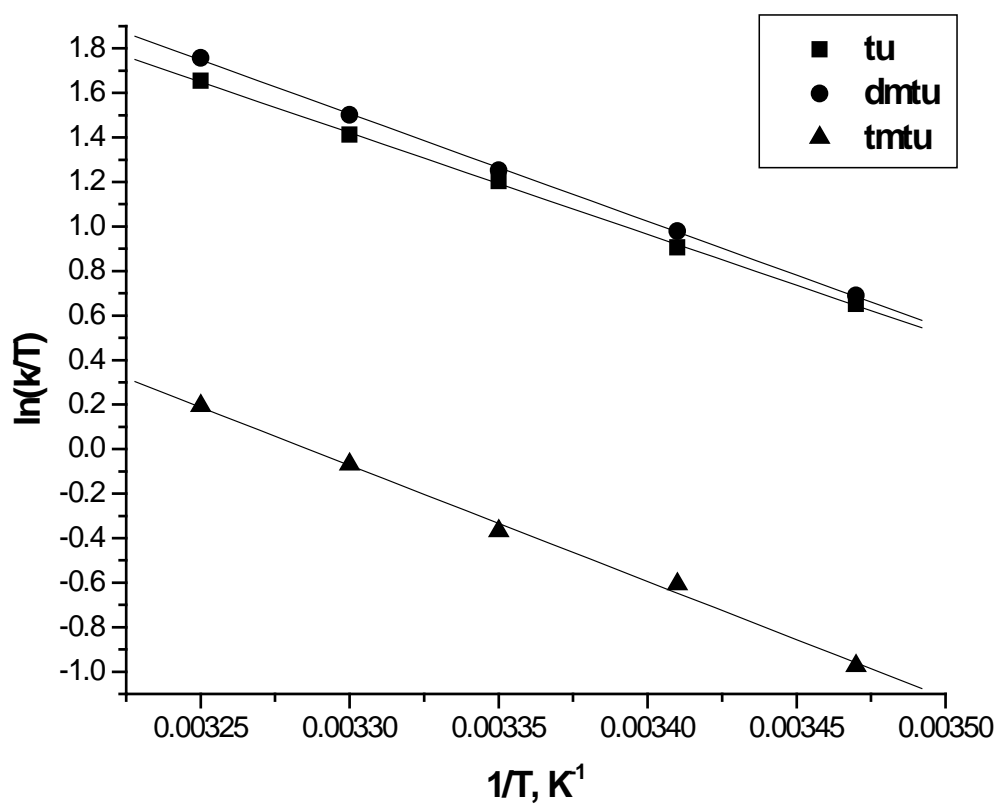


**Figure SI 5.5a** Temperature dependence of  $k_{2(1)}^{st}$ ,  $M^{-1} s^{-1}$ , for the simultaneous displacement of the first aqua ligand in **bpcHna** by thiourea nucleophiles, pH = 2.0, I = 0.02 M (0.01 M  $CF_3SO_3H$ , adjusted with  $Li(SO_3CF_3)$ ).

## Pt(II) complexes with rigid diamine bridges

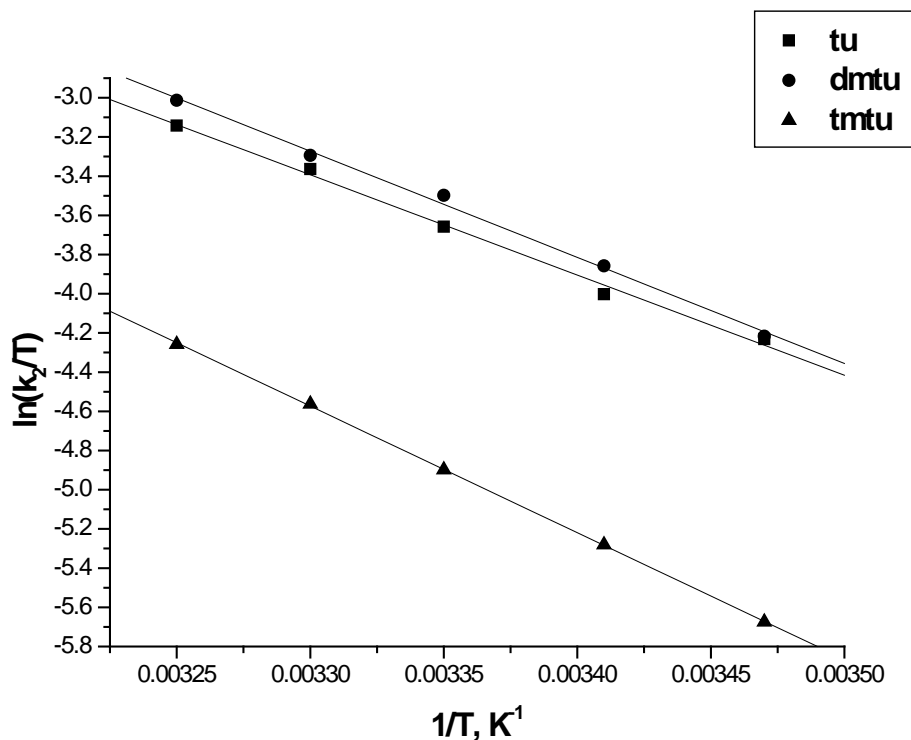


**Figure SI 5.5b** Temperature dependence of  $k_2$  ( $2^{\text{nd}}$ ),  $\text{M}^{-1} \text{s}^{-1}$ , for the dechelation of the pyridyl units in **bpcHna** by thiourea, pH = 2.0, I = 0.02 M (0.01 M  $\text{CF}_3\text{SO}_3\text{H}$ , adjusted with  $\text{Li}(\text{SO}_3\text{CF}_3)$ ).

**Table SI 5.3a** Average observed rate constants,  $k_{\text{obs},1}^{\text{st}}$ ,  $\text{s}^{-1}$ , for the simultaneous displacement of the aqua ligands in **dcHnm** by thiourea nucleophiles, pH = 2.0, T = 298 K, I = 0.02 M {0.01 M  $\text{CF}_3\text{SO}_3\text{H}$ , adjusted with  $\text{Li}(\text{SO}_3\text{CF}_3)$ }.

[tu], M	$k_{\text{obs},1}, \text{s}^{-1}$	[dmtu], M	$k_{\text{obs},1}, \text{s}^{-1}$	[tmtu], M	$k_{\text{obs},1}, \text{s}^{-1}$
0.00106	0.821	0.00107	0.9916	0.00107	0.224
0.00213	1.637	0.00213	1.983	0.00213	0.4554
0.00319	2.439	0.0032	2.965	0.0032	0.6678
0.00426	3.279	0.00426	4.001	0.00426	0.8921
0.00532	4.155	0.00533	5.016	0.00533	1.135

## *Pt(II) complexes with rigid diamine bridges*

**Table SI 5.3b** Average observed rate constants,  $k_{\text{obs.}(2^{\text{nd}})}$ ,  $\text{s}^{-1}$ , for the dechelation of the pyridyl units in **dcHnm** by thiourea nucleophiles,  $\text{pH} = 2.0$ ,  $T = 298 \text{ K}$ ,  $I = 0.02 \text{ M}$   $\{0.01 \text{ M CF}_3\text{SO}_3\text{H}$ , adjusted with  $\text{Li}(\text{SO}_3\text{CF}_3)\}$ .

[tu], M	$k_{\text{obs } 1}, \text{s}^{-1}$	[dmtu], M	$k_{\text{obs } 1}, \text{s}^{-1}$	[tmtu], M	$k_{\text{obs } 1}, \text{s}^{-1}$
0.00107	0.00826	0.00107	0.00925	0.00107	0.00259
0.00214	0.0176	0.00214	0.01971	0.00214	0.00551
0.0032	0.0249	0.0032	0.02789	0.0032	0.0078
0.00426	0.0325	0.00426	0.0364	0.00426	0.01017
0.00532	0.0413	0.00532	0.04626	0.00532	0.01293

**Table SI 5.3c** Temperature dependence of  $k_{2(1^{\text{st}})}$ ,  $\text{M}^{-1} \text{s}^{-1}$ , for the simultaneous displacement of the aqua ligands in **dcHnm** by thiourea nucleophiles,  $\text{pH} = 2.0$ ,  $I = 0.02 \text{ M}$  (0.01 M  $\text{CF}_3\text{SO}_3\text{H}$ , adjusted with  $\text{Li}(\text{SO}_3\text{CF}_3)$ ).

tu		dmtu		tmtu	
$1/T, \text{K}^{-1}$	$\ln(k/T)$	$1/T, \text{K}^{-1}$	$\ln(k/T)$	$1/T, \text{K}^{-1}$	$\ln(k/T)$
0.00325	1.452	0.00325	1.604	0.00325	0.2837
0.0033	1.203	0.0033	1.4265	0.0033	-0.0318
0.00335	0.963	0.00335	1.149	0.00335	-0.3366
0.00341	0.7257	0.00341	0.8833	0.00341	-0.6413
0.00347	0.4208	0.00347	0.5258	0.00347	-0.9573

**Table SI 5.3d** Temperature dependence of  $k_{2(2^{\text{nd}})}$ ,  $\text{M}^{-1} \text{s}^{-1}$ , for the dechelation of the pyridyl units in **dcHnm** by thiourea nucleophiles,  $\text{pH} = 2.0$ ,  $I = 0.02 \text{ M}$  (0.01 M  $\text{CF}_3\text{SO}_3\text{H}$ , adjusted with  $\text{Li}(\text{SO}_3\text{CF}_3)$ ).

tu		dmtu		tmtu	
$1/T, \text{K}^{-1}$	$\ln(k/T)$	$1/T, \text{K}^{-1}$	$\ln(k/T)$	$1/T, \text{K}^{-1}$	$\ln(k/T)$
0.00325	-3.078	0.00325	-3.005	0.00325	-4.104
0.0033	-3.356	0.0033	-3.264	0.0033	-4.449
0.00335	-3.643	0.00335	-3.53	0.00335	-4.80
0.00341	-3.939	0.00341	-3.805	0.00341	-5.172
0.00347	-4.244	0.00347	-4.088	0.00347	-5.549

## *Pt(II) complexes with rigid diamine bridges*

**Table SI 5.4a** Average observed rate constants,  $k_{\text{obs.}(1)^{\text{st}}}$ ,  $\text{s}^{-1}$ , for the simultaneous displacement of the aqua ligands in **pPh** by thiourea nucleophiles,  $\text{pH} = 2.0$ ,  $T = 298 \text{ K}$ ,  $I = 0.02 \text{ M}$  {0.01 M  $\text{CF}_3\text{SO}_3\text{H}$ , adjusted with  $\text{Li}(\text{SO}_3\text{CF}_3)$ }.

[tu], M	$k_{\text{obs } 1}, \text{s}^{-1}$	[dmtu], M	$k_{\text{obs } 1}, \text{s}^{-1}$	[tmtu], M	$k_{\text{obs } 1}, \text{s}^{-1}$
5.3366E-4	0.4904	5.3366E-4	0.397	5.3366E-4	0.1197
0.00107	0.9981	0.00107	0.7997	0.00107	0.2355
0.0016	1.495	0.0016	1.183	0.0016	0.3578
0.00213	2.03	0.00213	1.561	0.00213	0.4847
0.00267	2.498	0.00267	1.988	0.00267	0.588

**Table SI 5.4b** Average observed rate constants,  $k_{\text{obs.}(2)^{\text{nd}}}$ ,  $\text{s}^{-1}$ , for the dechelation of the pyridyl units in **pPh** by thiourea nucleophiles,  $\text{pH} = 2.0$ ,  $T = 298 \text{ K}$ ,  $I = 0.02 \text{ M}$  {0.01 M  $\text{CF}_3\text{SO}_3\text{H}$ , adjusted with  $\text{Li}(\text{SO}_3\text{CF}_3)$ }.

[tu], M	$k_{\text{obs } 2}, \text{s}^{-1}$	[dmtu], M	$k_{\text{obs } 2}, \text{s}^{-1}$	[tmtu], M	$k_{\text{obs } 2}, \text{s}^{-1}$
5.3366E-4	0.00307	5.3366E-4	0.00336	5.3366E-4	0.00185
0.00107	0.0061	0.00107	0.00674	0.00107	0.0037
0.0016	0.01013	0.0016	0.01016	0.0016	0.00524
0.00213	0.01305	0.00213	0.01354	0.00213	0.00705
0.00267	0.01698	0.00267	0.01684	0.00267	0.00888

**Table SI 5.4c** Temperature dependence of  $k_{2(1)^{\text{st}}}$ ,  $\text{M}^{-1} \text{s}^{-1}$ , for the simultaneous displacement of the aqua ligands in **pPh** by thiourea nucleophiles,  $\text{pH} = 2.0$ ,  $I = 0.02 \text{ M}$  {0.01 M  $\text{CF}_3\text{SO}_3\text{H}$ , adjusted with  $\text{Li}(\text{SO}_3\text{CF}_3)$ }.

tu		dmtu		tmtu	
$1/T, \text{K}^{-1}$	$\ln(k/T)$	$1/T, \text{K}^{-1}$	$\ln(k/T)$	$1/T, \text{K}^{-1}$	$\ln(k/T)$
0.00325	1.379	0.00325	1.558	0.00325	0.207
0.0033	1.131	0.0033	1.354	0.0033	-0.049
0.00335	0.927	0.00335	1.146	0.00335	-0.319
0.00341	0.655	0.00341	0.9108	0.00341	-0.6345
0.00347	0.315	0.00347	0.7042	0.00347	-0.8789

## *Pt(II) complexes with rigid diamine bridges*

---

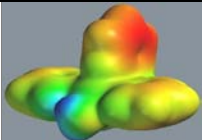
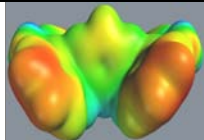
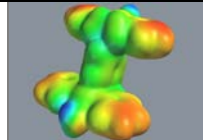
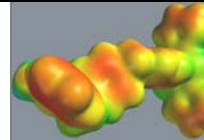
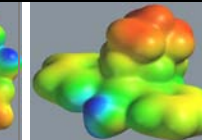
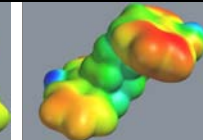
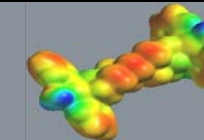
**Table SI 5.4d** Temperature dependence of  $k_2$  ( $2^{\text{nd}}$ ),  $\text{M}^{-1} \text{s}^{-1}$ , for the dechelation of the pyridyl units in **pPh** by thiourea nucleophiles,  $\text{pH} = 2.0$ ,  $I = 0.02 \text{ M}$  { $0.01 \text{ M CF}_3\text{SO}_3\text{H}$ , adjusted with  $\text{Li}(\text{SO}_3\text{CF}_3)$ }.

<b>tu</b>		<b>dmtu</b>		<b>tmtu</b>	
<b>1/T, K<sup>-1</sup></b>	<b>ln(k/T)</b>	<b>1/T, K<sup>-1</sup></b>	<b>ln(k/T)</b>	<b>1/T, K<sup>-1</sup></b>	<b>ln(k/T)</b>
0.00325	-3.253	0.00325	-3.258	0.00325	-3.511
0.0033	-3.546	0.0033	-3.494	0.0033	-3.859
0.00335	-3.852	0.00335	-3.781	0.00335	-4.195
0.00341	-4.148	0.00341	-4.057	0.00341	-4.601
0.00347	-4.465	0.00347	-4.386	0.00347	-5.018

## *Pt(II) complexes with rigid diamine bridges*

---

**Table SI 5.5** Electrostatic potential surface mappings of the dinuclear Pt(II) complexes bridged by rigid linkers and their mononuclear analogues.

Complex	bpPha	mPh	pPh	dPhm	bpcHna	cHn	dcHnm
EPS							

## *Pt(II) complexes with rigid diamine bridges*

---

### **5.7** Commentary notes (CN) to section 4.2.2.

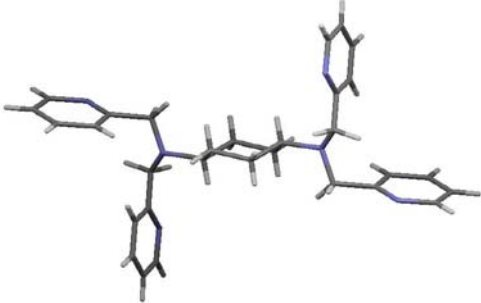
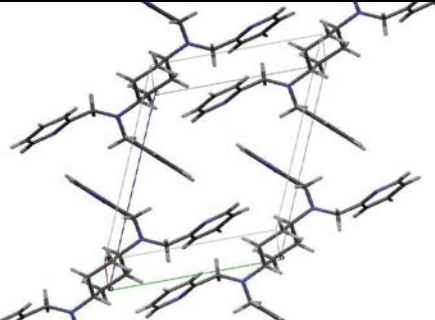
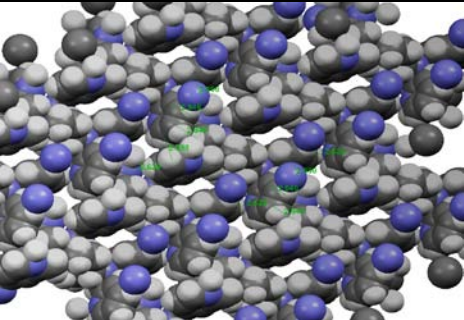
#### **5.7.1** *X-rays diffraction analysis of N,N,N',N'-tetrakis(2-pyridylmethyl)-trans-1,4-cyclohexyldiamine (L6).*

Colourless crystals were yielded for the ligands **L6** and **L7** through slow evaporation of the ethanol solvent over several days. The crystal structure of **L6** was solved X-ray diffraction analysis while **L7** gave a poor diffraction pattern.

The molecular structure was determined on an Oxford Diffraction Xcalibur2 CCD diffractometer equipped with Oxford cryojet operated at 100 K. Data collection was performed by the *CrystAlis CCD* program while cell refinement and data reduction were done using the *CrystAlis RED* suite of programs.<sup>1</sup> Crystal structures were solved and refined by the SHELXL97<sup>2</sup> software while the *Orterp*<sup>3</sup> and *WinGX*<sup>4</sup> were used for all molecular graphics. A summary of the crystal structure, packing and other important structural data for **L6** are given in Tables CN 4.1a and 4.1b. However, the data was not of sufficiently good quality to meet the stringent requirements for a crystallographic publication.

## *Pt(II) complexes with rigid diamine bridges*

**Table CN 5.1a** Summary of the crystal structure unit cell contents and CPK crystal packing of ligand L6.

Complex	Structure	Unit cell	CPK molecular packing
cHn			

## *Pt(II) complexes with rigid diamine bridges*

---

**Table CN 5.1b** A summary of the structural data of ligand **L6**.

---

Identification code	chex_100_4s_red1
Empirical formula	C <sub>15</sub> H <sub>17</sub> N <sub>3</sub>
Formula weight	239.32
Temperature	571(2) K
Wavelength	0.71073 Å
Unit cell dimensions	a = 6.1551(3) Å; α=70.817(6)°. b = 9.0775(6) Å; β=84.173(5)°. c = 12.6170(9) Å; γ=73.982(5)°.
Volume	639.91(7) Å <sup>3</sup>
Calculated density	1.242 Mg m <sup>-3</sup>
Absorption coefficient	0.076 mm <sup>-1</sup>
F(000)	256
Crystal size	0.60 x 0.55 x 0.20 mm
θ-range for data collection	3.83 to 31.92°.
Limiting indices	-6<=h<=9, -13<=k<=13, -18<=l<=18
Reflections collected/unique	6363/3895; [R <sub>(int)</sub> =0.0170]
Completeness to theta = 25.00	99.2 %
Max. and min. transmission	0.9850 and 0.9560
Refinement method	Full-matrix least-squares on F <sup>2</sup>
Data/restraints/parameters	3895/0/163
Goodness-of-fit on F <sup>2</sup>	1.168
Final R indices [I>2σ(I)]	R1 = 0.0847, wR <sup>2</sup> = 0.2460
R indices (all data)	R1 = 0.0960, wR <sup>2</sup> = 0.2515
Largest diff. peak and hole	0.776 and -0.313 e.Å <sup>-3</sup>

---

### **5.7.2 Comment on the crystal structure of ligand L4.**

In *N,N,N',N'*-tetrakis(2-pyridylmethyl)*trans*-1,4-diaminocyclohexane, C<sub>30</sub>H<sub>34</sub>N<sub>6</sub>, a new bis(tridentate) ligand has been synthesized. The molecules are linked face to face into a slip-up chain collinear to the axis containing the nitrogen atoms of the *trans*-1,4-diaminocyclohexane centre-piece. Each chain is stabilized by two sets of hydrogen bonding interactions. The first type is an unconventional (alkyl)C-H...N hydrogen bonds, involving the closest hydrogen atoms of the picolyl arm and the pyridyl N atoms, while the second type involves the N atoms and π-type C-H in neighbouring ring. The molecule has an inversion symmetry whose centre is located at the centroid of the *trans*-1,4-diaminocyclohexane.

Of interest is the packing arrangement of its molecules in the solid which shows some loose packing arrangements characterized by a two dimensional collinear networks of some cyclohexyl-shaped open voids as shown in Table CN 5.1a. Even though the existence of true channels within the lattice structure is not evident, **L4** can be a potentially useful agent for ultrapurification of cyclohexane solvents which are contaminated with smaller and difficult-to-

## *Pt(II) complexes with rigid diamine bridges*

---

remove gaseous contaminants. A modified distillation technique in which contaminated cyclohexane is vapourised and the vapour front of the mixture allowed to come into intimate contact with an adsorption bed of ligand **L4** would easily achieve the same kind of purification only achievable by costly techniques such as fractional distillation. In the vapour, the smaller molecular weight contaminants, especially those with similar boiling point ranges to cyclohexane or which form azeotropic mixtures with it can easily percolate through the open voids of **L4** in the cyclohexane adsorption bed. In this way, column bed of ligand **L4** is serving as molecular sieving bed or sorbents of cyclohexane since its molecules can snugly fit on the shape-specific open channels of the bed, thereby trapping them for a subsequent desorption step. A simple condensation step of the cyclohexane-impregnated column bed will afford the ultrapure cyclohexane solvent in which the undesirable (e.g. potentially wetting and smaller but difficult-to-separate nuisances) contaminants would have been efficiently removed. Large quantities of ultrapure cyclohexane solvent are required worldwide in the oleochemical and the pharmaceutical industries.

### **5.7.3 References to the commentary notes.**

- 1 Oxford Diffraction, *CrysAlis CCD* and *CrysAlis RED*, Versions 1.171.29.9 (Release 23-03-2006 CrysAlis 171. Net), 2006, Oxford Diffraction Ltd., Abingdon, Oxfordshire, England.
- 2 G. M. Sheldrick, *SHELXS97* and *SHELXL97*, 1997, University of Göttingen, Germany.
- 3 L. J. Farrugia, *J. Appl. Cryst.*, 1997, **30**, 565.
- 4 L. J. Farrugia, *J. Appl. Cryst.*, 1999, **32**, 837.

## Appendix

### Appendix A

#### Structural papers on the ligands.

<b>Paper A1</b>	D. Jaganyi, <b>A. Mambanda</b> and O. Q. Munro, A tripodal tris(thiophene) derivative of hexahydropyrimidine and its ladder-like extended structure' <i>Acta Cryst.</i> , 2007, <b>E63</b> , o2388–o2390.	<b>258</b>
<b>Paper A2</b>	<b>A. Mambanda</b> , D. Jaganyi, and O. Q. Munro, One-dimensional C-H...N hydrogen-bonded polymers in flexible tetrapyridyl systems, <i>Acta Cryst.</i> , 2007, <b>C63</b> , o676–o680.	<b>262</b>
<b>Paper A3</b>	<b>A. Mambanda</b> , D. Jaganyi and K. Stewart, <i>N,N</i> -bis(2-pyridylmethyl)- <i>tert</i> -butylamine, <i>Acta Cryst.</i> , 2009, <b>E65</b> , o402.	<b>268</b>

## Paper A1

electronic reprint

Acta Crystallographica Section E

Structure Reports

Online

ISSN 1600-5368

Editors: W. Clegg and D. G. Watson

### A tripodal tris(thiophene) derivative of hexahydropyrimidine and its ladder-like extended structure

Deogratius Jaganyi, Allen Mambanda and Orde Q. Munro

Copyright © International Union of Crystallography

Author(s) of this paper may load this reprint on their own web site provided that this cover page is retained. Republication of this article or its storage in electronic databases or the like is not permitted without prior permission in writing from the IUCr.

## organic papers

Acta Crystallographica Section E  
Structure Reports  
Online

ISSN 1600-5368

Deogratius Jaganyi, Allen  
Mambanda and Orde Q. Munro\*

School of Chemistry, University of KwaZulu-  
Natal, Pietermaritzburg, Private Bag X01,  
Scottsville 3209, South Africa

Correspondence e-mail: munroo@ukzn.ac.za

### Key indicators

Single-crystal X-ray study

$T = 110$  K

Mean  $\sigma(\text{C}-\text{C}) = 0.002$  Å

$R$  factor = 0.029

$wR$  factor = 0.082

Data-to-parameter ratio = 27.2

For details of how these key indicators were  
automatically derived from the article, see  
<http://journals.iucr.org/e>.

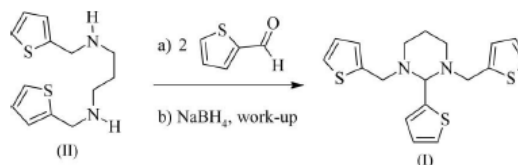
## A tripodal tris(thiophene) derivative of hexahydropyrimidine and its ladder-like extended structure

Received 20 March 2007  
Accepted 31 March 2007

In the title compound, 2-(2-thienyl)-1,3-bis(2-thienylmethyl)-perhydropyrimidine,  $\text{C}_{18}\text{H}_{20}\text{N}_2\text{S}_3$ , a new hexahydropyrimidine derivative with no formal crystallographic symmetry (but approximate  $C_3$  molecular symmetry), the thiophene rings are approximately orthogonal to the mean plane of the saturated pyrimidine 'core' of the molecule, with the three S atoms positioned on one side of the six-atom mean plane. The S atom of the directly attached thiophene ring is involved in an unconventional (alkyl)C—H...S hydrogen bond ( $\text{H}\cdots\text{S} = 2.87$  Å) with a thiophene CH group of the closest neighbouring molecule, leading to a ladder-like one-dimensional chain as the extended structure. The crystal specimen used for data collection was an inversion twin [twin fraction  $x = 0.41$  (4)].

### Comment

Sato *et al.* (1992) have described a method for the synthesis of *N,N'*-bis(2-pyridylmethyl)-*N,N'*-bis(2-thienylmethyl)-1,2-ethanediamine. Our goal was to synthesize the tetra(thiophene) analogue with a propyldiamine core for binding two  $\text{Pt}^{\text{II}}$  ions. Contrary to expectation, addition of two equivalents of thiophene-2-carbaldehyde to *N,N'*-bis(2-thienylmethyl)-1,2-propanediamine, (II), followed by  $\text{NaBH}_4$  reduction afforded the title compound, (I), the Mannich cyclization product (Buchen *et al.*, 1997).



Compound (I) is a hexahydropyrimidine derivative, and the six-membered ring core adopts a chair conformation (Fig. 1). This was confirmed quantitatively by Cremer–Pople ring puckering (CPRP) analysis (Cremer & Pople, 1975), which gave a  $\theta$  value closer to  $0^\circ$  (chair) than  $50.8^\circ$  (half-chair). [The CPRP amplitudes were  $Q = 0.594$  (2) Å,  $\theta = 4.1$  (1)° and  $\varphi = 89$  (2)°.] Each atom of the six-membered ring thus deviates systematically from the six-atom mean plane: atom N1 by 0.243 (1), C6 by  $-0.263$  (1), N2 by 0.263 (1), C16 by  $-0.241$  (2), C17 by 0.221 (2) and C18 by  $-0.221$  (2) Å. The weighted average absolute torsion angle for the six-membered ring is  $59$  (6)° and reflects a near-ideal (+)-synclinal conformation.

The thiophene rings are oriented with the three S atoms lying within the same plane. The dihedral angles of each

© 2007 International Union of Crystallography  
All rights reserved

02388 Jaganyi *et al.* •  $\text{C}_{18}\text{H}_{20}\text{N}_2\text{S}_3$

doi:10.1107/S1600536807016017

Acta Cryst. (2007). E63, o2388–o2390

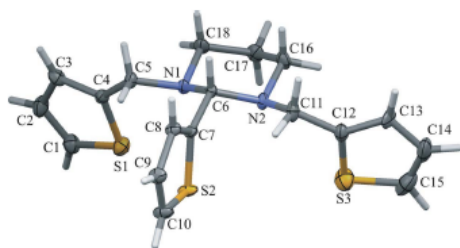


**Figure 1**  
The molecular structure of (I), with 60% probability displacement ellipsoids. H atoms are shown only as the end-points of bonds represented as cylinders.

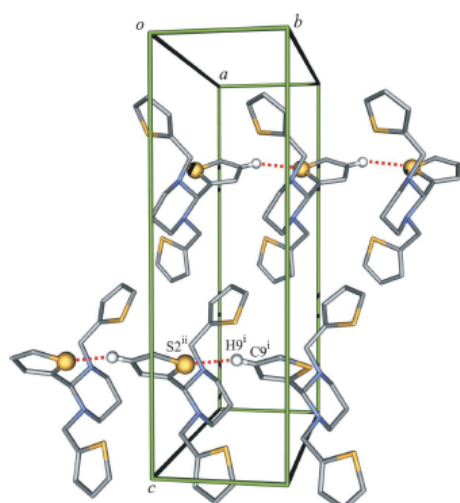


**Figure 2**  
A partial packing diagram for (I), showing two chains of interacting molecules with an interaction axis collinear with the unit-cell *b* axis. Dashed lines indicate hydrogen bonds. Interacting H and S atoms are represented as spheres of arbitrary radii. Non-interacting H atoms have been omitted for clarity. All other atoms are shown only as the intersections of bonds represented as cylinders. [Symmetry codes: (i)  $\frac{1}{2} - x, \frac{1}{2} + y, \frac{3}{2} + z$ ; (ii)  $\frac{1}{2} - x, -\frac{1}{2} + y, \frac{3}{2} + z$ .]

thiophene ring relative to the mean plane of the hexahydropyrimidine ring are  $81.6(1)^\circ$  (S1/C1–C4 ring),  $87.9(1)^\circ$  (S2/C7–C10 ring) and  $82.0(1)^\circ$  (S3/C12–C15 ring). The three thiophene rings exhibit significant in-plane libration, even at 110 K (*cf.* the displacements for atoms C14 and C15). However, the C–S bonds average  $1.712(6) \text{ \AA}$  (Table 1) and their precision is thus not overly affected by this thermal motion.

A significant attractive intermolecular interaction (Fig. 2, Table 2) exists between atom H9 and atom S2<sup>i</sup> of a neighbouring molecule [symmetry code: (i)  $x, y - 1, z$ ]. The H9...S2<sup>i</sup> distance ( $2.87 \text{ \AA}$ ) is shorter than the sum of the van der Waals radii of S and H by  $0.13 \text{ \AA}$  (Bondi, 1964). The geometry is consistent with an unconventional hydrogen bond

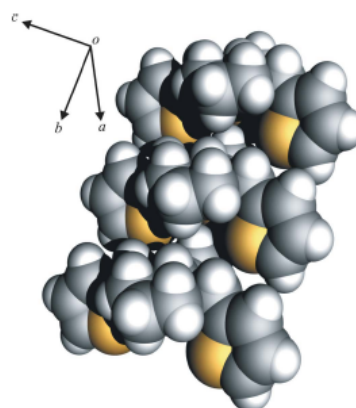


**Figure 3**  
A space-filling model of three interacting molecules of (I), showing the ladder-like one-dimensional hydrogen-bonded extended structure. The axis of the stack is collinear with the *b* axis of the unit cell.

between  $sp^2$ -hybridized S and a  $\pi$ -type C–H donor (Steiner, 2002). Molecules of (I) are thus held together (probably only weakly and in the condensed phase) to form a one-dimensional hydrogen-bonded stack whose axis is collinear with the *b* axis of the unit cell. Each molecule within the stack is translated by 1 along the *b*-axis direction [ $(x, y - 1, z)$ ,  $(x, y, z)$ ,  $(x, y + 1, z)$  *etc.*] to give a molecular sequence reminiscent of the steps in a conventional ladder (Fig. 3).

## Experimental

Under a flow of nitrogen, a solution of 2-thiophenecarbaldehyde (4.45 ml, 47.6 mmol) in absolute ethanol (16 ml) was added to a vigorously stirred solution of 1,3-propanediamine (2.0 ml, 23.9 mmol) in a dropwise manner. The mixture was stirred at room temperature for a further 2 h to afford a bright-yellow solution of the diimine Schiff base. The solvent was removed under reduced pressure and the residue redissolved in fresh absolute ethanol (60 ml), an excess of NaBH<sub>4</sub> (1.52 g, 40 mmol) added and the mixture stirred for a further 24 h after effervescence of the gas had ceased. The mixture was extracted with CH<sub>2</sub>Cl<sub>2</sub> ( $3 \times 40 \text{ ml}$ ), washed thoroughly with deionized water ( $3 \times 50 \text{ ml}$ ) and dried over Na<sub>2</sub>SO<sub>4</sub>. The extracting solvent was removed under reduced pressure to afford a light-yellow oil, (II).

The above imination-reduction step was repeated once, starting with the light-yellow oil of (II) as the amine source and 2-thiophenecarbaldehyde as the imination reagent. Slow addition of NaBH<sub>4</sub> in small portions is necessary as the second reduction step is highly exothermic. Colourless crystals of (I) were obtained by layering a concentrated CH<sub>2</sub>Cl<sub>2</sub> solution of (I) with a 1:1 (*v/v*) mixture of hexane and cyclohexane (yield 74%).

## Crystal data

$C_{18}H_{20}N_2S_3$	$V = 1802.62(11) \text{ \AA}^3$
$M_r = 360.54$	$Z = 4$
Orthorhombic, $Pna2_1$	Mo $K\alpha$ radiation
$a = 15.4391(6) \text{ \AA}$	$\mu = 0.41 \text{ mm}^{-1}$
$b = 5.9873(2) \text{ \AA}$	$T = 110(2) \text{ K}$
$c = 19.5007(7) \text{ \AA}$	$0.6 \times 0.5 \times 0.2 \text{ mm}$

## Paper A2

electronic reprint

Acta Crystallographica Section C

**Crystal Structure  
Communications**

ISSN 0108-2701

Editor: George Ferguson

### **One-dimensional C—H...N hydrogen-bonded polymers in flexible tetrapyridyl systems**

**Allen Mambanda, Deogratius Jaganyi and Orde Q. Munro**

Copyright © International Union of Crystallography

Author(s) of this paper may load this reprint on their own web site or institutional repository provided that this cover page is retained. Reproduction of this article or its storage in electronic databases other than as specified above is not permitted without prior permission in writing from the IUCr.

For further information see <http://journals.iucr.org/services/authorrights.html>

## organic compounds

Acta Crystallographica Section C  
**Crystal Structure  
 Communications**

ISSN 0108-2701

### One-dimensional C—H···N hydrogen-bonded polymers in flexible tetra-pyridyl systems

Allen Mambanda, Deogratius Jaganyi and Orde Q. Munro\*

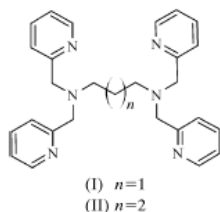
School of Chemistry, University of KwaZulu-Natal, Pietermaritzburg, Private Bag X01, Scottsville 3209, South Africa  
 Correspondence e-mail: munroo@ukzn.ac.za

Received 19 September 2007  
 Accepted 8 October 2007  
 Online 24 October 2007

In *N,N,N',N'*-tetrakis(2-pyridylmethyl)propane-1,3-diamine,  $C_{27}H_{30}N_6$ , (I), and *N,N,N',N'*-tetrakis(2-pyridylmethyl)butane-1,4-diamine,  $C_{28}H_{32}N_6$ , (II), the twofold rotational symmetry of (I) favours the formation of a one-dimensional hydrogen-bonded polymer with two columns of C—H···N hydrogen bonds, while the inversion symmetry of (II) allows the formation of a one-dimensional hydrogen-bonded polymer stabilized by four columns of C—H···N hydrogen bonds. The possible role played by the chain length of the linking alkanediamine in determining the type of supra-molecular architecture in this series of compounds is discussed.

#### Comment

The tetrapyridyl compounds formed by the reaction of four molar equivalents of 2-picoyl chloride with an  $\alpha,\omega$ -alkanediamine are versatile bis-tridentate ligands for the synthesis of binuclear transition metal complexes. Coordination compounds based on this ligand system were first reported by



Anderegg & Wenk (1967) and later by Toftlund & Yde-Andersen (1981). More recently, the *p*-phenylenediamine derivative was used to synthesize various copper complexes (Buchen *et al.*, 1997), while the *m*-phenylenediamine derivatives have been used to synthesize a range of copper(II), iron(II) and nickel(II) complexes (Schindler *et al.*, 1992; Foxon *et al.*, 2007).

Following the improved synthesis of *N,N,N',N'*-tetrakis(2-pyridylmethyl)- $\alpha,\omega$ -alkanediamines described by Sato *et al.* (1992), various binuclear metal complexes have been prepared. Thus, platinum(II) complexes of these ligands with varied bridging alkyl chain lengths have been used in mechanistic studies (Hoffmann & van Eldik, 2003). We have used several of these ligands for the coordination of platinum group metals in our laboratory and have obtained crystals suitable for X-ray diffraction analysis of two new metal-free derivatives, namely *N,N,N',N'*-tetrakis(2-pyridylmethyl)propane-1,3-diamine, (I), and *N,N,N',N'*-tetrakis(2-pyridylmethyl)butane-1,4-diamine, (II). The crystal structure of the ethane-1,2-diamine analogue ( $n = 0$  in the scheme) was reported only quite recently by Fujihara *et al.* (2004).

The structure of (I) has  $C_2$  molecular point group symmetry by virtue of the location of the central C atom of the propyl chain (C1) on a twofold rotation axis (Fig. 1). The methylene groups of the structure all adopt the expected staggered (lowest energy) conformation (Munro & Camp, 2003). The C—N $sp^2$  and C—N $sp^3$  bonds in the structure (Table 1) compare favourably with those reported for the related  $C_2$  symmetry ethane-1,2-diamine analogue of (I) (Fujihara *et al.*, 2004), but have been determined to a higher precision in the present structure. The pyridyl ring containing atom N2 is oriented at  $14(1)^\circ$  relative to the mean plane of the bridging propyl group, while that containing atom N3 is in a near-orthogonal orientation [ $81(1)^\circ$ ].

The underlying reason for the different relative orientations of the pyridyl rings is not immediately apparent from the crystal packing (Fig. 2), which reflects a rather loose interlocked arrangement of layers of (I) in which the propyl chains are all oriented in approximately the same direction as the diagonal plane perpendicular to the (101) direction. A plot of the unit-cell contents using the van der Waals radii of the atoms (not shown) clearly reflects the loose packing in this

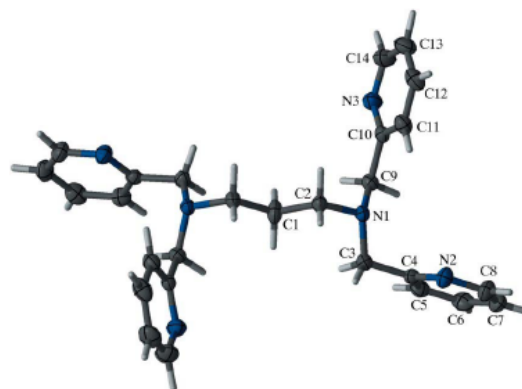


**Figure 1**  
 A plot of (I), showing the atom-numbering scheme. Displacement ellipsoids are drawn at the 60% probability level. H atoms are shown only as the intersections and endpoints of bonds represented as cylinders. Unlabelled atoms are related to labelled atoms by the symmetry operator  $(-x, y, -z + \frac{1}{2})$ .

system (there are no short van der Waals contacts less than the sum of the van der Waals radii). Weak (possibly stabilizing)  $\pi$ - $\pi$  intermolecular interactions do, however, occur in (I). Specifically, if  $Cg1$  defines the centre of gravity of the pyridyl ring containing atom N2, then the closest symmetry-related neighbouring ring centroid is located less than 6 Å away [ $Cg1 \cdots Cg1^1 = 5.057(2)$  Å; symmetry code: (i)  $-x, 1-y, -z$ ]. The interplanar separation is 3.395(2) Å, with a lateral offset (or slippage) of 3.747(2) Å. The metrics of this interaction reflect weak edge-to-edge  $\pi$ - $\pi$  overlap (at best) for the C4-C5  $\pi$  bonds in the inversion pair.

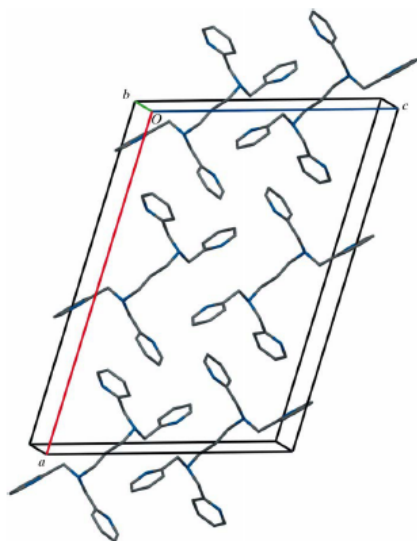


**Figure 2**  
The unit-cell contents for (I), viewed approximately down the  $b$  axis. H atoms have been omitted for clarity; all other atoms are shown only as the intersections and endpoints of bonds represented as cylinders.

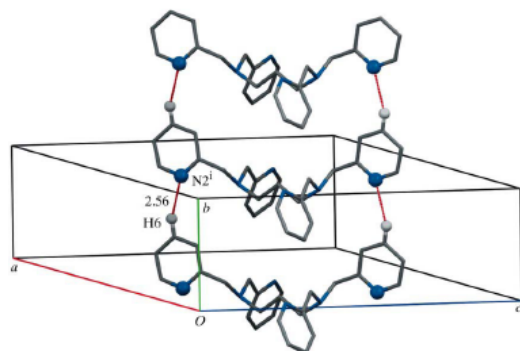


**Figure 3**  
A view of (I), illustrating a single one-dimensional hydrogen-bonded stack of molecules running collinear with the  $b$  axis of the unit cell. The symmetry-unique hydrogen-bond distance (in Å) is shown. [Symmetry code: (i)  $x, 1+y, z$ ].

The rather intriguing relative orientations of the pyridyl rings in (I), particularly the fact that the ring containing atom N2 points in the same direction as the  $b$  axis of the unit cell, reflect the formation of pairs of C-H $\cdots$ N hydrogen bonds [ $H \cdots N = 2.56(2)$  Å and  $C-H \cdots N = 145(1)^\circ$ ] that run collinear with the  $b$  axis (Table 2). These unconventional hydrogen bonds lead to the formation of one-dimensional hydrogen-bonded molecular stacks in the crystal structure (Fig. 3). Similar C-H $\cdots$ N hydrogen bonds are observed in the ethane-1,2-diamine analogue of (I) (Fujihara *et al.*, 2004), for which  $n = 0$  in the scheme [mean  $H \cdots N$  distance = 2.63(5) Å and mean C-H $\cdots$ N angle = 163(7)°]. However, as discussed below, the number of linker CH<sub>2</sub> groups that make up the diamine core of the molecule appears to dictate rather precisely the number of hydrogen-bonded columns (*i.e.* the supramolecular architecture) formed in this type of system. An additional noteworthy comment for (I) is that some stabilization of the interlocked packing evident in Fig. 2, due to the formation of weak C-H $\cdots$  $\pi$  bonds [averaging 2.91(4) Å; Table 2] roughly orthogonal to the stacking axis of each C-H $\cdots$ N hydrogen-bonded column, is likely. In effect, the hydrogen-bonded columns of (I) are tethered laterally by these significant, though often overlooked, interactions (Nishio, 2004).

Compound (II) has crystallographically required inversion symmetry, with the centroid of the central CH<sub>2</sub>-CH<sub>2</sub> bond located on the inversion centre (Fig. 4). As a result, the symmetry-unique pyridyl rings are oriented such that the pyridyl N atoms point in the same general direction (two up, two down), in marked contrast to the  $C_2$  symmetry structure of (I). The pyridyl ring containing atom N2 is oriented at 53(1)° relative to the mean plane of the bridging butyl group, and that containing atom N3 is similarly oriented [55(1)°]. The congruent pyridyl ring orientations for (II) directly reflect the supramolecular architecture within the system (see below),

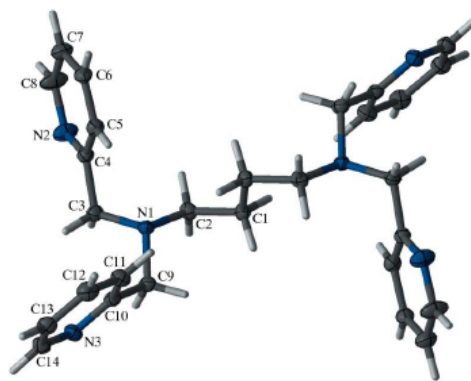


**Figure 4**  
A plot of (II), showing the atom-numbering scheme. Displacement ellipsoids are drawn at the 60% probability level. H atoms are shown only as the intersections and endpoints of bonds represented as cylinders. Unlabelled atoms are related to labelled atoms by the symmetry operator (2 -  $x, -y, -z$ ).

## organic compounds

which differs significantly from that of (I). The C–N distances listed in Table 3 are, as expected, in agreement with those of the propyl-bridged analogue, (I), and the ethyl-bridged analogue reported by Fujihara *et al.* (2004). Interestingly, the latter structure also crystallizes in the space group  $P\bar{1}$  on a special position ( $C_i$  point group symmetry). As discussed below, the significance of the molecular symmetry is that it most likely determines the type of supramolecular structure formed in this class of compounds.

The crystal packing of the unit-cell contents for (II) is similar in principle to that observed for (I). Specifically, the molecules interlock neatly within the (011) plane and are stacked in columns perpendicular to this plane, *i.e.* along the *a* axis (Fig. 5). The crystal packing is somewhat looser for (II), however, and two inversion-related voids at general positions measuring  $5.7 \text{ \AA}^3$  (probe radius =  $1.0 \text{ \AA}$ ) are located in the unit cell and are surrounded by pyridyl groups. (These voids are too small to accommodate a solvent molecule but do illustrate the low-density crystal packing in this system.) A possible reason for the low-density packing within the (011) layers is the formation of hydrogen-bonded stacks along the *a*-axis direction (Fig. 6). It is quite probable that optimization of hydrogen bonding in the crystal structure is energetically favoured over optimization of weaker van der Waals interactions. In the case of (II), the inversion symmetry clearly facilitates the formation of one-dimensional hydrogen-bonded polymers through two pairs of inversion-related C–H $\cdots$ N hydrogen bonds (Table 4). The hydrogen-bonded molecular stacks are thus held together by four columns of C–H $\cdots$ N hydrogen bonds with interaction vectors approximately along the *a*-axis direction. As noted above, the C–H $\cdots$ N hydrogen bonds in the ethane-1,2-diamine analogue of (II) have a mean H $\cdots$ N distance of  $2.63 (5) \text{ \AA}$  and a mean C–H $\cdots$ N angle of  $163 (7)^\circ$  (Fujihara *et al.*, 2004). The hydrogen bonding in (II) [mean H $\cdots$ N distance of  $2.5 (1) \text{ \AA}$  and a mean C–H $\cdots$ N

angle of  $166 (15)^\circ$ ] is therefore slightly tighter than in the ethane-1,2-diamine derivative, despite very similar angular interactions between the pyridyl rings within the hydrogen-bonded stacks. Interestingly, the C–H $\cdots$ N angle for (I) of  $145 (1)^\circ$  is significantly more acute than that for (II) and reflects a somewhat less ideal hydrogen-bonding interaction.

As with (I), there are several C–H $\cdots$  $\pi$  intermolecular interactions in (II) which are formed between molecules within adjacent hydrogen-bonded columns (Table 4) and which average  $2.79 (7) \text{ \AA}$ . These slightly weaker interactions roughly perpendicular to the direction of the C–H $\cdots$ N hydrogen bonds evidently further stabilize the interlocked supramolecular stacks. A significant additional packing stabilization, namely  $\pi$ – $\pi$  interactions between the pyridyl ring containing atom N2 and the inversion-related pyridine ring of the closest neighbour, is also evident in this system. Specifically, if  $Cg1$  defines the centre of gravity of this pyridyl ring in the asymmetric unit, then the  $Cg1 \cdots Cg1^i$  interaction is  $3.848 (2) \text{ \AA}$  [symmetry code: (i)  $-x, 2 - y, 1 - z$ ]. The mean plane separation of the coplanar rings is  $3.336 (2) \text{ \AA}$  (*i.e.* very similar to the graphite layer separation; Bacon, 1951) and the lateral shift or slippage is  $1.917 (2) \text{ \AA}$ . In effect, two pyridyl rings overlap by exact superposition of the C5–C6 bond of one molecule with the C6–C5 bond of the second through a centre of inversion midway between the planes passing through each bond.

Finally, it is intriguing to note that exactly the same supramolecular architecture observed for (II) (*i.e.* four C–H $\cdots$ N hydrogen-bonded columns) occurs in the  $C_i$  symmetry ethane-1,2-diamine analogue (Fujihara *et al.*, 2004), while the  $C_2$ -symmetry propyl-bridged derivative, (I), exhibits one-dimen-

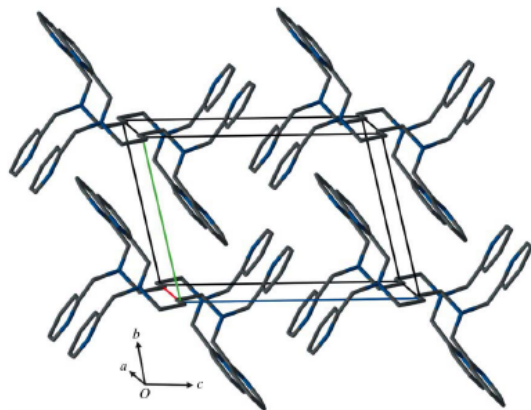


**Figure 5**  
The unit-cell contents for (II), viewed approximately down the *a* axis. H atoms have been omitted for clarity; all other atoms are shown only as the intersections and endpoints of bonds represented as cylinders.

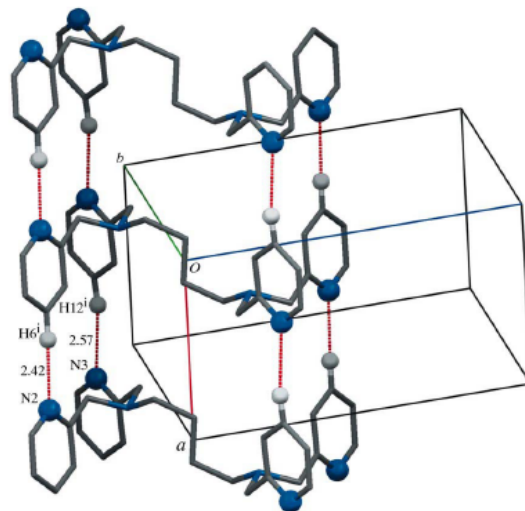


**Figure 6**  
A view of (II), illustrating a single one-dimensional hydrogen-bonded stack of molecules running collinear with the *a* axis of the unit cell. The symmetry-unique hydrogen-bond distances (in  $\text{\AA}$ ) are shown. [Symmetry code: (i)  $-1 + x, y, z$ .]

sional stacks based on only two columns of hydrogen bonds. Clearly, the number of methylene groups of the linking diamine core in these compounds affects the type of hydrogen-bonded stack that may be formed. Although based on relatively few data at present, a possible trend is that an even number of linking CH<sub>2</sub> groups favours hydrogen-bonded stacks with four columns of hydrogen bonds due to the C<sub>2</sub> symmetry of the constituent monomers.

### Experimental

Compounds (I) and (II) were synthesized following the literature method of Sato *et al.* (1992). Colourless crystals (X-ray quality) were obtained from solutions in ethanol by slow evaporation of the solvent over a period of several days.

Spectroscopic data for (I): <sup>1</sup>H NMR (500 MHz, D<sub>2</sub>O spiked with DCl): δ 8.60 (*d*, 4H), 8.38 (*t*, 4H), 7.94 (*d*, 4H), 7.82 (*t*, 4H), 4.20 (*s*, 8H), 2.50 (*t*, 4H), 1.71 (*m*, 2H); <sup>13</sup>C NMR (125 MHz, D<sub>2</sub>O spiked with DCl): δ 23.0, 52.5, 55.0, 127.1, 128.0, 128.0, 145.0, 148.0, 154.0; CHN analysis calculated for C<sub>27</sub>H<sub>30</sub>N<sub>6</sub>: C 73.94, H 6.89, N 19.17%; found: C 74.08, H 6.96, N 19.17%; MS-ES<sup>+</sup> *m/e*: 439.2453 (*M* + 1)<sup>+</sup>, 461.2428 (*M* + Na)<sup>+</sup>.

Spectroscopic data for (II): <sup>1</sup>H NMR (500 MHz, CD<sub>3</sub>OD): δ 8.41 (*d*, 4H), 7.77 (*td*, 4H), 7.58 (*d*, 4H), 7.26 (*tt*, 4H), 3.31 (*m*, 8H), 2.45 (*s*, br, 4H), 1.49 (*m*, 4H); CHN analysis calculated for C<sub>28</sub>H<sub>32</sub>N<sub>6</sub>: C 74.30, H 7.13, N 18.57%; found: C 74.30, H 7.13, N 18.53%; MS-ES<sup>+</sup> *m/e*: 453.2199 (*M* + 1)<sup>+</sup>, 475.2120 (*M* + Na)<sup>+</sup>.

### Compound (I)

#### Crystal data

C<sub>27</sub>H<sub>30</sub>N<sub>6</sub>  
*M<sub>r</sub>* = 438.57  
 Monoclinic, C<sub>2</sub>/c  
*a* = 24.615 (3) Å  
*b* = 6.0114 (11) Å  
*c* = 17.1066 (19) Å  
 $\beta$  = 106.702 (10)<sup>o</sup>

*V* = 2424.4 (6) Å<sup>3</sup>  
*Z* = 4  
 Mo *K*α radiation  
 $\mu$  = 0.07 mm<sup>-1</sup>  
*T* = 293 (2) K  
 0.6 × 0.4 × 0.3 mm

#### Data collection

Oxford Diffraction Xcalibur2 CCD diffractometer  
 Absorption correction: multi-scan [CrysAlis RED (Oxford Diffraction, 2006); Blessing, 1995]  
*T<sub>min</sub>* = 0.945, *T<sub>max</sub>* = 0.973

#### Refinement

$R[F^2 > 2\sigma(F^2)] = 0.041$   
 $wR(F^2) = 0.111$   
*S* = 0.99  
 3834 reflections  
 210 parameters  
 All H-atom parameters refined  
 $\Delta\rho_{\max} = 0.21 \text{ e } \text{Å}^{-3}$   
 $\Delta\rho_{\min} = -0.17 \text{ e } \text{Å}^{-3}$

**Table 1**

Selected geometric parameters (Å, °) for (I).

C2—N1	1.4757 (12)	C9—N1	1.4682 (12)
C3—N1	1.4772 (13)	C10—N3	1.3488 (13)
C4—N2	1.3455 (12)	C14—N3	1.3454 (15)
C8—N2	1.3436 (13)		
C9—N1—C2	112.96 (8)	C8—N2—C4	117.03 (9)
C9—N1—C3	111.56 (8)	C14—N3—C10	117.17 (10)
C2—N1—C3	111.47 (7)		
N1—C3—C4—N2	67.15 (11)	N1—C9—C10—N3	-155.42 (8)
N1—C3—C4—C5	-114.10 (11)	N1—C9—C10—C11	27.15 (13)

**Table 2**

Hydrogen-bond geometry (Å, °) for (I).

Cg2 is the centroid of the N3/C10—C14 ring.

<i>D</i> —H... <i>A</i>	<i>D</i> —H	H... <i>A</i>	<i>D</i> ... <i>A</i>	<i>D</i> —H... <i>A</i>
C6—H6...N2 <sup>i</sup>	0.97 (2)	2.56 (2)	3.404 (2)	145 (1)
C8—H8...Cg2 <sup>ii</sup>	0.98 (1)	2.94 (1)	3.700 (2)	135 (1)
C12—H12...Cg2 <sup>iii</sup>	0.96 (1)	2.88 (1)	3.586 (2)	131 (1)

Symmetry codes: (i) *x*, *y* + 1, *z*; (ii) *x*, -*y*, *z* - ½; (iii) -*x* + ½, *y* - ½, -*z* + ½

### Compound (II)

#### Crystal data

C<sub>28</sub>H<sub>32</sub>N<sub>6</sub>  
*M<sub>r</sub>* = 452.6  
 Triclinic, *P* $\bar{1}$   
*a* = 6.1942 (3) Å  
*b* = 9.2425 (3) Å  
*c* = 11.6798 (5) Å  
 $\alpha$  = 101.756 (3)<sup>o</sup>  
 $\beta$  = 96.953 (4)<sup>o</sup>  
 $\gamma$  = 106.289 (4)<sup>o</sup>  
*V* = 616.96 (5) Å<sup>3</sup>  
*Z* = 1  
 Mo *K*α radiation  
 $\mu$  = 0.07 mm<sup>-1</sup>  
*T* = 100 (2) K  
 0.5 × 0.4 × 0.2 mm

#### Data collection

Oxford Diffraction Xcalibur2 CCD diffractometer  
 Absorption correction: multi-scan [CrysAlis RED (Oxford Diffraction, 2006); Blessing, 1995]  
*T<sub>min</sub>* = 0.945, *T<sub>max</sub>* = 0.983  
 9960 measured reflections  
 4227 independent reflections  
 3241 reflections with *I* > 2σ(*I*)  
*R<sub>int</sub>* = 0.020

#### Refinement

$R[F^2 > 2\sigma(F^2)] = 0.045$   
 $wR(F^2) = 0.139$   
*S* = 1.01  
 4227 reflections  
 218 parameters  
 All H-atom parameters refined  
 $\Delta\rho_{\max} = 0.51 \text{ e } \text{Å}^{-3}$   
 $\Delta\rho_{\min} = -0.27 \text{ e } \text{Å}^{-3}$

**Table 3**

Selected geometric parameters (Å, °) for (II).

C2—N1	1.4687 (10)	C9—N1	1.4671 (11)
C3—N1	1.4651 (11)	C10—N3	1.3435 (11)
C4—N2	1.3363 (12)	C14—N3	1.3447 (11)
C8—N2	1.3506 (13)		
C3—N1—C9	110.03 (7)	C4—N2—C8	117.49 (8)
C3—N1—C2	109.96 (7)	C10—N3—C14	117.33 (8)
C9—N1—C2	111.55 (7)		
C1 <sup>1</sup> —C1—C2—N1	-56.58 (12)	N1—C9—C10—N3	120.23 (8)
N1—C3—C4—N2	136.20 (8)	N1—C9—C10—C11	-59.36 (10)
N1—C3—C4—C5	-46.42 (10)		

Symmetry code: (i) -*x* + 2, -*y*, -*z*.

**Table 4**

Hydrogen-bond geometry (Å, °) for (II).

Cg1 is the centroid of the N2/C4—C8 ring and Cg2 is the centroid of the N3/C10—C14 ring.

<i>D</i> —H... <i>A</i>	<i>D</i> —H	H... <i>A</i>	<i>D</i> ... <i>A</i>	<i>D</i> —H... <i>A</i>
C6—H6...N2 <sup>ii</sup>	0.98 (1)	2.42 (1)	3.405 (1)	177 (1)
C12—H12...N3 <sup>iii</sup>	0.98 (1)	2.57 (2)	3.484 (1)	155 (1)
C7—H7...Cg2 <sup>iii</sup>	0.98 (1)	2.79 (2)	3.663 (1)	149 (1)
C9—H9A...Cg2 <sup>iv</sup>	1.02 (1)	2.72 (2)	3.545 (1)	139 (1)
C14—H14...Cg1 <sup>v</sup>	0.99 (1)	2.86 (2)	3.756 (1)	151 (1)

Symmetry codes: (ii) *x* + 1, *y*, *z*; (iii) -*x*, -*y* + 2, -*z* + 1; (iv) -*x*, -*y* + 1, -*z*; (v) *x*, *y* - 1, *z*.

All H atoms were located in a final difference Fourier map and refined isotropically without restraints.

## organic compounds

---

For both compounds, data collection: *CrysAlis CCD* (Oxford Diffraction, 2006); cell refinement: *CrysAlis RED* (Oxford Diffraction, 2006); data reduction: *CrysAlis RED*; program(s) used to solve structure: *SHELXS97* (Sheldrick, 1997); program(s) used to refine structure: *SHELXL97* (Sheldrick, 1997); molecular graphics: *WinGX* (Farrugia, 1999); software used to prepare material for publication: *WinGX*.

The authors gratefully acknowledge financial support from the University of KwaZulu-Natal and the National Research Foundation (NRF, Pretoria). Any opinion, findings, conclusions or recommendations expressed in this paper are those of the authors and therefore the NRF does not accept any liability in regard thereto. We thank Mr C. Grimmer for the NMR analysis of the samples.

---

Supplementary data for this paper are available from the IUCr electronic archives (Reference: HJ3054). Services for accessing these data are described at the back of the journal.

---

## References

- Anderegg, G. & Wenk, F. (1967). *Helv. Chim. Acta*, **50**, 2330–2332.  
Bacon, G. E. (1951). *Acta Cryst.* **4**, 558–561.  
Blessing, R. H. (1995). *Acta Cryst.* **A51**, 33–38.  
Buchen, T., Hazell, A., Jessen, L., McKenzie, C. J., Nielson, L. P., Pedersen, J. Z. & Schollmeyer, D. (1997). *J. Chem. Soc. Dalton Trans.* pp. 2697–2704.  
Farrugia, L. J. (1999). *J. Appl. Cryst.* **32**, 837–838.  
Foxon, S., Xu, J., Turba, S., Leibold, M., Hampel, F., Heinemann, F. W., Walter, O., Wurtele, C., Holthausen, M. & Schindler, S. (2007). *Eur. J. Inorg. Chem.* pp. 429–443.  
Fujihara, T., Saito, M. & Nagasawa, A. (2004). *Acta Cryst.* **E60**, o262–o263.  
Hoffmann, A. van & Eldik, R. (2003). *Dalton Trans.* pp. 2979–2985.  
Munro, O. O. & Camp, G. L. (2003). *Acta Cryst.* **C59**, o672–o675.  
Nishio, M. (2004). *CrystEngComm*, **6**, 130–158.  
Oxford Diffraction (2006). *CrysAlis CCD* and *CrysAlis RED*. Versions 1.171.29.9. Oxford Diffraction Ltd, Abingdon, Oxfordshire, England.  
Sato, A., Mori, Y. & Lida, T. (1992). *Synthesis*, pp. 539–540.  
Schindler, S., Szalda, D. J. & Creutz, C. (1992). *Inorg. Chem.* **31**, 2255–2264.  
Sheldrick, G. M. (1997). *SHELXS97* and *SHELXL97*. University of Göttingen, Germany.  
Toftlund, H. & Yde-Andersen, S. (1981). *Acta Chem. Scand. Ser. A*, **35**, 575–581.

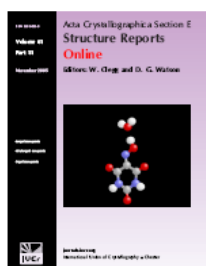
Acta Crystallographica Section E  
Structure Reports  
**Online**  
ISSN 1600-5368  
Editors: W. T. A. Harrison, J. Simpson and  
M. Weil

### *N,N*-Bis(2-pyridylmethyl)-*tert*-butylamine

Allen Mambanda, Deogratius Jaganyi and Kirsty Stewart

*Acta Cryst.* (2009). E65, o402

This open-access article is distributed under the terms of the Creative Commons Attribution Licence <http://creativecommons.org/licenses/by/2.0/uk/legalcode>, which permits unrestricted use, distribution, and reproduction in any medium, provided the original authors and source are cited.



*Acta Crystallographica Section E: Structure Reports Online* is the IUCr's highly popular open-access structural journal. It provides a simple and easily accessible publication mechanism for the growing number of inorganic, metal-organic and organic crystal structure determinations. The electronic submission, validation, refereeing and publication facilities of the journal ensure very rapid and high-quality publication, whilst key indicators and validation reports provide measures of structural reliability. In 2007, the journal published over 5000 structures. The average publication time is less than one month.

Crystallography Journals **Online** is available from [journals.iucr.org](http://journals.iucr.org)

## organic compounds

Acta Crystallographica Section E

Structure Reports

Online

ISSN 1600-5368

### *N,N*-Bis(2-pyridylmethyl)-*tert*-butylamine

Allen Mambanda, Deogratius Jaganyi and Kirsty Stewart\*

School of Chemical and Physical Sciences, University of KwaZulu-Natal, Scottsville 3209, South Africa

Correspondence e-mail: [stewart@ukzn.ac.za](mailto:stewart@ukzn.ac.za)

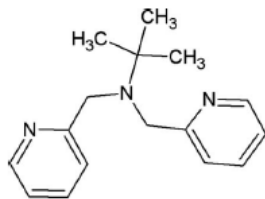
Received 29 October 2008; accepted 12 January 2009

Key indicators: single-crystal X-ray study;  $T = 293$  K; mean  $\sigma(\text{C}-\text{C}) = 0.003$  Å;  $R$  factor = 0.043;  $wR$  factor = 0.119; data-to-parameter ratio = 13.7.

In the title compound,  $\text{C}_{16}\text{H}_{21}\text{N}_3$ , the dihedral angle between the two pyridine rings is  $88.11$  ( $9$ )°. In the crystal, molecules are linked through intermolecular  $\text{C}-\text{H}\cdots\pi$  interactions, forming a layer expanding parallel to the  $(10\bar{1})$  plane.

#### Related literature

For related compounds, see: Mambanda *et al.* (2007); Foxon *et al.* (2007); Fujihara *et al.* (2004); Munro & Camp (2003). For metal complexes with the title compound as a ligand, see: Fujii *et al.* (2003); Lee & Lippard (2002); Mok *et al.* (1997). For the metal complex with *N,N*-bis(2-pyridylmethyl)ethylamine as a ligand, see: Pal *et al.* (1992).



#### Experimental

##### Crystal data

$\text{C}_{16}\text{H}_{21}\text{N}_3$   $V = 1496.62$  (12) Å<sup>3</sup>  
 $M_r = 255.36$   $Z = 4$   
 Monoclinic,  $Cc$   $\text{Mo } K\alpha$  radiation  
 $a = 6.1808$  (3) Å  $\mu = 0.07$  mm<sup>-1</sup>  
 $b = 17.9502$  (8) Å  $T = 293$  (2) K  
 $c = 13.7079$  (6) Å  $0.50 \times 0.50 \times 0.30$  mm  
 $\beta = 100.239$  (4)°

##### Data collection

Oxford Diffraction Xcalibur2 CCD diffractometer 7475 measured reflections  
 Absorption correction: multi-scan (CrysAlis RED; Oxford Diffraction, 2008) 2392 independent reflections  
 $R_{int} = 0.012$   
 $T_{min} = 0.967$ ,  $T_{max} = 0.980$   
 2024 reflections with  $I > 2\sigma(I)$

##### Refinement

$R[F^2 > 2\sigma(F^2)] = 0.043$  2 restraints  
 $wR(F^2) = 0.119$  H-atom parameters constrained  
 $S = 1.02$   $\Delta\rho_{max} = 0.21$  e Å<sup>-3</sup>  
 2392 reflections  $\Delta\rho_{min} = -0.22$  e Å<sup>-3</sup>  
 175 parameters

Table 1

Hydrogen-bond geometry (Å, °).

$D-H\cdots A$	$D-H$	$H\cdots A$	$D\cdots A$	$D-H\cdots A$
$C7-H1\cdots Cg2^{\ddagger}$	0.93	2.97	3.819 (2)	153
$C15-H16\cdots Cg1^{\ddagger}$	0.96	2.94	3.836 (2)	156

Symmetry codes: (i)  $x - \frac{1}{2}, y - \frac{1}{2}, z$ ; (ii)  $x, -y, z - \frac{1}{2}$

Data collection: CrysAlis CCD (Oxford Diffraction, 2008); cell refinement: CrysAlis RED (Oxford Diffraction, 2008); data reduction: CrysAlis RED; program(s) used to solve structure: SHELXS97 (Sheldrick, 2008); program(s) used to refine structure: SHELXL97 (Sheldrick, 2008); molecular graphics: ORTEP-3 (Farrugia, 1997); software used to prepare material for publication: WinGX (Farrugia, 1999).

The authors gratefully acknowledge financial support from the University of Kwazulu-Natal and the South African National Research Foundation. We thank Mr C. Grimmer for the NMR analysis of the samples. We also thank Professor O. Q. Munro and Professor J. Field for their guidance.

Supplementary data and figures for this paper are available from the IUCr electronic archives (Reference: IS2355).

#### References

- Farrugia, L. J. (1997). *J. Appl. Cryst.* **30**, 565.  
 Farrugia, L. J. (1999). *J. Appl. Cryst.* **32**, 837–838.  
 Foxon, S., Xu, J., Turba, S., Leibold, M., Hampel, F., Walter, O., Wurtele, C., Holthausen, M. & Schindler, S. (2007). *Eur. J. Inorg. Chem.* pp. 423–443.  
 Fujihara, T., Saito, M. & Nagasawa, A. (2004). *Acta Cryst.* **E60**, o262–o263.  
 Fujii, T., Naito, A., Yamaguchi, S., Wada, A., Funahashi, Y., Jitsukawa, K., Nagatomo, S., Kitagawa, T. & Masuda, H. (2003). *Chem. Commun.* pp. 2700–2701.  
 Lee, D. & Lippard, S. J. (2002). *Inorg. Chim. Acta*, **341**, 1–11.  
 Mambanda, A., Jaganyi, D. & Munro, O. Q. (2007). *Acta Cryst.* **C63**, o676–o680.  
 Mok, H. J., Davis, J. A., Pal, S., Mandal, S. K. & Armstrong, W. H. (1997). *Inorg. Chim. Acta*, **263**, 385–394.  
 Munro, O. Q. & Camp, G. L. (2003). *Acta Cryst.* **C59**, o672–o675.  
 Oxford Diffraction (2008). *CrysAlis CCD* and *CrysAlis RED*. Oxford Diffraction Ltd, Abingdon, England.  
 Pal, S., Chan, M. K. & Armstrong, W. H. (1992). *J. Am. Chem. Soc.* **114**, 6398–6404.  
 Sheldrick, G. M. (2008). *Acta Cryst.* **A64**, 112–122.

*Acta Cryst.* (2009). E65, o402 [ doi:10.1107/S1600536809001366 ]

## *N,N*-Bis(2-pyridylmethyl)-*tert*-butylamine

A. Mambanda, D. Jaganyi and K. Stewart

### Comment

The title compound is a versatile tridentate N-donor ligand, and it (Fujii *et al.*, 2003; Lee & Lippard, 2002; Mok *et al.*, 1997) and its analogue, *N,N*-bis(2-pyridylmethyl)ethylamine (Pal *et al.*, 1992) have been used extensively in metal coordination. The related crystal structures of symmetrical bis(tridentate) ligands have been reported (Mambanda *et al.*, 2007; Foxon *et al.*, 2007; Fujihara *et al.*, 2004).

The crystal structure of the title compound (Fig. 1) shows that the three nitrogen atoms (one  $sp^3$  and two pyridine  $sp^2$ ) are not suitably orientated for pincer-like coordination to a metal. Rotation about the C2—C3 and C8—C9 bonds are required for that to occur. The relative orientation of the two pyridine rings is reflected in a dihedral angle between their mean planes of 88.11 (9)°, clearly this angle would have to change were the ligand to bind to a metal centre. The steric influence of the bulky *tert*-butyl group is reflected in the C1—N1—C2 and C1—N1—C8 angles [113.90 (13) and 115.34 (13)°, respectively], being larger than the C2—N1—C8 angle of 110.08 (13)°. The methylene groups of the structure all adopt the expected staggered (lowest energy) conformation (Munro & Camp, 2003). The pyridyl ring containing atom N2 is orientated at 18 (1)° relative to the mean plane of the *N-tert*-butyl group (plane through C16—C1—N1), whilst that containing N3 is orientated at 74 (1)°.

There are no short van der Waals contacts less than the sum of the van der Waals radii in this system, reflected in the loose packing, however weak (possibly stabilizing) C—H... $\pi$  intermolecular interactions do occur. The metrics of such interactions reflect a T-shaped, edge-to-face geometry. Specifically, let us define *Cg*1 as the centre of gravity of the pyridyl N2/C3—C7 ring and *Cg*2 the centre of gravity of the pyridyl N3/C9—C13 ring. A C—H... $\pi$  interaction with a separation of 2.97 (1) Å exists between C7—H1 from the pyridyl ring containing atom N2 and *Cg*2 of neighbouring symmetry related molecule [symmetry code: (i)  $x - 1/2, y - 1/2, z$ ] (Table 1). A similar C—H... $\pi$  interaction with a separation of 2.94 (1) Å exists between C15—H16 from one of the methyl groups of the *tert*-butyl moiety and *Cg*1 on the symmetry related neighbouring molecule with symmetry code: (ii)  $x, -y, z - 1/2$ . Figure 2 shows the packing within the unit cell for the title compound.

### Experimental

The compound was synthesized following a literature method (Pal *et al.*, 1992). Under a high flow of nitrogen, 6 ml of 20% NaOH solution was added to an aqueous solution of 2-picolyl chloridehydrochloride [(3.937 g (24 mmol) in 0.5 ml ultra pure water] to form a pink emulsion solution. 2-Amino-2-methyl propane (12 mmol) was added and the mixture stirred at 60°C. 40 ml of 20% NaOH solution was then added over a period of 1 h and the mixture left to stir for a further 12 h. The crude product was extracted with CHCl<sub>3</sub> washed with ultra pure water and dried over Na<sub>2</sub>SO<sub>4</sub>. Excess solvent was removed under reduced pressure and the oil residue purified on a short chromatographic column packed with 0.5 g charcoal and 5 g of neutral alumina using CHCl<sub>3</sub> as an eluent to afford a light yellow solution. Colourless single crystals suitable for X-ray diffraction were obtained from slow evaporation of the solvent from its solution made from a 5% chloroform in ethanol solution (yield: 1.73 g, 60%).

# Appendices

Spectroscopic data:  $^1\text{H}$  NMR (400 MHz,  $\text{CDCl}_3$ )  $\delta$  / p.p.m.: 8.40 (d, 2H), 7.60 (t, 2H), 7.45 (d, 2H), 7.05 (t, 2H), 3.95 (s, 4H), 1.18 (s, 9H).  $^{13}\text{C}$  NMR (125 MHz,  $\text{CDCl}_3$ )  $\delta$  / p.p.m.: 27.0, 57.0, 122.0, 123.0, 136.0, 148.0, 160. Anal. Calc. for  $\text{C}_{16}\text{H}_{21}\text{N}_3$ : C 75.26, H 8.29, N 16.46; Found: C 74.89, H 7.97, N 17.37.

## Refinement

All Hydrogen atoms were positioned in geometrically idealized positions and constrained to ride on their parent atoms with C—H distances in the range 0.93–0.97 Å, and with  $U_{\text{iso}}(\text{H}) = 1.2$  or  $1.5U_{\text{eq}}(\text{C})$ . In the absence of significant anomalous scattering effects, Friedel pairs have been merged.

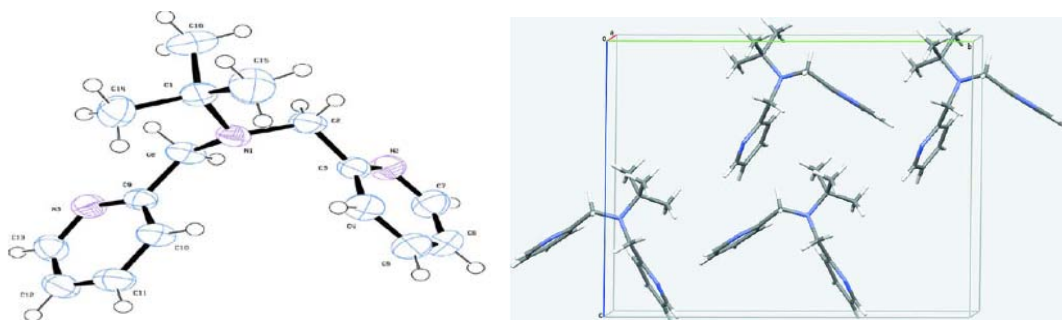


**Figure 1** Molecular structure of the title compound, showing 50% probability displacements ellipsoids and atomic numbering as well as the unit cell packing diagram.

## *N,N*-Bis(2-pyridylmethyl)-*tert*-butylamine

### Crystal data

$\text{C}_{16}\text{H}_{21}\text{N}_3$

$M_r = 255.36$

Monoclinic,  $Cc$

Hall symbol: C -2yc

$a = 6.1808$  (3) Å

$b = 17.9502$  (8) Å

$c = 13.7079$  (6) Å

$\beta = 100.239$  (4)°

$V = 1496.62$  (12) Å<sup>3</sup>

$Z = 4$

$F_{000} = 552$

$D_x = 1.133$  Mg m<sup>-3</sup>

Mo  $K\alpha$  radiation

$\lambda = 0.71073$  Å

Cell parameters from 4672 reflections

$\theta = 3.9$ – $32.0^\circ$

$\mu = 0.07$  mm<sup>-1</sup>

$T = 293$  (2) K

Plate, colourless

$0.50 \times 0.50 \times 0.30$  mm

### Data collection

Oxford Diffraction Xcalibur2 CCD diffractometer

2392 independent reflections

# Appendices

---

Radiation source: Enhance (Mo)X-Ray Source	2024 reflections with $I > 2\sigma(I)$
Monochromator: graphite	$R_{\text{int}} = 0.012$
Detector resolution: 8.4190 pixels $\text{mm}^{-1}$	$\theta_{\text{max}} = 31.9^\circ$
$T = 293(2)$ K	$\theta_{\text{min}} = 4.1^\circ$
$\omega$ -2 $\theta$ scans	$h = -8 \rightarrow 7$
Absorption correction: multi-scan ( <i>CrysAlis RED</i> ; Oxford Diffraction, 2008)	$k = -26 \rightarrow 26$
$T_{\text{min}} = 0.967$ , $T_{\text{max}} = 0.980$	$l = -18 \rightarrow 20$
7475 measured reflections	

## Refinement

Refinement on $F^2$	Secondary atom site location: difference Fourier map
Least-squares matrix: full	Hydrogen site location: inferred from neighbouring sites
$R[F^2 > 2\sigma(F^2)] = 0.043$	H-atom parameters constrained
$wR(F^2) = 0.119$	$w = 1/[\sigma^2(F_o^2) + (0.0873P)^2 + 0.017P]$
$S = 1.02$	where $P = (F_o^2 + 2F_c^2)/3$
2392 reflections	$(\Delta/\sigma)_{\text{max}} = 0.001$
175 parameters	$\Delta\rho_{\text{max}} = 0.21 \text{ e } \text{\AA}^{-3}$
2 restraints	$\Delta\rho_{\text{min}} = -0.21 \text{ e } \text{\AA}^{-3}$
Primary atom site location: structure-invariant direct methods	Extinction correction: none

## Special details

**Geometry.** All e.s.d.'s (except the e.s.d. in the dihedral angle between two l.s. planes) are estimated using the full covariance matrix. The cell e.s.d.'s are taken into account individually in the estimation of e.s.d.'s in distances, angles and torsion angles; correlations between e.s.d.'s in cell parameters are only used when they are defined by crystal symmetry. An approximate (isotropic) treatment of cell e.s.d.'s is used for estimating e.s.d.'s involving l.s. planes.

**Refinement.** Refinement of  $F^2$  against ALL reflections. The weighted  $R$ -factor  $wR$  and goodness of fit  $S$  are based on  $F^2$ , conventional  $R$ -factors  $R$  are based on  $F$ , with  $F$  set to zero for negative  $F^2$ . The threshold expression of  $F^2 > \sigma(F^2)$  is used only for calculating  $R$ -factors(gt) etc. and is not relevant to the choice of reflections for refinement.  $R$ -factors based on  $F^2$  are statistically about twice as large as those based on  $F$ , and  $R$ -factors based on ALL data will be even larger.

# Appendices

## Appendix B

### Pt(II Alkyldiamine-bridged) Complexes.

<b>Figure B 1a</b>	Infrared spectrum (KBr pellet) of the <i>N,N,N',N'</i> -tetrakis(2-pyridylmethyl)-1,4-butanediamine ligand.	274
<b>Figure B 1b</b>	Infrared spectrum (KBr pellet) of the $[\{\text{Pt}(\text{Cl})\}_2(\text{N,N,N',N'}$ -tetrakis(2-pyridylmethyl)-1,4-butanediamine)](ClO <sub>4</sub> ) complex.	274
<b>Figure B 2a</b>	UV-visible spectrum for the titration of 0.1 mM <b>Hex</b> with NaOH, pH range 2 - 9, 298 K. <i>Inset</i> the titration curve at 268 nm	275
<b>Figure B 2b</b>	UV-visible spectrum for the titration of 0.1 mM <b>Dec</b> with NaOH, pH range 2 - 9, T = 298 K. <i>Inset</i> the titration curve at 269 nm.	276
<b>Figure B 3a</b>	<sup>1</sup> H Spectrum of $[\{\text{Pt}(\text{DMF})\}_2(\text{N,N,N',N'}$ -tetrakis(2-pyridylmethyl)-1,4-butanediamine)](ClO <sub>4</sub> ) <sub>4</sub> .	277
<b>Figure B 3b</b>	<sup>195</sup> Pt Spectrum of $[\{\text{Pt}(\text{DMF})\}_2(\text{N,N,N',N'}$ -tetrakis(2-pyridylmethyl)-1,4-butanediamine)](ClO <sub>4</sub> ) <sub>4</sub> .	278
<b>Figure B 4a</b>	Plots of concentration dependence of $k_{\text{obs}(1)}^{\text{st}}$ , s <sup>-1</sup> , for the simultaneous displacement of the aqua ligands in <b>But</b> by thiourea nucleophiles, pH = 2.0, T = 298 K.	279
<b>Figure B 4b</b>	Plots of concentration dependence of $k_{2(2)}^{\text{nd}}$ , s <sup>-1</sup> , for the simultaneous displacement of the aqua ligands in <b>But</b> by thiourea nucleophiles, pH = 2.0, T = 298 K.	279
<b>Figure B 4c</b>	Temperature dependence of $k_{2(1)}^{\text{st}}$ , M <sup>-1</sup> s <sup>-1</sup> , for the simultaneous displacement of the first aqua ligand in <b>But</b> by thiourea nucleophiles, pH = 2.0.	280
<b>Figure B 4d</b>	Temperature dependence of $k_{2(2)}^{\text{nd}}$ , M <sup>-1</sup> s <sup>-1</sup> , for the dechelation of the pyridyl units in <b>but</b> by thiourea, pH = 2.0.	280
<b>Table B 1a</b>	Average observed rate constants, $k_{\text{obs}(1)}^{\text{st}}$ , s <sup>-1</sup> , for the simultaneous displacement of the aqua ligands in <b>But</b> by thiourea nucleophiles, pH = 2.0, T = 298 K.	280
<b>Table B 1b</b>	Average observed rate constants, $k_{\text{obs}(2)}^{\text{nd}}$ , s <sup>-1</sup> , for the dechelation of the pyridyl units in <b>But</b> by thiourea nucleophiles, pH = 2.0, T = 298 K.	281
<b>Table B 1c</b>	Temperature dependence of $k_{2(1)}^{\text{st}}$ , M <sup>-1</sup> s <sup>-1</sup> , for the simultaneous displacement of the first aqua ligand in <b>But</b> by thiourea nucleophiles, pH = 2.0.	281
<b>Table B 1d</b>	Temperature dependence of $k_{2(2)}^{\text{nd}}$ , M <sup>-1</sup> s <sup>-1</sup> , for the dechelation of the pyridyl units in <b>But</b> by thiourea nucleophiles, pH = 2.0.	282
<b>Table B 2a</b>	Concentration dependence of $k_{\text{obs}(1)}^{\text{st}}$ , s <sup>-1</sup> , for the substitution of the aqua ligand in <b>Dec</b> by thiourea nucleophiles, pH = 2.0, T = 298 K.	282
<b>Table B 2b</b>	Temperature dependence of $k_{2(1)}^{\text{st}}$ , M <sup>-1</sup> s <sup>-1</sup> , for the simultaneous displacement of the first aqua ligand in <b>Dec</b> by thiourea nucleophiles, pH = 2.0.	282

# Appendices

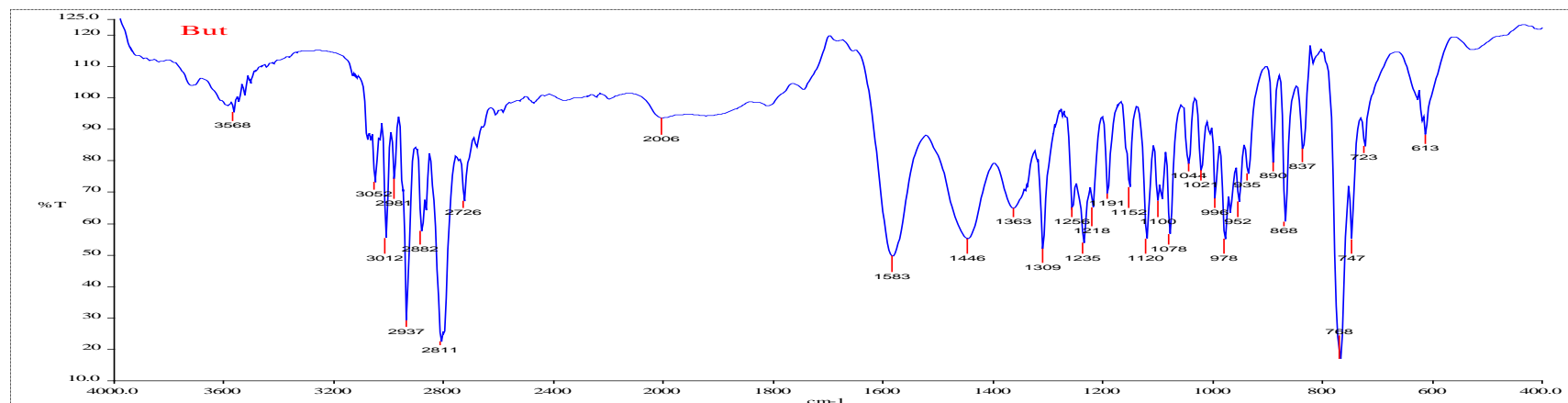


**Figure B 1a** Infrared spectrum (KBr pellet) of the *N,N,N',N'*-tetrakis(2-pyridylmethyl)-1,4-butanediamine ligand.

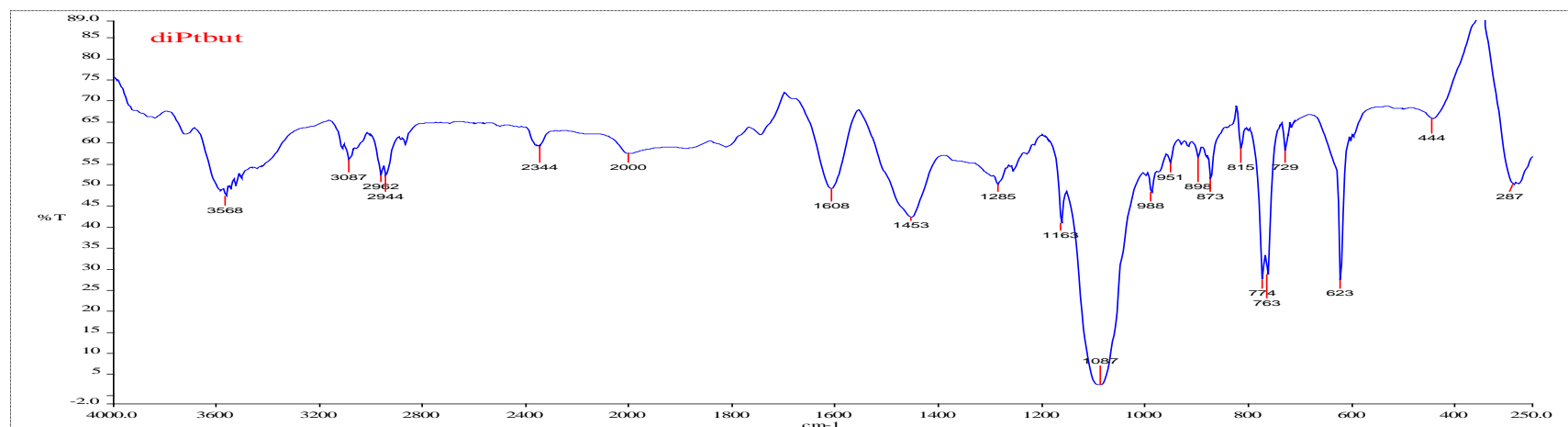


**Figure B 1b** Infrared spectrum (KBr pellet) of the  $[\{Pt(Cl)\}_2(N,N,N',N'$ -tetrakis(2-pyridylmethyl)-1,4-butanediamine)](ClO<sub>4</sub>) complex.

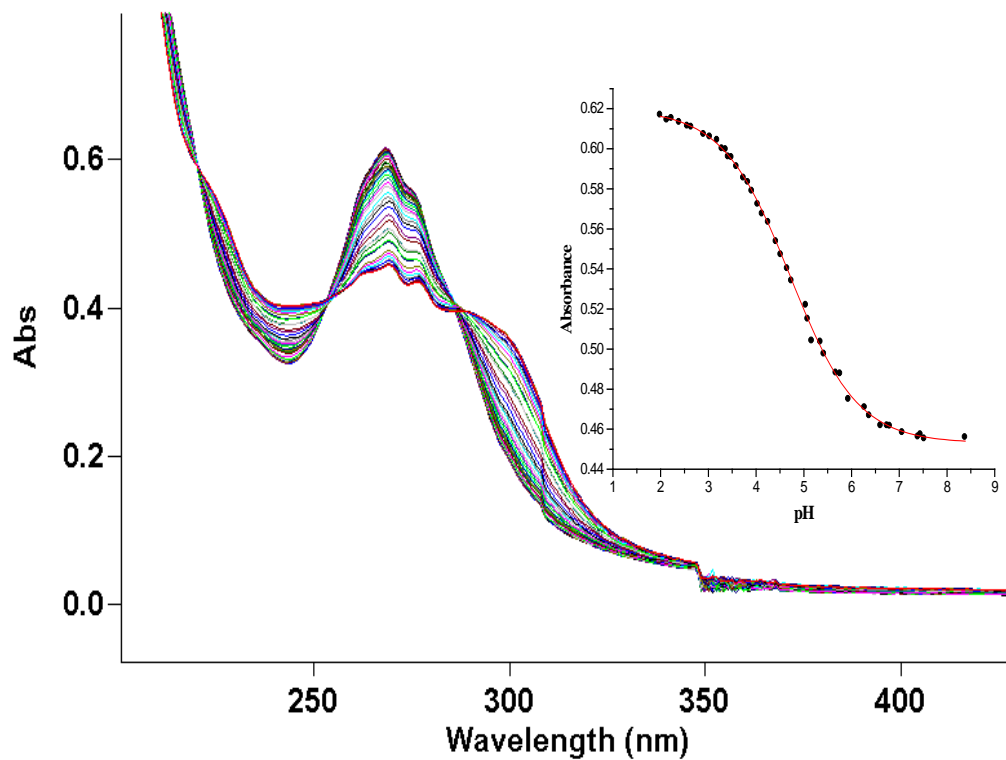


**Figure B 2a** UV-visible spectrum for the titration of 0.1 mM **Hex** with NaOH, pH range 2 - 9, 298 K. *Inset* the titration curve at 268 nm.

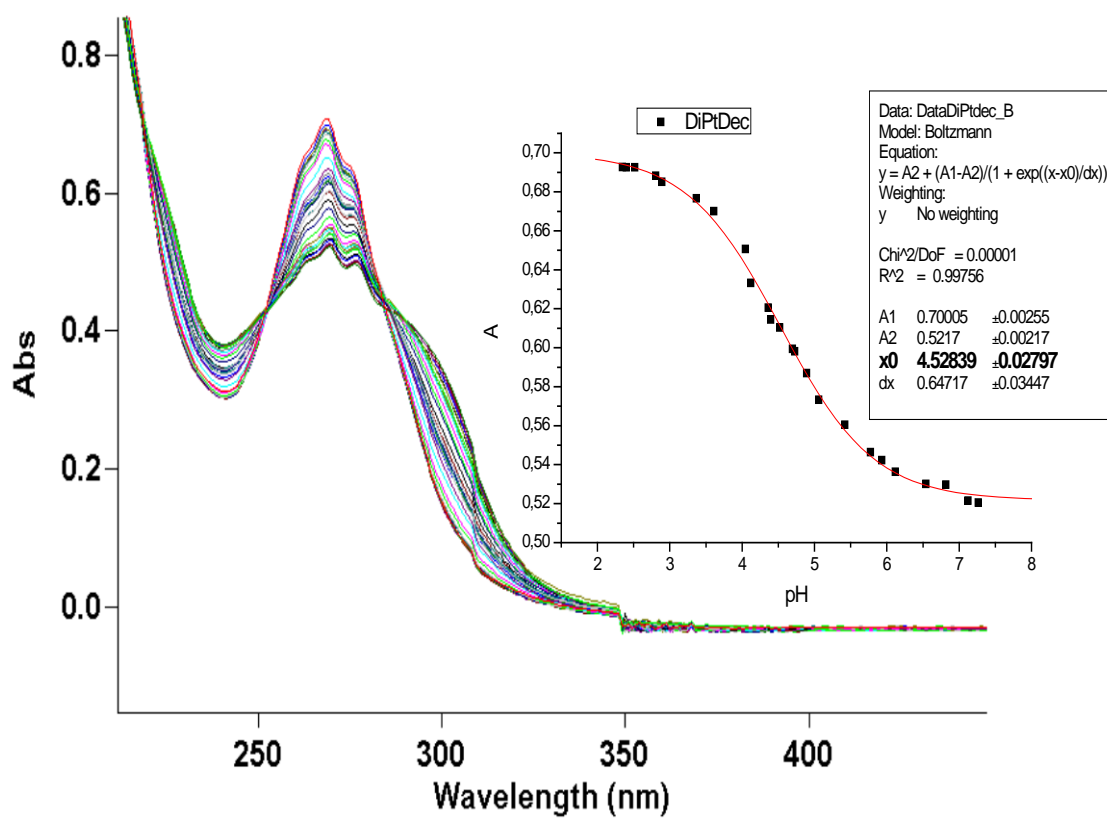


**Figure B 2b** UV-visible spectrum for the titration of 0.1 mM Dec with NaOH, pH range 2 - 9, T 298 K. *Inset* the titration curve at 269 nm.

# Appendices

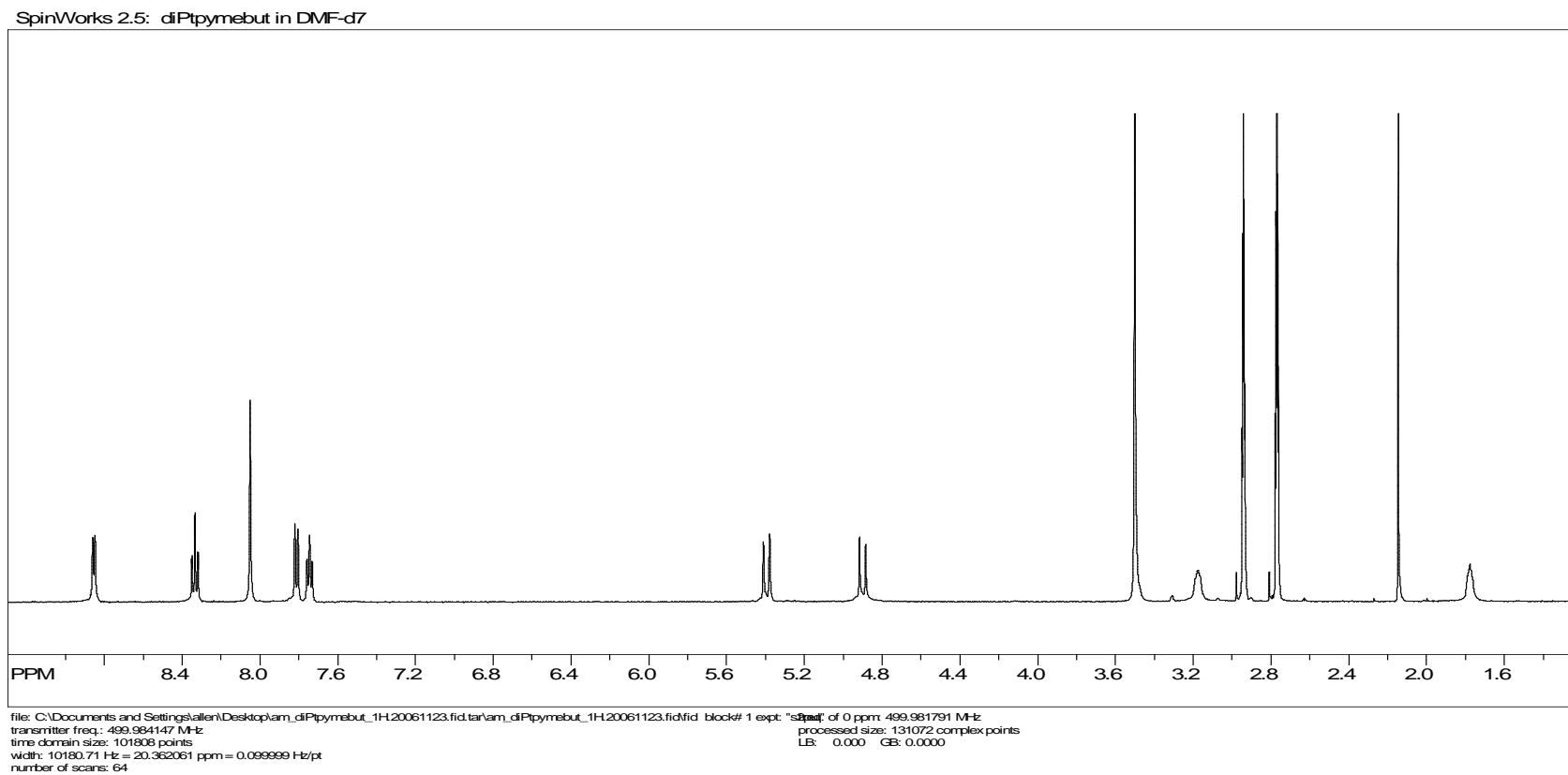


**Figure B 3a**  $^1\text{H}$  Spectrum of  $[\{\text{Pt}(\text{DMF})\}_2(\text{N},\text{N}',\text{N}',\text{N}'\text{-tetrakis}(2\text{-pyridylmethyl})\text{-}1,4\text{-butanediamine})](\text{ClO}_4)_4$  (**3**).

# Appendices

---

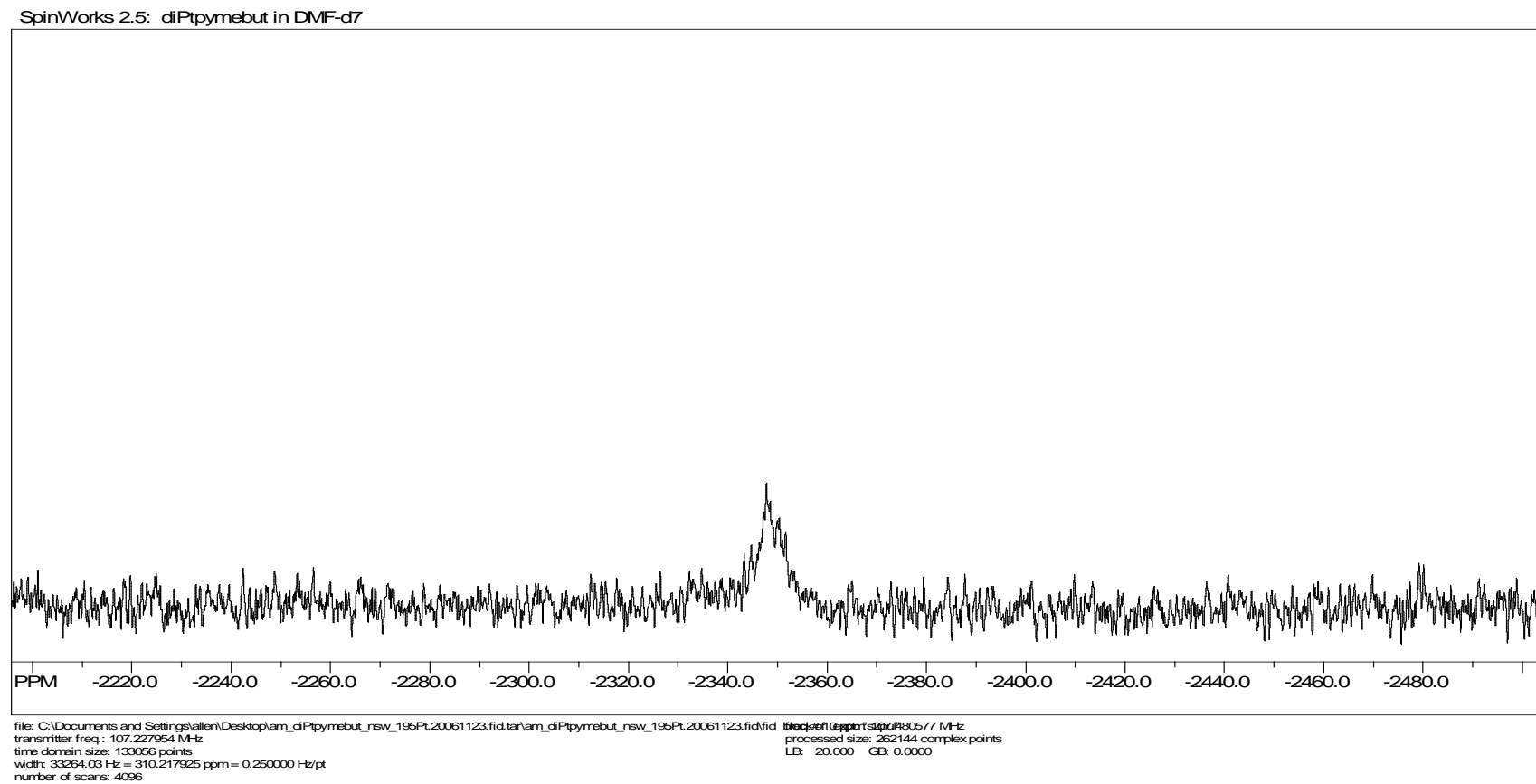


**Figure B 3b**  $^{195}\text{Pt}$  Spectrum of  $[\{\text{Pt}(\text{DMF})\}_2(\text{N},\text{N},\text{N}',\text{N}'\text{-tetrakis}(2\text{-pyridylmethyl})\text{-}1,4\text{-butanediamine})](\text{ClO}_4)_4$ .

## Appendices

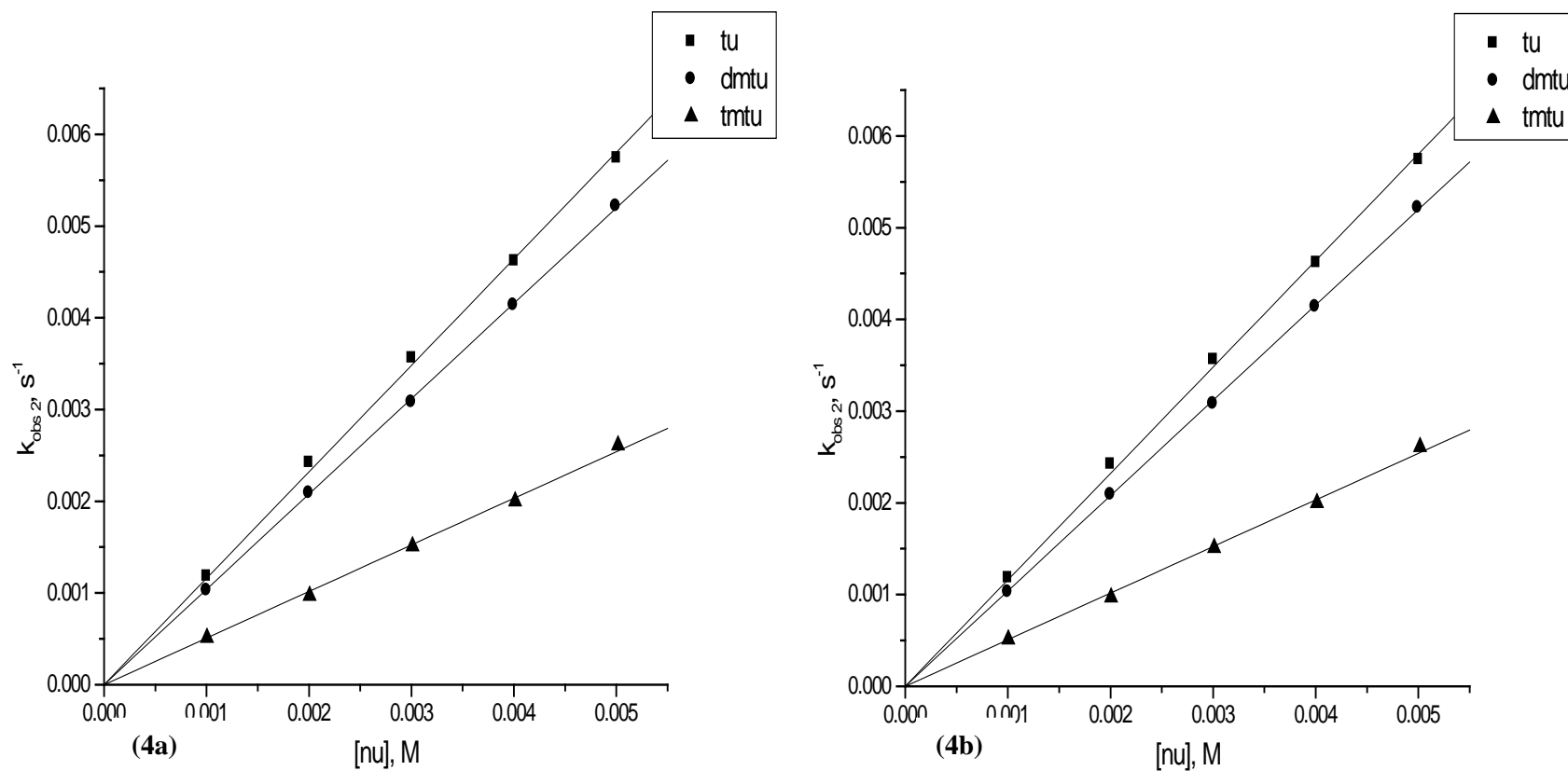


**Figure B 4a** Plots of concentration dependence of  $k_{\text{obs}(1^{\text{st}})}, \text{s}^{-1}$ , for the simultaneous displacement of the aqua ligands in **But** by thiourea nucleophiles,  $\text{pH} = 2.0$ ,  $T = 298 \text{ K}$ ,  $I = 0.02 \text{ M}$   $\{0.01 \text{ M } \text{CF}_3\text{SO}_3\text{H}$ , adjusted with  $\text{Li}(\text{SO}_3\text{CF}_3)\}$ .

**Figure B 4b** Plots of concentration dependence of  $k_{2(2^{\text{nd}})}, \text{s}^{-1}$ , for the simultaneous displacement of the aqua ligands in **But** by thiourea nucleophiles,  $\text{pH} = 2.0$ ,  $T = 298 \text{ K}$ ,  $I = 0.02 \text{ M}$   $\{0.01 \text{ M } \text{CF}_3\text{SO}_3\text{H}$ , adjusted with  $\text{Li}(\text{SO}_3\text{CF}_3)\}$ .

# Appendices

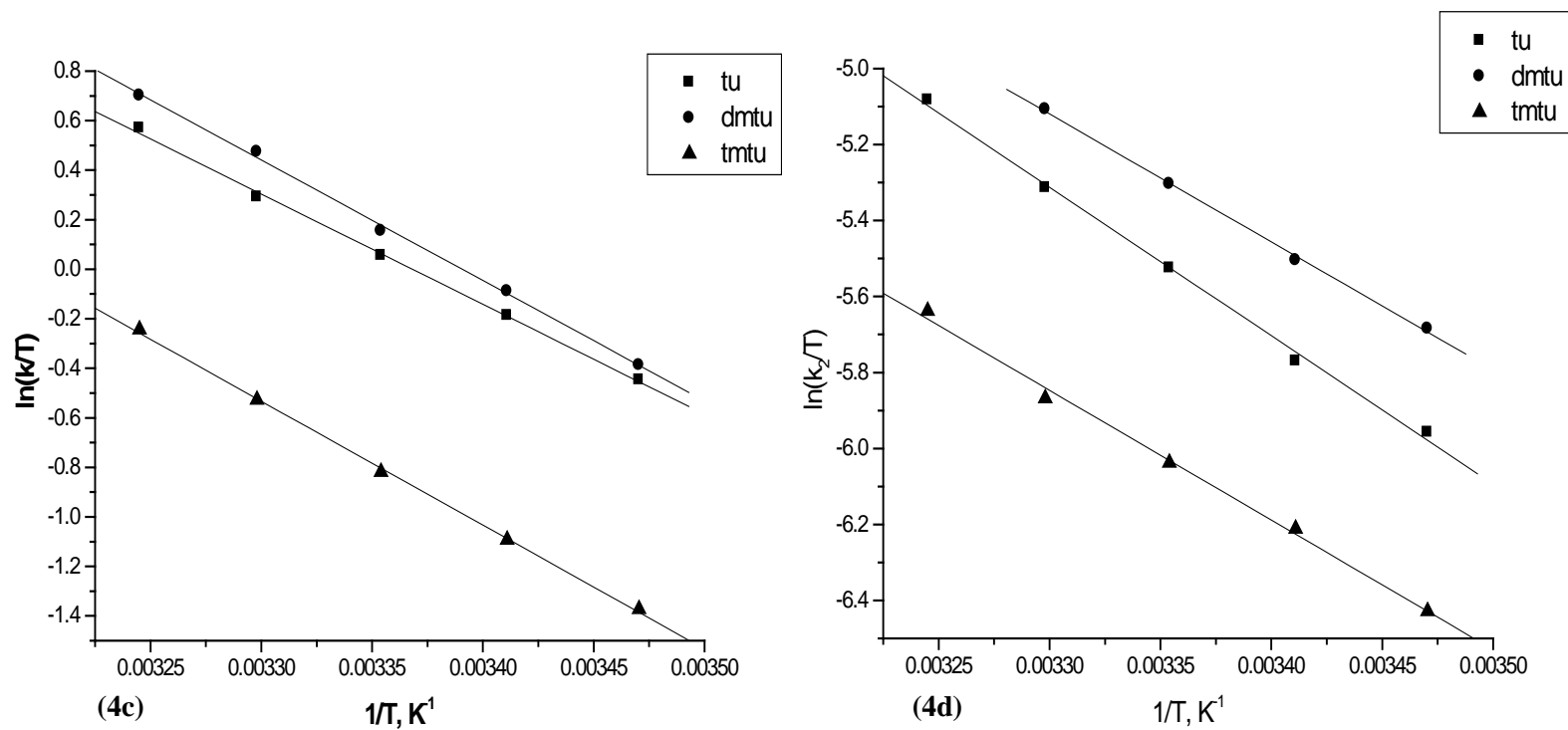


**Figure B 4c** Temperature dependence of  $k_{2(1^{st})}$ ,  $M^{-1} s^{-1}$ , for the simultaneous displacement of the first aqua ligand in **but** by thiourea nucleophiles, pH = 2.0, I = 0.02 M (0.01 M  $CF_3SO_3H$ , adjusted with  $Li(SO_3CF_3)$ ).

**Figure B 4d** Temperature dependence of  $k_{2(2^{nd})}$ ,  $M^{-1} s^{-1}$ , for the dechelation of the pyridyl units in **but** by thiourea, pH = 2.0, I = 0.02 M (0.01 M  $CF_3SO_3H$ , adjusted with  $Li(SO_3CF_3)$ ).

## Appendices

**Table B 1a.** Average observed rate constants,  $k_{\text{obs.}(1)}^{\text{st}}$ ,  $\text{s}^{-1}$ , for the simultaneous displacement of the aqua ligands in **But** by thiourea nucleophiles,  $\text{pH} = 2.0$ ,  $T = 298 \text{ K}$ ,  $I = 0.02 \text{ M}$   $\{0.01 \text{ M CF}_3\text{SO}_3\text{H}$ , adjusted with  $\text{Li}(\text{SO}_3\text{CF}_3)\}$ .

nucleophiles					
tu		dmtu		tmtu	
Conc., M	$k_{\text{obs.}, \text{s}^{-1}}$	Conc., M	$k_{\text{obs.}, \text{s}^{-1}}$	Conc., M	$k_{\text{obs.}, \text{s}^{-1}}$
0.001	0.3167	9.99E-4	0.3478	0.001	0.1383
0.002	0.639	0.002	0.6965	0.00201	0.2695
0.003	0.9457	0.003	1.043	0.00301	0.3954
0.004	1.266	0.004	1.349	0.00401	0.5218
0.005	1.5712	0.005	1.743	0.00502	0.6464

**Table B 1b** Average observed rate constants,  $k_{\text{obs.}(2)}^{\text{nd}}$ ,  $\text{s}^{-1}$ , for the dechelation of the pyridyl units in **But** by thiourea nucleophiles,  $\text{pH} = 2.0$ ,  $T = 298 \text{ K}$ ,  $I = 0.02 \text{ M}$   $\{0.01 \text{ M CF}_3\text{SO}_3\text{H}$ , adjusted with  $\text{Li}(\text{SO}_3\text{CF}_3)\}$ .

nucleophiles					
tu		dmtu		tmtu	
Conc., M	$k_{\text{obs.}, \text{s}^{-1}}$	Conc. M	$k_{\text{obs.}, \text{s}^{-1}}$	Conc. M	$k_{\text{obs.}, \text{s}^{-1}}$
0.001	0.00118	9.99E-4	0.00103	0.001	5.1E-4
0.002	0.00242	0.002	0.00209	0.00201	9.7E-4
0.003	0.00356	0.003	0.00308	0.00301	0.00151
0.004	0.00462	0.004	0.00414	0.00401	0.002
0.005	0.00574	0.005	0.00522	0.00502	0.00261

**Table B 1c** Temperature dependence of  $k_{2(1)}^{\text{st}}$ ,  $\text{M}^{-1} \text{s}^{-1}$ , for the simultaneous displacement of the first aqua ligand in **But** by thiourea nucleophiles,  $\text{pH} = 2.0$ ,  $I = 0.02 \text{ M}$   $(0.01 \text{ M CF}_3\text{SO}_3\text{H}$ , adjusted with  $\text{Li}(\text{SO}_3\text{CF}_3)$ ).

nucleophiles					
tu		dmtu		tmtu	
1/T., $\text{K}^{-1}$	$\ln(k/T)$	1/T., $\text{K}^{-1}$	$\ln(k/T)$	1/T., $\text{K}^{-1}$	$\ln(k/T)$
0.00325	0.5683	0.00325	0.7012	0.00325	-0.2443
0.0033	0.2911	0.0033	0.4736	0.0033	-0.5279
0.00335	0.0547	0.00335	0.1546	0.00335	-0.8197
0.00341	-0.1879	0.00341	-0.089	0.00341	-1.093
0.00347	-0.447	0.00347	-0.3886	0.00347	-1.373

## Appendices

**Table B 1d** Temperature dependence of  $k_{2(2^{nd})}$ ,  $M^{-1} s^{-1}$ , for the dechelation of the pyridyl units in **But** by thiourea nucleophiles, pH = 2.0, I = 0.02 M (0.01 M  $CF_3SO_3H$ , adjusted with  $Li(SO_3CF_3)$ ).

nucleophiles					
tu		dmtu		tmtu	
(1/T), $K^{-1}$	$\ln(k/T)$	(1/T), $K^{-1}$	$\ln(k/T)$	(1/T), $K^{-1}$	$\ln(k/T)$
0.00325	-5.083	0.00325		0.00325	-5.638
0.0033	-5.314	0.0033	-5.107	0.0033	-5.868
0.00335	-5.525	0.00335	-5.3038	0.00335	-6.038
0.00341	-5.77	0.00341	-5.505	0.00341	-6.212
0.00347	-5.958	0.00347	-5.685	0.00347	-6.429

**Table B 2a** Concentration dependence of  $k_{obs.(1^{st})}$ ,  $s^{-1}$ , for the substitution of the aqua ligand in **Dec** by thiourea nucleophiles, pH = 2.0, T = 298 K, I = 0.02 M {0.01 M  $CF_3SO_3H$ , adjusted with  $Li(SO_3CF_3)$ }.

nucleophiles					
tu		dmtu		tmtu	
Conc., M	$k_{obs.}, s^{-1}$	Conc., M	$k_{obs.}, s^{-1}$	Conc., M	$k_{obs.}, s^{-1}$
0.001	0.6036	0.00102	0.635	0.00101	0.1980
0.002	1.2610	0.00204	1.354	0.00201	0.3786
0.003	1.9160	0.00306	1.933	0.00301	0.5816
0.004	2.5830	0.00408	2.579	0.00401	0.8142
0.005	3.2212	0.00510	3.202	0.00502	0.9886

**Table B 2b** Temperature dependence of  $k_{2(1^{st})}$ ,  $M^{-1} s^{-1}$ , for the simultaneous displacement of the first aqua ligand in **Dec** by thiourea nucleophiles, pH = 2.0, I = 0.02 M (0.01 M  $CF_3SO_3H$ , adjusted with  $Li(SO_3CF_3)$ ).

nucleophiles					
tu		dmtu		tmtu	
Conc., M	$k_{obs.}, s^{-1}$	Conc. M	$k_{obs.}, s^{-1}$	Conc. M	$k_{obs.}, s^{-1}$
0.001	0.00606	0.00101	0.00348	0.00101	0.00167
0.002	0.01306	0.00202	0.00722	0.00201	0.00366
0.003	0.01932	0.00303	0.01071	0.00301	0.00565
0.004	0.02656	0.00405	0.01429	0.00402	0.00736
0.005	0.03256	0.00506	0.01740	0.00502	0.00914

# Appendices

## Appendix C

### Phenyldiamine and cyclohexyldiamine-bridged Pt(II) Complexes.

Figure C 1a	Mass spectrum (TOF-MS <sup>+</sup> ) for <i>N,N,N',N'</i> -tetrakis(2-pyridylmethyl)-1,4-phenyldiamine ligand.	285
Figure C 1b	Mass spectrum (TOF-MS <sup>+</sup> ) for <i>N,N</i> -bis(2-pyridylmethyl)cyclohexylamine ligand.	286
Figure C 2a	IR spectrum (KBr pellet) of <i>N,N,N',N'</i> -tetrakis(2-pyridylmethyl)-4,4'-methylenediaminocyclohexane ligand.	287
Figure C 2b	IR spectrum (KBr pellet) of [Pt(Cl)( <i>N,N</i> -bis(2-pyridylmethyl)phenylamine)](ClO <sub>4</sub> ).	287
Figure C 3a	<sup>1</sup> H Spectrum of [{Pt(Cl)} <sub>2</sub> ( <i>N,N,N',N'</i> -tetrakis(2-pyridylmethyl)-4,4'-methylenediaminocyclohexane)](ClO <sub>4</sub> ) <sub>2</sub> .	288
Figure C 3b	<sup>195</sup> Pt Spectrum of [{Pt(Cl)} <sub>2</sub> ( <i>N,N,N',N'</i> -tetrakis(2-pyridylmethyl)-4,4'-methylenediaminocyclohexane)](ClO <sub>4</sub> ) <sub>2</sub> .	289
Figure C 4a	<sup>1</sup> H Spectrum of [{Pt(Cl)} <sub>2</sub> ( <i>N,N,N',N'</i> -tetrakis(2-pyridylmethyl)- <i>trans</i> -1,4-cyclohexyldiamine)](ClO <sub>4</sub> ) <sub>2</sub> .	290
Figure C 4b	<sup>13</sup> C Spectrum of [{Pt(Cl)} <sub>2</sub> ( <i>N,N,N',N'</i> -tetrakis(2-pyridylmethyl)- <i>trans</i> -1,4-cyclohexyldiamine)](ClO <sub>4</sub> ) <sub>2</sub> .	291
Figure C 4c	Spectrum of [{Pt(Cl)} <sub>2</sub> ( <i>N,N,N',N'</i> -tetrakis(2-pyridylmethyl)- <i>trans</i> -1,4-cyclohexyldiamine)](ClO <sub>4</sub> ) <sub>2</sub> .	292
Figure C 5a	UV-visible spectrum for the titration of 0.1 mM <b>bpCHna</b> with NaOH, pH range 2 - 9, T 298 K. <i>Inset</i> the titration curve at 270 nm.	293
Figure C 5b	UV-visible spectrum for the titration of 0.1 mM <b>pPh</b> with NaOH, pH range 2 - 9, T 298 K. <i>Inset</i> the titration curve at 267 nm.	294
Figure C 6a	Concentration dependence of $k_{\text{obs.}(1)}^{\text{st}}$ , s <sup>-1</sup> , for the substitution of the aqua ligand in <b>mPh</b> by thiourea nucleophiles, pH = 2.0, T = 298 K.	295
Figure C 6b	Average observed rate constants, $k_{\text{obs.}(2)}^{\text{nd}}$ , s <sup>-1</sup> , for the dechelation of the pyridyl units in <b>mPh</b> by thiourea nucleophiles, pH = 2.0, T = 298 K.	295
Figure C 7a	Concentration dependence of $k_{\text{obs.}(1)}^{\text{st}}$ , s <sup>-1</sup> , for the substitution of the aqua ligand in <b>bpPha</b> by thiourea nucleophiles, pH = 2.0, T = 298 K.	296
Figure C 7b	Average observed rate constants, $k_{\text{obs.}(2)}^{\text{nd}}$ , s <sup>-1</sup> , for the dechelation of the pyridyl units in <b>bpPha</b> by thiourea nucleophiles, pH = 2.0, T = 298 K.	296
Figure C 8a	Temperature dependence of $k_{2(1)}^{\text{st}}$ , M <sup>-1</sup> s <sup>-1</sup> , for the simultaneous displacement of the first aqua ligand in <b>bpPha</b> by thiourea nucleophiles, pH = 2.0.	297
Figure C 8b	Temperature dependence of $k_{2(2)}^{\text{nd}}$ , M <sup>-1</sup> s <sup>-1</sup> , for the dechelation of the pyridyl units in <b>bpPha</b> by thiourea nucleophiles, pH = 2.0.	297
Table C 1a.	Average observed rate constants, $k_{\text{obs.}(1)}^{\text{st}}$ , s <sup>-1</sup> , for the simultaneous displacement of the aqua ligands in <b>mPh</b> by thiourea nucleophiles, pH = 2.0, T = 298 K.	298
Table C 1b	Average observed rate constants, $k_{\text{obs.}(2)}^{\text{nd}}$ , s <sup>-1</sup> , for the dechelation of the pyridyl units in <b>mPh</b> by thiourea nucleophiles, pH = 2.0, T = 298 K.	298
Table C 1c	Temperature dependence of $k_{2(1)}^{\text{st}}$ , M <sup>-1</sup> s <sup>-1</sup> , for the simultaneous displacement of the first aqua ligand in <b>mPh</b> by thiourea nucleophiles, pH = 2.0.	298

## Appendices

---

<b>Table C 1d</b>	Temperature dependence of $k_{2(2)^{\text{nd}}}$ , $\text{M}^{-1} \text{s}^{-1}$ , for the dechelation of the pyridyl units in <b>mPh</b> by thiourea nucleophiles, $\text{pH} = 2.0$ .	<b>298</b>
<b>Table C 2a.</b>	Average observed rate constants, $k_{\text{obs.}(1)^{\text{st}}}$ , $\text{s}^{-1}$ , for the simultaneous displacement of the aqua ligands in <b>bpPha</b> by thiourea nucleophiles, $\text{pH} = 2.0$ , $T = 298 \text{ K}$ .	<b>299</b>
<b>Table C 2b</b>	Average observed rate constants, $k_{\text{obs.}(2)^{\text{nd}}}$ , $\text{s}^{-1}$ , for the dechelation of the pyridyl units in <b>bpPha</b> by thiourea nucleophiles, $\text{pH} = 2.0$ , $T = 298 \text{ K}$ .	<b>299</b>
<b>Table C 2c</b>	Temperature dependence of $k_{2(1)^{\text{st}}}$ , $\text{M}^{-1} \text{s}^{-1}$ , for the simultaneous displacement of the first aqua ligand in <b>bpPha</b> by thiourea nucleophiles, $\text{pH} = 2.0$ .	<b>299</b>
<b>Table C 2d</b>	Temperature dependence of $k_{2(2)^{\text{nd}}}$ , $\text{M}^{-1} \text{s}^{-1}$ , for the dechelation of the pyridyl units in <b>bpPha</b> by thiourea nucleophiles, $\text{pH} = 2.0$ .	<b>299</b>

---

# Appendices

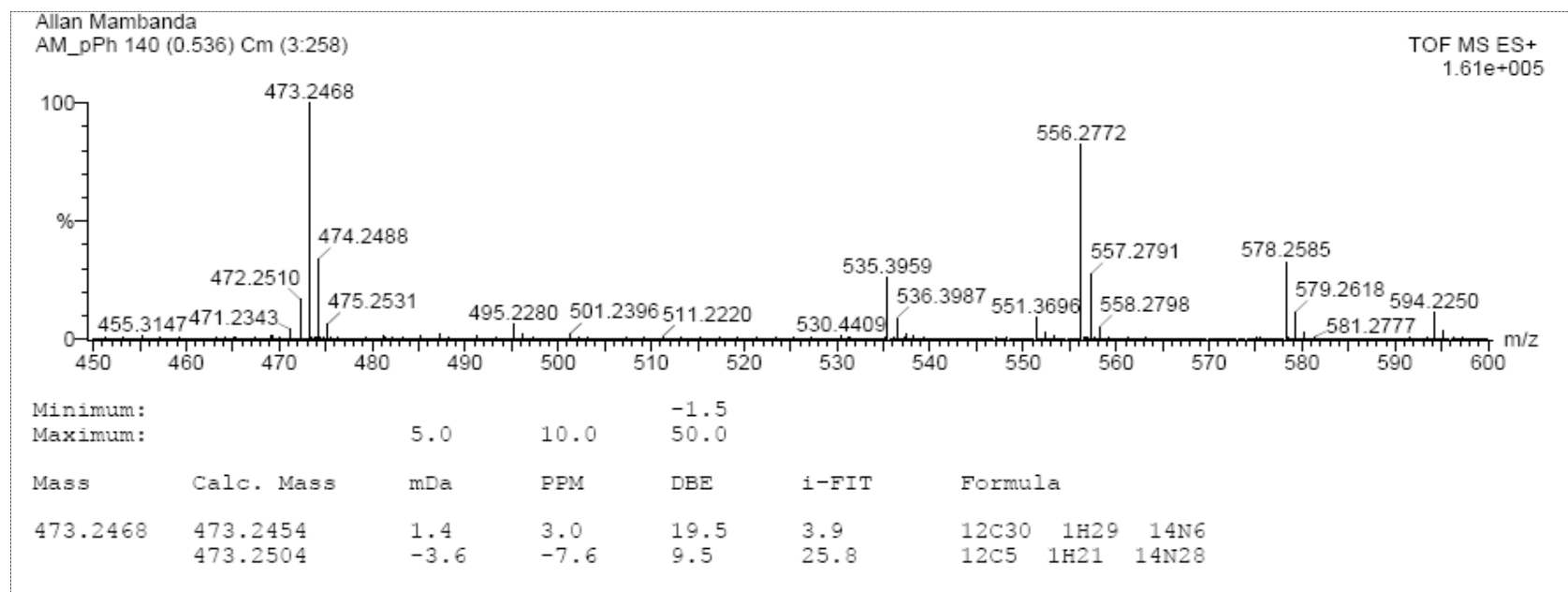


**Figure C 1a** Mass spectrum (TOF-MS<sup>+</sup>) for *N,N,N',N'*-tetrakis(2-pyridylmethyl)-1,4-phenyldiamine ligand.

# Appendices

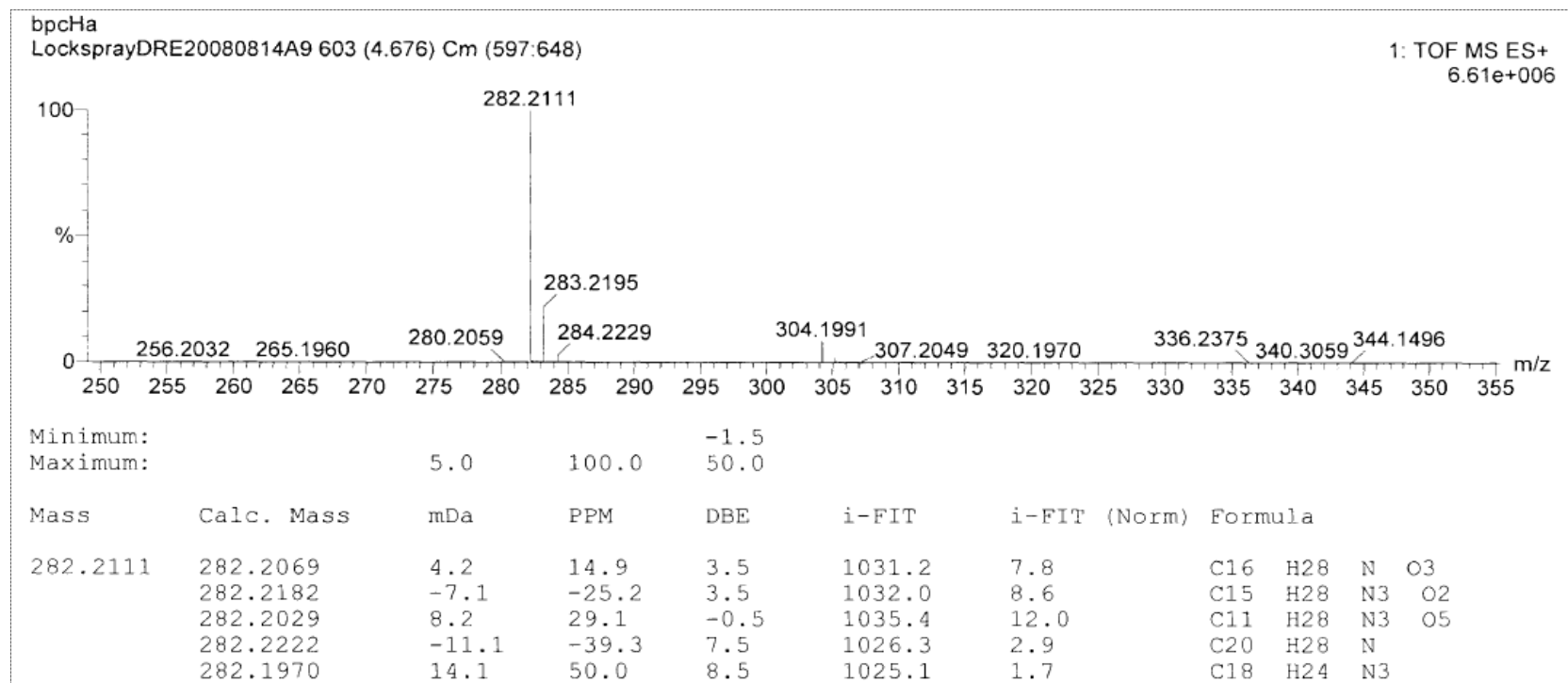


**Figure C 1b** Mass spectrum (TOF-MS<sup>+</sup>) for *N,N*-bis(2-pyridylmethyl)cyclohexylamine ligand.

# Appendices

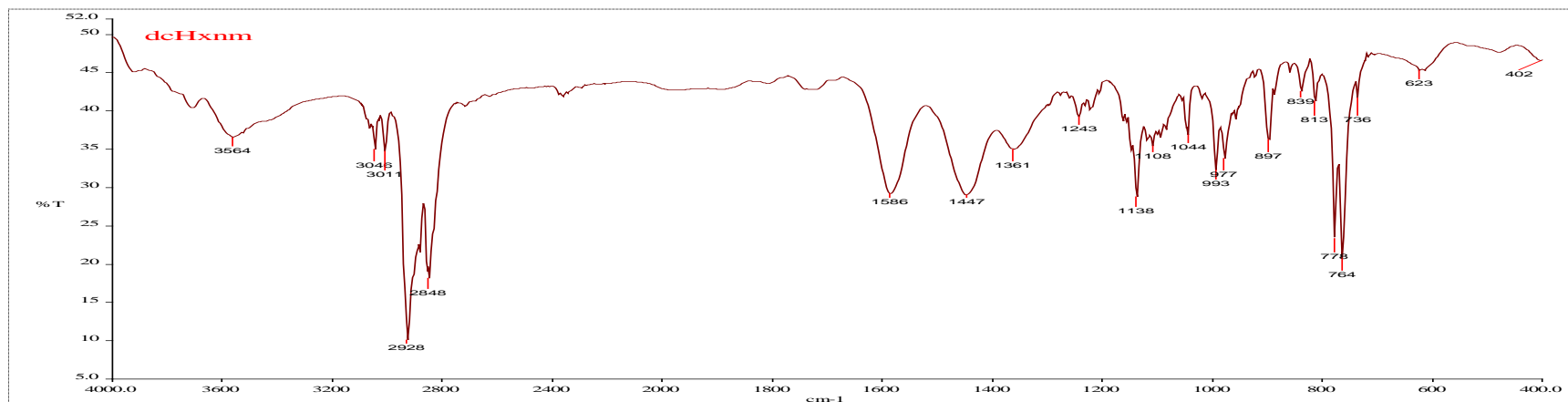


Figure C 2a IR spectrum (KBr pellet) of *N,N,N',N'*-tetrakis(2-pyridylmethyl)-4,4'-methylenediaminocyclohexane ligand.

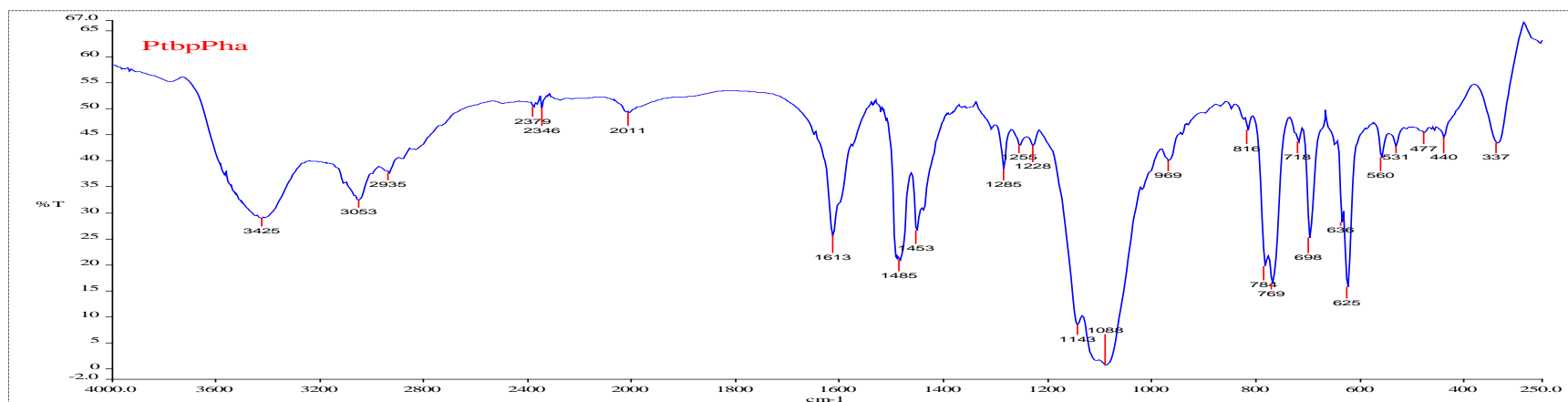
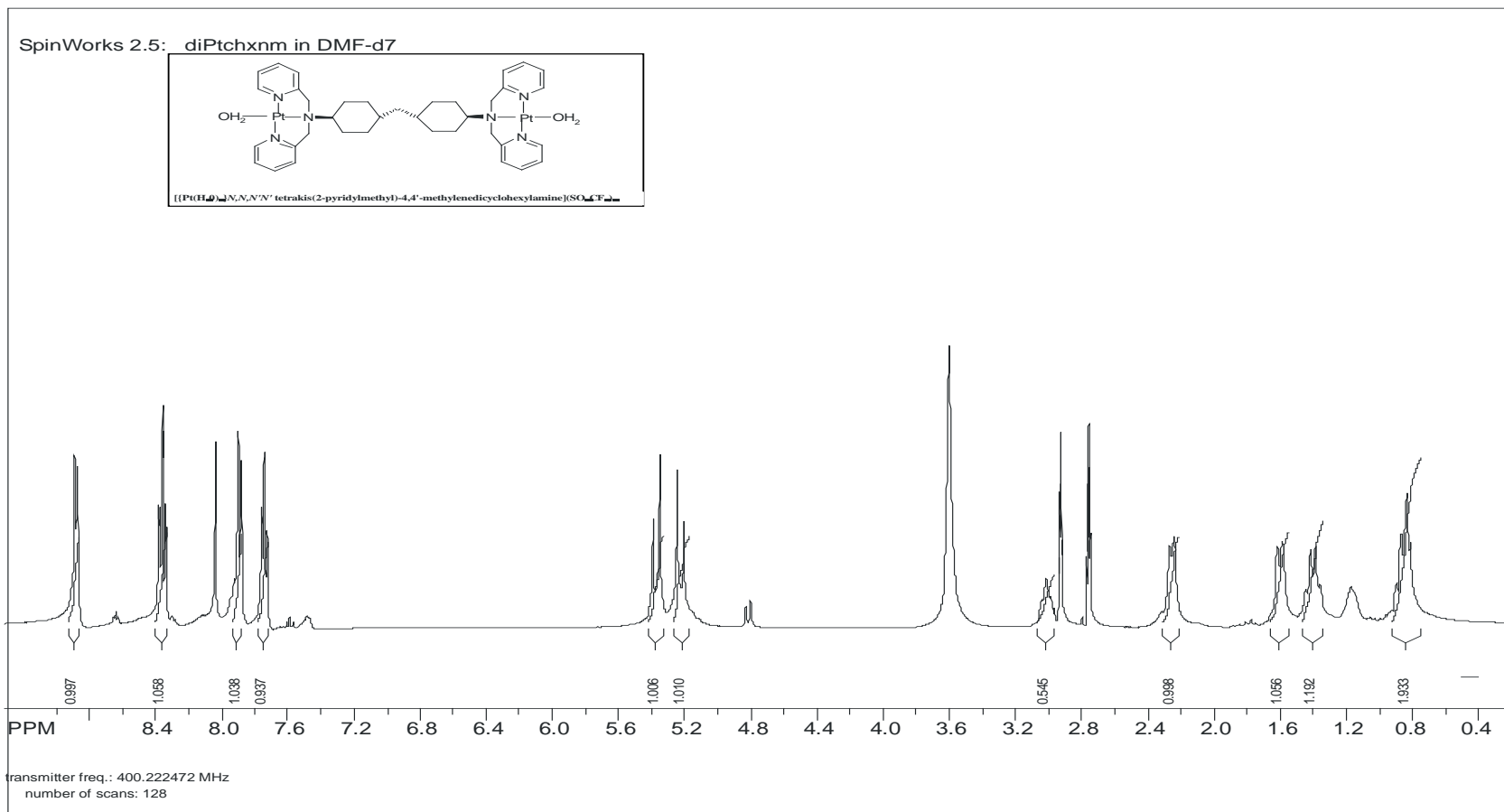


Figure C 2b IR spectrum (KBr pellet) of  $[\text{Pt}(\text{Cl})(\text{N},\text{N}\text{-bis}(2\text{-pyridylmethyl})\text{phenylamine})](\text{ClO}_4)$ .

# Appendices



**Figure C 3a**  $^1\text{H}$  Spectrum of  $[\{\text{Pt}(\text{Cl})\}_2(N,N,N',N'\text{-tetrakis}(2\text{-pyridylmethyl})\text{-}4,4'\text{-methylenediaminocyclohexane})](\text{ClO}_4)_2$

# Appendices

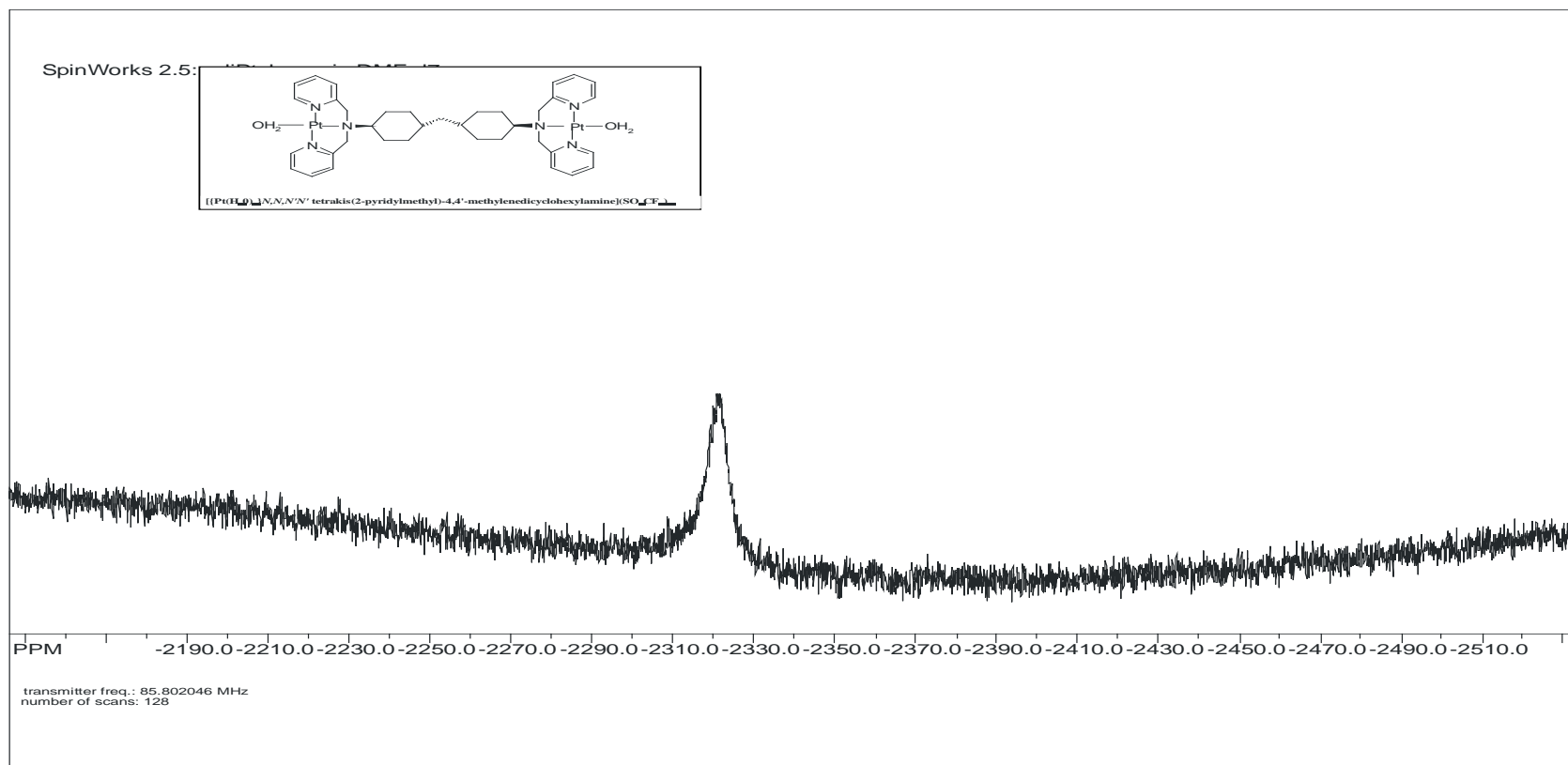


**Figure C 3b**  $^{195}\text{Pt}$  Spectrum of  $[\{\text{Pt}(\text{Cl})\}_2(\text{N},\text{N}',\text{N}',\text{N}'\text{-tetrakis}(2\text{-pyridylmethyl})\text{-}4,4'\text{-methylenediaminocyclohexane})](\text{ClO}_4)_2$ .

# Appendices

SpinWorks 2.5: Ptpbcha in DMF-d7

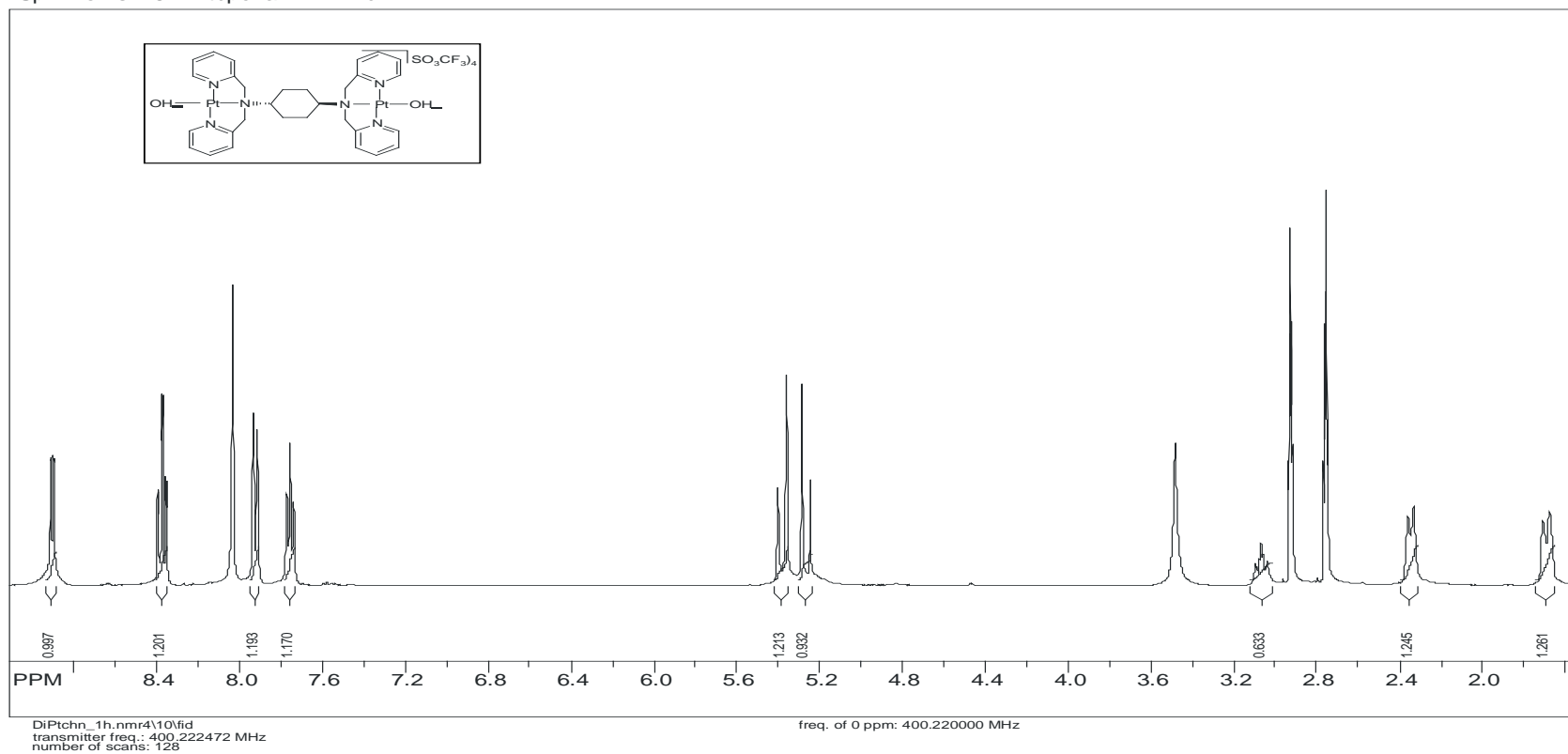


**Figure C 4a**  $^1\text{H}$  Spectrum of  $[\{\text{Pt}(\text{Cl})\}_2(\text{N,N,N',N'}\text{-tetrakis}(2\text{-pyridylmethyl})\text{-trans-1,4-cyclohexyldiamine})](\text{ClO}_4)_2$

# Appendices

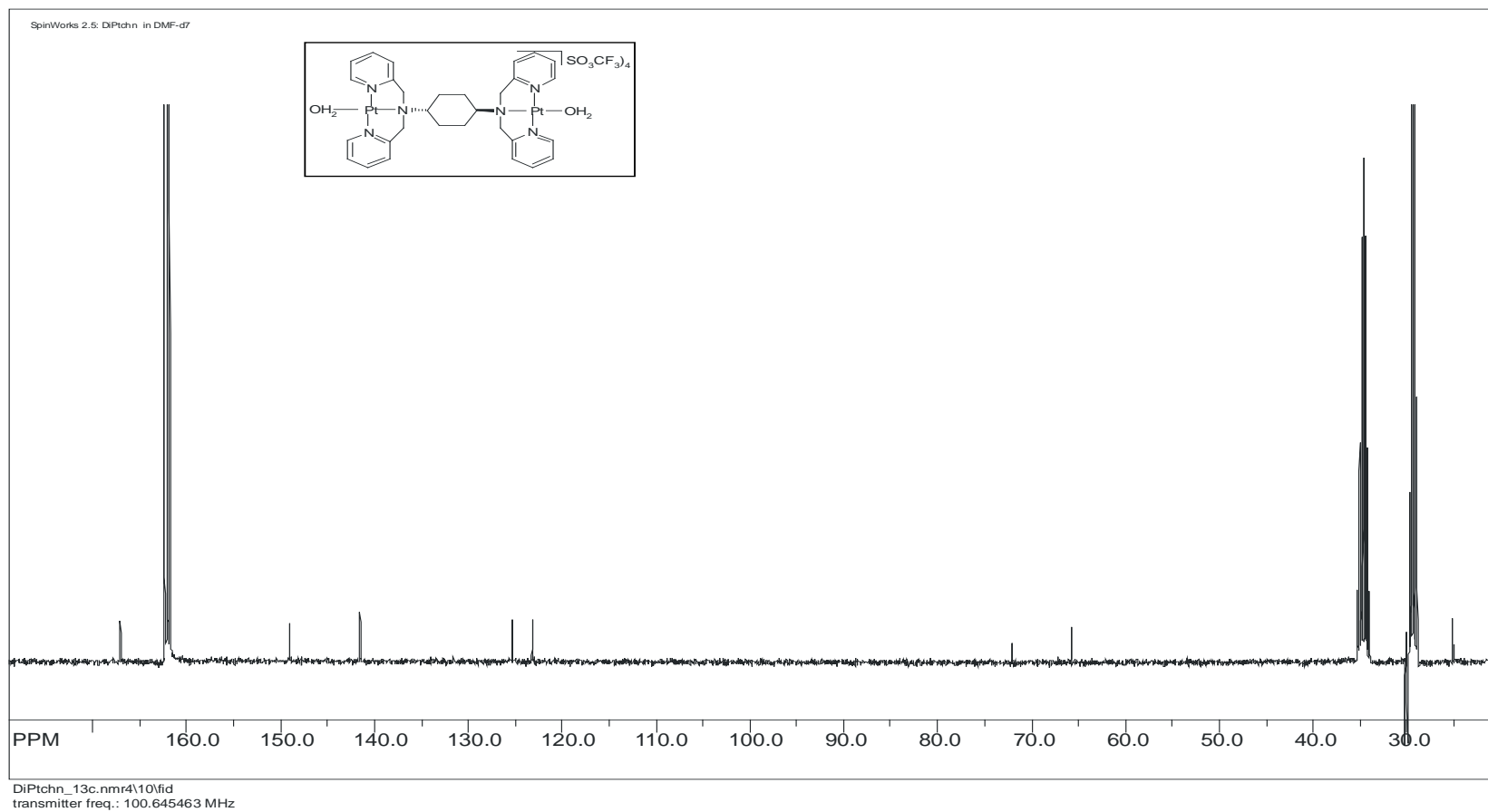
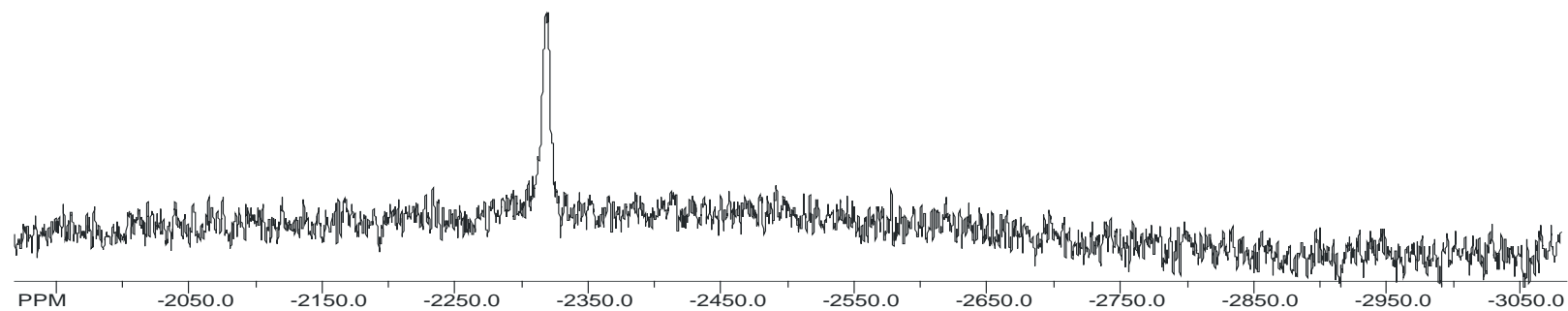
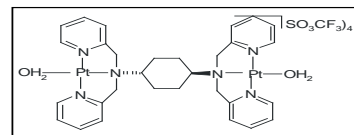


**Figure C 4b**  $^{13}\text{C}$  Spectrum of  $[\{\text{Pt}(\text{Cl})\}_2(\text{N,N,N',N'-tetrakis}(2\text{-pyridylmethyl})\text{-trans-1,4-cyclohexyldiamine})](\text{ClO}_4)_2$

# Appendices

SpinWorks 2.5: DiPtchn in DMF-d7



DiPtchn\_195pt.nmr41vid  
transmitter freq.: 85.819301 MHz

**Figure C 4c** Spectrum of [ $\{\text{Pt}(\text{Cl})\}_2(N,N,N',N'$ -tetrakis(2-pyridylmethyl)-*trans*-1,4-cyclohexyldiamine)](ClO<sub>4</sub>)<sub>2</sub>

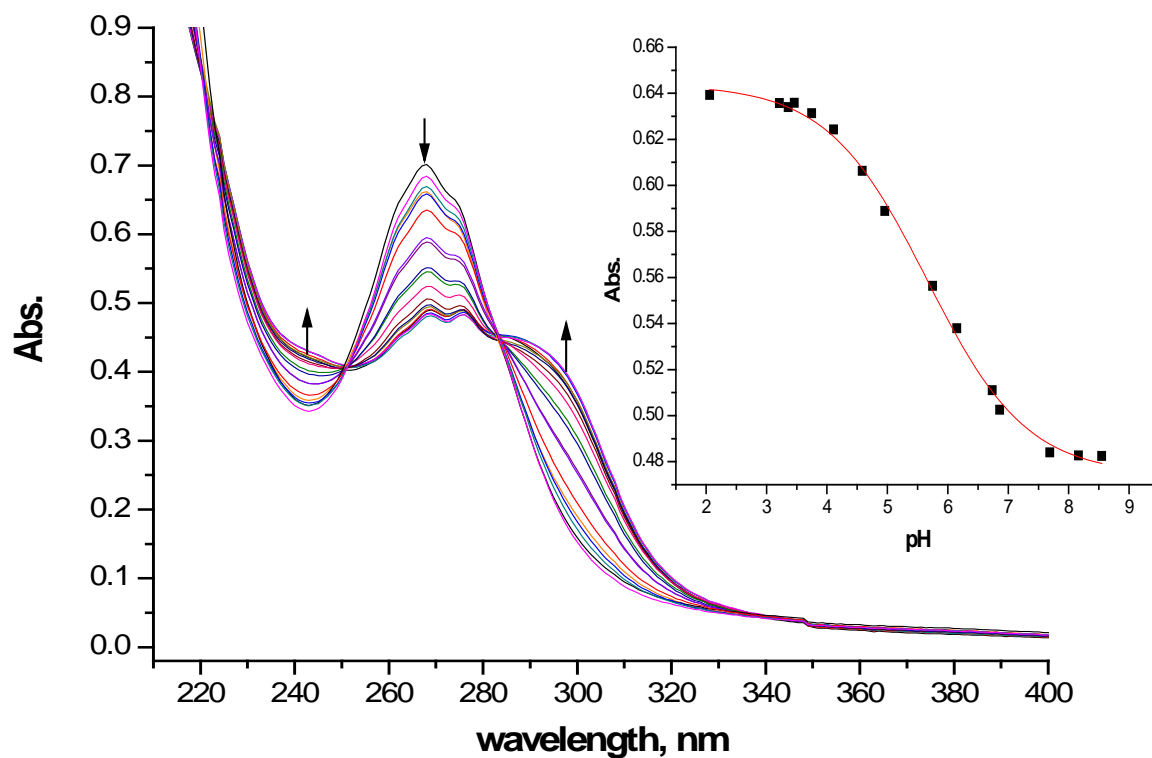


**Figure C 5a** UV-visible spectrum for the titration of 0.1 mM **bpcHna** with NaOH, pH range 2 - 9, T 298 K. *Inset* the titration curve at 270 nm.

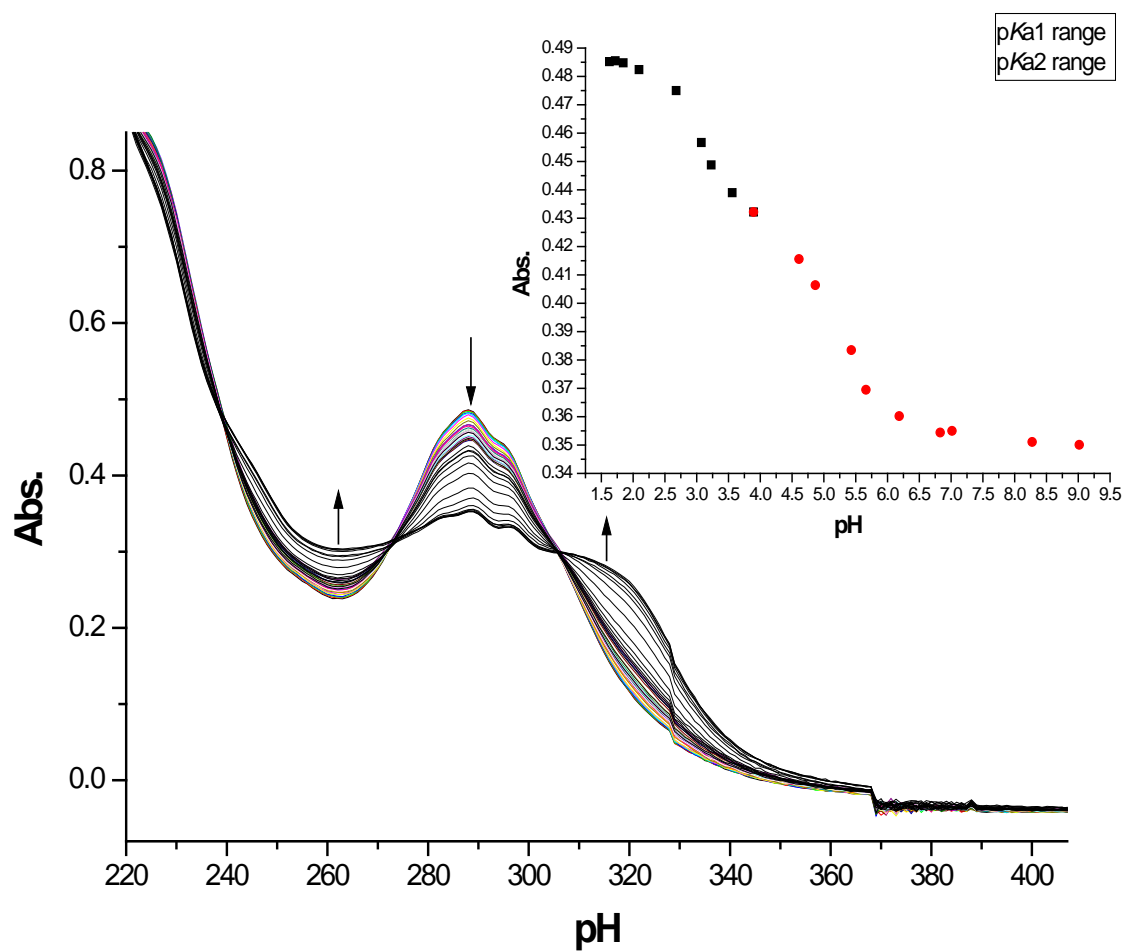


**Figure C 5b** UV-visible spectrum for the titration of 0.1 mM **pPh** with NaOH, pH range 2 - 9, T 298 K. *Inset* the titration curve at 267 nm.

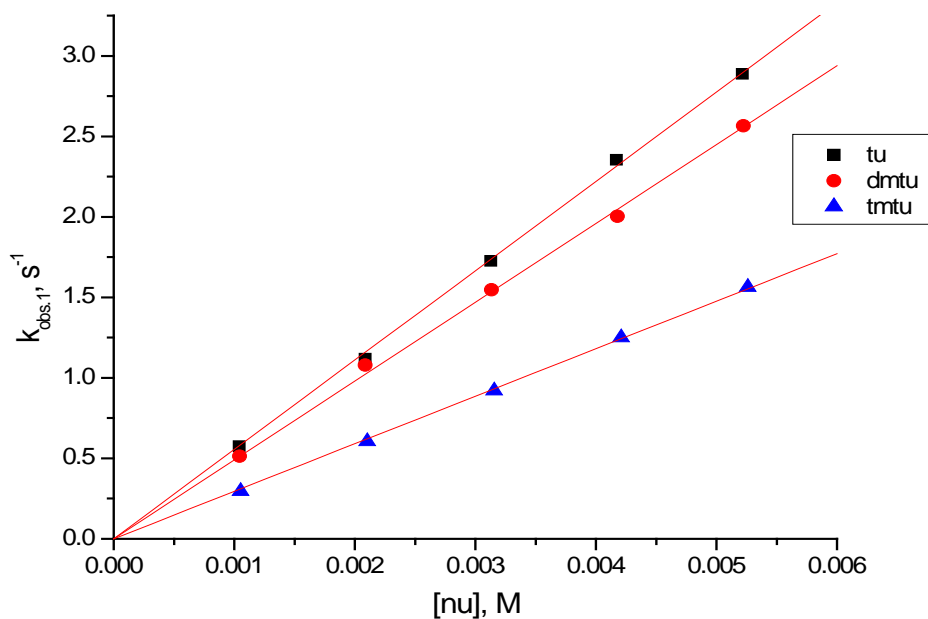


**Figure C 6a** Concentration dependence of  $k_{obs.(1)}, s^{-1}$ , for the substitution of the aqua ligand in **mPh** by thiourea nucleophiles, pH = 2.0, T = 298 K, I = 0.02 M {0.01 M  $CF_3SO_3H$ , adjusted with  $Li(SO_3CF_3)$ }.

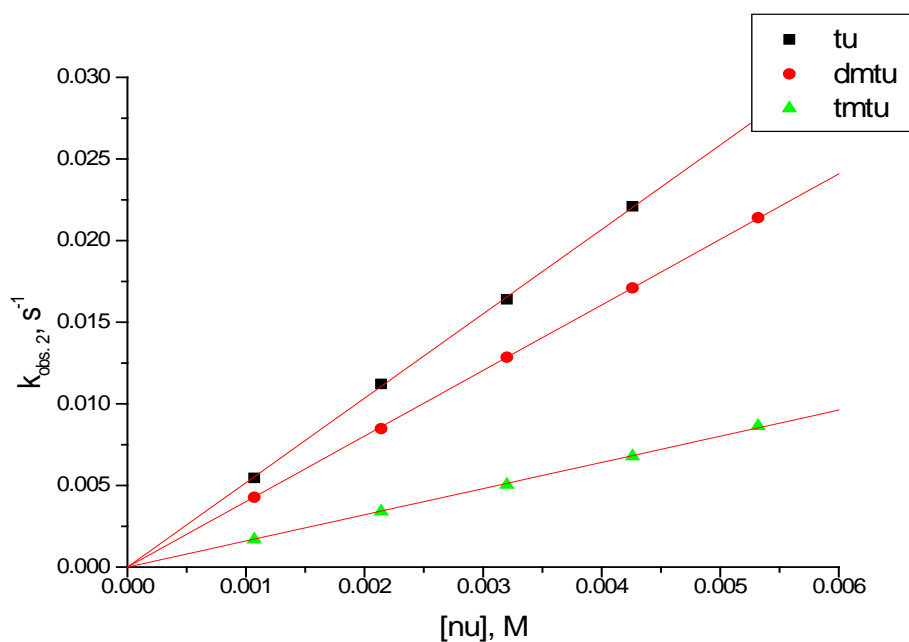


**Figure C 6b** Average observed rate constants,  $k_{obs.(2)}, s^{-1}$ , for the dechelation of the pyridyl units in **mPh** by thiourea nucleophiles, pH = 2.0, T = 298 K, I = 0.02 M {0.01 M  $CF_3SO_3H$ , adjusted with  $Li(SO_3CF_3)$ }.

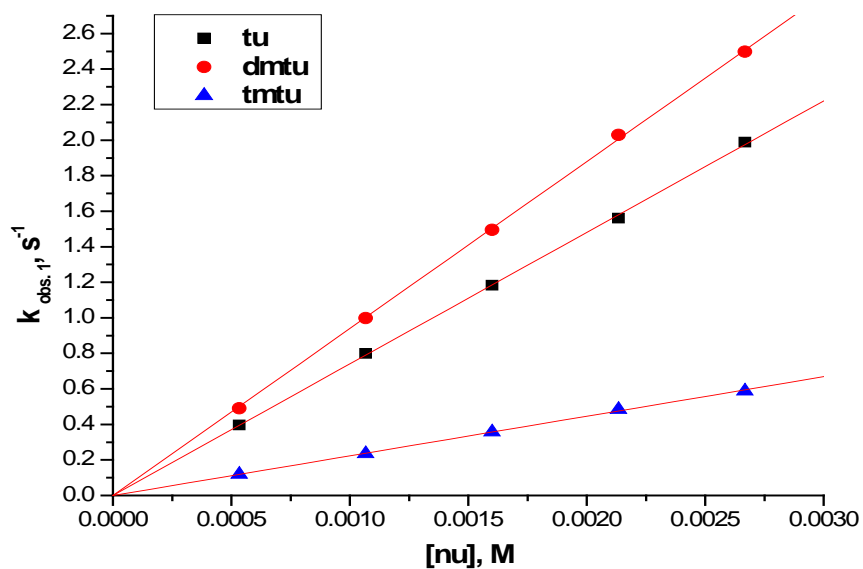


**Figure C 7a** Concentration dependence of  $k_{obs.(1^{st})}, s^{-1}$ , for the substitution of the aqua ligand in **bpPha** by thiourea nucleophiles, pH = 2.0, T = 298 K, I = 0.02 M {0.01 M  $CF_3SO_3H$ , adjusted with  $Li(SO_3CF_3)$ }.

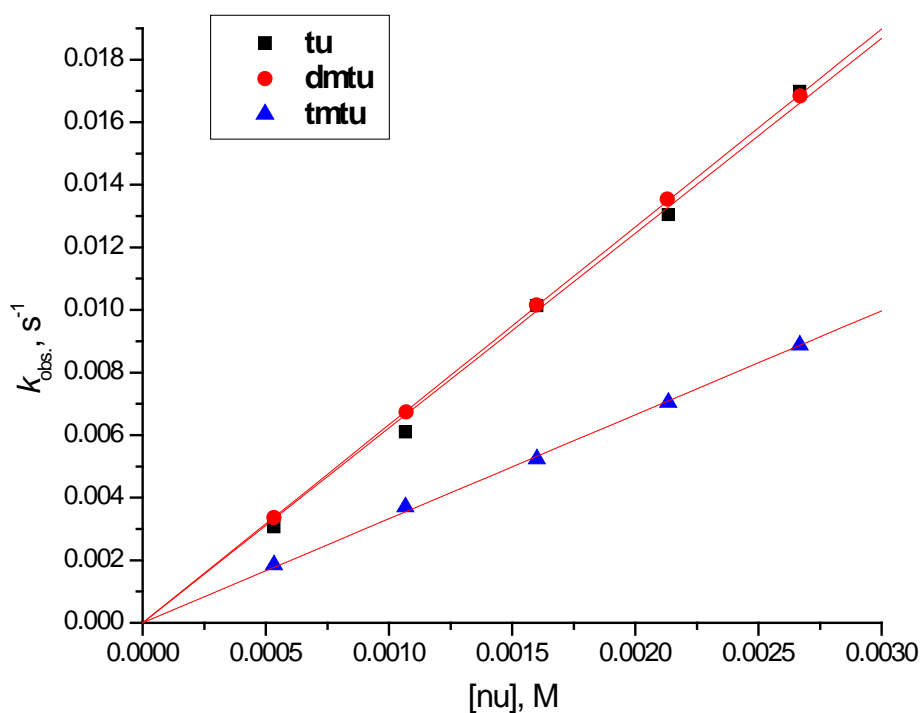


**Figure C 7b** Average observed rate constants,  $k_{obs.(2^{nd})}, s^{-1}$ , for the dechelation of the pyridyl units in **bpPha** by thiourea nucleophiles, pH = 2.0, T = 298 K, I = 0.02 M {0.01 M  $CF_3SO_3H$ , adjusted with  $Li(SO_3CF_3)$ }.

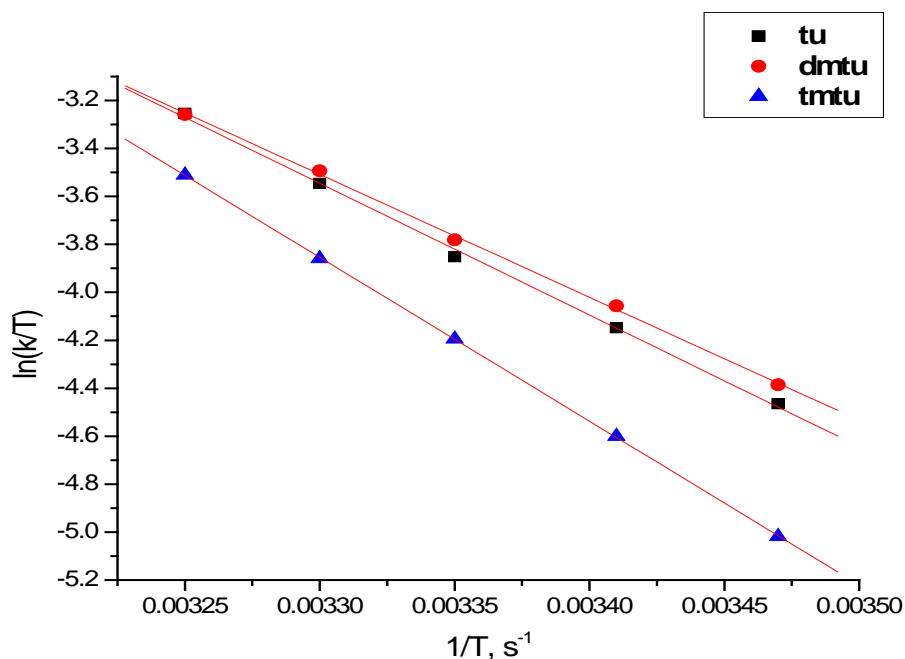


**Figure C 8a** Temperature dependence of  $k_{2(1)^{\text{st}}}$ ,  $\text{M}^{-1} \text{s}^{-1}$ , for the simultaneous displacement of the first aqua ligand in **bpPha** by thiourea nucleophiles,  $\text{pH} = 2.0$ ,  $I = 0.02 \text{ M}$  ( $0.01 \text{ M}$   $\text{CF}_3\text{SO}_3\text{H}$ , adjusted with  $\text{Li}(\text{SO}_3\text{CF}_3)$ ).

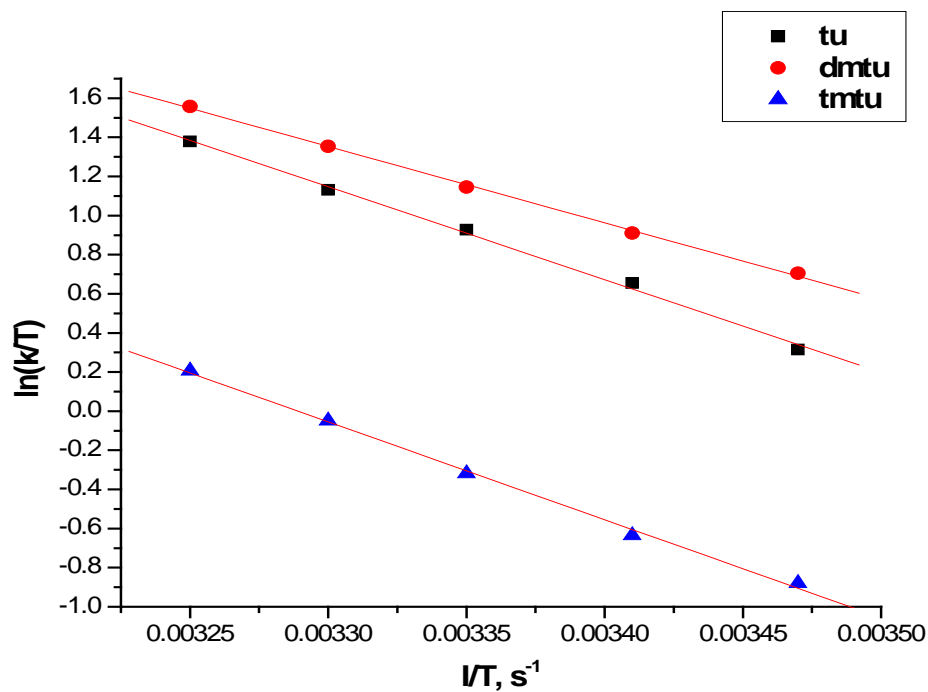


**Figure C 8b** Temperature dependence of  $k_{2(2)^{\text{nd}}}$ ,  $\text{M}^{-1} \text{s}^{-1}$ , for the dechelation of the pyridyl units in **bpPha** by thiourea nucleophiles,  $\text{pH} = 2.0$ ,  $I = 0.02 \text{ M}$  ( $0.01 \text{ M}$   $\text{CF}_3\text{SO}_3\text{H}$ , adjusted with  $\text{Li}(\text{SO}_3\text{CF}_3)$ ).

## Appendices

**Table C 1a.** Average observed rate constants,  $k_{\text{obs.}(1)^{\text{st}}}$ ,  $\text{s}^{-1}$ , for the simultaneous displacement of the aqua ligands in **mPh** by thiourea nucleophiles,  $\text{pH} = 2.0$ ,  $T = 298 \text{ K}$ ,  $I = 0.02 \text{ M}$   $\{0.01 \text{ M CF}_3\text{SO}_3\text{H}$ , adjusted with  $\text{Li}(\text{SO}_3\text{CF}_3)\}$ .

[tu]	$k_{\text{obs } 1}$	[dmtu]	$k_{\text{obs } 1}$	[tmtu]	$k_{\text{obs } 1}$
0.00104	0.5761	0.00104	0.5123	0.00105	0.2961
0.00209	1.118	0.00209	1.078	0.0021	0.6049
0.00313	1.725	0.00314	1.546	0.00316	0.9206
0.00417	2.354	0.00418	2.003	0.00421	1.251
0.00522	2.888	0.00522	2.565	0.00526	1.563

**Table C 1b** Average observed rate constants,  $k_{\text{obs.}(2)^{\text{nd}}}$ ,  $\text{s}^{-1}$ , for the dechelation of the pyridyl units in **mPh** by thiourea nucleophiles,  $\text{pH} = 2.0$ ,  $T = 298 \text{ K}$ ,  $I = 0.02 \text{ M}$   $\{0.01 \text{ M CF}_3\text{SO}_3\text{H}$ , adjusted with  $\text{Li}(\text{SO}_3\text{CF}_3)\}$ .

[tu]	$k_{\text{obs } 1}$	[dmtu]	$k_{\text{obs } 1}$	[tmtu]	$k_{\text{obs } 1}$
0.00107	0.00546	0.00107	0.00428	0.00107	0.00169
0.00214	0.01122	0.00214	0.00848	0.00214	0.0034
0.0032	0.0164	0.0032	0.01286	0.0032	0.00504
0.00426	0.0221	0.00426	0.0171	0.00426	0.00678
0.00532	0.0275	0.00532	0.0214	0.00532	0.00864

**Figure C 1c** Temperature dependence of  $k_{2(1)^{\text{st}}}$ ,  $\text{M}^{-1} \text{ s}^{-1}$ , for the simultaneous displacement of the first aqua ligand in **mPh** by thiourea nucleophiles,  $\text{pH} = 2.0$ ,  $I = 0.02 \text{ M}$  (0.01 M  $\text{CF}_3\text{SO}_3\text{H}$ , adjusted with  $\text{Li}(\text{SO}_3\text{CF}_3)$ ).

1/T	$\ln(k/T)$	1/T	$\ln(k/T)$	1/T	$\ln(k/T)$
0.00325	0.8619	0.00325	0.9561	0.00325	0.426
0.0033	0.6638	0.0033	0.7871	0.0033	0.256
0.00335	0.4689	0.00335	0.6051	0.00335	0.1003
0.00341	0.2712	0.00341	0.4208	0.00341	-0.101
0.00347	0.0204	0.00347	0.2084	0.00347	-0.278

**Table C 1d** Temperature dependence of  $k_{2(2)^{\text{nd}}}$ ,  $\text{M}^{-1} \text{ s}^{-1}$ , for the dechelation of the pyridyl units in **mPh** by thiourea nucleophiles,  $\text{pH} = 2.0$ ,  $I = 0.02 \text{ M}$  (0.01 M  $\text{CF}_3\text{SO}_3\text{H}$ , adjusted with  $\text{Li}(\text{SO}_3\text{CF}_3)$ ).

1/T	$\ln(k/T)$	1/T	$\ln(k/T)$	1/T	$\ln(k/T)$
0.00325	-3.55	0.00325	-3.79	0.00325	-4.596
0.0033	-3.755	0.0033	-4.043	0.0033	-4.868
0.00335	-4.064	0.00335	-4.306	0.00335	-5.243
0.00341	-4.368	0.00341	-4.68	0.00341	-5.619
0.00347	-4.677	0.00347	-4.934	0.00347	-5.995

## Appendices

**Table C 2a.** Average observed rate constants,  $k_{\text{obs.}(1)^{\text{st}}}$ ,  $\text{s}^{-1}$ , for the simultaneous displacement of the aqua ligands in **bpPha** by thiourea nucleophiles,  $\text{pH} = 2.0$ ,  $T = 298 \text{ K}$ ,  $I = 0.02 \text{ M}$   $\{0.01 \text{ M CF}_3\text{SO}_3\text{H}$ , adjusted with  $\text{Li}(\text{SO}_3\text{CF}_3)\}$ .

[tu]	$k_{\text{obs.}1}$	[dmtu]	$k_{\text{obs.}1}$	[tmtu]	$k_{\text{obs.}1}$
5.3366E-4	0.4904	5.3366E-4	0.397	5.3366E-4	0.1197
0.00107	0.9981	0.00107	0.7997	0.00107	0.2355
0.0016	1.495	0.0016	1.183	0.0016	0.3578
0.00213	2.03	0.00213	1.561	0.00213	0.4847
0.00267	2.498	0.00267	1.988	0.00267	0.588

**Table C 2b** Average observed rate constants,  $k_{\text{obs.}(2)^{\text{nd}}}$ ,  $\text{s}^{-1}$ , for the dechelation of the pyridyl units in **bpPha** by thiourea nucleophiles,  $\text{pH} = 2.0$ ,  $T = 298 \text{ K}$ ,  $I = 0.02 \text{ M}$   $\{0.01 \text{ M CF}_3\text{SO}_3\text{H}$ , adjusted with  $\text{Li}(\text{SO}_3\text{CF}_3)\}$ .

1/T	$\ln(k/T)$	1/T	$\ln(k/T)$	1/T	$\ln(k/T)$
0.00325	1.379	0.00325	1.558	0.00325	0.207
0.0033	1.131	0.0033	1.354	0.0033	-0.049
0.00335	0.927	0.00335	1.146	0.00335	-0.319
0.00341	0.655	0.00341	0.9108	0.00341	-0.6345
0.00347	0.315	0.00347	0.7042	0.00347	-0.8789

**Figure C 2c** Temperature dependence of  $k_{2(1)^{\text{st}}}$ ,  $\text{M}^{-1} \text{ s}^{-1}$ , for the simultaneous displacement of the first aqua ligand in **bpPha** by thiourea nucleophiles,  $\text{pH} = 2.0$ ,  $I = 0.02 \text{ M}$  (0.01 M  $\text{CF}_3\text{SO}_3\text{H}$ , adjusted with  $\text{Li}(\text{SO}_3\text{CF}_3)$ ).

[tu]	$k_{\text{obs.}2}$	[dmtu]	$k_{\text{obs.}2}$	[tmtu]	$k_{\text{obs.}2}$
5.3366E-4	0.00307	5.3366E-4	0.00336	5.3366E-4	0.00185
0.00107	0.0061	0.00107	0.00674	0.00107	0.0037
0.0016	0.01013	0.0016	0.01016	0.0016	0.00524
0.00213	0.01305	0.00213	0.01354	0.00213	0.00705
0.00267	0.01698	0.00267	0.01684	0.00267	0.00888

**Table C 2d** Temperature dependence of  $k_{2(2)^{\text{nd}}}$ ,  $\text{M}^{-1} \text{ s}^{-1}$ , for the dechelation of the pyridyl units in **bpPha** by thiourea nucleophiles,  $\text{pH} = 2.0$ ,  $I = 0.02 \text{ M}$  (0.01 M  $\text{CF}_3\text{SO}_3\text{H}$ , adjusted with  $\text{Li}(\text{SO}_3\text{CF}_3)$ ).

1/T	$\ln(k/T)$	1/T	$\ln(k/T)$	1/T	$\ln(k/T)$
0.00325	-3.253	0.00325	-3.258	0.00325	-3.511
0.0033	-3.546	0.0033	-3.494	0.0033	-3.859
0.00335	-3.852	0.00335	-3.781	0.00335	-4.195
0.00341	-4.148	0.00341	-4.057	0.00341	-4.601
0.00347	-4.465	0.00347	-4.386	0.00347	-5.018

# Appendices

## Appendix D Pt(II) complexes with alkyl pendants.

Figure D 1a	Low resolution ESI mass spectrum of <i>N,N</i> -bis(2-pyridylmethyl) <i>tert</i> -butylamine ligand.	301
Figure D 1b	Low resolution ESI mass spectrum of <i>N,N</i> -bis(2-pyridylmethyl)propylamine ligand.	302
Figure D 2a	IR spectrum (KBr pellet) of [Pt(Cl)( <i>N,N</i> -bis(2-pyridylmethyl)propylamine)](ClO <sub>4</sub> ).	303
Figure D 2b	IR spectrum (KBr pellet) of [Pt(Cl)( <i>N,N</i> -bis(2-pyridylmethyl)hexylamine)](ClO <sub>4</sub> ).	303
Figure D 3a	<sup>1</sup> H Spectrum of [Pt(DMF) <i>N,N</i> -bis(2-pyridylmethyl)amine](SO <sub>3</sub> CF <sub>3</sub> ) <sub>2</sub> .	304
Figure D 3b	<sup>13</sup> C Spectrum of [Pt(DMF) <i>N,N</i> -bis(2-pyridylmethyl)amine](SO <sub>3</sub> CF <sub>3</sub> ) <sub>2</sub> . 305	305
Figure D 3c	<sup>195</sup> Pt Spectrum of [Pt(DMF) <i>N,N</i> -bis(2-pyridylmethyl)amine](SO <sub>3</sub> CF <sub>3</sub> ) <sub>2</sub> .	306
Figure D 4a	<sup>1</sup> H NMR spectrum of <i>N,N</i> -bis(2-pyridylmethyl)ethylamine ligand.	307
Figure D 4b	<sup>13</sup> C spectrum of <i>N,N</i> -bis(2-pyridylmethyl)ethylamine ligand.	308
Figure D 5a	<sup>1</sup> H NMR spectrum of <i>N,N</i> -bis(2-pyridylmethyl) <i>tert</i> -butylamine ligand.	309
Figure D 5b 310	<sup>13</sup> C Spectrum of [Pt(DMF) <i>N,N</i> -bis(2-pyridylmethyl) <i>tert</i> -butylamine](SO <sub>3</sub> CF <sub>3</sub> ) <sub>2</sub> .	310
Figure D 6a	<sup>1</sup> H Spectrum of [Pt(DMF) <i>N,N</i> -bis(2-pyridylmethyl)butylamine](SO <sub>3</sub> CF <sub>3</sub> ) <sub>2</sub> .	311
Figure D 6b	<sup>13</sup> C Spectrum of [Pt(DMF) <i>N,N</i> -bis(2-pyridylmethyl)butylamine](SO <sub>3</sub> CF <sub>3</sub> ) <sub>2</sub> .	312
Figure D 7a	<sup>1</sup> H Spectrum of [Pt(DMF) <i>N,N</i> -bis(2-pyridylmethyl)decylamine](SO <sub>3</sub> CF <sub>3</sub> ) <sub>2</sub> .	313
Figure D 7b	<sup>13</sup> C Spectrum of [Pt(DMF) <i>N,N</i> -bis(2-pyridylmethyl)decylamine](SO <sub>3</sub> CF <sub>3</sub> ) <sub>2</sub> .	314
Figure D 7c	<sup>195</sup> Pt spectrum of [Pt(DMF) <i>N,N</i> -bis(2-pyridylmethyl)decylamine](SO <sub>3</sub> CF <sub>3</sub> ) <sub>2</sub> .	315
Figure D 8a	UV-visible spectrum for the titration of 0.1 mM <b>bppa</b> with NaOH, pH range 2 - 9, T 298 K. <i>Inset</i> the titration curve at 268 nm.	316
Figure D 8b	UV-visible spectrum for the titration of 0.1 mM <b>bpba</b> with NaOH, pH range 2 - 9, <i>Inset</i> the titration curve at 268 nm	316
Figure D 9a	Concentration dependence of $k_{\text{obs},(1)}^{\text{st}}$ , s <sup>-1</sup> , for the substitution of the aqua ligand in <b>bpha</b> by thiourea nucleophiles, pH = 2.0, T = 298 K.	317
Figure D 9b	Temperature dependence of $k_{2(1)}^{\text{st}}$ , M <sup>-1</sup> s <sup>-1</sup> , for the simultaneous displacement of the first aqua ligand in <b>bpha</b> by thiourea nucleophiles, pH = 2.0.	317
Figure D 10a	Concentration dependence of $k_{\text{obs},(1)}^{\text{st}}$ , s <sup>-1</sup> , for the substitution of the aqua ligand in <b>bpda</b> by thiourea nucleophiles, pH = 2.0, T = 298 K.	318
Figure D 10b	Temperature dependence of $k_{2(1)}^{\text{st}}$ , M <sup>-1</sup> s <sup>-1</sup> , for the simultaneous displacement of the first aqua ligand in <b>bpda</b> by thiourea nucleophiles, pH = 2.0.	318
Table D 1a	Average observed rate constants, $k_{\text{obs},(1)}^{\text{st}}$ , s <sup>-1</sup> , for the simultaneous displacement of the aqua ligands in <b>bpha</b> by thiourea nucleophiles, pH = 2.0, T = 298 K.	319
Table D 1b	Temperature dependence of $k_{2(1)}^{\text{st}}$ , M <sup>-1</sup> s <sup>-1</sup> , for the simultaneous displacement of the aqua ligands in <b>bpha</b> by thiourea nucleophiles, pH = 2.0.	319
Table D 2a.	Average observed rate constants, $k_{\text{obs},(1)}^{\text{st}}$ , s <sup>-1</sup> , for the simultaneous displacement of the aqua ligands in <b>bpda</b> by thiourea nucleophiles, pH = 2.0, T = 298 K.	319
Table D 2b	Temperature dependence of $k_{2(1)}^{\text{st}}$ , M <sup>-1</sup> s <sup>-1</sup> , for the simultaneous displacement of the aqua	319

# *Appendices*

---

ligands in **bpda** by thiourea nucleophiles, pH = 2.0.

---

**319**

## Appendices

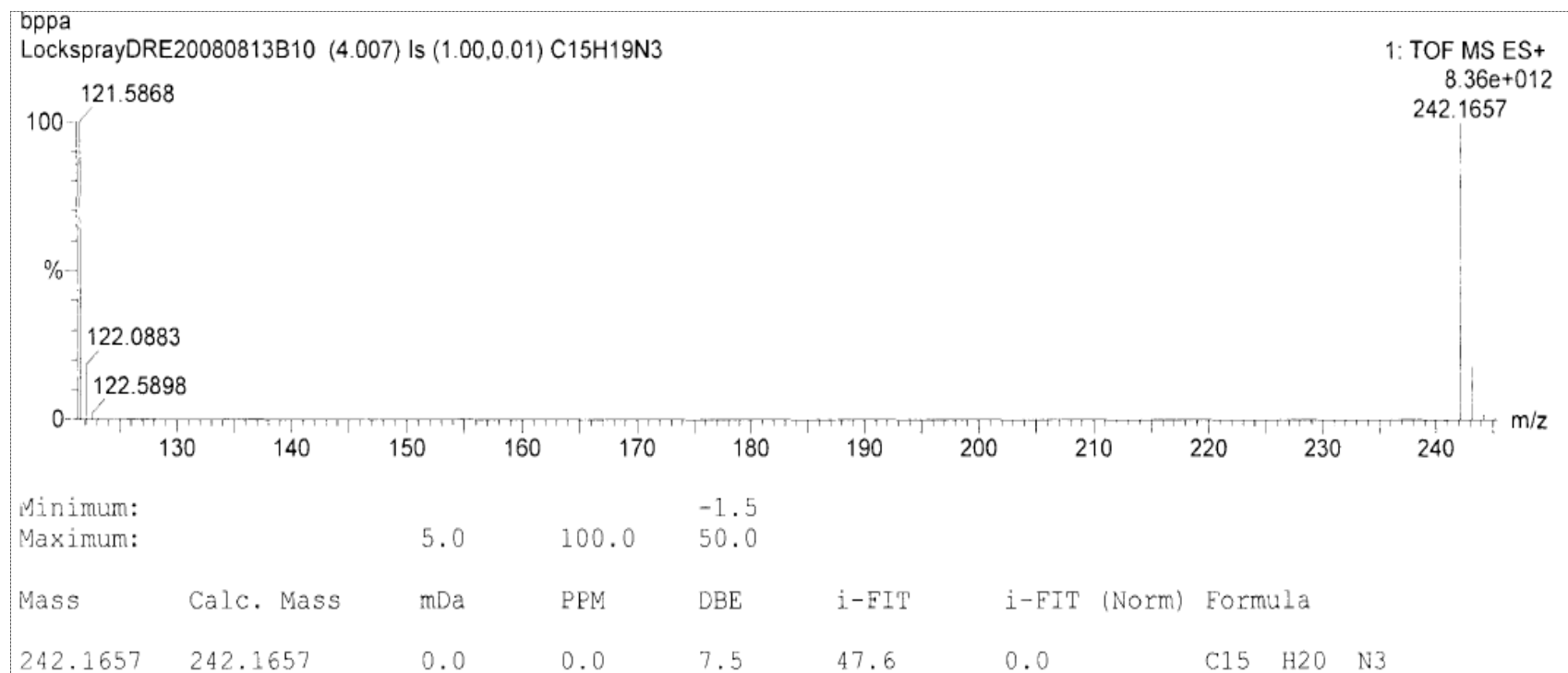


**Figure D 1a** Low resolution ESI mass spectrum of *N,N*-bis(2-pyridylmethyl)*tert*-butylamine ligand.

# Appendices

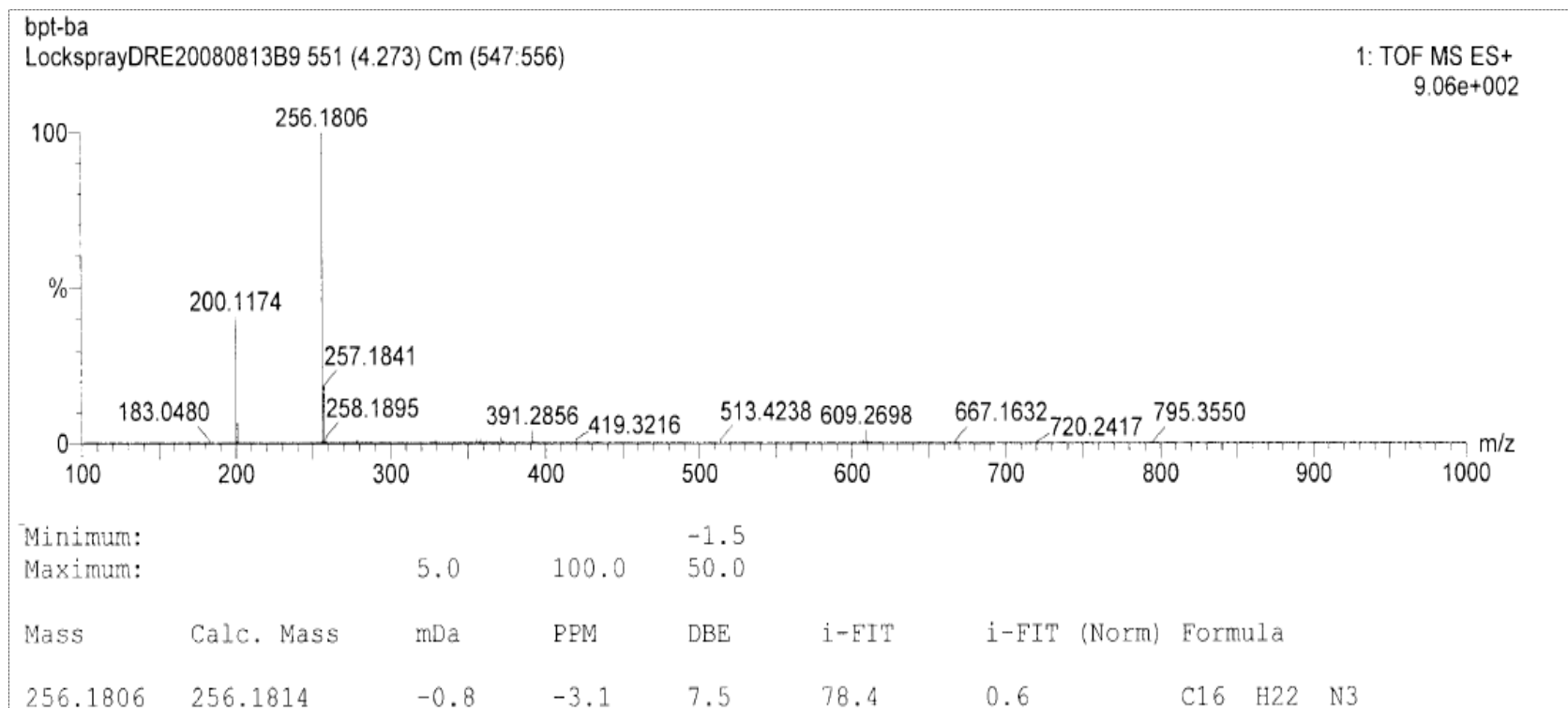


**Figure D 1b** Low resolution ESI mass spectrum of *N,N*-bis(2-pyridylmethyl)propylamine ligand.

# Appendices

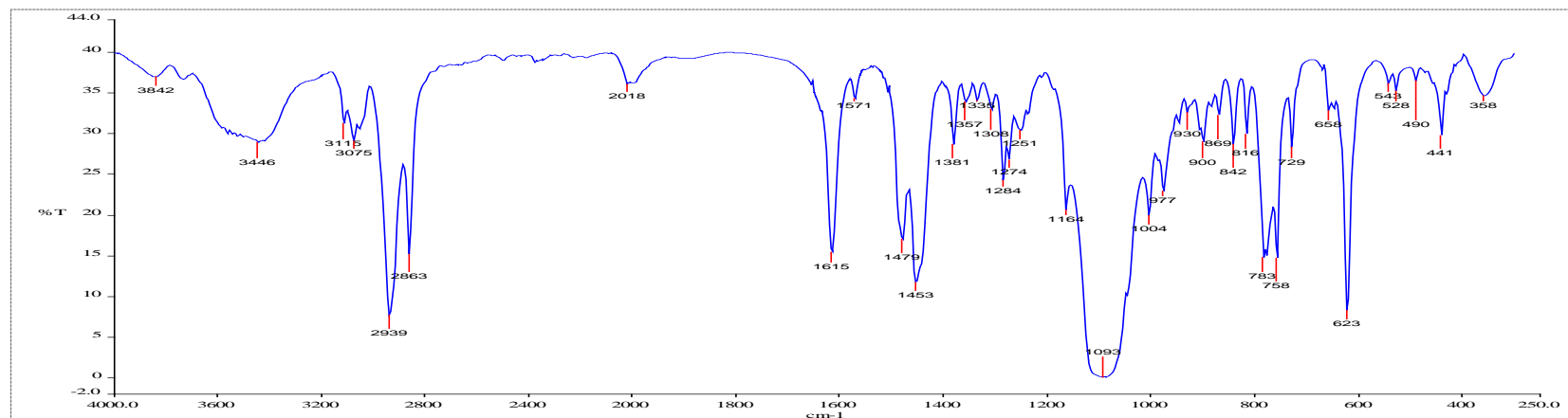


Figure D 2a IR spectrum (KBr pellet) of [Pt(Cl)(*N,N*-bis(2-pyridylmethyl)propylamine)](ClO<sub>4</sub>).

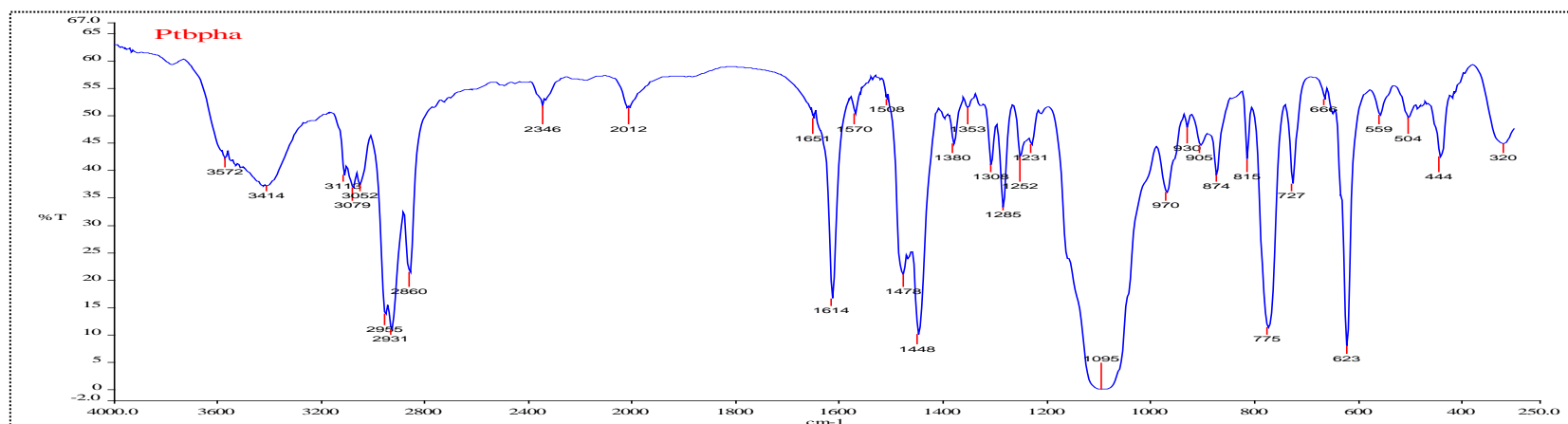
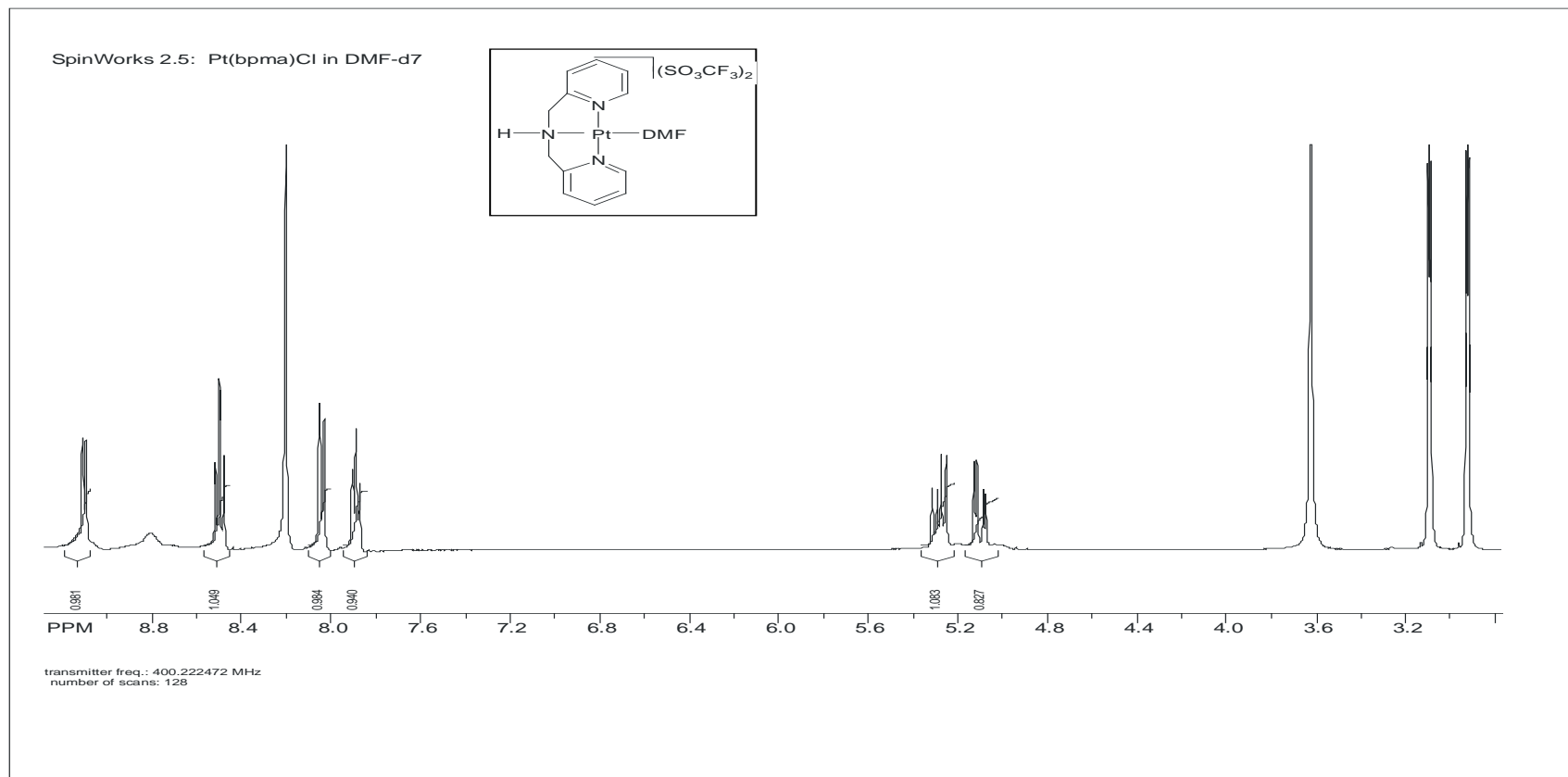


Figure D 2b IR spectrum (KBr pellet) of [Pt(Cl)(*N,N*-bis(2-pyridylmethyl)hexylamine)](ClO<sub>4</sub>).

# Appendices



**Figure D 3a**  $^1\text{H}$  Spectrum of  $[\text{Pt}(\text{DMF})N,N\text{-bis}(2\text{-pyridylmethyl})\text{amine}](\text{SO}_3\text{CF}_3)_2$

# Appendices

SpinWorks 2.5:

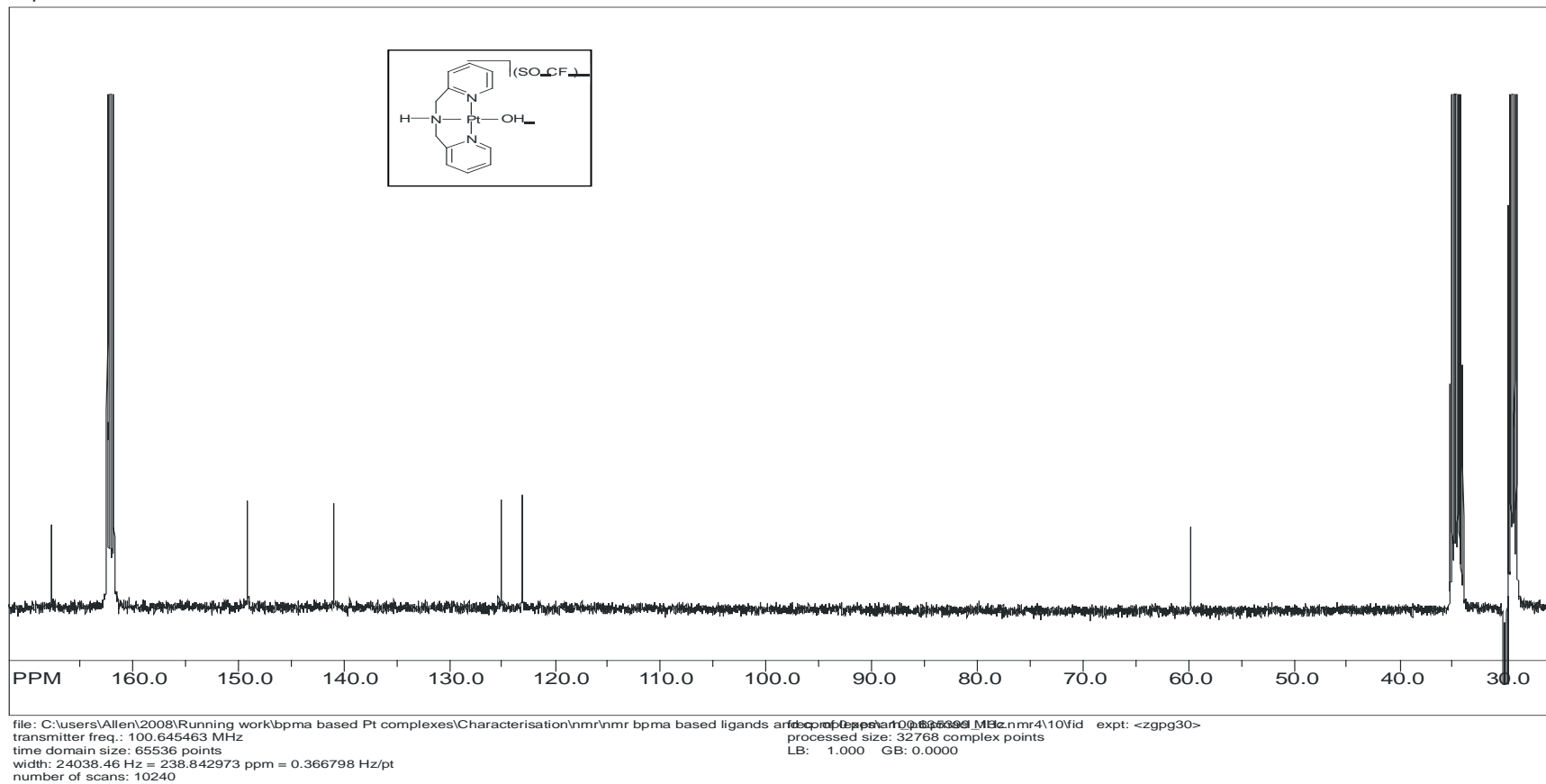


**Figure D 3b**  $^{13}\text{C}$  Spectrum of  $[\text{Pt}(\text{DMF})\text{N},\text{N}\text{-bis}(2\text{-pyridylmethyl})\text{amine}](\text{SO}_3\text{CF}_3)_2$

# Appendices

SpinWorks 2.5: Pt(bpma)Cl in DMF-d7

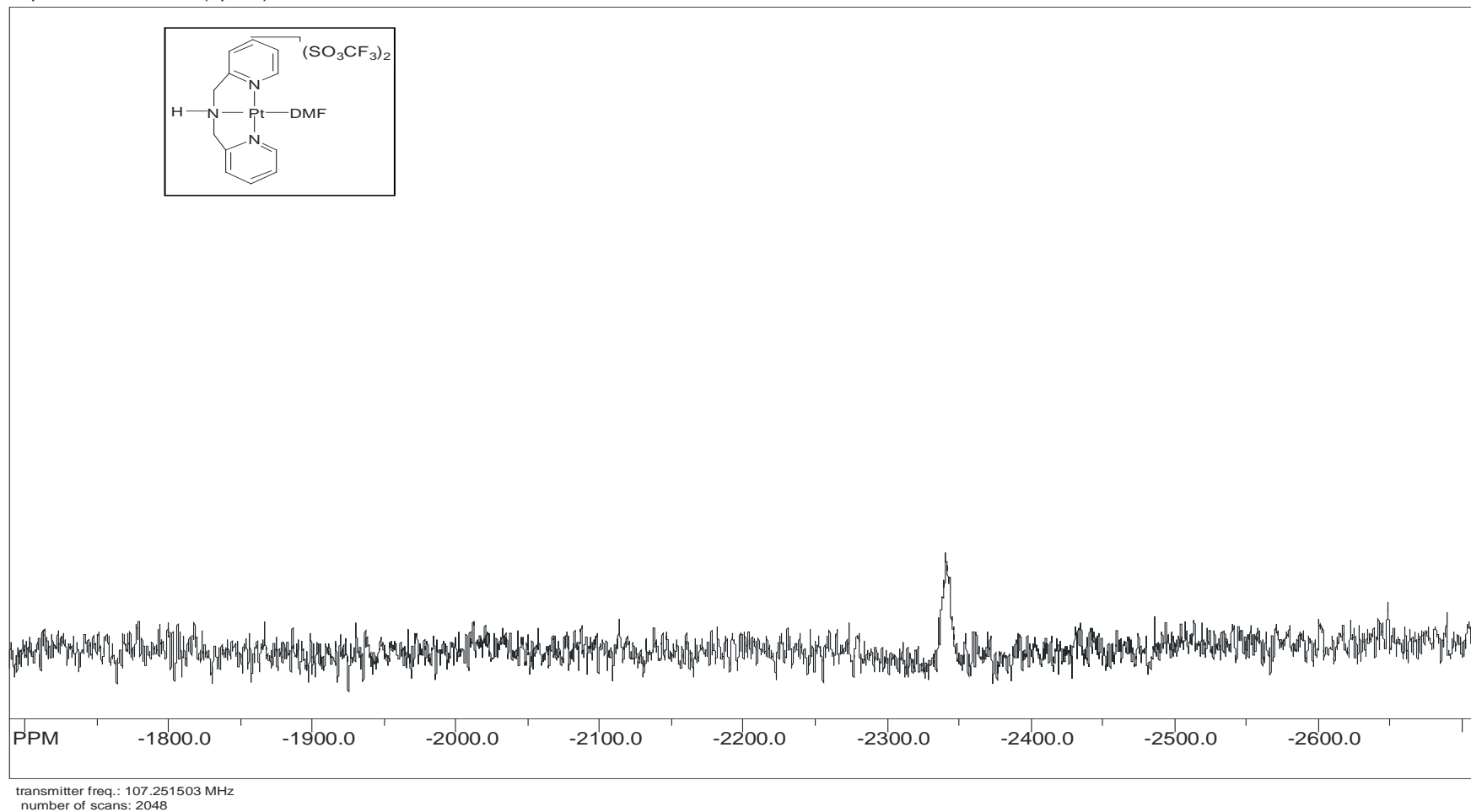


**Figure D 3c**  $^{195}\text{Pt}$  Spectrum of  $[\text{Pt}(\text{DMF})N,N\text{-bis}(2\text{-pyridylmethyl})\text{amine}](\text{SO}_3\text{CF}_3)_2$

# Appendices

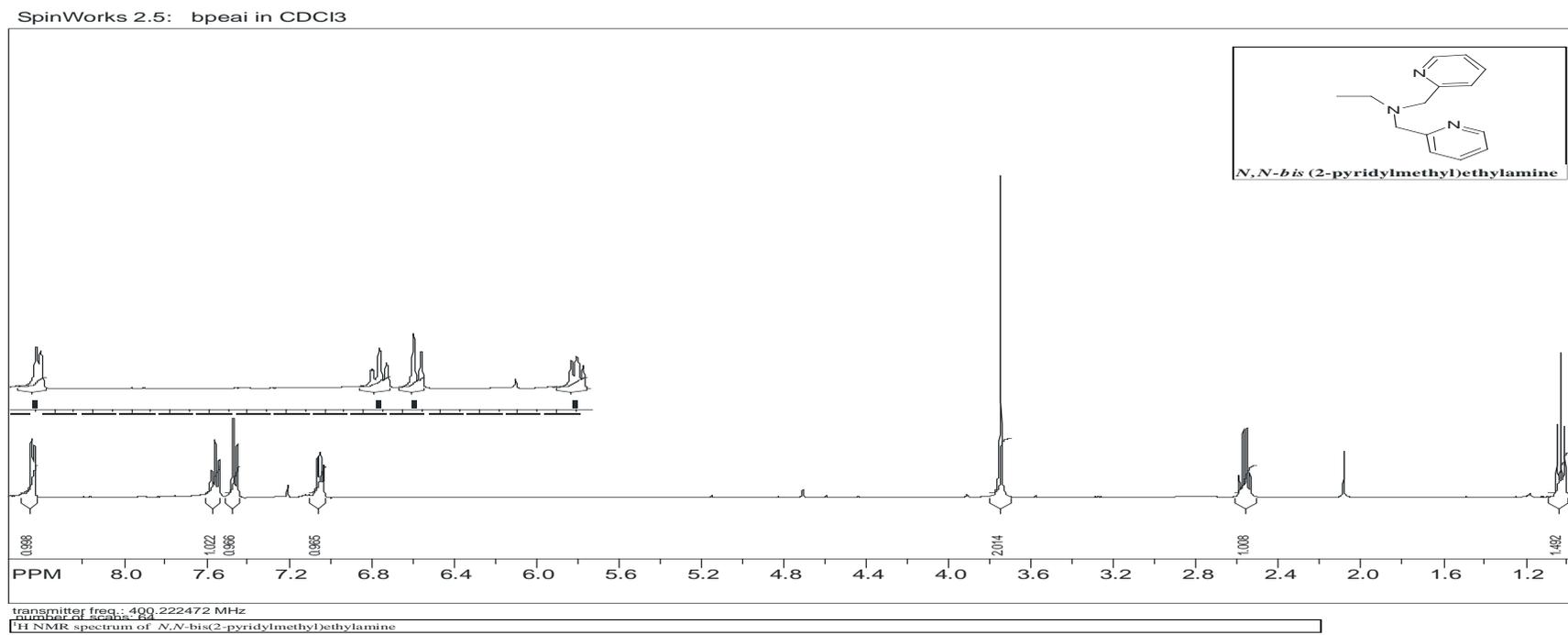


**Figure D 4a.** <sup>1</sup>H NMR spectrum of *N,N*-bis(2-pyridylmethyl)ethylamine ligand.

# Appendices

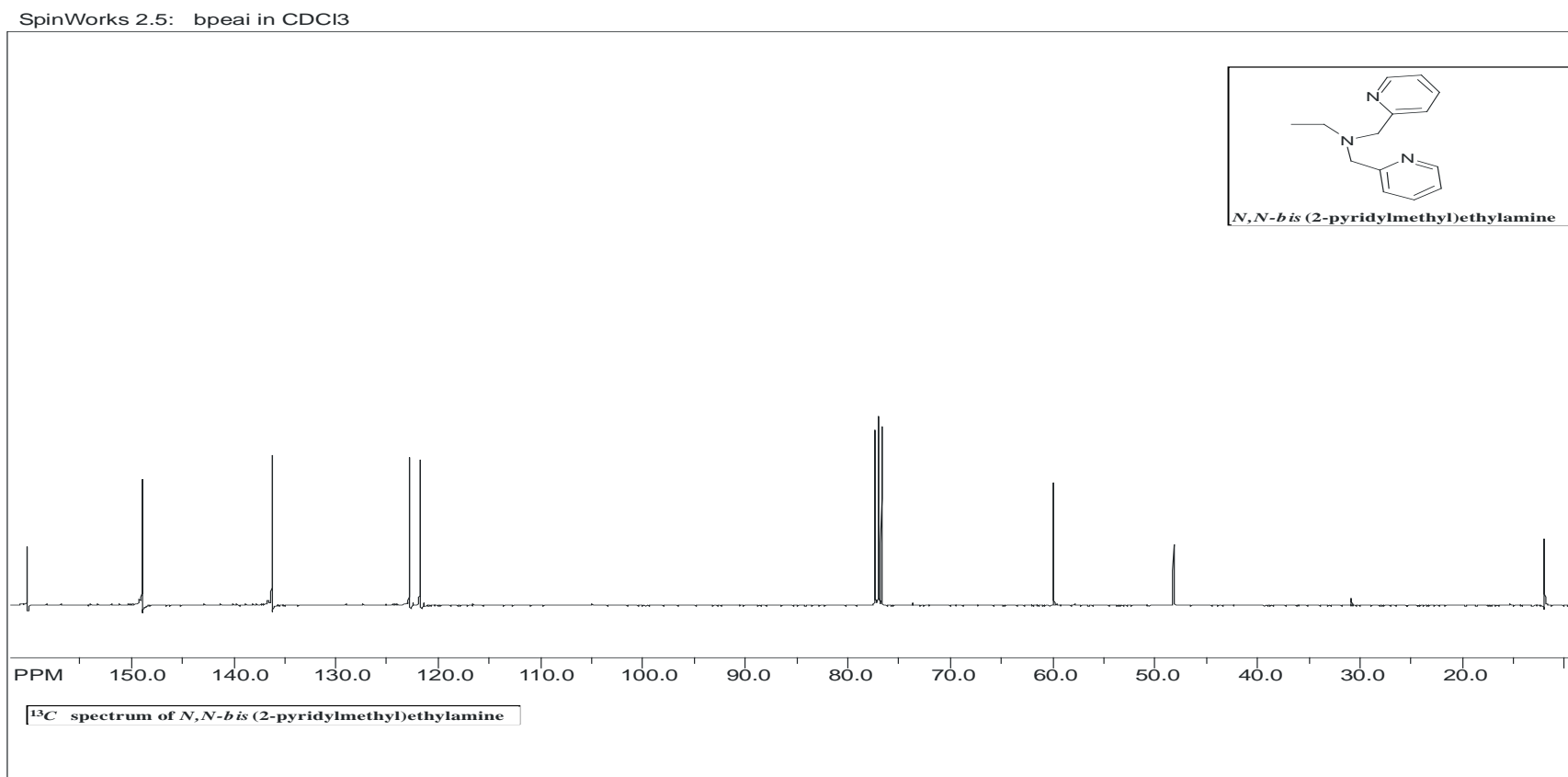


**Figure D 4b** <sup>13</sup>C spectrum of *N,N*-bis(2-pyridylmethyl)ethylamine ligand.

# Appendices

SpinWorks 2.5: Pt(bptbu)Cl in DMF-d7

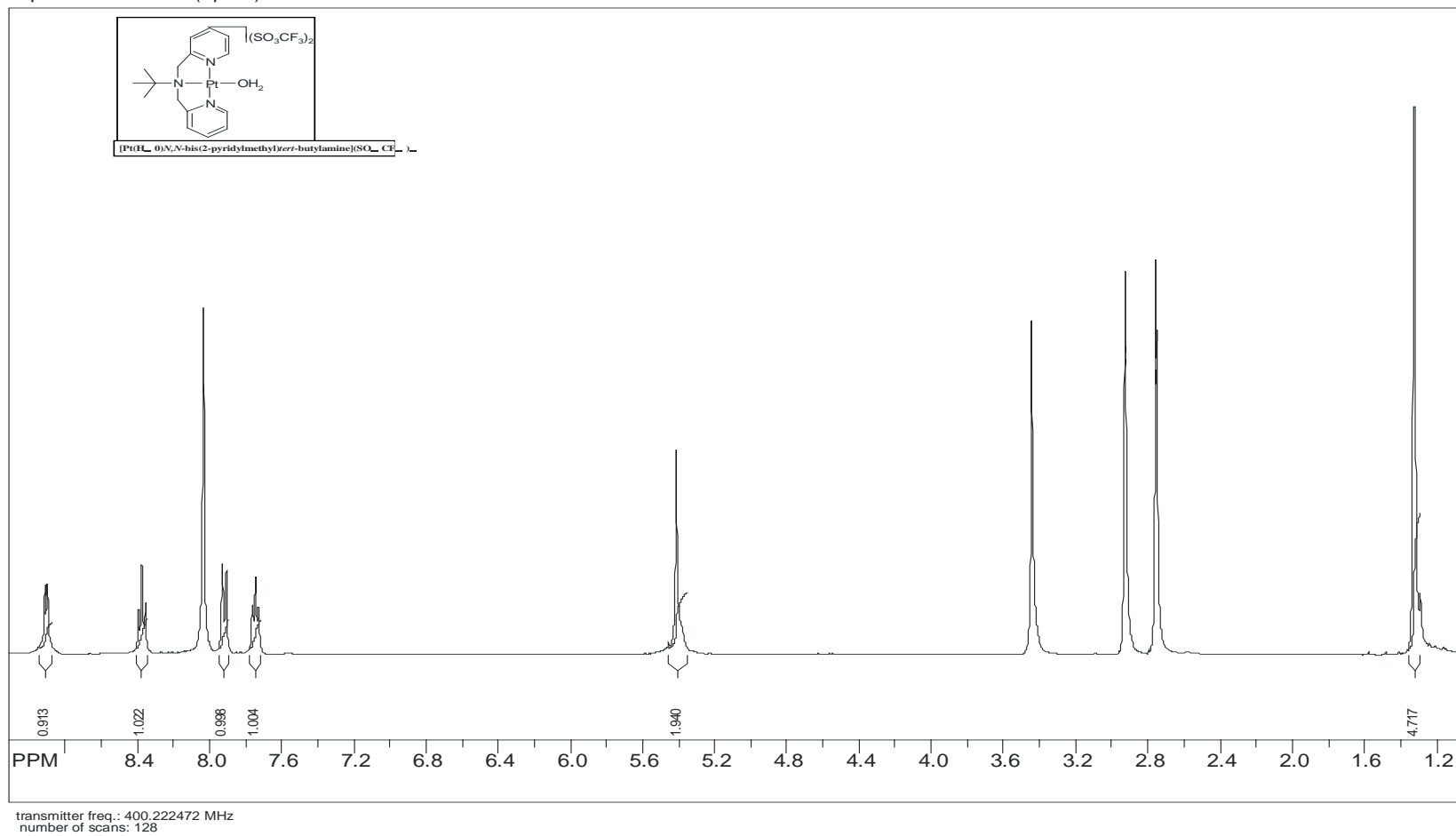


**Figure D 5a** <sup>1</sup>H NMR spectrum of *N,N*-bis(2-pyridylmethyl)*tert*-butylamine ligand.

# Appendices

SpinWorks 2.5: Pt(bptbu)Cl in DMF-d7

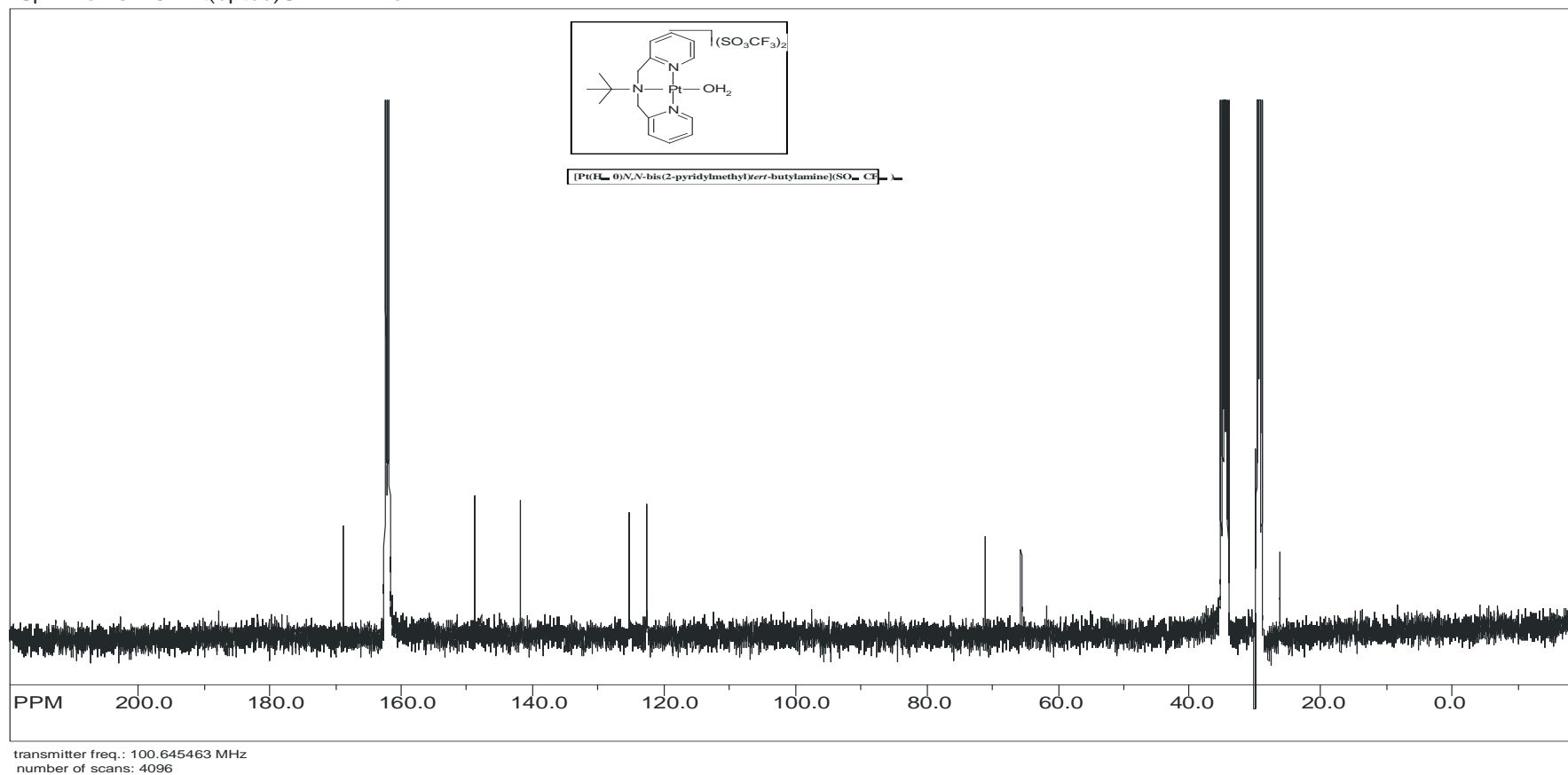


**Figure D 5b**  $^{13}\text{C}$  Spectrum of  $[\text{Pt}(\text{DMF})N,N\text{-bis}(2\text{-pyridylmethyl})\text{tert-butylamine}](\text{SO}_3\text{CF}_3)_2$

# Appendices

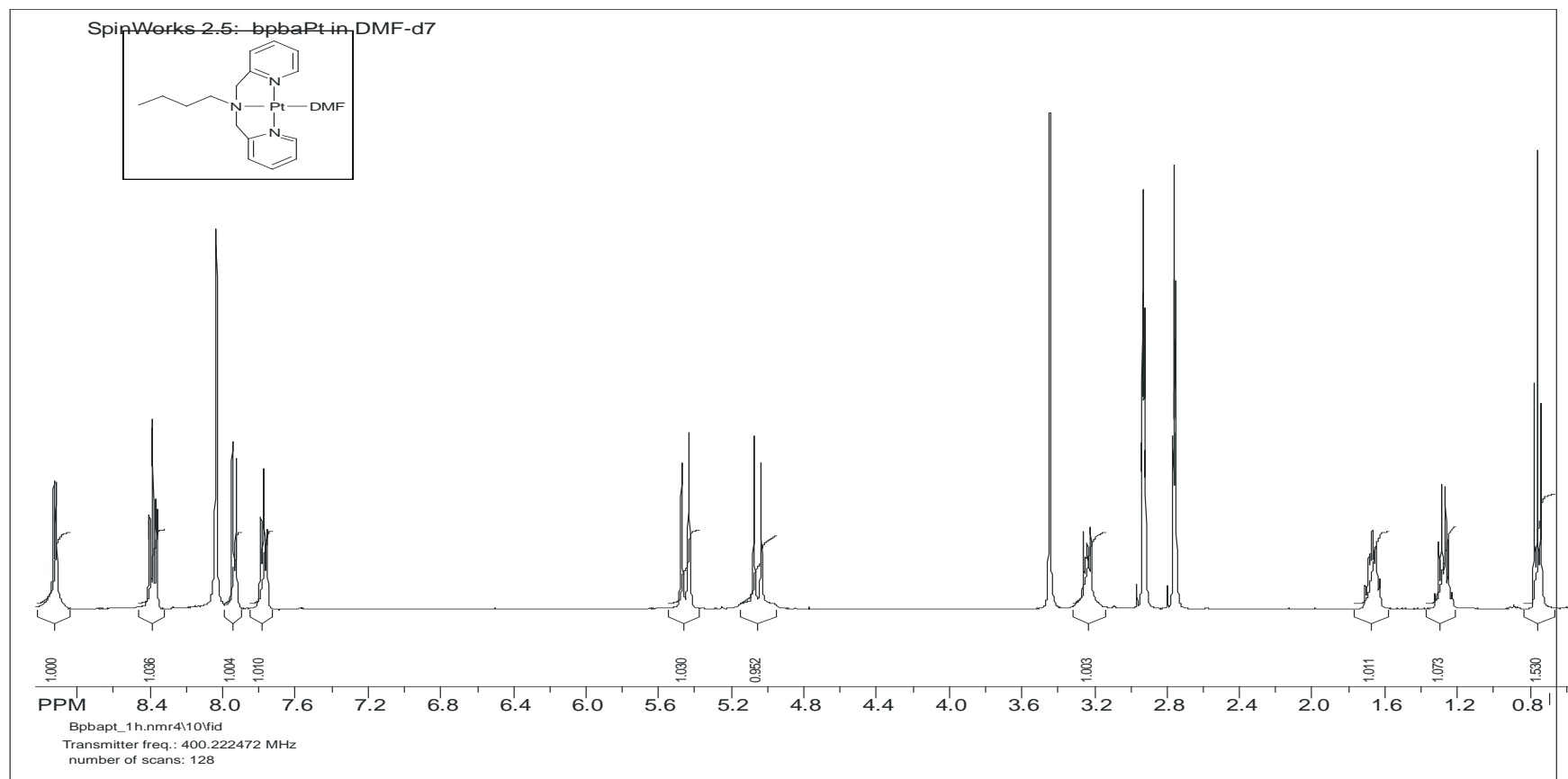


**Figure D 6a**  $^1\text{H}$  Spectrum of  $[\text{Pt}(\text{DMF})N,N\text{-bis}(2\text{-pyridylmethyl})\text{butylamine}](\text{SO}_3\text{CF}_3)_2$

# Appendices

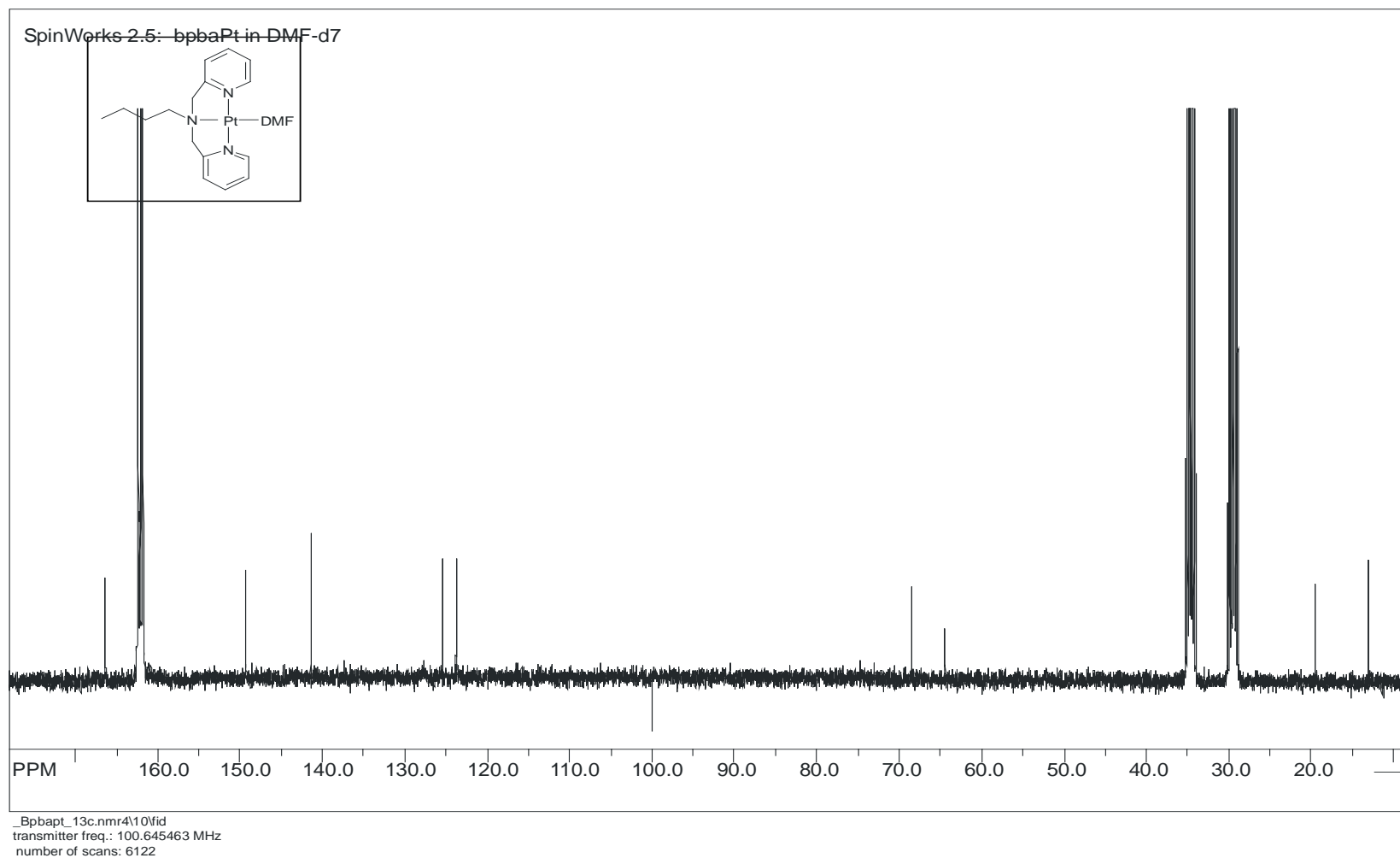
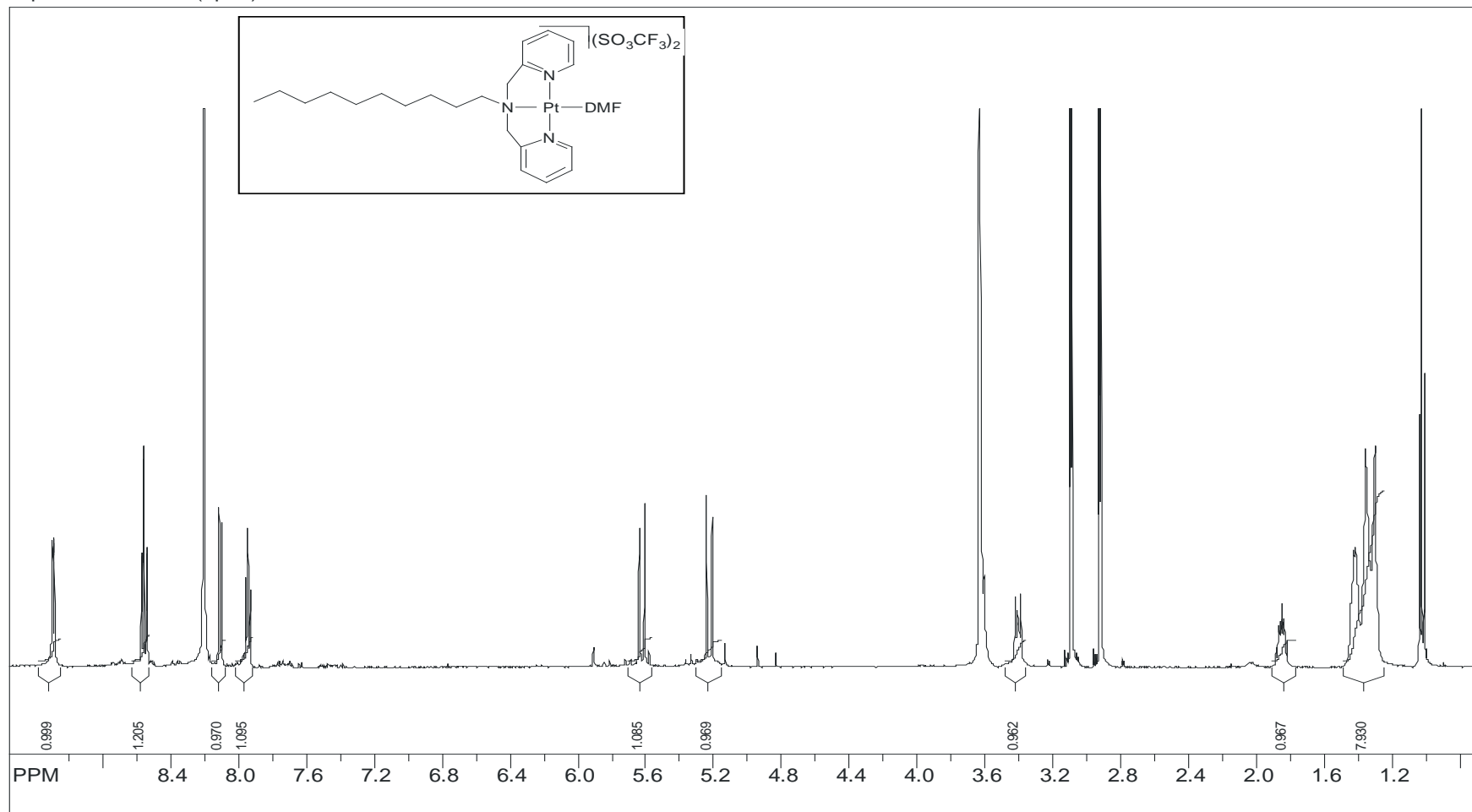


**Figure D 6b**  $^{13}\text{C}$  Spectrum of  $[\text{Pt}(\text{DMF})N,N\text{-bis}(2\text{-pyridylmethyl})\text{butylamine}](\text{SO}_3\text{CF}_3)_2$ .

# Appendices

SpinWorks 2.5: Pt(bpda)Cl in DMF-d7



transmitter freq.: 500.013088 MHz  
number of scans: 128

**Figure D 7a** <sup>1</sup>H Spectrum of [Pt(DMF)N,N-bis(2-pyridylmethyl)decylamine](SO<sub>3</sub>CF<sub>3</sub>)<sub>2</sub>

# Appendices

SpinWorks 2.5: Pt(bpda)Cl in DMF-d7

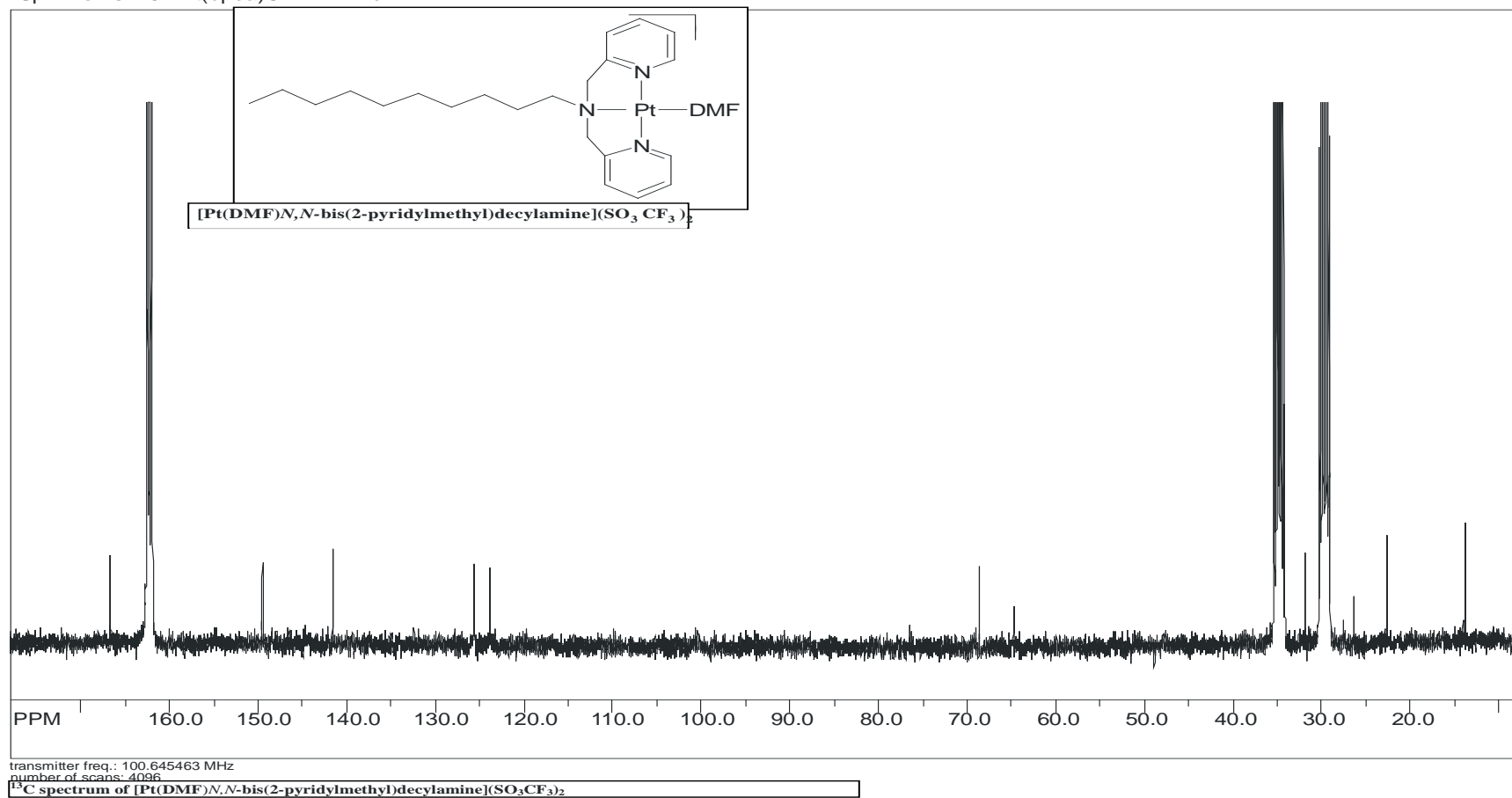


**Figure D 7b** <sup>13</sup>C Spectrum of [Pt(DMF)N,N-bis(2-pyridylmethyl)decylamine](SO<sub>3</sub>CF<sub>3</sub>)<sub>2</sub>

# Appendices

SpinWorks 2.5: Pt(bpda)Cl in DMF-d7

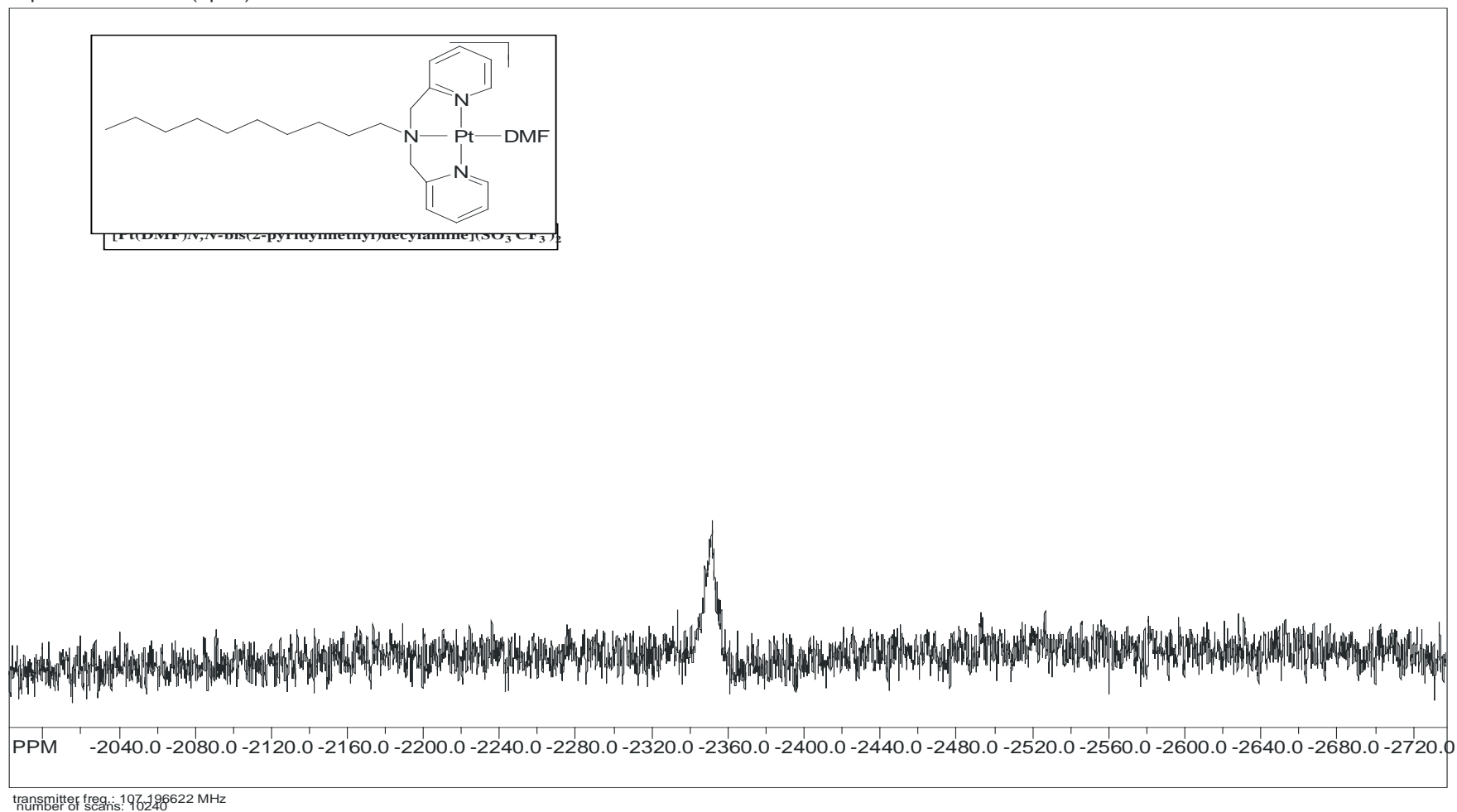


**Figure D 7c**  $^{195}\text{Pt}$  spectrum of  $[\text{Pt}(\text{DMF})N,N\text{-bis}(2\text{-pyridylmethyl})\text{decylamine}](\text{SO}_3\text{CF}_3)_2$ .

## Appendices

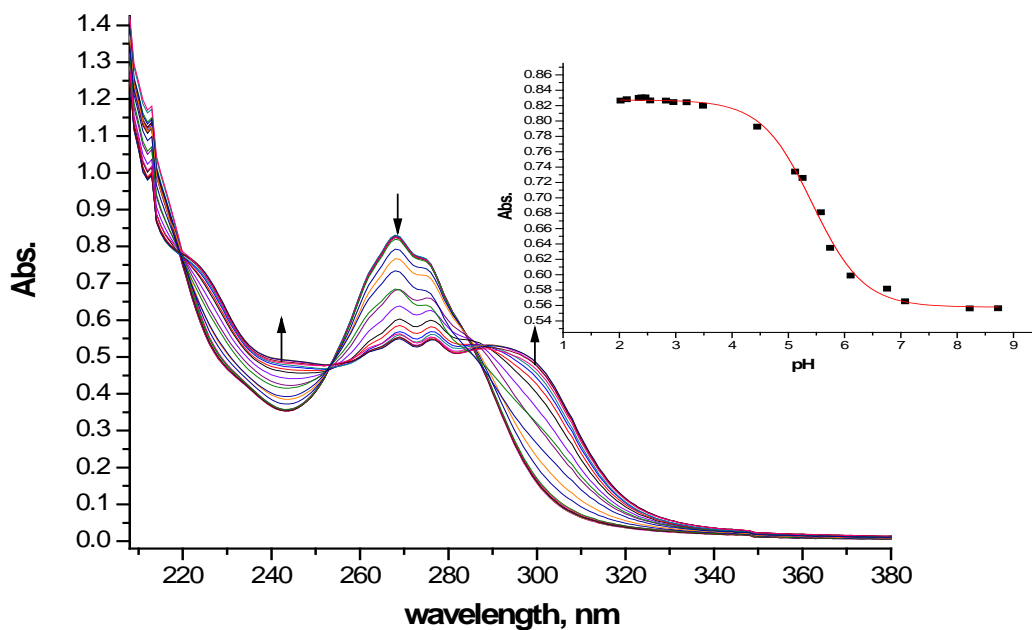


**Figure D 8a** UV-visible spectrum for the titration of 0.1 mM **bppa** with NaOH, pH range 2 - 9, T 298 K. *Inset* the titration curve at 268 nm.

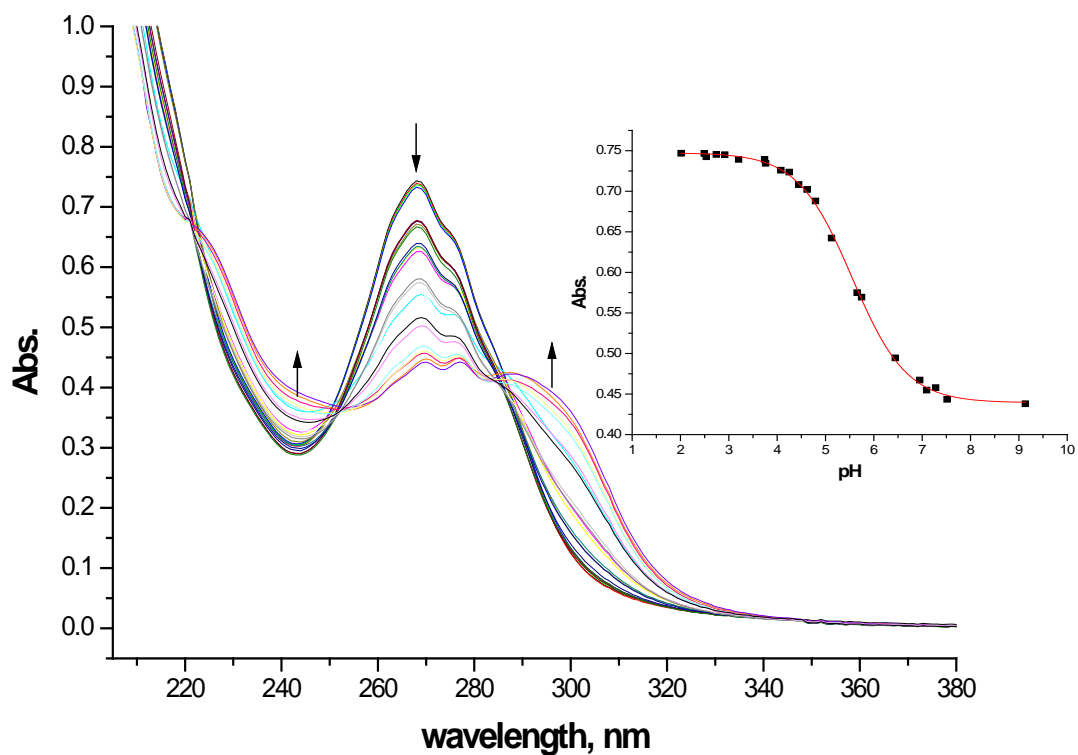


**Figure D 8b** UV-visible spectrum for the titration of 0.1 mM **bppta** with NaOH, pH range 2 - 9, T 298 K. *Inset* the titration curve at 268 nm.

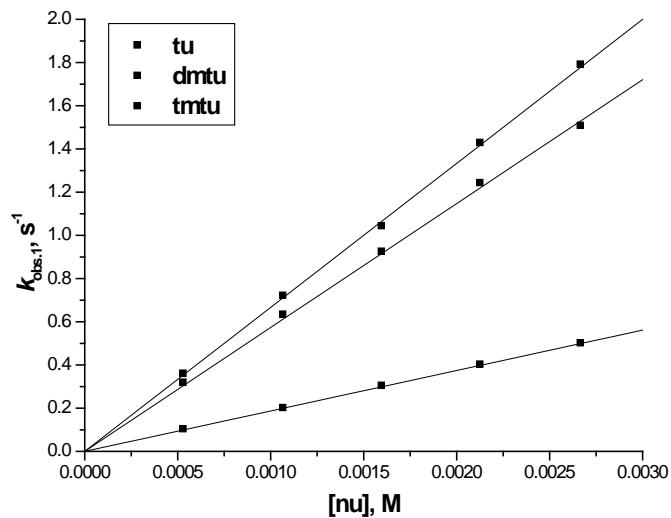


**Figure D 9a** Concentration dependence of  $k_{obs(1^st)}$ , s<sup>-1</sup>, for the substitution of the aqua ligand in **bpha** by thiourea nucleophiles, pH = 2.0, T = 298 K, I = 0.02 M {0.01 M CF<sub>3</sub>SO<sub>3</sub>H, adjusted with Li(SO<sub>3</sub>CF<sub>3</sub>)}.

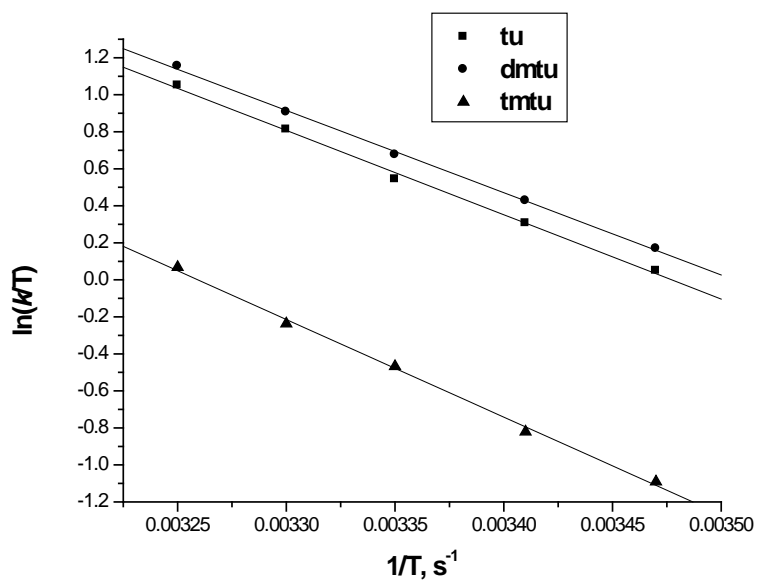


**Figure D 9b** Temperature dependence of  $k_{2(1^st)}$ , M<sup>-1</sup> s<sup>-1</sup>, for the simultaneous displacement of the first aqua ligand in **bpha** by thiourea nucleophiles, pH = 2.0, I = 0.02 M (0.01 M CF<sub>3</sub>SO<sub>3</sub>H, adjusted with Li(SO<sub>3</sub>CF<sub>3</sub>)).

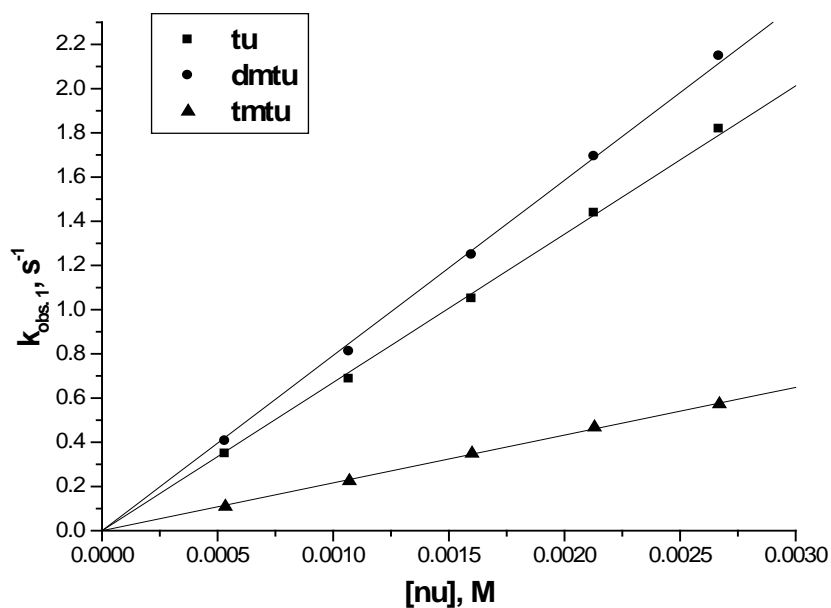


**Figure D 10a** Concentration dependence of  $k_{obs(1)}^{st}, s^{-1}$ , for the substitution of the aqua ligand in **bpda** by thiourea nucleophiles, pH = 2.0, T = 298 K, I = 0.02 M {0.01 M  $CF_3SO_3H$ , adjusted with  $Li(SO_3CF_3)$ }.

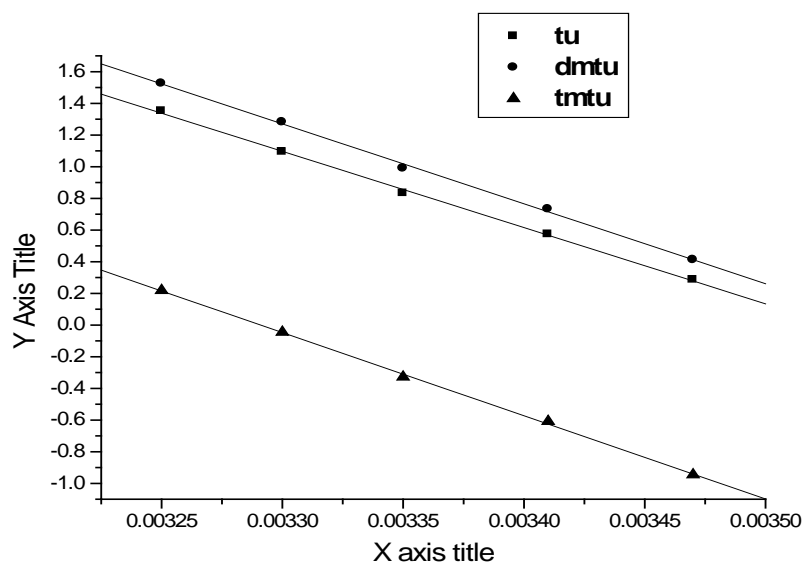


**Figure D 10b** Temperature dependence of  $k_{2(1)}^{st}, M^{-1} s^{-1}$ , for the simultaneous displacement of the first aqua ligand in **bpda** by thiourea nucleophiles, pH = 2.0, I = 0.02 M (0.01 M  $CF_3SO_3H$ , adjusted with  $Li(SO_3CF_3)$ ).

## Appendices

**Table D 1a.** Average observed rate constants,  $k_{\text{obs}(1^{\text{st}})}$ ,  $\text{s}^{-1}$ , for the simultaneous displacement of the aqua ligands in **bpha** by thiourea nucleophiles,  $\text{pH} = 2.0$ ,  $T = 298 \text{ K}$ .

[tu], M	$k_{\text{obs } 1}, \text{s}^{-1}$	[dm tu], M	$k_{\text{obs } 1}, \text{s}^{-1}$	[tmtu], M	$k_{\text{obs } 1}, \text{s}^{-1}$
5.334E-4	0.3163	5.327E-4	0.3576	5.3365E-4	0.1003
0.00107	0.6308	0.00107	0.7181	0.00107	0.1982
0.0016	0.9222	0.0016	1.041	0.0016	0.3015
0.00223	1.24	0.00213	1.426	0.00213	0.3992
0.00267	1.505	0.00266	1.788	0.00267	0.4985

**Table D 1b** Temperature dependence of  $k_{2(1^{\text{st}})}$ ,  $\text{M}^{-1} \text{s}^{-1}$ , for the simultaneous displacement of the aqua ligands in **bpha** by thiourea nucleophiles,  $\text{pH} = 2.0$ .

1/T, $\text{K}^{-1}$	$\ln(k/T)$	1/T, $\text{K}^{-1}$	$\ln(k/T)$	1/T, $\text{K}^{-1}$	$\ln(k/T)$
0.00325	1.051	0.00325	1.154	0.00325	0.068
0.0033	0.8125	0.0033	0.9061	0.0033	-0.237
0.00335	0.5427	0.00335	0.6757	0.00335	-0.4674
0.00341	0.3059	0.00341	0.4273	0.00341	-0.8208
0.00347	0.0489	0.00347	0.1692	0.00347	-1.091

**Table D 2a.** Average observed rate constants,  $k_{\text{obs}(1^{\text{st}})}$ ,  $\text{s}^{-1}$ , for the simultaneous displacement of the aqua ligands in **bpda** by thiourea nucleophiles,  $\text{pH} = 2.0$ ,  $T = 298 \text{ K}$ .

[tu]	$k_{\text{obs } 1}$	[dm tu]	$k_{\text{obs } 1}$	[tmtu]	$k_{\text{obs } 1}$
5.35E-4	0.3468	5.35E-4	0.4044	5.336E-4	0.1091
0.00107	0.6847	0.00107	0.8089	0.00107	0.225
0.00161	1.048	0.00161	1.2469	0.0016	0.349
0.00214	1.4363	0.00214	1.692	0.00213	0.468
0.00267	1.816	0.00267	2.146	0.00267	0.5729

**Table D 2b** Temperature dependence of  $k_{2(1^{\text{st}})}$ ,  $\text{M}^{-1} \text{s}^{-1}$ , for the simultaneous displacement of the aqua ligands in **bpda** by thiourea nucleophiles,  $\text{pH} = 2.0$ ,  $I = 0.02 \text{ M}$  ( $0.01 \text{ M CF}_3\text{SO}_3\text{H}$ , adjusted with  $\text{Li}(\text{SO}_3\text{CF}_3)$ ).

[tu]	$k_{\text{obs } 1}$	[dm tu]	$k_{\text{obs } 1}$	[tmtu]	$k_{\text{obs } 1}$
0.00325	1.352	0.00325	1.5257	0.00325	0.2185
0.0033	1.093	0.0033	1.2809	0.0033	-0.045
0.00335	0.8328	0.00335	0.9898	0.00335	-0.3283
0.00341	0.5731	0.00341	0.7321	0.00341	-0.6086
0.00347	0.2856	0.00347	0.411	0.00347	-0.9456